Sulfur(VI) Fluorides for Covalently Targeting Non-Cysteine Residues in Kinases: From Structure-Based Design to Covalent-First Approaches

Dissertation

der Mathematisch-Naturwissenschaftlichen Fakultät

der Eberhard Karls Universität Tübingen

zur Erlangung des Grades eines

Doktors der Naturwissenschaften

(Dr. rer. nat.)

vorgelegt von

Laura Hillebrand

aus Eschwege

Tübingen

2025

Gedruckt mit Genehmigung der Mathematisch-Naturwissenschaftlichen Fakultät der Eberhard Karls Universität Tübingen.

Tag der mündlichen Qualifikation:	19.09.2025
Dekan:	Prof. Dr. Thilo Stehle
1. Berichterstatter:	Prof. Dr. Matthias Gehringer
2. Berichterstatter:	Prof. Dr. Stefan A. Laufer
3. Berichterstatter:	Prof. Dr. Frank M. Böckler

Publication List

Hillebrand, L.; Gehringer, M. Never Gonna Give You Up – Current Developments in Covalent Protein Kinase Inhibitors. *CHIMIA* **2022**, *76* (5), 435–447.

Hillebrand, L.; Liang, X. J.; Serafim, R.; Gehringer, M. Emerging and Re-Emerging Warheads for Targeted Covalent Inhibitors: An Update. *J. Med. Chem.* **2024**, *67* (10), 7668–7758.

Hillebrand, L.; Wang, G.; Rasch, A.; Masberg, B.; Chaikuad, A.; Kronenberger, T.; Günther, E.; Forster, M.; Poso, A.; Lämmerhofer, M.; Laufer, S. A.; Knapp, S.; Gehringer M. A Twist in the Tale: Shifting from Covalent Targeting of a Tyrosine in JAK3 to a Lysine in MK2. *RSC Med. Chem.* **2025**, Advance Article.

“There is freedom waiting for you,
On the breezes of the sky,
And you ask, "What if I fall?"
Oh but my darling,
What if you fly?”
– *Erin Hanson*

Danksagung

Ich bedanke mich bei…

Prof. Dr. Matthias Gehringer für die Möglichkeit, diese Dissertation in einem freien und vertrauensvollen Arbeitsumfeld anfertigen zu dürfen. Besonders dankbar bin ich für die stets offene Tür und das offene Ohr – sowohl für fachliche Fragen als auch für persönliche Anliegen. Für die engagierte Betreuung meiner Arbeit, die zahlreichen hilfreichen Ratschläge bei chemischen Fragestellungen und den Austausch auf Augenhöhe danke ich ebenso wie für die Förderung eines kollegialen und wertschätzenden Arbeitsklimas. Mein Dank gilt darüber hinaus der finanziellen Unterstützung bei Tagungen sowie der Übernahme des Erstgutachtens.

Prof. Dr. Stefan Laufer für die Übernahme des Zweitgutachtens sowie für die Bereitstellung von Teilen der Infrastruktur, die die Durchführung der Synthese- und Analytikarbeiten ermöglicht haben.

Prof. Dr. Frank Böckler für die Erstellung des Drittgutachtens, die Teilnahme am Prüfungskomitee sowie für die Bereitstellung der Infrastruktur in der 8. Ebene. Außerdem gilt mein Dank seinen Mitarbeitenden für die freundliche Aufnahme und die angenehme Zusammenarbeit in der 8. Ebene. Ein besonderer Dank geht an **Jason Stahlecker** für die Unterstützung bei der kristallografischen Auswertung sowie an **Janosch Rheinganz** und **Martin Schwer** für das gelegentliche spontane Bereitstellen von Puffern.

Prof. Dr. Michael Lämmerhofer für die Teilnahme am Prüfungskomitee sowie bei seinem Mitarbeiter **Benedikt Masberg** für die Durchführung von (HR)MS Experimenten.

Unserem Kooperationspartner **Prof. Dr. Stefan Knapp** sowie seinen (ehemaligen) Mitarbeitern **Dr. Apirat Chaikuad** und **Guiqun Wang** für die Durchführung der Protein-MS Versuche und der Kristallstrukturanalyse.

Prof. Dr. Antti Poso, **Dr. Thales Kronenberger** und **Dr. Ina Pöhner** für die *in silico* Beiträge, das Modeling und alle Erklärungen dazu, sowie bei der Hilfe für die Auswahl der Tyrosin Library.

Our cooperation partners at the CMD in Oxford, **Dr. Jonathan Elkins** and **Dr. Eleanor Williams**, for welcoming me into their group and giving me the opportunity to benefit from their expertise and infrastructure for my project. I am especially grateful for the time they took to explain so many details to me and for their invaluable support during day-to-day work in the lab. Furthermore, I would like to thank everyone at the CMD for any support they have given me during my stay – in particular **Kory Wang**, **Dr. Souvika Bakshi**, **Anjhu Nair**, **Dong Wang**, and **Dr. Lee Harris** for their help in the lab, enjoyable lunch breaks, and all the other ways they made my time there easier and more pleasant. Finally, I would like to thank **Dr. Alexander Bullock** and, in particular, **William Seaton-Burn** from his group for providing me with proteins and for all the effort, especially by Will, that went into generating the final biological results of my thesis.

Der **Studienstiftung des deutschen Volkes** und der **Evonik-Stiftung** für die finanzielle und ideelle Förderung im Rahmen eines Stipendiums, die die Anfertigung dieser Arbeit in vielfältiger Weise unterstützt hat.

Dr. Raimund Nieß für die stets angenehme Zusammenarbeit im Praktikum, die Unterstützung bei der Abwicklung bürokratischer Aufgaben sowie für die zuverlässige und zügige Bearbeitung von Bestellungen aller Art.

Katharina Bauer, **Gerd Helms** und **Ursula Kurz** für die Unterstützung bei der Testung von Compounds, die Gespräche im Assay-Labor und im Kaffeeraum, und die Betreuung der NMR-Messungen.

Mechthild Seyboldt, **Birgit Kailer** und **Cornelia Neuhaus** für die zuverlässige Versorgung mit Chemikalien und Abfallkanistern sowie die reibungslose Verteilung der Bestellungen.

Kristine Schmidt für ihre immer freundliche Unterstützung bei bürokratischen Angelegenheiten und dem Versand zahlreicher Testverbindungen ins In- und Ausland.

Meinen Laborkollegen über die Jahre: **Dr. Stefan Gerstenecker** und **Dr. Lisa Haarer** für die Aufnahme ins Labor, die lustige Zeit und weitreichende Unterstützung im Laboralltag; **Janis Leske** (danke für die neverending Memes) und **Rebekka Fürst**, aka das *Musical Lab*, und, wenn auch nur für eine kurze Zeit, **Jana Strumberger**.

Allen anderen Mitgliedern des AK Gehringer: **Dr. Ricardo Serafim**, **Julia Liang**, **Maksym Kurkunov**, **Dr. Michela Puxeddu**, **Malte Hanne**, **Dr. Fabian Kraft**, **Simone Raimondi**, **Dr. Viktor Reshetnikov**, **Malte Mallossek**, **und Dr. Nikolaus Jork**.

Dem Nordlabor, das ich immer weiter „infiltrieren“ durfte: **Dr. Pascal Sander**, **Dr. Leon Katzengruber**, **Valentin Wydra**, **Eric Eberlein** und ganz besonders **Dr. Júlia Galvez**. Danke für die Gastaufnahme in den Club, die lustigen Zeiten im Labor und außerhalb. Júlia, thanks for the friendship outside of work, the BoB vacation, the LiB afternoons, the endless talks. One day we'll see Beyoncé together, I am sure of it.

Dr. Florian Wittlinger, Dr. Michael Forster, Dr. Claudia Albertini, Dr. Carine Abdelmalek, Gregor Schmidberger, Frederik Hacker, Nico Seidler für die gemeinsame Zeit auf den „AK Ausflügen“ nach Italien und Ägypten.

Dr. Florian Wittlinger, **Eric Eberlein** und **Janis Leske** fürs Korrekturlesen von Teilen dieser Arbeit.

Allen anderen Mitgliedern des AK Laufer: **Dr. Teodor Dimitrov**, **Dr. Philipp Nahidino**, **Raphael Ditzinger**, **Masanja Trautz**, **Mareike Möllers**, **Dr. Benedikt Wagner**, **Markus Friedrich**, **Moritz Schwarz**, **Dr. Alp Bayrak**, **Dr. Philipp Flury**, **Mirko Brandtjen**, **Dr. Thanigaimalai Pillayar**, **Mark Kudolo**, **Peter Weißhaupt**, **Dr. Florian Mohr**, **Dr. Juliander Reiner**, **Alexander Rasch**, **Roberta Cristofalo**, **Ekaterina Hermann**.

Meinen Freunden **Karoline Scheer**, für eine Freundschaft, die mich seit über 20 Jahren begleitet – vom Schulhof bis ins Erwachsenenleben, für unzählige gemeinsame Erlebnisse, und dafür, dass diese Verbindung bis heute geprägt ist von Vertrauen und einer Selbstverständlichkeit, die nicht selbstverständlich ist; (fast auch Dr.) **Magdalena Blei**, mit der ich mein Chemiestudium begonnen habe, für gemeinsame Urlaube, unvergessliche Momente voller Lachen und die beständige Unterstützung über all die Jahre; den Mädels vom **TV Rottenburg** und vom **TüMo**, für die herzliche Aufnahme in die Teams, den gemeinsam vergossenen Schweiß auf dem Volleyballfeld, die wertvolle Ablenkung vom Alltag und all die vielen schönen Momente abseits des Spielfelds, ganz besonders **Jule Vetter**, **Siggi Hanenberg** und **Stephanie Petzold** für die Zeit neben dem Spielfeld im Café, beim Frühstück, beim Laufen oder einfach so.

The whole **Collis family** – **Todd**, **Beth**, **Will** and especially **Zoe** – for taking me in when I was 16 years old, making me part of your family (the only honorary Collis there is!!!), probably

changing the trajectory of my life forever. Zoe, you're the closest person I have ever come to calling a sister – and truly the best one I could wish for.

Meinen Eltern **Annelie Bäumer** und **Ewald Hillebrand** für die bedingungslose Liebe und Unterstützung in absolut allen Lebenslagen. Dafür, dass sie mir stets mit Rat und Tat zur Seite standen, ohne mir je ihre Meinung aufzuzwingen oder Erwartungen an mich zu stellen, die mir Druck gemacht hätten – und mir so den Raum gegeben haben, meinen eigenen Weg zu gehen.

Zusammenfassung

Kovalente Proteinkinaseinhibitoren haben sich als wirksame Therapeutika etabliert, wobei der Fokus bisher vor allem auf der Adressierung reaktiver Cysteinreste lag. Viele Kinasen besitzen jedoch keine Cysteine an strategisch relevanten Positionen, was die Einsatzmöglichkeiten dieses Ansatzes einschränkt. Diese Arbeit untersucht daher die kovalente Hemmung mittels Aminosäureresten jenseits von Cystein, mit Fokus auf den weniger erforschten nucleophilen Aminosäuren Tyrosin und Lysin.

Erste Ansätze zielten auf die Nutzung von Schwefel(VI) Fluorid Chemie zur gezielten Adressierung von Tyrosinen in den Kinasen JAK3 und MK2 anhand strukturbasierten Designs ab. Die dargestellten Verbindungen mit Sulfonylfluorid- und Fluorsulfat-Warheads zeigten in einzelnen Fällen kovalente Modifikation, funktionelle Hemmung blieb jedoch häufig aus. Ein Fluorsulfat-Analogon modifizierte überraschenderweise statt eines Tyrosins das „katalytische“ Lysin in MK2, was die unerwartete, aber vielversprechende Reaktivität dieser Warheads verdeutlicht.

Wegen der eingeschränkten Erfolge mit struktur-basiertem, rationalem Design wurde daher ein „covalent-first“-Ansatz weiterverfolgt: Eine fokussierte Bibliothek mit verschiedenen Hinge-Bindungsmotiven, Linkern und S(VI)F-Warheads wurde an Kinasen mit Tyrosinresten in privilegierten strukturellen Positionen getestet. Dabei wurde eine Fluorsulfat-basierte Verbindung entdeckt, die das Lys338 (HRD+2) von ALK2 kovalent modifiziert, einer Kinase, die bei Fibrodysplasia Ossificans Progressiva (FOP) eine zentrale Rolle spielt. Dies stellt den ersten kovalenten Liganden für ALK2 dar, deren aktives Zentrum kein adressierbares Cystein besitzt und daher für Cystein-fokussierte Ansätze bisher unzugänglich war.

Strukturelle und kinetische Untersuchungen zeigten, dass Änderungen am Hinge-Bindungsmotif die Inaktivierungskinetik stark beeinflussen, während Variationen am Linker geringere Effekte hatten. Wie erwartet reagierten Sulfonylfluoride schneller als Fluorosulfate. Auch Substituenten am Arylring des Warheads beeinflussten die Reaktivität: Elektronenziehende Gruppen beschleunigten die Modifikation, elektronenschiebende verlangsamten sie, wobei sterische Hinderung diese Effekte abschwächen kann. Unerwartet zeigten mehrere Analogverbindungen, darunter der ursprüngliche Fluorsulfat-Hit, in biochemischen Assays eine scheinbare Aktivierung von ALK2. Obwohl der Mechanismus noch nicht geklärt ist, legen die Resultate nahe, dass komplexe Struktur-Funktions-Beziehungen vorliegen, die einer vertieften Erforschung bedürfen. Insgesamt erweitert diese Arbeit das Target-Spektrum kovalenter Kinaseinhibitoren durch die Validierung von Lysin als Target für Schwefel(VI) Fluorid Chemie über das „katalytische Lysin“ hinaus und eröffnet neue Möglichkeiten, bislang schwer zugängliche Kinasen kovalent zu modulieren.

Abstract

Covalent protein kinase inhibitors have firmly established themselves as a powerful therapeutic modality, with most efforts traditionally focused on targeting reactive cysteine residues. However, many kinases lack suitably positioned cysteines, limiting the reach of current covalent strategies. Motivated by this gap, this dissertation explores covalent inhibition beyond cysteine by leveraging underexplored nucleophilic residues – specifically tyrosines and lysines.

Initial efforts applied sulfur(VI) fluoride chemistry to target tyrosines through structure-based design, using the kinases JAK3 and MK2 as model systems. Tailored analogs bearing sulfonyl fluoride and fluorosulfate warheads were designed and synthesized to engage specific tyrosines. While intact protein mass spectrometry confirmed covalent modification in some cases, functional inhibition often proved elusive. In one striking example, a fluorosulfate designed to target a tyrosine in MK2 instead modified the “catalytic” lysine, highlighting the unpredictable yet promising reactivity of this warhead class.

In light of the challenges encountered using rational design alone, a covalent-first approach was adopted. A focused electrophilic library featuring diverse hinge binders, linker architectures, and S(VI)F warheads was screened against kinases with tyrosines in privileged structural positions. This led to the identification of several novel covalent binders, most notably a fluorosulfate that modified Lys338 (HRD+2) of ALK2, a kinase involved in fibrodysplasia ossificans progressiva (FOP). This represents the first reported covalent ligand for ALK2, which lacks a ligandable cysteine in its active site and has remained inaccessible to cysteine-focused strategies.

Further structural and kinetic studies on this hit revealed key structure–activity relationships. Variations to the hinge binder notably affected inactivation rates – e.g., replacing azaindole with aminopyridine slowed down the modification – while linker changes had minor impact. As expected, a sulfonyl fluoride showed greater reactivity than fluorosulfates, which translated into faster target modification. Substituents on the aryl ring bearing the warhead also influenced the rate of target inactivation: electron-withdrawing groups enhanced it, electron-donating groups reduced it, but steric bulk could offset these effects, underscoring the balance between reactivity and spatial fit. Unexpectedly, several analogs, including the original fluorosulfate hit, exhibited an apparent ALK2 activation in biochemical assays. Though the mechanism remains unclear, these results suggest a complex structure–function relationship meriting further investigation.

Altogether, this work expands the landscape of covalent kinase inhibition by validating lysines as viable targets for S(VI)F chemistry, offering new avenues beyond cysteine and enabling covalent targeting of kinases previously considered inaccessible to covalent drug modalities.

List of Abbreviations

#	5'-FSBA	5'-*p*-Fluorosulfonylbenzoyl adenosine
A	AChE	Acetylcholinesterase
	ACVR1	Activin A receptor, type I
	AGC	Protein A, G, and C kinases
	AISF	4-(Acetylamino)phenyl]imidodisulfuryl difluoride
	ALK	Activin receptor-like kinase
	AmPhos	[4-(N,N-Dimethylamino)phenyl]di-*tert*-butylphosphin
	APCI	Atmospheric pressure chemical ionization
	ASAP	Atmospheric solids analysis probe
	ATP	Adenosine triphosphate
	AURKA	Aurora kinase A
B	BCB	Bicyclo[1.1.0]butane
	Bcl-xL	B-Cell lymphoma extra-large
	BIR3	Baculovirus inhibitors of apoptosis proteins repeat 3
	BMP	Bone morphogenetic protein
	BMP2K	BMP-2-inducible protein kinase
	Bn	Benzyl
	Boc	*tert*-Butyloxycarbonyl
	BRSM	Based on recovered starting material
	BTK	Bruton's tyrosine kinase
C	CAII	Carbonic anhydrase II
	calcd.	Calculated
	CAMK	Calcium/calmodulin dependent kinases
	cataCXium A	Di(1-adamantyl)-*n*-butylphosphine
	CFA	Chlorofluoroacetamide
	ChEF	Chelation-enhanced fluorescence
	cIAP	Cellular inhibitor of apoptosis protein
	CK1	Casein kinases 1
	CMGC	Cyclin-dependent kinases, MAP kinases, glycogen synthase kinases, CDC-like kinases
	conc.	Concentrated
	CSNK2A2	Casein kinase II subunit alpha'
	CSNK2A1	Casein kinase II subunit alpha
D	DABSO	4-Diazabicyclo[2.2.2]octane bis(sulfur dioxide)
	dba	Dibenzylideneacetone

	DBU	1,8-Diazabicyclo[5.4.0]undec-7-ene
	DCM	Dichloromethane
	DELFIA	Dissociation-enhanced lanthanide fluorescence immunoassay
	DHFR	Dihydrofolate reductase
	DIPEA	*N*,*N*-Diisopropylethylamine
	DIPG	Diffuse intrinsic pontine glioma
	DMAP	4-Dimethylaminopyridine
	DMF	Dimethylformamide
	DMSO	Dimethyl sulfoxide
	DOM	Directed *ortho* metalation
	dppf	1,1'-Bis(diphenylphosphino)ferrocene
	DSF	Differential scanning fluorimetry
E	*E. coli*	*Escherichia coli*
	EDC	1-Ethyl-3-(3-dimethylaminopropyl)carbodiimide
	EDG	Electron-donating groups
	EGFR	Epidermal growth factor receptor
	eIF4E	Eukaryotic translation initiation factor 4E
	ELISA	Enzyme-linked immunosorbent assay
	ESI	Electrospray ionization
	EtOAc	Ethyl acetate
	EtOH	Ethanol
	EWG	Electron-withdrawing groups
F	FBDD	Fragment-based drug discovery
	FDA	US Food and Durg Administration
	FOP	Fibrodysplasia ossificans progressiva
G	G4	Fourth generation
	GEF	Guanine exchange factor
	GS	Glycine-serine-rich
	GSG2	Germ cell-specific gene 2 protein kinase
	GSK3B	Glycogen synthase kinase-3 beta
H	HATU	Hexafluorophosphate Azabenzotriazole Tetramethyl Uronium
	HBA	Hydrogen bond acceptors
	HBD	Hydrogen bond donors
	HER	Human epidermal growth factor receptor
	HIV-RT	Human immunodeficiency viruses reverse transcriptase
	HOBt	Hydroxybenzotriazole
	HPLC	High performance liquid chromatography

	Hsp90	Heat shock protein 90
	HTS	High-throughput screening
I	IL-6	Interleukin 6
	IMAC	Immobilized metal affinity chromatography
	IPTG	Isopropyl β-D-1-thiogalactopyranoside
	JAK	Janus kinase
K	KLIFS	Kinase ligand interaction fingerprints and structures
	KRAS	Kirsten rat sarcoma virus
L	LDA	Lithium diisopropylamide
	LG	Leaving group
M	MACH1	Max-activating cells for homologous recombination 1
	MAP2K1	Mitogen-activated protein kinase kinase 1
	MAPK	Mitogen-activated protein kinase
	MAPK1	Mitogen-activated protein kinase 1
	MAPKAPK2	MAP kinase-activated protein kinase 2
	*m*CPBA	*meta*-Chloroperoxybenzoic acid
	MeCN	Acetonitrile
	MK2	MAP kinase-activated protein kinase 2
	MOM	Methoxymethyl
	mRNA	Messenger ribonucleic acid
	MS	Mass spectrometry
	MSF	Methyl sulfonyl fluoride
N	NASA	*N*-Acyl-*N*-alkyl sulfonamides
	NBS	*N*-Bromosuccinimide
	NCS	*N*-Chlorosuccinimide
	NFSI	*N*-Fluorobenzenesulfonimide
	NMP	*N*-Methyl-2-pyrrolidone
	NMR	Nuclear magnetic resonance
	NSCLC	Non-small-cell lung cancer
P	PAK3	p21-Activated kinase 2
	PDB	Protein data bank
	PEI	Polyethylenimine
	PK	Protein kinase
	POI	Protein of interest
	PPI	Protein–protein interactions
	PROTAC	Proteolysis targeting chimera
	PSA	Polar surface area

	PTM	Post-translational modification
R	Ral	RAS-like
	rt	Room temperature
S	SAR	Structure-activity relationship
	SARS-CoV	Severe acute respiratory syndrome coronavirus
	sat.	Saturated
	SCID	Severe combined immunodeficiency
	SEM	2-(Trimethylsilyl)ethoxymethyl
	SF	Sulfonyl fluoride
	SIRT5	Sirtuin 5
	SMAD	Mothers against decapentaplegic homolog proteins
	S_NAr	Nucleophilic aromatic substitution
	Sox	Sulfonamido-oxine
	SRC	Sarcoma
	SRPK1	Serine/arginine-rich splicing factor (SRSF) protein kinase-1
	STAT	Signal transducer and activator of transcription proteins
	STE	Homologs of Sterile 7, Sterile 11, and Sterile 20 kinases
	STPK	Serine/threonine kinase
	SuFEx	Sulfur–fluoride exchange
	SuTEx	Sulfur–triazole exchange
T	TBAB	Tetrabutylammonium bromide
	TBAF	Tetrabutylammonium fluoride
	TBTU	2-(1*H*-Benzotriazole-1-yl)-1,1,3,3-tetramethylaminium tetrafluoroborate
	*t*BuOH	*tert*-Butanol
	TCI	Targeted covalent inhibitor
	TEA	Triethylamine
	TEC	Tyrosine-protein kinase expressed in hepatocellular carcinoma
	TEV	Tobacco Etch Virus
	Tf	Triflate
	TFA	Trifluoroacetic acid
	TFP	Tri(2-furyl)phosphine
	TGFBR1	Transforming growth factor beta receptor I
	TGF-β	Transforming growth factor beta
	THF	Tetrahydrofuran
	TIPS	Triisopropylsilyl
	TK	Tyrosine kinases
	TKL	Tyrosine kinase-like

	TLC-MS	Thin-layer chromatography mass spectrometry
	T_m	Melting temperature
	TMB	3,3',5,5'-Tetramethylbenzidine
	TNFα	Tumor necrosis factor
	TPK	Tyrosine protein kinases
	t_{ret}	Retention time
	TRF	Time resolved fluorescence
	TR-FRET	Time-resolved fluorescence energy transfer
	Ts	Tosyl
	TSA	Thermal shift assay
	TYK2	Tyrosine kinase 2
V	VRK1	Vaccinia-related kinase 1
W	WT	Wild type
X	Xantphos	(9,9-Dimethyl-9*H*-xanthene-4,5-diyl)bis(diphenylphosphane)
	XIAP	X-linked inhibitor of apoptosis protein
	XPhos	Dicyclohexyl[2′,4′,6′-tris(propan-2-yl)[1,1′-biphenyl]-2-yl]phosphane
Z	ZAK	Sterile alpha motif and leucine zipper containing kinase

Table of Contents

1. Introduction

1.1. Protein Kinases and their Structure

Kinases serve as vital conductors of cellular signaling networks, orchestrating a vast array of biological functions and maintaining cellular homeostasis. Through their role as key regulatory enzymes, they influence processes that are fundamental to cell proliferation, differentiation, apoptosis, and growth.[1] In the multitude of ways cells use to communicate, post-translational modifications (PTMs) – including acetylation, ubiquitination, methylation, and glycosylation – are central, with kinases conveying their signals specifically through phosphorylation. In this process, kinases catalyze the transfer of the terminal γ-phosphate of the nucleotide adenosine triphosphate (ATP) onto their substrates.[2] These substrates include lipids, nucleosides and carbohydrates, but most often, proteins. Protein kinases (PKs; from this point forward, the terms *protein kinase* and *kinase* will be used synonymously) account for about 2 % of the human genome and their complete set is usually referred to as the *kinome* as defined by MANNING *et al*.[3] In their seminal publication from 2002, 518 PKs were recognized as part of the kinome, a number which has since slowly risen.[3,4]

Phosphorylation of proteins can initiate a change in their secondary structure, which may influence their biological activity and behavior. Oftentimes, the substrates are PKs themselves. This mutual activation of kinases within the kinome generates a complex network that is used for signal transduction with a multitude of cascade-like but also recursive loop-like signaling pathways that may have both activating and/or inhibiting effects. Due to this fact, kinases are often referred to as *molecular* or *biological switches*.[4] Apart from intracellular factors, this network also reacts to neurotransmitters, extracellular hormonal stimuli or the presence of nutrients. While this system is responsible for a large part of intracellular signal transduction to modulate cellular processes, naturally, inherited or acquired genetic changes can lead to dysregulation and mutation of PKs which in turn can be responsible for numerous diseases such as cancer, inflammatory diseases, or cardiovascular disorders.[5,6] Phosphorylation is, however, not a one-way street: it is a reversible process in which the removal of phosphate groups is modulated by phosphatases.[1]

There are two major ways to classify eukaryotic protein kinases. The first is based on substrate specificity: most of these enzymes phosphorylate serine and/or threonine and a smaller fraction facilitates the phosphorylation of tyrosine. Consequentially, PKs have been separated into either serine/threonine kinases (STPKs) or tyrosine protein kinases (TPKs).[1] Dual specificity and histidine kinases exist as well, but the latter are not common in eukaryotes.[7,8] The other main classification, according to MANNING *et al*.,[3] takes into account their structural and functional similarities, leading to eight major groups: **(1)** tyrosine kinases (TK); **(2)** tyrosine

kinase-like (TKL); **(3)** cyclin-dependent kinases, MAP kinases, glycogen synthase kinases, CDC-like kinases (CMGC), **(4)** protein A, G, and C kinases (AGC); **(5)** calcium/calmodulin dependent kinases (CAMK); **(6)** homologs of Sterile 7, Sterile 11, and Sterile 20 kinases (STE); **(7)** casein kinases 1 (CK1); and **(8)** atypical kinases.[3,9] The last family, atypical kinases, are catalytically active, yet lacking typical structural elements in the kinase domain. Approx. 10 % of human kinases lack amino acid residues which are critical for catalysis and subsequently have been termed *pseudo kinases.* They nevertheless are thought to be useful through scaffolding function or other non-standard mechanisms.[3,10]

Since protein kinases all use ATP as their cofactor, the structural motifs of their key structural element, the *catalytic* or *kinase domain*, consisting of approx. 250 – 300 amino acids, is highly conserved across the kinome.[11,12] This domain consists of two lobes, the smaller N-terminal lobe and the larger C-terminal lobe which are connected through a flexible part: the so-called *hinge region*. While the N-lobe consists mostly of anti-parallel β-sheets and one conserved α-helix (the αC-helix), the C-lobe is mainly comprised of α-helices. Adjacent to the hinge region in between the two lobes is the ATP-binding pocket which is a deep binding cleft and the central anchoring point of the co-substrate. Overall, the kinase domain can be divided into 12 subdomains (**Figure 1**): subdomains I-IV can be found in the N-lobe while VI-XI are found in the C-lobe. Subdomain V is comprised of the hinge region, a β-sheet on the side of the N-lobe and an α-helix in the C-lobe.[12,13]

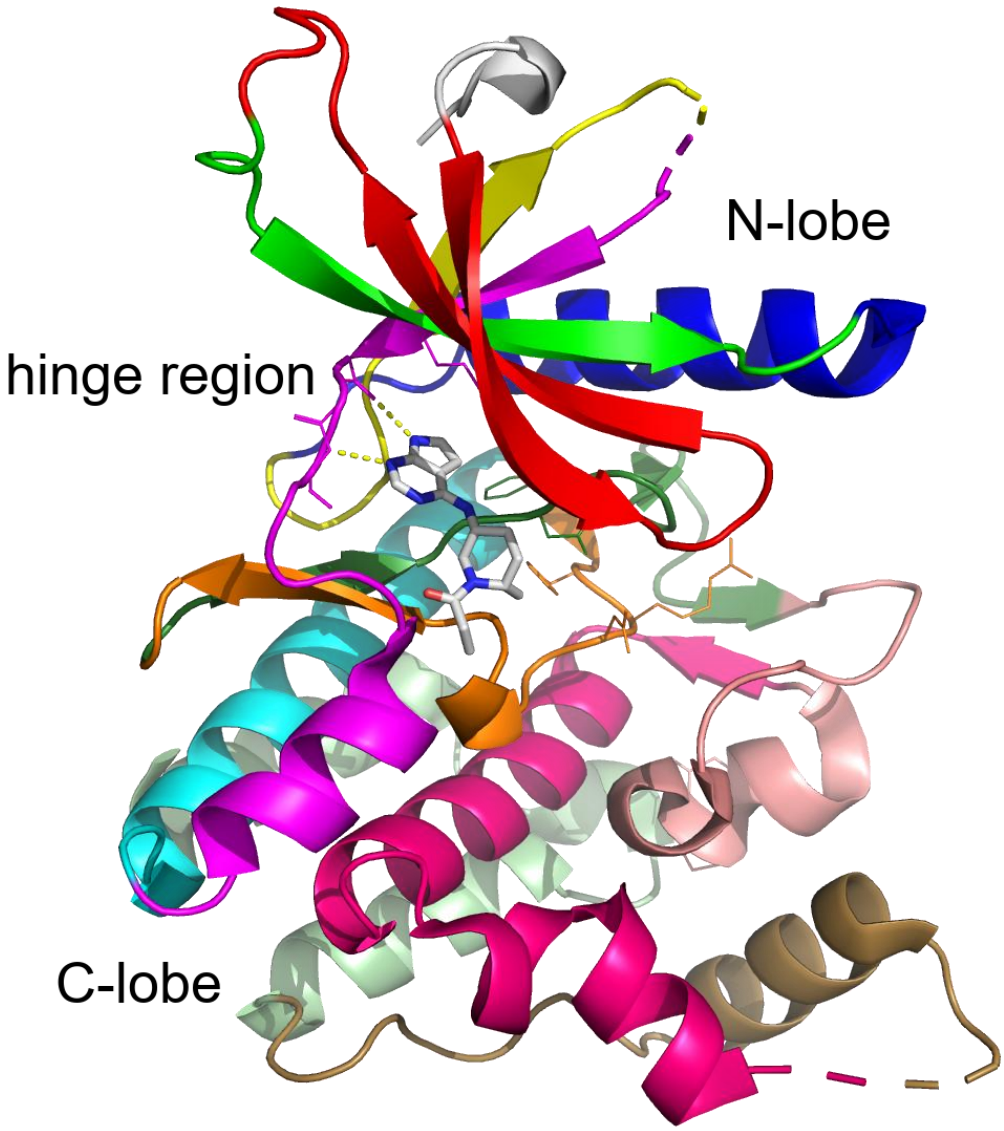

Figure 1: Conserved 12-subdomain structure of protein kinases exemplified through the JAK3 kinase domain (PDB: 5TOX). From subdomain I to subdomain XI: subdomain I: red; subdomain II: green; subdomain III: blue; subdomain IV: yellow; subdomain V: magenta (hinge region, side chain of GK methionine (M902) is depicted as lines, the main chain of the hinge region (E903, Y904, L905) is depicted as lines as well; the interactions from the inhibitor to the hinge region is shown as yellow dashed lines); subdomain VIa: cyan; subdomain VIb: orange (the side chains of the HRD motif are depicted as lines); subdomain VII: forest green (the side chains of the DFG motif are shown as lines); subdomain VIII: rose; subdomain IX: pink; subdomain X: brown; subdomain XI: sage.

The *glycine-rich loop* (also referred to as the *P-loop*) is located in subdomain I (red, **Figure 1**; the colors in parentheses in this paragraph all refer to **Figure 1**) and can be found in a flexible turn between β1 and β2. It is essential for ATP binding because it assists in correctly positioning the transferable phosphate group. In subdomain II (green), the *"catalytic" lysine* of kinases (Lys855 in JAK3) can be found – this lysine is essential for the catalytic activity of kinases because it positions and anchors the ATP α- and β-phosphate groups and forms a salt bridge to a glutamic acid which furthermore contributes to the stabilization of the position of the

phosphate groups. Subdomain III (blue) hosts the αC-helix which is an important regulatory element because it is positioned in such a way that it mediates interactions of the C-lobe with the N-lobe. In many kinases, it shows significant movement upon activation of the kinase.[4,12] Subdomain IV (yellow) preceding the hinge region (magenta) and subdomain VIa (cyan) following it, both do not play crucial roles in the catalytic function of the kinase. Subdomain VIb (orange) on the other hand, is critical for activity. Here, the *catalytic loop* containing the HRD motif can be found. The aspartate (D) residue acts as the catalytic base by abstracting the proton of the substrate hydroxyl group. Furthermore, another conserved lysine can be found here, which, through charge-assisted hydrogen bonding, further supports the activation of the γ-phosphate. The prominent DFG motif is located in the following subdomain VII (forest green). The aspartate of this motif coordinates the Mg^{2+} ion which bridges the β- and γ-phosphate and the motif thereby orients and activates the γ-phosphate for transfer. The DFG motif is also where the so-called *activation segment* begins, which contains the *activation loop* (*A-loop*) and consequently ends in subdomain VIII (rose) at the APE motif.[14] Subdomain IX (pink) is involved in stabilization of the catalytic loop, whereas subdomains X (brown) and XI (sage), located toward the C-terminal end of the kinase, do not play a crucial role in catalysis.

The transfer of the phosphate group always follows the same mechanism: ATP is fixated in the binding pocket with the help of two magnesium ions. These ions activate the terminal pyrophosphate bond for cleavage through polarization. As mentioned above, one of these ions is positioned by the aspartate of the DFG motif while the aspartate of the HRD motif activates the substrate hydroxyl group through a hydrogen bond. This is then followed by the attack of the hydroxyl group at the terminal phosphate.[15]

The main region that medicinal chemists are interested in, the hinge region, is very well understood through thousands of X-ray crystal structures that have been solved. It is here where the cofactor ATP binds and where most of the kinase small molecule inhibitors bind as well. This so-called *orthosteric pocket* was broken down into five distinct regions by TRAXLER and FURET (see **Figure 2**).[16] The *adenine binding site* includes the hinge region that fixates ATP via two hydrogen bonds. The binding site is limited by the gatekeeper (GK). This residue controls the size and access to a back pocket called *hydrophobic region I*. This region is not inhabited by ATP and therefore displays a lower degree of conservation than other parts of the binding cleft. More than 75 % of the kinome harbor large and hydrophobic GK amino acids such as methionine, leucine and phenylalanine. The GK and its mutations can markedly influence the activity of the kinase.[17] This residue is often exploited to generate selectivity when designing kinase inhibitors. The *hydrophobic region II* is another cavity not addressed by ATP that borders the hinge region and is at the solvent exposed front of the kinase. It is bordered by the *sugar pocket*, in which the ATP ribose is located, and which is hydrophilic in

nature. Finally, the hydrophilic *phosphate pocket* hosts the triphosphate tail that extends from the outer part of the solvent exposed front region toward the P-loop.[16]

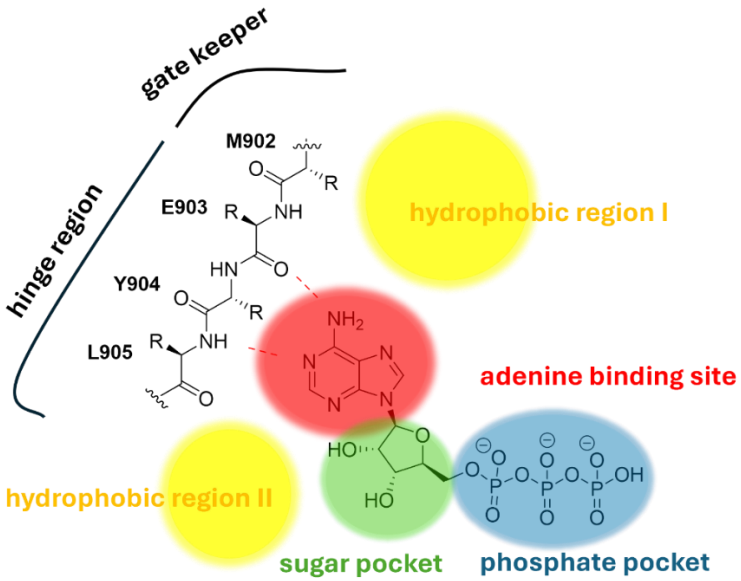

Figure 2: Depiction of the binding mode of ATP in JAK3 with distinct binding pockets according to TRAXLER *et al.*[16] The interactions between adenine and the hinge region are shown as dashed red lines. Adenine binding site: red; hydrophobic regions I and II: yellow; sugar pocket: green; phosphate pocket: blue.

The activation state of the kinase is highly influenced by the conformation of the DFG motif. In the *DFG-in* conformation, the kinase is in its active state. In the *DFG-out* conformation, the phenylalanine is oriented toward the binding pocket, blocking the binding of ATP, rendering the kinase inactive.[4]

1.2. Covalent (Kinase) Inhibition

Most small molecule drugs exert their biological effects by reversibly binding, in a noncovalent manner, to protein targets relevant to specific diseases. In the case of kinases, this is generally achieved by displacing ATP from the orthosteric pocket and thereby stopping the phosphorylation process altogether.[18] While this was long believed to be impossible because of the high intracellular concentrations of ATP and concerns about selectivity due to kinases being highly conserved across the kinome, more than 80 kinase inhibitors have been approved since the groundbreaking approval of imatinib in 2001, and kinases now constitute one of the major drug targets pursued.[19]

Conversely, medicinal chemists tended to avoid designing covalent drugs, which form a permanent bond with their target protein through a chemical reaction. This stemmed from the

belief that their reactivity could not be contained properly and would lead to severe off-target effects by modification of undesired proteins and idiosyncratic drug reactions.[20] Nevertheless, covalent drugs have been introduced and have remained in use for more than 120 years – with the most prominent example being aspirin (**1**). This drug, like other covalent "classics" including β-lactam antibiotics (e.g. penicillin V, **2**), proton-pump inhibitor omeprazole (**3,** all **Figure 3**) or the platelet agglutination inhibitor clopidogrel, however, are covalent not by design, with their mechanisms only uncovered retrospectively. It has only been in the last two decades that chemists have come back to look at covalent inhibition as a deliberate design strategy to overcome certain challenges that are difficult to solve with noncovalent drugs.[20,21]

The now intentionally designed covalent inhibitors are often referred to as *targeted covalent inhibitors* (TCIs). They address poorly conserved, noncatalytic amino acids through a *warhead*, which is the functional group forming the covalent bond with a specific residue.[20] The definition of TCIs is not handled entirely consistently – the restriction to noncatalytic residues is not always included and the concept can be extended beyond inhibitors to other types of ligands as well. The newfound interest into TCIs has been especially spurred because of their prolonged drug–target residence time and their potential for targets that had previously been deemed "undruggable" through noncovalent means. In the kinase field, TCIs are especially interesting due to their limited ATP competitivity and the additional, complementary selectivity filter that intrinsically comes with the need for a suitable nucleophilic amino acid in the binding pocket.[18,20–22]

These factors may be why TCIs have seen their biggest success in the field of kinase inhibition. In 2013, the first two covalent kinase inhibitors were approved by the US Food and Drug Administration (FDA), namely afatinib (**4**), an EGFR/pan-HER inhibitor, and ibrutinib (**5**), a BTK inhibitor.[22] Since then, a total of 11 covalent kinase inhibitors have been approved by the FDA, the majority of them for the treatment of oncological diseases – the most recent approval being lazertinib (in combination with amivantamab) for the treatment of non-small cell lung cancer (NSCLC) in august of 2024.[23] A notable exception is the JAK3 inhibitor ritlecitinib (**7**), which is used in the field of inflammatory and autoimmune disorders.[22] Beyond kinase inhibitors, another exciting TCI development was made in the field of KRAS inhibition. Sotorasib (not shown) and adagrasib (**6,** all **Figure 3**) are both FDA-approved inhibitors that target the oncogenic G12C mutation in the formerly deemed "undruggable" KRAS protein. Due to a lack of suitable binding pockets, KRAS had been unsuccessfully targeted for several decades. While it has become clear that different mechanisms convey resistance to these two drugs, they nevertheless are considered breakthroughs from a medicinal chemistry perspective. Other covalent drugs include the SARS-CoV-2 inhibitor nirmatrelvir, targeting the viral main protease (M^{pro}) or voxelotor, which is used to treat Sickle cell disease and allosterically addresses the N-terminal valine of the α chain of mutant hemoglobin. Beyond drug discovery,

covalency has also gained traction in chemical biology e.g. with covalent modulators being used as chemical probes.[22]

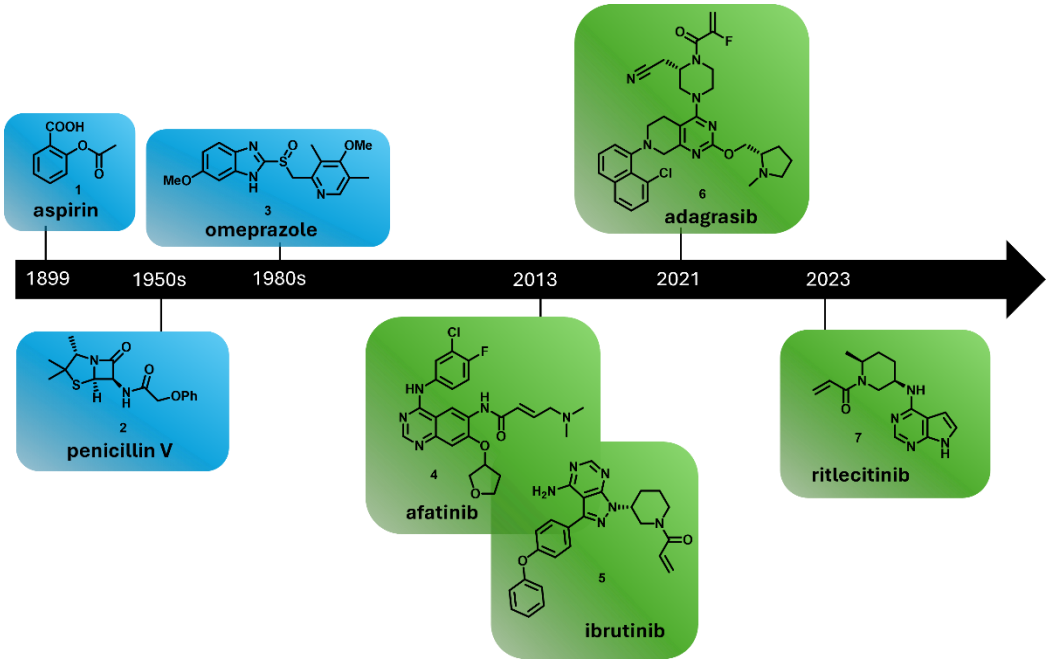

Figure 3: Timeline of the approval of selected covalent inhibitors. Blue boxes show drugs where the covalent mode of action has been discovered by serendipity while green boxes denote TCIs.

The growing interest in covalent ligands stems from their distinct advantages compared to noncovalent ones. Irreversible covalent ligands capitalize on their nonequilibrium binding profile to enhance (apparent) potency, which increases with time. Further benefits include **(1)** the possibility to boost selectivity through choosing a poorly conserved target amino acid or a disease-specific mutation; **(2)** the absence of competition from natural substrates (at least after the covalent binding event has occurred); and **(3)** prolonged pharmacological action, especially for targets with a low re-synthesis rate. In a clinical setting, this may lead to reduced drug metabolism and pharmacokinetic issues and possibly less frequent and/or lower dosing. Generally, these properties can facilitate high target occupancy and selectivity even when the noncovalent binding element shows only moderate affinity. Nevertheless, nonspecific binding due to high intrinsic reactivity of the warhead is something that needs to be carefully evaluated when designing covalent ligands. The balance between a promiscuous binder and one whose kinetics are too slow for meaningful covalent target engagement is central to the challenges in covalent inhibitor design.[18,24]

While (noncovalent) reversible binding (**Figure 4A**) is a one-step equilibrium process with ligand affinity characterized by the inhibition constant K_i – representing the ratio of the dissociation rate (k_{off} or k_{-1}) to the association rate (k_{on} or k_1) – irreversible covalent binding is a nonequilibrium process that proceeds in two distinct steps (**Figure 4B**). At first, a classical,

reversible binding event takes place. Noncovalent affinity is typically approximated by K_I, a constant that accounts for the ligand concentration necessary to attain a half-maximal rate of covalent modification. The second, i.e. the covalent step, is characterized by the first order rate constant k_{inact} which represents the maximal potential rate of covalent modification. The covalent step can also be reversible, but as this was not the topic of this dissertation, it will not be discussed here further. Finally, the second-order rate constant k_{inact}/K_I is what defines the total efficiency of covalent binding. While IC_{50} values can give a first indication of the efficiency of a covalent inhibitor, the mentioned rate constant gives a much more precise look into this time-dependent process since the apparent inhibitor potency increases with incubation time while k_{inact}/K_I covers both steps in a time-independent manner.[22,24,25]

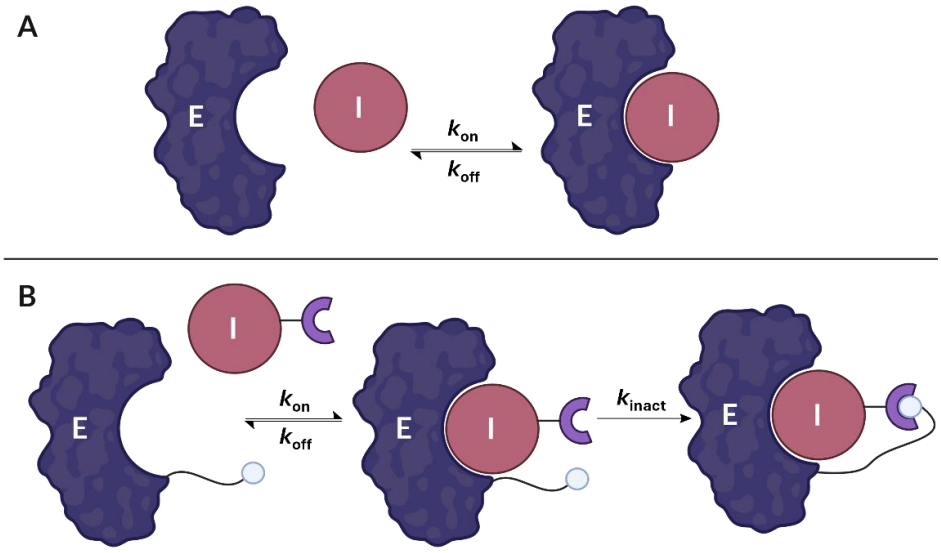

Figure 4: A Overview of the mechanism of one-step reversible, noncovalent binding. **B** Overview of the mechanism of two-step irreversible covalent binding. In the case of reversible covalent binding (not depicted here), the second step is also reversible and characterized through the 1st order rate constant k_{rev}. In the case of irreversible binding, $k_{rev} \approx 0$. (E = enzyme, I = inhibitor; graphic was created using BioRender.com).

There are several methods to detect a covalent mechanism of action: washout experiments or jump dilution, mutation of the target amino acid or the testing of nonreactive close analogs are more indirect methods that should be complemented by direct methods like intact protein MS and a corresponding trypsin digest or X-ray crystallography.[22]

1.2.1. Current State of the Art – Cysteine Targeting

As apparent from **Figure 3**, most of the recently approved TCIs bear a warhead belonging to the group of Michael acceptors and more specifically, acrylamide derivatives. They generally

bind to a cysteine side chain in their respective target (**Figure 5A**). This is because the nucleophilicity of the thiolate form of the cysteine side chain (pK_a ≈ 8.5) is the highest among the canonical amino acids.[26] While the chemical nature of the nucleophile is only one factor influencing its reactivity besides its location and its surrounding protein microenvironment, all 11 currently FDA-approved covalent kinase inhibitors target a cysteine through some form of Michael acceptor. The popularity of this warhead class comes back to its preference for "soft" nucleophiles, the relatively low intrinsic reactivity, the capacity to easily tune reactivity on a broad range and the synthetic accessibility.[18,22]

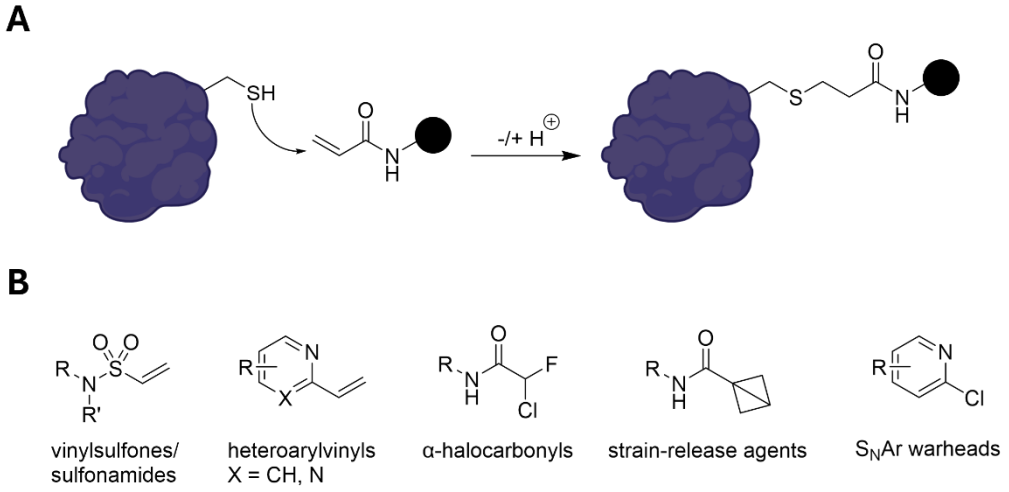

Figure 5: A Schematic depiction of the reaction of a cysteine with an acrylamide warhead. **B** Examples of warheads for cysteine targeting, some of which are well explored in research but are not yet used in approved drugs.

Beyond acrylamides, several other warheads for targeting cysteine have emerged (**Figure 5B**). Depending on the target, limitations such as steric constraints, (metabolic) stability issues (especially toward GSH) or limited adjustability of reactivity of carbonyl-based Michael acceptors may arise, rendering the investigation and implementation of other warheads worthwhile. Electrophiles such as vinyl sulfones/sulfonamides, heteroarylvinyls, α-halocarbonyls, strain-release agents or S_NAr warheads (mainly featuring haloaryls) have received significant attention albeit not being featured in approved drugs just yet.[22] A study by TOKUNAGA *et al.*[27] demonstrated the merits of altering the warhead on an otherwise unchanging probe: interchanging the classic acrylamide for a chlorofluoroacetamide (CFA) or a bicyclobutane (BCB) warhead led to new off-target profiles and considerably different proteome reactivity.

Cysteine reactivity is very well investigated, especially in the kinase field. Among the over 500 protein kinases, almost half contain a cysteine within or near the ATP binding site. As summarized by the groups of LAUFER and KNAPP,[28] targetable residues were found to be distributed over 27 distinct positions.

1.2.2. Novel Targets and Electrophiles

While the strategic targeting of cysteine residues has significantly advanced our understanding and therapeutic modulation of protein kinases and other enzymes, reliance on this singular approach limits the scope of drug discovery and chemical probe design. With the reactivity of cysteine being well-documented, there is growing recognition of the need to broaden this focus to include other amino acids that may serve as viable targets for covalent modification. Expanding beyond cysteine opens new avenues for targeting a wider range of proteins that lack cysteine residues in strategic positions but also necessitates a diversification of the available arsenal of electrophilic reactive groups.

An illustrative example that highlights the wide-ranging potential of diverse warheads and approaches is the aforementioned KRAS protein, and particularly its mutation of Gly12. As described in chapter 1.2, the development of KRAS G12C inhibitors adagrasib (**6**) and sotorasib was heralded as a great success by medicinal chemists, but mutations and other oncogenic mechanisms that were able to circumvent the effects of these drugs, quickly curbed the enthusiasm in a clinical setting. Scientists have therefore started to investigate other mutations at the same amino acid position. The SHOKAT group, inspired by natural products that form a covalent bond with a catalytic threonine, attached a strained β-lactone to the core of adagrasib (**6**) to target the G12S mutation, another oncogenic driver mutant.[29] While the drug-like properties of the optimized compound (**8**, **Figure 6**), especially hydrolytic stability, were not optimal, treatment with this compound led to a nearly complete loss of RAS·GTP and accompanying inhibition of ERK phosphorylation in cancer cell lines. The same group developed another inhibitor for the hot spot mutation G12R.[30] Attaching a vicinal dicarbonyl system to a compound similar to adagrasib (**6**) enables the formation of an imidazoline condensation product with arginine as confirmed via X-ray crystallography. While this compound (**9**, **Figure 6**) was hydrolytically more stable and did show promising effects *in vitro*, no effect on KRAS G12R mutant cells could be observed. Approaches like these are vital to advance our understanding of understudied biological processes but they also demonstrate that our level of comprehension of other warhead chemistries and target amino acids beyond acrylamides and cysteine is limited.

Among the most prevalent mutations of KRAS is the G12D mutation which has recently captured significant attention from the pharmaceutical industry. In an academic context, the SHOKAT group, similarly to their G12S approach, targeted the aspartate through a β-lactone,[31] while YU *et al.*[32] used an epoxide (**10**, **Figure 6**) that could target both the mutation to aspartate as well as to cysteine. Researchers from Boehringer Ingelheim very recently showed that carbodiimides (e.g. **11**, **Figure 6**) could be used to selectively target the aspartic acid in the G12D mutation.[33] Furthest along in their research is Revolution Medicines, who are

currently in Phase I trials (NCT06040541) with their inhibitor RMC-9805 (**12**, **Figure 6**),[34] that not only is a molecular glue, but also binds covalently via an aziridine. This highlights the pharmaceutical industry's active pursuit of innovative strategies beyond traditional cysteine targeting, embracing a broader spectrum of warhead chemistries. Each unique warhead demands precise tuning to effectively interact with specific target amino acids, underscoring the complexity and versatility required in advancing covalent strategies.

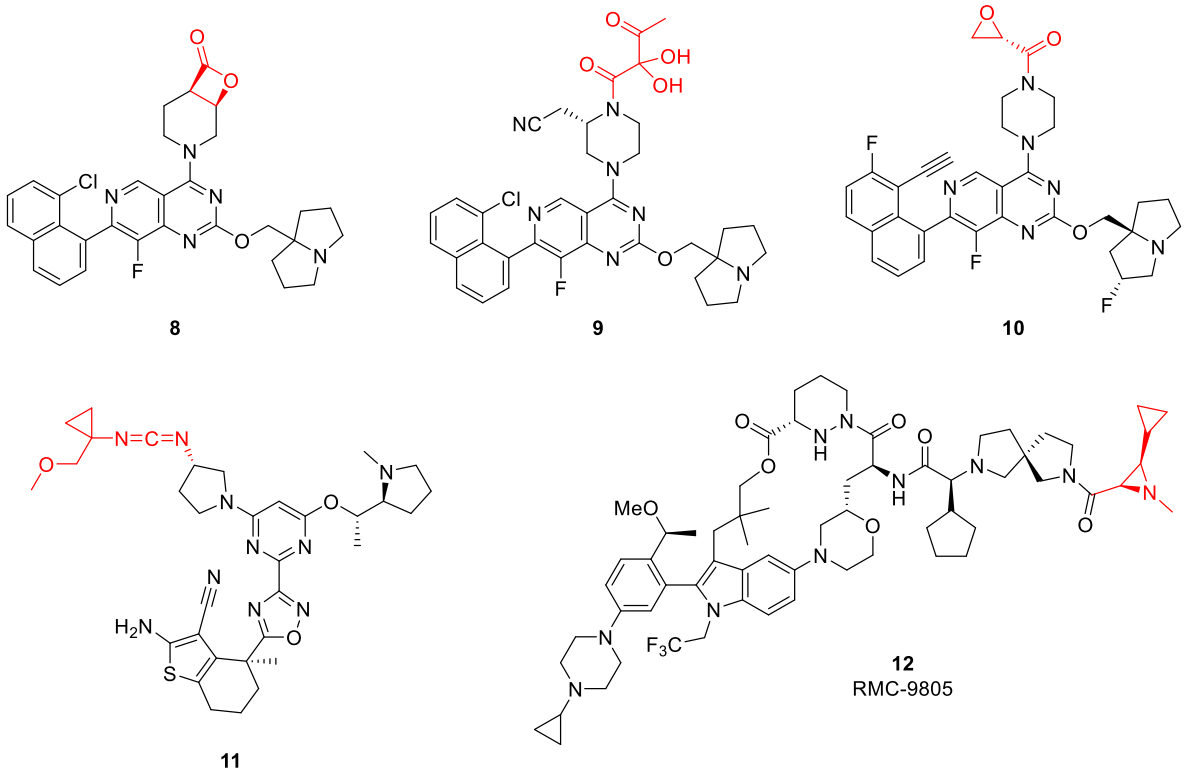

Figure 6: Inhibitors for targeting several different KRAS mutations showcasing the wide array of warheads (depicted in red) needed to selectively address various target amino acids.

Another sought after residue is lysine. A significant drawback of lysine is that at physiological pH, surface lysine residues are almost completely protonated (pK_a ≈ 10.5), rendering the side chain poorly nucleophilic. It has been established, however, that the pK_a, depending on the surrounding protein microenvironment, can be depressed up to 5 units leaving certain lysines much more nucleophilic.[35,36] Furthermore, lysine has a higher abundance than cysteine (5.8 % vs. 1.9 %)[37] thereby expanding the number of proteins suitable for covalent targeting – especially given the fact that many human proteins do not possess ligandable cysteine residues. Furthermore, it has been proposed that functional lysines are less likely to undergo mutation, as they frequently play a crucial role in catalysis by serving as nucleophiles or bases and are vital for maintaining a protein's structural integrity or for its regulation via PTMs.[38,39] These factors have encouraged scientists to pursue lysine as a promising site for covalent modification. Several electrophiles have been used to target lysines, among them (masked)

carbonyls, S_NAr warheads, activated esters, *N*-acyl-*N*-alkyl sulfonamides (NASA), and, prominently, sulfur(VI) fluorides.[22,26] As the latter are the main topic of this thesis, sulfur–fluoride exchange (SuFEx) chemistry will now be discussed in more detail.

1.2.2.1. Sulfur(VI) Fluoride Electrophiles and Related Warheads

Building on their prominence in lysine targeting, sulfonyl fluorides (and to a lesser extent their analogs, see **Figure 8**) have emerged as versatile electrophiles capable of engaging other nucleophilic residues such as tyrosine, serine, threonine, and histidine. They can also react with cysteines, but the resulting reaction product collapses to the corresponding sulfinic acid.[40,41] Sulfuryl fluoride (SO_2F_2) and small molecules containing sulfonyl fluorides have been known and utilized as insecticides for more than 100 years and in the 1960s scientists at Columbia University reported that their mechanism of action is the inhibition of esterases.[42] Beyond crop science, methyl sulfonyl fluoride (MSF, **13**, **Figure 7**), an irreversible inhibitor of acetylcholinesterase (AChE), has been successfully tested at very low doses for memory improvement in Alzheimer's disease patients in clinical trials.[43] Already in the last century, a pioneer in the field, BERNARD R. BAKER, realized that the sulfonyl fluoride group only shows minimal reaction with proteins unless the compound bearing the electrophile is reversibly associated with said protein. Once this happens though, he recognized that rapid covalent bond formation can take place.[44] His group went on to develop inhibitors of a range of target classes (e.g. NSC 127755, **14**, **Figure 7**, which binds to Tyr31 of dihydrofolate reductase (DHFR)).[45] Another major contributor to the field is ROBERTA F. COLMAN, whose group developed fluorosulfonylbenzoyl nucleoside probes such as 5'-*p*-fluorosulfonylbenzoyl adenosine (5'-FSBA, **15**, **Figure 7**) that was shown to specifically label NAD and ATP binding sites in over 50 proteins.[46,47] Nevertheless, the field was rather dormant until its recent revival by the group of Nobel laureate K. BARRY SHARPLESS who realized the potential of SuFEx chemistry as a valuable click-type reaction.[42]

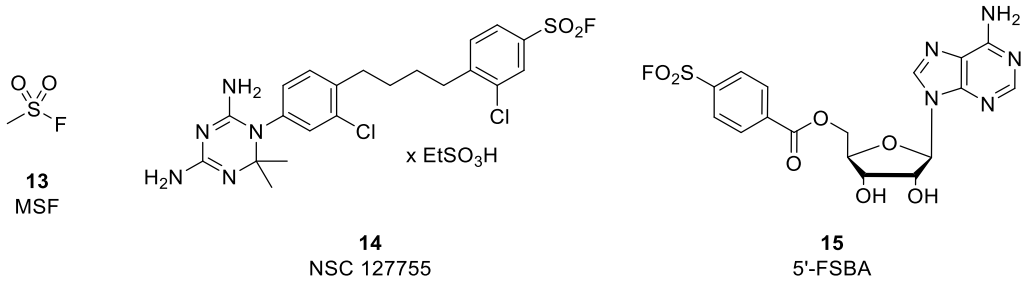

13
MSF

14
NSC 127755

15
5'-FSBA

Figure 7: Early examples of sulfonyl fluorides in drug discovery and chemical biology.

In contrast to sulfonyl fluorides, sulfonyl chlorides are well established electrophiles in the organic chemist's repertoire. Due to several unfavorable properties, however, they cannot be used as "connective units" in a biochemical context. Sulfonyl fluorides and their close analogs, on the other hand, behave very differently from their chloride counterparts in several ways:[42] **(1)** while homolytic scission of S–Cl bonds is common, S–F bond cleavage is exclusively heterolytic. This is due to fluorine being the most electronegative element of the periodic table, forming a stronger S–F bond. While sulfonyl fluorides are very resistant to reduction, sulfonyl chlorides are easily reduced to sulfinic acids or thiols; **(2)** while all sulfur(VI) substitution chemistry is commonly rather sluggish compared to sulfur centers at lower oxidation states, sulfonyl fluorides are much more stable toward nucleophilic substitution, including hydrolysis, than other sulfonyl halides; **(3)** while reactions of sulfonyl chlorides with e.g. carbon nucleophiles usually give mixtures of sulfonylation and chlorination products, sulfonyl fluorides exclusively provide sulfonylation outcomes. This difference is attributed to the high polarizability of the chlorine center in sulfonyl chlorides; additionally, the presence of a sigma hole facilitates nucleophilic attack on all halides except fluoride;[48] **(4)** SuFEx chemistry very much depends on the stabilization of the leaving fluoride ion in the substitution process. The fluoride ion is a unique base as shown by the stabilization in water by trapping a proton between two fluoride ions, rendering protons uniquely effective at stabilizing fluoride as a leaving group.[42]

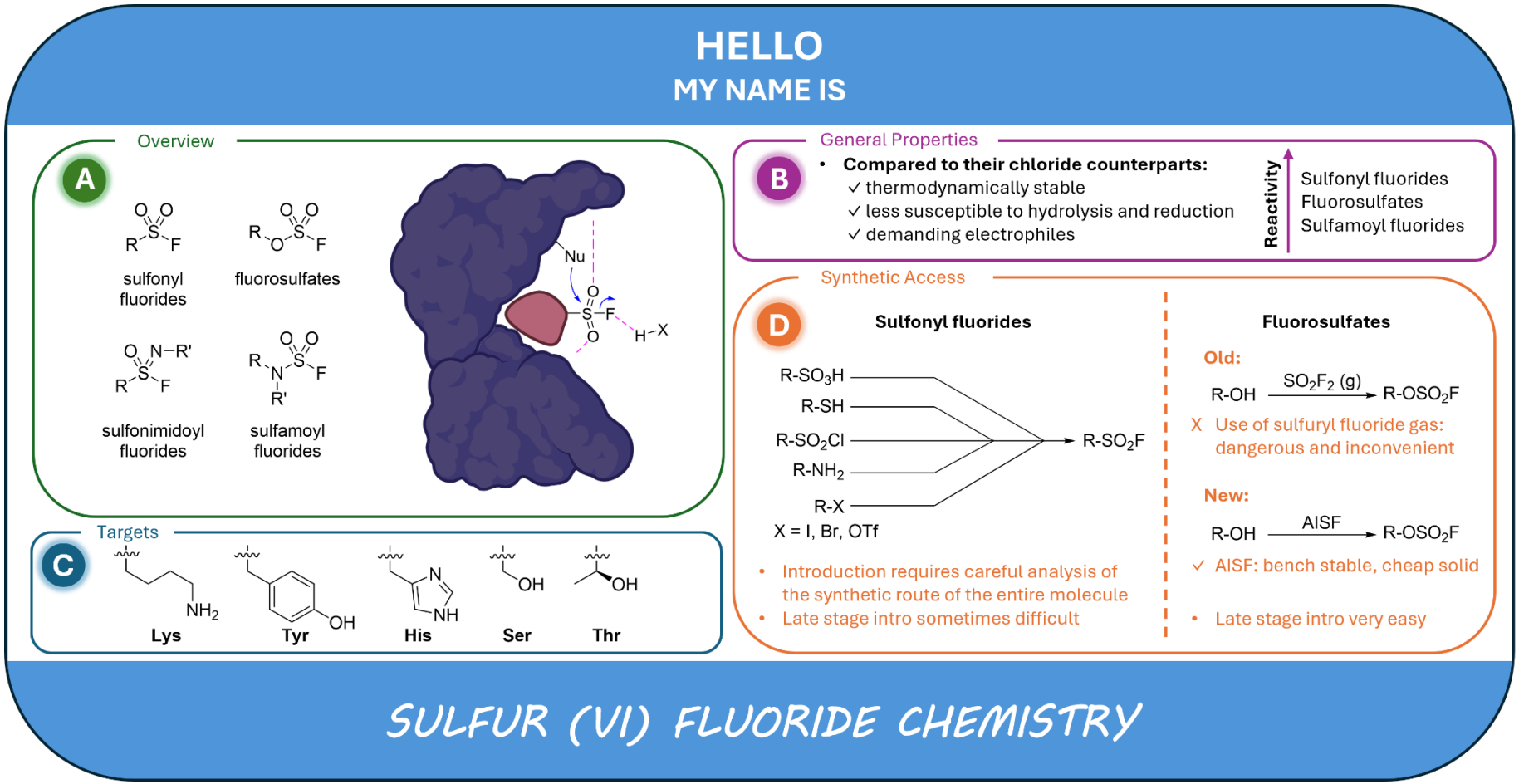

Figure 8: Overview over sulfur(VI) fluoride chemistry, its general properties, target amino acids (only lysine, tyrosine and histidine will be discussed here) and synthetic access (this topic will be further discussed in the chemical part of the thesis).

While sulfonyl fluorides are most widely used among the sulfur(VI) fluorides, other analogous electrophiles from the same group (see **Figure 8** for an overview) have begun to emerge. Within these, fluorosulfates have started to gain traction and have found more and more implementation. Albeit less reactive than sulfonyl fluorides, they show higher hydrolytic and general chemical stability. Several studies have now shown they possess more drug-like properties than sulfonyl fluorides (even though the latter can to a certain extent be tuned as well). Sulfonimidoyl fluorides contain an extra handle to tune reactivity, as the nitrogen substituent can easily be fitted with either electron-donating or -withdrawing groups. Nevertheless, they have found only very limited applications. Sulfamoyl fluorides, similarly understudied, are the least reactive among this warhead class.[22] As a side note, sulfur–triazole exchange (SuTEx) has recently been introduced,[49–53] which has been shown to preferentially address tyrosine over other nucleophiles in proteomes, but its use is so far mostly limited to chemoproteomic studies. Moreover, the factors driving a more pronounced preference for tyrosine compared to SuFEx electrophiles are poorly understood. Since these warheads only played a minor part in this work, they will not be discussed here further.

Generally, sulfur(VI) fluorides are often described as “latent” electrophiles as it has been suggested that activation only occurs if the departing fluoride ion is stabilized by the surrounding protein particularly through hydrogen bonding or protonation. Reactions may be further expedited when additionally, the sulfonyl oxygen atoms engage in hydrogen bonding which enhances the electrophilicity at the sulfur center. The exact aspects governing this, and importantly, factors to predict this in a design context are, however, not well understood.[22,26]

During the last 10 years, several studies looking at the general reactivity of sulfur(VI) fluoride groups have emerged. The first large systematic one came from researchers at AstraZeneca[40] examining the reactivity of molecules containing sulfonyl fluorides and related warheads toward nucleophilic amino acid side chains under physiological conditions. They synthesized a number of aryl sulfonyl fluorides bearing electron-donating (EDG) or -withdrawing (EWG) group in *para*-, *meta*-, and *ortho*-position. In an assay run in phosphate buffer at pH 7.5 at 37 °C, they first established again that the adducts of these warheads with cysteine are not stable, as they were unable to observe (via MS) the sulfonothioate ester intermediate that should form in a reaction between sulfonyl fluorides (SFs) and *N*-acetyl cysteine. When turning to *N*-acetyl tyrosine as the nucleophile, they could clearly establish a strong correlation between the rate of reaction and the electron-withdrawing properties (see **Figure 9** for an overview). Furthermore, by comparing *para*- vs. *ortho*-substitution they determined that electronic rather than steric factors guide the reactivity. When carrying out the same assay with *N*-acetyl lysine, they found slower reaction rates compared to the tyrosine surrogate at pH 7.5. Increasing the pH to 10, as expected, led to much higher reaction rates for all amino acids tested. From their findings, they deduced that the rate of covalent modification in a biological

context could be enhanced if the target residue is located close to a suitably positioned basic side chain. The hydrolytic stability as well as the plasma stability (as assessed in a rat plasma stability assay), predictably, mostly followed the opposite trend compared to reactivity. The same was not observed for metabolism, which seemingly did not primarily depend on intrinsic SF reactivity. The two fluorosulfates in their assay did not display any modification of *N*-acetyl tyrosine (they did conversely show extremely high stability) and of the eight sulfonimidoyl fluorides, only the four most electron-deficient afforded adducts with the tyrosine surrogate. Intriguingly, the modification of the N-substituent apparently could improve hydrolytic stability without compromising reactivity.

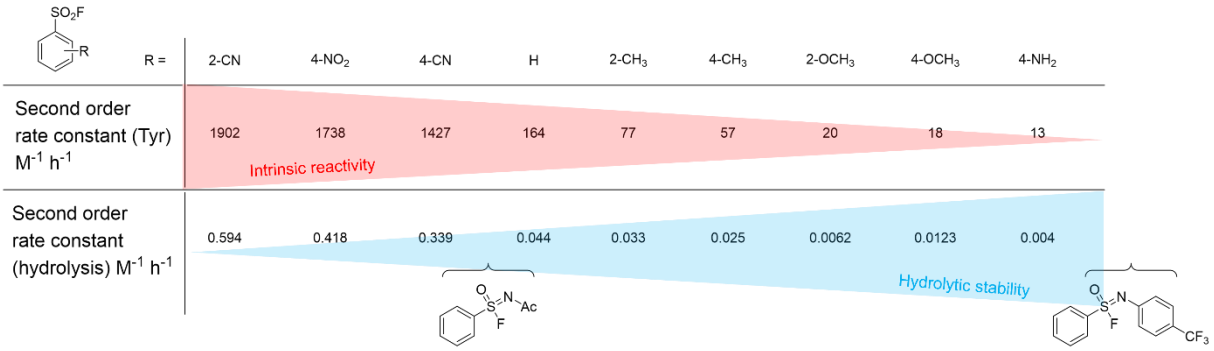

Figure 9: Overview over some of the examined fragments by MUKHERJEE *et al*.[40] Note that not all values follow the exact trend, but the general tendency remains valid. The corresponding sulfonimidoyl fluorides were inserted in the appropriate places. Fluorosulfates did not show measurable addition to *N*-acetyl tyrosine. The experiments were run in phosphate buffer (100 mM), pH 7.5 at 37 °C.

More recently, scientists from GSK conducted a similar study[41] using slightly more elaborate fragments, but also mostly focusing on sulfonyl fluorides, where they examined hydrolytic stability, intrinsic reactivity, protein modification, and proteome-wide reactivity in live cells. Nine distinct sulfur(VI) fluoride electrophiles featuring various electron-withdrawing and electron-donating substituents to evaluate electronic influences were selected for initial hydrolytic stability screening (see the upper half of **Figure 10**). The assessment was performed in PBS and HEPES buffers at pH 7 and 8, as well as in carbonate-bicarbonate buffer at pH 10, with fragment depletion monitored via HPLC. Observed half-lives ranged from 35 minutes to over 600 hours and showed a strong correlation with electronic factors. As anticipated, reaction rates increased under basic conditions, with half-lives approximately halved at pH 8 compared to pH 7. At both pH levels, compounds demonstrated twice the stability in HEPES compared to PBS, indicating a significant impact of buffer identity on stability. The fragments were also subjected to reactions with various *N*-acetylated amino acids, showing increased reactivity in the order: His < Lys < Tyr < Cys. Histidine did not form any adduct, while cysteine produced an unstable reaction product as previously described. However, in a protein context, reaction rates did not precisely mirror the trends observed in solution. To study the rate of protein

modification, the sulfur(VI) fluorides were linked to a carbonic anhydrase II (CAII) hit fragment (as depicted in the lower half of **Figure 10**), and their modification rate of CAII was evaluated, though the exact target residue remained unspecified. While reactivity at the extremes paralleled the solution trends, it differed in regions of moderate reactivity. Four of the nine original fragments were connected to two additional CAII binding elements, and kinetic analysis revealed that these rates were highly dependent on the specific CAII fragment, underscoring the importance of proper positioning and steric considerations of the warhead. Overall, the study confirms that sulfur(VI) fluorides are highly adaptable warheads, exhibiting a wide array of reactivity and stability. Notably, in areas of moderate reactivity, kinetics become more complex, with factors like the warhead's orientation, its geometry and general steric effects often outweighing electronic considerations. The research further demonstrates that less reactive warheads can be advantageous in certain contexts, as they engage only under specific conditions and exhibit considerably less promiscuity. At the same time, achieving effective inactivation kinetics may be more challenging with less reactive warheads.

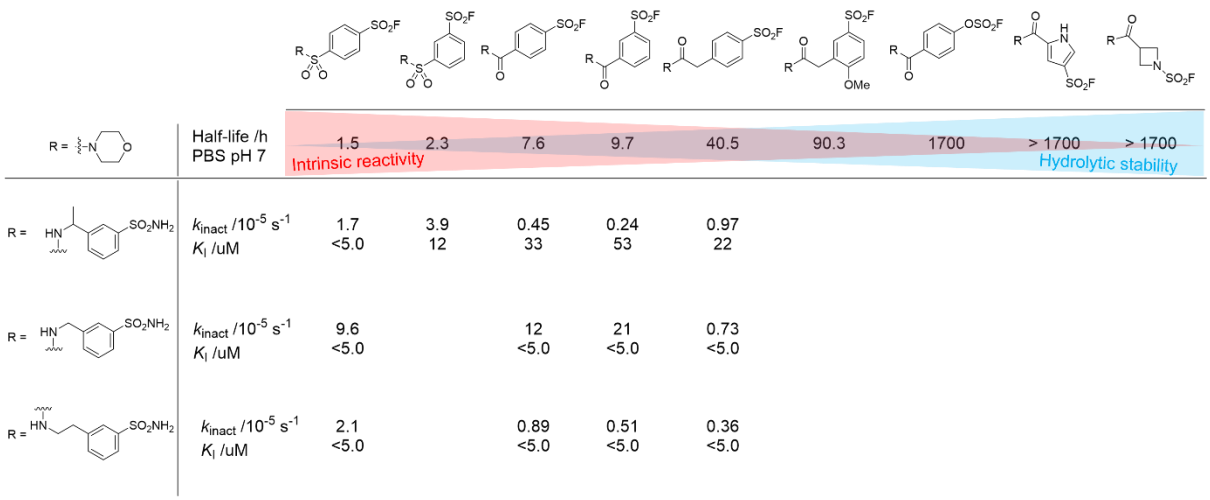

Figure 10: Overview of the examined fragments by GILBERT *et al*.[41] The upper half shows the clearly opposing trends of intrinsic reactivity and hydrolytic stability in solution. The kinetic data on the lower half for the modification of CAII does not strictly follow the same tendencies and is more influenced by other factors such as orientation and sterics. This graphic was reproduced from a literature review[22] published during the course of this PhD.

Reactivity and stability studies like these have played their part in increasing interest in this warhead class over the last decade, which has seen slow but steady growth in targeting many different protein families. Because protein–protein interactions (PPIs) are notoriously hard to target through noncovalent means because of their large surfaces, they represent an interesting target for covalent approaches. Since furthermore, cysteines are often underrepresented in these areas, which is not the case for lysine and tyrosine,[54] SuFEx chemistry has presented itself as a promising methodology to circumvent these problems. For instance, the group of PELLECHIA identified a unique lysine residue on the surface of the baculovirus inhibitors of apoptosis proteins repeat 3 (BIR3) domain of X-linked IAP (XIAP).

XIAP, together with its family members cellular IAP1 and 2 (cIAP1 and 2), can inhibit apoptosis and block caspase activation. The design of the inhibitors was based on a natural IAP ligand interacting via the tetrapeptide AVPI. When placing an aryl sulfonyl fluoride on the side chain of L-diaminopropionic acid, the warhead showed proper juxtaposition and distance toward the desired lysine.[55] Over the course of several studies,[55–59] the researchers were able to design and synthesize multiple probes bearing both sulfonyl fluorides and fluorosulfates that were able to either target XIAP selectively over its family members or in a way that targets the whole IAP family. Intriguingly, with one of their probes carrying a fluorosulfate (**16**, **Figure 11A**) they were able to show that these warheads can be similarly effective in terms of reaction rate, stability and cell permeability as acrylamides targeting cysteine. This PPI inhibitor also showed favorable cellular and pharmacological properties, corroborating the idea that fluorosulfates may be used as pharmacological tools and potentially even therapeutics.[58] Conversely, the same scientists were also able to show that with a clever substitution pattern, sulfonyl fluorides (e.g. **17**, **Figure 11A**) can also be made hydrolytically stable while retaining their reactivity *in vitro* and *in cellulo*.[60]

Since tyrosines are also often located at PPI “hot spots”, researchers at AstraZeneca targeted Tyr101 of the BH3 domain-binding groove of the PPI target B-cell lymphoma extra-large (Bcl-xL).[61] Their compound (**18**, **Figure 11A**) exhibited only modest covalent modification rates, resulting in no improved potency over noncovalent analogs *in vitro*, but achieving 50-fold selectivity over BCL-2. This approach, despite limited potency gains, proved the feasibility of identifying ligandable hotspots for PPI targets through screening sulfonyl fluoride-bearing fragments.

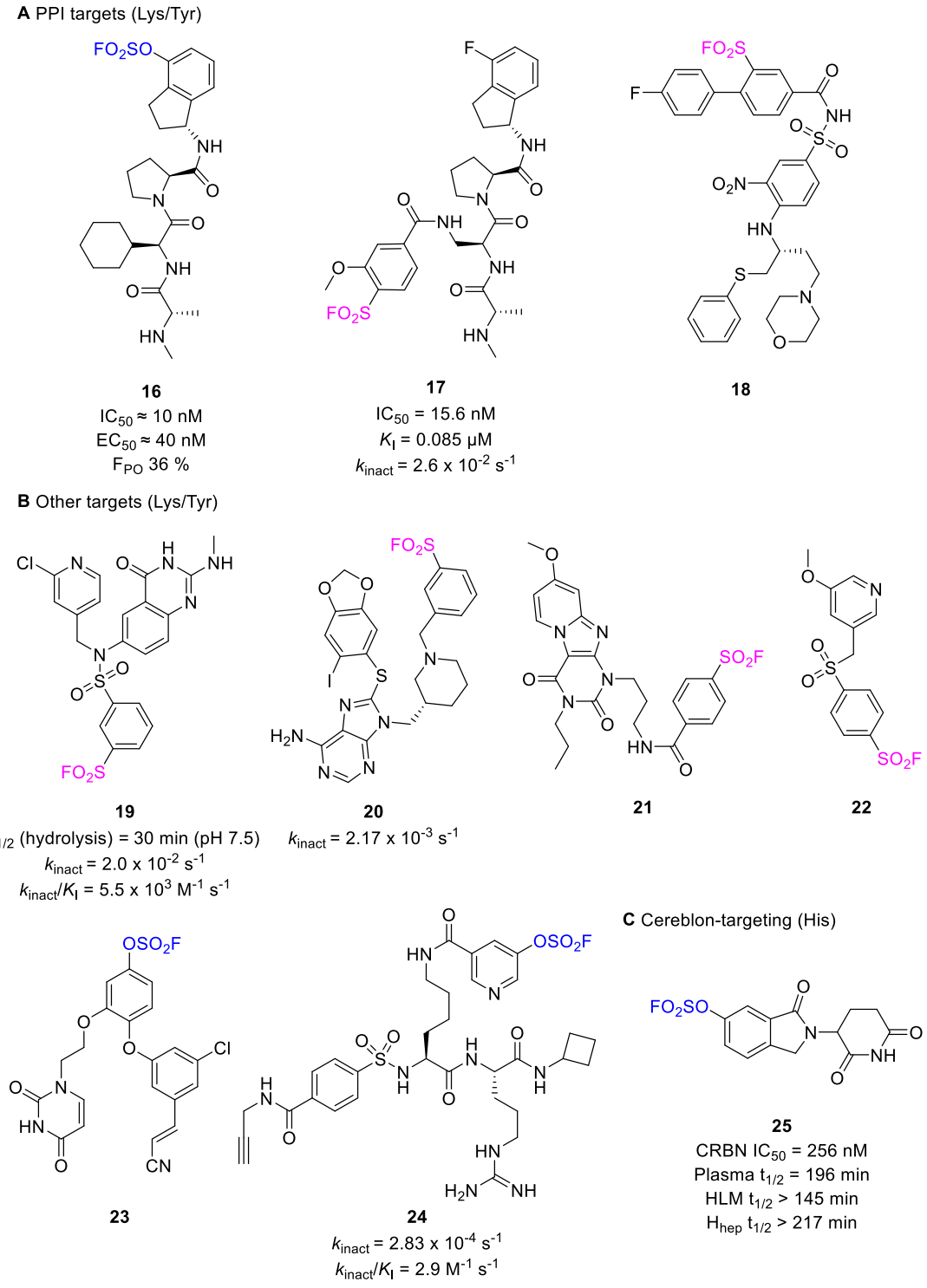

Figure 11: A Compounds targeting lysines or tyrosines in PPI targets. **B** Compounds targeting lysines or tyrosines in other selected targets. **C** Cereblon-targeted inhibitor targeting a histidine in the E3 ligase. Sulfonyl fluorides are depicted in magenta, while fluorosulfates are shown in blue. Selected kinetic and other values are shown where appropriate.

Beyond the realm of PPIs, the lab of JACK TAUNTON has made several strides using SuFEx chemistry. They developed eukaryotic translation initiation factor 4E (eIF4E) inhibitors (e.g. **19**, **Figure 11B**)[62] that circumvent the poor cell permeability of the usually utilized negatively

charged guanine nucleotide analogs. They also developed a heat shock protein 90 (Hsp90) inhibitor (**20**, **Figure 11B**) that targets the surface-exposed Lys58 which was smartly designed to use enantiodiscrimination to tune the kinetics of the probe.[63] The groups of VAN DER ES and IJZERMAN developed several covalent probes (e.g. **21**, **Figure 11B**) for different human adenosine receptors that could prove useful in the elucidation of some of these receptors.[64–68] Even in the earlier mentioned field of KRAS inhibition SuFEx has been utilized – because most RAS mutants and all RAS-like (Ral) proteins do not possess an addressable cysteine, BUM-ERDENE *et al*.[69] developed a sulfonyl fluoride-bearing probe (**22**, **Figure 11B**) that targets Tyr82 in RalB and thereby inhibits Ral nucleotide exchange by the guanine exchange factor (GEF) Rgl2.

Targets successfully addressed by rational design employing the more stable fluorosulfates include the wildtype (WT) HIV-1 reverse transcriptase (HIV-RT), where interestingly the fluorosulfate (**23**, **Figure 11B**)[70] displayed higher potency than the intrinsically more reactive sulfonyl fluoride and the sirtuin 5 (SIRT5) lysine deacylase where this particular warhead (see e.g. **24**, **Figure 11B**)[71] was chosen to reduce promiscuity albeit it turning out to show slow kinetics. In addition to lysine and tyrosine, histidine can also be targeted through SuFEx chemistry. Here, the lab of LYN H. JONES has played a pioneering role. They have developed several covalent cereblon blockers (e.g. **25**, **Figure 11C**)[72,73] as well as PROTACs that covalently bind to the E3 ligase instead of the protein of interest (POI), generating covalent PROTACs that keep and possibly even enhance the catalytic mechanism of these modalities while also displaying good plasma and metabolic stability.

In the kinase field, which is the focus of this dissertation, efforts to covalently target residues other than cysteine are relatively rare yet they do exist. An illustrative first step in this direction is the work by TAUNTON and his team published in 2017,[74] who employed sulfonyl fluorides as covalent reactive groups to develop a lysine-targeted broad-spectrum kinase inhibitor. This compound was designed as an active-site probe for chemical proteomics applications. Utilizing X-ray crystal structures, they identified a promiscuous pyrimidine 3-aminopyrazole scaffold and hypothesized that a carefully chosen linker at the 2-position of the pyrimidine ring would place a phenylsulfonyl fluoride in proximity to the conserved “catalytic” lysine. Using SRC as a model kinase, both MS and X-ray crystallography (PDB: 5K9I) confirmed that the optimized, clickable probe XO44 (**26**, **Figure 12**) selectively modified the target lysine (Lys295) without affecting the additional lysines and tyrosines, even at threefold excess. A similar binding mode was confirmed for the kinase domain of the EGFR tyrosine kinase receptor in another crystal structure (PDB: 5U8L). In Jurkat T-cells, the inhibitor successfully captured 133 protein kinases and inhibited more than 50 % of 219 kinases in a 375-kinase panel at 1 µM concentration. Although some non-kinase off-targets were also modified, kinases were the predominantly modified group in MS-based proteomics experiments, and competition experiments with

dasatinib, a tyrosine kinase inhibitor, further verified the probe's effectiveness for cellular selectivity profiling. Building on these advances, the GRAY lab then introduced SRPKIN-1 (**28**),[75] the first targeted kinase inhibitor addressing a tyrosine residue. Screening their compound library, they identified the anaplastic lymphoma kinase (ALK) inhibitor alectinib (**27**, both **Figure 12**) as a potent serine/arginine-rich splicing factor protein kinase-1 (SRPK1) inhibitor (IC_{50} = 11 nM). A co-crystal structure revealed the binding mode of alectinib in complex with SRPK1, suggesting that replacing the 4-morpholinopiperidine moiety with a *meta*-substituted phenyl ring containing a sulfonyl fluoride warhead could enable covalent targeting of a distinct tyrosine (Tyr227) near the solvent-exposed front region of the ATP binding site. The resulting modification retained SRPK1 activity (IC_{50} = 36 nM) while reducing ALK inhibition (IC_{50} = 195 nM). Selectivity for SRPK1 and 2 was demonstrated and washout experiments supported the covalent binding mode. The labeling of Tyr227 was tentatively confirmed by MS, but no kinetic data or any X-ray crystal structure was provided.

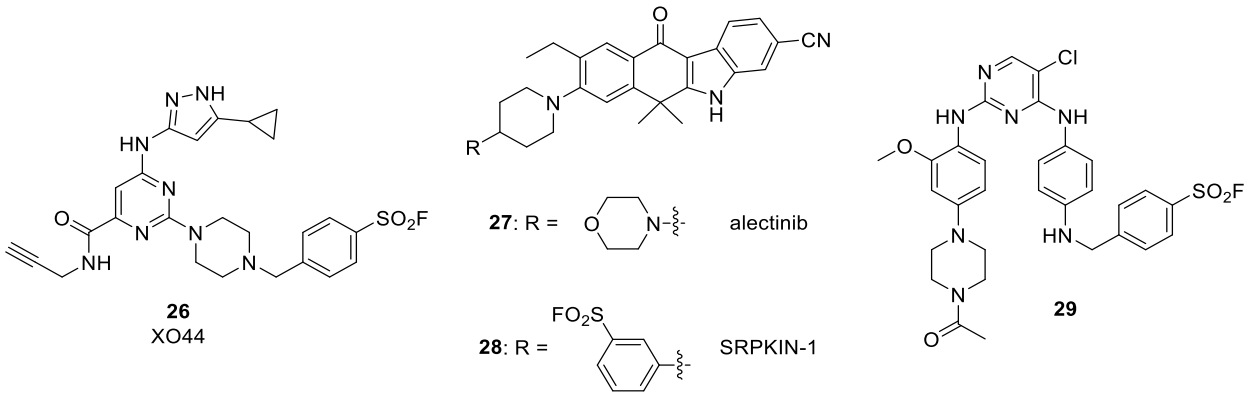

Figure 12: Semi-promiscuous kinase probe XO44 (**26**); first targeted covalent kinase inhibitor SRPKIN-1 (**28**) and its noncovalent design analog alectinib (**27**) and lysine-targeted EGFR inhibitor **29**.

At the start of this PhD project, XO44 (**26**) and SRPKIN-1 (**28**) were the only two SuFEx kinase-targeted probes/inhibitors available. In late 2021, FERLENGHI *et al.*[76] published their development of a lysine-targeted EGFR inhibitor revealing a sulfonyl fluoride as the best warhead for the task. Osimertinib, a third-generation EGFR inhibitor, faces a typical issue associated with covalent kinase inhibitors: decline of efficacy due to mutation of the target cysteine. This problem may be circumvented by targeting the "catalytic" lysine (in the case of EGFR Lys745) since this residue is vital for the function of the kinase. The possible downside of this approach is a potential lack of selectivity since this lysine is highly conserved across the kinome. The design strategy in this particular case was to link different lysine-targeting warheads to the 2-anilinopyrimidine hinge binding scaffold typical for third-generation EGFR inhibitors. From a chloroacetamide, vinyl sulfonamide, activated ester and different sulfonyl fluorides, the latter emerged as the most potent choice (**29**, TR-FRET assays revealed a 4-times higher potency on $EGFR^{L858R/T790M/C797S}$ than for Osimertinib itself). Docking simulations

revealed a high superimposition with the aforementioned XO44 (**26**). The covalent modification of Lys745 was finally proven through MS experiments, including a trypsin digest. Selectivity was only tested against 16 other kinases, but in this limited set it actually showed good results. Stability of the sulfonyl fluoride, however, was again an issue as exemplified by a short-lived effect on EGFR autophosphorylation and proliferation in Ba/F3 cells.

Another two years later, scientists from GSK published an interesting study using fluorosulfates to target both the “catalytic” lysine and a tyrosine in the lipid kinase PI4KIIIβ.[77] Based on a noncovalent inhibitor of the kinase, they identified Lys549 in the ATP binding pocket as their desired target residue but quickly realized that sulfonyl fluorides were too instable for their endeavor. Switching to a fluorosulfate (**30**, **Figure 13**) brought the desired potency against PI4KIIIβ while selectivity over other lipid kinases was high. Selective covalent engagement was shown via MS and the bond formation to Lys549 was apparent from an X-ray crystal structure (PDB: 8Q6F, magenta in **Figure 13**). Intriguingly, in this crystal structure a hydrogen bond between the pyridine ring of the compound and Tyr385 became apparent to the authors, and they decided to try to covalently trap this residue next. Again, they were able to covalently modify the desired residue (through compound **31**, **Figure 13**) as proven via MS and X-ray (PDB: 8Q6G, green in **Figure 13**). Interestingly, while both covalent modifications show rather slow kinetics (see **Figure 13** for the measured values), the modification of the desired tyrosine was even markedly slower than that of the lysine. This was attributed to the possibly lower nucleophilicity of the tyrosine compared to the lysine (the authors hypothesized the methoxy group next to the fluorosulfate in the lysine-targeting compound potentially increased the nucleophilicity of the lysine). Finally, a compound carrying both warheads was designed and synthesized (**32**) and indeed, covalent modification crosslinking both Lys549 and Tyr385 was observed (PDB: 8Q6H, orange in **Figure 13**).

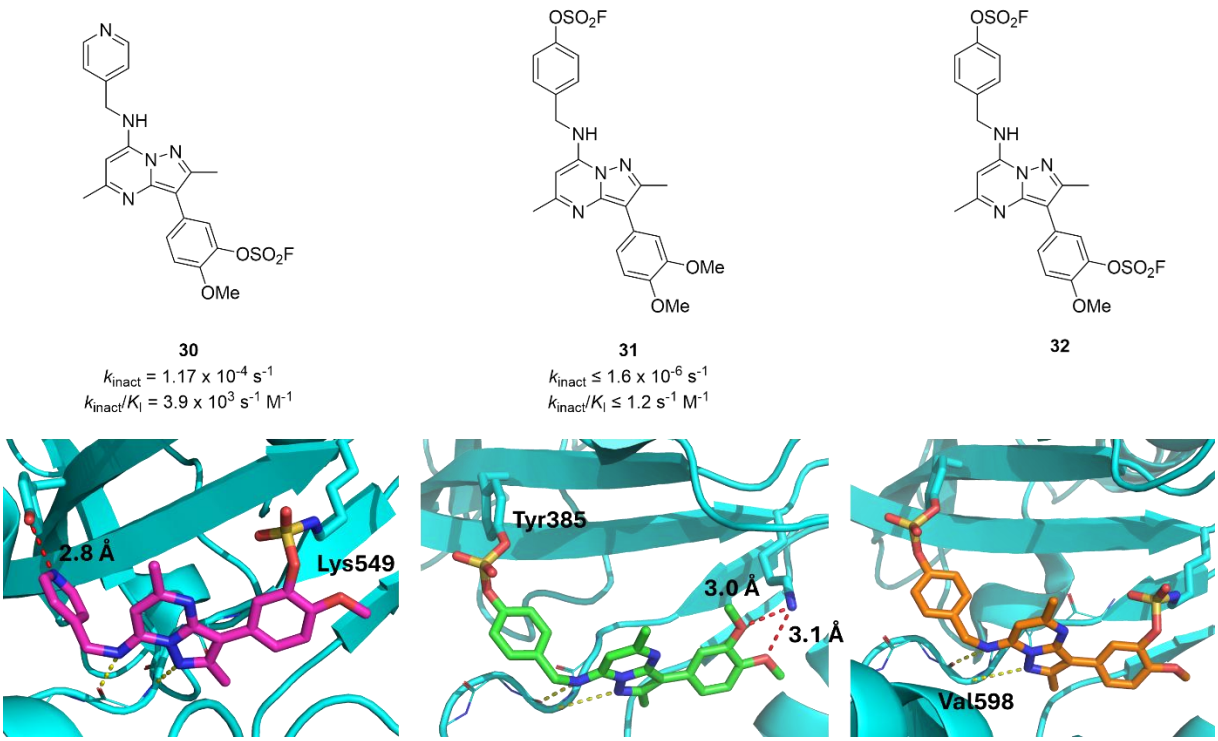

Figure 13: The three different inhibitors **30**, **31** and **32** by COSGROVE *et al.*[77] including their published kinetic parameters. The lower half shows the three crystal structures depicting the covalent bond formation with **left**: Lys549 (PDB: 8Q6F); **middle**: Tyr385 (PDB: 8Q6G); and **right**: both residues (PDB: 8Q6H). In all three depictions the interaction with Val598 in the hinge region is shown through yellow dashed lines. The distance to the two residues when not covalently bound is shown via red dashed lines.

To summarize, covalent targeting of cysteines in kinases suffers from two significant limitations: **(1)** despite the residues being highly nucleophilic and well characterized, their natural abundance is low leaving a vast part of the kinome "unaddressable" through classic cysteine-targeting means;[78] and **(2)** in a clinical setting resistance can, and often does, develop through single point mutation to serine, preventing covalent adduct formation.[79,80] These drawbacks affect both more basic research, including the design and application chemical probes, as well as translational research and actual drugs, thus impacting chemical biologists and medicinal chemists alike. While clearly only one piece of the "solution puzzle" and currently still in the early stages, SuFEx chemistry can offer answers for both aforementioned groups.

1. First, sulfur(VI) fluorides provide the possibility to address several different amino acid residues – lysine and tyrosine being the most commonly used so far. While the lysine side chain has a slightly higher pK_a compared to tyrosine (~10 vs 10.5, respectively, for the side chains of the unprotected amino acids),[81] the protein microenvironment can markedly influence this and furthermore, lysine is significantly more flexible than tyrosine – both offer their pros and cons that need to be considered. The lysinome and the tyrosinome equally offer much untapped potential.[82] Very recently, histidine has also gained more attention.[83]

2. While stability and reactivity of these warheads exist in a fine equilibrium that always needs to be balanced, it has been shown that both sulfonyl fluorides and fluorosulfates can be tuned to find the sweet spot between those two parameters. Although scarce, *in vitro* and *in vivo* studies have proven that good stability in plasma, microsomes and hepatocytes is possible (examples can be found throughout the literature cited in this chapter). And the "latent" reactivity of these electrophiles can also be seen as a positive: it makes unwanted side-reactions that are often feared in covalent targeting much less frequent.
3. Lastly, the fluoride leaving group seems to be safe up to millimolar concentrations *in vivo*[84] paving the way for more translational applications.

Taken together, these factors render SuFEx electrophiles a warhead class with great potential to broaden the landscape of covalent chemical probe and drug design, offering innovative solutions for both fundamental research and later on, clinical applications. This dissertation aims to contribute a piece to this evolving field by exploring new targets, methodologies and insights that address existing challenges and expand the possibilities of covalent targeting.

1.3. Structure-Based Design vs. Covalent-First Screens

In the realm of covalent drug discovery, especially for intentionally developed TCIs, there are two major hit finding approaches – structure-based design (also sometimes referred to as *binder-first*) and covalent-first screens. In the scope of drug design campaigns, fragment-based drug discovery (FBDD), which may be utilized also in a covalent manner, is seen as a successful and complementary method to the more "traditional" high-throughput screening (HTS). To date, eight FDA-approved drugs stem from an FBDD approach and over 50 such compounds have advanced to clinical stages.[85] Therefore, historically seen, this is a rather novel approach.

So far, rational TCI design has also often relied on binder-first approaches where a noncovalent inhibitor is analyzed for covalently addressable amino acid residues in its proximity in the target protein. A suitable warhead is then chosen and carefully placed on the noncovalent compound in order to balance reactivity and stability and achieve proper pre-orientation. This method was, for example, used in all three cases for targeted kinase inhibitors utilizing SuFEx warheads described in the previous chapter. While this method provides a clear design rationale from the beginning of the project, it also has two clear limitations: **(1)** the obligatory existence of a noncovalent binder as a starting point and thus, applicability only to "traditional" binding sites that are already known for hosting noncovalent ligands; and **(2)** that those ligands must be close to a reactive amino acid residue. This latter restriction is somewhat mitigated by the expansion of covalent targeting, which has progressed beyond its initial focus on cysteine

residues. Nevertheless, covalent screens including fragment-based approaches have gained popularity and have recently facilitated the identification of novel targets and binding sites, as well as ligands for targets once considered undruggable, most notably in the case of the FDA-approved drug sotorasib.[86]

Typically, a fragment is defined as a small molecule with a molecular weight below 300 Da. Arguably, the most well-known set of guidelines that most fragments follow is the 'rule of three' (Ro3), established by researchers at Astex Pharmaceuticals about twenty years ago.[87] They defined that to qualify as a fragment, a molecule should have **(1)** ≤3 hydrogen bond donors (HBD); **(2)** ≤3 hydrogen bond acceptors (HBA) and; **(3)** a cLogP/cLogD of ≤3. Additional criteria include ≤3 freely rotatable bonds and a polar surface area (PSA) of ≤60.[86] However, these should be regarded as guidelines rather than absolute rules. Covalent fragment-based approaches have enabled the sampling of a vast amount of chemical space with a rather small number of compounds (a few thousand compared to tens up to hundreds of thousands in the case of lead-like covalent libraries).[88] While hits from traditional (noncovalent) HTS campaigns generally display dissociation constant values (K_d) in the nM – µM range, fragments are often weak binders that require biophysical techniques for detection rather than biochemical assays. In the case of covalent fragments this usually means detection through liquid chromatography with tandem mass spectrometry (LC-MS/MS) which can be carried out in a high-throughput manner.[86] Despite its success and inherent benefits, hit-to-candidate progression in fragment-based drug discovery is often more difficult than with hits obtained through traditional high-throughput screening methods. Thus, optimization from fragments to leads is often a significant bottleneck in FBDD. This process can be especially time-consuming if the fragment hit offers limited opportunities for optimization and few handles to grow from. Researchers at Astex Pharmaceuticals therefore emphasize the importance of ensuring fragments are primed for swift hit-to-lead transitions and advise establishing the elaboration chemistry before screening begins.[87]

LONSDALE and WARD[89] suggested an interesting, nuanced way to look at this spectrum that is displayed in **Figure 14** (the subsequent description outlines the aspects of the figure sequentially from left to right). Chemoproteomic approaches are gaining more and more traction, such as for example in a strategy by SHARPLESS and colleagues that they termed “inverse drug discovery” that uses fluorosulfate[90] or sulfuramidimidoyl fluoride[91] probes to identify hotspots of reactivity across the cellular proteome. Afterwards, the exact targets can be identified and validated. This presents a direct way to identify an efficacious compound and requires only very little information about the target (at first). In a target-centric covalent screening approach, the target is known and isolated. This may be a valuable tactic if noncovalent binders of this respective target do not exist. Selectivity and reactivity might be harder to control though, especially if covalent fragment libraries are used, and this scenario

may require significant chemical optimization. Furthermore, as for chemoproteomic approaches, reactive molecules can bind anywhere in the protein – including in regions that will not result in the desired functional modification (e.g. inhibition). When screening covalent leads, the compounds tend to be more drug-like which can simplify medicinal chemistry optimization later on. While again, known noncovalent binders are not required for this approach, hit rates are typically lower, necessitating larger and more diverse libraries; additionally, the throughput and protein requirements of MS-based screens can pose practical challenges. In contrast – and returning to the binder-first paradigm discussed earlier – another viable strategy is to identify a reversible lead and subsequently append a covalent warhead. As previously noted, this is only possible if such a compound exists and sufficient structural information is available. This consideration becomes especially critical when the starting point is a fully optimized reversible inhibitor of the desired target.[89]

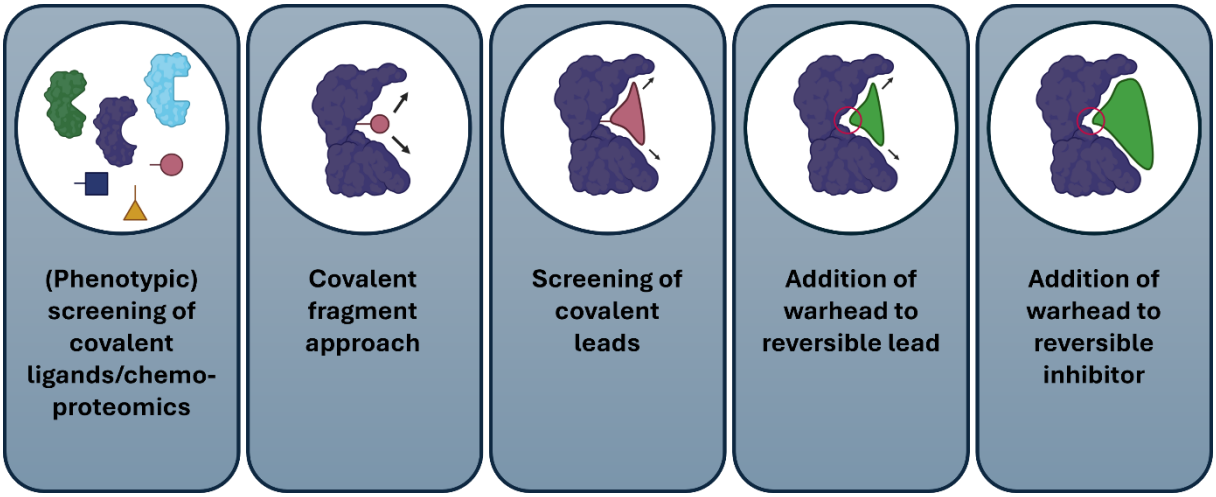

Figure 14: Overview over different covalent design strategies adapted from LONSDALE and WARD.[89] The methodologies progress from covalent-first strategies on the left to binder-first strategies on the right.

In conclusion, while both structure-based and covalent-first screening approaches offer distinct advantages and challenges in covalent drug discovery, the integration of fragment-based strategies continues to expand the horizons of this field. Furthermore, computational methods (e.g. virtual screenings), despite currently still being very prone to error and neglecting the reactivity part of covalent target engagement, provide complementary means to screen ultra-large fragment libraries before “lab validation”, creating a synergistic “computation-experiment” cycle.[85] As these methodologies evolve, they provide unprecedented opportunities to tackle both druggable and previously intractable targets, underscoring the importance of ongoing innovation and optimization in drug development.

1.4. Kinase Targets

Throughout this project, SuFEx chemistry was applied to target a variety of protein kinases. The following chapters will provide a short discussion of the three kinases that were central to this research.

1.4.1. JAK3

Janus kinase 3 (JAK3) is a member of the Janus kinase family, comprised of JAK1, JAK2, JAK3, and TYK2 (tyrosine kinase 2), which are cytosolic tyrosine kinases integral to the JAK/STAT (signal transducer and activator of transcription proteins) signaling pathway. These kinases play a pivotal role in transmitting signals from cytokine receptors to the nucleus, thereby affecting cell differentiation, proliferation, and apoptosis. JAK3, unlike the ubiquitously expressed JAK1, JAK2, and TYK2, is predominantly found in hematopoietic cells and is crucial for the development and function of immune cells such as T-cells, B-cells, and natural killer (NK) cells.[92,93] This specific expression pattern makes JAK3 a compelling target for the treatment of autoimmune diseases, as selective inhibition can lead to effective immunosuppression with potentially fewer side effects compared to pan-JAK inhibitors like tofacitinib.[93]

JAK3's unique structural feature – a cysteine residue (Cys909) located in the solvent-exposed front part of its ATP binding pocket – sets it apart from other JAK family members and serves as a valuable target for covalent inhibitors. Despite initial controversies regarding the necessity of concurrent JAK1 inhibition, recent studies indicate that selective JAK3 inhibition can effectively block downstream STAT phosphorylation and signaling, disproving earlier assumptions of JAK1's dominance in γ_c-dependent signaling pathways.[93,94]

JAK3's role in immune signaling is underscored by the severe immunological consequences of its deficiency, as evidenced by loss-of-function mutations leading to severe combined immunodeficiency (SCID). Patients with JAK3-SCID exhibit a marked absence of T- and NK-cells, emphasizing JAK3's critical role in immune function.[92] The promise of JAK3-selective inhibitors lies in their ability to achieve immunosuppression while minimizing adverse effects, presenting a more targeted therapeutic approach.[92,93] As research progresses, a deeper understanding of JAK3's structural and functional nuances continues to inform the development of targeted therapies which has culminated in the FDA-approval of ritlecitinib (**7**, **Figure 3**), a covalent (isoform-)selective JAK3 inhibitor (TEC-family kinases are its main "off-target" instead because they possess a cysteine in the same position).[95]

We selected JAK3, in which we have already successfully addressed cysteines, as the initial focus for this project due to the presence of a tyrosine residue at the GK+2 position (Tyr904), rendering it an ideal candidate for a proof-of-concept study utilizing SuFEx chemistry. As this tyrosine is also present in several other kinases (including JAK2 and TYK2) our primary objective was not to achieve selective inhibition of JAK3, but rather to demonstrate the feasibility of this approach. Choosing JAK3 allowed us to leverage the extensive body of research previously conducted in our group,[94,96,97] alongside established in-house testing methods. The concrete structure-based design strategy employed in this project will be detailed in chapter 3.1.1.

1.4.2. MK2/MAPKAPK2

Mitogen-activated protein kinase-activated protein kinase 2 (MK2, also known as MAPKAPK2) is a pivotal component in the p38–MAPK signaling pathway, which is central to the body's inflammatory and stress responses.[98] Newly uncovered roles of MK2 extend to tumor development and progression, highlighting its importance beyond inflammation. Activation of MK2 follows p38–MAPK stimulation and involves triple phosphorylation, primarily enacted by p38α/β, which allows MK2 to regulate the expression and stability of pro-inflammatory cytokines like TNFα and IL-6 through mRNA interactions.[99] This regulation renders MK2 a significant target for therapeutic intervention in inflammatory diseases, especially as direct p38 inhibitors have frequently failed (besides lack of efficacy) due to issues such as hepatotoxicity, cardiotoxicity, and tachyphylaxis. MK2 inhibitors, therefore, offer a promising avenue to suppress cytokine production without affecting upstream p38–MAPK functions that initiate both inflammatory and feedback mechanisms, thereby avoiding these pitfalls.[99,100]

Moreover, MK2 is ubiquitously expressed, with heightened levels observed in immune organs and gastrointestinal tissues, underscoring its integral role in immune regulation. Its position downstream of p38 makes it a viable target for selective blockade, potentially providing sustained anti-inflammatory effects critical for treating autoinflammatory and autoimmune conditions. While biochemically potent ATP-competitive inhibitors have been developed, achieving clinical efficacy remains challenging due to MK2’s high affinity for ATP and its deep, narrow ATP-binding cleft that complicates selective inhibitor design.[99] Nonetheless, ongoing research continues to illuminate MK2's therapeutic potential, paving the way for novel anti-inflammatory strategies that potentially circumvent the limitations of direct p38–MAPK targeting.[98,100]

Targeting MK2 covalently through its hinge cysteine (GK+2 position, Cys140) offers a promising strategy for the effective and selective inhibition of this kinase and has been a focal

point of our research group in recent years. However, given the constraints of MK2's narrow ATP binding site, exploring allosteric approaches is of considerable interest. In our investigation of non-cysteine residues using SuFEx chemistry, we identified a crystal structure (PDB: 6T8X) of an allosteric MK2 inhibitor featuring several proximal tyrosine residues. These residues provided a promising foundation for developing an alternative covalent strategy for MK2 inhibitors. The precise design concept, which remains rooted in structure-based methodology, will be elaborated upon in chapter 3.2.1.

1.4.3. ACVR1/ALK2

Activin receptor-like kinase 2 (ALK2), encoded by the *ACVR1* gene, is a critical member of the type I bone morphogenetic protein (BMP) receptor family, involved in the transforming growth factor-β (TGF-β) signaling pathway. As a serine/threonine kinase, ALK2 plays a vital role in the development and regulation of various physiological systems, including bone, heart, brain, and reproductive tissues. The receptor comprises an extracellular ligand-binding domain, a transmembrane region, and an intracellular kinase domain.[101] ALK2 is widely expressed throughout the body and serves as a receptor for multiple BMP ligands as well as activins. These ligands initiate receptor activation, leading to the phosphorylation of SMAD1/5/8 (mothers against decapentaplegic homolog proteins) and subsequent transcriptional regulation.[102,103]

Pathological gain-of-function mutations in *ACVR1* result in aberrant ALK2 signaling and are implicated in severe disorders like fibrodysplasia ossificans progressiva (FOP) and diffuse intrinsic pontine glioma (DIPG), both of which currently lack effective treatments. These mutations disrupt normal inhibitory mechanisms, such as FKBP12 binding, and increase sensitivity to ligands like activin A, causing excessive activation of downstream pathways.[104] Developing selective inhibitors targeting ALK2 presents challenges due to the high homology of the ATP-binding domain among ALK family members, particularly requiring careful differentiation from ALK5 to avoid cardiac toxicity.[101] The role of ALK2 in these detrimental diseases has also only been known for less than 20 years. Nonetheless, the potential to modulate ALK2’s aberrant activity holds promise for innovative therapeutic strategies in treating these genetic disorders and related pathologies.[101,102,105]

ALK2 became the center of attention in the latter half of this project, emerging from a different approach than our previous targets. While the initial two kinases were predetermined at the outset due to our binder-first strategy that depended on crystal structures of noncovalent binders, ALK2 was identified through a fragment/lead-like covalent-first screening of several preselected kinases (the selection process will be detailed in a chapter 4.4.1). Beyond its

intrinsic biological significance, ALK2 presents an intriguing target for a SuFEx-based covalent strategy because it lacks a targetable cysteine,[28] making it inaccessible to conventional covalent targeting methods.

2. Objectives

The cysteinome of the protein kinases represents a very well-established target for covalent inhibitors.[28] This strategy has led to the approval of over 10 targeted covalent kinase inhibitors by the FDA, nearly all of which address the same conserved front pocket cysteine position – except for futibatinib.[106] Despite this progress, approved covalent inhibitors are currently limited to fewer than 10 kinases, even though the human kinome comprises over 500 members. Additionally, more than half of all kinases lack a suitably positioned cysteine, making them inaccessible to current covalent approaches.[18,22,23,82] In clinical settings, moreover, resistance often arises from single point mutations of cysteine to serine, preventing covalent adduct formation.[79] These challenges underscore the need for broader strategies in covalent inhibitor design, with implications for both basic kinase research and therapeutic development.

While cysteine remains the most established nucleophilic target for covalent inhibitors, there is growing interest in expanding this strategy to other amino acids amenable to covalent modification. Broadening the scope beyond cysteine not only increases the chemical space of suitable electrophilic warheads but also enables access to proteins lacking strategically positioned cysteines. In particular, the lysinome and tyrosinome have emerged as promising targets. Despite their lower nucleophilicity compared to cysteine, lysine and tyrosine residues are more abundant, offering the potential to engage a broader range of the proteome. However, this shift also presents significant challenges: the reduced intrinsic reactivity of lysine and tyrosine necessitates more finely tuned electrophiles, and their higher abundance may lead to decreased selectivity and increased off-target (re)activity. Thus, while these residues hold great promise, realizing their full potential requires overcoming key chemical and biological hurdles.[22,82]

Although still in its early stages and only one component of a broader strategy, SuFEx chemistry has demonstrated potential for targeting both lysine and tyrosine residues. The most used congeners, sulfonyl fluorides and fluorosulfates, have been shown to be tunable to address both stability and reactivity issues. Importantly, they are not intrinsically so reactive that broad off-target modifications are a major concern, and the fluoride leaving group is considered safe up to millimolar concentrations *in vivo*.[22,41,42,82,84] Taken together, these factors position SuFEx chemistry as a promising warhead class capable of expanding the scope of covalent drug design, offering innovative solutions for both fundamental research and potentially clinical applications down the line. This dissertation aims to contribute to this evolving field by exploring new targets, developing methodologies, and providing insights that address current challenges and expand the possibilities for covalent targeting.

The first part of this thesis was centered on structure-based design starting from a noncovalent JAK3 inhibitor to which a warhead would be attached, creating a vector for covalent target engagement (**Figure 15**, the detailed design strategy is described in chapter 3.1.1). Initially, the project aimed to covalently target a tyrosine in the hinge region of JAK3, leading to the selection of fluorosulfates and sulfonyl fluorides as the designated warheads. While sulfonyl fluorides present the most established moieties used in SuFEx chemistry, fluorosulfates are more stable, exhibit more drug-like properties and are less explored. In a proof-of-concept study, the covalent probes were to be modified to achieve the proper geometry and pre-orientation to generate a covalent bond between the SuFEx warhead and the tyrosine nucleophile in the protein. The insights gained from this project were intended to be applied to other kinases, most notably the MAPK-kinase activated protein kinase MK2 (see chapter 3.2), leveraging the advantages of this chemistry to advance covalent kinase targeting beyond cysteine and Michael acceptors.

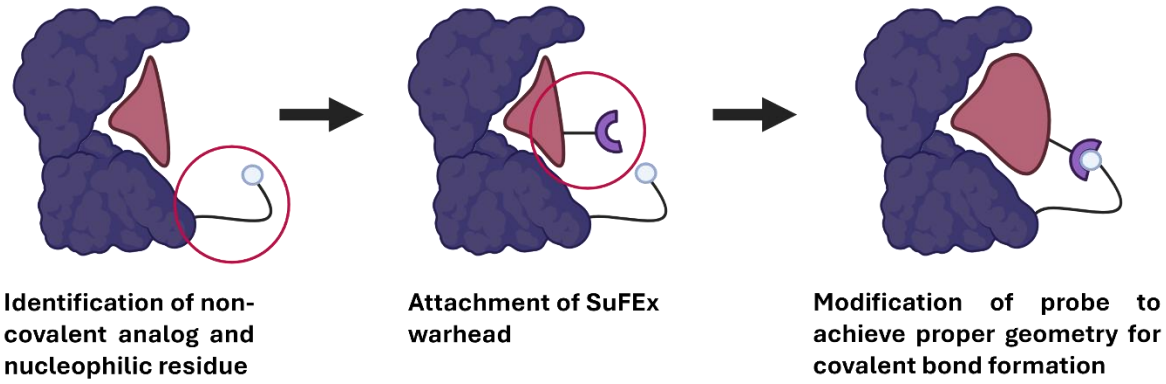

Figure 15: Structure-based design strategy to attain non-cysteine targeted covalent kinase inhibitors. Initially, a noncovalent ligand is selected, and a nearby nucleophilic residue is identified. Subsequently, an appropriate site for the SuFEx warhead is established. Finally, the probe is modified suitably to facilitate covalent bond formation. Graphic was created using BioRender.com.

In the later stages of the project, a covalent-first approach was adopted to develop a fragment-like yet kinase-focused SuFEx compound library (**Figure 16**) to probe a relevant selection of the kinome for covalent targeting beyond cysteine. The library was designed to include various hinge binders, along with different exit vectors linked to an aryl ring connecting the warhead. The probes were to be tested against a set of kinases (the details of the library and kinase selection are provided in chapters 3.3.1 and 4.4.1) using intact protein MS to identify modified proteins. Promising hits were to undergo additional biophysical experiments to confirm covalent bond formation and pinpoint the exact binding site. Compelling results from this approach would then be pursued further through a small structure–activity relationship (SAR) study, thereby offering new starting points for designing kinase TCIs beyond cysteine.

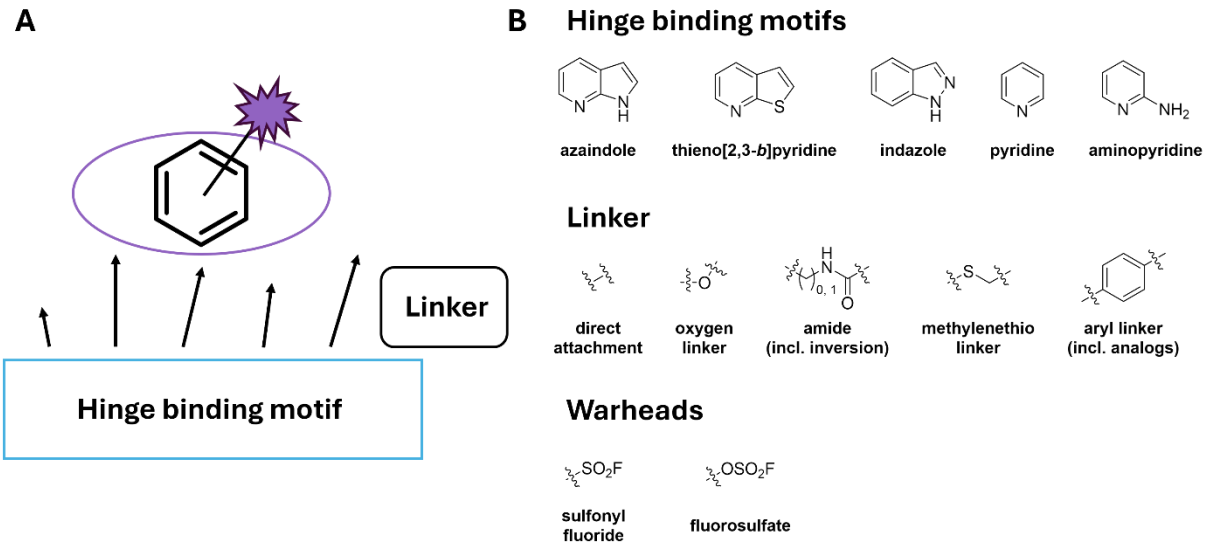

Figure 16: A Schematic depiction of the fragment-like library. Different hinge binding motifs were connected to various linkers via several exit vectors. These were attached to an aryl ring carrying the warhead (purple star). **B** Overview over the different hinge binding motifs, linkers and warheads used in the library.

3. Chemistry

3.1. Synthesis of JAK3-Targeted Inhibitors

3.1.1. Structure-Based Design Strategy for JAK3 Inhibitors

The design of the covalent JAK3 inhibitors was informed by the extensive research on JAK inhibitors previously conducted by our research group.[94,96,97,107] From an unpublished series in which modifications had been performed at the C-3 position of a tricyclic 1,6-dihydrodipyrrolo[2,3-*b*:2',3'-*d*]pyridine inhibitor scaffold,[107] compound **33** was identified as the most promising candidate. It features a cyano group in the *meta*-position of a 3-phenyl substituent (**Figure 17A**) and displays an IC_{50} value of 5.2 nM. An X-ray crystal structure confirmed the anticipated two hydrogen bonds formed by the azaindole core with the backbone of the hinge residues Glu903 and Leu905. The cyclohexyl group adopts a chair conformation, occupying the center of the ATP binding pocket. Notably, the C-3 phenyl substituent is situated in hydrophobic region II, with the cyano group exposed to the solvent and devoid of obvious interactions with the enzyme.

The X-ray structure (**Figure 17B**) also revealed that the mentioned phenyl ring is positioned near Tyr904 in the GK+2 position. The structure shows a 4 Å distance between the *meta*-position of the phenyl ring and the hydroxyl group of Tyr904, suggesting a suitable proximity for covalent bond formation. This observation led to the hypothesis that replacing the cyano group with a fluorosulfate (or sulfonyl fluoride) warhead, alongside a conformational flip of the phenyl moiety, could result in the first tyrosine-targeting covalent inhibitor of JAK3. Superimposing the crystal structure of **33** with a docking pose of the envisioned covalent inhibitor with the warhead in *meta*-position, modeled to covalently fit into the same crystal structure (**Figure 17C**) indicated that the proposed flip of the phenyl ring indeed leads to a favorable alignment of the fluorosulfate group toward the tyrosine residue without disturbing the inhibitor's overall orientation in the binding site. Based on this model, a small SAR series of related compounds was designed (**Figure 17A**). Fluorosulfates were preferred due to their improved stability and likely higher selectivity, stemming from their lower reactivity, but sulfonyl fluoride analogs were also included as well as compounds with the warhead in the *ortho*-position, featuring a distinct orientation toward the target nucleophile. Another series included inhibitors with the warhead in *meta*-position bearing an additional small *ortho*-substituent as well as a benzylic analog. These subtly different molecules were designed to achieve the optimal pre-orientation of the warhead, given that tyrosine is relatively inflexible, and docking indicated that twisting the phenyl ring out of plane may be advantageous.

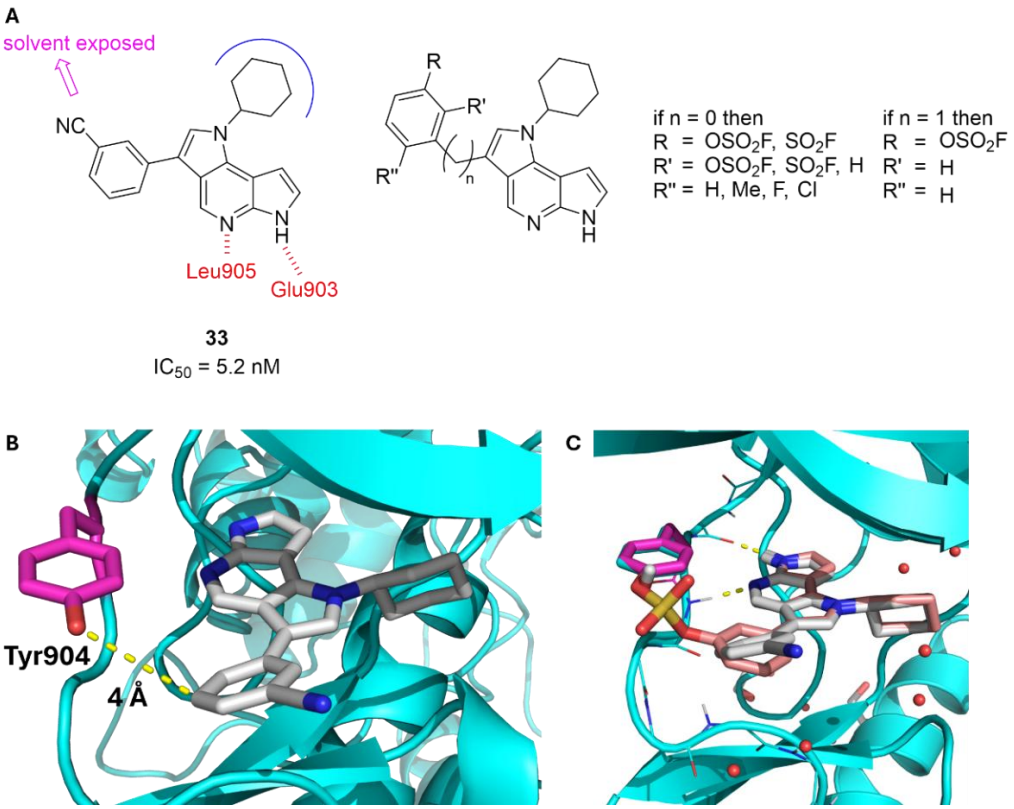

Figure 17: A Noncovalent JAK3 inhibitor **33** and its interactions with the ATP binding pocket of JAK3 from the dissertation of ELLEN PFAFFENROT[108] as well as a small SAR series of covalent compounds derived from **33**. **B** X-ray crystal structure of compound **33** bound to JAK3, highlighting the 4 Å distance between the *meta*-position of the phenyl ring and Tyr904. **C** X-ray structure of **33** (grey) and overlay of covalent docking of **34** (salmon) with a fluorosulfate replacing the nitrile. The fluorosulfate group is directed toward Tyr904 (magenta). This graphic was adapted from a paper[109] published during the course of this PhD.

The synthesis of the first three molecules (**34**, **35**, **36**) in this series, depicted in **Figure 18**, was carried out by ALEXANDER RASCH during his Master's thesis. From there, the envisioned SAR series was expanded in this project.

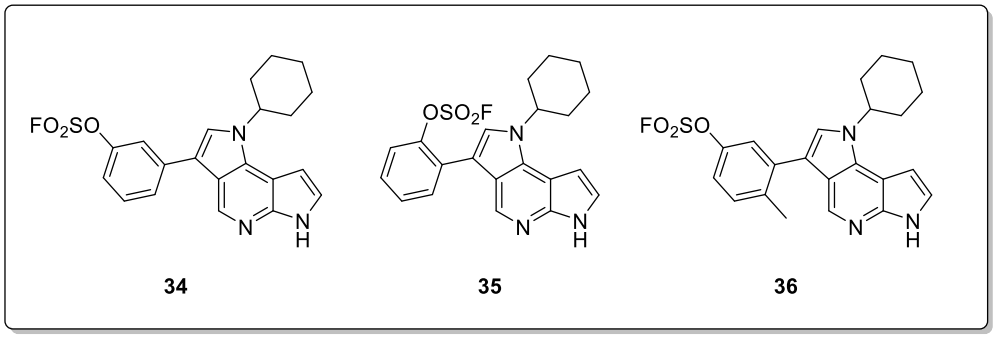

Figure 18: Initial JAK3-targeted compounds synthesized by ALEXANDER RASCH in his Master's thesis.[110]

3.1.2. Synthesis of Tricyclic Structures – Direct Aryl Ring Attachment for Subsequent Fluorosulfate Installation

The synthesis of the core structure **41** (**Scheme 1**) of the JAK3 inhibitors was based on research previously carried out in our group.[107] Starting from 4-chloro-7-azaindole (**37**), protection of the indole-N with a triisopropylsilyl (TIPS) group lead to compound **38**. This protection group is necessary for the next step, i.e. a metalation–bromination sequence. In azaindoles, the 2-position is typically the most reactive site in this type of reaction, but steric hindrance from the TIPS group effectively shields it. Bromination was achieved by lithiation with *sec*-BuLi, followed by quenching with CBr_4 as the electrophilic bromine source. The chlorine in 4-position has a weak directing effect for a directed *ortho* metalation (DOM), therefore directing it to the 5-position leading to intermediate **39**. The TIPS protection group was then removed with potassium fluoride (**40**) and a tosyl protection group was installed instead, yielding core structure **41**. The reason for the implementation of this new protection group is the next step in which the cyclohexylamine side chain was installed by S_NAr reaction. This nucleophilic substitution requires very high temperatures which the TIPS protection group cannot outlast. The bottom half of **Scheme 1** is in accordance with the thesis of ELLEN PFAFFENROT.[108] After the S_NAr reaction leading to compound **42**, the introduced bromide was reacted in a SUZUKI coupling with 2-ethoxyvinylboronic acid pinacol ester yielding enol ether intermediate **43**. The ethoxyvinyl side chain of **43** then underwent an acid-mediated intramolecular cyclization which led to tricyclic structure **44**. This was subsequently selectively brominated in the C-3 position via electrophilic bromination with NBS leading to key building block **45**.

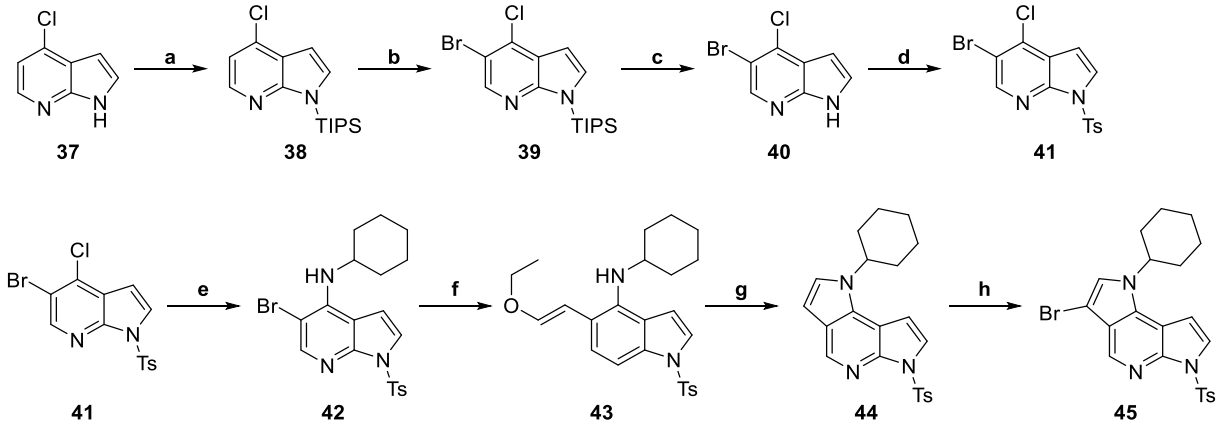

Scheme 1: (a) NaH, TIPSCl, THF, 0 °C to 50 °C, 17 h, 95 %; (b) *sec*-BuLi, CBr_4, THF, -78 °C, 2.5 h, 90 %; (c) KF, MeOH, rt, 1 h, 97 %; (d) NaH, TsCl, THF, 0 °C to rt, 3 h, 96 %; (e) cyclohexylamine, 145 °C, 6 h, 75 %; (f) 2-ethoxyvinylboronic acid pinacol ester, $Pd(PPh_3)_4$, K_3PO_4, MeCN/H_2O (3:2, V/V), 100 °C, 4.5 h; (g) AcOH, 100 °C, 2 h, 89 % (over two steps); (h) NBS, DCM, -16 °C, 20 min, 87 %.

The boronic esters for the following SUZUKI couplings to introduce the front-pocket residues were not commercially available and had to be synthesized first in a similar procedure as described in the Master's thesis of ALEXANDER RASCH[110] (**Scheme 2**). To this end, the respective phenols **46**, **47** and **52** were protected as methoxymethyl (MOM) ethers. The corresponding bromides **48**, **49** and **53** were then converted into the boronic acid pinacol esters **50**, **51** and **54** via a lithiation–borylation sequence employing isopropylpinacolylborate as the electrophile.

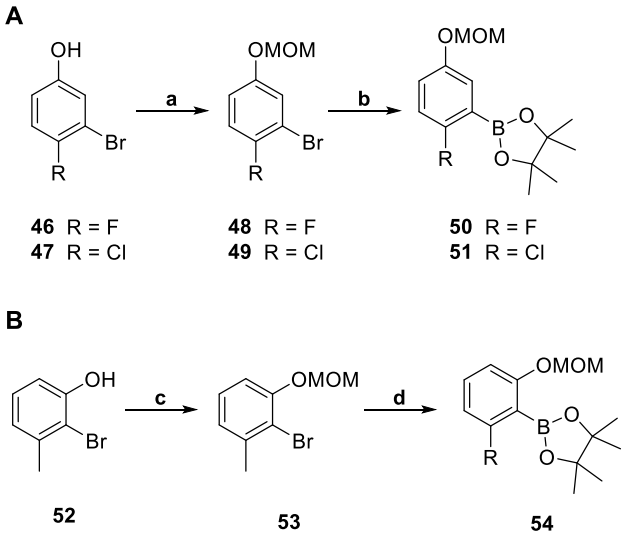

Scheme 2: A Synthesis of 1,2,4-subsituted (protected) phenols: (a) DIPEA, MOMBr, DCM, 0 °C to rt, 1 h, 87 – 93 %; (b) *n*BuLi, isopropylpinacolylborate, THF, -78 °C, 1.5 h, 42 – 73 %. **B** Synthesis of 1,2,3-subsituted (protected) phenols: (c) NaH, MOMBr, DMF, 0 °C to rt, 18 h, 64 %; (d) *n*BuLi, isopropylpinacolylborate, THF, -78 °C, 2 h, 80 %.

With these intermediates in hand, a SUZUKI coupling between brominated building block **45** and the boronic esters could now be carried out yielding **55**, **56** and **57** (**Scheme 3**). In the next step, these were deprotected. First, the tosyl group was removed under basic conditions and immediately after, the MOM group was deprotected under acidic conditions leading to phenols **58**, **59** and **60**. Finally, the fluorosulfate warhead was installed using 4-(acetylamino)phenyl]imidodisulfuryl difluoride (AISF, **64**) which led to the final fluorosulfate-containing molecules **61**, **62** and **63**. AISF (**64**) is a solid, bench-stable alternative to sulfuryl fluoride gas for the introduction of SO_2F groups onto hydroxyl groups or aliphatic amines. It reacts with hydroxyl substrates (which upon base (B)-mediated deprotonation form the phenolate) through nucleophilic attack at sulfur, cleaving the S–N bond and releasing (4-acetamidophenyl)sulfamoyl fluoride (**65**) as the byproduct. This method is significantly easier and less hazardous than the traditional route employing sulfuryl fluoride. AISF (**64**) is commercially available but can also easily be prepared in one step from acetanilide.[111]

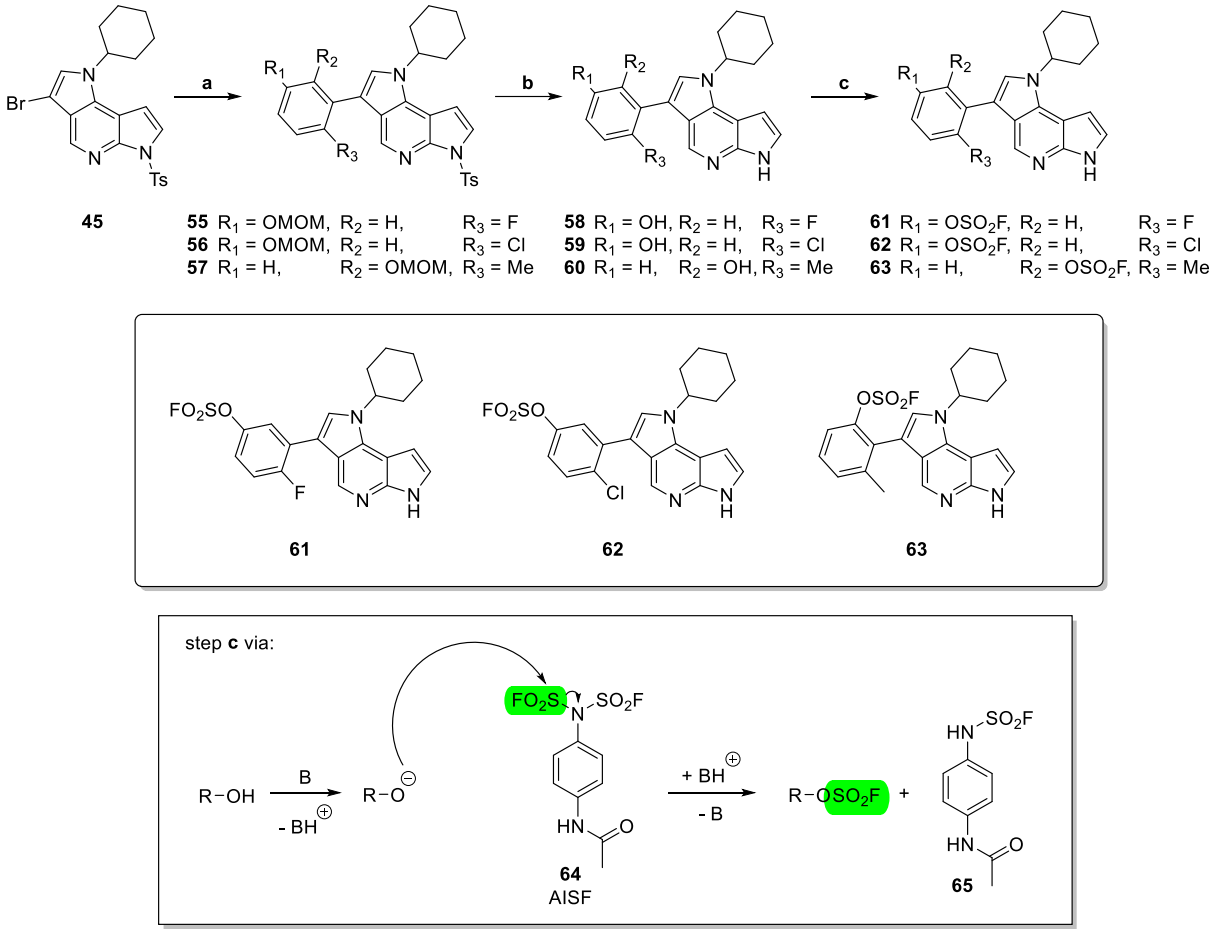

Scheme 3: (a) XPhos Pd G4, K_3PO_4, dioxane/H_2O (4:1, V/V), 70 – 90 °C, 3 h – 3 d, 41 – 82 %; (b) KOH, MeOH, 60 °C, 3 h, then HCl, rt, 2 h; crude products used in the next step: (c) AISF (**64**), DBU, THF, rt, 1.5 – 3 h, 25 – 74 %. The lower box depicts the mechanism through which the fluorosulfate group is generated from a hydroxyl group using AISF (**64**). B = base.

3.1.3. Synthesis of Tricyclic Structures – Direct Attachment of Sulfonyl Fluoride-Bearing Aryl Rings

Sulfonyl fluorides cannot be as easily attached in a late stage as fluorosulfates, therefore these molecules required a slightly different synthetic approach. The sulfonyl fluoride precursors were synthesized according to procedures from the WILLIS group.[112] This worked especially well for the *meta*-substituted aryl sulfonyl fluoride for which the conditions were taken over almost entirely from the literature (**Scheme 4**). Briefly, 3-bromobenzenesulfonyl chloride (**66**) was converted to the corresponding sulfonyl fluoride **67** using potassium bifluoride. The reaction yielded a highly pure product, eliminating the need for chromatographic purification. In the next step, the bromide was converted to the boronic acid pinacol ester **68** via a MIYAURA borylation with bis(pinacolato)diboron. Finally, the free boronic acid **69** was synthesized in an oxidative cleavage of the pinacol group by $NaIO_4$.[113]

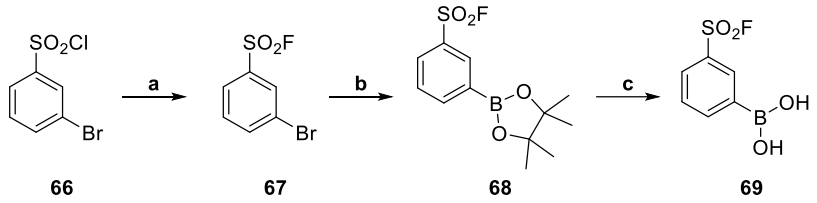

Scheme 4: (a) KHF_2, MeCN/H_2O (2:1, V/V), rt, 24 h, quant.; (b) B_2pin_2, KOAc, Pd(dppf)Cl_2, dioxane, 80 °C, 16 h, 79 %; (c) NH_4OAc, $NaIO_4$, acetone/H_2O (1:1, V/V), rt, 30 h, 75 %.

The synthesis of the *ortho*-sulfonyl fluoride analog of this compound required some more optimization. The direct *ortho*-lithiation–borylation of benzenesulfonyl fluoride (**70**, **Scheme 5A**) using LDA and triisopropyl borate, as described by LOU *et al.*[112] did not yield the desired boronic acid **71**. Instead, a similar tactic to that shown for the *meta*-analog was adopted (**Scheme 5B**). Conversion of 2-bromobenzenesulfonyl chloride (**72**) to the corresponding sulfonyl fluoride **73** worked as previously described. The following MIYAURA borylation, however, did not lead to the desired product **74**, presumably due to steric hindrances. An approach described by TALKO *et al.*[114] and subsequently adaptation of their methodology finally led to the desired product. In their paper, they describe a similar procedure as LOU *et al.*[112] but instead of acid-mediated cleavage of the isopropyl borate and isolation of the boronic acid, they use neopentyl glycol to generate boronic acid ester **75** (**Scheme 5C**). This method was then applied using pinacol instead to yield boronic acid pinacol ester **74** (**Scheme 5D**).

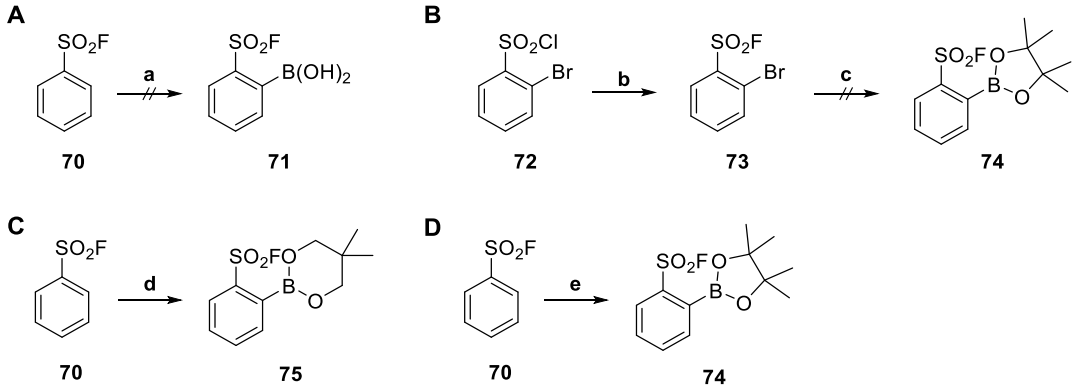

Scheme 5: A Direct *ortho*-lithiation of benzenesulfonyl fluoride as described by LOU *et al.*:[112] (a) 1. LDA, B(O^{i}Pr)$_3$, THF, -78 °C, 1 h, then 2. aq. HCl (10 %), rt. **B** Synthesis analogous to *meta*-substitution: (b) KHF_2, MeCN/H_2O (2:1, V/V), rt, 24 h, 97 %; (c) B_2pin_2, KOAc, Pd(dppf)Cl_2, dioxane, 80 °C. **C** Direct *ortho*-lithiation for test reaction leading to boronic acid ester **75**:[114] (d) 1. LDA, B(O^{i}Pr)$_3$, THF, -78 °C, 2 h, then 2. neopentyl glycol, toluene, rt, 20 h, 19 %. **D** Direct *ortho*-lithiation leading to pinacol ester **74** using similar conditions as in **C**: (e) 1. LDA, B(O^{i}Pr)$_3$, THF, -78 °C, 2 h; then 2. pinacol, toluene, rt, 22 h, 39 %.

The two aryl sulfonyl fluorides **69** and **74** were then to be attached to the hinge binding scaffold in a SUZUKI coupling reaction. Before this, however, a new protection group needed to be installed on the scaffold. While sulfonyl fluorides are much more stable than their chloride

counterparts, they will hydrolyze to the corresponding sulfonic acid/ester under basic aqueous/methanolic conditions employed for tosyl cleavage. The tosyl group of **45** was therefore removed in methanolic potassium hydroxide to yield the free azaindole **76** (**Scheme 6**). This compound was then protected again with a *tert*-butoxycarbonyl (Boc) protection group (**77**) which can later be deprotected under acidic conditions which sulfonyl fluorides are stable toward. Tricyclic structure **77** was therefore reacted with the respective aryl sulfonyl fluoride boronic esters **69** and **74** in a SUZUKI coupling yielding **78** (*meta*-substitution) and **79** (*ortho*-substitution). While **78** can be synthesized using fairly standard conditions, LOU *et al.*[112] found that the *ortho*-substitution, here found in **79**, requires the use of potassium fluoride as the base and a higher catalyst loading which was also successfully employed here. Acidic deprotection with HCl in dioxane then led to the expected final compounds **80** and **81**.

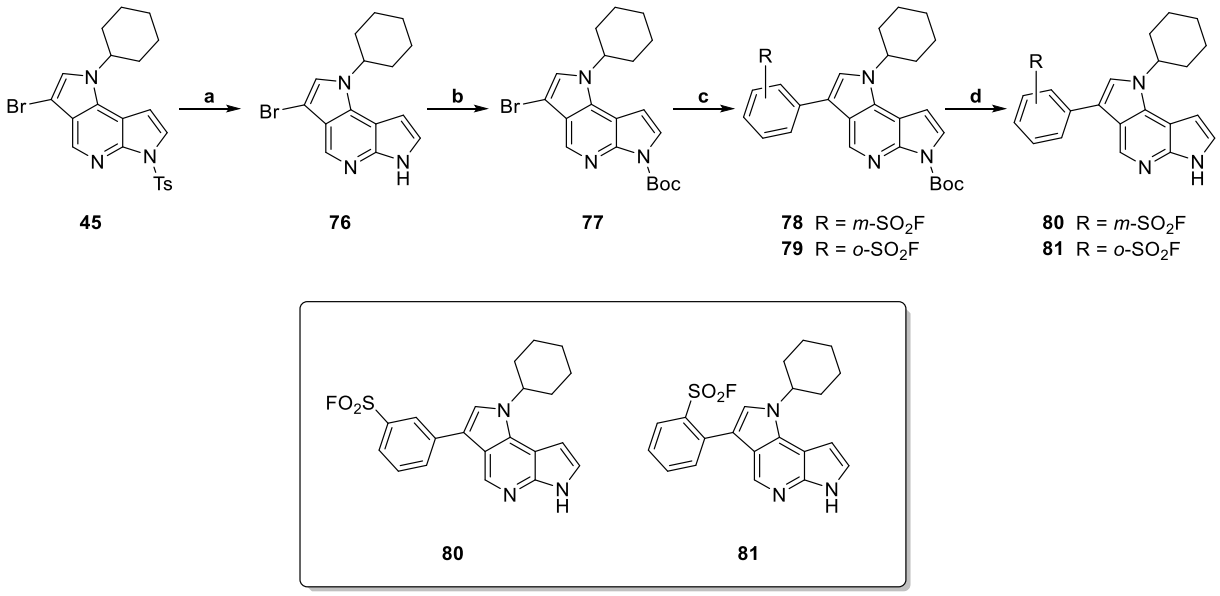

Scheme 6: (a) KOH, MeOH, reflux, 3 h, 62 %; (b) Boc_2O, DMAP, TEA, DCM, rt, 2 h, 83 %; (c) for R_1 = *m*-SO_2F (**78**): **69**, K_3PO_4, $Pd(OAc)_2$, XPhos, dioxane/H_2O (2:1, V/V), 40 °C, 4 h, 54 %; for R_1 = *o*-SO_2F (**79**): **74**, KF, $Pd(OAc)_2$, XPhos, THF, 40 °C then rt, 20 h, 32 %; (d) HCl in dioxane (4 M), rt, 18 – 20 h, 32 – 95 %.

3.1.4. Synthesis of Tricyclic Structures – Introduction of the Methylene-Bridged Aryl Ring

The final molecule synthesized in the initial JAK3 inhibitor series features a methylene bridge to link the aryl fluorosulfate warhead. The general procedure was again adapted from ELLEN PFAFFENROT'S dissertation.[108] The secondary amine in azaindole building block **42** (see **Scheme 10**) was to be substituted with cinnamic acid derived allylic S_N2 electrophiles, which would allow for building up the tricycle in an intramolecular HECK reaction. Prior to this, the corresponding S_N2 coupling partner had to be synthesized (**Scheme 7**). To this end, the carboxylic acid function of *meta*-hydroxy cinnamic acid (**82**) was transformed into an ethyl ester

(**83**) in a FISCHER esterification. Subsequently, the hydroxy group was protected as a MOM ether (**84**). The ester was then reduced to the corresponding alcohol **85** in a protocol according to WANG *et al.*[115] that uses lithium aluminum hydride and benzyl chloride to generate aluminum hydride *in situ*. This method was explicitly optimized for α,β-unsaturated carboxylic esters and ensures the full reduction of the ester to the alcohol while retaining the double bond in the molecule. In the final step, the obtained allylic alcohol was converted into the corresponding bromide through an APPEL reaction with PPh_3 and NBS to yield the intermediate **86**.

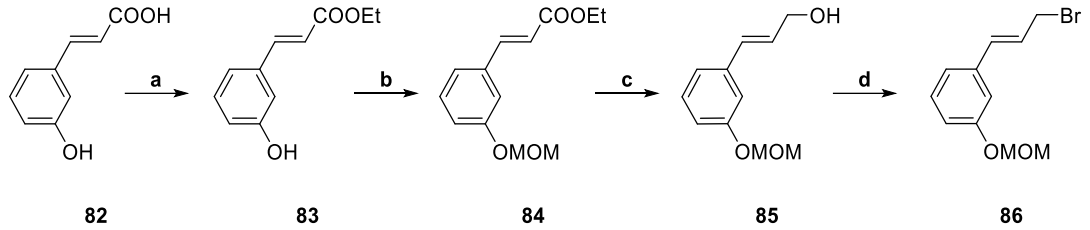

Scheme 7: (a) EtOH, H_2SO_4, reflux, 3.5 h, 94 %; (b) MOMBr, DIPEA, THF, 60 °C, 2 h, quant.; (c) $LiAlH_4$, BnCl, THF, -78 °C to -30 °C, 4 h, 66 %; (d) PPh_3, NBS, DCM, 0 °C, 1.5 h, 37 %.

A similar approach was chosen for the *ortho*-substituted analog (**Scheme 8**). Initially, the synthetic route proceeded in a manner comparable to the previous example. The carboxylic acid of *o*-coumaric acid (**87**) was protected through a FISCHER esterification leading to ethyl ester **88**, after which the phenol was protected as a MOM ether (**89**). The reduction as described before yielded α,β-unsaturated alcohol **90**. The following APPEL reaction to gain bromide **91**, however, proved to be difficult. Using the same method as for *meta*-analog **86** did not yield the desired product, even after several attempts and different workup techniques (e.g. precipitation of triphenylphosphine oxide with zinc chloride and subsequent evaporation of the solvent).[116]

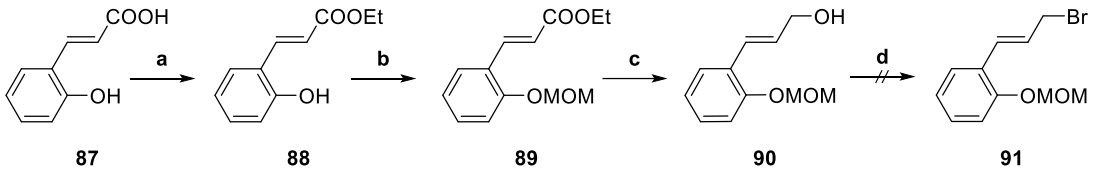

Scheme 8: (a) EtOH, H_2SO_4, reflux, 4 h, 96 %; (b) MOMBr, DIPEA, THF, 55 °C, 16 h, 92 %; (c) $LiAlH_4$, BnCl, THF, -78 °C to -30 °C, 6.5 h, 63 %; (d) PPh_3, NBS, DCM, 0 °C, 2 h.

An alternative strategy was therefore pursued to install the leaving group of the molecule (**Scheme 9**). Switching from *N*-bromosuccinimide to carbon tetrabromide did not yield any product. A procedure by XU *et al.*,[117] leading to the corresponding cinnamyl chloride **92** using NCS as the halogenating agent, did also not produce the desired product. Since not only halides can serve as leaving groups, the alcohol was then subjected to conversion into other

leaving groups. Nevertheless, neither the attempt to synthesize a mesylate[118] (**93**) nor two different protocols for tosylates[119,120] (**94**), using either sodium hydride or triethylamine as the base, led to the desired products. Finally, acylating the hydroxyl group utilizing acetic anhydride according to a procedure of KRÄTZSCHMAR *et al.*[121] yielded cinnamic acetate **95** which was then used in the next step.

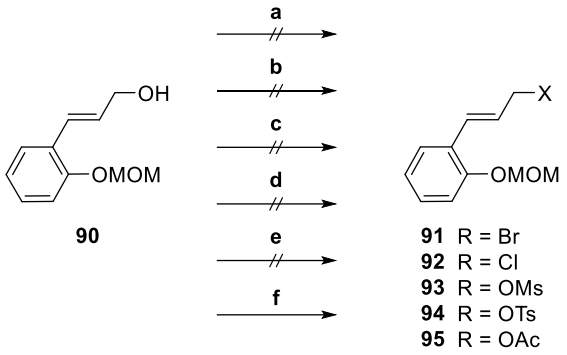

Scheme 9: Different attempts to install the leaving group (LG) needed for the following nucleophilic substitution. LG = Br (**91**): (a) PPh_3, CBr_4, DCM, 0 °C, 2.5 h; LG = Cl (**92**): (b) PPh_3, NCS, DCM, 0 °C, 3 h; LG = OMs (**93**): (c) TEA, MsCl, DCM, 0 °C, 3 h; LG = OTs (**94**): (d) NaH, TsCl, Et_2O, 0 °C to rt, 18 h; (e) TEA, TsCl, DCM, rt, 30 min; LG = OAc (**95**): (f) DMAP, Ac_2O, Et_2O, rt, 1 h, 80 %.

The cinnamyl precursors were finally to be coupled to hinge binding motif **42**. The synthesis of intermediate **96** (**Scheme 10A**) was based on the idea of performing an allylic amination via allyl acetates as described by ADAK *et al*.[122] This reaction uses tetrabutylammonium bromide (TBAB)-stabilized palladium nanoparticles to catalyze the reaction under basic conditions. While the authors show these conditions work for a range of amines and allyl acetates, product formation or even any significant conversion could not be observed here even after two days and continuous addition of reagents. The nucleophilic substitution between amine **42** and allyl bromide **86**, as previously described for similar compounds by ELLEN PFAFFENROT,[108] on the other hand, worked out as expected yielding **97** (**Scheme 10B**). This reaction was then followed by an intramolecular HECK reaction which should yield the exocyclic double bond. This was converted *in situ* to the endocyclic (and thus aromatic) double bond, as found in intermediate **98**, via the use of silica gel, which acts as a weak acid catalyst. Finally, both the tosyl and MOM protection groups were removed as described previously, leading to intermediate **99**, to which the fluorosulfate warhead was attached via AISF (**64**) to give final compound **100**.

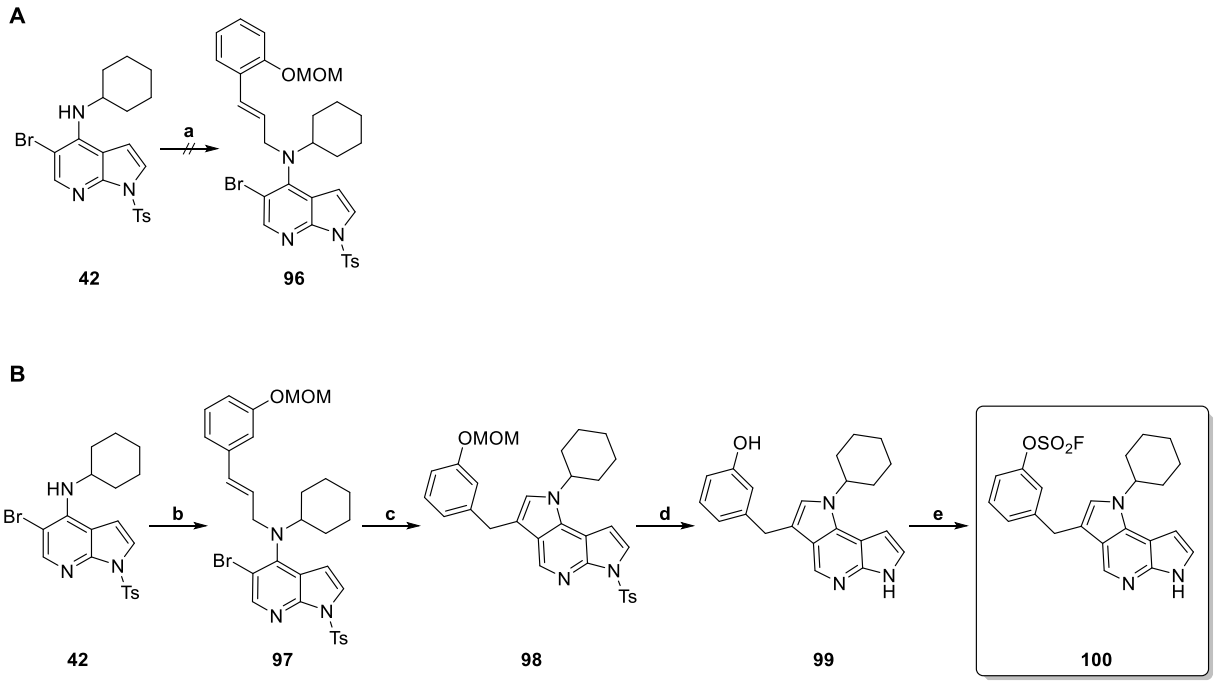

Scheme 10: A Failed synthesis of *ortho*-analog **96**: (a) **95**, $PdCl_2$, TBAB, K_2CO_3, toluene, 85 °C. **B** Synthesis of *meta*-analog **100**: (b) **86**, NaH, DMF, 0 °C, 20 h, 71 %; (c) 1. $Pd(PPh_3)_4$, Cs_2CO_3, DMF, 80 °C, 3 h; then 2. silica, EtOAc, 40 °C, 2.5 h, 12 %; (d) 1. KOH, MeOH, 65 °C, 2.5 h; then 2. conc. HCl, rt, 2 h; (e) AISF (**64**), DBU, THF, rt, 2 h, 33 % (over two steps).

3.1.5. Synthesis of Tricyclic Structures – Installation of SuTEx Warheads

Beyond SuFEx chemistry, there are very little other options to covalently target tyrosines.[22,26] In 2020, the group of HSU introduced sulfur–triazole exchange (SuTEx) chemistry[53] as a novel approach. According to their chemoproteomic studies,[50,52,53] SuTEx preferentially targets tyrosine over lysine. The mechanism behind this is, however, not elucidated and this functional group has barely been used in TCIs so far. The triazole group is, nevertheless, an interesting leaving group (LG), as it possesses the possibility to tune the LG properties, which is naturally impossible for fluoride. This chemistry was therefore to be incorporated so that a direct comparison could be made with the JAK3 inhibitors bearing sulfonyl fluorides and fluorosulfates.

Based on protocols from the HSU group,[50] bromophenylsulfonyl triazole **101** was synthesized starting from sulfonyl chloride **66** similarly to the strategy shown for sulfonyl fluorides in **Scheme 4** (**Scheme 11A**). The subsequent borylation proved to be a challenge, however. Neither did the attempts to obtain boronic acid **102** via bromide–lithium exchange and following borylation using *n*BuLi and $B(OiPr)_3$ lead to product formation, nor did a MIYAURA borylation utilizing B_2pin_2 yield the corresponding boronic acid pinacol ester **103**. A switch in polarities was therefore pursued where hinge binding motif **45** was borylated instead (**Scheme 11B**). Again, this strategy did not prove to be fruitful. The MIYAURA borylation did lead to the formation

of pinacol ester **104**, but dehalogenation of **45** also occurred in a significant amount and this side product could not be separated from the desired compound. Attempts to perform a halogen–lithium exchange and subsequent borylation with isopropylpinacolylborate showed significant formation of several side products and this approach was thus also discarded.

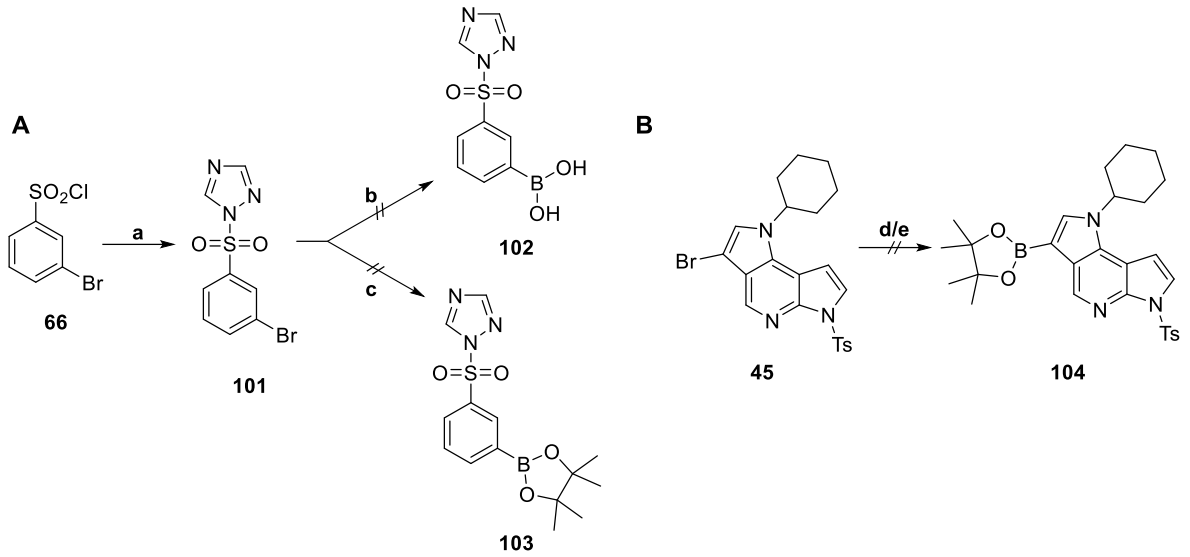

Scheme 11: A Attempt to generate a borylated aryl sulfonyl triazole: (a) 1*H*-1,2,4-triazole, TEA, rt, 3.5 h, 78 %; (b) *n*BuLi, $B(O^iPr)_3$, -78 °C to rt, 17 h; (c) B_2pin_2, KOAc, $Pd(dppf)Cl_2$, dioxane, 80 °C, 16 h. **B** Attempt for borylation of intermediate **45**: (d) B_2pin_2, KOAc, $Pd(dppf)Cl_2$, dioxane, 80 °C, 17 h; or (e) *n*BuLi, isopropylpinacolylborate, THF, -78 °C, 2 h.

3.1.6. Rigidization Approach and Synthesis of Tetracyclic Structure

Instead of further pursuing the SuTEx approach, the focus was shifted back to the more ”classic” fluorosulfate warheads. In the covalent modeling (see **Figure 17**), the warhead orients itself toward Tyr904, but since rotation around the bond connecting the warhead-bearing phenyl group to the hinge binding core is completely free and the crystal structure of the noncovalent design template **33** shows the orientation of the cyano group toward the solvent, it is also possible that the warhead may orient itself in this direction. A rigidization approach was therefore pursued to prevent this from happening.

In 2018, ELSAYED *et al.*[123] published a strategy to synthesize a tetracyclic benzo[*c*]pyrrolo[2,3-*h*][1,6]naphthyridin-5-one (BPN) series as JAK inhibitors that was used here to design a tetracyclic inhibitor with the warhead fixed toward the hinge region. To this end, 4-iodo-7-azaindole (**105**) was protected as the 2-(trimethylsilyl)ethoxymethyl (SEM) ether **106** (**Scheme 12A**) to attain the first required building block. Next, the commercially available 2-bromo-5-hydroxybenzoic acid (**107**) was converted into a carboxylic acid chloride through thionyl chloride and subsequently cyclohexylamine was added to yield amide **108** (**Scheme 12B**). The hydroxyl group was then protected with a MOM group (**109**) as described in previous

chapters. The SEM-protected 4-iodo-7-azaindole (**106**) and building block **109** were then subjected to a palladium-catalyzed CATELLANI-type reaction (the mechanism is described below, see **Scheme 13**) to yield key intermediate **110**. After sequential deprotection of both the SEM and MOM group (**111**), first under acidic conditions using TFA, followed by a basic treatment with DIPEA, the fluorosulfate was attached to the phenol hydroxyl group using AISF (**64**) leading to the final inhibitor **112**.

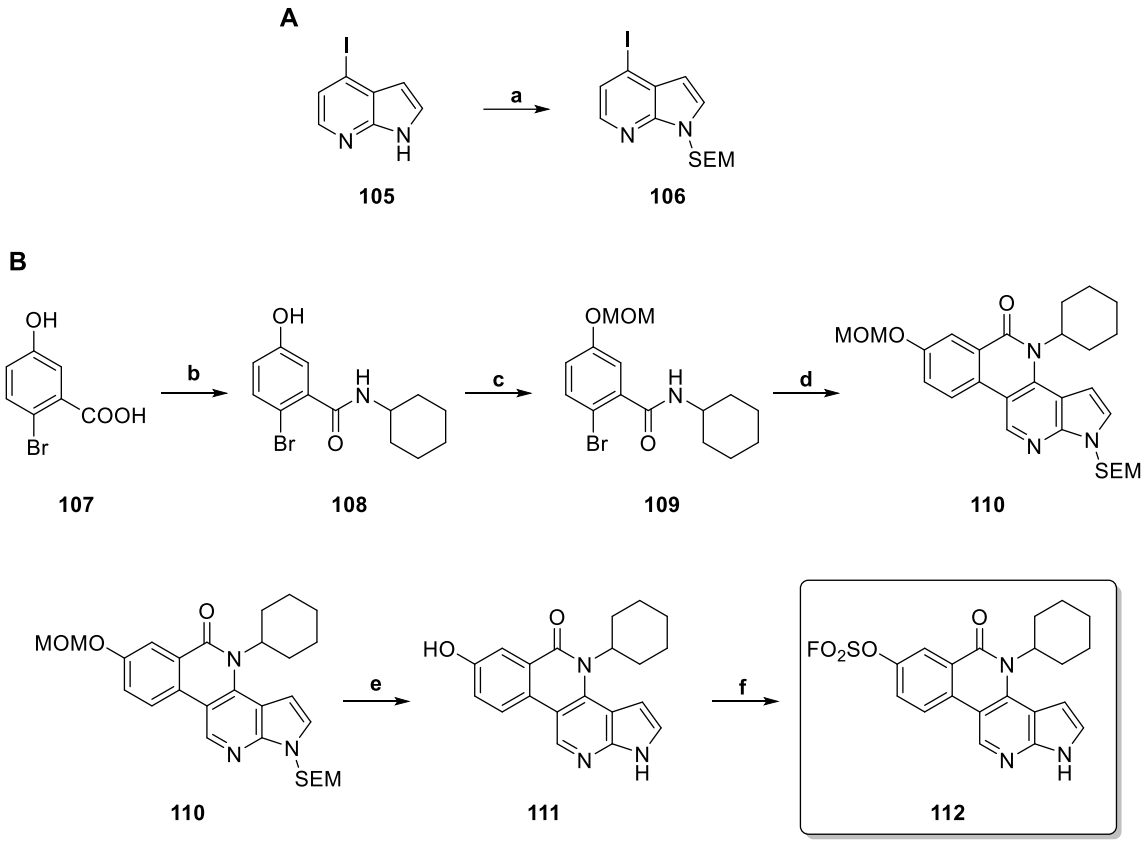

Scheme 12: A Synthesis of azaindole building block **106**: (a) NaH, SEMCl, DMF, 0 °C, 2 h, 81 %. **B** Synthesis of final tetracycle **112**: (b) 1. $SOCl_2$, DMF, reflux, 6 h; then 2. cyclohexylamine, DCM, TEA, rt, 16 h, 89 %; (c) MOMBr, DIPEA, DCM, rt, 2.5 h, 57 %; (d) **106**, norbornene, Cs_2CO_3, $Pd(TFA)_2$, TFP, toluene, 95 °C, 23 h, 26 %; (e) 1. TFA, DCM, rt, 2 h; then 2. DIPEA, MeOH, rt, 21 h, 52 %; (f) AISF (**64**), DBU, THF, rt, 3 h, 80 %.

The mechanism of the CATELLANI-type reaction as described by ELSAYED *et al.*[123] (**Scheme 13**) begins with the oxidative addition of Pd^0 into the C–I bond of azaindole **106**. Following this, the palladium(II) species **113** undergoes a carbopalladation with norbornene (**114**). In the resulting norbornylpalladium intermediate **115** β-hydride elimination is forbidden at both of its β-positions. In the next step, **115** participates in an electrophilic palladacycle formation through C–H activation leading to tricyclic structure **116**. The iodide is cleaved off in this step and the liberated hydroiodic acid scavenged by the added base (B). Subsequently, the palladacycle undergoes another oxidative addition with the aryl bromide of precursor **109**, forming a Pd^{IV} species, which immediately reacts in a reductive elimination to establish the first C–C bond of

the product in intermediate **117**. Norbornene (**114**) is now removed through β-carbon elimination and the resulting palladium(II) species **118** undergoes the final intramolecular BUCHWALD-type amidation to afford the desired tetracyclic intermediate **110**.

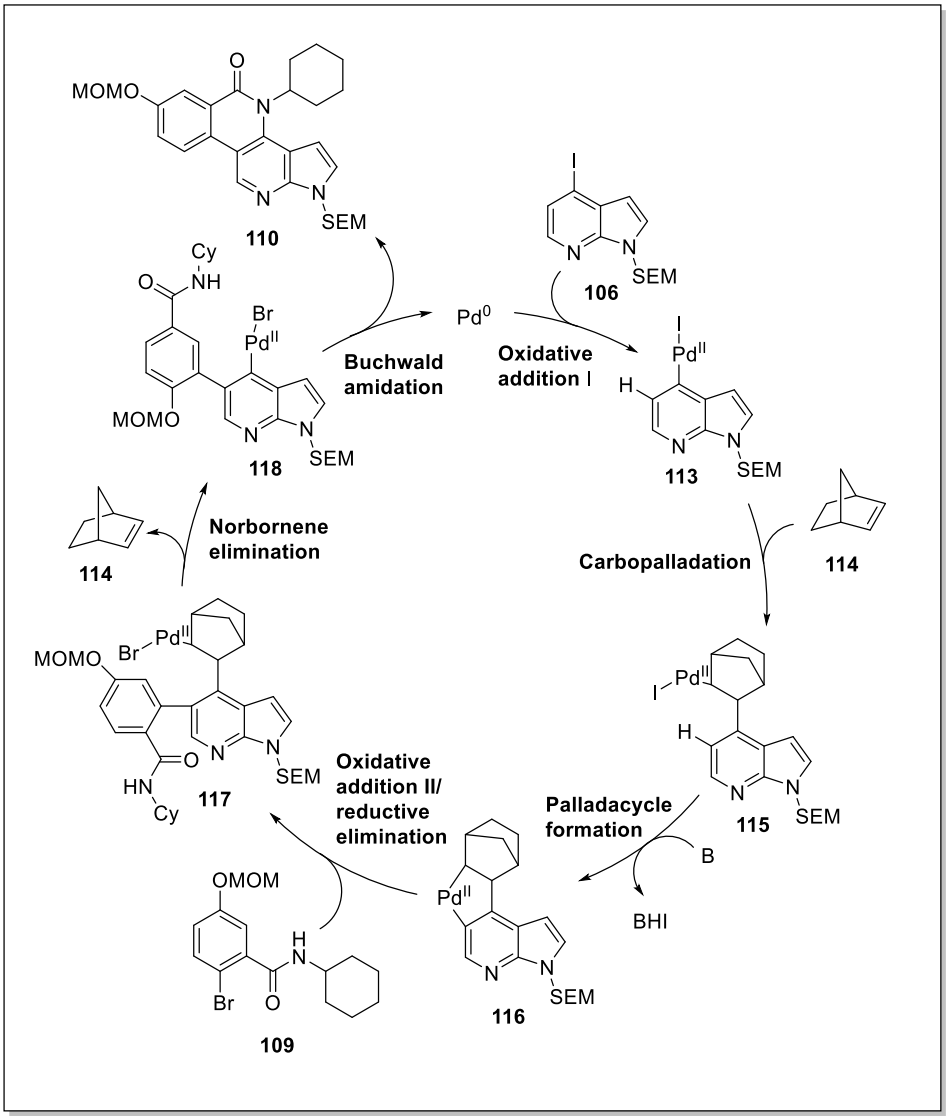

Scheme 13: CATELLANI-type reaction for the synthesis of key intermediate **110** according to ELSAYED *et al.*[123] B = base.

3.2. Synthesis of MK2-Targeted Inhibitors

3.2.1. Structure-Based Design Strategy for Allosteric MK2 Inhibitors

The second target of this project was the kinase MK2. In 2019, BARKER and BEAUMONT deposited a crystal structure (PDB: 6T8X), which became publicly available in 2021, reporting an allosteric MK2 inhibitor, although no associated publication was released. This inhibitor bears close structural resemblance to MK2 inhibitors previously disclosed by Merck in 2011. HUANG *et al.*[124] had identified a furan-2-carboxamide scaffold as a promising starting point for

MK2 inhibition through high-throughput screening. NMR and enzymatic analyses indicated that the binding mode was non-ATP-competitive; however, no crystal structure for this allosteric interaction was available at the time. Through a hit-to-lead optimization campaign, they developed compound **119** (**Figure 19A**), which showed substantial potency under high ATP conditions (IC_{50} = 110 nM at 100 µM ATP).

The crystal structure reported by BARKER and BEAUMONT was highly relevant to this project, as it revealed not just one, but multiple tyrosine residues in close proximity to the binding site of the inhibitor. This inhibitor shared a high degree of similarity with the Merck compound, differing only in the substitution of a chloro with a bromo atom. Upon examining the binding mode of compound **119**, four tyrosine residues located near the inhibitor were identified: Tyr225, Tyr228, Tyr260, and Tyr264. Among these, Tyr228 and Tyr260 interact with the amide carbonyl and the piperazine nitrogen, respectively. Tyr225 and Tyr264, however, are positioned adjacent to one of the two phenyl rings of the inhibitor.

Based on this observation, it was hypothesized that Tyr225 and Tyr264 could serve as chemically accessible targets for covalent inhibitor development. To investigate this, four putative covalent MK2 inhibitors were designed, each featuring a fluorosulfate warhead at either of the unsubstituted positions of the 1,4-disubstituted phenyl rings in the original scaffold. Noncovalent docking studies were performed to assess their spatial orientation relative to the tyrosines. Two candidates, compounds **120** and **121** (**Figure 19B**), exhibited a sulfur-to-hydroxyl distance of 4 Å or less between the fluorosulfate and the tyrosine residues. As illustrated in **Figure 19C**, placing the fluorosulfate warhead in the *ortho*-position relative to the halogen shows Tyr225 in close proximity with the electrophile. Conversely, **Figure 19D** depicts that positioning the warhead in *ortho* to the piperazine group places Tyr264 near the fluorosulfate moiety. Both configurations were subsequently evaluated experimentally in order to test the hypothesis.

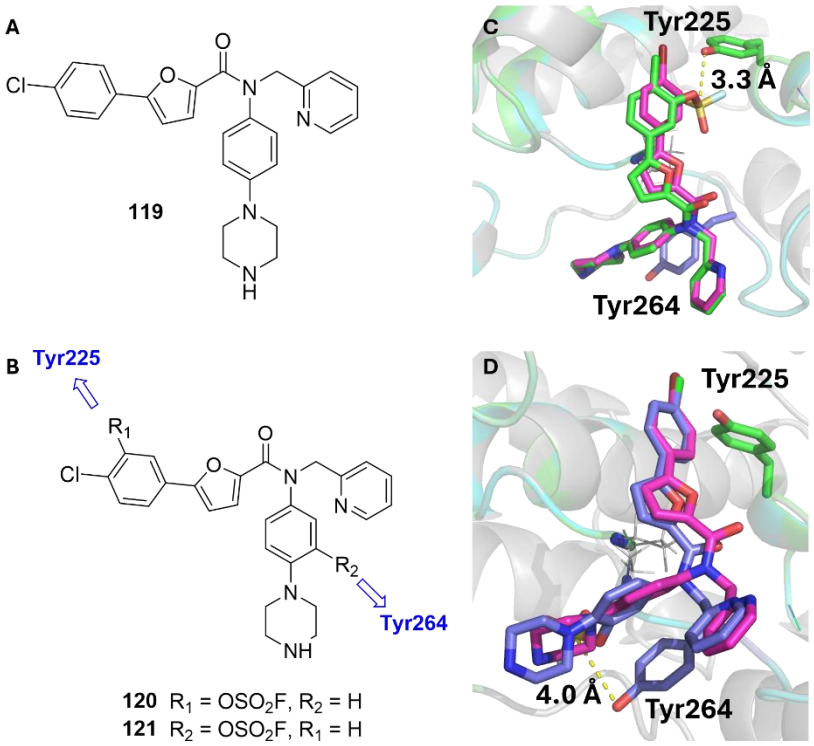

Figure 19: Allosteric inhibitor of MK2 by HUANG *et al.*[124] **B** Design strategy for proposed covalent allosteric inhibitors, indicating the tyrosine residues to be targeted by the respective warheads. **C** Superimposition of 6T8X (magenta) and the docking pose of **120** (green), illustrating a distance of 3.3 Å between the warhead and Tyr225 (green). **D** Superimposition of 6T8X (magenta) and the docking pose of **121** (blue), indicating a 4.0 Å distance between the warhead and Tyr264 (blue). This graphic was reproduced from a paper[109] published during the course of this PhD.

3.2.2. Synthesis of an Allosteric Inhibitor Targeting Tyr225 Through a Fluorosulfate

The proposed covalent inhibitors were synthesized using the strategy outlined by HUANG *et al.*[124] As the targeting of the two distinct tyrosine positions in MK2 was intended, a linear synthesis approach was deemed the only feasible option for each of the desired molecules. For the fluorosulfate-bearing compound targeting Tyr225 (**120**) the synthetic pathway (**Scheme 14**) began with the FISCHER esterification of 5-bromofuran-2-carboxylic acid (**122**) to simplify purification in subsequent steps. The resulting ethyl 5-bromofuran-2-carboxylate (**123**) was then coupled with the commercially available (4-chloro-3-methoxyphenyl)boronic acid in a SUZUKI coupling leading to biaryl compound **124**. Since the next steps required multiple orthogonal protection groups, the methoxy group on the phenol was initially removed with boron tribromide to yield compound **125**. A benzyl group was then introduced at the liberated phenol via benzyl bromide, resulting in benzyl ether **126**. Following the saponification of the ethyl ester using aqueous/methanolic lithium hydroxide, carboxylic acid **127** underwent an amide coupling with 1-Boc-4-(4'-aminophenyl)piperazine, utilizing HATU as the coupling reagent. Amide **128** subsequently underwent a base-promoted nucleophilic substitution

reaction with 2-(bromomethyl)pyridine, and the O-benzyl group was removed via hydrogenation over Pd/C, producing intermediate **129**. Importantly, the palladium-catalyzed debenzylation did not impact the previously incorporated benzylic pyridine group. Furthermore, it is imperative that the protecting groups on the phenol and the aliphatic amine are orthogonal. While aromatic amines do not react with AISF (**64**) to form sulfamoyl fluorides (*vide supra*, the pyrrole nitrogen of azaindoles did not need protecting groups in such reactions), aliphatic amines will indeed do so because of their higher nucleophilicity. Keeping the piperazine nitrogen protected with a suitable protection group that can be cleaved in the presence of the warhead is therefore essential to ensure clean conversion of the reaction from compound **129** to fluorosulfate **130**. In the final step, the Boc group on the piperazine was removed using TFA to yield final compound **120**.

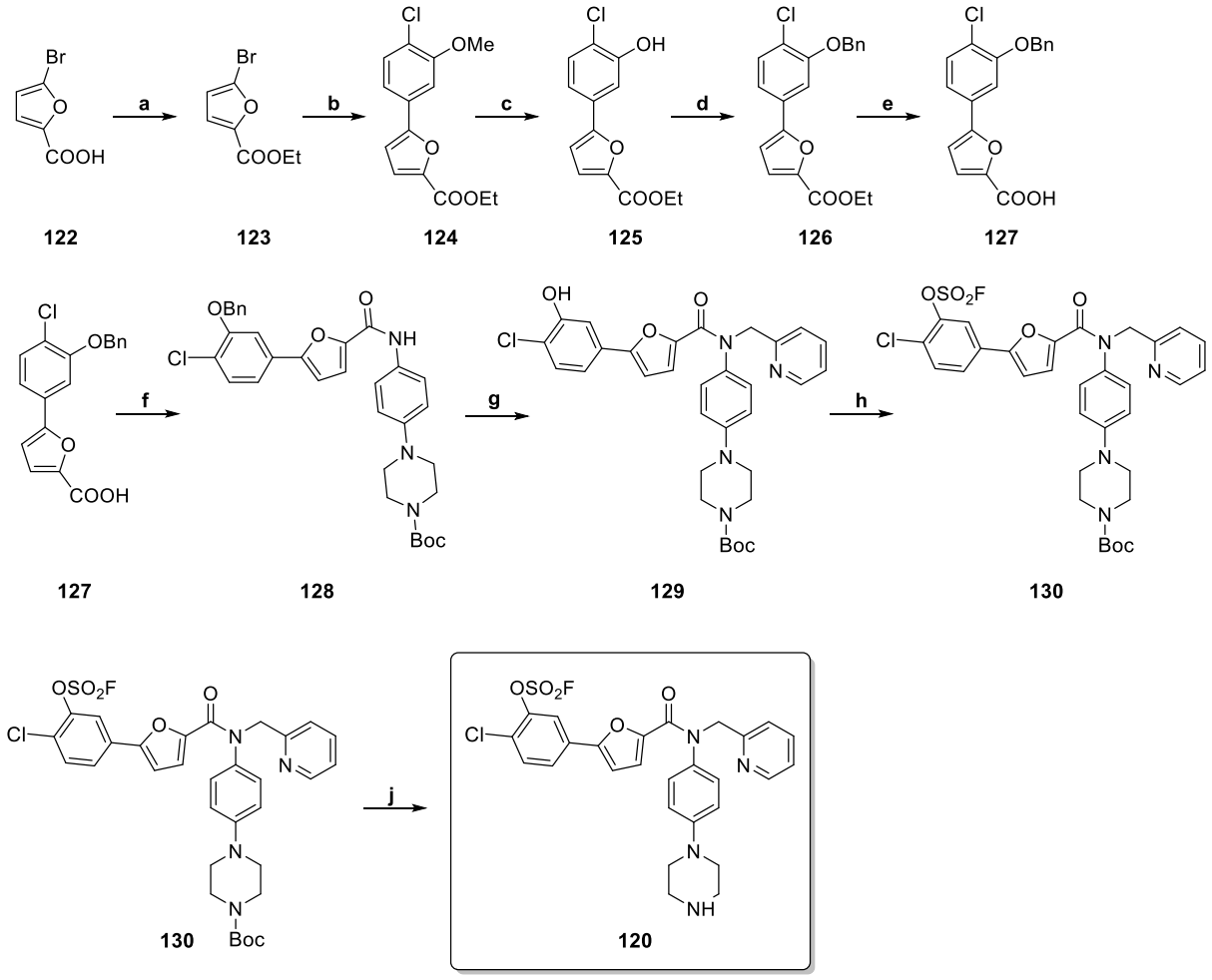

Scheme 14: (a) H_2SO_4, EtOH, reflux, 20 h, 94 %; (b) (4-chloro-3-methoxyphenyl)boronic acid, K_2CO_3, $Pd(PPh_3)_4$, dioxane/H_2O (1:1, V/V), 80 °C, 20 h, 39 %; (c) BBr_3, DCM, rt, 5 h, 85 %; (d) BnBr, K_2CO_3, DMF, rt, 3 h, 91 %; (e) LiOH, THF/H_2O (1:1, V/V), rt, 5 h, 95 %; (f) 1-Boc-4-(4′-aminophenyl)piperazine, HATU, DIPEA, DMF, rt, 3 h, quant.; (g) 1. 2-(bromomethyl)pyridine HBr, NaH, DMF, rt, 2 h; then 2. Pd/C, H_2 (1 atm), MeOH, rt, 2.5 h, 87 % over two steps; (h) AISF (**64**), DBU, THF, rt, 1.5 h, 75 %; (j) TFA, DCM, rt, 1.5 h, 76 %.

3.2.3. Synthesis of an Allosteric Inhibitor Targeting Tyr225 Through a Sulfonyl Fluoride

In analogy to the fluorosulfates, the synthesis of corresponding sulfonyl fluorides was also pursued. The first strategy was to follow a similar route as used for the fluorosulfate analog. To this end, 5-bromofuran-2-carboxylic acid (**122**) was subjected to an amide coupling with 1-Boc-4-(4′-aminophenyl)piperazine to yield compound **131** (**Scheme 15A**) using HATU as the coupling reagent. This was followed by a nucleophilic substitution with 2-(bromomethyl)pyridine to obtain intermediate **132** which would then be ready to use in a SUZUKI coupling. For the boronic acid, a similar strategy as detailed in chapter 3.1.3 was chosen. Starting from 5-bromo-2-chlorobenzenesulfonyl fluoride (**133**) the sulfonyl chloride was converted to sulfonyl fluoride **134** (**Scheme 15B**) with potassium bifluoride. The subsequent MIYAURA borylation with B_2pin_2 did yield boronic acid pinacol ester **135**, but the product could not be isolated in a clean fashion and the interfering side products could not be identified. SUZUKI test reactions between bromide **132** and impure boronic ester **135** did not yield any positive results.

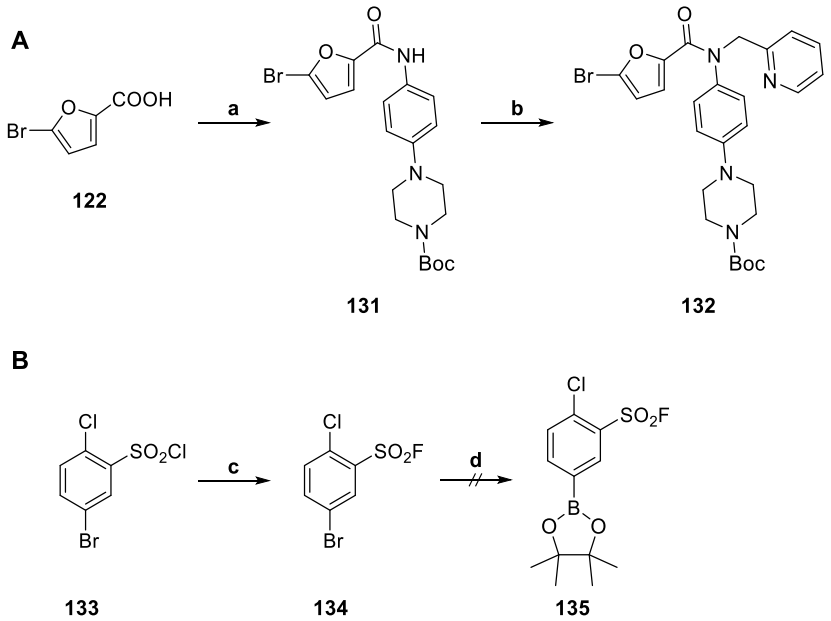

Scheme 15: A Synthesis of bromo furane intermediate **132**: (a) 1-Boc-4-(4′-aminophenyl)piperazine, HATU, DIPEA, DMF, rt, 1.5 h, 96 %; (b) 2-(bromomethyl)pyridine HBr, NaH, DMF, rt, 20 h, 84 %. **B** Attempted synthesis of boronic acid pinacol ester **135**: (c) KHF_2, $MeCN/H_2O$ (2:1, V/V), rt, 20 h, 95 %; (d) B_2pin_2, KOAc, $Pd(dppf)Cl_2$, dioxane, 80 °C.

A different approach was therefore pursued, and borylation of the furan was undertaken instead (**Scheme 16A**). First, the carboxylic acid of 5-bromofuran-2-carboxylic acid (**122**) was protected as *tert*-butyl ester **136**. This specific ester was chosen since the ester would have to be cleaved under acidic conditions later, as the warhead would be hydrolyzed under

saponification conditions. Unfortunately, both approaches, one as described by MORI *et al.*[125] using isopropylmagnesium chloride, dimethylaminoethyl ether and trimethyl borate as well as a more classical protocol utilizing halide–lithium exchange with *n*BuLi and trimethyl borate to borylate the furane ring for obtaining boronic acid **137** did not yield the desired product. To circumvent the borylation step, it was decided to use the commercially available boronic acid **138**, hoping that the ethyl ester of this molecule could be cleaved later under non-basic conditions (**Scheme 16B**). The SUZUKI coupling between **138** and bromide **134** led to the desired biaryl **137**. Regrettably, it was not possible to obtain the free carboxylic acid **140**. While the sulfonyl fluoride group was stable under acidic conditions at 120 °C, the carboxylic ester did not react at all, and the reaction did not show any conversion. At this point, the decision was made to discontinue further pursuit of this approach but potentially return to this particular problem in case the biological testing would show promising results in the targeting of Tyr225 via the fluorosulfate.

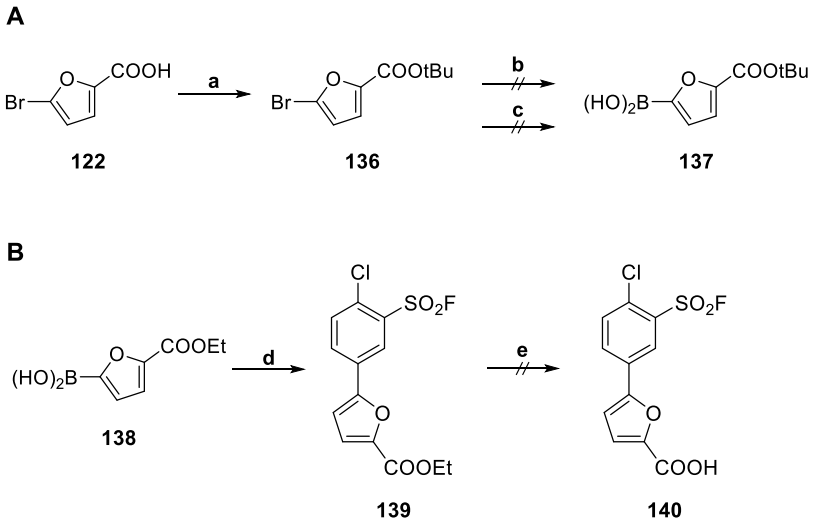

Scheme 16: A Efforts toward the synthesis of furanyl boronic acid **137**: (a) Boc_2O, DMAP, *t*BuOH, 40 °C, 5 h, 84 %; (b) 2-(dimethylamino)ethyl ether, ^{i}PrMgCl, $B(OMe)_3$, THF, 0 °C, 2 h; (c) *n*BuLi, $B(OMe)_3$, THF, -78 °C to 0 °C, 2 h. **B** Attempted synthesis of intermediate **140**: (d) **134**, K_2CO_3, $Pd(PPh_3)_4$, dioxane, reflux, 20 h, 43 %; (e) H_2SO_4, $MeOH/H_2O$ (1:7, V/V), 120 °C, 22 h.

3.2.4. Synthesis of an Allosteric Inhibitor Targeting Tyr264 Through a Fluorosulfate

To target the second suitable tyrosine residue in the allosteric pocket (Tyr264), the warhead had to be linked to the amide-bound phenyl piperazine. Consequently, the synthesis route (**Scheme 17**) was initiated by protecting the hydroxyl group of 2-fluoro-5-nitrophenol (**141**) with a benzyl group. Product **142** underwent a basic S_NAr reaction with 1-Boc-piperazine to afford intermediate **143**. This was followed by a BÉCHAMP reduction utilizing iron powder to produce aniline **144** (leaving the benzyl protection group untouched), which was then coupled with 5-

(4-chlorophenyl)furan-2-carboxylic acid (**162**) using HATU to yield amide **145**. The subsequent steps mirrored those in chapter 3.2.2: following the attachment of the methylene-linked pyridine (yielding **146**), the benzyl protecting group was removed via catalytic hydrogenation over Pd/C. The warhead was then introduced via AISF (**64**) to generate fluorosulfate **147**, and a final TFA-mediated acidic deprotection of the Boc group furnished the target compound **121**.

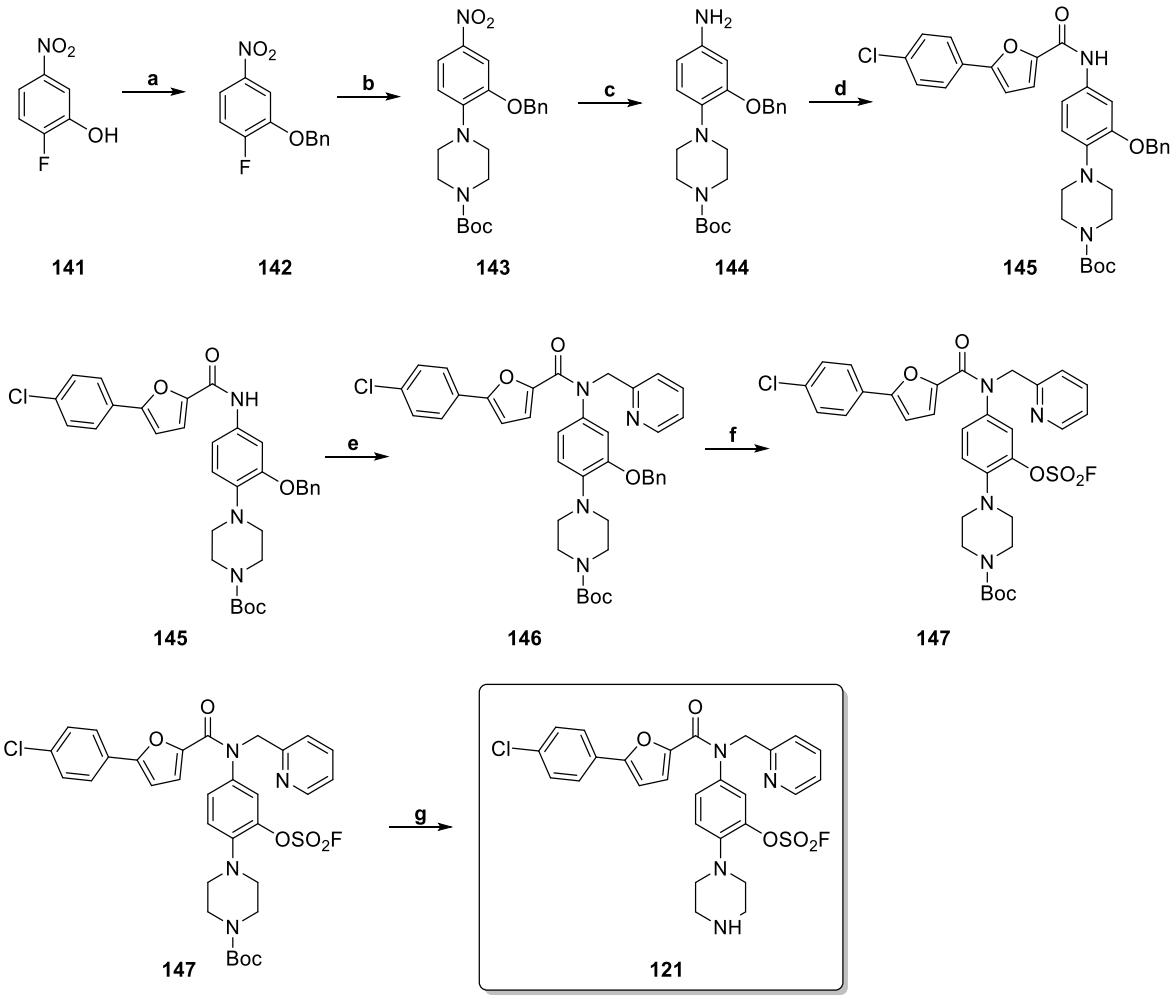

Scheme 17: (a) BnBr, K_2CO_3, DMF, rt, 1 h, 92 %; (b) 1-Boc-piperazine, DIPEA, DMF, 80 °C, 17 h, 89 %; (c) Fe, NH_4Cl, EtOH/H_2O (4:1, V/V), 40 °C, 20 h, 69 %; (d) 5-(4-chlorophenyl)furan-2-carboxylic acid (**162**), HATU, DIPEA, DMF, rt, 18 h, 84 %; (e) 2-(bromomethyl)pyridine HBr, NaH, DMF, rt, 40 h, 57 %; (f) 1. Pd/C, H_2 (1 atm), MeOH, rt, 2.5 h; then 2. AISF (**64**), DBU, THF, rt, 5 h, 60 % over two steps; (g) TFA, DCM, rt, 1 h, 47 %.

3.2.5. Synthesis of an Allosteric Inhibitor Targeting Tyr264 Through a Sulfonyl Fluoride

The synthesis of the sulfonyl fluoride analog to target Tyr264 fortunately turned out to be easier than for the SF analog targeting Tyr225. This is mostly due to the fact that 2-fluoro-5-nitrobenzenesulfonyl chloride (**148**) is commercially available which makes it possible to introduce the warhead early on. Importantly, all following steps were carried out under conditions that the warhead is stable toward. Taken together, this rendered it possible to pursue

a synthetic route similar to the corresponding fluorosulfate as described in the previous chapter (see **Scheme 18**). Briefly, sulfonyl chloride **148** was converted into sulfonyl fluoride **149** as previously described. 1-Boc-piperazine was attached in an S_NAr reaction (leading to **150**) at 80 °C, which was tolerated by the sulfonyl fluoride warhead. The nitro group was then reduced via palladium-catalyzed hydrogenation to form aniline **151**. As in the previous synthesis, coupling with 5-(4-chlorophenyl)furan-2-carboxylic acid (**162**) using HATU produced amide **152**. This was followed by attachment of the benzylic pyridine and TFA-mediated Boc deprotection, through which target compound **153** was obtained.

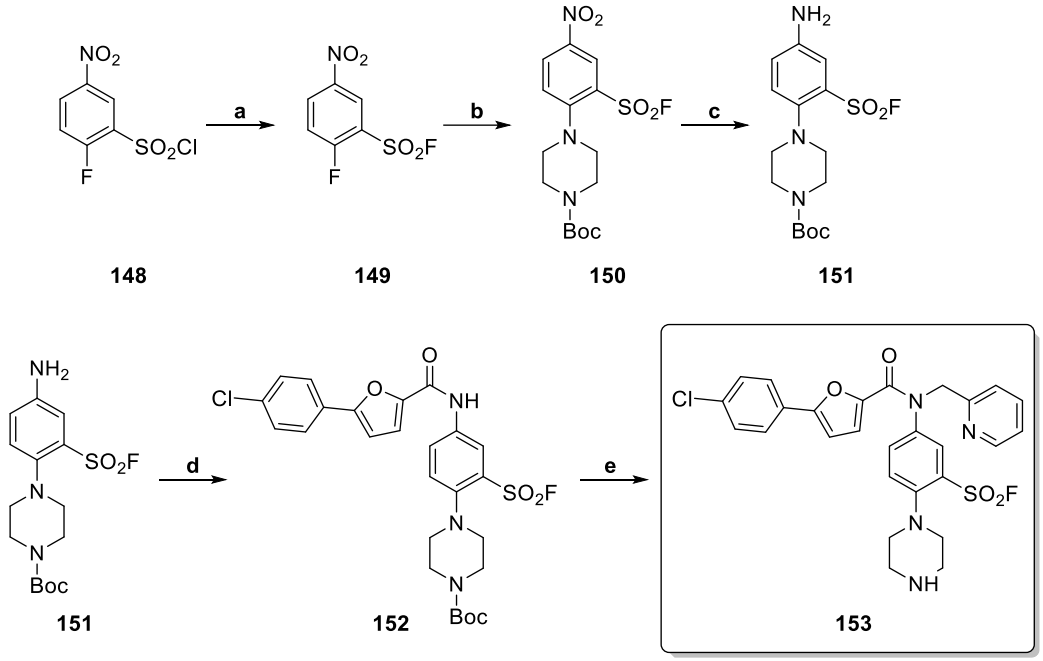

Scheme 18: (a) KHF_2, MeCN/H_2O (2:1, V/V), rt. 18 h, quant.; (b) 1-Boc-piperazine, DIPEA, DMF, 80 °C, 3 h, 54 %; (c) Pd/C, H_2 (1 atm), MeOH, rt, 1 h, quant.; (d) 5-(4-chlorophenyl)furan-2-carboxylic acid (**162**), HATU, DIPEA, DMF, 80 °C, 17 h, 37 %; (e) 1. 2-(bromomethyl)pyridine HBr, NaH, DMF, rt, 20 h; then 2. TFA, DCM, rt, 2 h, 42 % over two steps.

Alongside this synthetic route, another option to incorporate sulfonyl fluorides was explored. In the last 10 years, several similar protocols[126–128] have emerged that introduce SFs in a cross-coupling reaction from halides. Since these tactics were considered of value for later project stages, one such method was investigated in the context of the SF-bearing compound targeting Tyr264 (**Scheme 19**). To this end, the commercially available 2-bromo-1-fluoro-4-nitrobenzene (**154**) was used, the bromide being the handle to introduce the sulfonyl fluoride later in the synthesis. The synthesis route up to that point is very similar to the two approaches discussed before: the Boc-protected piperazine ring was introduced via a nucleophilic substitution, leading to nitro intermediate **155**. Through the BÉCHAMP reduction, amine **156** was obtained, followed by the HATU-mediated amide coupling with 5-(4-chlorophenyl)furan-2-carboxylic acid (**162**), generating amide **157**. After attaching the methylene-linked pyridine (to

yield **158**), the molecule was then at a point where the bromide should be converted into a sulfonyl fluoride. To this end, a protocol by DAVIES *et al.*[127] was followed, who found that $PdCl_2(AmPhos)_2$ was the best catalyst/ligand combination to generate a sulfinate (**160**) using 1,4-diazabicyclo[2.2.2]octane bis(sulfur dioxide) adduct (DABSO) as the sulfur dioxide surrogate while minimizing dehalogenation of the starting material. The catalytic cycle starts with Pd(0) undergoing oxidative addition to the aryl bromide, followed by insertion of sulfur dioxide from DABSO into the Pd–aryl bond to form a Pd–sulfinate intermediate. This intermediate then undergoes reductive elimination to release the aryl sulfinate (**160**) and regenerate Pd(0). In the following step, which is carried out in a one pot manner, *N*-fluorobenzenesulfonimide (NFSI) is utilized as the source of the "fluoride cation" (F^+). Unfortunately, when this methodology was applied to bromide **158** in an attempt to generate sulfonyl fluoride **159**, no product formation could be detected. While DAVIES *et al.*[127] showed that their protocol could be deployed to a wide range of substrates, in none of them is the bromide positioned in *ortho*-position to another substituent. It therefore appears plausible that the molecule here is sterically too encumbered to facilitate this reaction. Nevertheless, a similar methodology was revisited later in the project (see chapter 3.3.6.5).

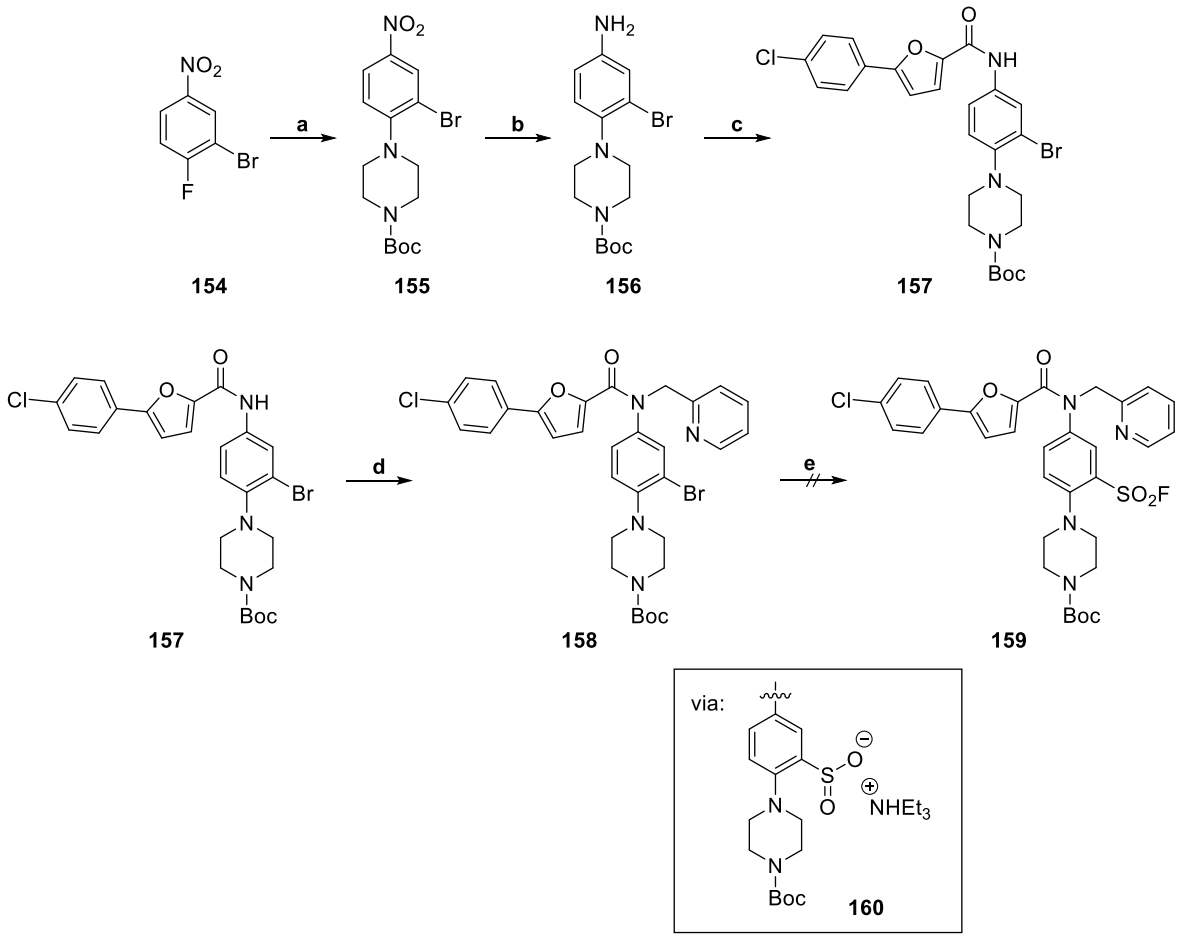

Scheme 19: (a) K_2CO_3, 1-Boc-piperazine, DMF, 60 °C, 18 h, 92 %; (b) Fe, NH_4Cl, EtOH/H_2O (4:1, V/V), 70 °C, 22 h, 56 %; (c) 5-(4-chlorophenyl)furan-2-carboxylic acid (**162**), HATU, DIPEA, DMF, rt, 3.5 h, quant.; (d) 2-

(bromomethyl)pyridine HBr, NaH, DMF, rt, 19 h, 72 %; (e) 1. TEA, DABSO, $PdCl_2(AmPhos)_2$, ^{i}PrOH, 75 °C, 48 h; then 2. NFSI, rt, 24 h.

3.2.6. Synthesis of Noncovalent Analogs

To assess binding and discern the impact of covalent bond formation, the corresponding noncovalent analogs to the covalent probes were to be synthesized as well as the original inhibitor described by HUANG *et al.*[124] To this end, furane ethyl ester **123** was coupled with (4-chlorophenyl)boronic acid in a SUZUKI coupling to obtain biaryl **161** (**Scheme 20**). The ester was cleaved under basic conditions (NaOH in MeOH/H_2O), yielding carboxylic acid **162**, which was subsequently coupled with 1-Boc-4-(4′-aminophenyl)piperazine, generating amide **163**. This was subjected to a nucleophilic substitution with 2-(bromomethyl)pyridine and TFA-mediated deprotection of the Boc group to yield noncovalent inhibitor **119** on which the design idea of the allosteric covalent inhibitors was based.

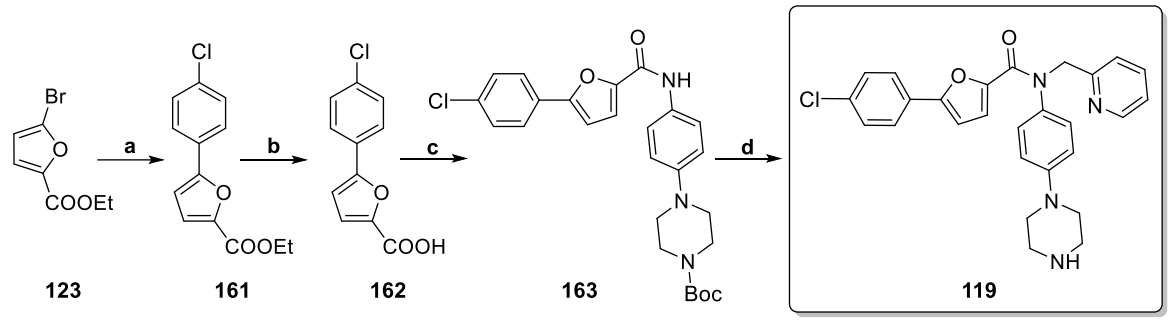

Scheme 20: (a) (4-Chlorophenyl)boronic acid, K_2CO_3, $Pd(PPh_3)_4$, dioxane/H_2O (3:1, V/V), 60 °C, 20 h, 94 %; (b) NaOH, MeOH/H_2O (1:1, V/V), rt, 3 h, 94 %; (c) 1-Boc-4-(4′-aminophenyl)piperazine, HATU, DIPEA, DMF, rt, 18 h, 74 %; (d) 1. 2-(bromomethyl)pyridine HBr, NaH, DMF, rt, 18 h; then 2. TFA, DCM, rt, 2 h, 89 % over two steps.

The synthesis of the hydroxyl-bearing compounds, which were also selected as noncovalent controls without the warhead, was closely related to the synthesis of the covalent compounds. 2-Fluoro-5-nitrophenol (**141**) was protected as a MOM ether (**164, Scheme 21**) instead of the benzyl ether (see **142**, **Scheme 17**) as this could be deprotected simultaneously with the Boc group later on. Intermediate **165** was generated through S_NAr with 1-Boc-piperazine as described before and the nitro group was reduced to amine **166** via hydrogenation over Pd/C as the concomitant work up is simpler than with a BÉCHAMP reduction carried out previously and the molecule does not feature any other functional groups that could be affected by this reaction. The following steps, i.e. the amide coupling leading to **167** and following attachment of the methylene-linked pyridine side chain were carried out as previously described. In the last step, the concurrent deprotection of both the Boc and MOM protecting groups under acidic conditions using TFA furnished noncovalent probe **168**.

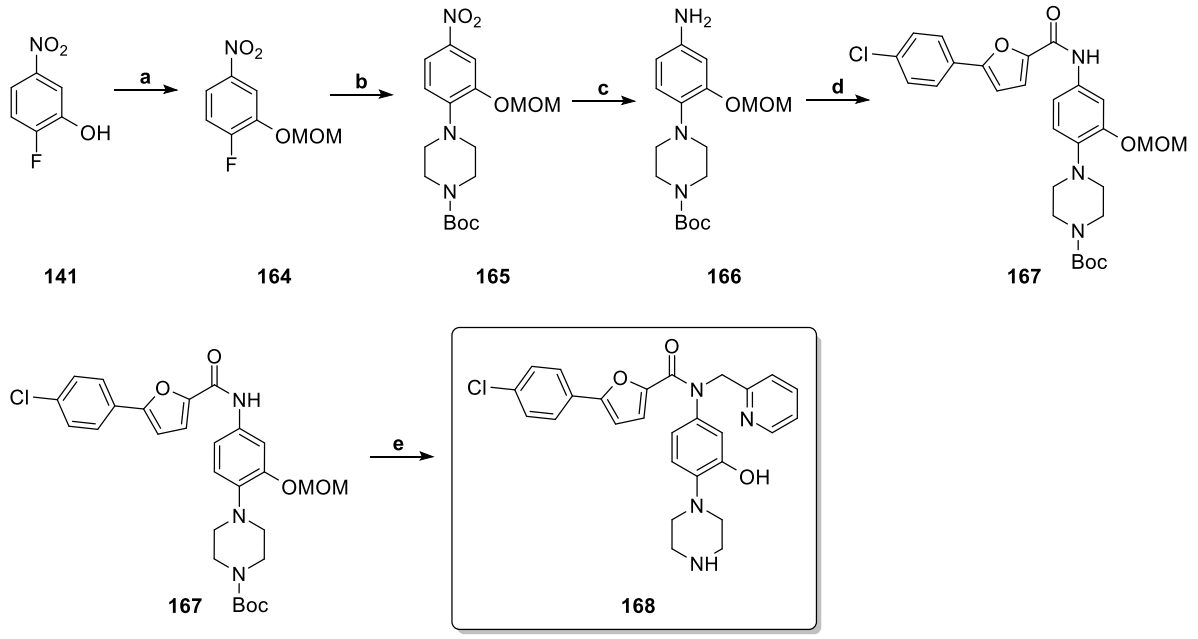

Scheme 21: (a) MOMCl, NaH, THF, 0°C to rt, 2 h, 92 %; (b) 1-Boc-piperazine, DIPEA, MeCN, reflux, 16 h, quant.; (c) Pd/C, H_2 (1 atm), MeOH, rt, 1.5 h 91 %; (d) 5-(4-chlorophenyl)furan-2-carboxylic acid (**162**), HATU, DIPEA, DMF, rt, 3.5 h, 88 %; (e) 1. 2-(Bromomethyl)pyridine HBr, NaH, DMF, rt, 20 h, 57 %; then 2. TFA, DCM, rt, 3 h, 88 % over two steps.

The synthesis of the noncovalent analog to fluorosulfate **121** began with biaryl intermediate **125**, which again was protected as a MOM ether (to yield **169**) in order to facilitate deprotection later on. After saponification of the ester using lithium hydroxide, carboxylic acid **170** was coupled with 1-Boc-4-(4′-aminophenyl)piperazine and amide **171** underwent nucleophilic substitution and deprotection (both steps were carried out as previously described) to obtain noncovalent analog **172**.

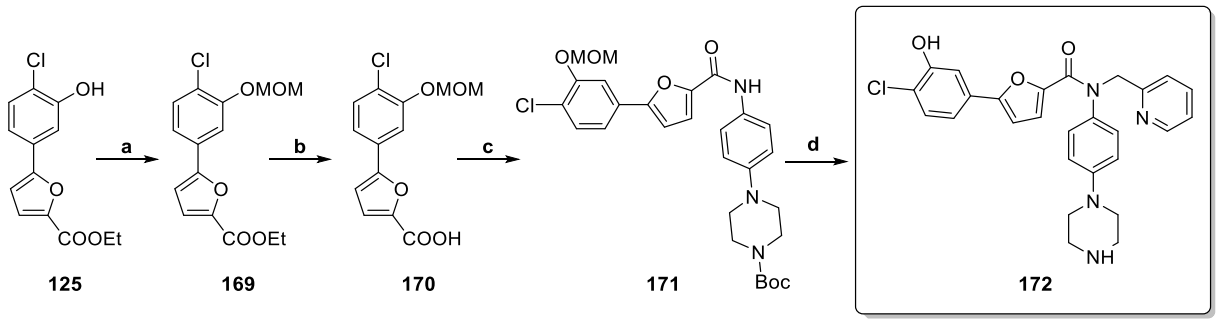

Scheme 22: (a) MOMCl, NaH, THF, 0°C to rt, 3 h, 81 %; (b) LiOH, THF/H_2O (1:1, V/V), rt, 4 h, 75 %; (c) 1-Boc-4-(4′-aminophenyl)piperazine, HATU, DIPEA, DMF, rt, 6.5 h, 98 %; (d) 1. 2-(bromomethyl)pyridine HBr, NaH, DMF, rt, 3 h; then 2. TFA, DCM, rt, 1.5 h, 66 % over two steps.

3.3. Synthesis of a Fragment-Like Covalent Library

3.3.1. Covalent-First Design Strategy

In the second half of this project, a covalent-first strategy was employed to generate a fragment-like library of covalent kinase probes, enabling a similar approach to the one recently published by our and the KNAPP group.[129] These molecules in this work were designed to combine non-cysteine targeting warheads – either sulfonyl fluorides or fluorosulfates – with diverse kinase hinge-binding motifs, connected via a modular linker system. The set of hinge-binding elements included 2-aminopyridine, pyridine, thieno[2,3-*b*]pyridine, indazole, and mostly azaindole cores, offering a range of hydrogen-bonding patterns and geometries. Various linker types were explored to modulate the spatial orientation and reactivity of the aryl sulfonyl fluoride or fluorosulfate electrophile, including direct attachment, oxygen linkers, methylene thioether groups, amides (including both inversions), and aryl-based spacers. The synthetic work detailed in this chapter describes the preparation of this library, which was intended for subsequent profiling across a curated kinase panel using intact protein MS, with the goal of identifying covalent binders that engage residues beyond cysteine. The selection of the kinases, which will be described in more detail in chapter 4.4.1, was based on the targeting of tyrosines but as sulfonyl fluorides and fluorosulfate can also be used for covalently binding to other amino acids, it was expected that residues other than tyrosine would engage as well.

3.3.2. Synthesis of SuFEx Compounds Featuring an Aminopyridine Hinge Binder

The first hinge-binding motif to be investigated was 2-aminopyridine. The aryl fluorosulfate analogs with a direct attachment between hinge binder and warhead-bearing phenyl ring, i.e. **176** (*meta*) and **177** (*para*) could be synthesized in two steps (**Scheme 23**). Phenols **174** and **175** were obtained through a SUZUKI coupling of 4-bromopyridin-2-amine (**173**) and the corresponding (hydroxyphenyl)boronic acids. Subsequently, the fluorosulfate groups were introduced with AISF (**64**) as described previously.

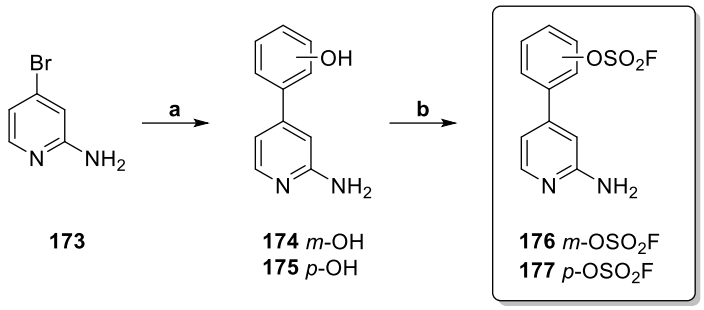

Scheme 23: (a) (3-/4-Hydroxyphenyl)boronic acid, XPhos Pd G4, K_2CO_3, dioxane/H_2O (5:3, V/V), 80 °C, 18 h, 85 – 87 %; (b) AISF (**64**), DBU, THF, rt, 1.5 – 4.5 h, 23 – 61 %.

The respective sulfonyl fluoride congeners **181** and **182**, meanwhile, could be prepared in one step after obtaining the boronic acid (esters). The synthesis of (3-(fluorosulfonyl)phenyl)boronic acid (**69**) was described in chapter 3.1.3. Synthesis for the *para*-analog was carried out in a similar way (**Scheme 24A**). 4-Bromobenzenesulfonyl chloride (**178**) was converted into sulfonyl fluoride **179** by means of potassium bifluoride and a subsequent MIYAURA borylation with B_2pin_2 led to boronic acid pinacol ester **180**. Similarly to the fluorosulfate analogs, the final compounds **181** and **182** were then obtained through a SUZUKI coupling with the brominated hinge binding motif **173** (**Scheme 24B**).

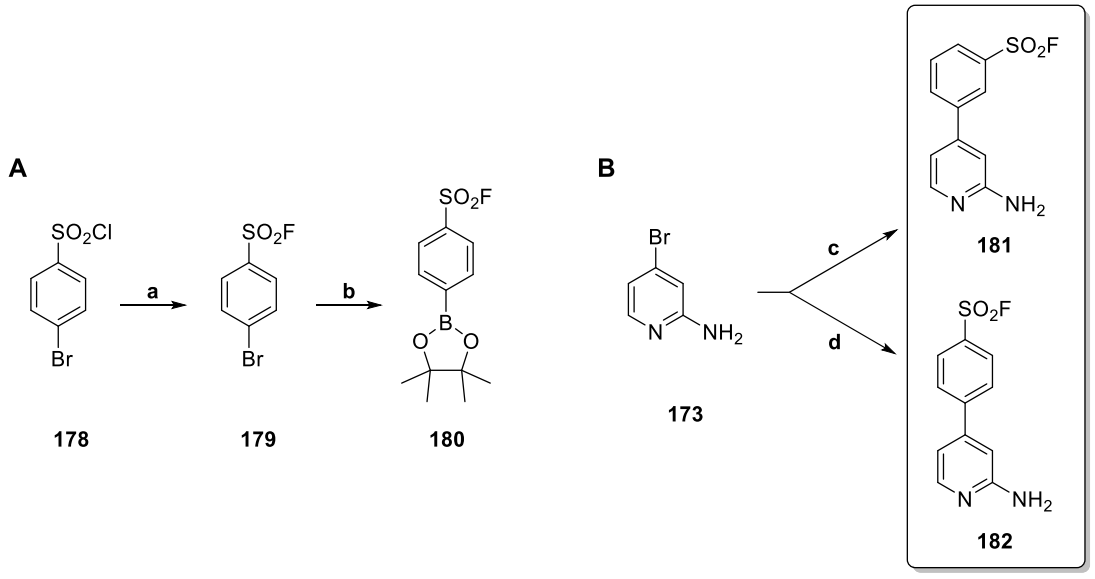

Scheme 24: A Synthesis of pinacol ester **180**: (a) KHF_2, MeCN/H_2O (2:1, V/V), rt, 18 h, 99 %; (b) B_2pin_2, KOAc, $Pd(dppf)Cl_2$, dioxane, 80 °C, 18 h, 76 %. **B** Synthesis of sulfonyl fluorides **181** and **182**: (c) (3-(fluorosulfonyl)phenyl)boronic acid (**69**), $Pd(OAc)_2$, XPhos, K_3PO_4, dioxane/H_2O (2:1, V/V), 40 °C, 18 h, 20 %; (d) **180**, $Pd(OAc)_2$, XPhos, K_3PO_4, dioxane/H_2O (2:1, V/V), 40 °C, 20 h, 12 %.

To increase flexibility and to a small extent also grow the linker length, the next step was to link the 2-aminopyridine hinge binding motif and the warhead-bearing phenyl ring via an ether. For

the fluorosulfate analogs this turned out to be more challenging than expected (**Scheme 25**). In the beginning, the synthesis route worked out as planned. 4-Fluoropyridin-2-amine (**183**) was subjected to a basic S_NAr reaction with the respective methoxyphenols to obtain biphenyl ethers **184** and **185**. The methyl groups were then removed using boron tribromide, yielding free phenols **186** and **187**. Following the usual procedure with AISF (**64**) to obtain the final fluorosulfates **188** and **189**, however, and somewhat surprisingly, did not show much conversion even after a long reaction time and the respective masses of the products could not be identified. While the free amine of the aminopyridine should not interfere with this reaction (*vide supra*), it was deemed the simplest solution to see if Boc-protecting the amine, leading to **190** and **191**, would facilitate the attachment of the warhead. Unfortunately, fluorosulfates **192** and **193** could not be detected once again. The reasons for this negative result remain unclear but they seem to be related to the ether linkage or a combination of the ether linkage and the aminopyridine motif as the direct linkage of the two phenyls was straightforward (*vide supra*) and a similar reaction with the azaindole hinge binding motif was also carried out successfully (see chapter 3.3.6.2). This approach was therefore discarded, and the focus was shifted onto other molecules of the conceived library.

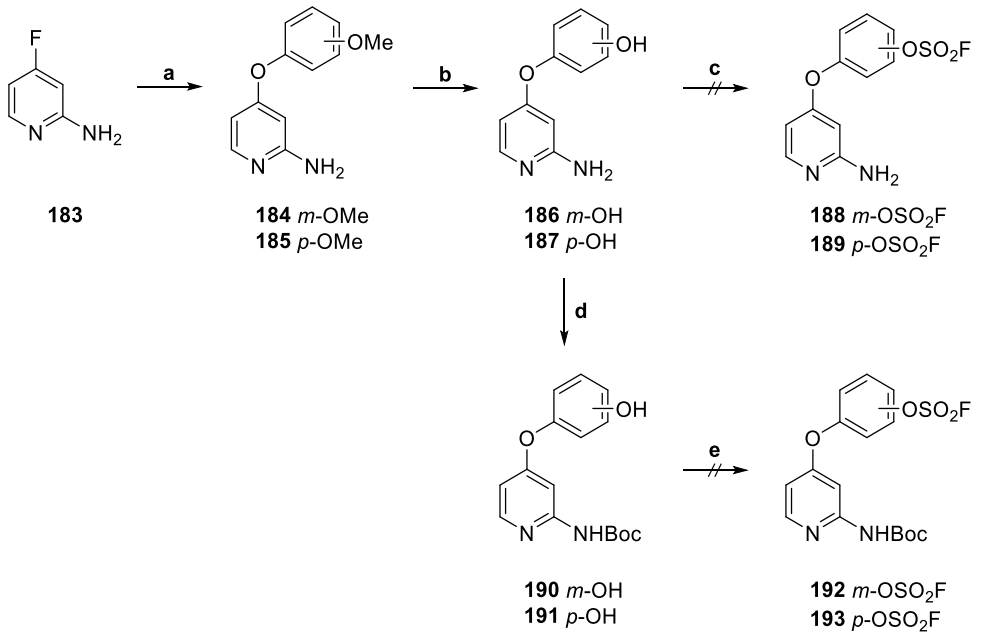

Scheme 25: (a) 3-/4-Methoxyphenol, NaH, NMP, 180 °C, 3 – 4 h, 78 – 88 %; (b) BBr_3, DCM, 0 °C to rt, 2 – 3 h, quant.; (c) AISF (**64**), DBU, THF, rt; (d) Boc_2O, *t*BuOH, 40 °C, 3 – 3.5 h, 44 – 63 %; (e) AISF (**64**), DBU, THF, rt.

For the ether-bridged aryl sulfonyl fluorides a protocol used by CRUITE *et al.*[130] was adapted that converts a bromide into the SF via several steps (**Scheme 26**). Initially, biaryl ethers **194** and **195** were again generated via a basic S_NAr reaction between 4-fluoropyridin-2-amine (**183**) and the respective bromophenols. In order to minimize possible side reactions, the free amine

at the pyridine was Boc-protected, yielding bromines **196** and **197**. Subsequently, benzyl thioethers **198** and **199** were obtained via a palladium-catalyzed BUCHWALD-type cross-coupling between the bromides and benzyl mercaptan. The desired oxidation state of the sulfur atom was then reached under acidic conditions utilizing *N*-chlorosuccinimide (NCS) as the oxidant. First, the benzyl group could be cleaved easily under mild acidic conditions with acetic acid which did not affect the Boc protection group. NCS was then used to perform an oxidative chlorination to yield sulfonyl chlorides **200** and **201** in good yields. Finally, these were converted into the respective sulfonyl fluorides via potassium bifluoride, and the Boc group was removed under harsher acidic conditions, utilizing HCl in dioxane, to obtain final compounds **202** and **203**. While this protocol required several steps to acquire the sulfonyl fluoride, it turned out to be a very reliable option, as both the palladium-catalyzed cross-coupling as well as the oxidative chlorination afforded the desired products in good to very good yields.

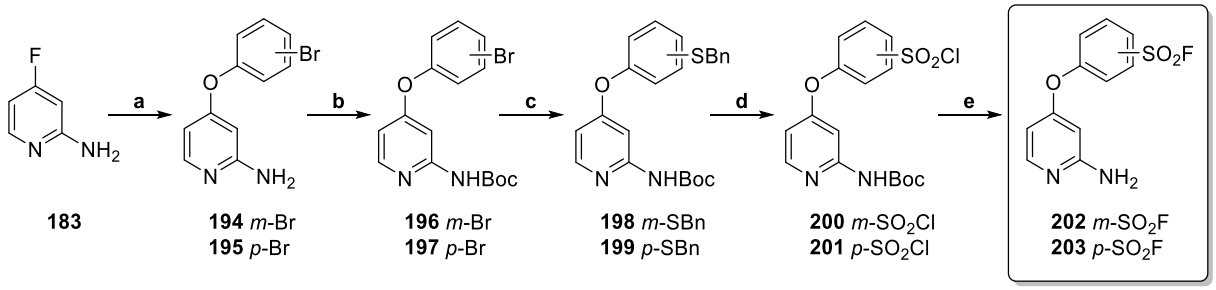

Scheme 26: (a) 3-/4-Bromophenol, NaH, NMP, 180 °C, 4 h, 71 – 77 %; (b) Boc_2O, *t*BuOH, 40 °C, 4 h, 57 – 76 %; (c) benzyl mercaptan, Pd_2dba_3, Xantphos, DIPEA, 90 °C, 18 h, 80 – 81 %; (d) NCS, AcOH/H_2O (3:1), rt, 3.5 h, 59 – 69 %; (e) 1. KHF_2, MeCN/H_2O (2:1, V/V), rt, 1 – 2 h; then 2. HCl in dioxane (4 M), 90 – 95 °C, 1 – 3.5 h, 4.6 – 88 %.

3.3.3. Synthesis of SuFEx Compounds Featuring a Pyridine Hinge Binder

Pyridines possess one less atom capable of interacting with the hinge region than 2-aminopyridines and therefore interact less strongly with the hinge region. However, a higher flexibility with respect to their orientation in the pocket can be assumed, which is why they were included in the library. The synthesis of fluorosulfates **207** and **208** (**Scheme 27**) is in analogy to the synthesis of the aminopyridines in chapter 3.3.2. Phenols **205** and **206** were synthesized via a SUZUKI coupling between 3-bromopyridine (**204**) and the respective (hydroxyphenyl)boronic acid. The resulting phenols were then converted to the corresponding fluorosulfates using AISF (**64**), following the previously described procedure.

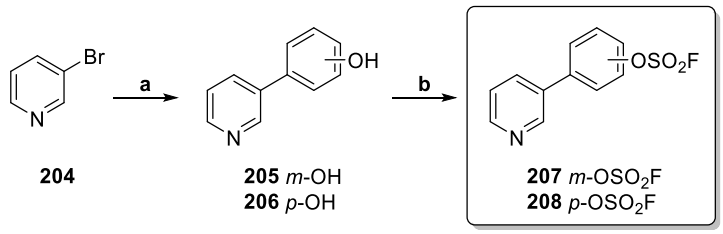

Scheme 27: (a) (3-/4-Hydroxyphenyl)boronic acid, XPhos Pd G4, K_2CO_3, dioxane/H_2O (5:3, V/V), 80 °C, 18 h, 88 – 91 %; (b) AISF (**64**), DBU, THF, rt, 20 h, 87 % – quant.

Throughout this project the synthesis of the fluorosulfates was usually simple, even in late stages of a synthetic route: the only thing needed is a phenol to attach the warhead in one of the last steps. There is a plethora of protection groups for phenols that can be cleaved under different conditions, rendering it very easy to carry the hydroxyl group through several steps. The situation is different when it comes to sulfonyl fluorides. There is no one-size-fits-all solution for the introduction of these warheads and every synthetic route should be carefully evaluated to determine the best stage to introduce a sulfonyl fluoride into the molecule. The synthesis of both fluorosulfate and sulfonyl fluoride from the same precursor is usually not possible and synthetic routes often need to be rearranged in order to obtain both molecules. In certain cases, however, it could be very useful to have the ability to generate both warheads from the same intermediate and it was therefore decided to briefly explore this. **Scheme 28** describes the possibility to convert a bromide into a sulfonyl fluoride via several steps that began with a palladium-catalyzed cross-coupling to introduce a thiol. Since it has been shown in other cross-couplings (e.g. SUZUKI couplings[131,132] or the MIYAURA borylation[133]) that pseudohalides such as the triflate group (-OTf) can be utilized as the leaving group, phenol **206** was used as a model compound to see if the conditions described in chapter 3.3.2 are applicable for this purpose. To this end, the phenol was converted into triflate **209** via treatment with trifluoromethanesulfonic anhydride. This fragment was then subjected to the same cross-coupling conditions using benzyl mercaptan and, to much satisfaction, benzyl thioether **210** was obtained in very good yield. Due to time constraints and the low priority of the pyridine hinge binder, this particular molecule was not further pursued but all following steps are well established and should not pose any problems. This method could be used to generate both the fluorosulfate and the sulfonyl fluoride from the same precursor without the need to reevaluate the synthetic route, possibly saving cost and time. It should be noted nevertheless that, since this protocol requires several steps, the synthesis of sulfonyl fluorides may still be achieved faster in a different way depending on the specific compound and building blocks availability.

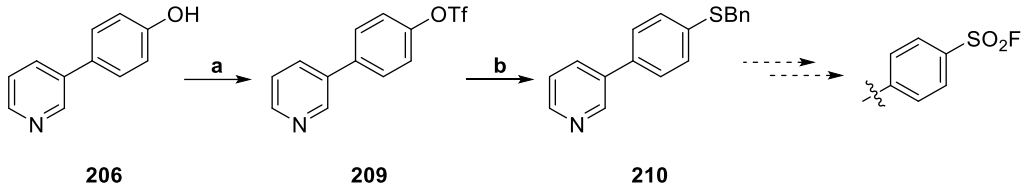

Scheme 28: (a) Tf_2O, DCM, 0 °C to rt, 1 h, 81 %; (b) benzyl mercaptan, Pd_2dba_3, Xantphos, DIPEA, 90 °C, 19 h, 83 %.

3.3.4. Synthesis of SuFEx Compounds Featuring a Thieno[2,3-*b*]pyridine Hinge Binder

The thieno[2,3-*b*]pyridine scaffold is a rather uncommon hinge binding motif, but it has gained some interest in recent years.[134–136] The azaindole scaffold is sometimes described as too promiscuous and while the sulfur atom in thienopyridines can engage in a chalcogen bond with the hinge region, this interaction is generally weaker than that of the pyrrole NH in azaindole.[135,137] As this core structure is less common than others, pre-functionalized precursors are not as readily available as those of e.g. azaindoles. The synthesis of fluorosulfates **216** and **217** therefore began from commercially available thieno[2,3-*b*]pyridine (**211**) which in the first step underwent an oxidation to *N*-oxide **212** (**Scheme 29**) using the oxidant *m*CPBA. A protocol established by LUCAS *et al.*[138] was followed to selectively brominate the 4-position. Trifluoromethanesulfonic anhydride is used here to activate the pyridine nitrogen, forming intermediate **218** with an excellent leaving group. This activation facilitates a conjugate-type S_NAr with a bromide nucleophile, enabling regioselective bromination of the thienopyridine core. The reaction proceeds via a MEISENHEIMER complex (**219**) before re-aromatization. To suppress bromination in the 6-position, the triflate group is absolutely necessary – mesylate or tosylate for example give a mixture of bromination in the 4- and 6-position. This led LUCAS *et al.*[138] to the conclusion that it cannot only be the size of the triflate group that shields the 6-position but also electronic factors. They hypothesized that the electronegative fluorine atoms of the activating group repel the incoming electron-rich bromide ion, thereby disfavoring nucleophilic attack at the 6-position adjacent to the activating group. As a result, only 4-bromothieno[2,3-*b*]pyridine (**213**) was formed. This compound could be handled as the other hinge binders before: SUZUKI coupling with the respective hydroxyphenyl boronic acids generated phenols **214** and **215** which were subjected to AISF (**64**) leading to fluorosulfates **216** and **217**.

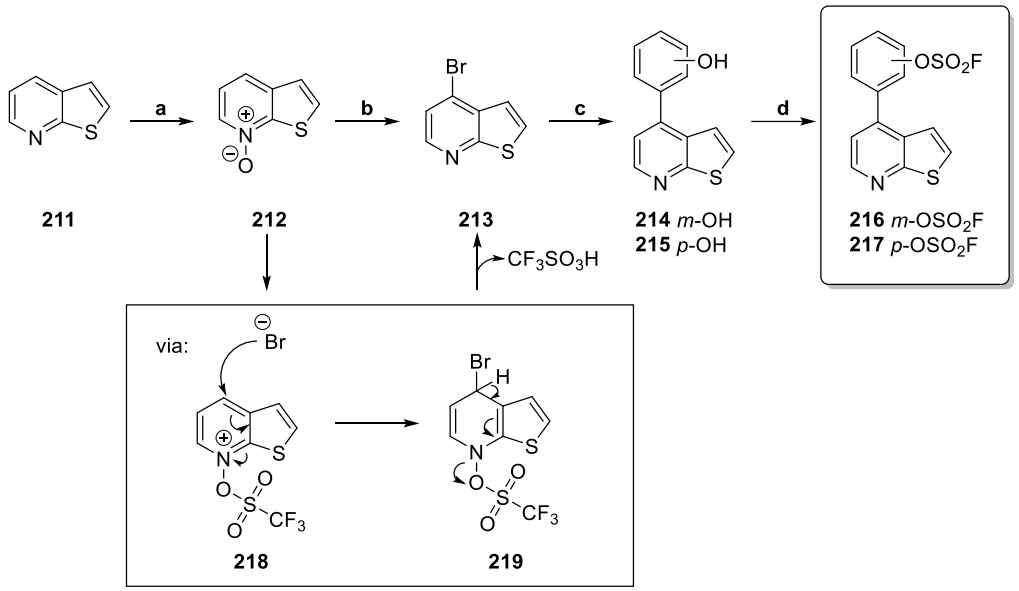

Scheme 29: (a) *m*CPBA, DCM/EtOAc (1:1, V/V), 0 °C to rt, 24 h, 86 %; (b) TBAB, Tf_2O, DCM, 0 °C to rt, 16 h, 85 %; (c) (3-/4-hydroxyphenyl)boronic acid, XPhos Pd G4, K_2CO_3, dioxane/H_2O (2:1, V/V), 80 °C, 17 h, 67 – 90 %; (d) AISF (**64**), DBU, THF, rt, 1 h, 86 – 89 %.

3.3.5. Synthesis of SuFEx Compounds Featuring an Indazole Hinge Binder

Indazoles typically engage the hinge region through a dual interaction: the NH group acts as a hydrogen bond donor, while the adjacent nitrogen serves as a hydrogen bond acceptor. This results in a binding orientation that differs markedly from that of azaindoles, aminopyridines, and related scaffolds. Consequently, it was decided to include an indazole in the library to incorporate a molecule with a completely different orientation relative to most of the other hinge binders employed here. Its synthesis is depicted in **Scheme 30**. 6-Bromo-1*H*-indazole (**220**) was Boc-protected (yielding **221**) to prepare it for the following palladium-catalyzed cross-coupling. This reaction was inspired by the cross-coupling with benzyl mercaptan as described in chapter 3.3.2 to introduce the phenyl ring onto which the warhead should be attached via a methylene thiol linker which should bring about a relatively high degree of linker flexibility. The methoxy group of **222** was removed using boron tribromide and the Boc protection group was deprotected concomitantly. The crude phenol was subjected to reaction with AISF (**64**) producing fluorosulfate **223**.

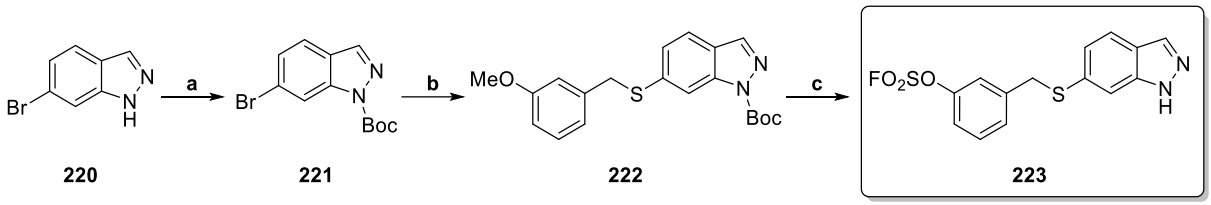

Scheme 30: (a) Boc_2O, DMAP, TEA, MeCN, rt, 2 h, 95 %; (b) (3-methoxyphenyl)methanethiol, Pd_2dba_3, Xantphos, DIPEA, 90 °C, 6 h, 66 %; (c) 1. BBr_3, DCM, rt, 18 h; then 2. AISF (**64**), DBU, DMF, rt, 18 h, 29 %.

3.3.6. Synthesis of SuFEx Compounds Featuring an Azaindole Hinge Binder

3.3.6.1. Azaindoles with a Direct Linkage to the Warhead-Bearing Phenyl

In the 7-azaindole series, the first compounds were synthesized by directly attaching aryl groups to the azaindole core via SUZUKI coupling, followed by introduction of the fluorosulfate warhead from a phenol precursor (**Scheme 31**). As shown in **Scheme 31A**, aryl substitution at the 4-position of 4-chloroazaindole (**224**) was achieved using 3- or 4-hydroxyphenylboronic acid, yielding phenolic intermediates **225** and **226**, which were subsequently converted to fluorosulfates **227** and **228** using AISF (**64**). Substitution at the 3-position was realized as shown in **Scheme 31B**, where 3-bromoazaindole (**229**) was coupled with the same boronic acids to give **230** and **231**, followed by fluorosulfation via AISF (**64**) to furnish **232** and **233**. Finally, as depicted in **Scheme 31C**, 5-bromoazaindole (**234**) served as the starting material for arylation, affording intermediates **235** and **236**, which were converted to fluorosulfates **237** and **238** under analogous conditions.

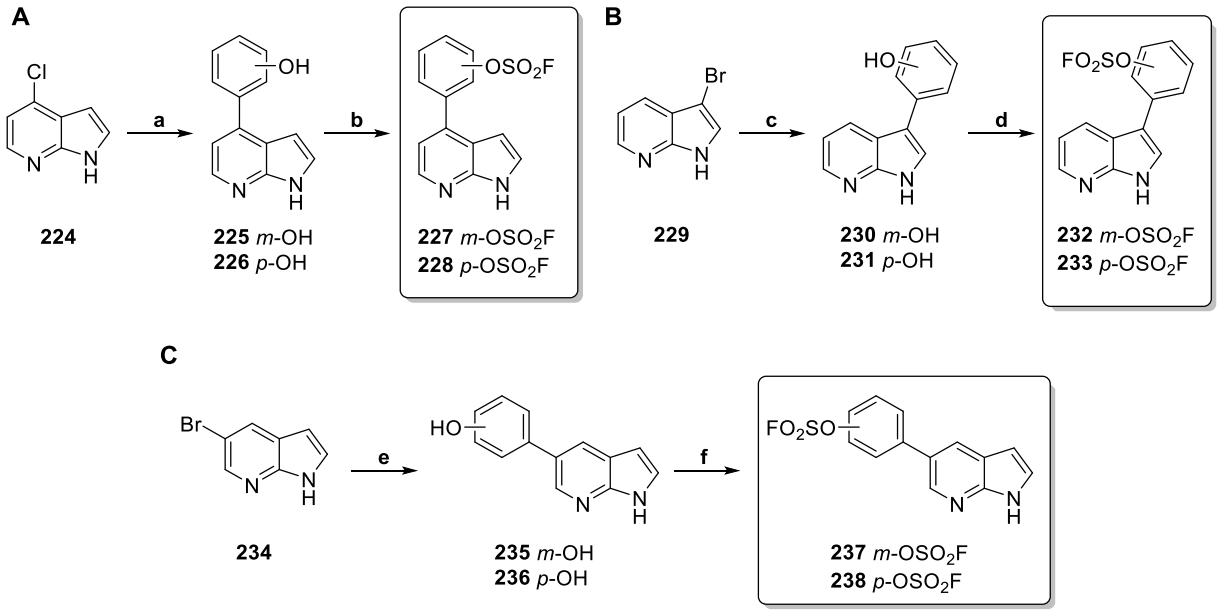

Scheme 31: A Direct linkage of the warhead-bearing phenyl in 4-position: (a) (3-/4-hydroxyphenyl)boronic acid, XPhos Pd G4, K_2CO_3, dioxane/H_2O (2:1, V/V), 80 °C, 18 h, 27 – 74 %; (d) AISF (**64**), DBU, THF, rt, 3 – 3.5 h, 69 %.

B Installation of the warhead-bearing phenyl group at the 3-position: (c) (3-/4-hydroxyphenyl)boronic acid, XPhos Pd G4, K_2CO_3, dioxane/H_2O (2:1, V/V), 80 °C, 2 d, 12 – 15 %; (d) AISF (**64**), DBU, THF, rt, 1 – 16 h, 11 – 12 %. **C** Direct linkage of the warhead-bearing phenyl in 5-position: (e) (3-/4-hydroxyphenyl)boronic acid, XPhos Pd G4, K_2CO_3, dioxane/H_2O (2:1, V/V), 80 °C, 3.5 h, 80 – 90 %; (f) AISF (**64**), DBU, THF, rt, 3 h, 71 – 76 %.

To complement the fluorosulfate analogs, a small set of sulfonyl fluorides directly linked via an aryl spacer was also synthesized (**Scheme 32**). Using the already prepared boronic acid derivatives equipped with the sulfonyl fluoride warhead, SUZUKI cross-couplings were carried out to attach the warhead-bearing aryl group directly onto the azaindole core. In **Scheme 32A**, installation at the 4-position of the core was achieved using either 3-(fluorosulfonyl)phenylboronic acid (**69**) or the corresponding *para*-substituted boronic ester **180**, affording products **239** and **240**. Additionally, 5-substituted analog **241** was accessed through a similar cross-coupling from bromo-azaindole **234** and the *meta*-substituted boronic acid **69** (**Scheme 32B**).

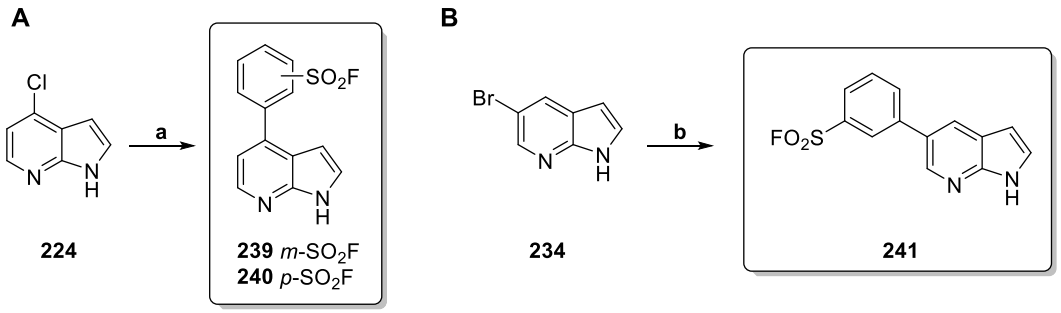

Scheme 32: A Direct linkage of the warhead-bearing phenyl in 4-position: (a) (3-(fluorosulfonyl)phenyl)boronic acid (**69**) or 4-(4,4,5,5-tetramethyl-1,3,2-dioxaborolan-2-yl)benzenesulfonyl fluoride (**180**), $Pd(OAc)_2$, XPhos, K_3PO_4, dioxane/H_2O (2:1, V/V), 40 °C, 18 – 20 h, 12 – 20 %. **B** Installation of the warhead-bearing phenyl group at the 5-position: (b) (3-(fluorosulfonyl)phenyl)boronic acid (**69**), $Pd(OAc)_2$, XPhos, K_3PO_4, dioxane/H_2O (2:1, V/V), 40 °C, 36 h, 3.6 %.

3.3.6.2. Azaindoles with an Ether Linkage to the Warhead-Bearing Phenyl

To explore the effects of increased conformational flexibility and altered spatial orientation of the electrophilic warhead, a subseries was designed in which the phenyl ring bearing the reactive group was connected to the azaindole core via an ether linkage. **Scheme 33** illustrates the synthesis of 4-fluoroazaindole (**245**) from 4-bromoazaindole (**242**) which was crucial to facilitate the upcoming S_NAr reactions. The pyrrole nitrogen was first protected with a TIPS group to afford intermediate **243**. In the next step, bromine–lithium exchange via *n*BuLi followed by electrophilic fluorination with NFSI yielded the fluorinated intermediate **244**. Finally, TIPS deprotection with TBAF furnished the target compound **245** in high overall yield.

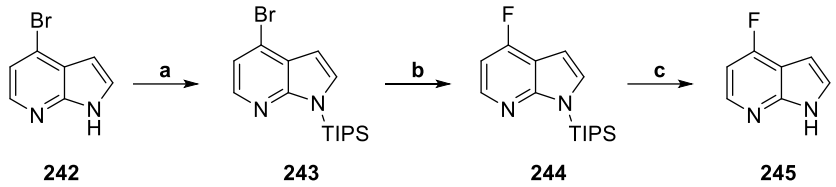

Scheme 33: (a) TIPSCl, NaH, THF, rt. 2.5 h, 88 %; (b) *n*BuLi, NFSI, THF, Et_2O, -78 °C, 3.5 h, 96 %; (c) TBAF, THF, 0 °C to rt, 16 h, 95 %.

As shown in **Scheme 34**, the 4-fluoroazaindole core (**245**) was further functionalized through nucleophilic aromatic substitution with 3- or 4-methoxyphenol to yield the corresponding aryl ethers **246** and **247**. Subsequent demethylation using BBr_3 provided the phenolic derivatives **248** and **249** in high yields. In the final step, the fluorosulfate warhead was introduced using AISF (**64**), affording the desired fluorosulfates **250** and **251**.

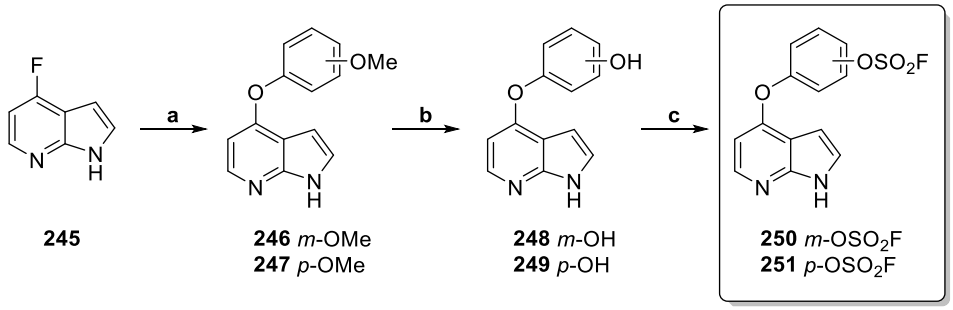

Scheme 34: (a) 3-/4-Methoxyphenol, NaH, NMP, 180 °C, 3.5 h, 21 – 41 %; (b) BBr_3, DCM, 0 °C to rt, 1.5 – 3 h, 85 – 86 %; (c) AISF (**64**), DBU, THF, rt, 1 h, 58 – 67 %.

3.3.6.3. Azaindoles with an Amine Linkage to the Warhead-Bearing Phenyl

For the introduction of the amine linker a BUCHWALD-HARTWIG reaction starting from 4-bromo-7-azaindole (**242**) seemed like the obvious option. The azaindole was therefore Boc-protected leading to analog **252**. The BUCHWALD-HARTWIG arylamination conditions were adapted from the dissertation of STEFAN GERSTENECKER.[139] Both intermediates **253** and **254** could be obtained this way, the yields were, however, rather low, i.e. 41 % for **253** and 48 % for **254** are the adjusted yields after re-isolation of unreacted starting material (BRSM). When not taking the recovered starting material into account, the yields drop to 10 % for **253** and 14 % for **254**. It was therefore decided to investigate a different approach.

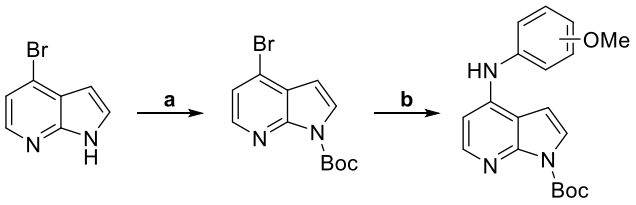

242 **252** **253** *m*-OMe **254** *p*-OMe

Scheme 35: (a) Boc_2O, DMAP, TEA, DCM, rt, 2 h, 92 %; (b) 3-/4-methoxyaniline, Xantphos Pd G4, Cs_2CO_3, 55 °C, 2 d, 41 – 48 % (BRSM).

Right around this time, researchers from Merck published a study on transition-metal free C–N cross-coupling.[140] In their methodology, they use 5,6-dichloropyrazine-2,3-dicarbonitrile (**263**) as a multifunctional reagent to enable the reaction between phenols and primary amines. As a new precursor was needed for this reaction, commercially available 4-hydroxy-7-azaindole (**255**) was Boc-protected leading to compound **256** (**Scheme 36**). Pleasingly, the cross-coupling between the methoxy anilines and 4-hydroxyazaindole **256** worked as described in the aforementioned publication furnishing both *meta*-methoxy intermediate **257** and *para*-intermediate **258**. The proposed reaction mechanism is depicted in **Scheme 36** using 3-methoxyaniline (**264**) and 4-hydroxyazaindole **256** as the model compounds. The commercially available and cheap 5,6-dichloropyrazine-2,3-dicarbonitrile (**263**) initially reacts with 3-methoxyaniline (**264**) in a first S_NAr reaction to yield monoamination product **265**. Generally, the first nucleophilic aromatic substitution deactivates toward diamination but in their study, the researchers also found that using ethereal solvents further favored monoamination. At this point of the one-pot reaction, the phenol (**256** in this case) is added to trigger the second S_NAr leading to **266**. In order to promote the rearrangement to intermediate **267**, highly polar solvents such as DMSO are necessary. In the final step, the reaction is quenched with acetic acid and zinc powder is added to trigger the reduction of the pyrazine ring and release of the cross-coupled product **257** and byproduct **268**. In this case, the final step also removed the Boc protecting group, which was unproblematic, as deprotection would have occurred in the following demethylation step using BBr_3 to yield the free phenols **259** and **260** anyway. Unfortunately, as previously observed for the ether-linked analogs described in chapter 3.3.2, the typically reliable reaction with AISF (**64**) to generate fluorosulfates **261** and **262** was unsuccessful in this case as well. The underlying reasons remain unclear and even extended reaction times failed to achieve full conversion or yield an isolable product. Consequently, the focus was shifted toward longer and more flexible linkers.

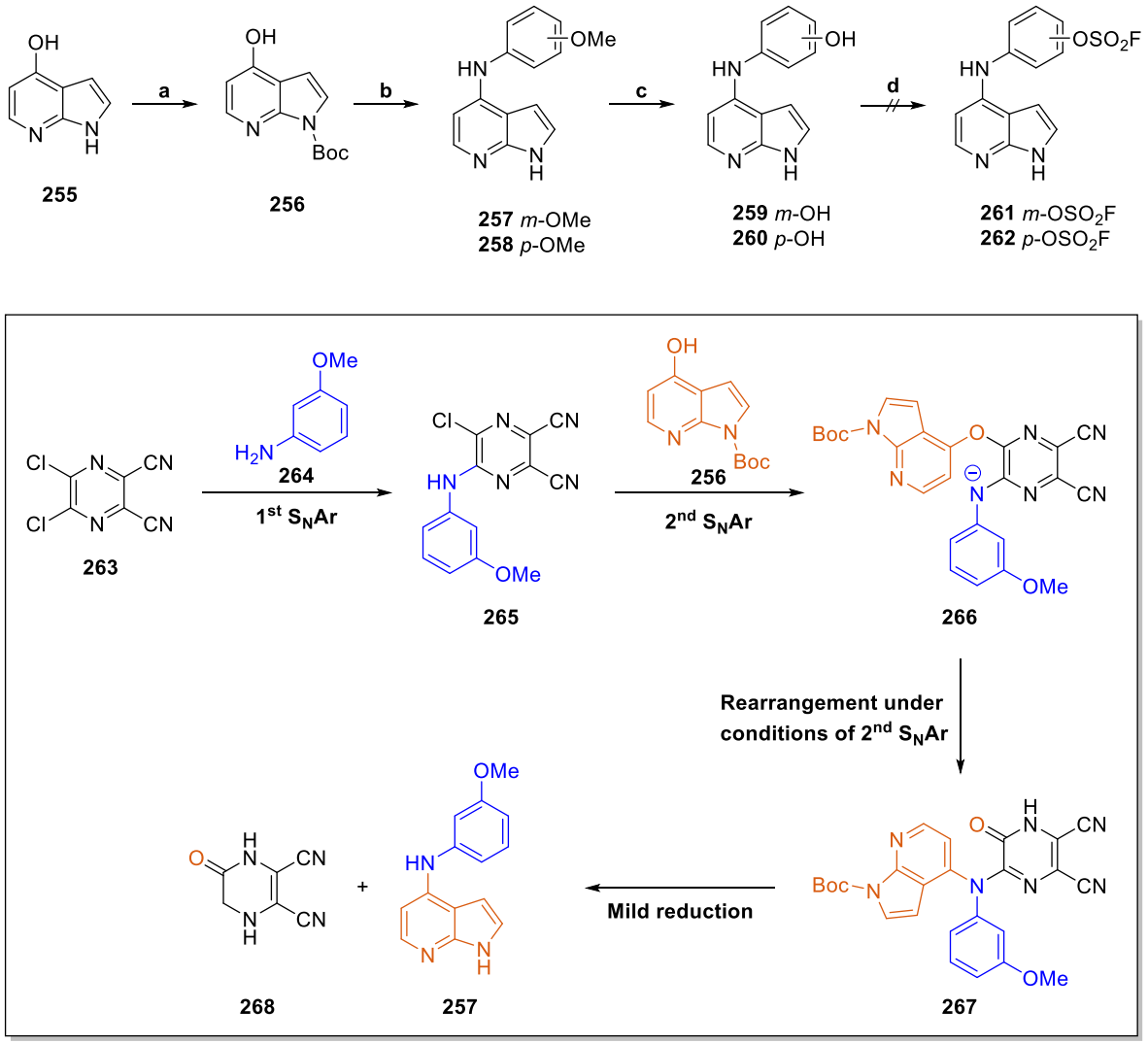

Scheme 36: (a) Boc_2O, DMAP, DCM, DMF, 0 °C to rt, 2.5 h, 58 %; (b) 3-/4-methoxyaniline, 5,6-dichloropyrazine-2,3-dicarbonitrile (**263**), K_3PO_4, Zn, AcOH, dioxane, DMSO, 50 to 100 °C, 3.5 h, 49 – 95 %; (c) BBr_3, DCM, 0 °C to rt, 2 h; (d) AISF (**64**), DBU, THF, rt.

3.3.6.4. Azaindoles with a Methylene Thioether Linkage to the Warhead-Bearing Phenyl

To explore the effect of increased linker length, a methylenethio linker was introduced, providing greater flexibility compared to the previously described direct and oxygen linkages. The synthesis of fluorosulfate derivatives **273** and **274** featuring this linker is outlined in **Scheme 37**. Starting from brominated Boc-protected azaindole **252**, a palladium-catalyzed cross-coupling with (3-/4-methoxyphenyl)methanethiol yielded thioether intermediates **269** and **270**. Subsequent demethylation using BBr_3 afforded the corresponding phenols **271** and **272**, which were then converted to the final fluorosulfates **273** and **274** via reaction with AISF (**64**) under the usual basic conditions.

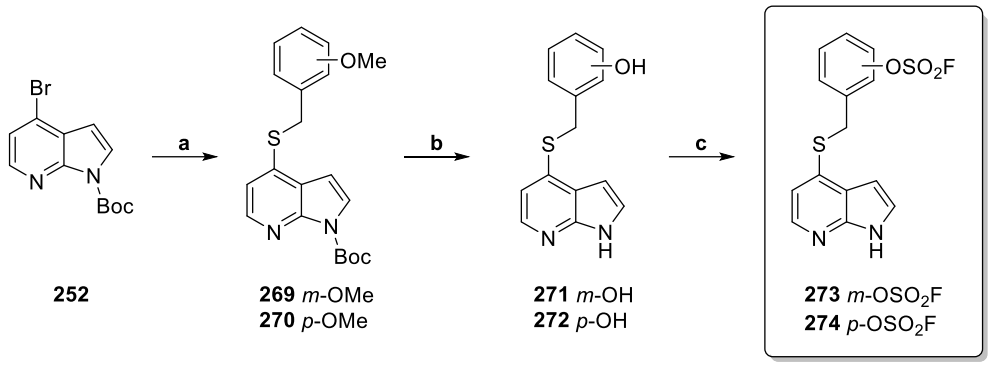

252 | **269** *m*-OMe, **270** *p*-OMe | **271** *m*-OH, **272** *p*-OH | **273** *m*-OSO_2F, **274** *p*-OSO_2F

Scheme 37: (a) (3-/4-Methoxyphenyl)methanethiol, Pd_2dba_3, Xantphos, DIPEA, 90 °C, 5 – 6 h, 57 – 96 %; (b) BBr_3, DCM, 0 °C to rt, 2 – 18 h, 64 – 73 %; (c) AISF (**64**), DBU, DMF, rt, 16 h, 3.9 – 19 %.

3.3.6.5. Azaindoles with an Amide Linkage to the Warhead-Bearing Phenyl

To further diversify the chemical space around the warhead attachment and explore different spatial orientations, azaindole derivatives bearing an amide linkage to the warhead-bearing phenyl ring were synthesized. This strategy enables a planar and more rigid connection between the hinge-binding core and the electrophilic moiety, potentially offering improved directional engagement with nucleophilic residues while at the same time elongating the linker some more. Moreover, the amide may undergo additional interactions within the binding pocket.

As depicted in **Scheme 38A**, starting from 4-aminoazaindole **275**, amide coupling with 3- or 4-methoxybenzoic acid using HATU provided intermediates **276** and **277**, which were subsequently demethylated and converted into fluorosulfates **278** and **279** in a two-step sequence involving BBr_3 and AISF (**64**). In addition to these fluorosulfates, a sulfonyl fluoride analog was also prepared. To this end, amide **280** was first synthesized from **275** and 4-iodobenzoic acid in a HATU-mediated amide coupling and then subjected to Boc-protection to afford aryl iodide **281**. This protection group was introduced to prepare the molecule for the upcoming palladium-catalyzed cross-coupling. During the MK2 project discussed in chapter 3.2.5, a palladium-catalyzed reaction was investigated to convert a bromide into a sulfonyl fluoride, but the reaction was not successful. Here, a different method by TRIBBY *et al.*[126] was implemented and sulfonyl fluoride **282** was successfully isolated in an acceptable yield of 33 %. This transformation also proceeds via an aryl ammonium sulfinate intermediate, but it is nevertheless slightly different to the previously mentioned one. It uses cataCXium A as the ligand and in the second step Selectfluor (also known as F-TEDA) as the electrophilic fluorine source. An advantage of this particular molecule is that the halogen is located in *para*-position (as compared to *ortho* in the molecule in chapter 3.2.5), so there is no steric hindrance – even though TRIBBY *et al.* actually do describe one example of this reaction in *ortho*-position to

another substituent. Furthermore, their methodology is based on aryl iodides which will generally react faster in these cross-coupling reactions. With the sulfonyl fluoride in hand, the Boc group was cleaved using TFA, yielding final molecule **283**. A very similar approach as described above for the fluorosulfate compounds was pursued for the amide linkage in the 5-position of the azaindole hinge binder (**Scheme 38B**): starting from 5-amino-7-azaindole (**284**) an amide coupling was performed, yielding methoxyphenyl intermediate **285**. This was demethylated utilizing BBr_3 and subsequently the fluorosulfate was attached via AISF (**64**) to afford the final compound **286**.

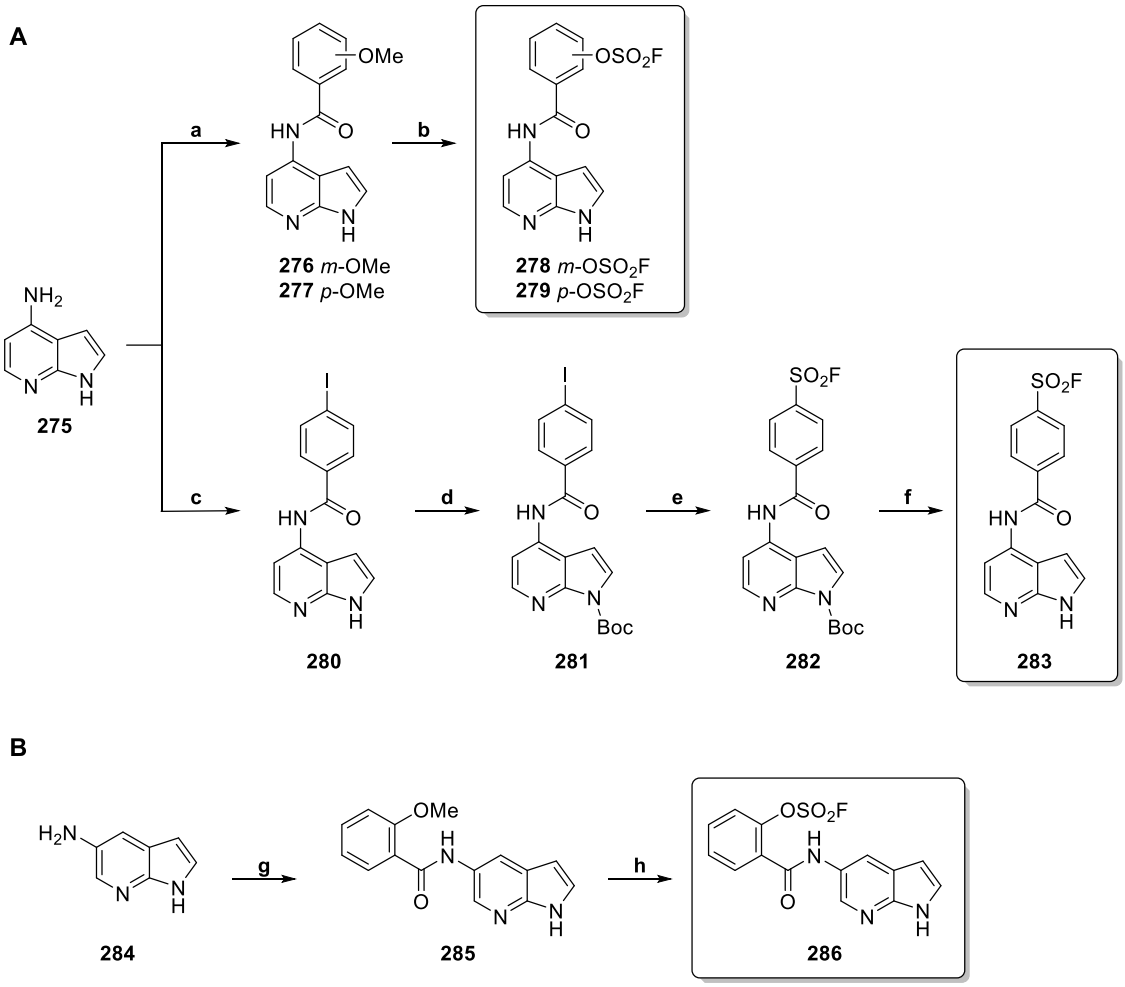

Scheme 38: A Synthesis of amide linkages in the 4-position of the azaindole: (a) 3-/4-methoxybenzoic acid, HATU, DIPEA, DMF, rt, 18 h, 11 – 58 %; (b) 1. BBr_3, DCM, 0 °C to rt, 18 h; then 2. AISF (**64**), DBU, DMF, rt, 5 – 7 h, 29 – 32 % over two steps; (c) 4-iodobenzoic acid, HATU, DIPEA, DMF, rt, 2 d, 32 %; (d) Boc_2O, DMAP, TEA, DMF, rt, 1 h, 37 %; (e) DABSO, $Pd(OAc)_2$, cataCXium A, TEA, Selectfluor, *i*PrOH, MeCN, rt to 75 °C, 7.5 h, 33 %; (f) TFA, DCM, rt, 18 h, 60 %. **B** Synthesis of amide linkages in the 5-position of the azaindole: (g) 2-methoxybenzoic acid, HATU, DIPEA, DMF, rt, 18 h, 84 %; (h) 1. BBr_3, DCM, rt, 18 h; then 2. AISF (**64**), DBU, DMF, rt, 18 h, 25 % over two steps.

For the inverted amide, an alternative strategy was pursued. Fluorosulfate-bearing anilines **289** and **290** could be synthesized in one step from the respective aminophenols **287** and **288**

(**Scheme 39A**), making the synthesis of the final fluorosulfate compounds a straightforward two-step sequence and eliminating the need for a deprotection step. To explore suitable conditions for amide coupling in the presence of the warhead, a small screening of amide coupling conditions was conducted using the reaction between 7-azaindole-4-carboxylic acid (**291**) and fluorosulfate **290** as the model system (**Scheme 39B**).

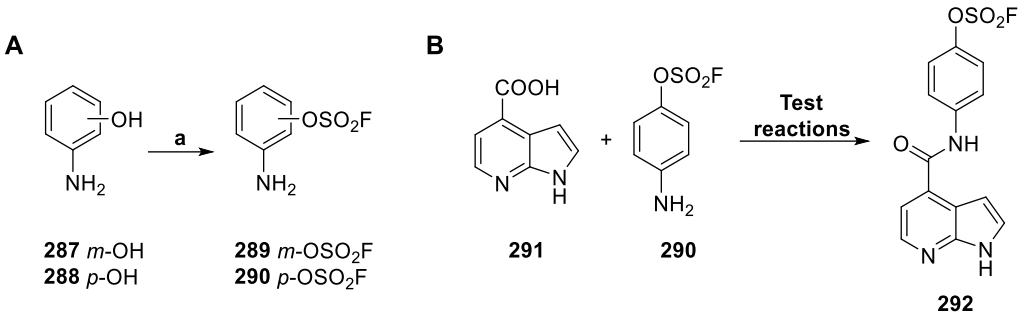

Scheme 39: A Synthesis of fluorosulfate anilines: (a) AISF (**64**), DBU, DMF, rt, 2 h, 65 – 72 %. **B** Test reactions to determine preferential amide coupling conditions. The exact conditions can be found in **Table 1**.

Among the conditions tested, only the use of HATU with DIPEA in DMF (entry **a**, **Table 1**) yielded the desired amide **292** as the main product, albeit accompanied by minor side products. In contrast, TBTU-mediated coupling (entry **b**) primarily resulted in unidentified side products, and only some formation of **292** was observed. Attempts involving *in situ* generation of the acid chloride (entry **c**), as well as EDC-based couplings either with HOBt (entry **d**) or DMAP (entry **e**), failed to produce the desired product entirely. These results highlighted the superior performance of HATU-mediated coupling under mild conditions for preserving the integrity of the fluorosulfate moiety.

Table 1: Conditions for amide coupling test reactions as depicted in **Scheme 39B**.

	Conditions	**Result**
a	HATU, DIPEA, DMF, rt	Main product: **292**, some side products
b	TBTU, DIPEA, DMF, rt	Mostly side products, **292** not main product
c	1. Carboxylic acid, oxalyl chloride, DMF, DCM; then 2. Aniline, reflux	**292** did not form
d	EDC, HOBt, TEA, DMF, rt	**292** did not form
e	EDC, DMAP, DCM, rt	**292** did not form

Unfortunately, when scaling up the HATU-mediated coupling, a persistent side product was formed that could not be separated despite extensive purification attempts. Due to time limitations, this approach was ultimately discontinued in favor of a slightly more flexible linker strategy. To this end, a methylene spacer was introduced between the azaindole core with the amide linker and the warhead-bearing phenyl ring and the previous approach of introducing the warhead after the amide coupling was resumed (**Scheme 40**). The HATU-mediated coupling of 7-azaindole-4-carboxylic acid (**291**) with (3- or 4-methoxyphenyl)methanamine afforded intermediates **293** and **294**, which were then subjected to the usual two-step deprotection and fluorosulfation sequence to yield fluorosulfates **295** and **296**. In a parallel approach for the sulfonyl fluoride, coupling of carboxylic acid **291** with (4-iodophenyl)methanamine furnished amide **297**, which was subsequently Boc-protected to yield intermediate **298**. Palladium-catalyzed sulfo-fluorination followed by final Boc-deprotection via TFA then provided the target sulfonyl fluoride **299**. This route allowed for the incorporation of a more flexible linker, enhancing spatial reach.

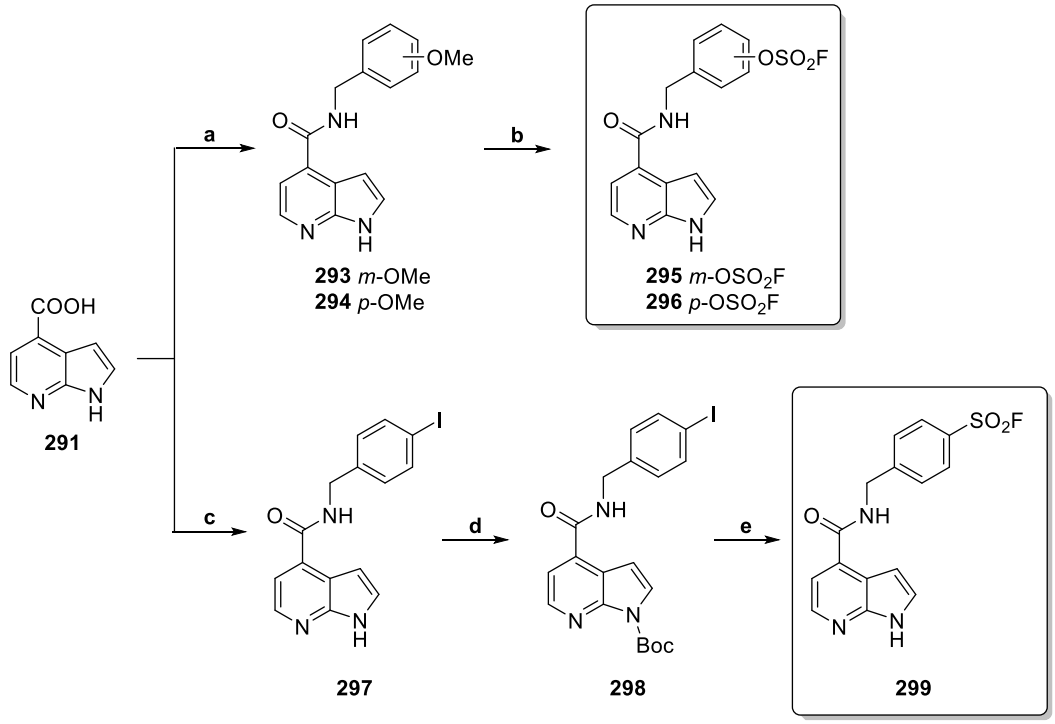

Scheme 40: (a) (3-/4-Methoxyphenyl)methanamine, HATU, TEA, DMF, rt, 3 – 17 h, 32 – 50 %; (b) 1. BBr_3, DCM, 0 °C to rt, 3 – 16 h; then 2. AISF (**64**), DBU, DMF, rt, 16 h, 17 – 54 % over two steps; (c) (4-iodophenyl)methanamine, HATU, DIPEA, DMF, rt, 6 h, 81 %; (d) Boc_2O, DMAP, TEA, DMF, rt, 2 h, 30 %; (e) 1. DABSO, $Pd(OAc)_2$, cataCXium A, TEA, Selectfluor, *i*PrOH, MeCN, rt to 90 °C, 18 h, 33 %; then 2. TFA, DCM, rt, 18 h, 12 % over two steps.

3.3.6.6. Azaindoles with a Larger Linkage to the Warhead-Bearing Phenyl

As a last step, even larger linkers were included to reach amino acids more distant from the hinge region, aiming to further expand the spatial reach of the electrophilic warhead (**Scheme 41**). Starting from bromo azaindole **242**, a BUCHWALD–HARTWIG coupling with 4-nitroaniline afforded intermediate **300**, which was subsequently reduced to the corresponding aniline **301** by hydrogenation over Pd/C. In parallel, ethyl esters **302** and **303** were first converted into the corresponding fluorosulfates **304** and **305**, followed by acidic ester cleavage using HCl in dioxane to yield the free acids **306** and **307**. Final amide coupling of these building blocks with the azaindole aniline **301** using HATU-mediated conditions furnished the fluorosulfate-bearing amides **308** and **309**, featuring extended and more flexible linkers.

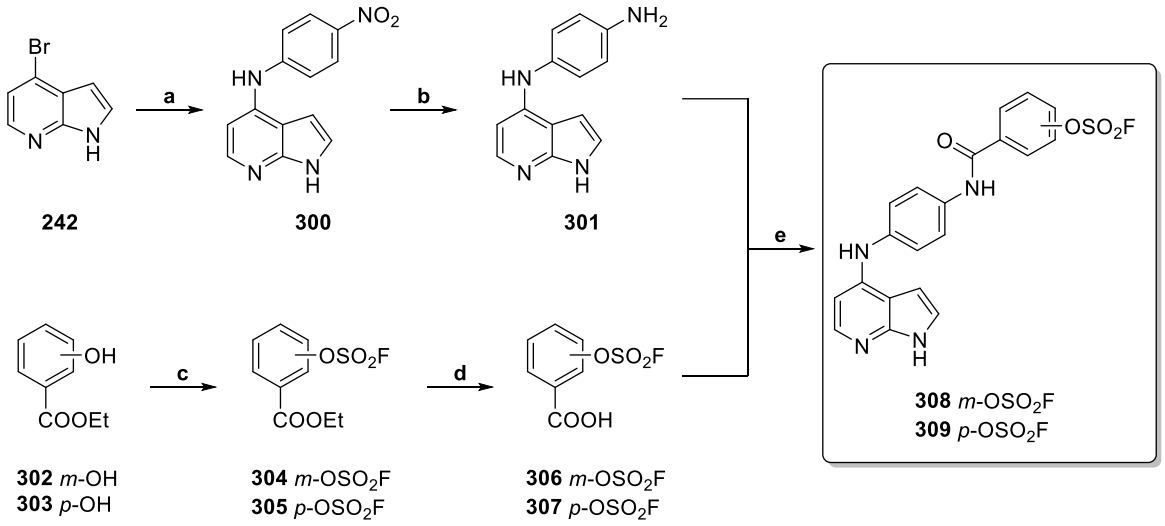

Scheme 41: (a) 4-Nitroaniline, Pd_2dba_3, XPhos, K_2CO_3, *t*BuOH, 80 °C, 16 h, 63 %; (b) Pd/C, H_2 (1 atm), MeOH, rt, 18 h, 99 %; (c) AISF (**64**), DBU, THF, rt, 5 h, 80 – 88 %; (d) HCl in dioxane (4 M), reflux, 16 h, 75 – 84 %; (e) HATU, DIPEA, DMF, rt, 6 – 18 h, 11 – 33 %.

3.4. Elaboration of the Screening Hit from the Covalent Library on ALK2

Building on the covalent-first library strategy, a promising covalent fragment hit targeting ALK2/ACVR1 was identified through intact protein MS and subsequent X-ray crystallographic experiments conducted during a research stay at the University of Oxford. The hit compound **308**, which features a 7-azaindole hinge-binding motif connected to a fluorosulfate warhead via a larger, more flexible linker, was found to covalently modify the protein. The co-crystal structure (see chapter 4.4.4 for a depiction of the structure and a more detailed discussion) revealed that **308** binds in the ATP-binding pocket and engages in a covalent interaction with Lys338, a residue located within the catalytic loop close to the conserved HRD motif that has so far never been covalently targeted. This structural insight provided a robust foundation for

the design of a small, focused SAR study. As depicted in **Figure 20**, there are three components to the molecule that may be modified: the hinge binding motif, the linker and the warhead-bearing aryl ring. The following chapters detail the synthesis of a series of analogs designed to refine the binding interactions, explore the impact of linker modifications, and assess the positioning and reactivity of the warhead to enhance covalent engagement with Lys338.

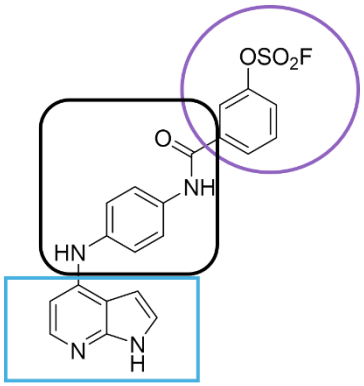

308

Figure 20: Hit molecule **308** and respective parts of the compound that should be modified: hinge region (blue), linker (black) and the warhead-bearing aryl ring (purple).

3.4.1. Modification of the Hinge Binder

To explore the impact of the hinge-binding motif, one alternative to the azaindole core, namely a 2-aminopyridine, was investigated (**Scheme 42**). Commercially available aminopyridine **310** was subjected to BUCHWALD–HARTWIG coupling with 4-nitroaniline to yield nitro compound **311**. Catalytic hydrogenation over Pd/C provided aniline **312**, which was subsequently coupled with fluorosulfate-bearing acid **306** using HATU to afford protected amide **313**. Final Boc-deprotection using TFA delivered the target compound **314**. While the SAR study focused predominantly on modifications to other regions of the molecule (such as the linker and the warhead-bearing aryl ring), this synthetic sequence provided initial access to a structurally slightly different hinge binder for comparison.

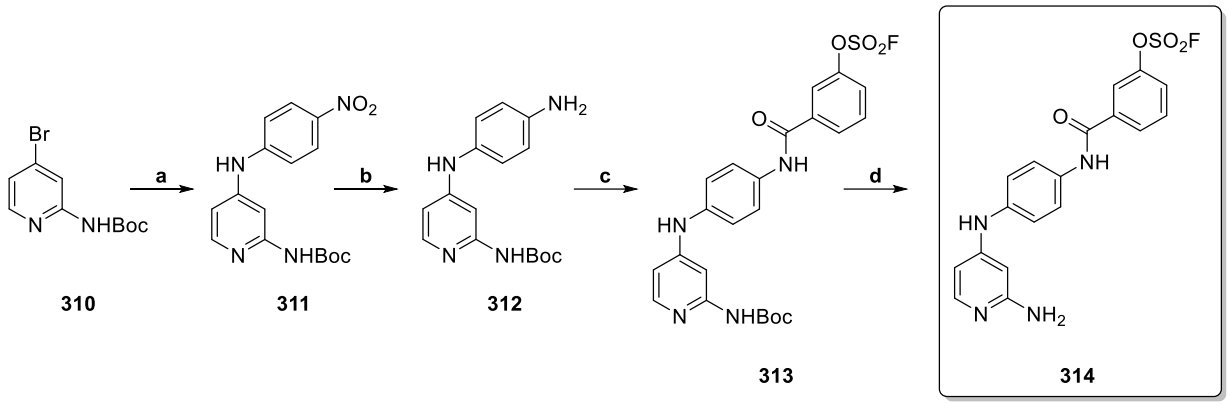

Scheme 42: (a) 4-Nitroaniline, Pd_2dba_3, Xantphos, Cs_2CO_3, dioxane, 95 °C, 18 h, 87 %; (b) Pd/C, H_2 (1 atm), MeOH, rt, 16 h, 71 %; (c) **306**, HATU, DIPEA, DMF, rt, 24 h, 92 %; (d) TFA, DCM, rt, 4 h, 66 %.

3.4.2. Modification of the Linker

Following the initial exploration of structural modifications around the hinge-binding motif, attention was next directed toward alterations of the linker region. A common medicinal chemistry strategy to probe linker flexibility and binding orientation is the inversion of the amide bond. This modification can significantly influence hydrogen bonding patterns and overall molecular conformation. To evaluate this approach, the inverted amide analog **317** was synthesized as outlined in **Scheme 43**. Coupling of 4-bromo-7-azaindole (**242**) with methyl 4-aminobenzoate under palladium catalysis in a BUCHWALD-HARTWIG reaction afforded intermediate **315**, which was subsequently hydrolyzed (LiOH in MeOH/H_2O) to the corresponding acid **316**. Final coupling with fluorosulfate warhead precursor **289** using HATU-mediated amidation yielded the target compound **317**.

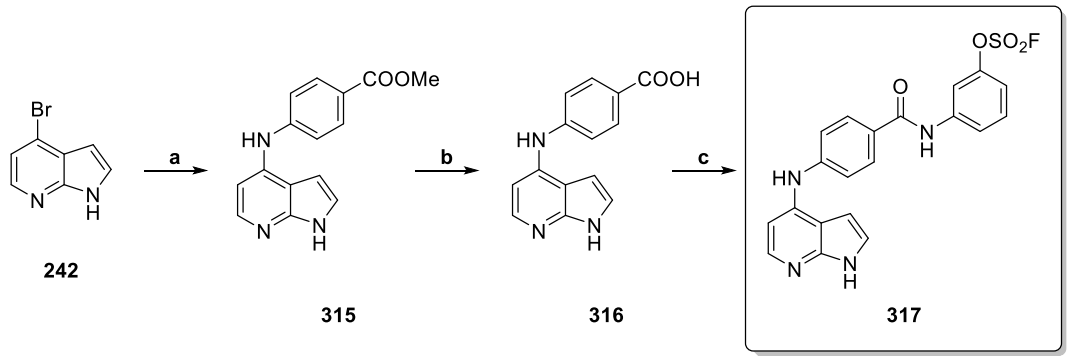

Scheme 43: (a) Methyl 4-aminobenzoate, Pd_2dba_3, XPhos, K_2CO_3, *t*BuOH, 80 °C, 16 h, 80 %; (b) LiOH, H_2O/THF (1:1, V/V), rt, 16 h, quant.; (c) **289**, HATU, DIPEA, DMF, rt, 18 h, 6.5 %.

Beyond the amide inversion strategy described above, further modifications to the linker region were explored to probe the influence of electronic effects and steric properties on binding and

reactivity. In particular, mono-fluorinated phenyl linkers were introduced to subtly alter the physicochemical characteristics and conformation of the molecule while maintaining the overall topology. As shown in **Scheme 44**, coupling of 4-bromo-7-azaindole (**242**) with 2- or 3-fluoro-4-nitroaniline via a BUCHWALD–HARTWIG amination provided nitro intermediates **318** and **319**. Subsequent hydrogenation over palladium on carbon yielded the corresponding anilines **320** and **321**, which were then coupled with warhead precursor **306** under HATU activation to afford fluorosulfate analogs **322** and **323**. These derivatives allowed for the assessment of how subtle electronic modifications in the linker affect the orientation and reactivity of the electrophilic warhead in the context of ALK2 binding.

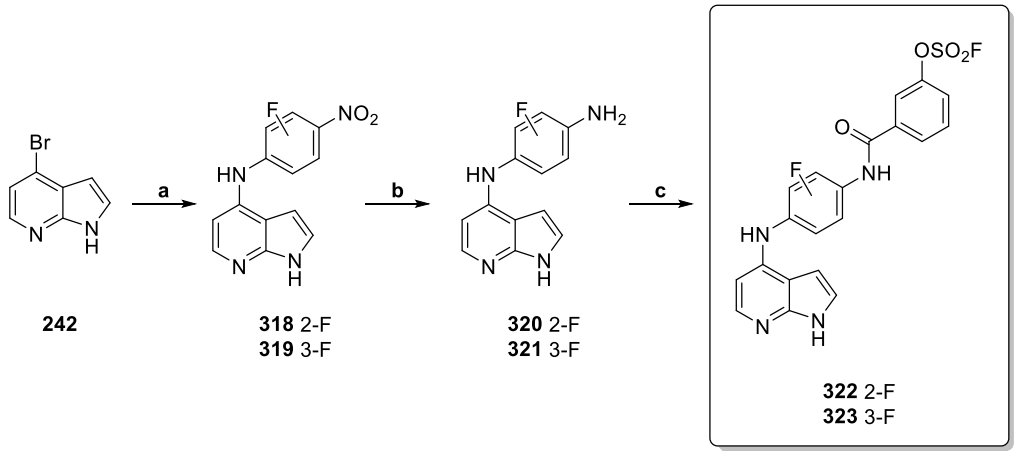

Scheme 44: (a) 2-/3-Fluoro-4-nitroaniline, Pd_2dba_3, XPhos, K_2CO_3, *t*BuOH, 80 °C, 18 h, 72 – 84 %; (b) Pd/C, H_2 (1 atm), MeOH, rt, 18 h, 82 – 88 %; (c) **306**, HATU, DIPEA, DMF, rt, 18 h, 8.8 – 9.4 %.

3.4.3. Modification of the Warhead-Bearing Aryl Ring

In a final effort to systematically optimize the electrophilic moiety of the inhibitor series, particular attention was given to structural variation on the warhead-bearing aryl ring. This region of the molecule offered a versatile platform for fine-tuning both electronic properties and steric environment, which are known to significantly influence the rate and selectivity of covalent modification. A series of electron-donating and electron-withdrawing substituents were introduced to investigate their effects on the reactivity of the appended electrophilic warhead. Furthermore, a sulfonyl fluoride analog was prepared to directly compare the behavior of the two different warhead classes. The synthesis of the required carboxylic acid building blocks is outlined in **Scheme 45**. Aromatic carboxylic acids **324** and **325** were first converted to their corresponding methyl esters **326** and **327** under acidic esterification conditions. The other methyl esters shown here, **328** – **332**, with the exception of **331** (*vide infra*), were commercially available. Methyl esters were preferred due to the simplification of the work up in the next step, the fluorosulfation using AISF (**64**) to yield intermediates **333** –

339. Acidic hydrolysis of the esters furnished the desired fluorosulfate-substituted acids **340** – **346**, which were used in their crude state as key precursors for the final amidation step. A special case was the synthesis of nitrile-containing ester **331**, which was accessed in a ROSENMUND-VON-BRAUN reaction from bromo ester **330** using copper(I) cyanide (**Scheme 45B**). **Scheme 45C** outlines the synthesis of sulfonyl fluoride precursor **348** which was obtained from sulfonyl chloride **347** using potassium bifluoride.

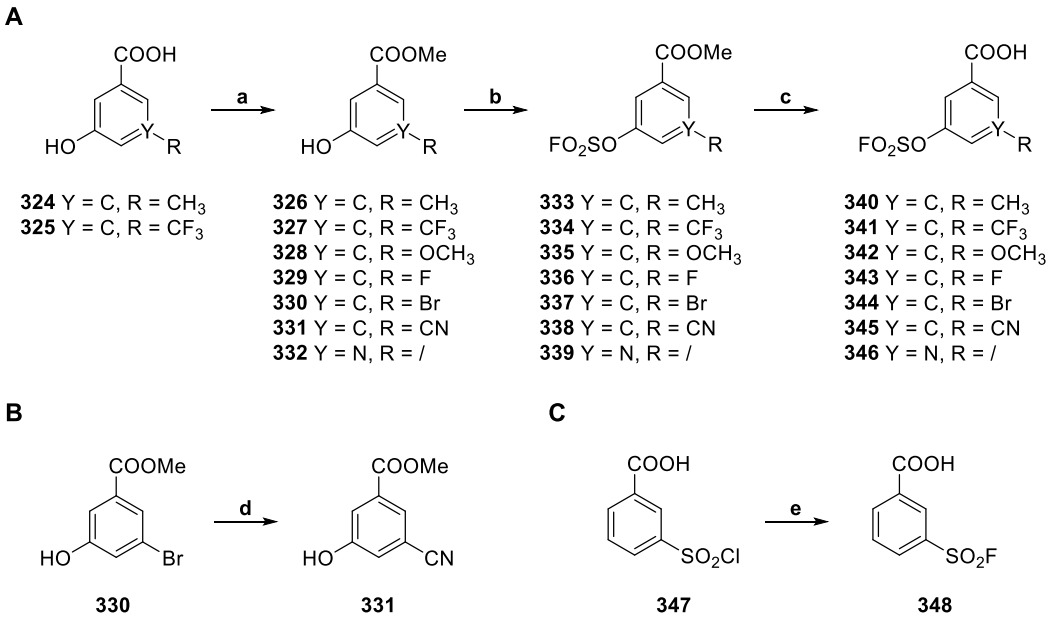

Scheme 45: A General synthesis of carboxylic acid precursors: (a) conc. H_2SO_4, MeOH, reflux, 20 h, 97 – 99 %; (b) AISF (**64**), DBU, THF, rt, 1.5 – 16 h, 30 – 88 %; (c) HCl in dioxane (4 M)/aq. HCl (1 M) (1:5, V/V), reflux, 7 – 24 h. The carboxylic acids were used in the next step without further purification. **B** ROSENMUND-VON-BRAUN reaction to obtain **331**: (d) CuCN, NMP, 180 °C, 6 h, 78 %. **C** Synthesis of sulfonyl fluoride precursor **348**: (e) KHF_2, MeCN/H_2O (2:1, V/V), rt, 20 h, 95 %.

Amide coupling of the warhead-bearing carboxylic acids with the aniline intermediate **301** was achieved under standard amide coupling conditions using HATU and DIPEA in DMF (**Scheme 46**). This final step successfully delivered the targeted covalent inhibitors **349** – **356** as well as the noncovalent analogs **357** and **358**, encompassing a broad spectrum of electronic and steric environments on the aryl ring. The series included electron-withdrawing substituents such as trifluoromethyl (**350**), cyano (**354**), bromo (**353**) and fluoro (**352**), as well as electron-donating motifs including methoxy (**351**) and methyl (**349**). Notably, compound **356** incorporated a sulfonyl fluoride warhead in place of the fluorosulfate, enabling direct comparison of these electrophilic functional groups within the same molecular framework. This comprehensive set of analogs provided a robust platform to evaluate how warhead electronics and positioning impact covalent reactivity and binding efficacy toward ALK2, setting the stage for detailed biochemical and biophysical characterization.

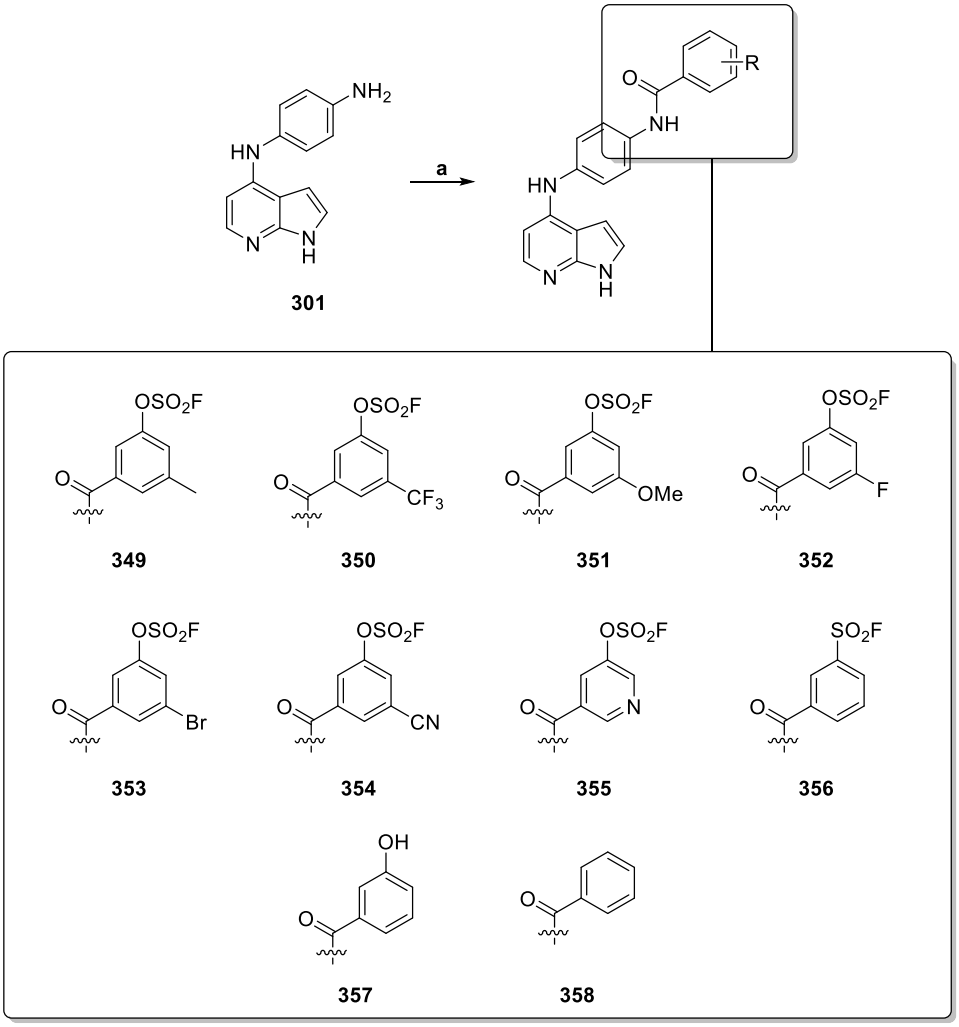

Scheme 46: (a) Carboxylic acid, HATU, DIPEA, DMF, rt, 16 – 18 h, 6.8 – 38 %.

4. Biochemical Evaluation and Discussion

4.1. Evaluation of Putative JAK3 Inhibitors

4.1.1. Biochemical Evaluation through JAK3-ELISA

The evaluation of the JAK3-targeted inhibitors was carried out in an enzyme-linked immunosorbent assay (ELISA) developed in house by SILKE BAUER (**Figure 21**).[141] In this assay, a synthetic polypeptide substrate composed of L-glutamic acid and L-tyrosine in a 4:1 ratio is pre-adsorbed on the walls of the assay wells. Serial dilutions of the test compounds are introduced to generate dose–response curves for IC_{50} determination, using tofacitinib (**359**) as a reference inhibitor. A positive control, in which the kinase reaction proceeds without any inhibitor, is used to define maximal activity, while a negative control lacking both JAK3 and inhibitor serves to assess background signal. Phosphorylation of the tyrosine residues is detected via a peroxidase-conjugated anti-phosphotyrosine antibody. This antibody not only binds the phosphorylated substrate but also catalyzes the conversion of the redox dye 3,3',5,5'-tetramethylbenzidine (TMB) into a colored product upon addition of hydrogen peroxide, enabling quantitative analysis via absorbance measurement.

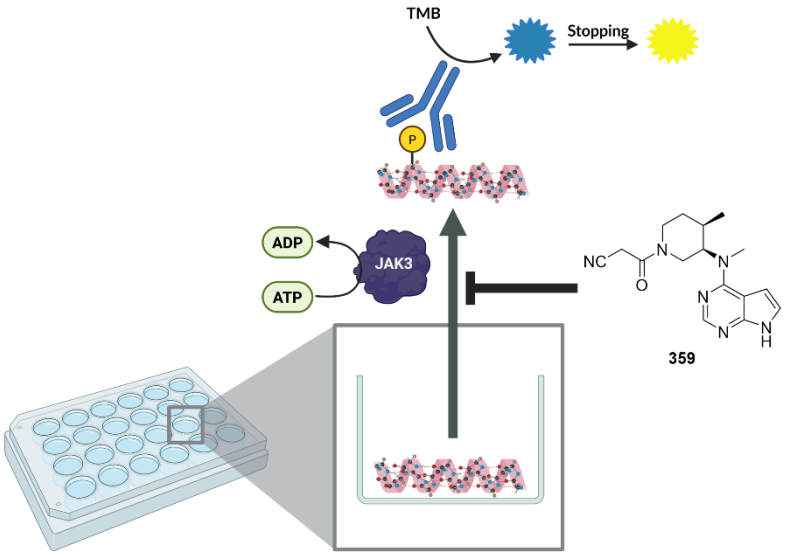

Figure 21: Schematic depiction of the JAK3-ELISA developed by SILKE BAUER.[141] This representation shows tofacitinib (**359**) as the inhibitor. Graphic was created using BioRender.com.

The assay workflow begins with the immobilization of the synthetic polypeptide substrate onto the walls of a well plate by incubating a stock solution of the substrate at 4 °C for 17 hours. Following adsorption, nonspecific binding sites are blocked by treatment with a blocking buffer. The kinase reaction is initiated by adding a mixture of JAK3 and ATP, along with the compound

under investigation or the reference inhibitor tofacitinib (both dissolved in DMSO), to the wells. After incubation for one hour at 37 °C, the reaction is terminated by washing off the reaction mixture. Subsequently, a peroxidase-conjugated anti-phosphotyrosine antibody is added to detect phosphorylated tyrosine residues and incubated for one hour at 37 °C, followed by another washing step. Detection is carried out by adding a hydrogen peroxide-containing TMB reagent, which is incubated for five minutes in the dark. This reaction yields a blue-colored product that is converted to yellow by the addition of 1 M sulfuric acid, thereby stopping the reaction. The absorbance is then measured at 450 nm, and the resulting signal correlates with the degree of substrate phosphorylation and, thus, JAK3 activity. To ensure assay reliability, the substrate is used in excess at ATP concentrations near the K_m value so that kinase activity is influenced solely by the presence of the inhibitor and not limited by the availability of substrate. Moreover, a linear correlation between the absorbance values and the kinase activity is essential for accurate interpretation of inhibitor potency.

It is important to note that determination of IC_{50} values for covalent inhibitors after a set time simultaneously encompasses contributions from both reversible and irreversible binding. While it is common to utilize this value for noncovalent inhibitors, the comparison between irreversible agents based on this value is not as accurate since the formation of the covalent bond is a time-dependent process, rendering also IC_{50} values time-dependent.[25] Nevertheless, as the determination of kinetic parameters is a more complicated and less established process, IC_{50} values can be and often are used to gain first insights into binding. Unfortunately, most of the compounds did not display inhibitory activity toward JAK3 during the time frame of the assay (**Table 2**). The only compound that showed nanomolar potency (IC_{50} = 26 nM) was compound **80**, which contains a sulfonyl fluoride warhead in the *meta*-position. For both unsubstituted fluorosulfate-bearing compounds **34** and **35** an IC_{50} value > 1 µM was determined, but all other compounds did not show any inhibition in this assay format.

Table 2: Inhibitory activity of JAK3 inhibitors as determined by the previously described ELISA assay. At high concentrations of the inhibitors, Cremophor® EL had to be added to ensure solubility of the compounds. n/a: No inhibitory activity could be observed. IC_{50} estimation was based on 4-point triplicate measurements with 10-fold dilution steps starting from 10 µM.

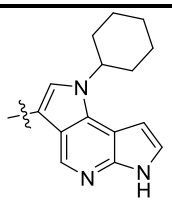

Structure	#	IC_{50} [nM]
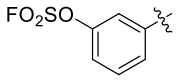	**34**	1432
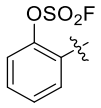	**35**	1076
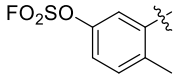	**36**	n/a
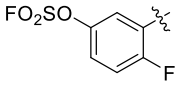	**61**	n/a
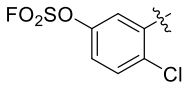	**62**	n/a
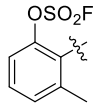	**63**	n/a
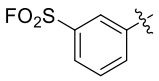	**80**	26
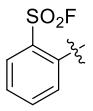	**81**	n/a
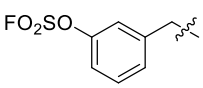	**100**	n/a

4.1.2. Intact Protein MS and X-ray Crystallography of Putative JAK3 Inhibitors

To validate potential covalent interactions, intact protein MS experiments (3-fold excess of compound over JAK3, 4 °C, 24 h) were conducted by APIRAT CHAIKUAD in the KNAPP group (Institute for Pharmaceutical Chemistry, Structural Genomics Consortium, Goethe University, Frankfurt) in order to assess whether covalent bond formation with the target had occurred. However, no mass shift indicative of covalent modification was detected, suggesting that none of the tested compounds was able to form a covalent bond with JAK3. It was hypothesized that, although inhibitor **80** exhibits nanomolar inhibitory activity, it is likely oriented similarly to the noncovalent design template **33**, in which the nitrile group is directed away from the target tyrosine residue. As a result, the electrophilic warhead is presumed to be solvent exposed rather than positioned toward the hinge region containing the reactive tyrosine.

This hypothesis was confirmed by solving the X-ray crystal structure of compound **80** in complex with JAK3 (**Figure 22**, PDB: 9R5Z). The experiment was performed by APIRAT CHAIKUAD and GUIQUN WANG of the KNAPP group. The structure revealed that no covalent bond formation occurs, as **80** indeed adopts an analogous orientation as compound **33**. The same expected hydrogen bonds of the azaindole core to the backbone of hinge residues Glu903 and Leu905 could be observed and the cyclohexyl group is arranged in a similar chair conformation located in a hydrophobic region in the center of the ATP pocket. As mentioned above, this confirms that the warhead is indeed solvent-exposed and oriented away from Tyr904 and thus rendered inaccessible for covalent bond formation.

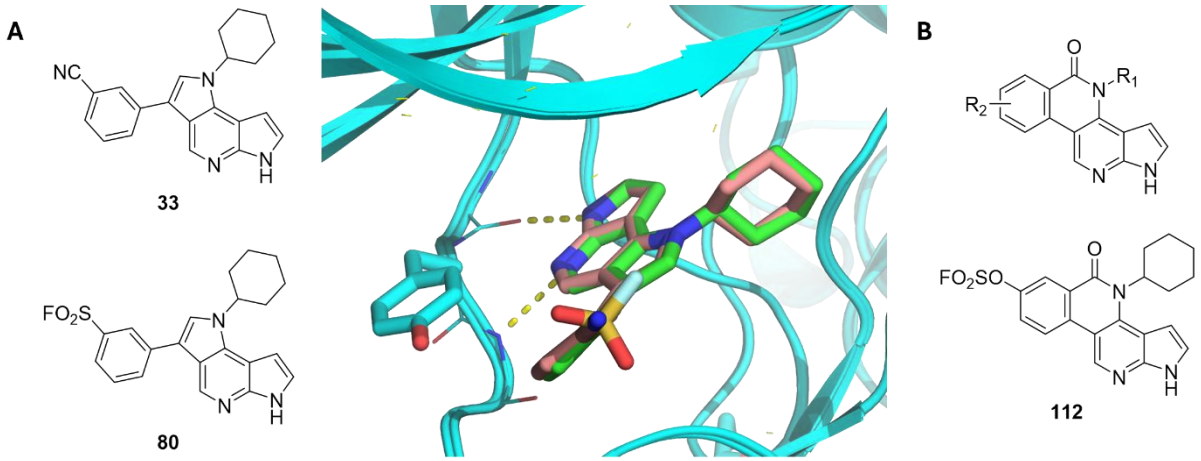

Figure 22: A Structures and overlay of noncovalent design template **33** (salmon) and sulfonyl fluoride-bearing inhibitor **80** (green, PDB: 9R5Z) in JAK3. The overlay shows a very high overlap of the two compounds. **B** BPN structures of ELSAYED *et al.*[123] (top) and tetracyclic, rigidized fluorosulfate compound **112** (bottom).

4.1.3. Rigidization Approach of Putative JAK3 Inhibitors

To position the warhead correctly, the rigidization strategy outlined in chapter 3.1.6 was subsequently employed. As previously mentioned, this approach was based on the work of ELSAYED *et al.,*[123] who reported a synthetic procedure to access a series of tetracyclic benzo[*c*]pyrrolo[2,3-*h*][1,6]naphthyridin-5-ones (BPNs) developed as JAK inhibitors. The tetracyclic inhibitor synthesized during this project, **112**, was then tested in the ELISA assay, but also failed to demonstrate any inhibition (in the same assay setup as mentioned above, see **Table 2** for details).

Since this project was meant as a proof-of-concept study to covalently address a tyrosine via fluorosulfates (or sulfonyl fluorides), the approach was dropped in favor of the MK2 project (*vide infra*). The cause of this lack of success could not be attributed to a single definitive factor; however, several plausible explanations have been proposed. The absence of a basic residue in vicinity of Tyr904 may hinder covalent targeting, as basic side chains are thought to facilitate phenol deprotonation and thereby enhance its reactivity.[22,142] Furthermore, the limited flexibility of the tyrosine side chain places increased importance on achieving an optimal pre-orientation of the electrophilic warhead. Although various geometric configurations were explored in this project, it remains plausible that none successfully aligned the warhead for effective covalent bond formation. In particular, the rotational flexibility of the warhead-bearing aryl group in the tricyclic compounds appears to compromise effective positioning, as evidenced by the obtained crystal structure. While a rigidization strategy was employed to address this issue, it simultaneously reduced the ability to fine-tune the direction and angle of warhead presentation and may lead to steric clashes. Although further optimization around compound **112** might have been feasible to achieve covalent modification, the approach was ultimately discontinued due to the substantial synthetic effort required and the limited success achieved. Moreover, previous work within our group has suggested that covalent engagement of the GK+2 position can be inherently challenging,[129] necessitating a precise “U-shaped” inhibitor conformation that can be difficult to realize with this scaffold.

4.2. Evaluation of Putative MK2 Inhibitors

4.2.1. Reaction Biology HotSpot™ Kinase Assay for Putative MK2 Inhibitors

Initially, the IC_{50} values of the putative MK2 inhibitors were determined by Reaction Biology Corp. at their site in Malvern, PA, USA. Their HotSpot™ kinase assay is a radioactive assay format that is based on the transfer of ^{33}P-labelled phosphate from ATP to the kinase substrate. The advantage of such a radiometric assay is the fact that they directly measure enzyme

activity – the catalytic product (the phosphorylated substrate) is directly detected. This way, false positives and negatives, which occur in indirect formats of detection, can typically be avoided. Importantly, this format does not only allow for detection of ATP-competitive inhibitors, but also allosteric ones as were synthesized in this project. The relative amount of phosphorylated substrate, compared to a reference sample, serves as an indicator of the percentage of inhibition and is plotted against varying inhibitor concentrations. The IC_{50} value is subsequently derived as the concentration corresponding to half-maximal inhibition, based on the fitted dose–response curve.

The protocol by Reaction Biology is performed as follows:[143]

(1) The substrate (peptide [KKLNRTLSVA] in the case of MK2) is added to the buffer, followed by the necessary cofactors (excluding ATP) and the respective kinase (for MK2: residues 1 – 370, untagged).
(2) In the initial noncompetitive phase, the putative inhibitor is added and incubated at rt for 20 min.
(3) Subsequently, in the competitive phase, ^{33}P-ATP (10 µM) is added and incubated at rt for 2 h.
(4) Excess ATP is removed by spotting onto P81 ion exchange filter paper and washing.
(5) Kinase activity is measured by a radiometric readout.

The three covalent inhibitors **120** (targeting Tyr225), **121** and **153** (both targeting Tyr264), the unreactive analogs **168** and **172** as well as the noncovalent design template by HUANG *et al.*,[124] **119**, were all tested in this assay format in a 10-dose IC_{50} mode with 3-fold serial dilution starting at 5 µM. Unfortunately, none of the compounds showed any inhibition in this assay format. This is especially surprising for reference compound **119** which according to the literature,[124] should display an IC_{50} of 110 nM. Given that IC_{50} values are inherently assay-dependent, minor variations between different experimental setups are expected; however, the magnitude of this discrepancy exceeds what can be attributed to such variability alone.

The assay used to determine the IC_{50} value of compound **119** in the literature was a dissociation-enhanced lanthanide fluorescent immunoassay (DELFIA). This is a technique that combines time resolved fluorescence (TRF) with the use of lanthanide chelates. The kinase reaction is carried out with a biotinylated substrate. Subsequently, the reaction mixture is transferred into a *capture plate* coated with streptavidin. After multiple washing steps, a europium-labeled antibody is added to detect phosphorylated substrate. To dissociate the europium ions into solution for detection, an enhancement solution is added. Components of this solution form highly fluorescent chelates with the europium ions, allowing for a fluorescence readout.[144] Even though this is a different readout format than in the Reaction Biology assay, there appeared to be no obvious reason why these two assays should give

such different results in inhibitory activity. A second, complementary assay was therefore carried out to validate the observed results.

4.2.2. AssayQuant Phosphosens® Kinase Assay for Putative MK2 Inhibitors

The second determination of IC_{50} values for the MK2 compounds was carried out by AssayQuant Technologies in their Phosphosens® assay format. In contrast to the radiometric readout at Reaction Biology, this protocol uses a fluorescence-based readout. The Phosphosens® assay is also a direct assay, circumventing complications observed in indirect assays. Furthermore, it is a continuous format that measures initial reaction rates without assumptions of linearity. The technique uses the sulfonamido-oxine (Sox) fluorophore which is covalently attached in close proximity (± 2 – 5 residues) to the Ser/Thr/Tyr phosphorylation site.[145] This fluorophore, developed by the IMPERIALI lab,[146] is relatively small, reducing steric hindrance, is neutral and only nominally hydrophobic, minimizing nonspecific binding. After phosphorylation of the substrate, magnesium ions, present in large excess, chelate between the Sox group and the newly added phosphate group, triggering fluorescence. This provides a direct signal (similarly as in the Reaction Biology assay, despite the different readout) of the phosphorylation state of the proximal hydroxyl group of the substrate. This is known as chelation-enhanced fluorescence (ChEF), which is directly proportional to the phosphorylation level, allowing real-time kinetic measurements.[147]

The protocol by AssayQuant is carried out as follows:

(1) The sensor peptide is added to the *master mix*, including reaction buffer and ATP (K_m).
(2) Inhibitor dilutions are added.
(3) Plates are sealed and incubated at 30 °C for 5 min to equilibrate the plate.
(4) The kinase (MK2: residues 1 – 400, N-terminal GST tag) is added in the enzyme dilution buffer.
(5) Kinase activity is monitored at 30 °C for 120 min by collecting fluorescence intensity readings.

This presents the setup of the assay when run without preincubation. When a 60 min preincubation step is added, ATP is only added after that step. In this case, the 11-point serial dilution started at 10 µM and (putative) covalent inhibitors **120**, **121** and **153** were tested as well as design template **119** (**Figure 23**). Regardless of the preincubation step, the covalent compounds again did not show any inhibitory activity. The noncovalent analog **119** displayed only weak activity, still showing a large discrepancy to the reported literature value.[124] In both assays performed here, those findings of an IC_{50} = 110 nM could not be recreated. Notably,

the literature construct consisted of residues 46 – 400 with an A399G mutation and an N-terminal GST tag, whereas the constructs used here spanned residues 1 – 370 (untagged, RBC assay) and 1 – 400 (N-terminal GST tag, AQ assay) without the mutation. These differences in construct design may contribute to the observed discrepancies in inhibitor potency, alongside other factors such as e.g. the phosphorylation state.

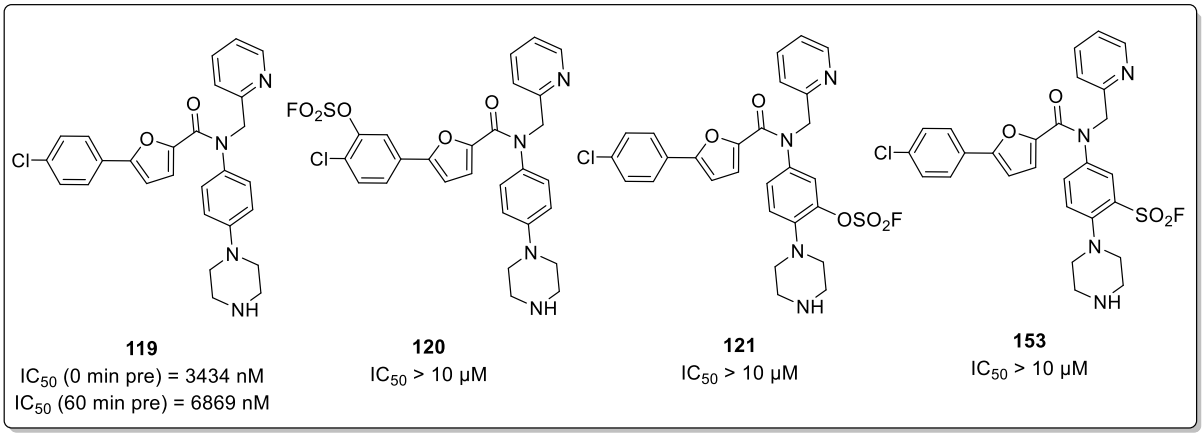

Figure 23: Compounds tested in the Phosphosens® kinase assay at AssayQuant. pre = preincubation. For the covalent agents, the IC_{50} values were above 10 µM regardless of preincubation.

4.2.3. Intact Protein MS of Putative MK2 Inhibitors

Nevertheless, further investigation into the covalent binding characteristics of the compounds was conducted, as it was anticipated that covalent binding might still occur despite a lack of catalytic inhibition. Given that fluorosulfates and sulfonyl fluorides are known to exhibit relatively slow rates of covalent modification, it is plausible that the assay duration was insufficient to detect such binding events. This possibility was further supported by the weak activity observed with the known allosteric ligand **119** in the employed assay system.

Consequently, intact-protein MS analysis was performed, initially by GUIQUN WANG in the KNAPP group. Results were validated by BENEDIKT MASBERG from the LÄMMERHOFER lab (Institute of Pharmaceutical Sciences, Eberhard Karls University, Tübingen). Encouragingly, moderate to high levels of covalent bond formation with MK2 were observed for several compounds (**Figure 24**) within a relatively short incubation period (5-fold excess of compound over MK2, rt, 3 h), especially when compared to previously reported experiments involving fluorosulfates and sulfonyl fluorides.[61,69,70,148] While no covalent binding was detected for compound **121** (bearing a fluorosulfate adjacent to the piperazine), 15% covalent modification was observed for compound **153** (the sulfonyl fluoride analog), and compound **120** (bearing a fluorosulfate adjacent to the chloride) achieved an impressive 95% covalent binding to MK2 under the experimental conditions.

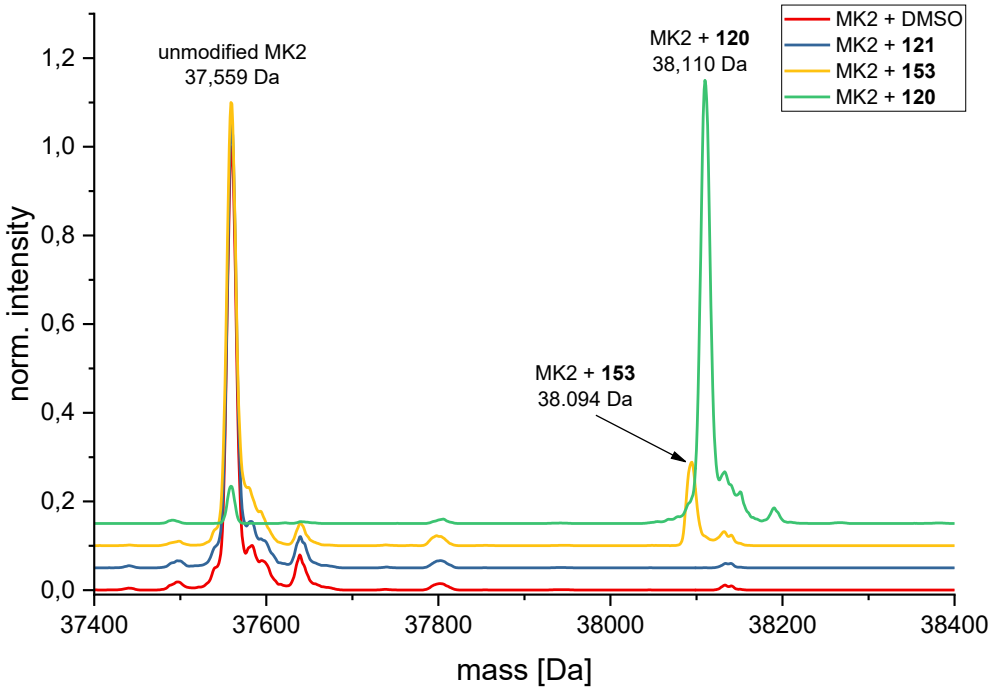

Figure 24: Intact protein MS experiments between MK2 (red, DMSO was added as a control) and the three different covalent inhibitors (**120**, green; **121**, blue; **153**, yellow). The depiction was adapted from a figure by BENEDIKT MASBERG published in a paper[109] during the course of this PhD.

4.2.4. X-ray Crystallography of MK2 Binders

To determine the exact binding site of the compounds, co-crystallization experiments were carried out by GUIQUN WANG in the KNAPP lab. Attempts to crystallize a bound complex of **153** and MK2 were unsuccessful, likely due to the only moderate covalent modification. Experiments with the most efficient binder, compound **120**, however, yielded an X-ray crystal structure (**Figure 25**, PDB: 9R59). Unexpectedly, compound **120** was not found to bind within the allosteric pocket but instead occupied the ATP binding site, where it formed a covalent bond with the “catalytic” lysine residue, Lys93. The limited activity observed in enzymatic assays, despite this orthosteric binding mode, may be attributed to the typically slow inactivation kinetics of fluorosulfates, which might be insufficient to overcome a relatively weak noncovalent affinity within the timeframe of the assay and under ATP-competitive conditions. Supporting this, the measured k_{inact}/K_I value of 1.12 $M^{-1}s^{-1}$ (**Figure 26**) reflects a low intrinsic reactivity of the covalent warhead, limiting the compound’s ability to effectively inactivate the target enzyme under these conditions. Although this outcome was not anticipated, the resulting crystal structure is of considerable interest due to its revelation of an uncommon binding mode. Notably, only a few examples have been reported[77] in which a fluorosulfate forms a covalent bond with a kinase, regardless of the specific target residue. In addition to the covalent interaction, the hinge-binding behavior of the compound is noteworthy, particularly because

the molecule was not designed for orthosteric engagement and lacks a traditional hinge-binding motif. Instead, the carbonyl oxygen of the amide moiety forms a hydrogen bond with the backbone amide NH of Leu141, resembling the hinge interaction observed for skepinone-type inhibitors of the upstream kinase p38α,[149] albeit without the peptide flip characteristic of the latter.

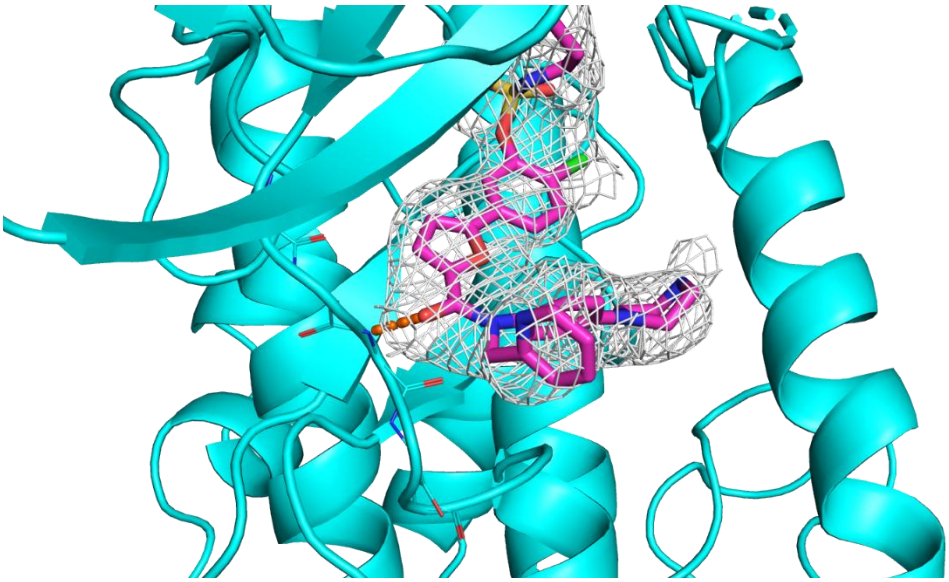

Figure 25: X-ray co-crystal structure of compound **120** (pink) in complex with MK2 displaying the orthosteric binding mode and the covalent bond to the "catalytic" Lys93. The interactions between the carbonyl of **120** and Leu141 in the hinge region are depicted as orange dashes. The grey mesh is the unbiased omit map prepared by JASON STAHLECKER. For this depiction, residues Val78 – Lys84 were deleted.

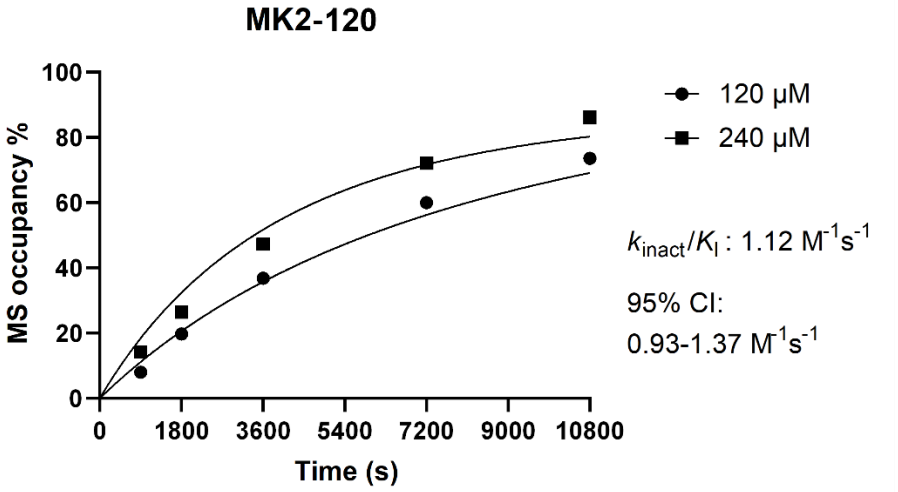

Figure 26: Determination of k_{inact}/K_I conducted by GUIQUN WANG showcasing the slow inactivation kinetics of compound **120**. The figure was adapted from a figure by GUIQUN WANG published in a paper[109] during the course of this PhD.

4.3. Investigation of the Intrinsic Reactivity of Fluorosulfates

Several studies have examined the intrinsic reactivity of sulfur(VI) fluorides, with most focusing primarily on sulfonyl fluorides.[41,150] Other electrophilic warheads within this class, however, have been less frequently explored. For instance, researchers at AstraZeneca conducted a study[40] investigating the reactivity of sulfur(VI) fluorides with nucleophilic amino acid side chains under physiological conditions. Their work included over 20 aryl sulfonyl fluorides but only two aryl fluorosulfates. Similarly, a study by researchers at GSK[41] evaluated six aryl sulfonyl fluorides alongside a single fluorosulfate (and other congeners of this group). In both investigations, the fluorosulfates exhibited remarkable hydrolytic stability and showed no reactivity toward nucleophilic amino acids at neutral pH.

Consequently, a preliminary investigation was conducted to examine this phenomenon more closely. Three different aryl fluorosulfates, **360**, **361** and **362** were evaluated for their buffer stability and reactivity toward *N*-acetyl tyrosine. These three fluorosulfates were selected due to their distinct *para*-substituents, which exhibit varying electronic properties that consequently are expected to influence the reactivity of the fluorosulfate warheads, as illustrated in **Figure 27**.

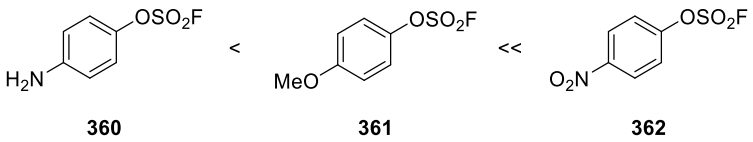

Figure 27: Aryl fluorosulfates studied for their stability and intrinsic reactivity toward *N*-acetyl tyrosine as a nucleophile. They are ranked here according to their reactivity toward nucleophiles, which is determined by their electronic properties.

At pH 8 (PBS buffer), all three molecules remained stable throughout the 13.5-hour experiment, showing no evidence of hydrolysis. While this stability was encouraging, a similar trend was observed in their reactivity toward *N*-acetyl tyrosine – no reaction with the nucleophile was detected. In line with the study conducted by GILBERT *et al.*,[41] the experiment was subsequently repeated at pH 10 using a carbonate-bicarbonate buffer. Under these conditions, the expected reactivity trend emerged: the least reactive compound, **360**, exhibited a half-life of 4.8 hours in buffer containing *N*-acetyl tyrosine, where competing reactions with both the buffer and the tyrosine surrogate occur. Compound **361** showed a half-life of 2.5 hours under the same conditions. For the most reactive analog, **362**, no half-life could be determined, as the compound underwent complete decomposition in the buffer alone within just 4 hours. Although these results confirmed the anticipated reactivity order, the reaction rates at this elevated pH were exceedingly rapid, thereby limiting the ability to resolve subtle differences among more closely related analogs.

The pK_a value of the tyrosine side chain in its free amino acid form is approximately 10.[81] While this value is well established and readily measurable in solution, the pK_a of tyrosine residues within proteins can vary significantly due to the local chemical environment. Studies have demonstrated that tyrosine pK_a values in proteins can range from as low as ≈ 6.1 to as high as ≈ 12.5,[151,152] reflecting the influence of factors such as hydrogen bonding, solvent accessibility, and electrostatic interactions within the protein matrix. Given the limited insight obtained from pH variation – where no reactivity was observed at pH 8 and reactions proceeded too rapidly at pH 10 – an alternative approach was adopted. To better reflect the variability in tyrosine sidechain pK_a values observed in protein environments, the experiment was repeated at pH 8 using a series of tyrosine mimetics with differing pK_a values as depicted in **Figure 28**.

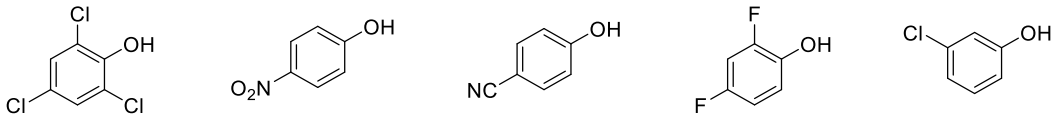

363 pK_a = 6 | **364** pK_a = 7.2 | **365** pK_a = 7.9 | **366** pK_a = 8.5 | **367** pK_a = 9

Figure 28: Tyrosine „mimetics“ used in stability and intrinsic reactivity studies. The pK_a values depicted here were accessed from http://ibond.nankai.edu.cn/ in May of 2023.

Despite the rationale behind using tyrosine mimetics with varying pK_a values, these compounds also exhibited negligible to no reactivity with the aryl fluorosulfates under the tested conditions. While it might have been possible to further explore pH values in the intermediate range – such as around pH 9 – this was ultimately not pursued. Such conditions raise questions about physiological relevance and may not accurately reflect the complex microenvironments found within proteins. Attempting to artificially construct an experimental environment optimized for observing reactivity could have introduced conditions that no longer faithfully represent the biochemical context, thereby limiting the translatability of the findings. Moreover, the previously mentioned studies on sulfonyl fluorides[41,150] have shown that trends observed in simple solution-phase experiments do not always translate to protein systems, where steric constraints, local polarity, and structural context can override purely electronic considerations. Taken together, these findings support the conclusion that, while the experimental approach was conceptually sound, additional efforts along the same line were unlikely to yield significantly more insight without transitioning to a protein-based system.

4.4. Biophysical Evaluation of the Covalent-First Approach

4.4.1. Selection of Target Kinases

By June 2025, X-ray crystal structures for 326 distinct kinases were documented in the kinase-ligand interaction fingerprints and structure (KLIFS) database.[153] At the beginning of this part of the doctoral project, in spring of 2024, structures of 277 kinases were available. To identify the kinases suitable for the proposed covalent-first approach, it was necessary to narrow down the original pool (**Figure 29**). The initial steps of this were carried out by INA PÖHNER of the POSO group (School of Pharmacy, University of Eastern Finland). A script was developed that screened the protein data bank (PDB) for all kinases that met the following requirements: **(1)** the binding pocket features a tyrosine residue; and **(2)** a basic lysine or arginine functionality is within max. 6 Å of the tyrosine hydroxyl oxygen. Through this script, the number of kinases could be narrowed down from 277 to 126. This number was then further reduced through manual selection. To this end, the list was first screened for structures that might be “artifacts” because the respective tyrosine (or basic residue in proximity) was not naturally present but a mutation. After these were removed from the list, the structures of the other kinases were investigated more closely through evaluation of the structures in PyMOL. 13 of the structures included a tyrosine in the GK+2 position with an arginine close by while 14 structures possessed a tyrosine in this position with a lysine in proximity. In general, when targeting a tyrosine residue, the presence of a nearby arginine is preferred, as the warheads employed here can also bind to lysine. Nonetheless, at this stage, both residue types were retained in the selection. Furthermore, five kinases with a histidine in the GK+2 position were selected, as sulfur(VI) fluorides are also able to target histidine. Finally, an additional 10 kinases were selected from the list, each containing a tyrosine residue located elsewhere within the binding pocket at an accessible position. The remaining kinases were excluded from the list because their tyrosine residues were either deeply buried or positioned too far from the hinge region to be reached by the fragment-like molecules used in the covalent library. In total, this approach led to the selection of 42 kinases. These were then further filtered down to 28 kinases together with collaboration partners JONATHAN ELKINS and ELEANOR WILLIAMS (Centre for Medicines Discovery, Nuffield Department of Medicine, University of Oxford). This selection was based on an evaluation of the proteins available within their groups or the established protein expression systems in their laboratories, as the subsequent research described in the following chapters was conducted during a research stay in their labs in Oxford.

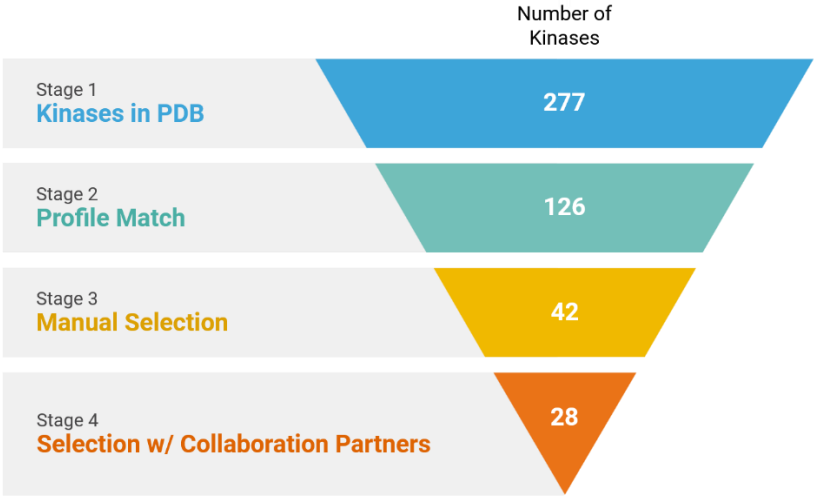

Figure 29: Selection process for kinase library. **Stage 1:** At the time of the selection process, 277 distinct kinases had corresponding available structures. **Stage 2:** 126 kinases matched the profile description set on the onset of the project. **Stage 3:** 42 kinases were selected manually based on the location and accessibility of the tyrosine. **Stage 4:** 28 kinases were finally nominated based on their availability in the group of the collaboration partners in Oxford. Graphic was created using BioRender.com.

4.4.2. Protein Expression of Selected Kinases

At the outset of the research stay in Oxford, recombinant protein production was carried out using a bacterial expression system (**Figure 30**). The process began with a plasmid vector encoding the gene of interest that was stored in *E. coli* MACH1 cells. The respective constructs and plasmids had been designed and produced before in the groups of JONANTHAN ELKINS and ELEANOR WILLIAMS. Following plasmid isolation, which was carried out through commercially available Miniprep Kits, the construct was transformed into Rosetta competent cells to enhance expression of eukaryotic proteins. These cells are specialized bacterial cells that have been engineered to easily take up foreign DNA from their surroundings. Transformed cells were plated, incubated, and selected colonies were gradually expanded in antibiotic-containing media. After growing colonies in a Petri dish (step I, **Figure 30**), they were picked and first grown overnight (step II) in a small volume of media. In the next step, they were transferred into their final, larger volume of media (step III). Protein expression was induced using isopropyl β-D-1-thiogalactopyranoside (IPTG, this removes a repressor from the lac operon to induce gene expression) after cultures reached an appropriate optical density, and cells were subsequently harvested by centrifugation. Cell lysis was performed via sonication. Polyethyleneimine (PEI) was added subsequently to remove nucleic acids. The resulting lysate underwent an initial purification by immobilized metal ion affinity chromatography (IMAC), exploiting a His-tag engineered into the protein. After TEV protease cleavage to remove the

His-tag and a second round of reverse IMAC, the sample was concentrated and subjected to size-exclusion chromatography to achieve final purification.

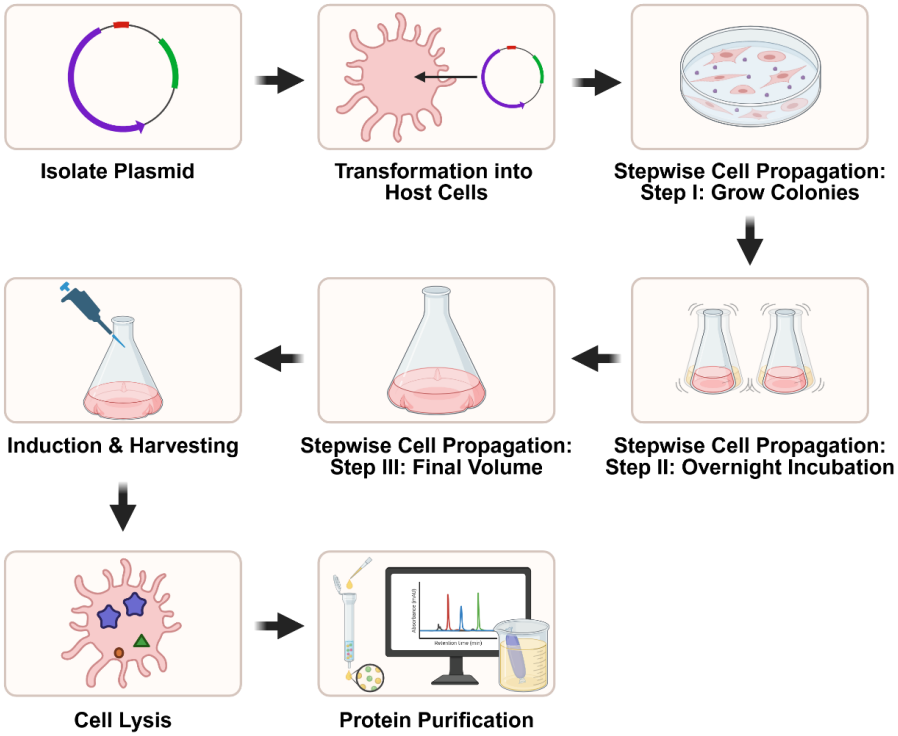

Figure 30: Schematic depiction of protein expression and subsequent purification using a bacterial expression system. Graphic was created using BioRender.com.

Through this protocol, the five kinases CSNK2A1, CSNK2A2, BMP2K, MAPK1 and MAP2K1 were produced. Other kinases (GSK3B, AURKA, PAK3, VRK1, GSG2 and ZAK) were already available in the host groups. Two kinases (TGFBR1 and ACVR1) were obtained from WILLIAM SEATON-BURN from the BULLOCK lab (Centre for Medicines Discovery, Nuffield Department of Medicine, University of Oxford). TYK2, JAK3, NTRK1, CDK8, LIMK2, and BTK could not be obtained within the project's timeframe, as their expression requires a viral system (Sf9), which is considerably more time-consuming than bacterial expression. BRSK2 and CDK6 were ruled out after further investigation of the expression systems available. The expression and purification of the kinases STK17B, RPS6KA3, BMX, ULK1, NEK2, S6K1, and ATM were pursued using the described *E. coli* protocol but proved unsuccessful due to failures at various stages, either during expression or purification. The tyrosine residues targeted in this study are summarized in **Table 3**.

Table 3: Kinases that were tested for covalent modification against the covalent library described in chapter 3.3, and the location of the targeted tyrosine and the corresponding basic residue in proximity of this tyrosine are provided.

Kinase	Location of targeted tyrosine	Basic residue in proximity
CSNK2A1	GK+2 *(His, not Tyr)*	-
CSNK2A2	GK+2	Arg
BMP2K	GK+2	Arg
MAPK1	αC loop	Arg
MAP2K1	A-loop	Arg
GSK3B	GK+2	Arg
AURKA	GK+2	Arg
PAK3	GK+2	Lys
VRK1	αC loop	Lys
GSG2	αC loop	Lys
ZAK	GK+2	Arg
TGFBR1	αC loop	Lys
ACVR1	P-loop	Arg

4.4.3. Intact Protein MS of Covalent Library

The successfully obtained kinases were then tested in intact protein MS with the compounds described in chapter 3.3. To this end, the respective compounds and proteins were incubated (100 µM compound, 4 µM protein) at room temperature for 24 hours and then measured with a RapidFire mass spectrometry system to determine which compounds would show covalent binding to the proteins. Only modifications greater than 50 % are shown here. Although numerous additional hits showed modifications below 50 %, given the already extended incubation time, these were considered insufficiently promising to pursue further.

An opposing trend was observed for Aurora kinase A (AURKA), which was detected in a phosphorylated state (+80 Da indicating one phosphorylation; AURKA displayed multiple phosphorylation events). Notably, AURKA showed extensive modification upon treatment with several compounds, particularly the aminopyridine sulfonyl fluorides **181**, **182**, and **203** (**Figure 31**). The extent of modification was so pronounced that the unmodified protein (red trace) was

no longer detectable for any of these compounds. All three derivatives induced multiple modifications, suggesting unspecific binding. For compounds **181** (blue trace) and **203** (green trace), both singly and doubly modified species were observed. However, compound **182** (yellow trace) bound so readily and frequently that only species with up to four modifications were detected, with no clear evidence of a single modification event. As discussed previously, multiple modifications are indicative of unspecific interactions – the desired outcome being a complete, single-site modification without over-modification. Consequently, these compounds were not pursued further on this kinase.

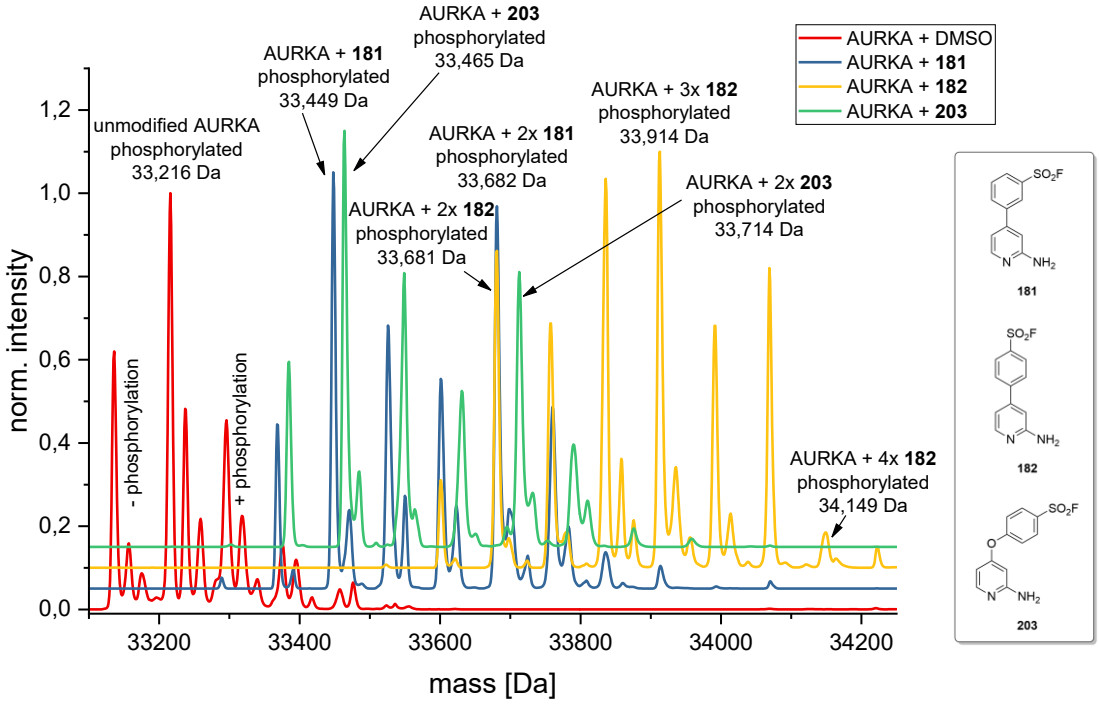

Figure 31: Intact protein MS experiments between AURKA (red, DMSO was added as a control) and the three different covalent inhibitors (**181**, blue; **182**, yellow; **203**, green). No other compounds showed covalent modification > 50 %.

In contrast, GSG2 (also known as Haspin) exhibited a single, well-defined binding event with azaindole sulfonyl fluoride **240** (blue trace, **Figure 32**). This compound modified the kinase nearly completely within the experimental timeframe, without evidence of a second binding event – representing the ideal modification profile. In addition to the phosphorylation-related mass shift (*vide supra*), the spectrum also revealed a distinct peak corresponding to a +23 Da increase, indicative of sodium ion adduction. Among all tested kinases, GSG2 was the only one to exhibit more than 50 % covalent modification by compound **240**, and it did so with a favorable modification pattern. As a result, this hit was selected for further investigation through X-ray crystallography (see chapter 4.4.4).

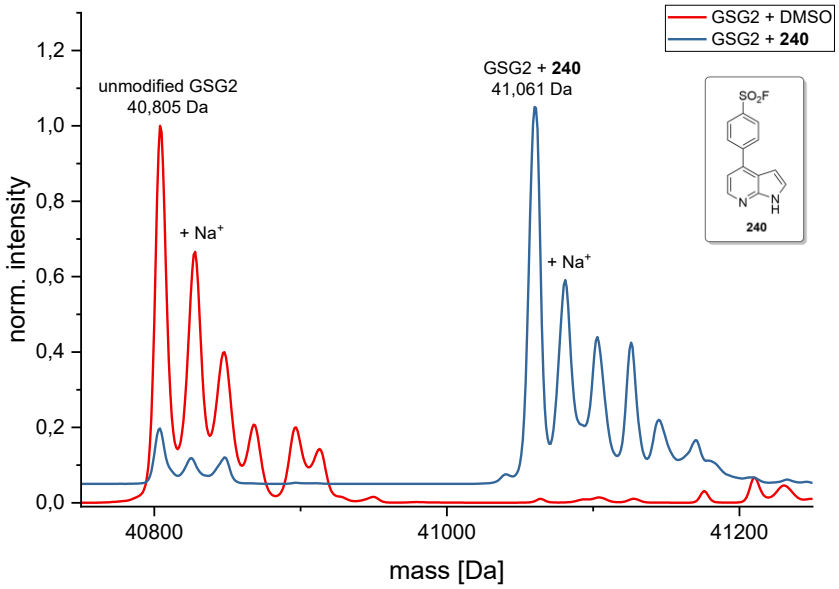

Figure 32: Intact protein MS experiments between GSG2 (red) and covalent compound **240** (blue). A small increment of +23 Da indicates addition of a sodium ion.

A comparable modification profile was observed for ZAK in combination with the ether-linked aminopyridine sulfonyl fluoride **203** (blue trace, **Figure 33**). The initial covalent modification appeared nearly complete; however, a second binding event was already detectable. Additionally, compound **203** exhibited significant reactivity with other proteins, suggesting limited selectivity. For these reasons, this kinase-compound pair was not pursued further in X-ray crystallography experiments.

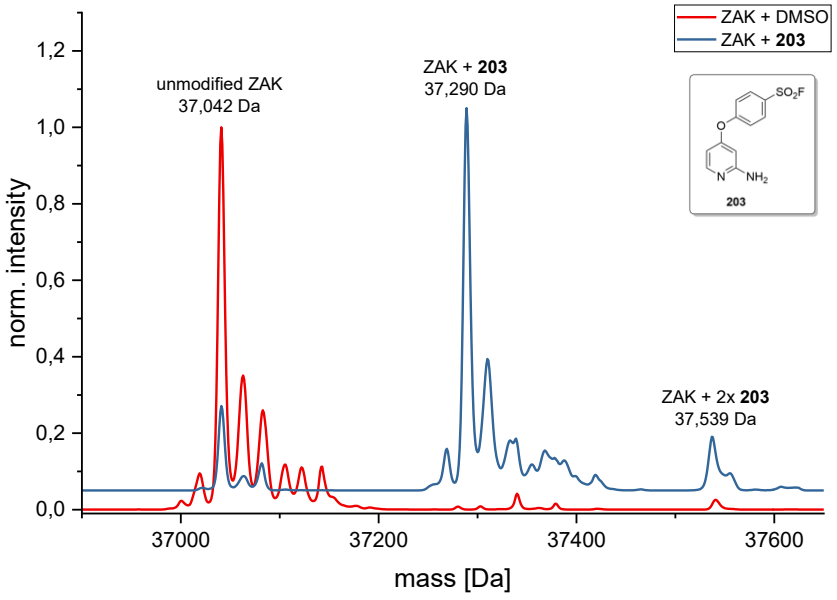

Figure 33: Intact protein MS experiments between ZAK (red) and covalent compound **203** (blue).

A slightly more favorable profile, characterized by the presence of only a single covalent modification, was observed for the combination of amide-linked azaindole fluorosulfate **286** (blue trace) with CSNK2A2 (**Figure 34**). Although the extent of this modification remained moderate – exceeding 50% but falling short of complete modification – no evidence of a second binding event was detected over the course of the experiment. Notably, compound **286** features a geometric configuration that could plausibly reach the target tyrosine residue in CSNK2A2, located at the GK+2 position. If appropriately oriented, **286** may adopt the "U-shaped" conformation required for this interaction. Given that CSNK2A2 belongs to the *dark kinome*[154] and the compound-protein pair exhibited a promising binding profile, this combination was included in subsequent X-ray crystallography experiments. The compound was considered a solid starting point, with the potential for further structural optimization to enhance the so far moderate covalent engagement. It also did not engage in any significant modification with any other kinases.

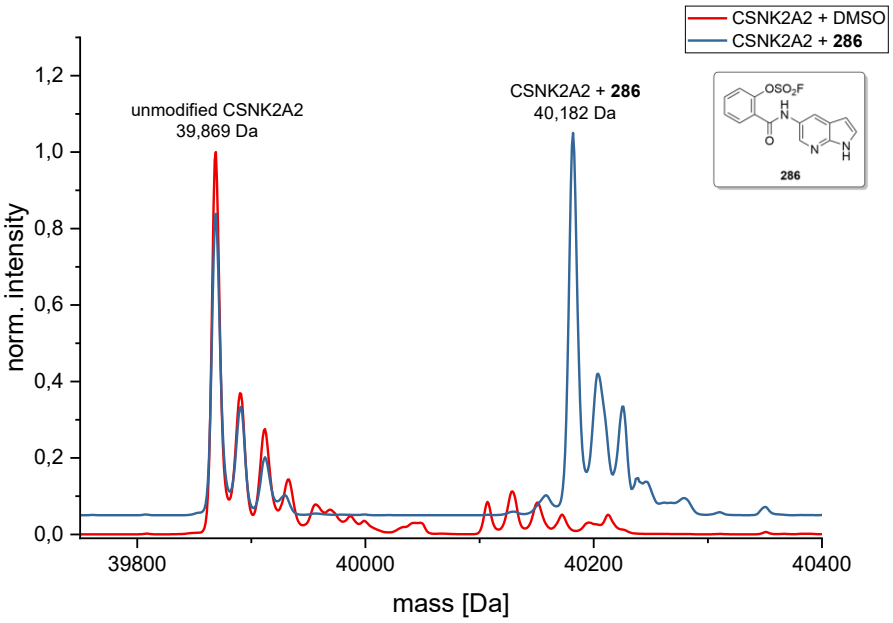

Figure 34: Intact protein MS experiments between CSNK2A2 (red) and covalent compound **286** (blue).

MAPK1 was among the kinases that exhibited substantial covalent modification, with several compounds achieving labeling efficiencies reaching at least 50 % (**Figure 35**). The most pronounced single modification was observed with compound **239** (green trace), which resulted in nearly complete covalent labeling of the kinase. Compounds **181** (blue trace), **202** (yellow trace), and **283** (grey-blue trace) also modified MAPK1, each achieving approximately 50 % single-site modification. However, all four compounds additionally showed a second, less pronounced modification event, suggesting possible nonspecific interactions. Despite this,

compounds **181** and **239** were selected for follow-up in X-ray crystallography experiments. This decision was based on the shared spatial orientation of their warheads relative to the hinge-binding region, which provided a unique opportunity to compare two distinct hinge binders with similarly positioned reactive groups. Additionally, compound **239** displayed a favorable selectivity profile, as it did not covalently modify any other kinase above 50 %, in contrast to **181**.

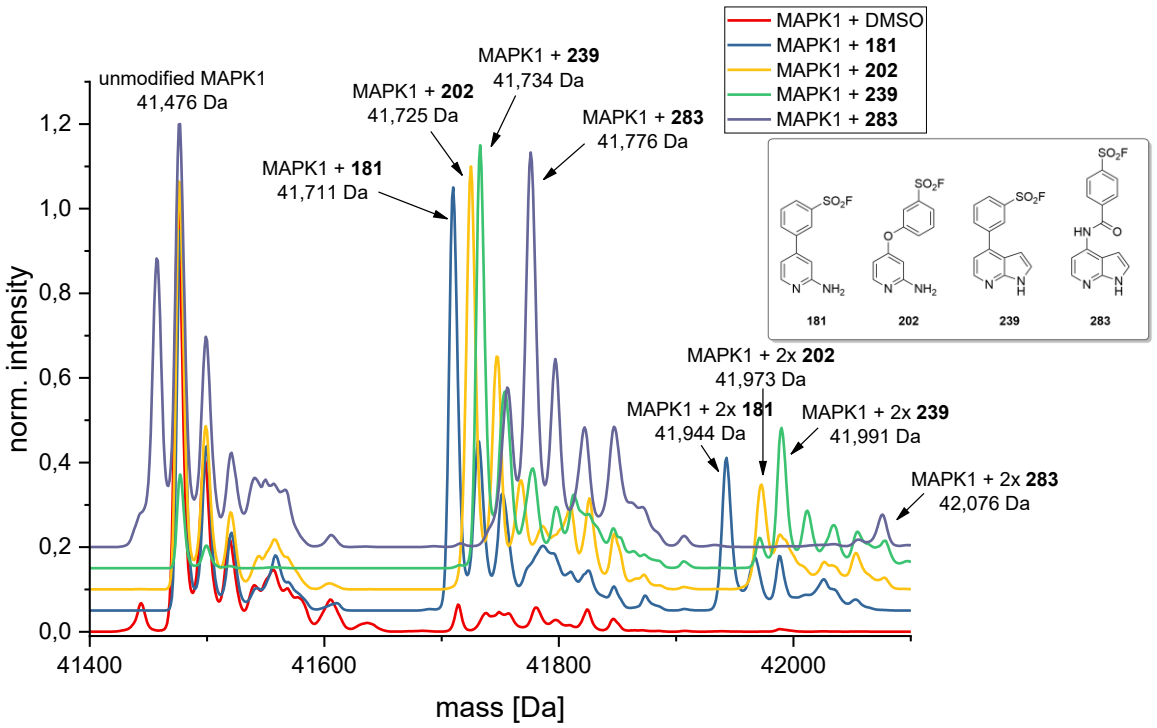

Figure 35*:* Intact protein MS experiments between MAPK1 (red) and the four different covalent inhibitors (**181**, blue; **202**, yellow; **239**, green; **283**, grey-blue).

Lastly, ACVR1 emerged as another kinase exhibiting significant covalent modification (**Figure 36**). Two compounds, **181** (blue trace) and **308** (yellow trace), demonstrated strong binding. While compound **181** modified ACVR1 substantially, it also showed a second, weaker modification peak. Moreover, this fragment was found to modify nearly all kinases tested in the screen to varying degrees, indicating a high level of nonspecific reactivity. As a result, **181** was not pursued further. In contrast, compound **308** represented one of the most promising and specific hits. It achieved near-complete single modification of ACVR1 and did not covalently bind to any other kinase in the panel. This selectivity, combined with its relatively large molecular size, made it particularly intriguing (especially because of the long linker), as the targeted tyrosine in ACVR1 is located within the P-loop – a region requiring a more extended molecule to be reached effectively. Additionally, **308** is one of the few fluorosulfate-containing hits, a class of warheads known for their potential selectivity and favorable drug-like properties.

Based on these combined factors, ACVR1 in complex with **308** was selected for follow-up in X-ray crystallography experiments.

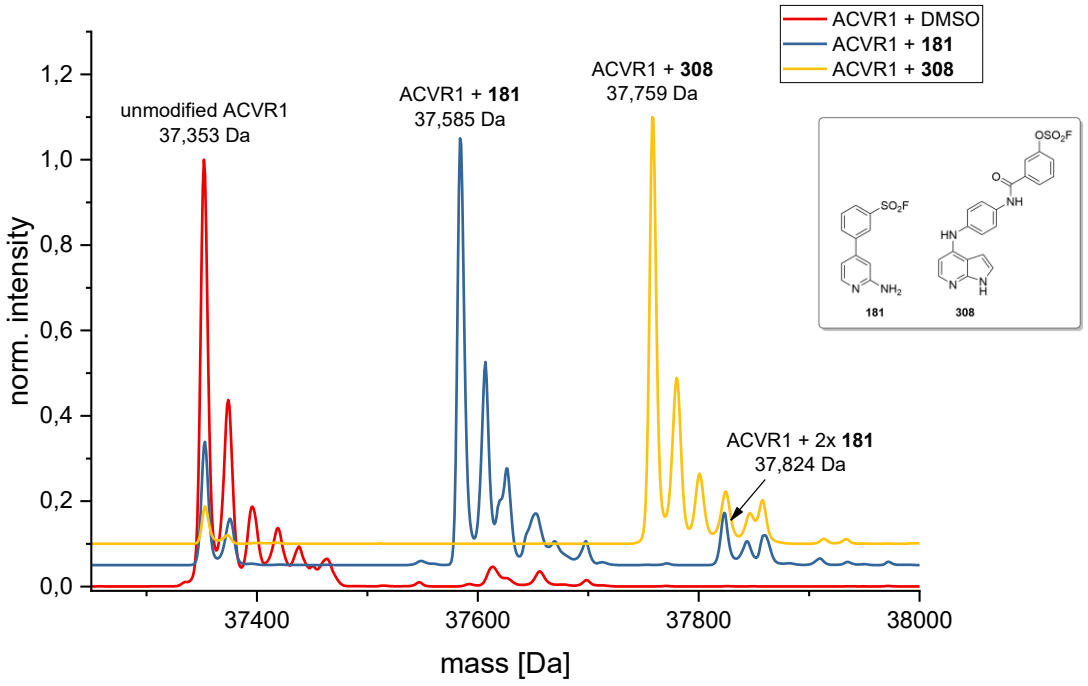

Figure 36: Intact protein MS experiments between ACVR1 (red) and the two different covalent inhibitors (**181**, blue; **308**, yellow).

4.4.4. X-ray Crystallography for Selected Hits

As detailed in the previous chapter, crystallization plates were prepared for CSNK2A2 with compound **286**, MAPK1 with compounds **181** or **239**, respectively, GSG2 with molecule **240** as well as ACVR1 with compound **308**. For the initial crystallization trials, *coarse screening* approaches were employed for the first three proteins, as their optimal crystallization conditions were not yet established. In such cases, it is advisable to explore a broad range of conditions to identify suitable starting points for further optimization. In contrast, for the final protein, ACVR1, previously established *fine screening* conditions were available and were therefore utilized directly. In addition to the crystallization conditions themselves, the success of crystallization is often highly dependent on the specific protein construct used. For both CSNK2A2 and MAPK1, the initial crystallization attempts did not yield any crystals.

For GSG2, on the other hand, crystals formed very rapidly even under the coarse screening conditions. The intended target was Tyr580 in the αC loop; however, the crystal structure (**Figure 37**) revealed that compound **240** instead binds to the “catalytic” lysine of GSG2, Lys511. The structure clearly showed that compound **240** is too short to reach Tyr580 and that the orientation of the warhead vector is likely incorrect. While the compound formed the

expected interactions with Gly608 and Gly609 in the hinge region, no additional significant contacts with the protein were observed. Given that this lysine is conserved across the entire kinome, this hit was not pursued further. Nevertheless, it provides an interesting proof of concept that this lysine can be consistently targeted via sulfur(VI) fluoride chemistry (compare with the MK2 crystal structure in chapter 4.2.4). Moreover, compound **240** selectively modified only GSG2 within this small kinase panel, despite being a relatively small molecule not specifically designed for this target. This tentative selectivity suggests that exploiting this conserved lysine as a covalent modification site could enable the development of covalent inhibitors that are resistant to mutation of the target residue, while still maintaining selectivity across the kinome despite the residue's high conservation.

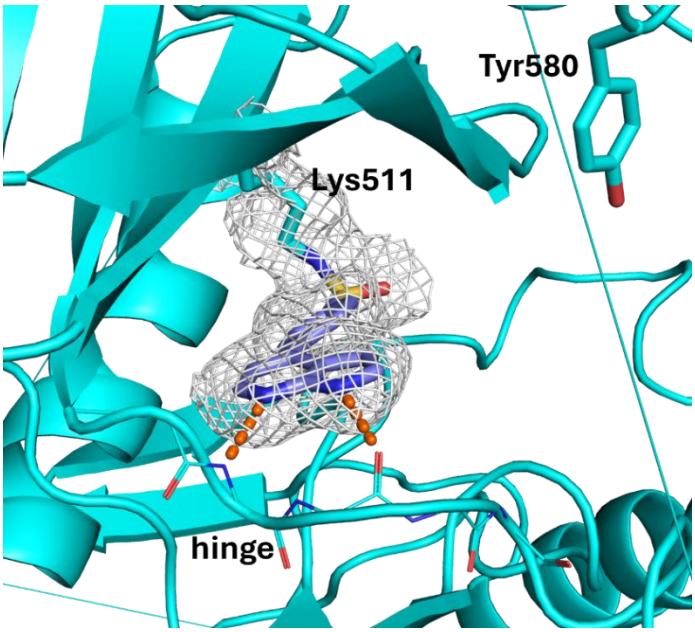

Figure 37: X-ray co-crystal structure of compound **240** (dark blue) in complex with GSG2. Noncovalent interactions to the hinge region are depicted as orange dashes. The grey mesh is the unbiased omit map prepared by JASON STAHLECKER.

The ACVR1 complex likewise yielded a high-quality crystal structure, providing valuable insights into the binding mode of compound **308**, revealing an unexpected mode of covalent engagement (**Figure 38**). While the design of **308** was aimed at targeting Tyr219, located in the P-loop of the kinase, the electron density unambiguously showed the formation of a covalent bond with Lys338, situated in the catalytic loop at the HRD+2 position. This lysine has not previously been reported as a site of covalent modification in any kinase. Notably, ACVR1 lacks a cysteine residue within the ATP-binding pocket,[28] the common nucleophilic target for covalent inhibitors, making non-cysteine-targeted strategies particularly valuable. To date, the only lysine that has been successfully targeted through sulfur(VI) fluoride chemistry in kinases has been the canonical "catalytic" lysine.[76] Compound **308** retains the expected noncovalent

interactions within the active site: its azaindole hinge-binding motif forms hydrogen bonds with His284 and His286. The amide carbonyl engages in a polar interaction with Tyr219, the original design target. Additionally, an interaction between Thr378 and one of the sulfonyl oxygens of the fluorosulfate warhead is observed, potentially stabilizing the covalent adduct with Lys338, as previously suggested in the context of sulfonyl fluoride-based inhibitors.[155] This structure represents both the first covalent inhibitor of ACVR1 and the first reported instance of lysine targeting via sulfur(VI) fluoride chemistry beyond the “catalytic” lysine site in any kinase.

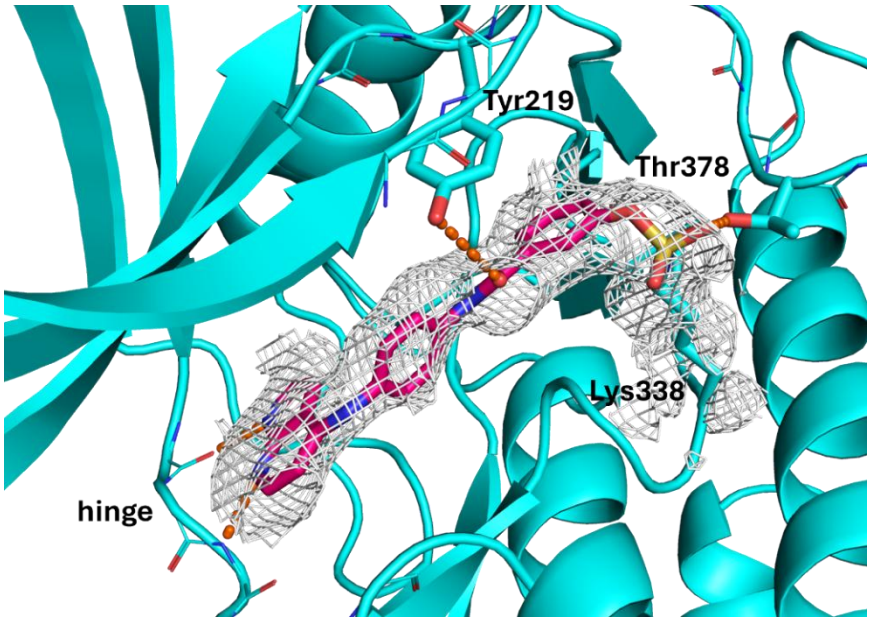

Figure 38: X-ray co-crystal structure of compound **308** (pink) in complex with ACVR1. Noncovalent interactions (to the hinge region and other residues) are depicted as orange dashes. The grey mesh is the unbiased omit map prepared by JASON STAHLECKER.

4.4.5. Efforts Toward Trypsin-Mediated Digestion of the Protein Adducts of Selected Hits

In parallel with the X-ray crystallography experiments, efforts were undertaken to identify the site of covalent modification via trypsin digestion. Trypsin is a serine protease that specifically cleaves peptide bonds at the carboxyl side of lysine and arginine residues. It is commonly used in protein analysis to determine the exact covalent binding site of a molecule by producing well-defined peptide fragments that can be analyzed using techniques like mass spectrometry.[156] While X-ray crystallography is generally seen as the best way to determine the exact binding site and mode, trypsin digest may be used in cases where crystallography fails or simply to validate the crystallography data in a less artificial setting.

Trypsin digestion protocols are widely available and generally applicable to sulfur(VI) fluoride chemistry,[75,76,148,157] so it has been shown that the enzyme may be used without impacting the

covalent bond with the target residue. Since the technique had not yet been established in the Oxford group where the research stay was conducted, several different ratios of protease to protein were tested, including 1:20, 1:50 and 1:100. GSG2 was selected as the model system because the covalent modification site had previously been identified via X-ray crystallography as the “catalytic” lysine residue, Lys511, of the kinase. Because the binding site was already established, the trypsin digest experiment might have been employed to confirm the binding site and validate the effectiveness of the technique and protocol as intended. Unfortunately, the experiments conducted did not produce any meaningful results. The sequence coverage was very low: 27 % for the 1:20 protease-to-protein ratio (**Figure 39A**), 24 % for the 1:50 ratio (**Figure 39B**) and again 27 % for the 1:100 ratio (**Figure 39C**). When taking all three experiments into account, the sequence coverage was still only 32 % combined, far too low to draw any meaningful conclusions. Moreover, the “catalytic” lysine is indeed present in the sequences observed in the experiment, but it consistently appears in its unmodified, natural form rather than covalently modified.

It became evident that substantial optimization of sample preparation, data processing, or both was necessary to develop a robust protocol capable of reliably identifying binding sites of modifications not previously characterized by X-ray crystallography. One potential avenue for improving sequence coverage would be to employ alternative proteolytic enzymes that generate complementary peptide fragments. For example, chymotrypsin cleaves specifically at the carboxyl side of aromatic residues such as phenylalanine, tyrosine, and tryptophan, while GluC targets the carboxyl side of glutamic acid residues, with some variability depending on buffer conditions. AspN, in contrast, cleaves at the amino side of aspartic acid residues, producing peptides with acidic N-termini. Additionally, enzymes with broader or less specific cleavage patterns, such as pepsin, which preferentially cleaves N-terminal to hydrophobic and aromatic residues under acidic conditions, and proteinase K, known for its broad specificity and robustness in harsh environments, could further enhance peptide coverage and increase the likelihood of detecting covalently modified residues.[158,159]

Given the need for extensive method development and the challenges encountered, attention was redirected toward the ACVR1 target, whose binding site had also been characterized by X-ray crystallography. This target presented a promising starting point for further SAR analysis due to the novel binding site identified and the geometry of the molecule.

Figure 39: A Sequence of GSG2 with peptides identified, highlighted in pink, from the 1:20 protease-to-protein ratio experiment. The “catalytic“ lysine is indicated by an arrow. **B** Sequence coverage in the 1:50 experiment. **C** Sequence coverage in the 1:100 experiment.

4.5. Evaluation of Putative ACVR1 Inhibitors

4.5.1. Reaction Biology HotSpot™ Kinase Assay for Putative ACVR1 Inhibitors

The small ACVR1 SAR library, which had been prepared based on the screening hit **308** (see chapter 3.4 for the synthesis) was evaluated via the Reaction Biology HotSpot™ kinase assay as described in chapter 4.2.1 by RBC at their site in Malvern, PA, USA, and the results are displayed in **Table 4**. The assay was performed in a 10-fold dilution series starting at 50 µM, as weak activity was expected due to the typically slow kinetics of these warheads and the short pre-incubation time of only 20 minutes. At first glance, the results did not meet expectations. Pyridinyl analog **355** showed some activity at higher assay concentrations but not enough to determine an IC_{50} value. The sulfonyl fluoride **356** on the other hand, is the only compound out of the series that displayed a measurable IC_{50} value of 997 nM. When looking beyond the IC_{50} values, however, an interesting discovery was made – several of the “inhibitors” (the original hit **308**, **349**, **350**, **353** and **354**) showed a clear activating effect (more than 130 % kinase activity at the highest concentration). This activating effect is not something that is usually encountered with ACVR1 or kinases in general. However, since the assay has

previously been used to evaluate activators and the results showed consistent, concentration-dependent values across duplicate measurements, it was concluded that the observed values were not merely assay artifacts and merited further investigation.

Table 4: Inhibitory activity of ACVR1 inhibitors as determined by Reaction Biology in their HotSpot™ kinase assay. Experiments were conducted via 5-point duplicate measurements with 10-fold dilution steps starting from 50 µM. The values depicted here for the IC_{50} values, and the activity are the mean of two measurements. Compounds showing no effect are color coded in grey, inhibitors are marked in green and activators (highest activation > 130 %) in red. n/a: No inhibitory activity could be observed.

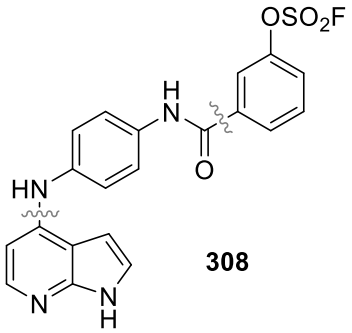

308

Structure	#	IC_{50} [nM]	Activity [%]
See above	**308**	n/a	167.03
			130.09
			123.84
			117.33
			119.13
Variation of Hinge Binder			
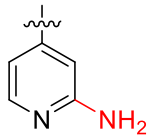	**314**	n/a	93.86
			98.32
			98.48
			98.98
			99.42
Variation of Linker			
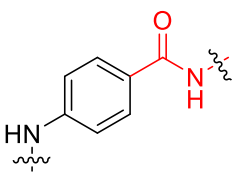	**317**	n/a	93.06
			102.66
			100.34
			102.66
			104.54

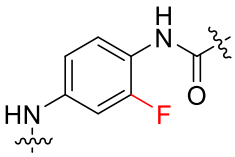	**322**	n/a	94.42 108.68 105.34 102.25 101.19
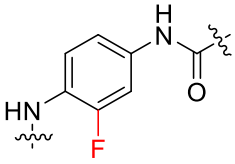	**323**	n/a	113.45 104.13 105.79 104.26 107.14
Variation of Warhead-Bearing Aryl Ring			
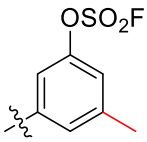	**349**	n/a	161.42 107.19 108.48 104.05 105.06
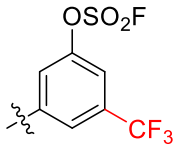	**350**	n/a	148.05 108.80 108.25 104.85 105.11
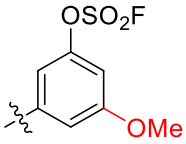	**351**	n/a	112.44 114.33 105.68 107.69 105.02
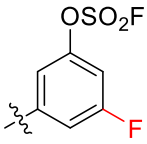	**352**	n/a	121.54 101.84 101.78 98.60 104.27
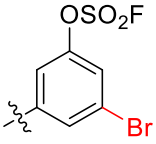	**353**	n/a	169.36 109.70 108.91 105.37 106.37

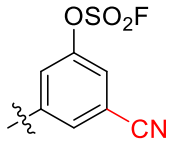	**354**	n/a	139.71 108.99 113.26 111.18 110.78
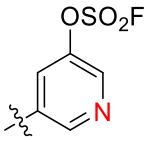	**355**	> 50,000	56.08 87.18 94.30 101.24 99.49
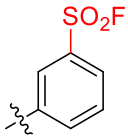	**356**	997	3.96 26.53 59.45 94.18 99.07
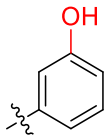	**357**	n/a	126.76 105.48 102.75 101.84 102.24
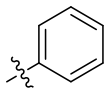	**358**	n/a	105.53 103.07 102.84 103.99 101.10

In kinase structural biology, RAF kinases are a well-known example where ATP-competitive inhibitors can paradoxically activate signaling. Sorafenib stabilizes the kinase in a type 2 conformation with the DFG-loop flipped out, while e.g. vemurafenib, dabrafenib, and LGX818 stabilize the active type 1 conformation with the DFG-loop in. Despite their inhibitory binding, these compounds can activate RAF–MEK–ERK signaling in cells with wild-type BRAF, especially in the presence of activating RAS mutations.[160] The assay format utilized here has generally been used to successfully assess activators in the past and the values here do not seem to be artifacts of the assay. There are several conceivable theories regarding the underlying cause of the activating effect. An apparent activation could be due to dimerization of ACVR1 – an inactivated ACVR1 molecule could bind to and thereby activate another ACVR1

molecule. This effect could be increased at higher compound concentrations if compound binding occurs slowly, which is the case here (see also chapter 4.5.3 for intact protein MS measurements of the compounds). BATTISTI *et al.*[161] describe a phenomenon where their covalently bound compounds are outcompeted by ATP causing the compounds to become displaced and then in their new position possibly help to coordinate a metal ion (Mn^{2+}) in the active site, enhancing the rate of catalysis. In his preliminary NanoBRET assays, WILLIAM SEATON-BURN found that treatment of cells with 5 – 50 µM of **308** resulted in a marked increase in signal, with up to a tenfold elevation observed after eight hours of incubation. Although the NanoBRET assay is not designed or validated to measure target activation, and the observed effect may be an artifact, this increase was not detected in cells treated with other compounds, and all controls performed as expected. Notably, a comparable activating effect in the same concentration range was confirmed in the Reaction Biology radiometric assay. A key distinction between the two assays is that NanoBRET is independent of ATP and metal ions. In this system, **308** competes for binding to ACVR1 with a small-molecule inhibitor conjugated to a fluorescent dye. One possible explanation is that **308** is displaced from the binding pocket by a more potent compound but remains in proximity, thereby stabilizing the newly bound molecule. The structural modification in **355**, specifically the addition of a nitrogen atom, may enhance binding affinity, reduce the likelihood of such displacement, and thus account for the observed inhibitory rather than activating behavior. Additionally, enhanced substrate binding by **308** could also contribute to the increased signal observed in the Reaction Biology assay. However, this remains speculative, and further experiments will be necessary to validate these hypotheses. In a thermal shift assay performed by WILLIAM SEATON-BURN, the potential for further stabilization of ACVR1 covalently bound to **308** was evaluated by the addition of ATP mimetics, nanomolar inhibitors, or metal ions. While metal ions produced no measurable effect, the other compounds demonstrated increased stabilization relative to the DMSO control. Although this assay is not definitive, the results suggest that additional compounds are capable of binding the pocket following covalent modification of Lys338 by **308**. Confirmation of this binding through crystallographic analysis would be highly desirable. A crystallization experiment attempting to crystallize **308** besides an ATP mimetic in ACVR1 has therefore been set up.

It is especially interesting that there is such a pronounced difference between the initial fluorosulfate **308** and the sulfonyl fluoride analog **356**. These molecules only differ by one atom, namely the removal of the O-linker, but while the more flexible but less reactive fluorosulfate has an activating effect, the intrinsically more reactive sulfonyl fluoride acts as an inhibitor. Further experiments are needed to elucidate this different effect of the warhead on the kinase.

4.5.2. Thermal Shift Assay of ACVR1 Binders

Following the evaluation of compound potency through biochemical IC_{50} measurements, the next step was to assess compound–protein interactions using biophysical approaches. A thermal shift assay (TSA), also known as differential scanning fluorimetry (DSF), carried out by WILLIAM SEATON-BURN was employed to determine changes in protein thermal stability upon ligand binding. This method provides insight into target engagement by monitoring shifts in the protein's melting temperature (T_m), which typically increases when a stabilizing interaction occurs.[162] TSA offers an orthogonal perspective on compound binding, complementing both biochemical data and the intact protein mass spectrometry analyses presented in the subsequent chapter.

Interestingly, all compounds that were tested, i.e. the original hit **308**, as well as compounds **322**, **352** and **354**, show a "biphasic unfolding" to a certain extent (**Figure 40**). A consistent thermal shift of approximately 11.5 °C was observed; however, this represents a secondary melting transition following an initial unfolding event.

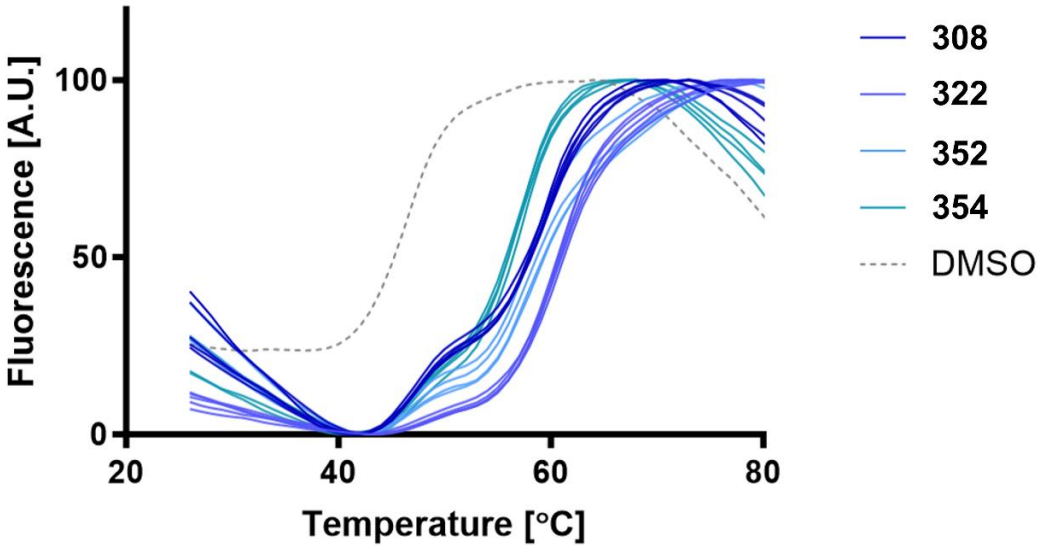

Figure 40: Thermal shift assay performed by WILLIAM SEATON-BURN that shows biphasic unfolding of the ACVR1 binders. All four compounds show a shift in melting temperature greater than 10 °C. The experiment was repeated four times for each compound as displayed here. The depiction was provided by WILLIAM SEATON-BURN.

This biphasic unfolding becomes especially clear when comparing the negative control (DMSO) and positive control (saracatinib), which both do not show this behavior (**Figure 41A**). Saracatinib was used as a positive control based on in-house validation demonstrating a strong thermal stabilization of ACVR1 ($\Delta T_m \approx +15$ °C) and biochemical potency in the low nanomolar range ($IC_{50} \approx 5 - 10$ nM; unpublished data). The biphasic unfolding, that is consistently

observed for e.g. compound **308**, as depicted in **Figure 41B**, is not something that is necessarily uncommon, but it does complicate analysis. Multiple thermal transitions observed during protein unfolding may arise from distinct structural domains, increased aggregation at elevated temperatures, or heterogeneous populations within the sample. In some cases, a melting event near the native T_m is accompanied by one or more higher-temperature transitions. One possible explanation is that certain ligands selectively stabilize a subset of the protein population, potentially reflecting partial activation or conformational heterogeneity; however, alternative explanations – such as incomplete labeling or sample heterogeneity – cannot be excluded.[163] These interpretations are based on preliminary data and require further validation; additional experiments will be necessary to clarify the underlying mechanisms. One point that is clear, however, is that the compounds tested consistently stabilize ACVR1 to a similar extent as the validated positive control.

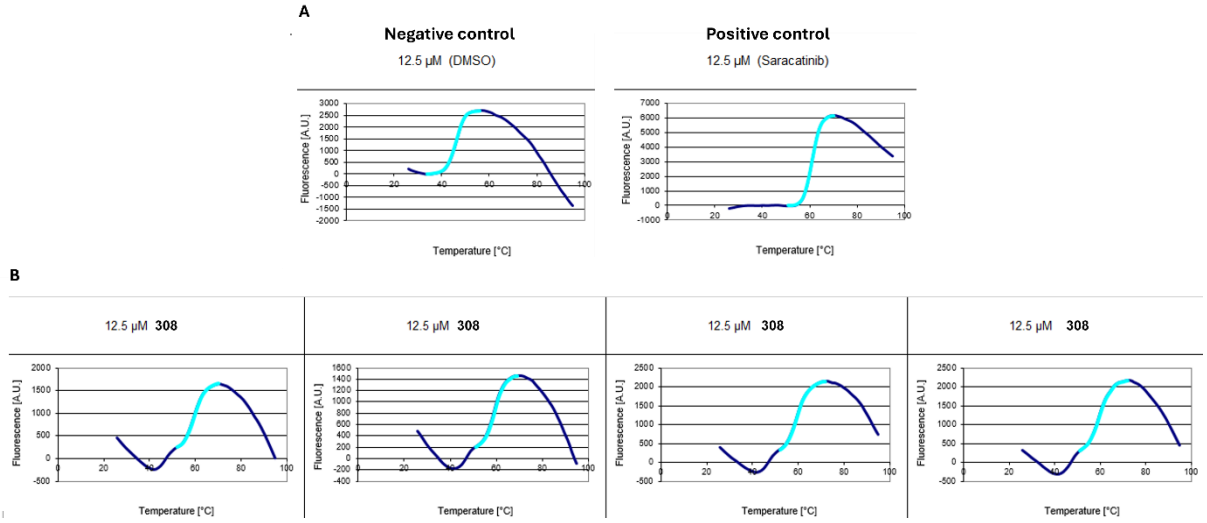

Figure 41: A Graphs showing the negative control (DMSO) and positive control (saracatinib) in the TSA of ACVR1. **B** Graphs depicting the biphasic unfolding behavior consistently observed with compound **308**. The graphs were provided by WILLIAM SEATON-BURN.

4.5.3. Intact Protein MS of ACVR1 Binders

The newly developed ACVR1-targeted compounds were subsequently evaluated by WILLIAM SEATON-BURN using intact protein MS to assess the impact of structural modifications on the rate of covalent binding (25-fold excess compound over ACVR1, rt, 30 h). Initially, alterations to the hinge-binding moiety – specifically the substitution with 2-aminopyridine (compound **314**) – as well as modifications to the linker region, including the introduction of a fluorine atom to the central phenyl ring (compounds **322** and **323**) and amide bond inversion (compound **317**), were examined (**Figure 42**). For comparative purposes, data for the unmodified protein (red trace) and the original hit compound **308** (blue trace) are also presented. Incorporation of a fluorine substituent at either the 2- or 3-position of the central phenyl ring (yellow and green

traces, respectively) did not produce a measurable change in the rate of covalent modification. Although fluorine is sterically similar to hydrogen, its distinct electronic properties did not appear to influence binding kinetics in this context. In contrast, inversion of the amide bond (grey-blue trace) resulted in a modest decrease in covalent binding efficiency, with a slightly reduced extent of protein modification observed over the assay duration; however, this effect was not substantial. The most pronounced effect was observed with the replacement of the azaindole hinge-binding motif by 2-aminopyridine (grey trace), which led to a marked reduction in the rate of covalent modification. Under the experimental conditions, significantly less than 50 % of the protein was modified, indicating that the 2-aminopyridine moiety is significantly less effective as a hinge binder in this system. While this finding does not necessarily identify azaindole as the optimal hinge-binding motif for ACVR1, it seems that 2-aminopyridine is a suboptimal choice in comparison.

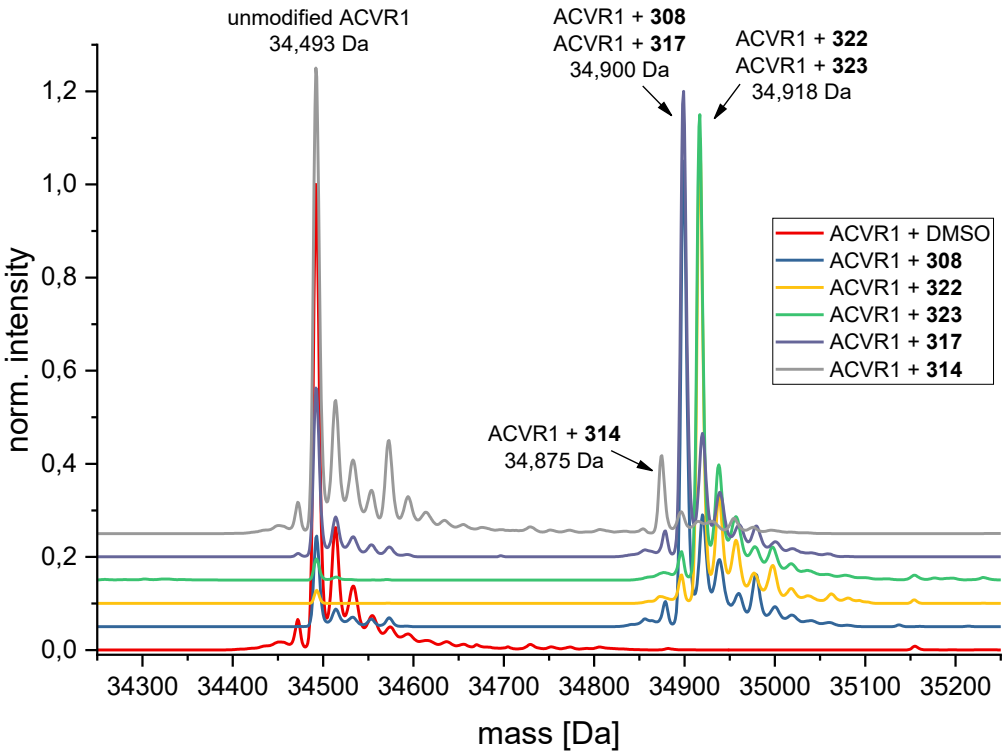

Figure 42: Intact protein MS experiments between ACVR1 (red) and the different covalent inhibitors (**308**, original hit, blue; **322**, 2-F, yellow; **323**, 3-F, green; **317**, amide inversion, grey-blue; **314**, 2-aminopyridine hinge binder, grey). Note that a different ACVR1 construct was used as above.

The incorporation of electron-donating substituents onto the aryl ring bearing the electrophilic warhead yielded results consistent with the initial hypothesis. Specifically, the increased electron density within the aromatic system reduced the electrophilicity of the warhead, thereby attenuating its reactivity toward covalent modification of ACVR1. This effect was evident in both

the methoxy-substituted analog (compound **351**, blue trace) and the methyl-substituted analog (compound **349**, yellow trace), as shown in **Figure 43**, both of which exhibited slower covalent modification. Although the methoxy group is expected to exert a stronger electron-donating effect than the methyl group, compound **351** still resulted in approximately 50 % protein modification, while compound **349** showed clearly less than 50 %. This difference may be influenced by steric and conformational factors rather than electronic factors alone. Nonetheless, the general trend remains clear: electron-donating groups on the aryl ring decrease the rate of covalent modification by reducing the warhead's electrophilicity.

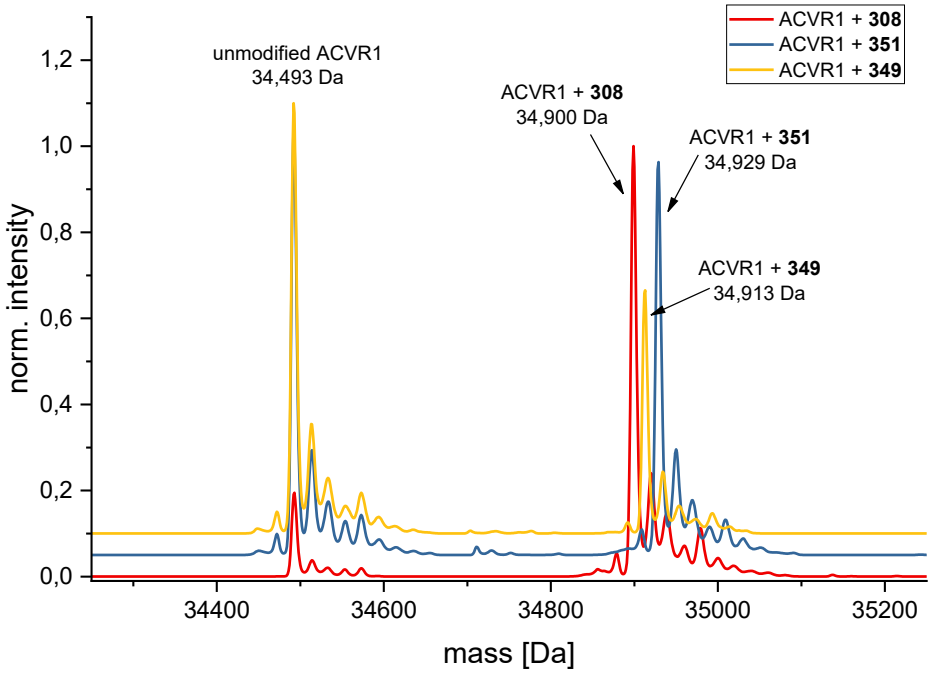

Figure 43: Intact protein MS experiments between ACVR1 and the different covalent inhibitors (**308**, red; **351**, -OMe, blue; **349**, -Me, yellow).

The introduction of electron-withdrawing groups would be expected to exert the opposite effect of electron-donating substituents, enhancing the electrophilicity of the warhead and thereby increasing the rate of covalent modification. This trend was indeed observed for most of the compounds tested (**Figure 44**). The fluorine-substituted analog (compound **352**, blue trace) and the pyridinyl analog (compound **355**, yellow trace) exhibited slightly increased on-target reactivity compared to the original hit compound **308**. Notably, the cyano-substituted analog (compound **354**, grey-blue trace) underwent a second covalent modification event with ACVR1, consistent with the strong electron-withdrawing nature of the cyano group, the most electron-withdrawing of the three substituents. However, this trend did not hold for the bromo-substituted compound (**353**, green trace) and the trifluoromethyl-substituted compound (**350**, grey trace). While the bromine analog exhibited marginally greater than 50 % modification, the

trifluoromethyl analog failed to reach the 50 % threshold over the course of the experiment. This deviation may be attributed to steric factors, as bromine and trifluoromethyl are the largest among the electron-withdrawing substituents examined, suggesting that steric hindrance or conformational changes disrupting warhead orientation may outweigh electronic effects in these cases.

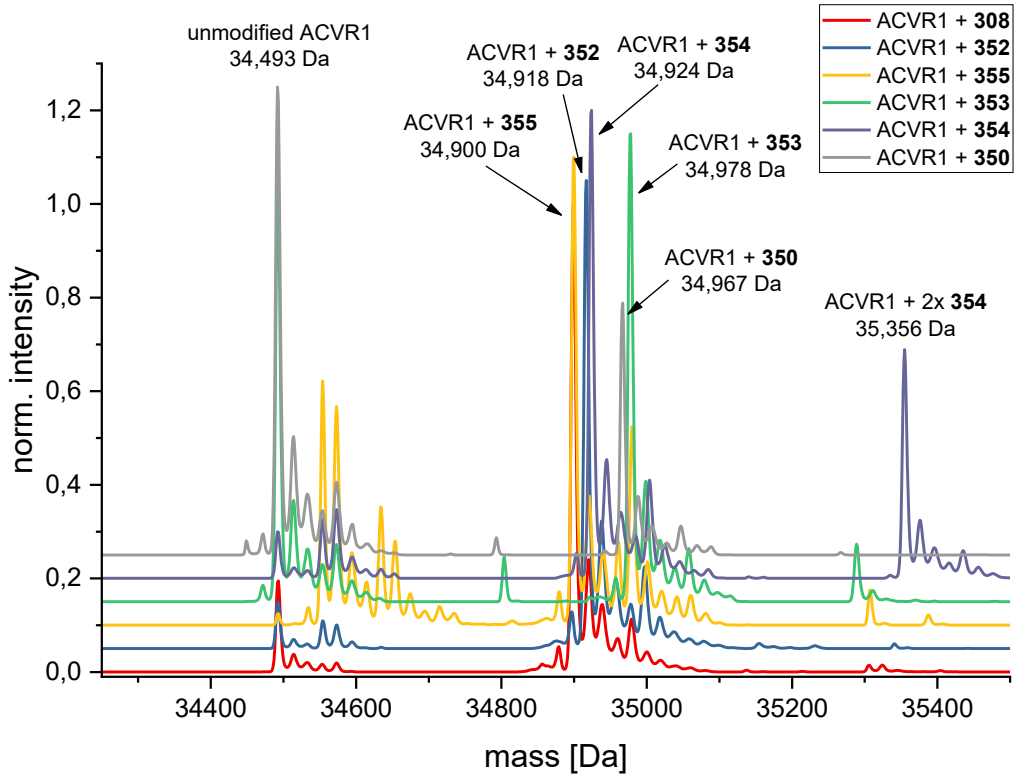

Figure 44: Intact protein MS experiments between ACVR1 and the different covalent inhibitors (**308**, original hit, red; **352**, -F, blue; **355**, pyrdinyl, yellow; **353**, -Br, green; **354**, -CN, grey-blue; **350**, -CF_3, grey).

Finally, the sulfonyl fluoride analog **356** was also examined in intact protein MS. As this warhead is intrinsically more reactive than fluorosulfate, it was not surprising to see that the unmodified protein could not be observed anymore after incubation with compound **356** (yellow trace, **Figure 45**). Indeed, a second and even third binding event could be observed instead, highlighting the higher level of promiscuity of the sulfonyl fluoride warhead.

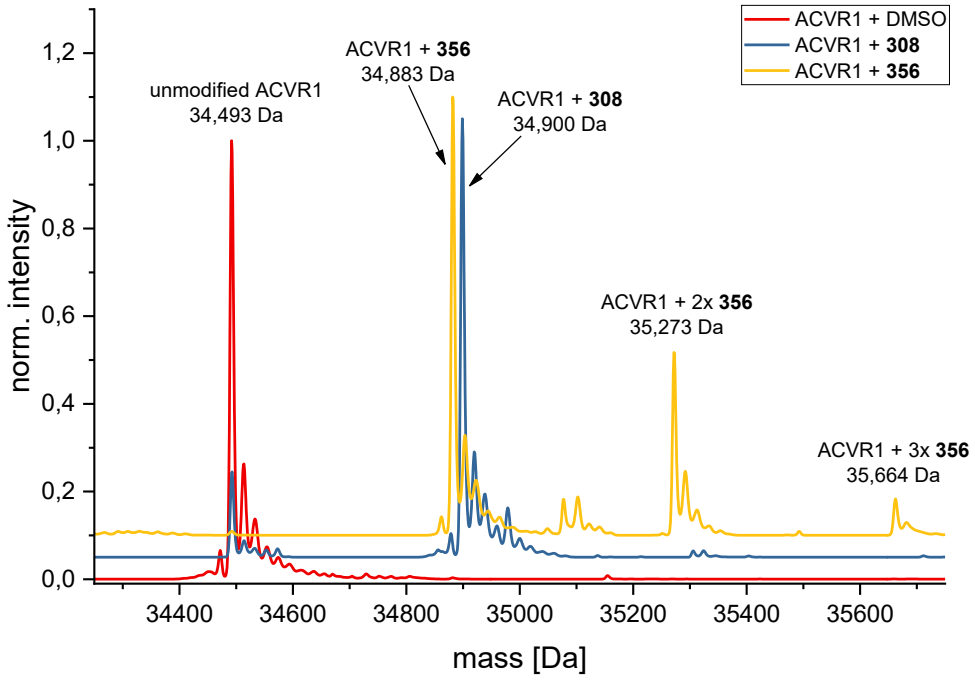

Figure 45: Intact protein MS experiments between ACVR1 (red) and the two different covalent inhibitors (fluorosulfate **308**, blue; sulfonyl fluoride **356**, yellow).

4.5.4. Preliminary Selectivity Assessments for ACVR1 Binders

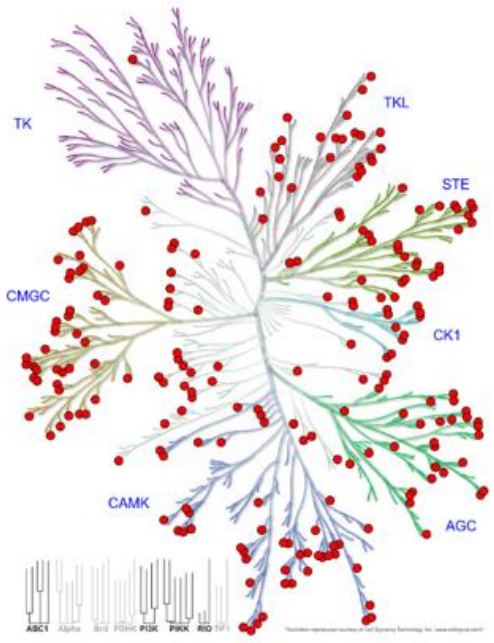

Figure 46: Kinome tree with red dots marking all kinases that possess an equivalently positioned lysine to Lys338 in ACVR1. The graphic was created using the KLIFS database [153] (accessed on July 4, 2025).

The lysine targeted by compound **308**, Lys338 at the HRD+2 position, is less conserved than the universally present “catalytic” lysine found in all kinases. Yet, a significant level of conservation can also be claimed for this lysine (**Figure 46**, 215 out of 326 kinases according to the KLIFS database).[153] This prompted concerns as to how selective the covalent binders would be. In the initial MS screening (see chapter 4.4.3), several kinases that contain a lysine at the same position – AURKA, CSNK2A1, CSNK2A2, GSK3B, ZAK, MAPK1, PAK3, and VRK1 – were fortuitously included. None of these exhibited binding with compound **308**. Although this represents only a limited subset, it suggests that compound **308** (and its analogs) may not universally react with all kinases possessing this

lysine across the kinome. To assess selectivity in a more encompassing way, further experiments that cover more of the kinome would be necessary.

Instead, the preliminary efforts here were focused more on assessing the other kinases in the ACVR1 family. ACVR1 is a transmembrane receptor Ser/Thr kinase. This group can be split into type I (also known as ALKs) and type II receptors (**Figure 47**). Type I receptors are designated ALK1 through ALK7. Type II receptors lack the glycine-serine-rich (GS) domain, which is located just N-terminal to the kinase domain in type I receptors, and therefore they function mainly to phosphorylate the GS domain of type I receptors.[164] The conservation level of the residues found in the ATP binding pocket of ACVR1 vs. other type I receptors is about 85 %. The gatekeeper varies across the ALKs – ALK1/2/3/6 feature a threonine in this position while ALK4/5/7 possess a serine. The lysine targeted through **308** is present in all type I and II receptors except for BMPR2, where the residue is an asparagine and AMHR2, where a serine can be found in the HRD+2 position. During the development of ALK2 inhibitors, particular emphasis has been placed on achieving selectivity over TGFBR1/ALK5, as potent inhibition of TGFBR1/ALK5 has been associated with cardiac toxicity.[165] For this reason, **308** was tested against ALK5 (**Figure 48**), as well as ALK6 (**Figure 49**) and BMPR2 in intact protein MS. As expected, since the lysine residue is not conserved in BMPR2, **308** did not covalently bind BMPR2 and did not prevent its autophosphorylation activity. However, the outcome was markedly different for TGFBR1/ALK5 and ALK6 which both feature the same lysine. Both kinases were modified by **308** in a similar fashion as ACVR1 was. Unfortunately, since the lysine is so conserved across the family, covalent inhibition alone does not bring a direct advantage for selectivity in this case. To achieve selectivity across the family, further assessment of the binding pockets and their differences will be necessary. As some of the kinases under investigation differ at the gatekeeper position, this commonly exploited feature may offer a viable route toward selective inhibitor design.

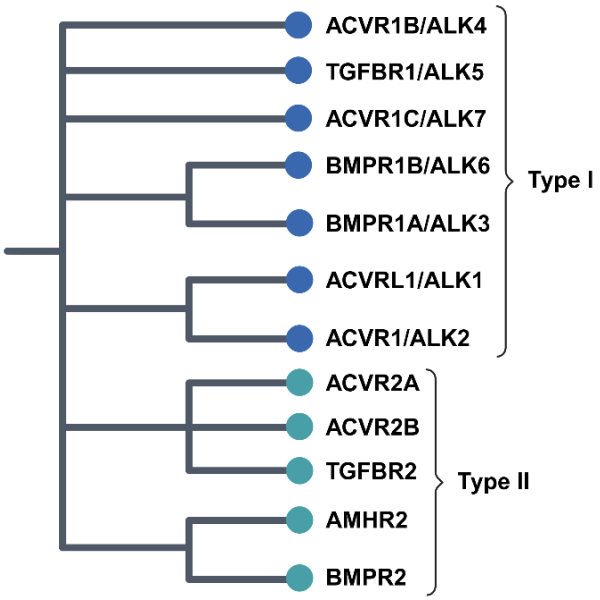

Figure 47: Overview over type I and II transmembrane receptor Ser/Thr kinases.[164,171] Graphic was created using BioRender.com.

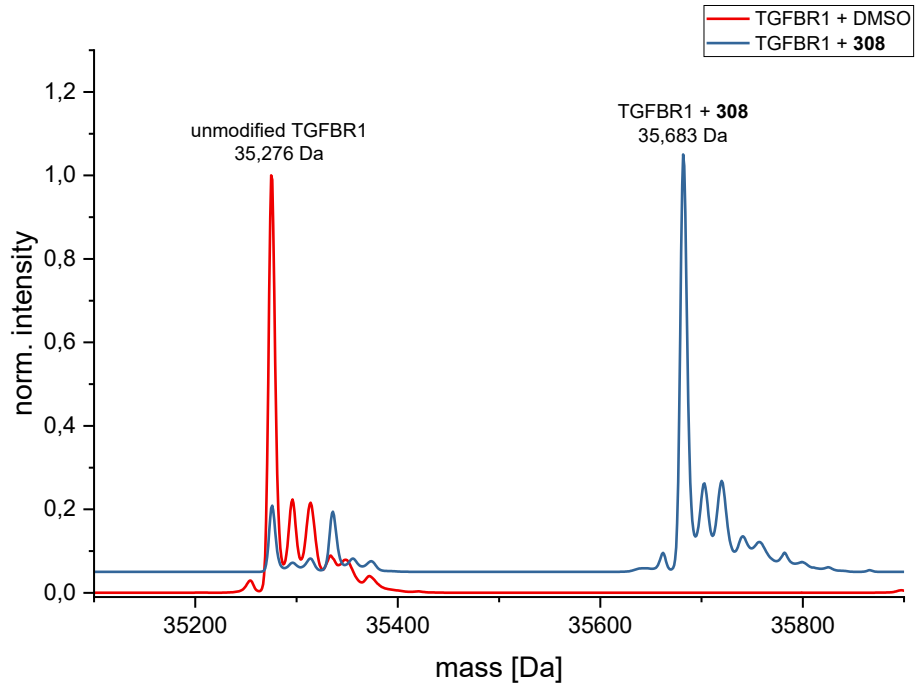

Figure 48: Intact protein MS experiments between TGFRB1/ALK5 (red) and covalent binder **308** (blue).

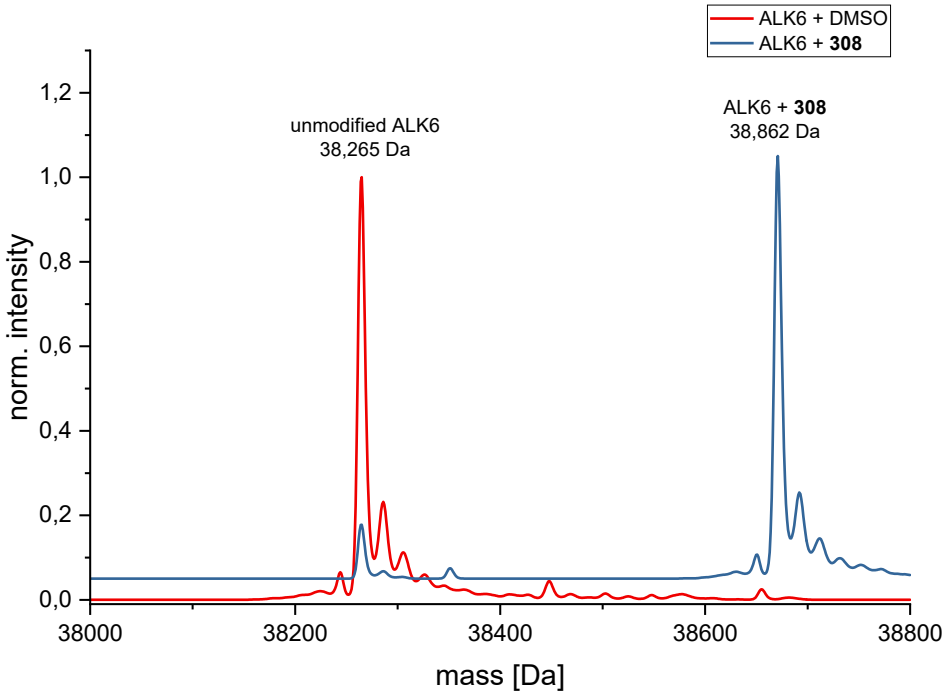

Figure 49: Intact protein MS experiments between ALK6 (red) and covalent binder **308** (blue).

5. Conclusions and Outlook

This dissertation set out to explore covalent inhibition strategies beyond the well-trodden path of cysteine targeting in kinases. While cysteine-directed covalent inhibitors are well established and widely used, the potential of engaging other nucleophilic amino acids – such as lysines and tyrosines – remains comparatively underexplored. Kinases represent a compelling target class in this context: although the covalent addressability of cysteines has been extensively characterized, systematic efforts to target alternative residues have lagged behind, despite structural and chemoproteomic evidence suggesting ample opportunity. Originally aimed at applying sulfur(VI) fluoride chemistry to selectively target tyrosines using structure-based design, this work evolved into a broader covalent-first strategy. This ultimately led to the discovery of the first covalent ligand for ACVR1, a kinase involved in fibrodysplasia ossificans progressiva (FOP), which notably lacks a targetable cysteine in its binding pocket. Additionally, this research provides the first demonstration of sulfur(VI) fluoride chemistry being used to covalently engage a lysine beyond the “catalytic” lysine residue in a kinase, underscoring the untapped potential of this warhead class for expanding the covalently ligandable proteome.

The initial investigations centered on JAK3 and aimed to establish a proof-of-concept demonstrating the feasibility of employing S(VI) F chemistry to target tyrosine residues. Guided by the crystal structure of a highly potent noncovalent JAK3 inhibitor, a small series of putative covalent inhibitors bearing sulfonyl fluorides and fluorosulfates (**Figure 50**) was designed and synthesized to engage Tyr904 at the GK+2 position. Using a fluorosulfate-containing compound, in which the warhead-bearing aryl ring was otherwise unsubstituted, docking studies were performed to guide systematic variation of the warhead’s position and chemical nature, as well as further substitutions and linker length. An ELISA assay revealed that only the sulfonyl fluoride analog exhibited low nanomolar potency comparable to the noncovalent reference compound. However, intact protein MS failed to detect any covalent modification. This discrepancy was resolved by solving a co-crystal structure, which revealed that the warhead of the “covalent” compound was misoriented – pointing away from the target tyrosine. A rigidization strategy, involving the conversion of the tricyclic scaffold into a tetracyclic system to enforce proper warhead alignment, also failed to achieve tyrosine-directed covalent inhibition of JAK3.

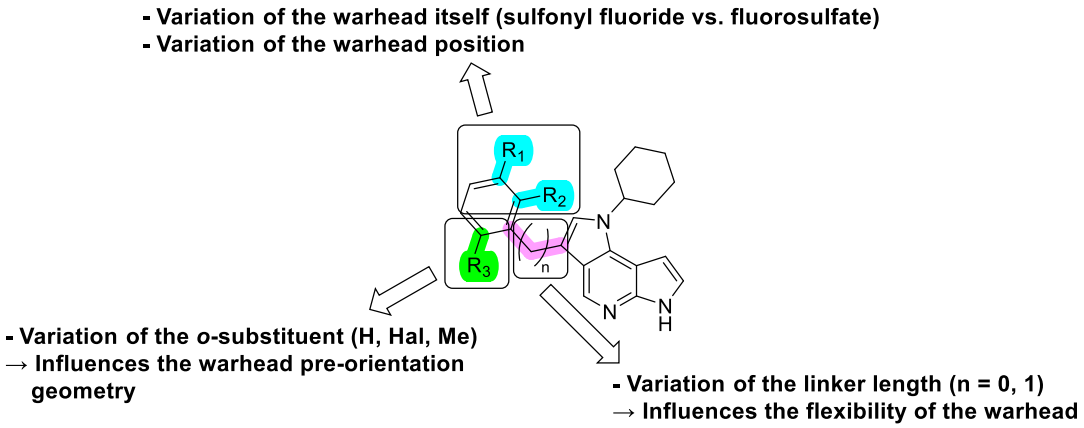

Figure 50: Schematic overview over the modifications applied to a tricyclic JAK3 inhibitor structure to achieve covalent binding of Tyr904 in the GK+2 position.

In a second structure-based design approach, an allosteric noncovalent inhibitor (compound **119**) of MK2 was chosen as the starting point of the investigation. Among the four tyrosine residues located near the inhibitor's binding site, computational modeling identified two – Tyr225 and Tyr264 – as accessible targets. A subsequent synthetic campaign, involving extensive optimization across multiple routes, yielded two fluorosulfates, one sulfonyl fluoride analog, their corresponding noncovalent hydroxy analogs, and the parent compound (**Figure 51**). Despite these efforts, two complementary biochemical assays failed to detect any inhibitory activity, even for the original noncovalent analog, which according to literature data[124] should have an IC_{50} of 110 nM. However, intact protein MS did confirm covalent modification. Sulfonyl fluoride **153**, designed to target Tyr264, exhibited only moderate modification over the experimental timeframe. In contrast, fluorosulfate **120**, targeting Tyr225, showed nearly complete covalent modification. Co-crystallization studies revealed an unexpected and highly intriguing binding mode: instead of occupying the allosteric site, compound **120** bound within the ATP-binding pocket, adopting a pose reminiscent of skepinone-type inhibitors of the upstream kinase p38α. In this configuration, the amide carbonyl oxygen interacts with the hinge region. Remarkably, the covalent modification occurred at Lys93 – the "catalytic" lysine – rather than a tyrosine residue. This finding not only underscores the potential of fluorosulfates as covalent warheads but also provides a rare example of successful lysine targeting by a fluorosulfate in a kinase context.

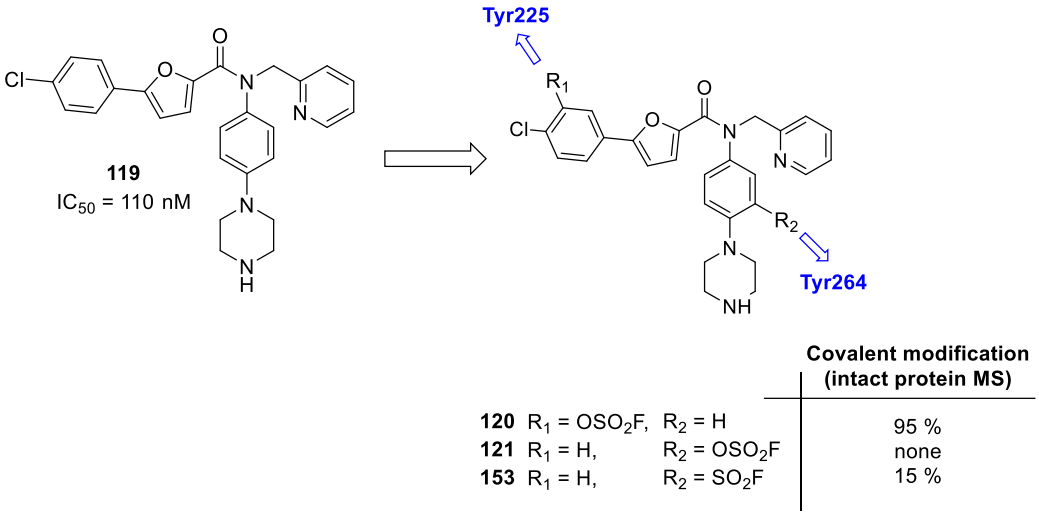

Figure 51: Noncovalent allosteric MK2 inhibitor **119** was used as a design analog to design covalent inhibitors that should target Tyr225 or Tyr264. While none of the compounds showed inhibitory activity in two complementary assays, **120** and **153** showed moderate to very high covalent modification of MK2 in intact protein MS measurements (5-fold excess compound over MK2, rt, 3 h).

The limited success of the initial two approaches underscored the challenges and inherent limitations of traditional structure-based TCI design when aiming at less nucleophilic residues such as tyrosines. To overcome these obstacles, a covalent-first strategy was adopted. A focused library was designed and synthesized, incorporating five distinct hinge-binding motifs, a variety of linker architectures differing in length, geometry, and exit vectors, as well as both sulfonyl fluorides and fluorosulfates as warheads. In parallel, kinases featuring a tyrosine residue within the ATP-binding pocket and a nearby basic residue (to potentially enhance the tyrosine's nucleophilicity) were selected for screening against this library. Intact protein mass spectrometry identified several promising covalent binders, and select hits were further validated through X-ray crystallography to determine their exact sites of modification. Among the most intriguing hits was a fluorosulfate that covalently modified ACVR1. This compound elaborately mimicked ATP binding and targeted Lys338 – an unprecedented site in kinase covalent inhibition – located in the catalytic loop at the HRD+2 position. Notably, this represents the first known covalent inhibitor of ACVR1, a kinase lacking a covalently ligandable cysteine within its binding pocket.

In the final project of this dissertation, the original ACVR1 hit (compound **308**) was diversified into a small SAR series to explore the impact of modifications to the hinge-binding moiety, the linker, and the warhead-bearing aryl ring. As shown in **Figure 52A**, this exploration yielded both expected and unexpected findings. Substituting the azaindole hinge binder with an aminopyridine significantly slowed down the reaction, while modifications to the linker had little apparent effect. Expectedly, electron-donating groups (EDGs) on the aryl ring led to a marked decrease in reactivity. While electron-withdrawing groups (EWGs) generally accelerated

covalent modification as anticipated, a steric threshold was observed – bulkier EWGs ultimately hindered the reaction despite their electronic properties generally enhancing electrophilicity. Unsurprisingly, switching from the less reactive fluorosulfate to the sulfonyl fluoride warhead resulted in much faster covalent modification of the protein. Although these SAR variations provided valuable insights, several promising avenues remain unexplored. Future investigations could include evaluating a broader range of hinge-binding motifs, exploring alternative linkers (e.g., incorporating more sp^3-rich elements), fine-tuning of sulfonyl fluoride reactivity using EDG substitutions, and assessing entirely different electrophilic warhead classes.

A particularly puzzling discovery emerged during the biochemical evaluation of the ACVR1-targeted compounds. While sulfonyl fluoride **356** exhibited the expected inhibitory activity, the original hit **308** – and several analogs – unexpectedly demonstrated an apparent activating effect (**Figure 52B**). The underlying mechanism of this activation remains unclear, but it is especially striking that the simple addition of an oxygen linker to the warhead can transform an inhibitor into an activator. This phenomenon observed in biochemical *in vitro* assays was further cautiously supported by qualitative signals from both NanoBRET and thermal shift assays. Additional structural studies, including co-crystallization of ACVR1 with compound **308** in the presence of an ATP mimetic are currently in progress. However, further biochemical and biophysical investigations will be essential to elucidate the origin of this activation effect and to understand its potential functional and mechanistic implications.

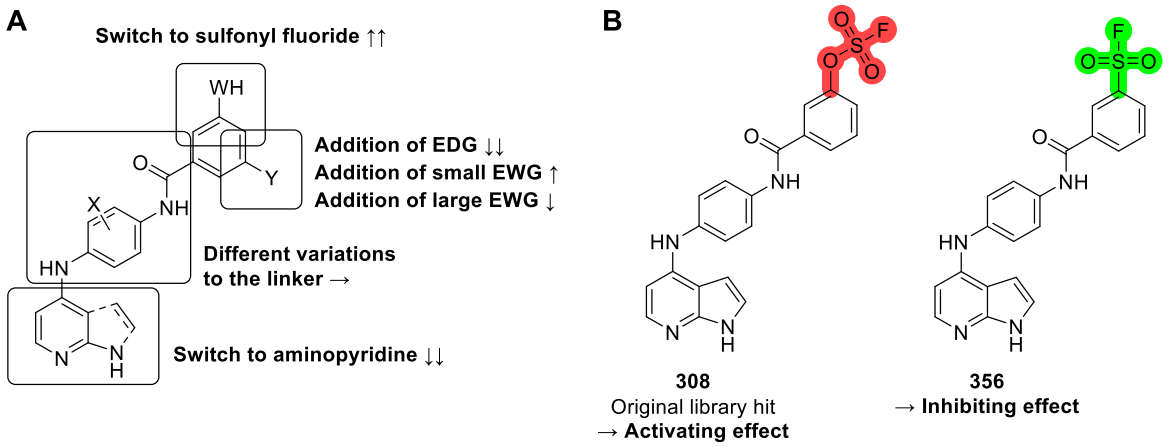

Figure 52: A Summary of SAR findings for analogs of compound **308**. Substitution of the fluorosulfate warhead with a sulfonyl fluoride significantly increased covalent modification rates. The addition of electron-donating groups (EDGs) slowed down the reaction, while small electron-withdrawing groups (EWGs) accelerated it; larger EWGs reduced reactivity, presumably due to steric effects. Variations to the linker had a minimal impact, and replacing the azaindole hinge binder with an aminopyridine decreased covalent inactivation efficiency. **B** Comparison of two key analogs: fluorosulfate **308**, the original hit, unexpectedly displayed an activating effect on ACVR1, while sulfonyl fluoride **356** exhibited the anticipated inhibitory activity.

6. Experimental Part

6.1. Materials and Methods

Chemistry

All starting materials and reagents used in the chemical syntheses were obtained from commercial sources and employed without further purification, unless otherwise noted. Solvents used were anhydrous and oxygen-free, procured commercially and stored over molecular sieves under an inert atmosphere. Unless otherwise specified, reactions were conducted under an argon atmosphere with continuous stirring. Thin layer chromatography (TLC) was carried out using Merck 60 F254 silica gel plates (Merck KGaA, Darmstadt, Germany), and compound visualization was achieved under UV light at either 254 nm or 366 nm. Product purification was performed by preparative column chromatography utilizing the Interchim PuriFlash XS420/430 (Interchim® S.A., Montluçon, Allier, France). For normal phase chromatography, Grace Davison Davisil LC60A silica (20–45 µm; W.R. Grace and Company, Columbia, MD, USA), Merck Geduran Si60 (63–200 µm; Merck KGaA, Darmstadt, Germany), or pre-packed puriFlash® SIHP silica columns (60 Å, 500 m²/g, 30 µm dp, sizes 12/25/40 g; Interchim S.A.) were employed. Reverse phase chromatography was performed using a CHROMABOND® Flash RS 40 C18 ec column (Macherey-Nagel GmbH & Co. KG, Düren, Germany). Preparative HPLC was performed using a puriFlash® 5.250P system (Interchim® S.A., Montluçon, Allier, France) equipped with US5C18HQ-150/212 and US10C18HQ-250/300 reverse-phase C18 columns for high-resolution compound purification.

HPLC

Compound purity, as well as buffer and *N*-Ac-tyrosine stability assays were determined using an Agilent 1100 series HPLC system (equipped with an injection module, thermostat module, ColCom column compartment, degasser, and binary pump; Agilent Technologies Inc., Santa Clara, CA, USA) coupled to an Agilent 1260 diode array detector (DAD). Analyses were performed using a Phenomenex Kinetex® C8 column (2.6 µm, 100 Å, 150 × 4.6 mm; Phenomenex Inc., Torrance, CA, USA) with an injection volume of 5 µL and a flow rate of 0.5 mL/min at 23 °C. UV detection was carried out at 254 nm and 230 nm. Two different methods were used:

Method A:

0 min: 40% MeOH, 60% phosphate buffer (0.01 M) pH 2.3

9 min: 85% MeOH, 15% phosphate buffer (0.01 M) pH 2.3

10 min: 85% MeOH, 15% phosphate buffer (0.01 M) pH 2.3

11 min: 40% MeOH, 60% phosphate buffer (0.01 M) pH 2.3

16 min: 40% MeOH, 60% phosphate buffer (0.01 M) pH 2.3

Method B:

0 min: 40% MeOH, 60% phosphate buffer (0.01 M) pH 2.3

15 min: 85% MeOH, 15% phosphate buffer (0.01 M) pH 2.3

20 min: 85% MeOH, 15% phosphate buffer (0.01 M) pH 2.3

22 min: 40% MeOH, 60% phosphate buffer (0.01 M) pH 2.3

28 min: 40% MeOH, 60% phosphate buffer (0.01 M) pH 2.3

NMR Spectroscopy

NMR spectra were acquired using Bruker Avance III HD 200/400/600 MHz spectrometers (Bruker Corporation, Billerica, MA, USA). Samples were dissolved in deuterated solvents, and chemical shifts were referenced to the residual solvent signals as described by FULMER *et al.*,[166] with tetramethylsilane (TMS) defined as δ = 0 ppm. Signal multiplicities were indicated as follows: s = singlet, d = doublet, dd = doublet of doublets, dt = doublet of triplets, ddd = doublet of doublet of doublets, t = triplet, td = triplet of doublets, q = quartet, hept = heptett, and m = multiplet.

Mass Spectrometry

TLC-MS: Mass spectrometric data for reaction intermediates were obtained using an Advion TLC-MS interface (Advion, Ithaca, NY, USA) employing electrospray ionization (ESI) in both positive and negative ion modes. Instrument settings were as follows: ESI voltage at 3.50 kV, capillary voltage at 187 V, source voltage at 44 V, capillary temperature at 250 °C, desolvation gas temperature at 250 °C, and a nitrogen gas flow rate of 5 L/min.

LC-MS: In cases where TLC-MS measurements were unsuccessful, mass spectrometric measurements for compound verification were performed at the mass spectrometry department of the Institute of Organic Chemistry, University of Tübingen, using a Bruker maXis ESI-TOF system (Bruker Corporation, Billerica, MA, USA) operated in positive or negative ESI mode. Samples were analyzed by flow injection without chromatographic separation. The instrument was run under standard conditions with a capillary voltage of 4500 V, end plate

offset of −500 V, nebulizer pressure of 1.2 bar, dry gas flow rate of 6.0 L/min, and a dry heater temperature of 200 °C.

ASAP: Mass spectrometric analysis for rapid reaction monitoring was performed, where applicable, using an Advion ASAP® (Atmospheric Solid Analysis Probe) system (Advion, Ithaca, NY, USA) operated in both positive and negative ion modes. Samples were introduced via glass capillaries and analyzed directly without prior chromatographic separation. Standard operating conditions were applied, including a vaporization temperature of 250 °C and ionization was achieved via a heated gas stream under standard APCI-like conditions. The ASAP probe was coupled to an Advion expression® Compact Mass Spectrometer (CMS).

HRMS: Measurements were performed by the MS department of the Institute of Organic Chemistry at Eberhard Karls University of Tübingen. Analyses were carried out using a Bruker maXis 4G ESI-TOF instrument (Bruker Corporation, Billerica, MA, USA) operating in positive electrospray ionization (ESI) mode. Instrument parameters were set as follows: dry heater temperature at 200 °C, nebulizer pressure at 1.2 bar, dry gas flow rate at 6.0 L/min, capillary voltage at 4500 V, and endplate offset voltage at 2500 V. The measurements for the ALK2 library were carried out by BENEDIKT MASBERG of the LÄMMERHOFER group (Institute of Pharmaceutical Sciences, Eberhard Karls University, Tübingen). These measurements were performed using a 1290 Infinity I LC system (Agilent Technologies, Waldbronn, Germany) coupled to a SCIEX TripleTOF 5600+ mass spectrometer (SCIEX, Darmstadt, Germany) equipped with a DuoSpray ESI source and operated in SWATH-MS acquisition mode. Sample injection was carried out using an HTC-xt PAL autosampler (CTC Analytics, Zwingen, Switzerland), and a Cheminert 6-port valve (Valco Instruments Co. Inc., TX, USA) was installed to divert salts and buffers away from the ion source.

Intact Protein Measurements:

JAK3: These measurements were conducted by APIRAT CHAIKUAD from the KNAPP group (Institute for Pharmaceutical Chemistry, Structural Genomics Consortium, Goethe University, Frankfurt). A solution containing 50 µM of protein and 150 µM of the test compound was incubated at 4 °C for 24 hours. For the negative control, an equivalent volume of DMSO was added to the protein solution. The reaction was quenched by adding 0.1 % formic acid in double-distilled water (ddH_2O) at a 1:10 (v/v) ratio, followed by sample desalting using C8 stage tips according to a previously published protocol.[167] MS data acquisition was carried out on a Time-of-Flight (TOF) LC/MS system (Agilent 6200 series) equipped with a positive electrospray ionization (ESI) source. A volume of 5 µL of the desalted sample was injected for mass spectrometry (MS) analysis. To prevent cross-sample contamination, blank injections were run between each sample. Data were deconvoluted and analyzed using Agilent's

MassHunter Bioconfirm software, applying a scan range of 600 – 2000 m/z, a mass range of 10 – 100 kDa, a mass step of 1 Da, and a baseline subtraction value of 7.

MK2: Sample preparation was performed by GUIQUN WANG from the KNAPP group. A solution of 50 µM protein and 250 µM test compound was incubated at room temperature for 3 hours. For the negative control, an equivalent volume of DMSO was added to the protein solution. The reaction was quenched by adding 0.1 % formic acid in double-distilled water (ddH_2O) at a 1:10 (v/v) ratio, followed by sample desalting using C8 stage tips, according to a previously published protocol.[167]

Mass spectrometric measurements were carried out by BENEDIKT MASBERG from the LÄMMERHOFER group using a SCIEX TripleTOF 5600+ mass spectrometer (SCIEX, Darmstadt, Germany) coupled to an Agilent 1290 Infinity UHPLC system (G4220A binary pump, G1316C column compartment, G1170A valve drive; Agilent Technologies, Waldbronn, Germany). Online desalting was performed via a 2-position 6-port valve. Chromatographic separation was achieved on a BIOshell Protein C4 column (5 cm × 2.1 mm, 3.4 µm, 400 Å; Merck, Darmstadt, Germany) using a gradient of water/acetonitrile with 0.1 % formic acid at a flow rate of 1.0 mL/min and a column temperature of 60 °C. The DuoSpray ion source was operated in positive ESI mode with standard settings (CUR: 30 psi; GS1: 50 psi; GS2: 40 psi; ISVF: 5500 V; source temperature: 450 °C; CE: 30 V; DP: 230 V). Data were acquired in TOF mode (100 – 5000 m/z, 100 ms accumulation) and optimized for intact protein detection using the IntactProteinMode script. Analyst TF 1.8.1 and PeakView 2.2.0 were used for data acquisition and analysis, and deconvolution was performed using the BioToolKit 2.2.0 software. Relative quantification was based on AUC integration of deconvoluted protein species.

$$Ratio\ [\%] = \frac{AUC[mod]}{AUC[unmod] + AUC[mod]} \times 100$$

Table 5 Relative Quantification of covalent modification to the MK2 protein.

Compound	AUC[unmod] in cts	AUC[mod] in cts	Ratio [%]
153	1.01E+05	1.71E+04	14.51
120	8.86E+03	1.46E+05	94.28

Covalent Fragment Screening: Covalent fragment screening was carried out using a RapidFire high-throughput liquid chromatography system (Agilent Technologies, Waldbronn, Germany) coupled to a quadrupole time-of-flight mass spectrometer (Agilent Technologies, Waldbronn,

Germany). Samples were prepared in 384-well plates (Greiner Bio-One, Kremsmünster, Austria), each containing 50 µL of assay solution composed of 100 µM compound and 4 µM of the respective protein. Compounds were dispensed from 50 mM DMSO stock solutions using an Echo 520 acoustic liquid dispenser (Labcyte Inc., Sunnyvale, CA, USA), and the plates were incubated at room temperature for 24 hours. The reaction was quenched by adding 0.1 % formic acid in double-distilled water (ddH_2O) at a 1:10 (v/v) ratio. All measurements were performed in singlicates. During analysis, each sample was aspirated onto a C4 solid-phase extraction (SPE) cartridge using 0.1% formic acid as the loading solvent and eluted with 0.1% formic acid in 85% acetonitrile. Mass spectrometric data were acquired and processed using MassHunter Qualitative Analysis software (Agilent Technologies, Waldbronn, Germany).

Determination of Kinetic Parameters

k_{inact}/K_I was measured by GUIQUN WANG based on time- and concentration-dependent analysis of intact protein mass spectra using the bimolecular model described by the equations seen below, as reported recently by LI *et al.*,[168] [PI]: concentration of the protein-compound complex, [PI*]: concentration of the covalent protein-compound complex, [PI*] ≈ [PI] if k_{inact} is relatively high. $[P]_0$, $[I]_0$: concentration of initial protein and compound. *t*: incubation time(s).

Briefly, MK2 was adjusted to 2 mg/mL (53 µM), then incubated with 2 different concentrations (120 µM, 240 µM) of **120** separately at room temperature. When reaching each time point of incubation (15 min, 30 min, 60 min, 120 min, 180 min), an aliquot of the reaction mixture was transferred into 1 % formic acid in ddH2O using a multichannel pipette (10 µL of sample added to 90 µL ddH2O/1% formic acid), to stop the reaction at the exact time point. MS was performed and % occupancy was calculated in the same way (see equations below).

To extract the k_{inact}/K_I, Prism 8.0.2 (Graphpad Software, San Diego, CA) was used to fit the data of time- and concentration-dependent % occupancy: import data as XY table. A nonlinear regression fit was chosen to fit the curves, k_{inact}/K_I was set up as the constraint type of “Shared value for all datasets”, initial value as 0, the rest settings are as default.

$$Occupancy\ [\%] = \frac{I_{mod}}{(I_{mod} + I_{unmod})} \times 100$$

$$[PI^*] = [P]_0[I]_0 \frac{e^{([P]_0-[I]_0)\times k_{inact}/K_i \times t} - 1}{[P]_0 \times e^{([P]_0-[I]_0)\times k_{inact}/K_i \times t} - [I]_0}$$

$$Occupancy\ [\%] = \frac{[PI]}{[P]_0} \times 100$$

Stability and Intrinsic Reactivity Assays

The assay determining buffer stability and intrinsic reactivity toward *N*-Ac-tyrosine was derived from the assay established by GILBERT *et al*.[41] Briefly, each S(VI)-F compound as described in chapter 4.3 (60 µL, 10 mM in DMSO) was added to a glass HPLC vial containing 80 µL DMSO and 60 µL of a 10 mM internal standard solution of 1,4-dicyanobenzene in DMSO. Finally, 800 µL of 0.1 M aqueous buffer was added, and the mixture was vortexed thoroughly. Assays were performed using either phosphate-buffered saline (PBS, pH 8.0) or carbonate-bicarbonate buffer (pH 10.0). The final solution had a total volume of 1 mL, with 0.6 mM S(VI)-F compound, 0.6 mM internal standard, and 20 % DMSO by volume. Samples were incubated at room temperature and monitored at approximately 20-minute intervals via HPLC.

For intrinsic reactivity measurements, S(VI)-F compounds (20 µL, 10 mM in DMSO) were added to 980 µL of amino acid stock solution containing *N*-acetyl-tyrosine (2 mM) and 1,4-dicyanobenzene (0.6 mM) in aqueous buffer containing 20 % DMSO by volume. The final concentration of the S(VI)-F compound was 0.2 mM. Reactions were mixed by pipetting and analyzed by HPLC at ~20-minute intervals.

The reaction was monitored by the decreasing area under the curve (AUC) of the compound peak, normalized to the AUC of the internal standard (1,4-dicyanobenzene). Kinetic analysis was performed by plotting the natural logarithm of the normalized AUC at each time point relative to the initial AUC ($\ln[AUC/AUC_0]$) against time. Linear regression of this plot yielded the pseudo-first-order rate constant (k), from which the half-life ($t_{1/2}$) was calculated using the standard equation:[169]

$$t_{1/2} = \ln\left(\frac{2}{k}\right)$$

As discussed in chapter 4.3, at pH 8 (PBS buffer), all three compounds remained stable over the 13.5-hour experiment with no evidence of hydrolysis or reaction with *N*-acetyl-tyrosine. However, when the experiment was repeated under more basic conditions at pH 10 using a carbonate-bicarbonate buffer, the expected reactivity trend was observed: the least reactive compound, **360**, exhibited a half-life of 4.8 hours in its reaction with the tyrosine surrogate (**Figure 53**), while compound **361** showed a shorter half-life of 2.5 hours (**Figure 54**). The most reactive analog, **362**, underwent complete decomposition in the buffer alone within 4 hours, precluding determination of its half-life in reaction with the tyrosine surrogate.

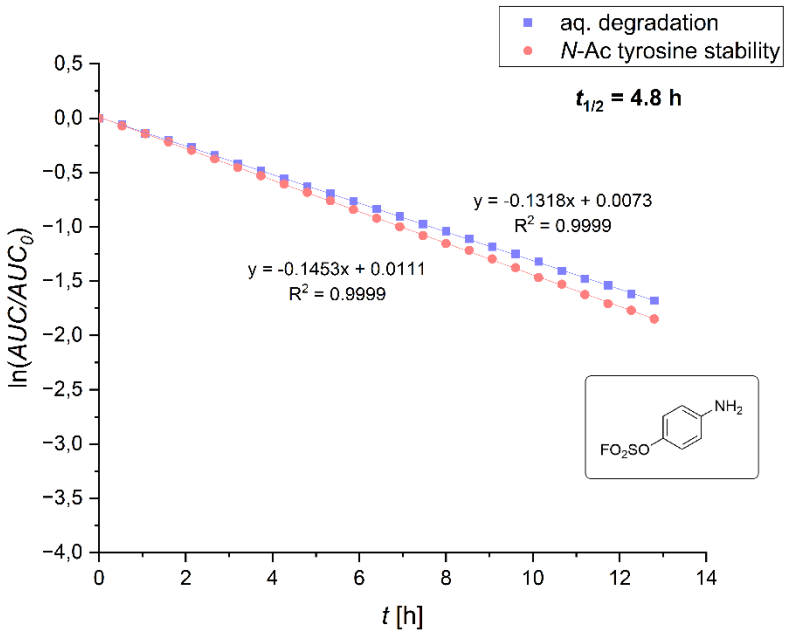

Figure 53: *N*-Ac tyrosine intrinsic reactivity assay of 4-aminophenyl sulfurofluoridate in carbonate-bicarbonate buffer (pH 10).

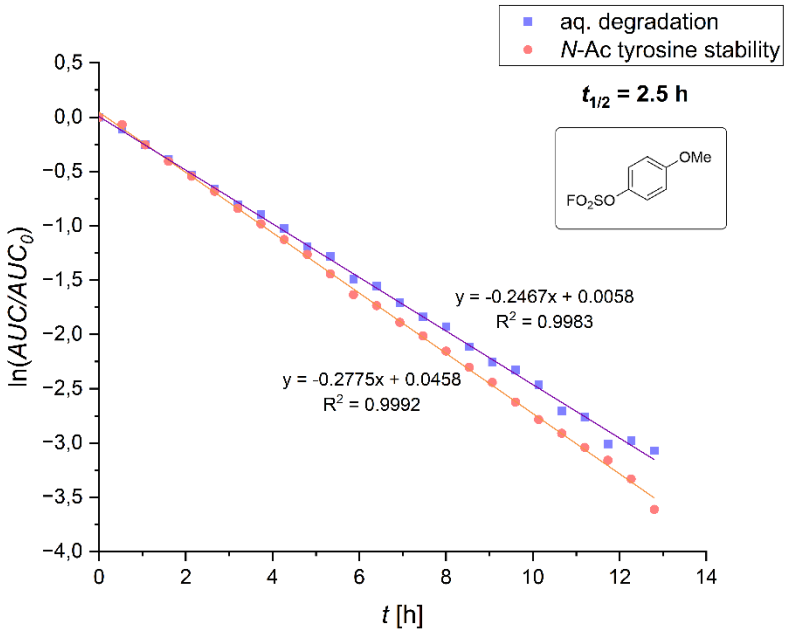

Figure 54: *N*-Ac tyrosine intrinsic reactivity assay of 4-methoxyphenyl sulfurofluoridate in carbonate-bicarbonate buffer (pH 10).

Biochemical Assays

The determination of the IC_{50} values for the putative JAK3 inhibitors was performed by KATHARINA BAUER of the LAUFER group as described in chapter 4.1.1 according to the protocol

of BAUER *et al.*[141] IC_{50} values for the putative MK2 inhibitors were determined commercially by either Reaction Biology Corp. as described in chapter 4.2.1 or by AssayQuant Technologies as described in chapter 4.2.2. The activity of the ALK2 compounds was also determined by Reaction Biology Corp. as described in chapter 4.5.1.

Protein Expression and Purification

Recombinant human protein kinases were expressed in *Escherichia coli* Rosetta™ (DE3) competent cells. Bacterial cultures were grown in LB medium supplemented with 50 µg/mL kanamycin at 37 °C with shaking at 250 rpm. Protein expression was induced at an optical density (OD_{600}) of 0.8 – 1.0 by the addition of 400 µL of 1 M IPTG per liter of culture (final concentration: 0.4 mM). Cultures were then incubated overnight at 18 °C to allow for protein expression. Protein-specific details are summarized in **Table 6**.

Table 6: Summary of expressed protein constructs.

Protein name	Residues	Plasmid	Tag Type	Antibiotic
BMP2KA	S38 – E345	pNIC-ZB	ZB-fusion	Kanamycin
CSNK2A1A	M1 – S337	pNIC28-Bsa4	N-terminal His_6	Kanamycin
CSNK2A2A	M1 – P335	pNIC28-Bsa4	N-terminal His_6	Kanamycin
MAP2K1A	E62 – V393	pNIC-CTHF	C-terminal His_6-FLAG	Kanamycin
MAPK1A	M1 – S360	pNIC28-Bsa4	N-terminal His_6	Kanamycin

Cells were harvested by centrifugation and resuspended in 40 mL of Ni-IMAC binding buffer (25 mM HEPES (pH 7.4), 150 mM NaCl, 10 mM imidazole, 5 % glycerol). Cell lysis was performed by sonication on ice for 5 minutes using pulses of 5 s on and 10 s off. Following lysis, 1 mL of polyethyleneimine (PEI) was added from a 5 % (w/v) stock solution (pH 7.4) to precipitate nucleic acids. The lysate was clarified by centrifugation at 21,000 rpm for 1 hour at 4 °C using a JA25.50 rotor (Beckman Coulter).

The clarified supernatant was applied to a gravity flow column containing 2 mL of Ni-Sepharose resin, equilibrated with water and then with binding buffer. To enhance binding efficiency, the flow-through was reapplied to the column. The resin was washed sequentially with 50 mL

(Wash 1) and 30 mL (Wash 2) of wash buffer (binding buffer containing 30 mM imidazole), followed by elution with four 5 mL fractions of elution buffer (binding buffer containing 300 mM imidazole), each after a 10-minute incubation (Elutions 1 – 4).

Eluted fractions were pooled, and fusion tags were cleaved overnight at 4 °C using TEV protease during dialysis into Ni-IMAC binding buffer. The cleaved sample was then re-applied to a re-equilibrated Ni-Sepharose column to remove uncleaved protein and TEV protease. The column was washed with 20 mL of wash buffer, followed by two 5 mL elutions (E1 and E2) after 10-minute incubations with elution buffer.

Final purification was achieved by size-exclusion chromatography using a Superdex 75 16/60 column equilibrated in gel filtration buffer (50 mM HEPES (pH 7.4), 150 mM NaCl, 0.5 mM TCEP, 5 % glycerol). Protein-containing fractions were pooled and flash-frozen in liquid nitrogen and kept at -80 °C.

Co-Crystallization Experiments

JAK3: Protein crystallization of JAK3 was carried out by APIRAT CHAIKUAD in the KNAPP group, as previously described.[97] Briefly, JAK3 protein was concentrated to 15 mg/mL in a buffer containing 20 mM Tris-HCl (pH 8.0), 250 mM NaCl, 10 mM DTT, and 10 % glycerol. To promote crystal formation, *N*-phenyl urea was added to a final concentration of 0.25 %, and the protein was incubated on ice for 1 hour with 1 mM of the inhibitor to allow complex formation. Crystallization trials were conducted using the sitting-drop vapor diffusion method at 4 °C. Crystals were obtained from a condition containing 31 % PEG 3350, 0.2 M $MgCl_2$, and 0.1 M MES (pH 5.5).

MK2: Protein crystallization of MK2 was carried out by GUIQUN WANG in the KNAPP group. The protein was concentrated to 12 mg/mL in a buffer containing 20 mM HEPES (pH 8.0), 200 mM NaCl, 0.5 mM TCEP, and 5 % glycerol. The compound was added at a 1.5-fold molar excess, and the mixture was incubated at room temperature for 3 hours to allow complex formation. Crystallization trials were performed at 4 °C using the sitting-drop vapor diffusion method. Crystals were obtained from a condition containing 1 M succinic acid, 1 % PEG 2000 MME, and 0.1 M HEPES (pH 7.0).

Crystals were carefully harvested and briefly soaked in cryo-protectant solutions prepared using their respective mother liquors: 25 % ethylene glycol for JAK3 and 25 % glycerol for MK2. After cryo-protection, crystals were flash-cooled in liquid nitrogen. X-ray diffraction data were collected at the Diamond Light Source (Didcot, UK). Both structures have been deposited in

the Protein Data Bank under the accession numbers PDB: 9R59 (JAK3) and PDB: 9R5Z (MK2).

GSG2: The purified protein was concentrated to 9.5 mg/mL in a buffer containing 50 mM HEPES (pH 7.5) and 150 mM NaCl. The compound was added to a final concentration of 1 mM, and the protein–ligand mixture was incubated on ice for 24 hours to allow complex formation. Crystallization trials were carried out using the sitting-drop vapor diffusion method at 4 °C. Crystals of GSG2 were obtained by mixing 150 nL of the protein–compound solution with an equal volume of reservoir solution containing 0.1 M citrate (pH 5.0) and 20 % (w/v) PEG 6000. Crystals were cryoprotected by brief soaking in mother liquor supplemented with 25 % ethylene glycol and subsequently flash-cooled in liquid nitrogen. X-ray diffraction data were collected at the Diamond Light Source

ALK2: The ALK2 sample was further polished using a Superdex 200 Increase 10/300 GL column by WILLIAM-SEATON BURN from the group of ALEXANDER BULLOCK (Centre for Medicines Discovery, Nuffield Department of Medicine, University of Oxford), and concentrated to 5 mg/mL buffered in 50 mM HEPES, pH 7.5, and 150 mM NaCl. The protein was incubated with 1 mM compound for 24 hours on ice. The sample was then concentrated to 10mg/mL. Crystallization was performed using the sitting drop vapor diffusion method at 4°C. Viable crystals of ALK2 grew in a 150 nL drop mixing 10 mg/mL protein:compound solution, with a reservoir solution of 1.4 M ammonium sulfate, 0.1 M tris pH 7.5 and 16 % glycerol. Crystals were transferred into a cryoprotective solution prepared from the mother liquor supplemented with 25 % ethylene glycol. Diffraction data were collected at Diamond Light Source.

Differential Scanning Fluorimetry (DSF) Assay

Differential scanning fluorimetry (DSF), also known as a thermal shift assay, is a high-throughput method commonly used in drug discovery to assess the binding of small molecules to target proteins, such as kinases. The assay relies on the principle that ligand binding can stabilize the folded structure of a protein, resulting in an increase in its melting temperature (T_m) – the temperature at which 50 % of the protein population is unfolded. This thermal stabilization is indicative of binding affinity and can provide insights into selectivity and potential off-target interactions. The assay monitors protein unfolding by tracking the fluorescence of an environment-sensitive dye, such as SYPRO Orange, which exhibits low fluorescence in aqueous solution but fluoresces strongly upon interaction with hydrophobic regions exposed during protein unfolding.[163] Differential Scanning Fluorimetry was performed by WILLIAM-SEATON BURN of the BULLOCK group as described by FEDOROV *et al*.[170] The purified kinase domain of ALK2 containing the Q207D mutation was screened at 4 µM concentration against

308, **322**, **352** and **354** in a 96-well plate format. The inhibitors were prepared in 100 % DMSO stock solutions leading to 2.5 % DMSO final concentration in each well. Compounds were added to a final concentration of 12.5 µM in an assay buffer containing 10 mM HEPES, pH 7.4, 150 mM NaCl, and SYPRO Orange (1:1000 dilution, MilliporeSigma). Samples were heated from 2 5°C to 96 °C in a Mx3005P real-time PCR instrument (Stratagene). Fluorescence was monitored with excitation and emission filters set to 465 and 590 nm, respectively. Data was analysed with MxPro software. Positive controls were run in wells containing protein and 12.5 µM Saracatinib, a validated nanomolar inhibitor of ALK2.

Visualization Tools

Figures were prepared using Microsoft PowerPoint or BioRender.com. Images of protein crystal structures and models were generated using the PyMOL Molecular Graphics System (Version 3.0.3, Schrödinger). Graphs were created with Origin 2025 (OriginLab Corporation, Northampton, MA, USA).

6.2. Synthesis

6.2.1. Synthesis of Putative JAK3 Inhibitors

4-Chloro-1-(triisopropylsilyl)-1H-pyrrolo[2,3-b]pyridine (38)

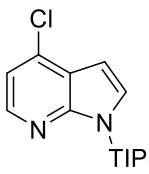

Chemical Formula: $C_{16}H_{25}ClN_2Si$
Exact Mass: 308.14755
Molecular Weight: 308.92500

4-Chloro-1*H*-pyrrolo[2,3-*b*]pyridine (**37**, 5.00 g, 32.8 mmol, 1.00 eq.) was dissolved in THF (50 mL) and the solution was cooled to 0 °C. NaH (60 % dispersion in mineral oil, 1.46 g, 36.4 mmol, 1.11 eq.) was added portion wise and the suspension was stirred for 30 min. Subsequently, TIPSCl (7.70 mL, 36.1 mmol, 1.10 eq.) was added dropwise and the solution was heated to 50 °C. After stirring for 17 h, the mixture was cooled to rt and quenched with sat. NH_4Cl (20 mL). Extraction was carried out with EtOAc (5 x 40 mL). The combined organic phases were dried over Na_2SO_4, the solvent was evaporated, and the residue was purified via flash column chromatography (silica gel, hexane) which afforded the product **38** (9.60 g, 31.1 mmol, 95 %) as a colorless oil.

^{1}H-NMR (400 MHz, $CDCl_3$) δ 8.14 (d, J = 5.1 Hz, 1H), 7.33 (d, J = 3.5 Hz, 1H), 7.06 (d, J = 5.2 Hz, 1H), 6.65 (d, J = 3.5 Hz, 1H), 1.85 (hept, J = 7.5 Hz, 3H), 1.12 (d, J = 7.5 Hz, 18H). ^{13}C-NMR (101 MHz, $CDCl_3$) δ 154.5, 142.7, 135.1, 131.8, 121.8, 116.2, 101.6, 18.2, 12.4. TLC-

MS: ESI(+) calcd. for $[M+H]^+$: *m/z* = 309.2; found: 309.2. HPLC: t_{ret} = 12.90 min (85.0 % at 254 nm, 98.2 % at 230 nm, method B).

5-Bromo-4-chloro-1-(triisopropylsilyl)-1H-pyrrolo[2,3-b]pyridine (39)

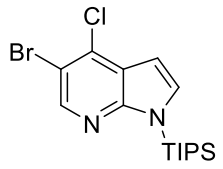

Chemical Formula: $C_{16}H_{24}BrClN_2Si$
Exact Mass: 386.05807
Molecular Weight: 387.82100

4-Chloro-1-(triisopropylsilyl)-1*H*-pyrrolo[2,3-*b*]pyridine (**38**, 4.02 g, 10.4 mmol, 1.00 eq.) was dissolved in THF (60 mL) and cooled to -78 °C. *sec*-Butyllithium (1.4 M in cyclohexane, 1.60 mL, 23.0 mmol, 2.21 eq.) was added very slowly and the solution was stirred for 30 min. CBr_4 (5.15 g, 12.5 mmol, 1.20 eq.) was dissolved in THF (15 mL) and added dropwise to the first solution. The reaction was stirred at -78 °C for a further 2 h, then warmed up and quenched with sat. NH_4Cl (50 mL). It was extracted with DCM (2 x 60 mL), washed with brine (50 mL) and dried over Na_2SO_4. After evaporating the solvent, the residue was purified via flash column chromatography (silica gel, hexane) which afforded the product **39** (4.48 g, 11.6 mmol, 90 %) as a white solid.

^{1}H-NMR (400 MHz, $CDCl_3$) δ 8.34 (s, 1H), 7.32 (d, J = 3.4 Hz, 1H), 6.64 (d, J = 3.5 Hz, 1H), 1.82 (hept, J = 7.6 Hz, 3H), 1.11 (d, J = 7.6 Hz, 18H). ^{13}C-NMR (101 MHz, $CDCl_3$) δ 152.7, 144.2, 134.4, 133.0, 123.3, 112.3, 102.2, 18.2, 12.3. TLC-MS: ESI(-) calcd. for $[M\text{-TIPS-H}]^+$: *m/z* = 228.9; found: 229.0. An HPLC could not be measured due to the high nonpolarity of the product.

5-Bromo-4-chloro-1H-pyrrolo[2,3-b]pyridine (40)

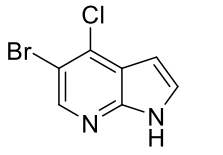

Chemical Formula: $C_7H_4BrClN_2$
Exact Mass: 229.92464
Molecular Weight: 231.47700

5-Bromo-4-chloro-1-(triisopropylsilyl)-1*H*-pyrrolo[2,3-*b*]pyridine (**39**, 4.44 g, 11.5 mmol, 1.00 eq.) was dissolved in MeOH (45 mL). KF (735 mg, 12.7 mmol, 1.10 eq.) was added and the reaction was stirred at rt for 1 h. Sat. NH_4Cl (50 mL) was added and extracted with EtOAc (5 x 50 mL). The organic phases were dried over Na_2SO_4, the solvent was removed under reduced pressure and the residue was triturated from DCM to yield the desired product **40** (2.57 g, 11.1 mmol, 97 %) as a white solid.

^{1}H-NMR (400 MHz, DMSO) δ 12.23 (s, 1H), 8.40 (s, 1H), 7.65 (d, J = 3.4 Hz, 1H), 6.53 (d, J = 3.5 Hz, 1H). ^{13}C-NMR (101 MHz, DMSO) δ 147.4, 144.1, 133.2, 128.9, 120.2, 110.6, 98.6. TLC-MS: ESI(-) calcd. for $[M-H]^+$: *m/z* = 228.9; found: 228.8. HPLC: t_{ret} = 16.80 min (96.6 % at 254 nm, 94.4 % at 230 nm, method B).

5-Bromo-4-chloro-1-tosyl-1H-pyrrolo[2,3-b]pyridine (41)

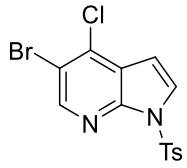

Chemical Formula: $C_{14}H_{10}BrClN_2O_2S$
Exact Mass: 383.93349
Molecular Weight: 385.66000

5-Bromo-4-chloro-1*H*-pyrrolo[2,3-*b*]pyridine (**40,** 2.63 g, 11.4 mmol, 1.00 eq.) was dissolved in THF (80 mL) and the solution was cooled to 0 °C. NaH (60 % dispersion in mineral oil, 909 mg, 22.7 mmol, 2.00 eq.) was added portionwise and the suspension was stirred for 1 h. TsCl (4.32 g, 22.7 mmol, 2.00 eq.) was dissolved in THF (15 mL) and was added to the first solution. After stirring at rt for 2 h, the reaction was quenched by adding sat. NH_4Cl (50 mL). The aq. phase was extracted with EtOAc (3 x 80 mL). The combined org. phases were washed with 1 M K_2CO_3 (3 x 100 mL), dried over Na_2SO_4 and the solvent was removed under reduced pressue. The residue was purified via flash column chromatography (silica gel, 0 – 100 % hexane/EtOAc) which afforded the product **41** (4.21 g, 10.9 mmol, 96 %) as a beige solid.

^{1}H-NMR (400 MHz, $CDCl_3$) δ 8.50 (s, 1H), 8.08 – 7.99 (m, 2H), 7.76 (d, J = 4.0 Hz, 1H), 7.34 – 7.27 (m, 2H), 6.68 (d, J = 4.0 Hz, 1H), 2.38 (s, 3H). ^{13}C-NMR (101 MHz, $CDCl_3$) δ 146.9, 145.9, 145.8, 136.4, 134.9, 130.0, 128.3, 128.2, 123.7, 115.7, 103.7, 21.8. TLC-MS: ESI(+) calcd. for $[M+Na]^+$: *m/z* = 406.9; found: 407.2. HPLC: t_{ret} = 10.04 min (100 % at 254 nm, 99.4 % at 230 nm, method A).

5-Bromo-N-cyclohexyl-1-tosyl-1H-pyrrolo[2,3-b]pyridin-4-amine (42)

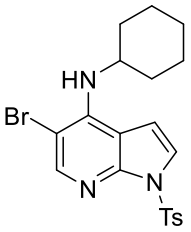

Chemical Formula: $C_{20}H_{22}BrN_3O_2S$
Exact Mass: 447.06161
Molecular Weight: 448.37900

5-Bromo-4-chloro-1-tosyl-1*H*-pyrrolo[2,3-*b*]pyridine (**41**, 2.00 g, 5.19 mmol, 1.00 eq.) and cyclohexylamine (9.00 mL, 78.3 mmol, 15.1 eq.) were stirred at 145 °C for 6 h. The solution was cooled to rt, H_2O (20 mL) was added, and it was extracted with DCM (3 x 30 mL). The organic phases were dried over Na_2SO_4, the solvent was removed under reduced pressure and the residue was purified via flash column chromatography (silica gel, DCM) to yield the desired product **42** (1.73 g, 3.87 mmol, 75 %) as a beige solid.

^{1}H-NMR (400 MHz, $CDCl_3$) δ 8.18 (s, 1H), 8.07 – 7.99 (m, 2H), 7.51 (d, J = 4.2 Hz, 1H), 7.30 – 7.22 (m, 2H), 6.56 (d, J = 4.2 Hz, 1H), 5.01 (d, J = 8.2 Hz, 1H), 3.82 – 3.75 (m, 1H), 2.37 (s, 3H), 2.10 – 2.00 (m, 2H), 1.86 – 1.75 (m, 2H), 1.73 – 1.60 (m, 1H), 1.49 – 1.20 (m, 5H). ^{13}C-NMR (101 MHz, $CDCl_3$) δ 147.9, 146.2, 145.2, 144.2, 135.5, 129.7, 128.4, 123.3, 108.6, 104.5, 102.1, 52.7, 34.1, 25.6, 24.6, 21.8. TLC-MS: ESI(+) calcd. for $[M+Na]^+$:

m/z = 470.1; found: 470.4. HPLC: t_{ret} = 20.53 min (99.2 % at 254 nm, 99.4 % at 230 nm, method B).

(E)-N-Cyclohexyl-5-(2-ethoxyvinyl)-1-tosyl-1H-pyrrolo[2,3-b]pyridin-4-amine (43)

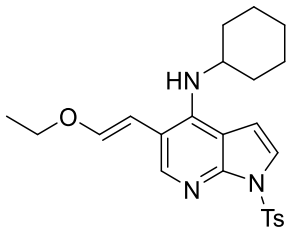

Chemical Formula: $C_{24}H_{29}N_3O_3S$
Exact Mass: 439.19296
Molecular Weight: 439.57400

5-Bromo-*N*-cyclohexyl-1-tosyl-1*H*-pyrrolo[2,3-*b*]pyridin-4-amine (**42**, 1.73 g, 3.86 mmol, 1.00 eq.), 2-ethoxyvinylboronic acid pinacol ester (1.55 g, 7.83 mmol, 2.03 eq.) and K_3PO_4 (2.50 g, 11.8 mmol, 3.05 eq.) were added to a mixture of MeCN (12 mL) and H_2O (8 mL). $Pd(PPh_3)_4$ (223 mg, 0.193 mmol, 0.05 eq.) was added and the mixture was stirred at 100 °C for 4.5 h. After cooling down, H_2O (20 mL) was added, and the solution was extracted with EtOAc (3 x 30 mL). The organic phases were dried over Na_2SO_4 and the solvent was evaporated. The product (**43**) was used in the next step without further purification.

1-Cyclohexyl-6-tosyl-1,6-dihydrodipyrrolo[2,3-b:2',3'-d]pyridine (44)

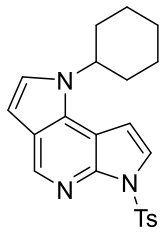

Chemical Formula: $C_{22}H_{23}N_3O_2S$
Exact Mass: 393.15110
Molecular Weight: 393.50500

(*E*)-*N*-Cyclohexyl-5-(2-ethoxyvinyl)-1-tosyl-1*H*-pyrrolo[2,3-*b*]pyridin-4-amine (**43**) was dissolved in AcOH (40 mL) and stirred at 100 °C for 2 h. After cooling down, the solvent was evaporated, and residual acid was removed by adding toluene (3 x 15 mL) and removing this under reduced pressure. The residue was purified via flash column chromatography (silica gel, 0 – 30 % hexane/EtOAc) which afforded the product **44** (1.36 g, 3.46 mmol, 89 % over two steps) as a yellow solid.

^{1}H-NMR (400 MHz, $CDCl_3$) δ 8.70 (s, 1H), 8.12 – 8.02 (m, 2H), 7.70 (d, J = 4.0 Hz, 1H), 7.25 – 7.19 (m, 2H), 7.18 (d, J = 3.4 Hz, 1H), 6.77 (d, J = 4.0 Hz, 1H), 6.65 (d, J = 3.3 Hz, 1H), 4.43 (tt, J = 11.8, 3.7 Hz, 1H), 2.32 (s, 3H), 2.25 – 2.13 (m, 2H), 2.07 – 1.92 (m, 2H), 1.88 – 1.77 (m, 1H), 1.69 (qd, J = 12.4, 3.3 Hz, 2H), 1.53 (qt, J = 13.2, 3.4 Hz, 2H), 1.40 – 1.22 (m, 1H). ^{13}C-NMR (101 MHz, $CDCl_3$) δ 144.9, 143.0, 139.8, 135.8, 133.5, 129.6, 128.1, 123.6, 123.2, 121.3, 107.4, 102.6, 102.0, 57.1, 33.7, 26.0, 25.6, 21.7. TLC-MS: ESI(+) calcd. for $[M+Na]^+$: *m/z* = 416.1; found: 416.1. HPLC: t_{ret} = 19.23 min (94.3 % at 254 nm, 96.2 % at 230 nm, method B).

3-Bromo-1-cyclohexyl-6-tosyl-1,6-dihydrodipyrrolo[2,3-b:2',3'-d]pyridine (45)

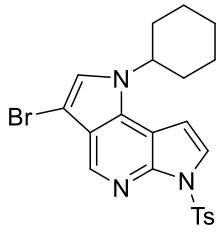

Chemical Formula: $C_{22}H_{22}BrN_3O_2S$
Exact Mass: 471.06161
Molecular Weight: 472.40100

1-Cyclohexyl-6-tosyl-1,6-dihydrodipyrrolo[2,3-*b*:2',3'-*d*]pyridine (**44**, 1.36 g, 3.46 mmol, 1.00 eq.) was dissolved in DCM (70 mL) and cooled to -16 °C. NBS (615 mg, 3.46 mmol, 1.00 eq.) was also dissolved in DCM (35 mL) and slowly added dropwise to the first solution. After 20 min, the reaction is quenched by adding sat. $NaHCO_3$ (50 mL). The aq. phase was extracted with DCM (3 x 30 mL). The combined org. phases were dried over Na_2SO_4 and the solvent was evaporated. The residue was purified via flash column chromatography (silica gel, 0 – 80 % hexane/EtOAc) which afforded the product **45** (1.42 g, 3.01 mmol, 87 %) as a beige solid.

^{1}H-NMR (400 MHz, $CDCl_3$) δ 8.63 (s, 1H), 8.13 – 8.05 (m, 2H), 7.75 (d, J = 4.0 Hz, 1H), 7.25 – 7.21 (m, 2H), 7.18 (s, 1H), 6.74 (d, J = 4.0 Hz, 1H), 4.41 (tt, J = 11.7, 3.6 Hz, 1H), 2.33 (s, 3H), 2.22 – 2.12 (m, 2H), 2.07 – 1.92 (m, 2H), 1.89 – 1.77 (m, 1H), 1.72 – 1.59 (m, 2H), 1.59 – 1.46 (m, 2H), 1.42 – 1.26 (m, 1H).^{13}C-NMR (101 MHz, $CDCl_3$) δ 145.1, 143.4, 138.7, 135.6, 133.4, 129.6, 128.3, 124.2, 122.5, 120.2, 107.0, 102.3, 90.6, 57.7, 33.6, 25.9, 25.5, 21.7. TLC-MS: ESI(+) calcd. for $[M+Na]^+$: *m/z* = 494.1; found: 494.3. HPLC: t_{ret} = 20.77 min (95.9 % at 254 nm, 94.9 % at 230 nm, method B).

2-Bromo-1-fluoro-4-(methoxymethoxy)benzene (48)

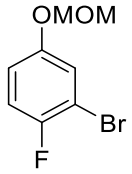

Chemical Formula: $C_8H_8BrFO_2$
Exact Mass: 233.96917
Molecular Weight: 235.05240

3-Bromo-4-fluorophenol (**46**, 2.00 g, 10.1 mmol, 1.00 eq) was dissolved in DCM (21 mL), DIPEA (3.27 mL, 18.8 mmol, 1.80 eq.) was added and the solution was cooled to 0 °C. MOMBr (1.10 mL, 13.6 mmol, 1.30 eq.) was added dropwise and the solution was slowly warmed up to rt. After 1 h of stirring, the reaction was quenched with sat. $NaHCO_3$ (20 mL) and extracted with DCM (3 x 20 mL). The combined organic phases were then washed with water (50 mL) and brine (50 mL), dried over Na_2SO_4 and the solvent was evaporated. The residue was purified via flash column chromatography (silica gel, 0 – 10 % hexane/EtOAc) which afforded the product **48** (2.07 g, 8.81 mmol, 87 %) as a colorless oil.

^{1}H-NMR (400 MHz, $CDCl_3$) δ 7.28 – 7.23 (m, 1H), 7.03 (dd, J = 9.0, 8.0 Hz, 1H), 6.98 – 6.92 (m, 1H), 5.11 (s, 2H), 3.47 (s, 3H). ^{13}C-NMR (101 MHz, $CDCl_3$) δ 154.7 (d, J = 241.2 Hz), 153.8 (d, J = 2.2 Hz), 121.2, 116.9 (d, J = 6.7 Hz), 116.7 (d, J = 23.6 Hz), 109.1 (d, J = 22.2 Hz), 95.2, 56.2. GC-MS: EI(+) calcd. for $[M]^+$: *m/z* = 234.0; found: 234.0. HPLC: t_{ret} = 11.42 min (99.9 % at 254 nm, 98.9 % at 230 nm, method A).

2-(2-Fluoro-5-(methoxymethoxy)phenyl)-4,4,5,5-tetramethyl-1,3,2-dioxaborolane (50)

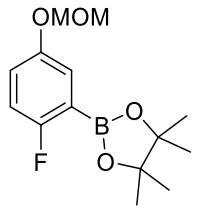

Chemical Formula: $C_{14}H_{20}BFO_4$
Exact Mass: 282.14387
Molecular Weight: 282.11840

2-Bromo-1-fluoro-4-(methoxymethoxy)benzene (**48**, 752 mg, 3.20 mmol, 1.00 eq.) was dissolved in THF (11 mL) and cooled to -78 °C. *n*-Butyllithium (2.5 M in hexane, 3.80 mL, 9.51 mmol, 2.98 eq.) was added dropwise and the solution was then stirred for 30 min. Consequently, isopropylpinacolylborate (2.30 mL, 11.3 mmol, 3.54 eq.) was added slowly and the mixture was stirred for another hour. It was then warmed up and quenched with sat. NH_4Cl (20 mL). Extraction was carried out with EtOAc (3 x 20 mL). The combined organic phases were then washed with water (2 x 40 mL) and brine (40 mL) and subsequently dried over Na_2SO_4, after which the solvent was evaporated. The residue was purified via flash column chromatography (silica gel, 0 – 10 % hexane/EtOAc) which afforded the product **50** (381 mg, 1.35 mmol, 42 %) as a colorless oil.

^{1}H-NMR (400 MHz, $CDCl_3$) δ 7.34 (dd, J = 4.6, 3.2 Hz, 1H), 7.09 (ddd, J = 9.0, 4.4, 3.2 Hz, 1H), 6.95 (t, J = 8.7 Hz, 1H), 5.14 (s, 2H), 3.48 (s, 3H), 1.35 (s, 12H). ^{13}C-NMR (101 MHz, $CDCl_3$) δ 162.5 (d, J = 245.0 Hz), 153.0 (d, J = 2.7 Hz), 123.7 (d, J = 8.1 Hz), 121.5 (d, J = 8.8 Hz), 116.3, 116.0, 95.1, 84.1, 56.1, 24.9. TLC-MS: ESI(+) calcd. for $[M+Na]^+$: *m/z* = 305.1; found: 305.1. HPLC measurements were not possible due to decomposition on the column.

2-Bromo-1-chloro-4-(methoxymethoxy)benzene (49)

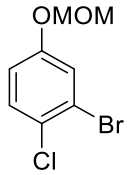

Chemical Formula: $C_8H_8BrClO_2$
Exact Mass: 249.93962
Molecular Weight: 251.50400

3-Bromo-4-chlorophenol (**47**, 2.02 g, 9.74 mmol, 1.00 eq) was dissolved in DCM (20 mL), DIPEA (3.03 mL, 17.4 mmol, 1.79 eq.) was added and the solution was cooled to 0 °C. MOMBr (1.01 mL, 12.5 mmol, 1.28 eq.) was added dropwise and the solution was slowly warmed up to rt. After 1 h of stirring, the reaction was quenched with sat. $NaHCO_3$ (20 mL) and extracted with DCM (3 x 20 mL). The combined organic phases were then washed with water (50 mL) and brine (50 mL), dried over Na_2SO_4 and the solvent was evaporated. The residue was purified via flash column chromatography (silica gel, 0 – 10 % hexane/EtOAc) which afforded the product **49** (2.25 g, 8.95 mmol, 93 %) as a colorless oil.

^{1}H-NMR (400 MHz, $CDCl_3$) δ 7.36 – 7.31 (m, 2H), 6.94 (dd, J = 8.8, 2.8 Hz, 1H), 5.14 (s, 2H), 3.47 (s, 3H). ^{13}C-NMR (101 MHz, $CDCl_3$) δ 156.3, 130.7, 127.3, 122.7, 121.6, 116.9, 94.8, 56.3. GC-MS: EI(+) calcd. for $[M]^+$: *m/z* = 249.9; found: 249.8. HPLC: t_{ret} = 12.15 min (98.9 % at 254 nm, 95.7 % at 230 nm, method A).

2-(2-Chloro-5-(methoxymethoxy)phenyl)-4,4,5,5-tetramethyl-1,3,2-dioxaborolane (51)

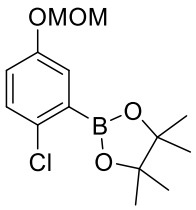

Chemical Formula: $C_{14}H_{20}BClO_4$
Exact Mass: 298.11432
Molecular Weight: 298.57000

2-Bromo-1-chloro-4-(methoxymethoxy)benzene (**49**, 751 mg, 2.99 mmol, 1.00 eq.) was dissolved in THF (10 mL) and cooled to -78 °C. *n*-Butyllithium (2.5 M in hexane, 3.60 mL, 8.99 mmol, 3.01 eq.) was added dropwise and the solution was then stirred for 30 min. Consequently, isopropylpinacolylborate (2.10 mL, 10.8 mmol, 3.61 eq.) was added slowly and the mixture was stirred for another hour. It was then warmed up and quenched with sat. NH_4Cl (20 mL). Extraction was carried out with EtOAc (3 x 20 mL). The combined organic phases were then washed with water (2 x 40 mL) and brine (40 mL) and subsequently dried over Na_2SO_4, after which the solvent was evaporated. The residue was purified via flash column chromatography (silica gel, 0 – 10 % hexane/EtOAc) which afforded the product **51** (650 mg, 2.18 mmol, 73 %) as a colorless oil.

^{1}H-NMR (400 MHz, $CDCl_3$) δ 7.33 (d, J = 3.1 Hz, 1H), 7.28 (s, 1H), 7.04 (dd, J = 8.8, 3.1 Hz, 1H), 5.18 (s, 2H), 3.48 (s, 3H), 1.39 (s, 12H). ^{13}C-NMR (101 MHz, $CDCl_3$) δ 155.3, 132.2, 130.5, 123.8, 119.9, 94.6, 84.4, 77.5, 77.2, 76.8, 56.2, 24.9. TLC-MS: ESI(+) calcd. for $[M+Na]^+$: *m/z* = 321.1; found: 321.3. HPLC measurements were not possible due to decomposition on the column.

2-Bromo-1-(methoxymethoxy)-3-methylbenzene (53)

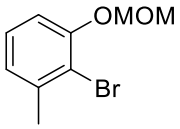

Chemical Formula: $C_9H_{11}BrO_2$
Exact Mass: 229.99424
Molecular Weight: 231.08900

2-Bromo-3-methylphenol (**52**, 2.01 g, 10.7 mmol, 1.00 eq.) was dissolved in DMF (22 mL) and cooled to 0 °C. NaH (60 % dispersion in mineral oil, 555 mg, 13.9 mmol, 1.30 eq.) was added, followed by dropwise addition of MOMBr (1.00 mL, 12.9 mmol, 1.15 eq.). The reaction was then stirred at rt for 18 h. After cooling down to 0 °C again, the reaction was quenched with H_2O (20 mL), extracted with DCM (3 x 30 mL) and dried over Na_2SO_4. The solvent was removed under reduced pressure and the residue was purified via flash column chromatography (silica gel, 0 – 25 % hexane/EtOAc) which afforded the product **53** (1.58 g, 6.84 mmol, 64 %) as a colorless oil.

^{1}H-NMR (400 MHz, $CDCl_3$) δ 7.14 (dd, J = 8.2, 7.5 Hz, 1H), 7.01 – 6.95 (m, 1H), 6.92 (ddd, J = 7.6, 1.5, 0.8 Hz, 1H), 5.25 (s, 2H), 3.52 (s, 3H), 2.42 (s, 3H). ^{13}C-NMR (101 MHz, $CDCl_3$) δ 154.0, 139.9, 127.6, 124.3, 115.7, 113.5, 95.3, 56.5, 23.5. HPLC: t_{ret} = 11.64 min (88.7 % at 254 nm, 81.2 % at 230 nm, method A).

2-(2-(Methoxymethoxy)-6-methylphenyl)-4,4,5,5-tetramethyl-1,3,2-dioxaborolane (54)

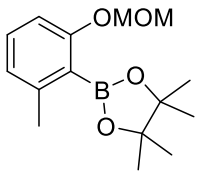

Chemical Formula: $C_{15}H_{23}BO_4$
Exact Mass: 278.16894
Molecular Weight: 278.15500

2-Bromo-1-(methoxymethoxy)-3-methylbenzene (**53**, 1.58 g, 6.84 mmol, 1.00 eq.) was dissolved in THF (23 mL) and cooled to -78 °C. *n*-Butyllithium (2.5 M in hexane, 2.90 mL, 7.18 mmol, 1.05 eq.) was added dropwise and the solution was then stirred for 30 min. Consequently, isopropylpinacolylborate (2.80 mL, 9.71 mmol, 1.42 eq.) was added slowly and the mixture was stirred for another 1.5 h. It was then warmed up and quenched with sat. NH_4Cl (30 mL). Extraction was carried out with EtOAc (3 x 30 mL). The combined organic phases were then washed with water (50 mL) and brine (50 mL) and subsequently dried over Na_2SO_4, after which the solvent was evaporated. The residue was purified via flash column chromatography (silica gel, 0 – 20 % hexane/EtOAc) which afforded the product **54** (1.51 g, 5.43 mmol, 80 %) as a colorless oil.

^{1}H-NMR (400 MHz, $CDCl_3$) δ 7.16 (dd, J = 8.3, 7.5 Hz, 1H), 6.88 – 6.76 (m, 2H), 5.14 (s, 2H), 3.46 (s, 3H), 2.35 (s, 3H), 1.39 (s, 12H). ^{13}C-NMR (101 MHz, $CDCl_3$) δ 160.2, 143.0, 130.4, 123.2, 110.8, 94.4, 83.9, 56.1, 24.9, 21.8. LC-MS: ESI(+) calcd. for $[M+Na]^+$: *m/z* = 301.2; found: 301.2. HPLC: t_{ret} = 11.56 min (98.7 % at 254 nm, 98.8 % at 230 nm, method A).

1-Cyclohexyl-3-(2-fluoro-5-(methoxymethoxy)phenyl)-6-tosyl-1,6-dihydrodipyrrolo[2,3-b:2',3'-d]pyridine (55)

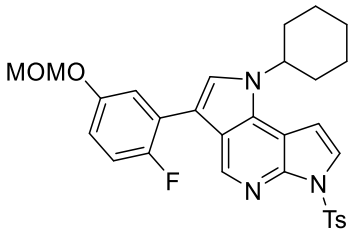

Chemical Formula: $C_{30}H_{30}FN_3O_4S$
Exact Mass: 547.19411
Molecular Weight: 547.64540

5-Bromo-*N*-cyclohexyl-1-tosyl-1*H*-pyrrolo[2,3-*b*]pyridin-4-amine (**45**, 250 mg, 0.539 mmol, 1.00 eq.) and 2-(2-fluoro-5-(methoxymethoxy)phenyl)-4,4,5,5-tetramethyl-1,3,2-dioxaborolane (**50**, 299 mg, 1.06 mmol, 2.00 eq.) were dissolved in 1,4-dioxane (8 mL). XPhos Pd G4 (9.11 mg, 10.6 µmol, 0.02 eq.) and K_3PO_4 (0.8 M in H_2O, 2.00 mL, 1.59 mmol, 3.00 eq.) were added and the solution was stirred at 85 °C for 3 h. After cooling to rt, sat. NH_4Cl (10 mL) was added, and the aq. solution was extracted with DCM (3 x 20 mL). After drying over Na_2SO_4, the solvent was evaporated. The residue was purified via flash column chromatography (silica gel, 0 – 60 % hexane/EtOAc) leading to the product **55** (118 mg, 0.215 mmol, 41 %) as a white solid.

^{1}H-NMR (400 MHz, $CDCl_3$) δ 8.92 (d, J = 1.2 Hz, 1H), 8.30 – 7.95 (m, 2H), 7.74 (d, J = 4.0 Hz, 1H), 7.44 (d, J = 2.1 Hz, 1H), 7.35 (dd, J = 6.2, 3.0 Hz, 1H), 7.24 – 7.17 (m, 2H), 7.10 (dd, J = 10.0, 8.9 Hz, 1H), 6.94 (ddd, J = 8.9, 3.9, 3.0 Hz, 1H), 6.79 (d, J = 4.0 Hz, 1H), 5.19 (s,

2H), 4.48 (tt, J = 11.8, 3.6 Hz, 1H), 3.51 (s, 3H), 2.32 (s, 3H), 2.25 (d, J = 12.4 Hz, 2H), 2.07 – 1.96 (m, 2H), 1.84 (d, J = 13.3 Hz, 1H), 1.75 (qd, J = 12.5, 3.4 Hz, 2H), 1.55 (qt, J = 13.0, 3.3 Hz, 2H), 1.42 – 1.29 (m, 1H). ^{13}C-NMR (101 MHz, $CDCl_3$) δ 155.0 (d, *J* = 240.6 Hz), 153.6 (d, *J* = 2.5 Hz), 145.0, 143.2, 139.3 (d, *J* = 3.1 Hz), 135.7, 134.0, 129.6, 128.2, 124.0, 123.2 (d, *J* = 6.6 Hz), 123.0 (d, *J* = 16.5 Hz), 119.3, 118.0 (d, *J* = 3.7 Hz), 116.7 (d, *J* = 24.9 Hz), 115.5 (d, *J* = 8.4 Hz), 111.0, 107.3, 102.6, 95.2, 57.4, 56.2, 33.6, 26.0, 25.5, 21.7. TLC-MS: ESI(+) calcd. for $[M+H]^+$: *m/z* = 548.2; found: 548.3. HPLC: t_{ret} = 13.51 min (93.1 % at 254 nm, 90.4 % at 230 nm, method A).

3-(1-Cyclohexyl-1,6-dihydrodipyrrolo[2,3-b:2',3'-d]pyridin-3-yl)-4-fluorophenol (58)

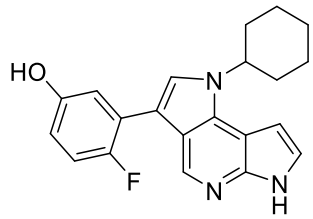

Chemical Formula: $C_{21}H_{20}FN_3O$
Exact Mass: 349.15904
Molecular Weight: 349.40940

1-Cyclohexyl-3-(2-fluoro-5-(methoxymethoxy)phenyl)-6-tosyl-1,6-dihydrodipyrrolo[2,3-*b*:2',3'-*d*]pyridine (**55**, 118 mg, 0.215 mmol, 1.00 eq.) was dissolved in KOH solution (3 M in MeOH, 100 mL) and stirred at 65 °C for 2 h. The solution was cooled to 0 °C and slowly acidified with conc. HCl. It was stirred a further 2 h at rt, after which the MeOH was evaporated under reduced pressure. The solution was again cooled to 0 °C, neutralized with sat. Na_2CO_3 and extracted with DCM (6 x 50 mL). It was dried over Na_2SO_4 and the solvent was evaporated under reduced pressure. The product **58** was then used in the next step without further purification.

TLC-MS: ESI(+) calcd. for $[M+H]^+$: *m/z* = 350.2; found: 350.3.

3-(1-Cyclohexyl-1,6-dihydrodipyrrolo[2,3-b:2',3'-d]pyridin-3-yl)-4-fluorophenyl sulfurofluoridate (61)

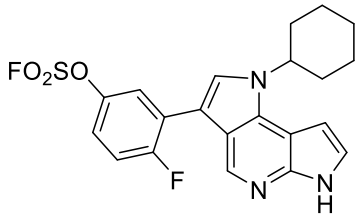

Chemical Formula: $C_{21}H_{19}F_2N_3O_3S$
Exact Mass: 431.11152
Molecular Weight: 431.45781

3-(1-Cyclohexyl-1,6-dihydrodipyrrolo[2,3-*b*:2',3'-*d*]pyridin-3-yl)-4-fluorophenol (**58**, 69.2 mg, 0.198 mmol, 1.00 eq.) and AISF (**64**, 75.9 mg, 0.242 mmol, 1.22 eq.) were dissolved in THF (10 mL). DBU (65.3 µL, 0.438 mmol, 2.21 eq.) was added and the reaction was stirred at rt for 1.5 h. EtOAc (25 mL) was added and the organic phase was washed with sat. NH_4Cl (2 x 20 mL) and brine (20 mL). The organic phase was dried over Na_2SO_4 and the solvent was evaporated under reduced pressure. The residue was purified via flash column chromatography (silica gel, 0 – 100 % hexane/EtOAc) and subsequently triturated from DCM leading to the product **61** (23.0 mg, 53.3 µmol, 25 % over two steps) as a beige solid.

^{1}H-NMR (400 MHz, $CDCl_3$) δ 10.19 (s, 1H), 8.75 (d, J = 1.6 Hz, 1H), 7.72 (dd, J = 5.9, 2.9 Hz, 1H), 7.51 (d, J = 1.9 Hz, 1H), 7.38 (d, J = 3.5 Hz, 1H), 7.35 – 7.27 (m, 2H), 6.74 (d, J = 3.5 Hz, 1H), 4.65 (tt, J = 11.8, 3.6 Hz, 1H), 2.36 (d, J = 12.2 Hz, 2H), 2.10 – 2.01 (m, 2H), 1.92 – 1.73 (m, 3H), 1.62 (qt, J = 13.1, 3.4 Hz, 2H), 1.37 (qt, J = 13.0, 3.7 Hz, 1H). ^{13}C-NMR (101 MHz, $CDCl_3$) δ 158.7 (d, J = 249.1 Hz), 146.0, 145.9, 144.9, 136.3, 135.0, 125.7 (d, J = 17.9 Hz), 122.5 (d, J = 5.8 Hz), 122.4, 119.3 (d, J = 9.0 Hz), 117.7 (d, J = 25.8 Hz), 116.6, 109.2, 104.9, 97.7, 57.3, 33.6, 25.9, 25.5. ^{19}F NMR (376 MHz, $CDCl_3$) δ 37.3, -113.8. HRMS: ESI(+) [*m/z*]: calcd. mass $[M+H]^+$ = 432.11880; found = 432.11876; rel. deviation 0.1 ppm. HPLC: t_{ret} = 12.24 min (96.7 % at 254 nm, 97.7 % at 230 nm, method A).

3-(2-Chloro-5-(methoxymethoxy)phenyl)-1-cyclohexyl-6-tosyl-1,6-dihydrodipyrrolo[2,3-b:2',3'-d]pyridine (56)

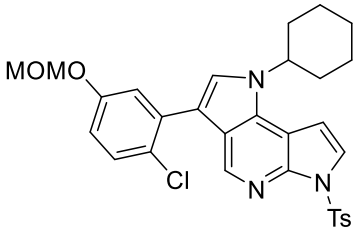

Chemical Formula: $C_{30}H_{30}ClN_3O_4S$
Exact Mass: 563.16456
Molecular Weight: 564.09700

5-Bromo-*N*-cyclohexyl-1-tosyl-1*H*-pyrrolo[2,3-*b*]pyridin-4-amine (**45**, 401 mg, 0.849 mmol, 1.00 eq.) and 2-(2-chloro-5-(methoxymethoxy)phenyl)-4,4,5,5-tetramethyl-1,3,2-dioxaborolane (**51**, 484 mg, 1.72 mmol, 2.02 eq.) were dissolved in 1,4-dioxane (12 mL). XPhos Pd G4 (14.6 mg, 17.0 µmol, 0.02 eq.) and K_3PO_4 (0.8 M in H_2O, 3.50 mL, 2.79 mmol, 3.29 eq.) were added and the solution was stirred at 70 °C for 4.5 h. After cooling to rt, sat. NH_4Cl (15 mL) was added, and the aq. solution was extracted with DCM (3 x 25 mL). After drying over Na_2SO_4, the solvent was evaporated. The residue was purified via flash column chromatography (silica gel, 0 – 60 % hexane/EtOAc) leading to the product **56** (392 mg, 0.695 mmol, 82 %) as a beige solid.

^{1}H-NMR (400 MHz, $CDCl_3$) δ 8.75 (s, 1H), 8.13 – 8.03 (m, 2H), 7.74 (d, J = 4.0 Hz, 1H), 7.45 – 7.36 (m, 2H), 7.26 – 7.17 (m, 3H), 6.96 (dd, J = 8.8, 3.0 Hz, 1H), 6.80 (d, J = 4.0 Hz, 1H), 5.19 (s, 2H), 4.48 (tt, J = 11.8, 3.6 Hz, 1H), 3.49 (s, 3H), 2.32 (s, 3H), 2.30 – 2.21 (m, 2H), 2.03 – 1.94 (m, 2H), 1.84 (d, J = 13.4 Hz, 1H), 1.74 (qd, J = 12.5, 3.3 Hz, 2H), 1.56 (qt, J = 13.3, 3.5 Hz, 2H), 1.41-1.29 (m, 1H). ^{13}C-NMR (101 MHz, $CDCl_3$) δ 155.9, 144.9, 143.0, 139.3, 135.6, 133.8, 133.5, 130.9, 129.5, 128.1, 125.7, 123.8, 123.3, 119.7, 119.6, 116.0, 114.3, 107.3, 102.5, 94.6, 77.4, 77.0, 76.7, 57.2, 56.1, 33.6, 25.8, 25.4, 21.6. TLC-MS: ESI(+) calcd. for $[M+H]^+$: *m/z* = 564.2; found: 564.3. HPLC: t_{ret} = 13.71 min (78.2 % at 254 nm, 76.2 % at 230 nm, method A).

4-Chloro-3-(1-cyclohexyl-1,6-dihydrodipyrrolo[2,3-b:2',3'-d]pyridin-3-yl)phenol (59)

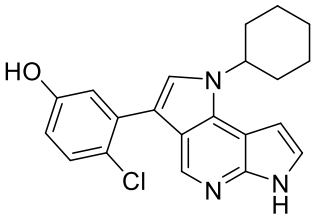

Chemical Formula: $C_{21}H_{20}ClN_3O$
Exact Mass: 365.12949
Molecular Weight: 365.86100

3-(2-Chloro-5-(methoxymethoxy)phenyl)-1-cyclohexyl-6-tosyl-1,6-dihydrodipyrrolo[2,3-*b*:2',3'-*d*]pyridine (**56**, 373 mg, 0.681 mmol, 1.00 eq.) was dissolved in KOH solution (3 M in MeOH, 200 mL) and stirred at 65 °C for 3 h. The solution was cooled to 0 °C and slowly acidified with conc. HCl. It was stirred a further 2 h at rt, after which the MeOH was evaporated under reduced pressure. The solution was again cooled to 0 °C, neutralized with sat. Na_2CO_3 and extracted with DCM (6 x 70 mL). It was dried over Na_2SO_4 and the solvent was evaporated under reduced pressure. The product **59** was then used in the next step without further purification.

TLC-MS: ESI(+) calcd. for $[M+H]^+$: *m/z* = 366.1; found: 366.3.

4-Chloro-3-(1-cyclohexyl-1,6-dihydrodipyrrolo[2,3-b:2',3'-d]pyridin-3-yl)phenyl sulfurofluoridate (62)

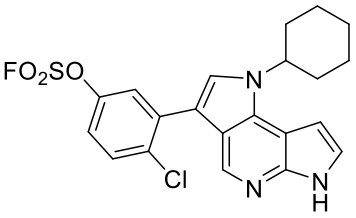

Chemical Formula: $C_{21}H_{19}ClFN_3O_3S$
Exact Mass: 447.08197
Molecular Weight: 447.90940

3-(2-Chloro-5-(methoxymethoxy)phenyl)-1-cyclohexyl-6-tosyl-1,6-dihydrodipyrrolo[2,3-*b*:2',3'-*d*]pyridine (**59**, 173 mg, 0.473 mmol, 1.00 eq.) and AISF (**64**, 178 mg, 0.567 mmol, 1.20 eq.) were dissolved in THF (23 mL). DBU (157 µL, 1.05 mmol, 2.22 eq.) was added and the reaction was stirred at rt for 2 h. EtOAc (50 mL) was added and the organic phase was washed with sat. NH_4Cl (2 x 40 mL) and brine (40 mL). The organic phase was dried over Na_2SO_4, and the solvent was evaporated under reduced pressure. The residue was purified via flash column chromatography (silica gel, 0 – 100 % hexane/EtOAc) leading to the product **62** (135 mg, 0.301 mmol, 43 % over two steps) as a white solid.

^{1}H-NMR (400 MHz, DMSO) δ 11.77 (s, 1H), 8.40 (s, 1H), 7.89 (d, J = 3.0 Hz, 1H), 7.84 (d, J = 8.9 Hz, 1H), 7.72 (s, 1H), 7.62 (dd, J = 8.9, 3.0 Hz, 1H), 7.42 (t, J = 3.0 Hz, 1H), 6.77 – 6.72 (m, 1H), 4.78 – 4.56 (m, 1H), 2.17 (d, J = 11.9 Hz, 2H), 1.91 (d, J = 13.6 Hz, 2H), 1.87 – 1.73 (m, 3H), 1.71 – 1.54 (m, 2H), 1.49 – 1.25 (m, 1H). ^{13}C-NMR (101 MHz, $CDCl_3$) δ ^{13}C NMR (101 MHz, DMSO) δ 148.1, 144.2, 136.0, 135.8, 133.6, 132.4, 132.2, 124.2, 123.2, 123.0, 120.4, 116.0, 111.7, 104.1, 97.1, 32.9, 25.1, 25.0. ^{19}F NMR (376 MHz, DMSO) δ 39.0. HRMS: ESI(+) [*m/z*]: calcd. mass $[M+H]^+$ = 448.08924; found = 448.08955; rel. deviation 0.7 ppm. HPLC: t_{ret} = 12.43 min (96.1 % at 254 nm, 96.8 % at 230 nm, method A).

1-Cyclohexyl-3-(2-(methoxymethoxy)-6-methylphenyl)-6-tosyl-1,6-dihydrodipyrrolo[2,3-b:2',3'-d]pyridine (57)

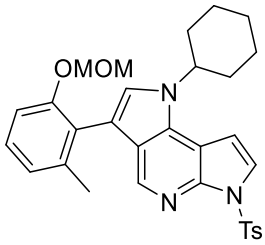

Chemical Formula: $C_{31}H_{33}N_3O_4S$
Exact Mass: 543.21918
Molecular Weight: 543.68200

5-Bromo-*N*-cyclohexyl-1-tosyl-1*H*-pyrrolo[2,3-*b*]pyridin-4-amine (**45**, 400 mg, 0.847 mmol, 1.00 eq.) and 2-(2-(methoxymethoxy)-6-methylphenyl)-4,4,5,5-tetramethyl-1,3,2-dioxaborolane (**54**, 473 mg, 1.70 mmol, 2.01 eq.) were dissolved in 1,4-dioxane (12 mL). XPhos Pd G4 (14.6 mg, 16.9 µmol, 0.02 eq.) and K_3PO_4 (0.8 M in H_2O, 3.50 mL, 2.79 mmol, 3.29 eq.) were added and the solution was stirred at 85 °C for 3 d. After cooling to rt, sat. NH_4Cl (15 mL) was added, and the aq. solution was extracted with DCM (3 x 25 mL). After drying over Na_2SO_4, the solvent was evaporated. The residue was purified via flash column chromatography (silica gel, 0 – 40 % hexane/EtOAc) leading to the product **57** (170 mg, 0.313 mmol, 37 %) as a red solid. 43 % of starting material were recovered which leads to an adjusted yield of the reaction of 65 %.

^{1}H-NMR (400 MHz, $CDCl_3$) δ 8.38 (s, 1H), 8.13 – 8.04 (m, 2H), 7.72 (d, J = 4.0 Hz, 1H), 7.25 – 7.18 (m, 3H), 7.09 (s, 1H), 7.05 (dd, J = 8.3, 1.0 Hz, 1H), 6.99 (dt, J = 7.3, 1.1 Hz, 1H), 6.80 (d, J = 4.0 Hz, 1H), 5.00 – 4.88 (m, 2H), 4.48 (tt, J = 11.7, 3.6 Hz, 1H), 3.22 (s, 3H), 2.33 (s, 3H), 2.32 – 2.22 (m, 2H), 2.12 (s, 3H), 2.00 (d, *J* = 13.3 Hz, 2H), 1.84 (d, *J* = 13.4 Hz, 1H), 1.72 (t, *J* = 11.4 Hz, 2H), 1.65 – 1.48 (m, 2H), 1.39 – 1.23 (m, 1H). ^{13}C-NMR (101 MHz, $CDCl_3$) δ 156.0, 144.9, 143.1, 139.7, 139.7, 135.8, 133.5, 129.5, 128.3, 128.3, 124.0, 123.8, 123.5, 122.3, 120.8, 112.9, 112.1, 107.4, 102.6, 95.1, 57.2, 56.1, 33.9, 33.6, 26.0, 25.6, 21.7, 20.9. TLC-MS: ESI(+) calcd. for $[M+H]^+$: *m/z* = 544.2; found: 544.0. HPLC: t_{ret} = 13.33 min (97.9 % at 254 nm, 95.2 % at 230 nm, method A).

2-(1-Cyclohexyl-1,6-dihydrodipyrrolo[2,3-b:2',3'-d]pyridin-3-yl)-3-methylphenol (60)

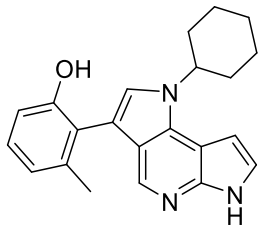

Chemical Formula: $C_{22}H_{23}N_3O$
Exact Mass: 345.18411
Molecular Weight: 345.44600

1-Cyclohexyl-3-(2-(methoxymethoxy)-6-methylphenyl)-6-tosyl-1,6-dihydrodipyrrolo[2,3-*b*:2',3'-*d*]pyridine (**57**, 170 mg, 0.313 mmol, 1.00 eq.) was dissolved in KOH solution (3 M in MeOH, 100 mL) and stirred at 70 °C for 2 h. The solution was cooled to 0 °C and slowly acidified with conc. HCl. It was stirred a further 2 h at rt, after which the MeOH was evaporated under reduced pressure. The solution was again cooled to 0 °C, neutralized with sat. Na_2CO_3 and extracted with DCM (6 x 40 mL). It was dried over Na_2SO_4, and the solvent was evaporated under reduced pressure. The residue was purified via flash

column chromatography (silica gel, 0 – 10 % DCM/MeOH) leading to the product **60** (102 mg, 0.295 mmol, 94 %) as a red solid.

^{1}H-NMR (400 MHz, DMSO) δ 11.58 (s, 1H), 8.89 (s, 1H), 8.02 (s, 1H), 7.38 – 7.32 (m, 1H), 7.24 (s, 1H), 7.11 – 7.01 (m, 1H), 6.81 – 6.73 (m, 2H), 6.70 (dd, J = 3.4, 1.8 Hz, 1H), 4.59 (tt, J = 11.6, 3.6 Hz, 1H), 2.15 (d, J = 12.1 Hz, 2H), 2.09 (s, 3H), 2.01 – 1.85 (m, 2H), 1.85 – 1.69 (m, 3H), 1.62 (qt, J = 13.0, 3.5 Hz, 2H), 1.41 – 1.21 (m, 1H).^{13}C-NMR (101 MHz, DMSO) δ 155.8, 144.4, 138.5, 137.1, 133.3, 127.5, 122.1, 121.1, 121.1, 120.7, 117.6, 112.9, 111.1, 104.2, 96.9, 56.1, 33.1, 25.3, 25.1, 20.7. TLC-MS: ESI(+) calcd. for $[M+H]^+$: *m/z* = 346.2; found: 346.1. HPLC: t_{ret} = 10.45 min (93.5 % at 254 nm, 91.8 % at 230 nm, method A).

2-(1-Cyclohexyl-1,6-dihydrodipyrrolo[2,3-b:2',3'-d]pyridin-3-yl)-3-methylphenyl sulfurofluoridate (63)

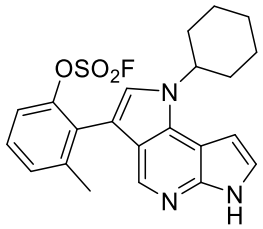

Chemical Formula: $C_{22}H_{22}FN_3O_3S$
Exact Mass: 427.13659
Molecular Weight: 427.49440

2-(1-Cyclohexyl-1,6-dihydrodipyrrolo[2,3-*b*:2',3'-*d*]pyridin-3-yl)-3-methylphenol (**60**, 84.8 mg, 0.245 mmol, 1.00 eq.) and AISF (**64**, 93.0 mg, 0.295 mmol, 1.20 eq.) were dissolved in THF (12 mL). DBU (81.2 µL, 0.544 mmol, 2.21 eq.) was added and the reaction was stirred at rt for 3 h. EtOAc (25 mL) was added, and the organic phase was washed with sat. NH_4Cl (2 x 15 mL) and brine (15 mL). The organic phase was dried over Na_2SO_4, and the solvent was evaporated under reduced pressure. The residue was purified via flash column chromatography (silica gel, 0 – 10 % DCM/MeOH) leading to the product **63** (77.7 mg, 0.182 mmol, 74 %) as a light orange solid.

^{1}H-NMR (400 MHz, DMSO) δ 11.73 (s, 1H), 8.03 (s, 1H), 7.54 – 7.50 (m, 3H), 7.47 (s, 1H), 7.41 (t, J = 3.0 Hz, 1H), 6.75 (dd, J = 3.4, 1.9 Hz, 1H), 4.71 – 4.60 (m, 1H), 2.23 (s, 3H), 2.19 – 2.06 (m, 2H), 1.90 (d, J = 12.9 Hz, 2H), 1.86 – 1.72 (m, 3H), 1.71 – 1.57 (m, 2H), 1.36 – 1.21 (m, 1H). ^{13}C NMR (101 MHz, DMSO) δ 148.8, 144.5, 141.2, 135.9, 133.5, 130.6, 128.9, 127.6, 122.7, 122.2, 118.6, 116.9, 107.4, 104.2, 97.0, 56.2, 33.1, 32.9, 25.2, 25.1, 25.1, 20.3. ^{19}F NMR (376 MHz, DMSO) δ 41.3. HRMS: ESI(+) [*m/z*]: calcd. mass $[M+H]^+$ = 428.14387; found = 428.14420; rel. deviation 0.8 ppm. HPLC: t_{ret} = 12.05 min (96.0 % at 254 nm, 97.7 % at 230 nm, method A).

3-Bromobenzenesulfonyl fluoride (67)

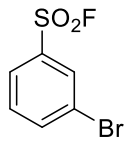

Chemical Formula: $C_6H_4BrFO_2S$
Exact Mass: 237.90994
Molecular Weight: 239.05840

3-Bromobenzenesulfonyl chloride (**66**, 2.00 g, 7.83 mmol, 1.00 eq.) was dissolved in MeCN (8 mL). KHF_2 (1.41 g, 18.0 mmol, 2.31 eq.) was dissolved in H_2O (4 mL) and added to the first solution. After stirring at rt for 24 h, the mixture was extracted with EtOAc (3 x 10 mL) and dried over Na_2SO_4. The solvent was evaporated under reduced pressure which afforded the product **67** (1.84 g, 7.70 mmol, quant.) as a yellow oil.

^{1}H-NMR (400 MHz, $CDCl_3$) δ 8.16 (t, J = 1.9 Hz, 1H), 7.96 (ddd, J = 7.9, 1.9, 1.0 Hz, 1H), 7.91 (ddt, J = 8.1, 1.8, 0.8 Hz, 1H), 7.52 (td, J = 8.0, 1.1 Hz, 1H). ^{13}C-NMR (101 MHz, $CDCl_3$) δ 138.8, 134.9 (d, J = 25.7 Hz), 131.4, 131.3, 127.1, 123.7. ^{19}F NMR (376 MHz, $CDCl_3$) δ 66.2. TLC-MS: ESI(-) calcd. for $[M-H]^+$: *m/z* = 236.9; found: 236.8. HPLC: t_{ret} = 11.07 min (99.7 % at 254 nm, 98.7 % at 230 nm, method A).

3-(4,4,5,5-Tetramethyl-1,3,2-dioxaborolan-2-yl)benzenesulfonyl fluoride (68)

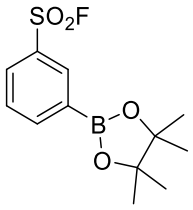

Chemical Formula: $C_{12}H_{16}BFO_4S$
Exact Mass: 286.08464
Molecular Weight: 286.12440

3-Bromobenzenesulfonyl fluoride (**67**, 1.83 g, 7.65 mmol, 1.00 eq.), bis(pinacolato)diboron (2.12 g, 8.34 mmol, 1.09 eq.), KOAc (2.33 g, 23.7 mmol, 3.10 eq.) and $Pd(dppf)Cl_2 \cdot CH_2Cl_2$ (188 mg, 0.231 mmol, 0.03 eq.) were suspended in 1,4-dioxane (25 mL) and heated to 80 °C. After 16 h, the solution was cooled to rt, EtOAc (50 mL) was added, washed with H_2O (50 mL) and brine (50 mL) and dried over Na_2SO_4. The solvent was removed under reduced pressure and the residue was purified by flash column chromatography (silica gel, 5 – 20 % hexane/EtOAc) to yield the product **68** (1.73 g, 6.05 mmol, 79 %) as a white solid.

^{1}H-NMR (400 MHz, $CDCl_3$) δ 8.44 (s, 1H), 8.17 (dd, J = 7.4, 1.3 Hz, 1H), 8.07 (ddd, J = 8.0, 2.0, 1.2 Hz, 1H), 7.66 – 7.58 (m, 1H), 1.36 (s, 12H). ^{13}C-NMR (101 MHz, $CDCl_3$) δ 141.7, 134.6, 133.0 (d, J = 24.1 Hz), 130.7, 129.1, 84.9, 25.0. TLC-MS: ESI(+) calcd. for $[M+Na]^+$: *m/z* = 309.1; found: 309.3. HPLC: t_{ret} = 9.57 min (95.4 % at 254 nm, 98.7 % at 230 nm, method A).

(3-(Fluorosulfonyl)phenyl)boronic acid (69)

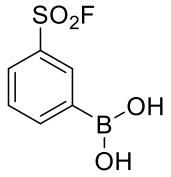

Chemical Formula: $C_6H_6BFO_4S$
Exact Mass: 204.00639
Molecular Weight: 203.97840

3-(4,4,5,5-Tetramethyl-1,3,2-dioxaborolan-2-yl)benzenesulfonyl fluoride (**68**, 1.73 g, 6.05 mmol, 1.00 eq.) was dissolved in acetone (30 mL). NH_4OAc (2.35 g, 30.5 mmol, 5.05 eq.) was dissolved in H_2O (30 mL) and was added to the first solution. Finally, $NaIO_4$ (5.17 g, 24.2 mmol, 4.00 eq.) was added and the solution was stirred vigorously at rt for 30 h. The acetone was evaporated, EtOAc (30 mL) was added. The organic phase was washed with brine (30 mL) and the combined aq. phases were extracted with EtOAc (3 x 30 mL). After drying over Na_2SO_4 and removing the solvent under reduced pressure, the residue was triturated from hexane/DCM (4:1) which afforded the product **69** (919 mg, 4.51 mmol, 75 %) as a beige solid.

^{1}H-NMR (400 MHz, DMSO) δ 8.59 (s, 2H), 8.47 (s, 1H), 8.30 (dt, J = 7.4, 1.3 Hz, 1H), 8.16 (ddd, J = 8.0, 2.2, 1.2 Hz, 1H), 7.78 (t, J = 7.7 Hz, 1H). ^{13}C-NMR (101 MHz, DMSO) δ 142.4, 137.5, 133.7, 131.6 (d, J = 22.1 Hz), 130.1, 130.1. MS: ESI(+) calcd. for $[M+Na]^+$: *m/z* = 227.0; found: 227.0. HPLC: t_{ret} = 6.22 min (100 % at 254 nm, 99.3 % at 230 nm, method A).

2-Bromobenzenesulfonyl fluoride (73)

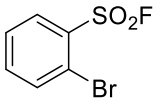

Chemical Formula: $C_6H_4BrFO_2S$
Exact Mass: 237.90994
Molecular Weight: 239.05840

2-Bromobenzenesulfonyl chloride (**72**, 500 mg, 1.96 mmol, 1.00 eq.) was dissolved in MeCN (2 mL). KHF_2 (350 mg, 4.50 mmol, 2.30 eq.) was dissolved in H_2O (1 mL) and added to the first solution. After stirring at rt for 24 h, the mixture was extracted with EtOAc (3 x 10 mL) and dried over Na_2SO_4. The solvent was evaporated under reduced pressure which afforded the product **73** (455 mg, 1.90 mmol, 97 %) as a beige solid.

^{1}H-NMR (400 MHz, $CDCl_3$) δ 8.19 – 8.09 (m, 1H), 7.90 – 7.80 (m, 1H), 7.63 – 7.51 (m, 2H). ^{13}C-NMR (101 MHz, $CDCl_3$) δ 136.1, 135.9, 134.1 (d, *J* = 24.5 Hz), 132.1, 128.0, 121.1. TLC-MS: ESI(-) calcd. for $[M-H]^+$: *m/z* = 236.9; found: 236.6. HPLC: t_{ret} = 10.56 min (99.1 % at 254 nm, 98.8 % at 230 nm, method A).

2-(4,4,5,5-Tetramethyl-1,3,2-dioxaborolan-2-yl)benzenesulfonyl fluoride (74)

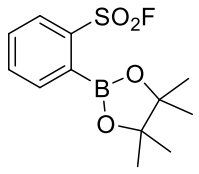

Chemical Formula: $C_{12}H_{16}BFO_4S$
Exact Mass: 286.08464
Molecular Weight: 286.12440

Benzenesulfonyl fluoride (**70**, 600 mg, 3.75 mmol, 1.00 eq.) was dissolved in THF (4 mL) and the solution was cooled to -78 °C. Triisopropyl borate (2.10 mL, 9.10 mmol, 2.43 eq.) was added. Subsequently, a freshly prepared LDA solution (diisopropylamine (680 µL, 4.87 mmol, 1.30 eq.) was dissolved in THF (4 mL), cooled to 0 °C and *n*-butyllithium (2.5 M in hexane, 1.80 mL, 4.50 mmol, 1.21 eq.) was added dropwise) was added over the course of 1 min. The solution was stirred for 2 h. It was then warmed up and quenched with HCl (3.5 %, 20 mL). Extraction was carried out with EtOAc (3 x 20 mL), the combined org. phases were dried over Na_2SO_4, and the solvent was removed under reduced pressure. The residue was dissolved in toluene (16 mL) and pinacol (531 mg, 4.50 mmol, 1.20 eq.) was added. The solution was stirred at rt for 24 h, after which the solvent was evaporated and the residue was purified by flash column chromatography (silica gel, 0 – 20 % hexane/EtOAc) to yield the product **74** (409 mg, 1.43 mmol, 38 %) as a colorless oil.

^{1}H-NMR (400 MHz, $CDCl_3$) δ 8.06 (dd, J = 7.9, 1.1 Hz, 1H), 7.78 – 7.67 (m, 2H), 7.62 (dddd, J = 8.1, 7.0, 1.8, 1.2 Hz, 1H), 1.40 (s, 12H). ^{13}C-NMR (101 MHz, $CDCl_3$) δ 136.5, 136.2, 134.8, 134.4, 130.4, 129.2, 85.3, 24.9, 22.1. ASAP: APCI(+) calcd. for $[M+H]^+$: *m/z* = 287.1; found: 286.7. HPLC: t_{ret} = 11.51 min (83.7 % at 254 nm, 87.0 % at 230 nm, method A).

2-(5,5-Dimethyl-1,3,2-dioxaborinan-2-yl)benzenesulfonyl fluoride (75)

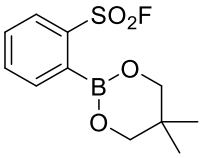

Chemical Formula: $C_{11}H_{14}BFO_4S$
Exact Mass: 272.06899
Molecular Weight: 272.09740

Benzenesulfonyl fluoride (**70**, 1.02 g, 6.37 mmol, 1.00 eq.) was dissolved in THF (6 mL) and the solution was cooled to -78 °C. Triisopropyl borate (3.50 mL, 15.2 mmol, 2.38 eq.) was added. Subsequently, a freshly prepared LDA solution (diisopropylamine (1.15 mL, 8.22 mmol, 1.30 eq.) was dissolved in THF (6 mL), cooled to 0 °C and *n*-butyllithium (2.5 M in hexane, 3.00 mL, 7.57 mmol, 1.20 eq.) was added dropwise) was added over the course of 1 min. The solution was stirred for 2 h. It was then warmed up and quenched with HCl (3.5 %, 20 mL). Extraction was carried out with EtOAc (4 x 20 mL), the combined org. phases were dried over Na_2SO_4, and the solvent was removed under reduced pressure. The residue was dissolved in toluene (24 mL) and neopentyl glycol (809 mg, 7.77 mmol, 1.22 eq.) was added. The solution was stirred at rt for 20 h, after which the solvent was evaporated and the residue was purified by flash column chromatography (silica gel, 0 – 20 % hexane/EtOAc) to yield the product **75** (332 mg, 1.22 mmol, 19 %) as a colorless oil.

^{1}H-NMR (400 MHz, $CDCl_3$) δ 8.07 – 8.01 (m, 1H), 7.76 – 7.65 (m, 2H), 7.58 (dddd, *J* = 8.1, 7.0, 1.9, 1.1 Hz, 1H), 3.81 (s, 4H), 1.09 (s, 6H). ^{13}C-NMR (101 MHz, $CDCl_3$) δ 136.0, 135.8, 134.4, 134.0, 129.8, 129.0, 73.0, 32.0, 22.1. HPLC: t_{ret} = 6.77 min (89.1 % at 254 nm, 86.6 % at 230 nm, method A).

3-Bromo-1-cyclohexyl-1,6-dihydrodipyrrolo[2,3-b:2',3'-d]pyridine (76)

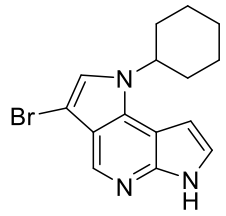

Chemical Formula: $C_{15}H_{16}BrN_3$
Exact Mass: 317.05276
Molecular Weight: 318.21800

3-Bromo-1-cyclohexyl-6-tosyl-1,6-dihydrodipyrrolo[2,3-*b*:2',3'-*d*]pyridine (**45**, 400 mg, 0.847 mmol, 1.00 eq.) was dissolved in KOH solution (4 M in MeOH, 6.5 mL) and refluxed for 3 h. The solution was neutralized with HCl (2 M), extracted with DCM (5 x 15 mL), dried over Na_2SO_4 and the solvent was removed under reduced pressure. The residue was purified by flash column chromatography (silica gel, 0 – 10 % DCM/MeOH, 1 % NH_3) to yield the product **76** (166 mg, 0.522 mmol, 62 %) as a beige solid.

^{1}H-NMR (400 MHz, $CDCl_3$) 12.07 (s, 1H), 8.61 (s, 1H), 7.42 (d, J = 3.4 Hz, 1H), 7.17 (s, 1H), 6.68 (d, J = 3.4 Hz, 1H), 4.57 (tt, J = 11.7, 3.6 Hz, 1H), 2.32 – 2.23 (m, 2H), 2.05 – 1.96 (m, 2H), 1.89 – 1.80 (m, 1H), 1.70 (qd, J = 12.3, 3.1 Hz, 2H), 1.58 (qt, J = 13.2, 3.3 Hz, 2H), 1.32 (qt, J = 12.9, 3.7 Hz, 1H). ^{13}C-NMR (101 MHz, $CDCl_3$) δ 145.3, 136.3, 134.3, 122.5, 120.9, 117.9, 104.6, 97.6, 90.6, 57.6, 33.7, 26.0, 25.6. TLC-MS: ESI(+) calcd. for $[M+H]^+$: *m/z* = 318.1; found: 318.2. HPLC: t_{ret} = 15.87 min (93.5 % at 254 nm, 92.3 % at 230 nm, method B).

tert-Butyl 3-bromo-1-cyclohexyldipyrrolo[2,3-b:2',3'-d]pyridine-6(1H)-carboxylate (77)

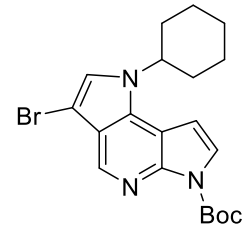

Chemical Formula: $C_{20}H_{24}BrN_3O_2$
Exact Mass: 417.10519
Molecular Weight: 418.33500

3-Bromo-1-cyclohexyl-1,6-dihydrodipyrrolo[2,3-*b*:2',3'-*d*]pyridine (**76**, 166 mg, 0.522 mmol, 1.00 eq.) was dissolved in DCM (6 mL). DMAP (6.37 mg, 52.2 µmol, 0.10 eq.), TEA (1.00 mL, 0.715 mmol, 1.37 eq.) and Boc_2O (150 µL, 0.699 mmol, 1.34 eq.) were added and the solution was stirred at rt for 2.5 h. Subsequently, sat. NH_4Cl (10 mL) was added, and the aq. phase was extracted with EtOAc (3 x 15 mL). After washing with H_2O (30 mL) and brine (30 mL), the org. phase was dried over Na_2SO_4 and the solvent was evaporated to afford the product **77** (182 mg, 0.435 mmol, 83 %) as a beige solid.

^{1}H-NMR (400 MHz, $CDCl_3$) δ 8.70 (s, 1H), 7.65 (d, J = 4.0 Hz, 1H), 7.20 (s, 1H), 6.65 (d, J = 4.1 Hz, 1H), 4.47 (tt, J = 11.8, 3.6 Hz, 1H), 2.27 – 2.17 (m, 2H), 2.05 – 1.94 (m, 2H), 1.89 – 1.78 (m, 1H), 1.69 (s, 9H), 1.62 – 1.43 (m, 4H), 1.38 – 1.27 (m, 1H). ^{13}C-NMR (101 MHz,

$CDCl_3$) δ 148.3, 144.5, 138.8, 133.5, 124.4, 122.5, 120.1, 107.0, 101.4, 90.5, 84.1, 57.6, 33.6, 28.3, 25.9, 25.5. TLC-MS: ESI(+) calcd. for $[M+Na]^+$: *m/z* = 440.1; found: 440.2. HPLC: t_{ret} = 19.82 min (92.9 % at 254 nm, 94.6 % at 230 nm, method B).

tert-Butyl 1-cyclohexyl-3-(3-(fluorosulfonyl)phenyl)dipyrrolo[2,3-b:2',3'-d]pyridine-6(1H)-carboxylate (78)

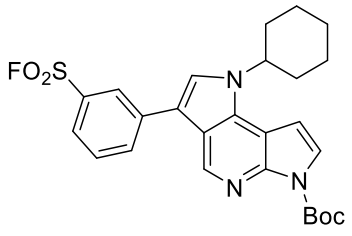

Chemical Formula: $C_{26}H_{28}FN_3O_4S$
Exact Mass: 497.17846
Molecular Weight: 497.58540

(3-(Fluorosulfonyl)phenyl)boronic acid (**69**, 129 mg, 0.633 mmol, 1.50 eq.), $Pd(OAc)_2$ (4.75 mg, 21.1 µM, 0.05 eq) and XPhos (22.2 mg, 46.5 µM, 0.11 eq.) were suspended in 1,4-dioxane (2 mL). K_3PO_4 (179 mg, 0.844 mmol, 2.00 eq.) was dissolved in H_2O (1 mL) and added to the first solution. Finally, *tert*-butyl 3-bromo-1-cyclohexyldipyrrolo[2,3-*b*:2',3'-*d*]pyridine-6(1*H*)-carboxylate (**77**, 177 mg, 0.423 mmol, 1.00 eq.) was added and the mixture was stirred at 40 °C for 24 h. After cooling down to rt, the solution is diluted with EtOAc (20 mL), dried over Na_2SO_4 and the solvent is removed under reduced pressure. The residue was purified by flash column chromatography (silica gel, 0 – 40 % hexane/EtOAc) to yield the product **78** (112 mg, 0.225 mmol, 54 %) as a beige solid.

^{1}H-NMR (400 MHz, $CDCl_3$) δ 9.05 (s, 1H), 8.25 (t, J = 1.8 Hz, 1H), 8.09 (dt, J = 7.9, 1.4 Hz, 1H), 7.90 (dt, J = 8.1, 1.3 Hz, 1H), 7.75 – 7.64 (m, 2H), 7.48 (s, 1H), 6.72 (d, J = 4.1 Hz, 1H), 4.56 (tt, J = 11.8, 3.6 Hz, 1H), 2.36 – 2.28 (m, 2H), 2.05 (dt, J = 13.6, 3.5 Hz, 2H), 1.92 – 1.72 (m, 3H), 1.70 (s, 9H), 1.60 (qt, J = 13.2, 3.4 Hz, 2H), 1.36 (qt, J = 13.0, 3.7 Hz, 1H). ^{13}C-NMR (101 MHz, $CDCl_3$) δ 148.3, 144.3, 138.3, 137.3, 134.8, 134.1, 133.9 (d, J = 23.9 Hz), 130.4, 126.8, 125.6, 124.6, 121.9, 118.4, 115.6, 107.5, 101.5, 84.2, 57.4, 33.7, 28.3, 26.0, 25.6. TLC-MS: ESI(+) calcd. for $[M+H]^+$: *m/z* = 498.2; found: 498.4. HPLC: t_{ret} = 21.19 min (97.2 % at 254 nm, 94.9 % at 230 nm, method B).

3-(1-Cyclohexyl-1,6-dihydrodipyrrolo[2,3-b:2',3'-d]pyridin-3-yl)benzenesulfonyl fluoride (80)

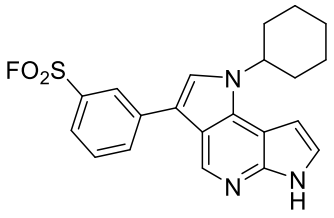

Chemical Formula: $C_{21}H_{20}FN_3O_2S$
Exact Mass: 397.12603
Molecular Weight: 397.46840

tert-Butyl 1-cyclohexyl-3-(3-(fluorosulfonyl)phenyl)dipyrrolo[2,3-*b*:2',3'-*d*]pyridine-6(1*H*)-carboxylate (**78**, 90.6 mg, 0.182 mmol, 1.00 eq.) was dissolved in DCM (4 mL) and HCl in dioxane (4 M, 4 mL) was added. The solution was stirred at rt for 18 h, neutralized with sat. $NaHCO_3$ and extracted with EtOAc (3 x 20 mL). The org. phase was dried over Na_2SO_4, the solvent was evaporated,

and the residue was triturated from hexane/DCM 4:1 to yield the product **80** (68.7 mg, 0.173 mmol, 95 %) as an off-white solid.

^{1}H-NMR (400 MHz, DMSO) δ 11.81 (s, 1H), 8.82 (s, 1H), 8.43 – 8.35 (m, 2H), 8.10 (s, 1H), 7.97 (dt, J = 8.0, 1.4 Hz, 1H), 7.85 (t, J = 7.8 Hz, 1H), 7.43 (t, J = 3.0 Hz, 1H), 6.75 (dd, J = 3.5, 1.9 Hz, 1H), 4.70 – 4.59 (m, 1H), 2.15 (d, J = 11.5 Hz, 2H), 2.03 – 1.82 (m, 4H), 1.78 (d, J = 12.9 Hz, 1H), 1.71 – 1.58 (m, 2H), 1.38 – 1.25 (m, 1H). ^{13}C-NMR (101 MHz, DMSO) δ 144.8, 137.6, 135.5, 134.5, 134.2, 132.4 (d, J = 22.6 Hz), 131.1, 125.4, 124.8, 123.1, 122.5, 115.2, 113.8, 104.2, 97.1, 56.3, 32.9, 25.1, 25.1. ^{19}F NMR (376 MHz, DMSO) δ 66.0. HRMS: ESI(+) [*m/z*]: calcd. mass $[M+H]^+$ = 398.13330; found = 398.13360; rel. deviation 0.8 ppm. HPLC: t_{ret} = 17.94 min (97.4 % at 254 nm, 97.3 % at 230 nm, method B).

tert-Butyl 1-cyclohexyl-3-(2-(fluorosulfonyl)phenyl)dipyrrolo[2,3-b:2',3'-d]pyridine-6(1H)-carboxylate (79)

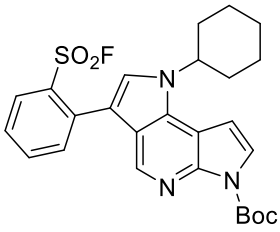

Chemical Formula: $C_{26}H_{28}FN_3O_4S$
Exact Mass: 497.17846
Molecular Weight: 497.58540

tert-Butyl 3-bromo-1-cyclohexyldipyrrolo[2,3-*b*:2',3'-*d*]pyridine-6(1*H*)-carboxylate (**77**, 200 mg, 0.478 mmol, 1.00 eq.) was dissolved in THF (2 mL). KF (92.0 mg, 1.58 mmol, 3.31 eq.), $Pd(OAc)_2$ (21.5 mg, 95.6 µmol, 0.20 eq.) and XPhos (93.4 mg, 0.196 mmol, 0.41 eq.) were added to the solution. After heating up to 40 °C, 2-(4,4,5,5-tetramethyl-1,3,2-dioxaborolan-2-yl)benzenesulfonyl fluoride (**74**, 205 mg, 0.717 mmol, 1.50 eq.) in THF (0.4 mL) was added. The reaction was stirred at 40 °C for another 30 min and then at rt for 20 h. H_2O (10 mL) was added, and extraction was carried out with EtOAc (3 x 15 mL). The organic phase was dried over Na_2SO_4, and the solvent was evaporated. The residue was triturated from hexane and used in the next step without further purification.

LC-MS: ESI(+) calcd. for $[M+NH_4]^+$: *m/z* = 515.2; found: 515.3.

2-(1-Cyclohexyl-1,6-dihydrodipyrrolo[2,3-b:2',3'-d]pyridin-3-yl)benzenesulfonyl fluoride (81)

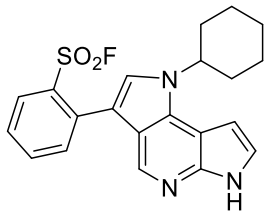

Chemical Formula: $C_{21}H_{20}FN_3O_2S$
Exact Mass: 397.12603
Molecular Weight: 397.46840

tert-Butyl, 1-cyclohexyl-3-(2-(fluorosulfonyl)phenyl)dipyrrolo[2,3-*b*:2',3'-*d*]pyridine-6(1*H*)-carboxylate (**79**, 75.0 mg, 0.151 mmol, 1.00 eq.) was dissolved in HCl in dioxane (4 M, 5 mL) and stirred at rt for 20 h. The reaction was neutralized with sat. $NaHCO_3$ and extracted with EtOAc (4 x 10 mL). After drying over Na_2SO_4 the solvent was evaporated and residue was purified by flash column chromatography (silica gel, 0 – 5 % DCM/MeOH) to yield the product **81** (46.7 mg, 0.117 mmol, 32 %) as a beige solid.

^{1}H-NMR (400 MHz, $CDCl_3$) δ 10.73 (s, 1H), 8.51 (s, 1H), 8.23 (dd, J = 8.1, 1.2 Hz, 1H), 7.82 (qd, J = 7.8, 1.7 Hz, 2H), 7.57 (ddt, J = 8.4, 6.7, 1.6 Hz, 1H), 7.49 (s, 1H), 7.36 (t, J = 2.9 Hz, 1H), 6.73 (dd, J = 3.5, 1.8 Hz, 1H), 4.64 (tt, J = 11.8, 3.7 Hz, 1H), 2.40 – 2.32 (m, 2H), 2.08 – 1.97 (m, 2H), 1.89 – 1.71 (m, 3H), 1.60 (qt, J = 13.1, 3.4 Hz, 2H), 1.36 (qt, J = 12.8, 3.7 Hz, 1H).^{13}C-NMR (101 MHz, $CDCl_3$) δ 145.2, 136.5, 136.0, 134.8, 134.5, 134.2, 133.3 (d, J = 19.9 Hz), 130.6, 127.3, 123.0 (d, J = 3.6 Hz), 122.1, 118.4, 112.1, 104.8, 97.9, 57.4, 33.7, 26.0, 25.6. ^{19}F NMR (376 MHz, $CDCl_3$) δ 65.2. HRMS: ESI(+) [*m/z*]: calcd. mass $[M+H]^+$ = 398.13330; found = 398.13372; rel. deviation 1.1 ppm. HPLC: t_{ret} = 11.27 min (99.7 % at 254 nm, 99.3 % at 230 nm, method A).

Ethyl (E)-3-(3-hydroxyphenyl)acrylate (83)

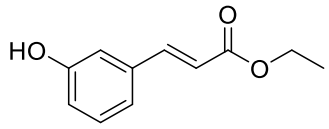

Chemical Formula: $C_{11}H_{12}O_3$
Exact Mass: 192.07864
Molecular Weight: 192.21400

3-Hydroxycinnamic acid (**82**, 3.00 g, 18.3 mmol, 1.00 eq.) was dissolved in EtOH (75 mL). Concentrated H_2SO_4 (1.5 mL) was added, and the reaction was stirred at reflux for 3.5 h. After cooling to rt, EtOAc (75 mL) was added. The organic phase was washed with sat. $NaHCO_3$ (3 x 50 mL) and subsequently dried over Na_2SO_4. The solvent was removed under reduced pressure which afforded the product **83** (3.29 g, 17.1 mmol, 94 %) as a light pink solid.

^{1}H-NMR (400 MHz, DMSO) δ 9.62 (s, 1H), 7.55 (d, J = 16.0 Hz, 1H), 7.21 (t, J = 7.8 Hz, 1H), 7.13 (dt, J = 7.7, 1.3 Hz, 1H), 7.03 (t, J = 2.0 Hz, 1H), 6.83 (ddd, J = 8.1, 2.6, 1.1 Hz, 1H), 6.50 (d, J = 16.0 Hz, 1H), 4.18 (q, J = 7.1 Hz, 2H), 1.25 (t, J = 7.1 Hz, 3H). ^{13}C-NMR (101 MHz, DMSO) δ 166.2, 157.7, 144.6, 135.3, 129.9, 119.2, 117.9, 117.6, 114.7, 60.0, 14.2. TLC-MS: ESI(-) calcd. for $[M-H]^-$: *m/z* = 191.1; found: 191.2. HPLC: t_{ret} = 13.30 min (99.5 % at 254 nm, 99.0 % at 230 nm, method B).

Ethyl (E)-3-(3-(methoxymethoxy)phenyl)acrylate (84)

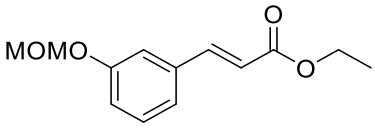

Chemical Formula: $C_{13}H_{16}O_4$
Exact Mass: 236.10486
Molecular Weight: 236.26700

Ethyl (*E*)-3-(3-hydroxyphenyl)acrylate (**83**, 1.20 g, 6.23 mmol, 1.00 eq.) was dissolved in THF (20 mL) and DIPEA (3.26 mL, 18.7 mmol, 3.00 eq.) was added dropwise. Methoxymethyl bromide (1.00 mL, 12.5 mmol, 2.00 eq.) was dissolved in THF (5 mL) and this was added to the first solution. After stirring at 60 °C for 2 h, the mixture was cooled down to rt and H_2O (40 mL) was added. The aq. phase was extracted with DCM (3 x 40 mL). The combined organic phases were washed with brine (80 mL), dried over Na_2SO_4 and the solvent was removed under reduced pressure. This afforded the product **84** (1.46 g, 6.18 mmol, quant.) as an orange oil.

^{1}H-NMR (400 MHz, $CDCl_3$) δ 7.65 (d, J = 16.0 Hz, 1H), 7.30 (t, J = 7.9 Hz, 1H), 7.23 – 7.13 (m, 2H), 7.06 (ddd, J = 8.2, 2.5, 1.0 Hz, 1H), 6.42 (d, J = 16.0 Hz, 1H), 5.19 (s, 2H), 4.26 (q, J = 7.1 Hz, 2H), 3.49 (s, 3H), 1.34 (t, J = 7.1 Hz, 3H). ^{13}C-NMR (101 MHz, $CDCl_3$) δ 167.1, 157.8, 144.5, 136.1, 130.0, 122.0, 118.9, 118.4, 115.5, 94.6, 60.7, 56.2, 14.4. TLC-MS: ESI(+) calcd. for $[M+Na]^+$: *m/z* = 259.1; found: 259.1. HPLC: t_{ret} = 16.29 min (98.0 % at 254 nm, 98.2 % at 230 nm, method B).

(E)-3-(3-(Methoxymethoxy)phenyl)prop-2-en-1-ol (85)

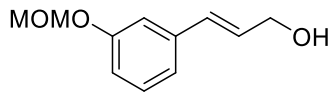

Chemical Formula: $C_{11}H_{14}O_3$
Exact Mass: 194.09429
Molecular Weight: 194.23000

$LiAlH_4$ (482 mg, 12.7 mmol, 1.50 eq.) was suspended in THF (15 mL). Benzyl chloride (1.70 mL, 14.4 mmol, 1.70 eq.) was dissolved in THF (5 mL) and added dropwise tot he suspension. After stirring at rt for 15 min, the solution was cooled to -78 °C. Ethyl (*E*)-3-(3-(methoxymethoxy)phenyl)acrylate (**84**, 2.00 g, 8.46 mmol, 1.00 eq.) was dissolved in THF (10 mL) and added dropwise to the cooled solution. After stirring at -78 °C for 2 h, the solution was slowly warmed up to -30 °C and stirred another 2 h at this temperature. It was then warmed up to rt and carefully quenched with as little as possible H_2O. The solution was filtered and the solvent evaporated under reduced pressure. The residue was purified by flash column chromatography (silica gel, 0 – 50% hexane/EtOAc) which afforded the product **85** (1.09 g, 5.61 mmol, 66 %) as a light yellow oil.

^{1}H-NMR (400 MHz, $CDCl_3$) δ 7.24 (t, J = 7.9 Hz, 1H), 7.07 (t, J = 2.0 Hz, 1H), 7.04 (dt, J = 7.6, 1.4 Hz, 1H), 6.93 (ddd, J = 8.3, 2.5, 1.0 Hz, 1H), 6.59 (dt, J = 15.8, 1.6 Hz, 1H), 6.36 (dt, J = 15.9, 5.6 Hz, 1H), 5.18 (s, 2H), 4.32 (dd, J = 5.7, 1.5 Hz, 2H), 3.48 (s, 3H).^{13}C-NMR (101 MHz, $CDCl_3$) δ 157.7, 138.4, 130.9, 129.7, 129.2, 120.4, 115.7, 114.3, 94.6, 63.7, 56.1. TLC-MS: ESI(+) calcd. for $[M+Na]^+$: *m/z* = 217.1; found: 217.1. HPLC: t_{ret} = 8.87 min (98.8 % at 254 nm, 99.9 % at 230 nm, method A).

(E)-1-(3-Bromoprop-1-en-1-yl)-3-(methoxymethoxy)benzene (86)

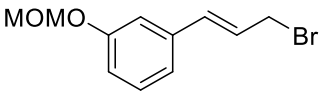

Chemical Formula: $C_{11}H_{13}BrO_2$
Exact Mass: 256.00989
Molecular Weight: 257.12700

(*E*)-3-(3-(Methoxymethoxy)phenyl)prop-2-en-1-ol (**85**, 985 mg, 5.07 mmol, 1.00 eq.) was dissolved in DCM (17 mL) and the solution was cooled to 0 °C. Triphenylphosphine (1.54 g, 5.88 mmol, 1.16 eq.) and subsequently NBS (1.08 g, 6.09 mmol, 1.20 eq.) were added and the reaction was stirred at 0 °C for 1 h. After warming up to rt, the reaction was stirred at this temperature for another 15 min. The solvent was removed under reduced pressure at room temperature and the residue was purified by flash column chromatography (silica gel, 0 – 20 % hexane/EtOAc) to yield the product **86** (476 mg, 1.85 mmol, 37 %) as a light yellow oil.

^{1}H-NMR (400 MHz, $CDCl_3$) δ 7.26 – 7.21 (m, 1H), 7.08 – 7.01 (m, 2H), 6.95 (ddd, J = 8.2, 2.5, 1.0 Hz, 1H), 6.61 (d, J = 15.5 Hz, 1H), 6.39 (dt, J = 15.6, 7.7 Hz, 1H), 5.18 (s, 2H), 4.14 (dd, J = 7.8, 1.0 Hz, 2H), 3.48 (s, 3H). ^{13}C-NMR (101 MHz, $CDCl_3$) δ 157.7, 137.5, 134.4, 129.8, 125.8, 120.7, 116.5, 114.5, 94.6, 56.2, 33.4. HPLC: t_{ret} = 11.59 min (86.7 % at 254 nm, 84.1 % at 230 nm, method A).

Ethyl (E)-3-(2-hydroxyphenyl)acrylate (88)

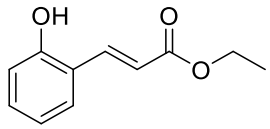

Chemical Formula: $C_{11}H_{12}O_3$
Exact Mass: 192.07864
Molecular Weight: 192.21400

trans-*o*-Coumaric acid (**87**, 2.00 g, 12.2 mmol, 1.00 eq.) was dissolved in EtOH (50 mL). Concentrated H_2SO_4 (1.0 mL) was added, and the reaction was stirred at reflux for 3 h. After cooling to rt, EtOAc (50 mL) was added. The organic phase was washed with sat. $NaHCO_3$ (3 x 40 mL) and brine (40 mL) and subsequently dried over Na_2SO_4. The solvent was removed under reduced pressure which afforded the product **88** (2.29 g, 11.9 mmol, 98 %) as a white solid.

^{1}H-NMR (400 MHz, $CDCl_3$) δ 8.03 (d, J = 16.2 Hz, 1H), 7.47 (dd, J = 7.8, 1.7 Hz, 1H), 7.26 – 7.20 (m, 1H), 6.92 (td, J = 7.6, 1.1 Hz, 1H), 6.85 (dd, J = 8.1, 1.2 Hz, 1H), 6.63 (d, J = 16.2 Hz, 1H), 6.44 (s, 1H), 4.29 (q, J = 7.1 Hz, 2H), 1.35 (t, J = 7.1 Hz, 3H). ^{13}C-NMR (101 MHz, $CDCl_3$) δ 168.9, 155.8, 141.1, 131.5, 129.2, 121.7, 120.5, 118.1, 116.5, 60.9, 14.3. TLC-MS: ESI(-) calcd. for $[M-H]^-$: *m/z* = 191.1; found: 191.0. HPLC: t_{ret} = 10.30 min (99.3 % at 254 nm, 99.4 % at 230 nm, method A).

Ethyl (E)-3-(2-(methoxymethoxy)phenyl)acrylate (89)

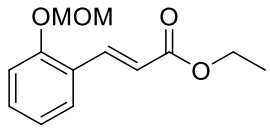

Chemical Formula: $C_{13}H_{16}O_4$
Exact Mass: 236.10486
Molecular Weight: 236.26700

Ethyl (*E*)-3-(2-hydroxyphenyl)acrylate (**88**, 2.27 g, 11.8 mmol, 1.00 eq.) was dissolved in THF (37 mL) and DIPEA (6.20 mL, 35.5 mmol, 3.01 eq.) was added dropwise. Methoxymethyl bromide (1.90 mL, 23.4 mmol, 2.00 eq.) was dissolved in THF (10 mL) and this was added to the first solution. After stirring at 55 °C for 16 h, the mixture was cooled down to rt and H_2O (50 mL) was added. The aq. phase was extracted with DCM (3 x 50 mL). The combined organic phases were washed with brine (80 mL), dried over Na_2SO_4 and the solvent was removed under reduced pressure. The residue was purified via flash column chromatography (silica gel, 0 – 1 % DCM/MeOH) leading to the product **89** (2.56 g, 10.8 mmol, 92 %) as a colorless oil.

^{1}H-NMR (400 MHz, $CDCl_3$) δ 8.04 (d, J = 16.2 Hz, 1H), 7.54 (dd, J = 7.8, 1.7 Hz, 1H), 7.32 (ddd, J = 8.4, 7.3, 1.7 Hz, 1H), 7.16 (dd, J = 8.4, 1.1 Hz, 1H), 7.01 (td, J = 7.3, 1.0 Hz, 1H), 6.50 (d, J = 16.2 Hz, 1H), 5.26 (s, 2H), 4.27 (q, J = 7.1 Hz, 2H), 3.50 (s, 3H), 1.34 (t, J = 7.1 Hz, 3H). ^{13}C-NMR (101 MHz, $CDCl_3$) δ 167.6, 156.1, 139.9, 131.6, 128.5, 124.3, 122.1, 119.0, 115.0, 94.7, 60.5, 56.4, 14.5. TLC-MS: ESI(+) calcd. for $[M+Na]^+$: *m/z* = 259.1; found: 259.1. HPLC: t_{ret} = 11.38 min (98.6 % at 254 nm, 98.8 % at 230 nm, method A).

(E)-3-(2-(Methoxymethoxy)phenyl)prop-2-en-1-ol (90)

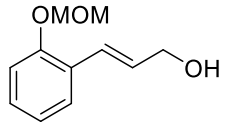

Chemical Formula: $C_{11}H_{14}O_3$
Exact Mass: 194.09429
Molecular Weight: 194.23000

$LiAlH_4$ (617 mg, 18.4 mmol, 1.50 eq.) was suspended in THF (18 mL). Benzyl chloride (2.10 mL, 18.4 mmol, 1.70 eq.) was dissolved in THF (6 mL) and added dropwise to the suspension. After stirring at rt for 15 min, the solution was cooled to -78 °C. Ethyl (*E*)-3-(2-(methoxymethoxy)phenyl)acrylate (**89**, 2.56 g, 10.8 mmol, 1.00 eq.) was dissolved in THF (12 mL) and added dropwise to the cooled solution. The solution was slowly warmed up to -30 °C and stirred 6 h at this temperature. It was then warmed up to rt and carefully quenched with as little as possible H_2O. The solution was filtered and the solvent evaporated under reduced pressure. The residue was purified by flash column chromatography (silica gel, 0 – 50% hexane/EtOAc) which afforded the product **90** (1.32 g, 6.80 mmol, 63 %) as a colorless oil.

^{1}H-NMR (400 MHz, $CDCl_3$) δ 7.47 (dd, J = 7.7, 1.7 Hz, 1H), 7.21 (ddd, J = 8.2, 7.2, 1.7 Hz, 1H), 7.10 (dd, J = 8.4, 1.2 Hz, 1H), 7.03 – 6.92 (m, 2H), 6.38 (dt, J = 16.1, 5.8 Hz, 1H), 5.22 (s, 2H), 4.34 (dd, J = 5.9, 1.6 Hz, 2H), 3.49 (s, 3H).^{13}C-NMR (101 MHz, $CDCl_3$) δ 154.6, 129.5, 128.9, 127.0, 126.6, 126.1, 122.1, 114.9, 94.8, 64.3, 56.3. TLC-MS: ESI(+) calcd. for $[M+Na]^+$:

m/z = 217.1; found: 217.1. HPLC: t_{ret} = 5.71 min (97.3 % at 254 nm, 97.7 % at 230 nm, method B).

(E)-3-(2-(Methoxymethoxy)phenyl)allyl acetate (95)

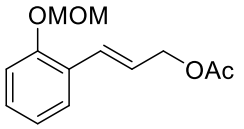

Chemical Formula: $C_{13}H_{16}O_4$
Exact Mass: 236.10486
Molecular Weight: 236.26700

(*E*)-3-(2-(Methoxymethoxy)phenyl)prop-2-en-1-ol (**90**, 101 mg, 0.520 mmol, 1.00 eq.) and DMAP (71.2 mg, 0.582 mmol, 1.12 eq.) were dissolved in Et_2O (1 mL). Ac_2O (59.0 µL, 0.624 mmol, 1.20 eq.) was added and the solution was stirred at rt for 1 h. EtOAc (15 mL) was added, and the solution was washed with sat. $NaHCO_3$ (15 mL) and sat. NH_4Cl (15 mL). After extraction with EtOAc (3 x 20 mL), the org. phases were dried over Na_2SO_4, and the solvent was removed under reduced pressure. The residue was purified by flash column chromatography (silica gel, 0 – 20% hexane/EtOAc) which afforded the product **95** (96.7 mg, 0.409 mmol, 80 %) as a yellow oil.

^{1}H-NMR (400 MHz, $CDCl_3$) δ 7.46 (dd, J = 7.7, 1.7 Hz, 1H), 7.22 (ddd, J = 8.3, 7.3, 1.7 Hz, 1H), 7.10 (dd, J = 8.3, 1.2 Hz, 1H), 7.05 – 6.94 (m, 2H), 6.30 (dt, J = 16.0, 6.6 Hz, 1H), 5.22 (s, 2H), 4.75 (dd, J = 6.6, 1.4 Hz, 2H), 3.50 (s, 3H), 2.10 (s, 3H).^{13}C-NMR (101 MHz, $CDCl_3$) δ 171.0, 154.7, 129.3, 129.2, 127.1, 126.1, 124.0, 122.1, 114.9, 94.9, 65.7, 56.3, 21.2. HPLC: t_{ret} = 10.79 min (88.5 % at 254 nm, 94.6 % at 230 nm, method A).

(E)-5-Bromo-N-cyclohexyl-N-(3-(3-(methoxymethoxy)phenyl)allyl)-1-tosyl-1H-pyrrolo[2,3-b]pyridin-4-amine (97)

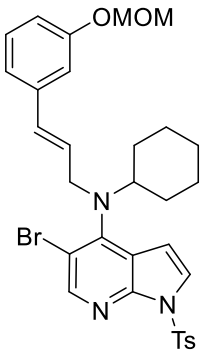

Chemical Formula: $C_{31}H_{34}BrN_3O_4S$
Exact Mass: 623.14534
Molecular Weight: 624.59400

5-Bromo-*N*-cyclohexyl-1-tosyl-1*H*-pyrrolo[2,3-*b*]pyridin-4-amine (**42**, 295 mg, 0.658 mmol, 1.00 eq.) was dissolved in DMF (19 mL) and cooled to 0 °C. NaH (60 % dispersion in mineral oil, 32.2 mg, 0.790 mmol, 1.20 eq.) was added and the suspension was stirred for 30 min. (*E*)-1-(3-Bromoprop-1-en-1-yl)-3-(methoxymethoxy)benzene (**86**, 186 mg, 0.724 mmol, 1.10 eq.) was dissolved in DMF (4.5 mL) and added dropwise to the first solution. This was stirred for 20 h and then quenched with sat. NH_4Cl (25 mL). The aq. phase was extracted with DCM (3 x 20 mL). The combined organic phases were dried over Na_2SO_4, and the solvent was removed under reduced pressure. The residue was purified by flash column chromatography (silica gel, 0 – 100 % hexane/DCM) to yield the product **97** (290 mg, 0.464 mmol, 71 %) as a white solid.

^{1}H-NMR (400 MHz, $CDCl_3$) δ 8.42 (s, 1H), 8.07 – 8.00 (m, 2H), 7.63 (d, J = 4.1 Hz, 1H), 7.25 – 7.23 (m, 2H), 7.15 (td, J = 7.5, 1.2 Hz, 1H), 6.91 – 6.81 (m, 3H), 6.63 (d, J = 4.1 Hz, 1H), 6.41 (dt, J = 15.8, 1.6 Hz, 1H), 6.03 (dt, J = 15.8, 6.0 Hz, 1H), 5.14 (s, 2H), 4.12 (dd, J = 6.0, 1.6 Hz, 2H), 3.46 (s, 3H), 3.31 (tt, J = 10.8, 3.4 Hz, 1H), 2.36 (s, 3H), 1.87 (d, J = 12.3 Hz, 2H), 1.74 (d, J = 12.9 Hz, 2H), 1.54 – 1.40 (m, 2H), 1.28 – 1.02 (m, 4H). ^{13}C-NMR (101 MHz, $CDCl_3$) δ 157.6, 150.4, 148.4, 147.5, 145.4, 138.6, 135.4, 130.8, 129.8, 129.6, 128.8, 128.3, 125.6, 122.4, 120.1, 115.6, 115.2, 114.2, 104.4, 94.6, 61.7, 56.1, 49.6, 31.5, 25.9, 25.7, 21.8. TLC-MS: ESI(+) calcd. for $[M+Na]^+$: *m/z* = 646.2; found: 646.4. HPLC: t_{ret} = 20.68 min (69.8 % at 254 nm, 75.3 % at 230 nm, method B).

1-Cyclohexyl-3-(3-(methoxymethoxy)benzyl)-6-tosyl-1,6-dihydrodipyrrolo[2,3-b:2',3'-d]pyridine (98)

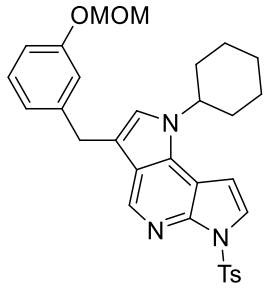

Chemical Formula: $C_{31}H_{33}N_3O_4S$
Exact Mass: 543.21918
Molecular Weight: 543.68200

(*E*)-5-Bromo-*N*-cyclohexyl-*N*-(3-(3-(methoxymethoxy)phenyl)allyl)-1-tosyl-1*H*-pyrrolo[2,3-*b*]pyridin-4-amine (**97**, 566 mg, 0.906 mmol, 1.00 eq.) and Cs_2CO_3 (360 mg, 1.11 mmol, 1.22 eq.) were suspended in DMF (18 mL). $Pd(PPh_3)_4$ (94.2 mg, 81.6 µM, 0.09 eq.) was added and the solution was stirred at 80 °C for 3 h. It was cooled to rt and sat. NH_4Cl (20 mL) was added. Extraction was carried out with DCM (3 x 25 mL) and the combined organic phases were dried over Na_2SO_4 and the solvent was evaporated. The residue was redissolved in EtOAc (30 mL), silica is added, and the suspension is concentrated to dryness. This process is repeated 5x, after which the residue was purified by flash column chromatography (silica gel, 0 – 100 % hexane/EtOAc) to yield the product **98** (57.6 mg, 0.106 mmol, 12 %) as a yellow solid.

^{1}H-NMR (400 MHz, $CDCl_3$) δ 8.56 (s, 1H), 8.13 – 7.99 (m, 2H), 7.69 (d, J = 4.0 Hz, 1H), 7.24 – 7.19 (m, 2H), 7.16 (d, J = 7.8 Hz, 1H), 6.97 – 6.84 (m, 4H), 6.75 (d, J = 4.0 Hz, 1H), 5.13 (s, 2H), 4.39 (tt, J = 11.8, 3.6 Hz, 1H), 4.10 (s, 2H), 3.45 (s, 3H), 2.32 (s, 3H), 2.21 – 2.12 (m, 2H), 1.96 (dt, J = 13.8, 3.4 Hz, 2H), 1.87 – 1.76 (m, 1H), 1.66 (qd, J = 12.6, 3.4 Hz, 2H), 1.52 (qt, J = 13.0, 3.4 Hz, 2H), 1.35 – 1.28 (m, 1H). ^{13}C-NMR (101 MHz, $CDCl_3$) δ 154.5, 144.8, 143.1, 142.6, 138.1, 135.9, 134.1, 129.6, 128.2, 123.5, 122.4, 121.2, 120.5, 116.9, 116.0, 113.5, 107.9, 102.6, 94.6, 57.0, 56.1, 33.6, 31.8, 26.0, 25.6, 21.7. TLC-MS: ESI(+) calcd. for $[M+H]^+$: m/z = 544.2; found: 544.3. HPLC: t_{ret} = 21.37 min (82.3 % at 254 nm, 85.2 % at 230 nm, method B).

3-((1-Cyclohexyl-1,6-dihydrodipyrrolo[2,3-b:2',3'-d]pyridin-3-yl)methyl)phenol (99)

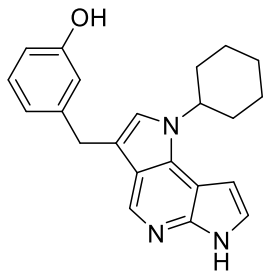

Chemical Formula: $C_{22}H_{23}N_3O$
Exact Mass: 345.18411
Molecular Weight: 345.44600

1-Cyclohexyl-3-(3-(methoxymethoxy)benzyl)-6-tosyl-1,6-dihydrodipyrrolo[2,3-*b*:2',3'-*d*]pyridine (**98**, 58.1 mg, 0.107 mmol, 1.00 eq.) was dissolved in KOH solution (3 M in MeOH, 50 mL) and stirred at 65 °C for 2.5 h. The solution was cooled to 0 °C and slowly acidified with conc. HCl. It was stirred a further 2 h at rt, after which the MeOH was evaporated under reduced pressure. The solution was again cooled to 0 °C, neutralized with sat. Na_2CO_3 and extracted with DCM (6 x 30 mL). It was dried over Na_2SO_4, and the solvent was evaporated under reduced pressure. The product **99** was then used in the next step without further purification.

TLC-MS: ESI(+) calcd. for $[M+H]^+$: *m/z* = 346.2; found: 346.3.

3-((1-Cyclohexyl-1,6-dihydrodipyrrolo[2,3-b:2',3'-d]pyridin-3-yl)methyl)phenyl sulfurofluoridate (100)

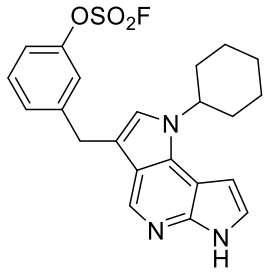

Chemical Formula: $C_{22}H_{22}FN_3O_3S$
Exact Mass: 427.13659
Molecular Weight: 427.49440

3-((1-Cyclohexyl-1,6-dihydrodipyrrolo[2,3-*b*:2',3'-*d*]pyridin-3-yl)methyl)phenol (**99**, 37.0 mg, 0.107 mmol, 1.00 eq.) and AISF (**64**, 41.1 mg, 0.131 mmol, 1.22 eq.) were dissolved in THF (5.4 mL). DBU (35.3 µL, 0.237 mmol, 2.21 eq.) was added and the reaction was stirred at rt for 2 h. EtOAc (15 mL) was added and the organic phase was washed with sat. NH_4Cl (3 x 10 mL) and brine (10 mL). The organic phase was dried over Na_2SO_4 and the solvent was evaporated under reduced pressure. The residue was purified via flash column chromatography (silica gel, 0 – 10 % DCM/MeOH) leading to the product **100** (15.3 mg, 35.8 µmol, 33 % over two steps) as a yellow solid.

^{1}H-NMR (400 MHz, $CDCl_3$) δ 11.03 (s, 1H), 8.43 (s, 1H), 7.43 – 7.31 (m, 3H), 7.30 – 7.26 (m, 1H), 7.19 (d, J = 7.7 Hz, 1H), 6.93 (s, 1H), 6.69 (d, J = 3.4 Hz, 1H), 4.56 (tt, J = 11.8, 3.7 Hz, 1H), 4.25 (s, 2H), 2.32 – 2.23 (m, 2H), 2.00 (dt, J = 13.5, 3.3 Hz, 2H), 1.84 (d, J = 13.3 Hz, 1H), 1.71 (qd, J = 12.3, 3.2 Hz, 2H), 1.58 (qt, J = 13.2, 3.3 Hz, 2H), 1.40 – 1.28 (m, 1H). ^{13}C-NMR (101 MHz, $CDCl_3$) δ 150.4, 144.5, 144.2, 135.6, 135.2, 130.4, 129.0, 122.0, 121.1, 120.4, 118.5, 118.1, 114.3, 105.1, 97.9, 57.1, 33.7, 31.7, 26.0, 25.7. ^{19}F NMR (376 MHz, $CDCl_3$) δ 37.7. HRMS: ESI(+) [*m/z*]: calcd. mass $[M+H]^+$ = 428.14387; found = 428.14415; rel. deviation 0.7 ppm. HPLC: t_{ret} = 11.40 min (96.4 % at 254 nm, 99.0 % at 230 nm, method A).

1-((3-Bromophenyl)sulfonyl)-1H-1,2,4-triazole (101)

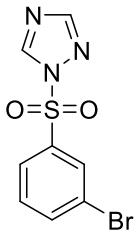

Chemical Formula: $C_8H_6BrN_3O_2S$
Exact Mass: 286.93641
Molecular Weight: 288.11900

3-Bromobenzenesulfonyl chloride (**66**, 2.00 g, 7.83 mmol, 1.00 eq.) was dissolved in DCM (20 mL). 1*H*-1,2,4-Triazole (541 mg, 7.83 mmol, 1.00 eq.) and TEA (1.30 mL, 9.39 mmol, 1.20 eq.) were added and the reaction was stirred at rt for 3.5 h. H_2O (25 mL) was added and it was extracted with DCM (3 x 20 mL). The org. phase was dried over Na_2SO_4, the solvent was evaporated, and the residue was purified by flash column chromatography (silica gel, 0 – 50 % hexane/EtOAc) to yield the product **101** (1.76 g, 6.11 mmol, 78 %) as a white solid.

^{1}H-NMR (400 MHz, $CDCl_3$) δ 8.75 (s, 1H), 8.22 (t, J = 1.9 Hz, 1H), 8.06 (s, 1H), 8.04 (ddd, J = 8.0, 1.9, 1.0 Hz, 1H), 7.86 (ddd, J = 8.0, 1.9, 1.0 Hz, 1H), 7.49 (t, J = 8.0 Hz, 1H). ^{13}C-NMR (101 MHz, $CDCl_3$) δ 154.8, 144.9, 138.8, 137.6, 131.5, 131.3, 127.4, 123.8, 77.5, 77.2, 76.8. HPLC: t_{ret} = 9.28 min (98.6 % at 254 nm, 97.1 % at 230 nm, method A).

4-Iodo-1-((2-(trimethylsilyl)ethoxy)methyl)-1H-pyrrolo[2,3-b]pyridine (106)

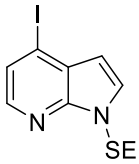

Chemical Formula: $C_{13}H_{19}IN_2OSi$
Exact Mass: 374.03113
Molecular Weight: 374.29747

4-Iodo-1*H*-pyrrolo[2,3-b]pyridine (**105**, 500 mg, 2.05 mmol, 1.00 eq.) was dissolved in DMF (4.5 mL). The solution was cooled to 0 °C and NaH (60 % dispersion in mineral oil, 120 mg, 3.07 mmol, 1.50 eq.) was added. The suspension was stirred for 1h. Subsequently, SEMCl (440 µL, 2.46 mmol, 1.19 eq.) was added dropwise and the reaction stirred for another hour. It was then quenched with H_2O (10 mL), extracted with EtOAc (2 x 15 mL), dried over Na_2SO_4 and the solvent was removed under reduced pressure. The residue was purified by flash column chromatography (silica gel, 0 – 20 % hexane/EtOAc) to yield the product **106** (622 mg, 1.66 mmol, 81 %) as a colorless oil.

^{1}H-NMR (400 MHz, $CDCl_3$) δ 7.96 (d, J = 5.0 Hz, 1H), 7.51 (d, J = 5.0 Hz, 1H), 7.41 (d, J = 3.6 Hz, 1H), 6.42 (d, J = 3.6 Hz, 1H), 5.64 (s, 2H), 3.57 – 3.48 (m, 2H), 0.95 – 0.85 (m, 2H), -0.07 (s, 9H). ^{13}C-NMR (101 MHz, $CDCl_3$) δ 146.4, 143.2, 128.4, 126.5, 125.9, 104.3, 99.0, 73.4, 66.5, 17.9, -1.3. TLC-MS: ESI(+) calcd. for $[M+Na]^+$: *m/z* = 397.0; found: 396.7. HPLC: t_{ret} = 13.57 min (98.2 % at 254 nm, 99.5 % at 230 nm, method A).

2-Bromo-N-cyclohexyl-5-hydroxybenzamide (108)

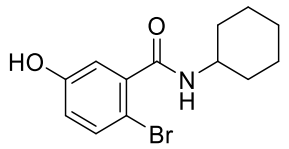

Chemical Formula: $C_{13}H_{16}BrNO_2$
Exact Mass: 297.03644
Molecular Weight: 298.18000

2-Bromo-5-hydroxybenzoic acid (**107**, 500 mg, 2.30 mmol, 1.00 eq.) was dissolved in $SOCl_2$ (5 mL) and DMF (20 drops) was added. The solution was refluxed for 6 h and then cooled to rt. Thionyl chloride was removed and the residue was dissolved in DCM (5 mL). TEA (1.00 mL, 7.21 mmol, 3.13 eq.) was added and the solution was cooled to 0 °C. Cyclohexylamine (1.00 mL, 8.75 mmol, 3.80 eq.) was added dropwise and the mixture was stirred at rt for 16 h. Sat. Na_2CO_3 (10 mL) was added, and it was extracted with DCM (3 x 20 mL). After drying over Na_2SO_4 the solvent was evaporated. The residue was purified by flash column chromatography (silica gel, 0 – 10 % DCM/MeOH) to yield the product **108** (612 mg, 2.05 mmol, 89 %) as a brown solid.

^{1}H-NMR (400 MHz, $CDCl_3$) δ 8.21 (s, 1H), 7.35 (d, J = 8.7 Hz, 1H), 7.26 (s, 1H), 6.77 (dd, J = 8.7, 3.0 Hz, 1H), 6.21 (d, J = 8.3 Hz, 1H), 4.06 – 3.91 (m, 1H), 2.10 – 1.98 (m, 2H), 1.83 – 1.71 (m, 2H), 1.71 – 1.58 (m, 1H), 1.50 – 1.37 (m, 2H), 1.36 – 1.20 (m, 3H). ^{13}C-NMR (101 MHz, $CDCl_3$) δ 167.3, 156.6, 137.4, 134.5, 119.9, 117.7, 108.1, 49.5, 32.8, 25.6, 24.8. TLC-MS: ESI(+) calcd. for $[M+Na]^+$: *m/z* = 320.0; found: 320.1. HPLC: t_{ret} = 9.50 min (90.5 % at 254 nm, 95.3 % at 230 nm, method A).

2-Bromo-N-cyclohexyl-5-(methoxymethoxy)benzamide (109)

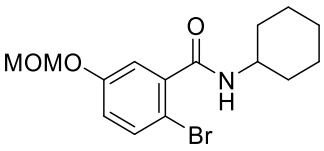

Chemical Formula: $C_{15}H_{20}BrNO_3$
Exact Mass: 341.06266
Molecular Weight: 342.23300

2-Bromo-*N*-cyclohexyl-5-hydroxybenzamide (**108**, 612 mg, 2.05 mmol, 1.00 eq.) was dissolved in DCM (4.5 mL). DIPEA (650 µL, 3.74 mmol, 1.82 eq.) was added and the solution was cooled to 0 °C. MOMBr (220 µL, 2.71 mmol, 1.32 eq.) was added and the reaction was stirred at rt for 2.5 h. Subsequently, the reaction was quenched with sat. $NaHCO_3$ (10 mL) and extracted with DCM (3 x 10 mL). After drying over Na_2SO_4 the solvent was removed under reduced pressure and the residue was purified by flash column chromatography (silica gel, 0 – 50 % hexane/EtOAc) to yield the product **109** (400 mg, 1.17 mmol, 57 %) as an off-white solid.

^{1}H-NMR (400 MHz, $CDCl_3$) δ 7.44 (d, J = 8.8 Hz, 1H), 7.21 (d, J = 3.0 Hz, 1H), 6.95 (dd, J = 8.8, 3.0 Hz, 1H), 5.82 (d, J = 8.3 Hz, 1H), 5.16 (s, 2H), 3.99 (tdt, J = 10.4, 8.1, 3.9 Hz, 1H), 3.45 (s, 3H), 2.05 (dt, J = 12.4, 3.9 Hz, 2H), 1.75 (dt, J = 13.4, 4.0 Hz, 2H), 1.64 (dq, J = 12.7, 4.0 Hz, 1H), 1.50 – 1.35 (m, 2H), 1.34 – 1.14 (m, 3H). ^{13}C-NMR (101 MHz, $CDCl_3$) δ 166.4, 156.7, 139.2, 134.3, 119.3, 117.6, 110.9, 94.6, 56.3, 49.1, 33.0, 25.7, 24.9. TLC-MS: ESI(+) calcd. for

[M+Na]$^+$: *m/z* = 364.1; found: 364.1. HPLC: t_{ret} = 10.76 min (92.4 % at 254 nm, 95.9 % at 230 nm, method A).

4-Cyclohexyl-6-(methoxymethoxy)-1-((2-(trimethylsilyl)ethoxy)methyl)-1,4-dihydro-5H-benzo[c]pyrrolo[2,3-h][1,6]naphthyridin-5-one (110)

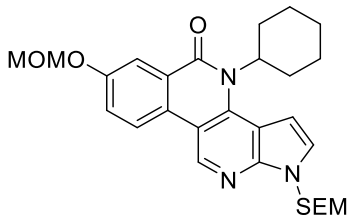

Chemical Formula: $C_{28}H_{37}N_3O_4Si$
Exact Mass: 507,25533
Molecular Weight: 507,70600

4-Iodo-1-((2-(trimethylsilyl)ethoxy)methyl)-1*H*-pyrrolo[2,3-*b*]pyridine (**106**, 415 mg, 1.11 mmol, 1.00 eq.) and 2-bromo-*N*-cyclohexyl-5-(methoxymethoxy)benzamide (**109**, 398 mg, 1.16 mmol, 1.05 eq.) were dissolved in toluene (17 mL). Norbornene (**114**, 110 mg, 1.16 mmol, 1.05 eq.), Cs_2CO_3 (1.09 g, 3.35 mmol, 3.02 eq.), $Pd(TFA)_2$ (40.6 mg, 0.122 mmol, 0.11 eq.) and TFP (51.5 mg, 0.222 mmol, 0.20 eq.) were added and the reaction was stirred at 95 °C for 23 h. After cooling to rt, the suspension was filtered over celite, and the solvent was evaporated. The residue was purified by flash column chromatography (silica gel, 0 – 40 % hexane/EtOAc) to yield the product **110** (144 mg, 0.284 mmol, 26 %) as a beige solid.

^{1}H-NMR (400 MHz, $CDCl_3$) δ 9.16 (s, 1H), 8.26 (d, J = 8.9 Hz, 1H), 8.07 (d, J = 2.7 Hz, 1H), 7.45 (dd, J = 8.8, 2.8 Hz, 1H), 7.38 (d, J = 3.7 Hz, 1H), 6.78 – 6.73 (m, 1H), 5.74 (s, 2H), 5.31 (s, 2H), 5.05 – 4.69 (m, 1H), 3.65 – 3.55 (m, 2H), 3.52 (s, 3H), 3.01 – 2.88 (m, 2H), 2.03 – 1.95 (m, 4H), 1.81 – 1.77 (m, 1H), 1.52 – 1.29 (m, 3H), 0.99 – 0.86 (m, 2H), -0.04 (s, 9H). ^{13}C-NMR (101 MHz, $CDCl_3$) δ 163.3, 156.5, 148.8, 140.4, 139.1, 128.2, 127.1, 126.2, 123.4, 122.6, 112.9, 109.5, 107.7, 102.0, 94.7, 73.4, 66.6, 61.7, 56.4, 29.5, 26.7, 25.5, 18.0, -1.3. TLC-MS: ESI(+) calcd. for [M+Na]$^+$: *m/z* = 530.3; found: 530.2. HPLC: t_{ret} = 14.76 min (99.7 % at 254 nm, 95.3 % at 230 nm, method A).

4-Cyclohexyl-6-hydroxy-1,4-dihydro-5H-benzo[c]pyrrolo[2,3-h][1,6]naphthyridin-5-one (111)

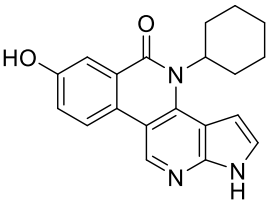

Chemical Formula: $C_{20}H_{19}N_3O_2$
Exact Mass: 333.14773
Molecular Weight: 333.39100

4-Cyclohexyl-6-(methoxymethoxy)-1-((2-(trimethylsilyl)ethoxy)methyl)-1,4-dihydro-5*H*-benzo[*c*]pyrrolo[2,3-*h*][1,6]naphthyridin-5-one (**110**, 144 mg, 0.284 mmol, 1.00 eq.) was dissolved in DCM (4 mL) and TFA (4 mL) was added. The solution was stirred at rt for 2 h and then the solvent was evaporated. The residue was dissolved in MeOH (8 mL) and DIPEA (2 mL) was added. The reaction was stirred

another 21 h at rt after which the precipitate was filtered off. Washing with very little MeOH afforded the product **111** (48.6 mg, 0.146 mmol, 52 %) as a white solid.

^{1}H-NMR (400 MHz, DMSO) δ 12.03 (s, 1H), 10.03 (s, 1H), 9.19 (s, 1H), 8.44 (d, J = 8.9 Hz, 1H), 7.62 (d, J = 2.7 Hz, 1H), 7.53 (t, J = 3.1 Hz, 1H), 7.26 (dd, J = 8.8, 2.8 Hz, 1H), 6.60 (dd, J = 3.9, 2.0 Hz, 1H), 4.87 (t, J = 11.9 Hz, 1H), 2.80 (q, J = 12.0 Hz, 2H), 1.95 – 1.81 (m, 4H), 1.74 (d, J = 12.6 Hz, 1H), 1.45 (q, J = 13.1 Hz, 2H), 1.36 – 1.23 (m, 1H).^{13}C-NMR (101 MHz, DMSO) δ 162.2, 156.6, 149.0, 139.8, 137.3, 126.2, 125.5, 124.6, 123.3, 122.3, 111.3, 108.2, 106.2, 100.3, 60.3, 29.0, 26.0, 25.1. LC-MS: ESI(+) calcd. for $[M+H]^+$: *m/z* = 334.2; found: 334.3. HPLC: t_{ret} = 12.71 min (99.3 % at 254 nm, 95.3 % at 230 nm, method A).

4-Cyclohexyl-5-oxo-4,5-dihydro-1H-benzo[c]pyrrolo[2,3-h][1,6]naphthyridin-6-yl sulfurofluoridate (112)

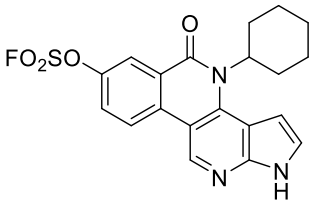

Chemical Formula: $C_{20}H_{18}FN_3O_4S$
Exact Mass: 415.10021
Molecular Weight: 415.43940

4-Cyclohexyl-6-hydroxy-1,4-dihydro-5*H*-benzo[*c*]pyrrolo[2,3-*h*][1,6]naphthyridin-5-one (**111**, 48.0 mg, 0.144 mmol, 1.00 eq.) and AISF (**64**, 54.0 mg, 0.173 mmol, 1.20 eq.) were dissolved in THF (5 mL). DBU (48.1 µL, 0.322 mmol, 2.21 eq.) was added and the reaction was stirred at rt for 3 h. NH_4Cl (15 mL) was added, and the aq. phase was extracted with EtOAc (3 x 15 mL). The organic phase was dried over Na_2SO_4, and the solvent was evaporated under reduced pressure. The residue was triturated from MeOH, followed by a trituration from DCM leading to the product **112** (48.1 mg, 0.116 mmol, 80 %) as a white solid.

^{1}H-NMR (400 MHz, DMSO) δ 12.26 (s, 1H), 9.36 (s, 1H), 8.87 (d, J = 9.2 Hz, 1H), 8.33 (d, J = 2.8 Hz, 1H), 8.05 (dd, J = 9.0, 2.9 Hz, 1H), 7.63 – 7.59 (m, 1H), 6.69 – 6.63 (m, 1H), 4.92 (t, J = 11.9 Hz, 1H), 2.84 – 2.71 (m, 2H), 1.98 – 1.84 (m, 4H), 1.75 (d, J = 12.7 Hz, 1H), 1.56 – 1.39 (m, 2H), 1.35 – 1.20 (m, 1H).^{13}C-NMR (101 MHz, DMSO) δ 161.1, 149.9, 148.1, 141.0, 139.1, 134.3, 126.0, 125.9, 125.3, 125.1, 119.3, 106.9, 106.1, 100.8, 60.7, 28.8, 25.9, 25.1. ^{19}F NMR (376 MHz, DMSO) δ 39.0. HRMS: ESI(+) [*m/z*]: calcd. mass $[M+H]^+$ = 416.10748; found = 416.10786; rel. deviation 0.9 ppm. HPLC: t_{ret} = 13.55 min (95.3 % at 254 nm, 96.0 % at 230 nm, method A).

6.2.2. Synthesis of Putative MK2 Inhibitors

Ethyl 5-bromofuran-2-carboxylate (123)

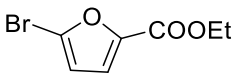

Chemical Formula: $C_7H_7BrO_3$
Exact Mass: 217.95786
Molecular Weight: 219.03400

5-Bromofuran-2-carboxylic acid (**122**, 2.02 g, 10.6 mmol, 1.00 eq.) was dissolved in EtOH (42 mL) and conc. H_2SO_4 (0.8 mL) was added. The reaction was refluxed for 20 h and then cooled to rt. The solution was diluted with EtOAc (50 mL), washed with sat. $NaHCO_3$ (3 x 30 mL) and brine (30 mL). The organic phase was dried over Na_2SO_4, and the solvent was removed under reduced pressure to yield the product **123** (2.17 g, 9.91 mmol, 94 %) as a yellow oil.

^{1}H-NMR (400 MHz, $CDCl_3$) δ 7.12 (d, J = 3.5 Hz, 1H), 6.45 (d, J = 3.5 Hz, 1H), 4.36 (q, J = 7.1 Hz, 2H), 1.37 (t, J = 7.1 Hz, 3H). ^{13}C-NMR (101 MHz, $CDCl_3$) δ 157.8, 146.7, 127.5, 120.0, 114.0, 61.4, 14.4. LC-MS: ESI(+) calcd. for $[M+Na]^+$: *m/z* = 241.0; found: 240.9. HPLC: t_{ret} = 10.31 min (99.3 % at 254 nm, 99.0 % at 230 nm, method A).

Ethyl 5-(4-chloro-3-methoxyphenyl)furan-2-carboxylate (124)

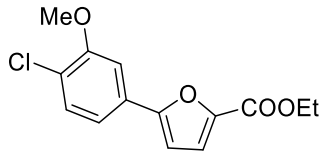

Chemical Formula: $C_{14}H_{13}ClO_4$
Exact Mass: 280.05024
Molecular Weight: 280.70400

Ethyl 5-bromofuran-2-carboxylate (**123**, 2.17 g, 9.91 mmol, 1.00 eq.) was dissolved in 1,4-dioxane (25 mL) and (4-chloro-3-methoxyphenyl)boronic acid (2.31 g, 12.4 mmol, 1.25 eq.) was added. K_2CO_3 (2.79, 20.2 mmol, 2.04 eq.) was dissolved in H_2O (25 mL) and this was added to the first solution. $Pd(PPh_3)_4$ (286 mg, 0.248 mmol, 0.025 eq.) was added and the reaction was heated to 80 °C and stirred for 20 h. After cooling down to rt, sat. NH_4Cl (15 mL) was added, and the solution was extracted with EtOAc (3 x 30 mL). The combined organic phases were dried over Na_2SO_4, and the solvent was removed under reduced pressure. The residue was purified by flash column chromatography (silica gel, 0 – 20 % hexane/EtOAc) to yield the product **124** (1.08 g, 3.85 mmol, 39 %) as a white solid.

^{1}H-NMR (400 MHz, $CDCl_3$) δ 7.40 (d, J = 8.2 Hz, 1H), 7.33 (d, J = 1.9 Hz, 1H), 7.30 (dd, J = 8.2, 1.9 Hz, 1H), 7.23 (d, J = 3.6 Hz, 1H), 6.74 (d, J = 3.6 Hz, 1H), 4.39 (q, J = 7.1 Hz, 2H), 3.99 (s, 3H), 1.40 (t, J = 7.1 Hz, 3H). ^{13}C-NMR (101 MHz, $CDCl_3$) δ 158.9, 156.6, 155.5, 144.3, 130.7, 129.5, 123.4, 119.9, 118.0, 108.3, 107.5, 77.5, 77.2, 76.8, 61.2, 56.5, 14.5. TLC-MS: ESI(+) calcd. for $[M+Na]^+$: *m/z* = 303.1; found: 303.1. HPLC: t_{ret} = 12.37 min (98.9 % at 254 nm, 96.5 % at 230 nm, method A).

Ethyl 5-(4-chloro-3-hydroxyphenyl)furan-2-carboxylate (125)

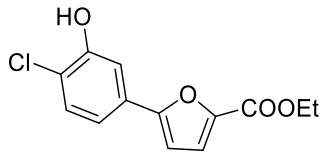

Chemical Formula: $C_{13}H_{11}ClO_4$
Exact Mass: 266.03459
Molecular Weight: 266.67700

Ethyl 5-(4-chloro-3-methoxyphenyl)furan-2-carboxylate (**124**, 1.08 g, 3.85 mmol, 1.00 eq.) was dissolved in DCM (40 mL) and the solution was cooled to 0 °C. BBr_3 (1 M in DCM, 10.0 mL, 10.0 mmol, 2.60 eq.) was added dropwise. The reaction mixture was stirred at rt for 5 h. After cooling to 0 °C, the reaction was carefully quenched with H_2O (40 mL). The reaction was extracted with DCM (3 x 20 mL), washed with H_2O (50 mL) and dried over Na_2SO_4. After evaporating the solvent, the residue was purified by flash column chromatography (silica gel, 0 – 50 % hexane/EtOAc) to yield the product **125** (875 mg, 3.28 mmol, 85 %) as a white solid.

^{1}H-NMR (400 MHz, $CDCl_3$) δ 7.44 (d, J = 2.0 Hz, 1H), 7.36 (d, J = 8.4 Hz, 1H), 7.30 (dd, J = 8.4, 2.0 Hz, 1H), 7.22 (d, J = 3.6 Hz, 1H), 6.71 (d, J = 3.6 Hz, 1H), 5.74 (s, 1H), 4.39 (q, J = 7.1 Hz, 2H), 1.40 (t, J = 7.1 Hz, 3H). ^{13}C-NMR (101 MHz, $CDCl_3$) δ 158.9, 156.2, 151.9, 144.3, 130.1, 129.6, 120.6, 119.9, 118.0, 112.6, 107.7, 61.2, 14.5. LC-MS: ESI(-) calcd. for $[M-H]^+$: *m/z* = 265.0; found: 265.2. HPLC: t_{ret} = 11.25 min (99.3 % at 254 nm, 98.0 % at 230 nm, method A).

Ethyl 5-(3-(benzyloxy)-4-chlorophenyl)furan-2-carboxylate (126)

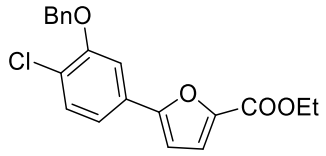

Chemical Formula: $C_{20}H_{17}ClO_4$
Exact Mass: 356.08154
Molecular Weight: 356.80200

Ethyl 5-(4-chloro-3-hydroxyphenyl)furan-2-carboxylate (**125**, 250 mg, 0.937 mmol, 1.00 eq.) and K_2CO_3 (259 mg, 1.87 mmol, 2.00 eq.) were suspended in DMF (5 mL) and benzyl bromide (224 µL, 1.88 mmol, 2.01 eq.) was added. The reaction was stirred at rt for 3 h and then sat. NH_4Cl (15 mL) was added. The mixture was extracted with EtOAc (3 x 15 mL), dried over Na_2SO_4 and the solvent was evaporated. The residue was purified by flash column chromatography (silica gel, 0 – 20 % hexane/EtOAc) to yield the product **126** (304 mg, 0.852 mmol, 91 %) as a white solid.

^{1}H-NMR (400 MHz, $CDCl_3$) δ 7.52 (ddt, J = 7.5, 1.4, 0.7 Hz, 2H), 7.46 – 7.38 (m, 4H), 7.37 – 7.29 (m, 2H), 7.22 (d, J = 3.6 Hz, 1H), 6.69 (d, J = 3.6 Hz, 1H), 5.23 (s, 2H), 4.39 (q, J = 7.1 Hz, 2H), 1.41 (t, J = 7.1 Hz, 3H). ^{13}C-NMR (101 MHz, $CDCl_3$) δ 158.9, 156.5, 154.7, 144.2, 136.4, 130.8, 129.4, 128.8, 128.3, 127.4, 124.2, 119.9, 118.3, 110.2, 107.5, 71.2, 61.1, 14.5. LC-MS: ESI(+) calcd. for $[M+Na]^+$: *m/z* = 379.0; found: 379.2. HPLC: t_{ret} = 13.14 min (98.6 % at 254 nm, 98.3 % at 230 nm, method A).

5-(3-(Benzyloxy)-4-chlorophenyl)furan-2-carboxylic acid (127)

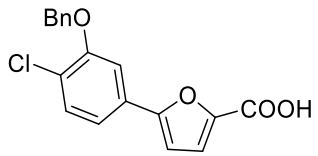

Chemical Formula: $C_{18}H_{13}ClO_4$
Exact Mass: 328.05024
Molecular Weight: 328.74800

Ethyl 5-(3-(benzyloxy)-4-chlorophenyl)furan-2-carboxylate (**126**, 286 mg, 0.802 mmol, 1.00 eq.) was dissolved in THF (4 mL) and H_2O (4 mL) and LiOH (101 mg, 2.40 mmol, 3.00 eq.) was added. The reaction mixture was stirred at rt for 5 h, THF was removed and then the aq. phase was acidified with HCl (2 M) to achieve pH 4 – 5. The precipitate was filtered off and washed with water to afford the product **127** (251 mg, 0.763 mmol, 95 %) as a white solid.

^{1}H-NMR (400 MHz, DMSO) δ 7.62 (d, J = 2.0 Hz, 1H), 7.59 – 7.48 (m, 3H), 7.46 – 7.39 (m, 3H), 7.38 – 7.32 (m, 2H), 7.24 (d, J = 3.6 Hz, 1H), 5.31 (s, 2H). ^{13}C-NMR (101 MHz, DMSO) δ 159.2, 155.2, 154.1, 144.4, 136.4, 130.7, 129.3, 128.6, 128.1, 127.7, 122.2, 119.9, 117.7, 109.9, 108.9, 70.3. LC-MS: ESI(-) calcd. for $[M-H]^+$: *m/z* = 327.1; found: 327.0. HPLC: t_{ret} = 12.07 min (96.1 % at 254 nm, 98.2 % at 230 nm, method A).

tert-Butyl 4-(4-(5-(3-(benzyloxy)-4-chlorophenyl)furan-2-carboxamido)phenyl)piperazine-1-carboxylate (128)

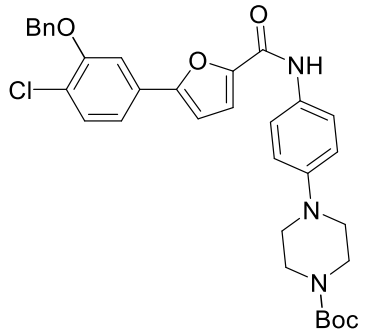

Chemical Formula: $C_{33}H_{34}ClN_3O_5$
Exact Mass: 587.21870
Molecular Weight: 588.10100

5-(3-(Benzyloxy)-4-chlorophenyl)furan-2-carboxylic acid (**127**, 244 mg, 0.742 mmol, 1.00 eq.) and HATU (427 mg, 0.757 mmol, 1.02 eq.) were dissolved in DMF (10 mL). Subsequently, 1-Boc-4-(4′-aminophenyl)piperazine (257 mg, 0.928 mmol, 1.25 eq.) and DIPEA (260 µL, 1.49 mmol, 2.01 eq.) were added and the reaction was stirred at rt for 3 h. The solvent was removed under reduced pressure and the residue was purified by flash column chromatography (silica gel, 0 – 60 % hexane/EtOAc) to yield the product **128** (436 mg, 0.741 mmol, quantitative) as a yellow solid.

^{1}H-NMR (400 MHz, $CDCl_3$) δ 7.93 (s, 1H), 7.61 – 7.53 (m, 2H), 7.53 – 7.48 (m, 2H), 7.46 – 7.38 (m, 3H), 7.38 – 7.32 (m, 1H), 7.30 – 7.25 (m, 3H), 6.96 (d, J = 8.6 Hz, 2H), 6.72 (d, J = 3.6 Hz, 1H), 5.25 (s, 2H), 3.60 (t, J = 5.0 Hz, 4H), 3.12 (t, J = 5.1 Hz, 4H), 1.49 (s, 9H). ^{13}C-NMR (101 MHz, $CDCl_3$) δ 156.0, 154.8, 154.7, 148.5, 147.3, 136.4, 130.9, 130.3, 129.3, 128.4, 124.1, 121.8, 118.1, 117.4, 117.3, 110.3, 108.4, 80.1, 71.3, 49.9, 43.6, 28.6. TLC-MS: ESI(+) calcd. for $[M+Na]^+$: *m/z* = 610.2; found: 610.7. HPLC: t_{ret} = 13.27 min (99.5 % at 254 nm, 99.7 % at 230 nm, method A).

tert-Butyl 4-(4-(5-(3-(benzyloxy)-4-chlorophenyl)-N-(pyridin-2-ylmethyl)furan-2-carboxamido)phenyl)piperazine-1-carboxylate

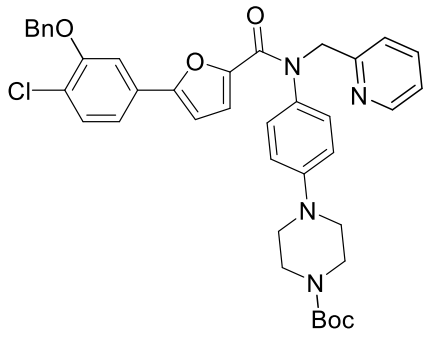

Chemical Formula: $C_{39}H_{39}ClN_4O_5$
Exact Mass: 678.26090
Molecular Weight: 679.21400

tert-Butyl 4-(4-(5-(3-(benzyloxy)-4-chlorophenyl)furan-2-carboxamido)phenyl)piperazine-1-carboxylate (**128**, 404 mg, 0.687 mmol, 1.00 eq.) was dissolved in DMF (10 mL). NaH (60 % dispersion in mineral oil, 60.0 mg, 2.70 mmol, 2.20 eq.) and 2-(bromomethyl)pyridine hydrobromide (382 mg, 1.51 mmol, 1.23 eq.) were added and the reaction was stirred at rt for 2 h. The solvent was then removed under reduced pressure and the residue was used in the next step without further purification.

TLC-MS: ESI(+) calcd. for $[M+Na]^+$: *m/z* = 701.3; found: 701.7.

tert-Butyl 4-(4-(5-(4-chloro-3-hydroxyphenyl)-N-(pyridin-2-ylmethyl)furan-2-carboxamido)phenyl)piperazine-1-carboxylate (129)

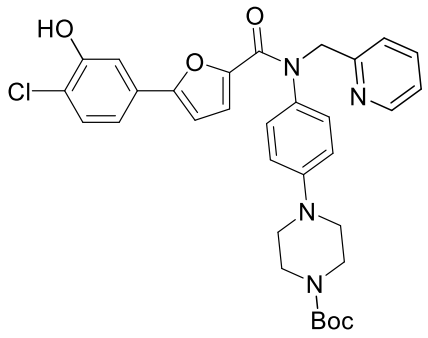

Chemical Formula: $C_{32}H_{33}ClN_4O_5$
Exact Mass: 588.21395
Molecular Weight: 589.08900

The residue from the previous reaction, *tert*-Butyl 4-(4-(5-(3-(benzyloxy)-4-chlorophenyl)-*N*-(pyridin-2-ylmethyl)furan-2-carboxamido)phenyl)piperazine-1-carboxylate was dissolved in MeOH (10 mL). Palladium on carbon (45 mg) was suspended in EtOAc (1.5 mL) and added to the first solution. H_2 was bubbled through the solution and the reaction was stirred under H_2 atmosphere for 2.5 h. The reaction mixture was filtered over celite and was purified by flash column chromatography (silica gel, 0 – 5 % DCM/MeOH) to yield the product **129** (352 mg, 0.598 mmol, 87 % over two steps) as a light green solid.

^{1}H-NMR (400 MHz, $CDCl_3$) δ 8.50 (ddd, J = 4.9, 1.8, 0.9 Hz, 1H), 7.66 (td, J = 7.6, 1.8 Hz, 1H), 7.51 (dt, J = 7.9, 1.1 Hz, 1H), 7.42 (s, 1H), 7.24 – 7.12 (m, 4H), 7.02 – 6.95 (m, 2H), 6.91 (d, J = 3.6 Hz, 1H), 6.87 (dd, J = 8.3, 2.0 Hz, 1H), 6.48 (d, J = 3.6 Hz, 1H), 6.29 (d, J = 2.0 Hz, 1H), 5.16 (s, 2H), 3.65 (t, J = 5.2 Hz, 4H), 3.20 (t, J = 5.1 Hz, 4H), 1.49 (s, 9H). ^{13}C-NMR (101 MHz, $CDCl_3$) δ 158.7, 157.3, 154.7, 154.3, 152.1, 150.1, 149.2, 146.8, 136.9, 136.5, 129.6, 129.6, 129.5, 123.0, 122.5, 120.6, 120.6, 117.5, 117.0, 112.3, 106.9, 80.3, 56.5, 49.5, 43.4, 28.5. TLC-MS: ESI(+) calcd. for $[M+Na]^+$: *m/z* = 611.2; found: 611.8. HPLC: t_{ret} = 11.94 min (87.6 % at 254 nm, 90.6 % at 230 nm, method A).

tert-Butyl 4-(4-(5-(4-chloro-3-((fluorosulfonyl)oxy)phenyl)-N-(pyridin-2-ylmethyl)furan-2-carboxamido)phenyl)piperazine-1-carboxylate (130)

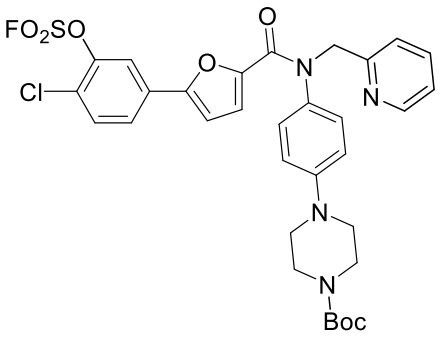

Chemical Formula: $C_{32}H_{32}ClFN_4O_7S$
Exact Mass: 670.16643
Molecular Weight: 671.13740

tert-Butyl 4-(4-(5-(4-chloro-3-hydroxyphenyl)-*N*-(pyridin-2-ylmethyl)furan-2-carboxamido)phenyl)piperazine-1-carboxylate (**129**, 150 mg, 0.255 mmol, 1.00 eq.) and AISF (**64**, 96.8 mg, 0.163 mmol, 1.21 eq.) were dissolved in THF (13 mL). DBU (83.6 µL, 0.560 mmol, 2.20 eq.) was added and the reaction was stirred at rt for 1.5 h. Sat. NH_4Cl (25 mL) was added and the aq. phase was extracted with EtOAc (3 x 35 mL). The organic phase was dried over Na_2SO_4, and the solvent was evaporated under reduced pressure. The residue was purified via flash column chromatography (silica gel, 0 – 100 % hexane/EtOAc) leading to the product **130** (128 mg, 0.191 mmol, 75 %) as a yellow solid.

^{1}H-NMR (400 MHz, $CDCl_3$) δ 8.52 (ddd, J = 5.0, 1.8, 0.9 Hz, 1H), 7.68 (td, J = 7.7, 1.8 Hz, 1H), 7.51 (d, J = 7.9 Hz, 1H), 7.44 (d, J = 8.5 Hz, 1H), 7.38 (dd, J = 8.5, 1.9 Hz, 1H), 7.35 – 7.30 (m, 1H), 7.23 – 7.16 (m, 1H), 7.16 – 7.08 (m, 2H), 6.90 – 6.82 (m, 2H), 6.59 (d, J = 3.7 Hz, 1H), 6.45 (d, J = 3.6 Hz, 1H), 5.16 (s, 2H), 3.58 (t, J = 5.1 Hz, 4H), 3.14 (t, J = 5.2 Hz, 4H), 1.48 (s, 9H). ^{13}C-NMR (101 MHz, $CDCl_3$) δ 159.0, 157.1, 154.8, 152.1, 151.0, 149.2, 147.8, 146.2, 137.0, 134.8, 131.7, 130.7, 128.9, 126.5, 125.3, 123.0, 122.5, 119.6, 118.6, 116.7, 108.5, 80.2, 56.5, 49.0, 43.6, 28.6. TLC-MS: ESI(+) [*m/z*]: calcd. mass $[M+Na]^+$ = 693.2; found = 694.0. HPLC: t_{ret} = 12.96 min (88.4 % at 254 nm, 90.3 % at 230 nm, method A).

2-Chloro-5-(5-((4-(piperazin-1-yl)phenyl)(pyridin-2-ylmethyl)carbamoyl)furan-2-yl)phenyl sulfurofluoridate (120)

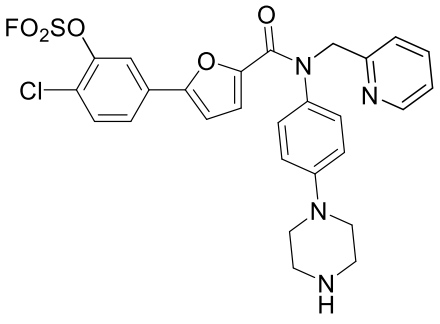

Chemical Formula: $C_{27}H_{24}ClFN_4O_5S$
Exact Mass: 570.11400
Molecular Weight: 571.02040

tert-Butyl 4-(4-(5-(4-chloro-3-((fluorosulfonyl)oxy)phenyl)-*N*-(pyridin-2-ylmethyl)furan-2-carboxamido)phenyl)piperazine-1-carboxylate (**130**, 60.7 mg, 90.4 µmol, 1.00 eq.), was dissolved in DCM (3 mL) and TFA (3 mL) and stirred at rt for 1.5 h. The solvent was evaporated, and the residue was purified by reverse phase column chromatography (CHROMABOND® Flash RS 40 C18 ec, 10 – 60 % H_2O/MeCN, 0.2% TFA). The fractions containing product

were lyophilized to afford the product **120** (TFA salt: 47.2 mg, 68.9 µmol, 76 %) as a light yellow solid.

^{1}H-NMR (400 MHz, DMSO) δ 8.82 (s, 2H), 8.57 – 8.51 (m, 1H), 7.87 (td, J = 7.7, 1.8 Hz, 1H), 7.78 (d, J = 8.5 Hz, 1H), 7.70 (d, J = 1.9 Hz, 1H), 7.53 (d, J = 8.0 Hz, 1H), 7.48 (dd, J = 8.5, 2.0 Hz, 1H), 7.40 – 7.33 (m, 1H), 7.30 – 7.22 (m, 2H), 7.20 (d, J = 3.7 Hz, 1H), 7.04 – 6.94 (m, 2H), 6.61 – 6.56 (m, 1H), 5.10 (s, 2H), 3.36 – 3.30 (m, 4H), 3.27 – 3.15 (m, 4H). ^{13}C-NMR (101 MHz, DMSO) δ 158.1, 156.2, 151.2, 149.4, 148.1, 147.4, 145.5, 138.2, 134.5, 132.1, 130.4, 128.6, 125.6, 125.0, 122.9, 122.7, 119.4, 118.3, 116.1, 110.0, 55.0, 45.2, 42.8. ^{19}F NMR (376 MHz, DMSO) δ 42.4, -74.5. HRMS: ESI(+) [*m/z*]: calcd. mass $[M+H]^+$ = 571.12127; found = 571.12175; rel. deviation 0.8 ppm. HPLC: t_{ret} = 11.04 min (90.5 % at 254 nm, 90.4 % at 230 nm, method A).

tert-Butyl 4-(4-(5-bromofuran-2-carboxamido)phenyl)piperazine-1-carboxylate (131)

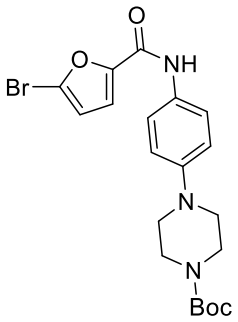

Chemical Formula: $C_{20}H_{24}BrN_3O_4$
Exact Mass: 449.09502
Molecular Weight: 450.33300

5-Bromofuran-2-carboxylic acid (**122**, 250 mg, 1.31 mmol, 1.00 eq.) and HATU (503 mg, 1.32 mmol, 1.01 eq.) were dissolved in DMF (18 mL). Subsequently, 1-Boc-4-(4′-aminophenyl)piperazine (552 mg, 1.99 mmol, 1.52 eq.) and DIPEA (450 µL, 2.58 mmol, 1.97 eq.) were added and the reaction was stirred at rt for 1.5 h. The solvent was removed under reduced pressure and the residue was purified by flash column chromatography (silica gel, 0 – 50 % hexane/EtOAc) to yield the product **131** (565 mg, 1.25 mmol, 96 %) as a yellow solid.

^{1}H-NMR (400 MHz, $CDCl_3$) δ 7.88 (s, 1H), 7.58 – 7.49 (m, 2H), 7.16 (d, J = 3.5 Hz, 1H), 6.97 – 6.88 (m, 2H), 6.49 (d, J = 3.5 Hz, 1H), 3.61 – 3.54 (m, 4H), 3.11 (t, J = 5.1 Hz, 4H), 1.48 (s, 9H). ^{13}C-NMR (101 MHz, $CDCl_3$) δ 154.9, 149.7, 148.7, 130.0, 124.7, 121.6, 117.3, 117.3, 114.7, 80.1, 49.8, 28.6. TLC-MS: ESI(+) calcd. for $[M+Na]^+$: *m/z* = 472.1; found: 472.1. HPLC: t_{ret} = 11.50 min (99.5 % at 254 nm, 96.1 % at 230 nm, method A).

tert-Butyl 4-(4-(5-bromo-N-(pyridin-2-ylmethyl)furan-2-carboxamido)phenyl)piperazine-1-carboxylate (132)

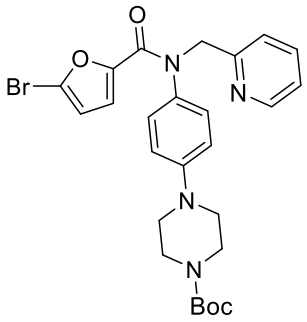

Chemical Formula: $C_{26}H_{29}BrN_4O_4$
Exact Mass: 540.13722
Molecular Weight: 541.44600

tert-Butyl 4-(4-(5-bromofuran-2-carboxamido)phenyl)piperazine-1-carboxylate (**131**, 555 mg, 1.23 mmol, 1.00 eq.) was dissolved in DMF (17 mL). NaH (60 % dispersion in mineral oil, 108 mg, 2.71 mmol, 2.20 eq.) and 2-(bromomethyl)pyridine hydrobromide (374 mg, 1.48 mmol, 1.20 eq.) were added and the reaction was stirred at rt for 20 h. The solvent was then removed under reduced pressure and the residue was purified by flash column chromatography (silica gel, 0 – 80 % hexane/EtOAc) to yield the product **132** (562 mg, 1.04 mmol, 84 %) as an off-white solid.

^{1}H-NMR (400 MHz, $CDCl_3$) δ 8.49 (ddd, J = 4.9, 1.8, 0.9 Hz, 1H), 7.67 (td, J = 7.7, 1.8 Hz, 1H), 7.51 (dt, J = 7.9, 1.1 Hz, 1H), 7.17 (ddd, J = 7.5, 4.9, 1.2 Hz, 1H), 7.08 – 7.00 (m, 2H), 6.88 – 6.79 (m, 2H), 6.13 (d, J = 3.6 Hz, 1H), 5.65 (s, 1H), 5.11 (s, 2H), 3.60 – 3.53 (m, 4H), 3.14 (t, J = 5.2 Hz, 4H), 1.48 (s, 9H). ^{13}C-NMR (101 MHz, $CDCl_3$) δ 158.4, 157.0, 154.7, 151.0, 148.9, 148.7, 136.9, 134.1, 129.0, 125.8, 123.1, 122.4, 119.0, 116.7, 113.1, 80.1, 56.1, 48.9, 28.4. TLC-MS: ESI(+) calcd. for $[M+Na]^+$: *m/z* = 563.1; found: 562.9. HPLC: t_{ret} = 11.53 min (99.9 % at 254 nm, 99.1 % at 230 nm, method A).

5-Bromo-2-chlorobenzenesulfonyl fluoride (134)

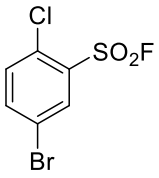

Chemical Formula: $C_6H_3BrClFO_2S$
Exact Mass: 271.87097
Molecular Weight: 273.50040

5-Bromo-2-chlorobenzenesulfonyl chloride (**133**, 544 mg, 1.88 mmol, 1.00 eq.) was dissolved in MeCN (2 mL). KHF_2 (337 mg, 4.32 mmol, 2.30 eq.) was dissolved in H_2O (1 mL) and added to the first solution. The reaction mixture was stirred at rt for 20 h. More H_2O was added (10 mL) and it was extracted with EtOAc (3 x 10 mL). After drying over Na_2SO_4, the solvent was removed under reduced pressure to afford the product **134** (486 mg, 1.78 mmol, 95 %) as a beige solid.

^{1}H-NMR (400 MHz, $CDCl_3$) δ 8.24 (d, J = 2.3 Hz, 1H), 7.79 (ddd, J = 8.5, 2.3, 0.5 Hz, 1H), 7.51 (d, J = 8.5 Hz, 1H). ^{13}C-NMR (101 MHz, $CDCl_3$) δ 139.3, 134.4, 133.8, 133.5 (d, J = 25.7 Hz), 132.6, 121.0. ^{19}F NMR (376 MHz, $CDCl_3$) δ 59.2. GC-MS: EI(+) calcd. for $[M]^+$: *m/z* = 271.9; found: 271.8.

tert-Butyl 5-bromofuran-2-carboxylate (136)

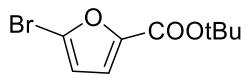

Chemical Formula: $C_9H_{11}BrO_3$
Exact Mass: 245.98916
Molecular Weight: 247.08800

Bromofuran-2-carboxylic acid (**122**, 500 mg, 2.62 mmol, 1.00 eq.) was dissolved in *t*BuOH (25 mL) and DMAP (99.1 mg, 0.812 mool, 0.31 eq.) and Boc_2O (1.10 mL, 5.16 mmol, 1.97 eq.) were added. The reaction was stirred at 40 °C for 5 h and then cooled to rt. The solvent was removed under reduced pressure and the residue was purified by flash column chromatography (silica gel, 0 – 10 % hexane/EtOAc) to yield the product **136** (542 mg, 2.19 mmol, 84 %) as a colorless oil.

^{1}H-NMR (400 MHz, $CDCl_3$) δ 7.01 (d, J = 3.5 Hz, 1H), 6.41 (d, J = 3.5 Hz, 1H), 1.56 (s, 9H). ^{13}C-NMR (101 MHz, $CDCl_3$) δ 157.1, 147.7, 126.8, 119.2, 113.8, 82.5, 28.3. LC-MS: ESI(+) calcd. for $[M+Na]^+$: *m/z* = 269.0; found: 268.8. HPLC: t_{ret} = 11.49 min (99.7 % at 254 nm, 98.9 % at 230 nm, method A).

Ethyl 5-(4-chloro-3-(fluorosulfonyl)phenyl)furan-2-carboxylate (139)

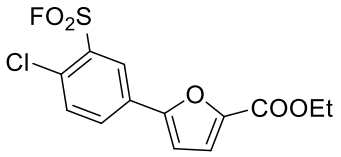

Chemical Formula: $C_{13}H_{10}ClFO_5S$
Exact Mass: 331.99215
Molecular Weight: 332.72640

5-Bromo-2-chlorobenzenesulfonyl fluoride (**134**, 45.0 mg, 0.165 mmol, 1.00 eq.) was dissolved in 1,4-dioxane (1 mL). (5-(Ethoxycarbonyl)furan-2-yl)boronic acid (40.0 mg, 0.217 mmol, 1.32 eq.), K_2CO_3 (68.2 mg, 0.494 mmol, 3.00 eq.) and $Pd(PPh_3)_4$ (12.7 mg, 18.1 µmol, 0.11 eq.) were added and the reaction was refluxed for 20 h. After cooling down to rt, H_2O (5 mL) was added, and the solution was extracted with EtOAc (3 x 5 mL). The combined organic phases were dried over Na_2SO_4, and the solvent was removed under reduced pressure. The residue was purified by flash column chromatography (silica gel, 0 – 20 % hexane/EtOAc) to yield the product **139** (23.6 mg, 70.9 µmol, 43 %) as a yellow solid.

^{1}H-NMR (400 MHz, $CDCl_3$) δ 8.42 (dd, J = 2.2, 0.8 Hz, 1H), 8.06 (ddd, J = 8.4, 2.3, 0.9 Hz, 1H), 7.69 (d, J = 8.4 Hz, 1H), 7.29 – 7.24 (m, 1H), 6.90 (d, J = 3.6 Hz, 1H), 4.40 (q, J = 7.1 Hz, 2H), 1.41 (t, J = 7.1 Hz, 3H). ^{13}C-NMR (101 MHz, $CDCl_3$) δ 158.5, 153.4, 145.6, 133.1, 133.1, 133.0, 132.8, 129.5, 127.7, 119.8, 109.5, 61.5, 14.5. LC-MS: ESI(+) calcd. for $[M+Na]^+$: *m/z* = 355.0; found: 355.0. HPLC: t_{ret} = 12.15 min (94.4 % at 254 nm, 94.9 % at 230 nm, method A).

2-(Benzyloxy)-1-fluoro-4-nitrobenzene (142)

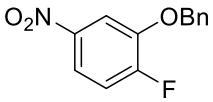

Chemical Formula: $C_{13}H_{10}FNO_3$
Exact Mass: 247.06447
Molecular Weight: 247.22540

2-Fluoro-5-nitrophenol (**141**, 750 mg, 4.77 mmol, 1.00 eq.) and K_2CO_3 (1.33 g, 9.60 mmol, 2.01 eq.) were suspended in DMF (24 mL) and benzyl bromide (1.15 mL, 9.69 mmol, 2.03 eq.) was added. The reaction was stirred at rt for 1 h and then sat. NH_4Cl (40 mL) was added. The mixture was extracted with EtOAc (3 x 40 mL), dried over Na_2SO_4 and the solvent was evaporated. The residue was purified by flash column chromatography (silica gel, 0 – 20 % hexane/EtOAc) to yield the product **142** (1.08 g, 4.37 mmol, 92 %) as a light yellow solid.

^{1}H-NMR (400 MHz, $CDCl_3$) δ 7.97 (dd, J = 7.2, 2.7 Hz, 1H), 7.91 (ddd, J = 8.9, 3.9, 2.7 Hz, 1H), 7.54 – 7.36 (m, 5H), 7.32 – 7.22 (m, 1H), 5.27 (s, 2H). ^{13}C-NMR (101 MHz, $CDCl_3$) δ 156.8 (d, J = 258.8 Hz), 147.2 (d, J = 12.4 Hz), 144.4, 135.2, 129.0, 128.8, 127.8, 117.5 (d, J = 8.1 Hz), 116.5 (d, J = 21.1 Hz), 110.8 (d, J = 3.7 Hz), 71.8. LC-MS: ESI(+) calcd. for $[M+Na]^+$: *m/z* = 270.1; found: 270.0. HPLC: t_{ret} = 11.71 min (97.6 % at 254 nm, 97.8 % at 230 nm, method A).

tert-Butyl 4-(2-(benzyloxy)-4-nitrophenyl)piperazine-1-carboxylate (143)

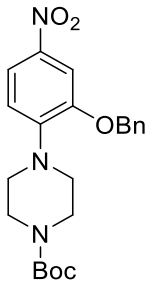

Chemical Formula: $C_{22}H_{27}N_3O_5$
Exact Mass: 413.19507
Molecular Weight: 413.47400

2-(Benzyloxy)-1-fluoro-4-nitrobenzene (**142**, 1.00 g, 4.04 mmol, 1.00 eq.) was dissolved in DMF (15 mL). 1-Boc-piperazine (1.13 g, 6.07 mmol, 1.50 eq.) and DIPEA (2.10 mL, 12.1 mmol, 2.98 eq.) were added and the reaction was stirred at 80 °C for 17 h. After cooling to rt, sat. NH_4Cl (25 mL) was added, the aq. phase was extracted with EtOAc (3 x 30 mL) and the org. phase dried over Na_2SO_4. The solvent was evaporated, and the residue was purified by flash column chromatography (silica gel, 0 – 100 % hexane/EtOAc) to yield the product **143** (1.48 g, 3.58 mmol, 89 %) as a yellow solid.

^{1}H-NMR (400 MHz, $CDCl_3$) δ 7.88 (dd, J = 8.8, 2.5 Hz, 1H), 7.83 (d, J = 2.5 Hz, 1H), 7.51 – 7.32 (m, 5H), 6.88 (d, J = 8.9 Hz, 1H), 5.17 (s, 2H), 3.58 – 3.51 (m, 4H), 3.20 (t, J = 5.0 Hz, 4H), 1.48 (s, 9H). ^{13}C-NMR (101 MHz, $CDCl_3$) δ 154.8, 150.5, 147.7, 142.3, 136.0, 128.9, 128.6, 127.5, 118.2, 117.1, 108.4, 80.2, 71.2, 50.1, 43.8, 28.6. TLC-MS: ESI(+) calcd. for $[M+Na]^+$: *m/z* = 436.2; found: 436.1. HPLC: t_{ret} = 12.94 min (99.0 % at 254 nm, 97.8 % at 230 nm, method A).

tert-Butyl 4-(4-amino-2-(benzyloxy)phenyl)piperazine-1-carboxylate (144)

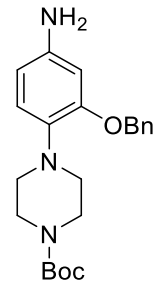

Chemical Formula: $C_{22}H_{29}N_3O_3$
Exact Mass: 383.22089
Molecular Weight: 383.49200

tert-Butyl 4-(2-(benzyloxy)-4-nitrophenyl)piperazine-1-carboxylate (**143**, 1.00 g, 2.42 mmol, 1.00 eq.), iron powder (1.35 g, 24.2 mmol, 10.0 eq.) and NH_4Cl (1.29 g, 24.2 mmol, 10.0 eq.) were suspended in EtOH (48 mL) and H_2O (12 mL). The reaction mixture was then stirred at 40 °C for 20 h. Sat. $NaHCO_3$ (50 mL) was added and the aq. phase was extracted with EtOAc (3 x 50 mL). After drying over Na_2SO_4 and removing the solvent, the residue was purified by flash column chromatography (silica gel, 0 – 70 % hexane/EtOAc) to yield the product **144** (643 mg, 1.68 mmol, 69 %) as a beige solid.

^{1}H-NMR (400 MHz, $CDCl_3$) δ 7.48 – 7.28 (m, 5H), 6.76 (d, J = 8.3 Hz, 1H), 6.35 (d, J = 2.5 Hz, 1H), 6.28 (dd, J = 8.3, 2.5 Hz, 1H), 5.08 (s, 2H), 3.58 – 3.48 (m, 6H), 2.94 (t, J = 5.0 Hz, 4H), 1.48 (s, 9H). ^{13}C-NMR (101 MHz, $CDCl_3$) δ 155.0, 152.8, 142.9, 137.4, 134.0, 128.6, 127.9, 127.1, 119.9, 107.7, 102.2, 79.7, 70.4, 51.4, 44.6, 28.6. TLC-MS: ESI(+) calcd. for $[M+H]^+$: *m/z* = 384.2; found: 384.2. HPLC: t_{ret} = 10.30 min (89.7 % at 254 nm, 82.2 % at 230 nm, method A).

tert-Butyl 4-(2-(benzyloxy)-4-(5-(4-chlorophenyl)furan-2-carboxamido)phenyl)piperazine-1-carboxylate (145)

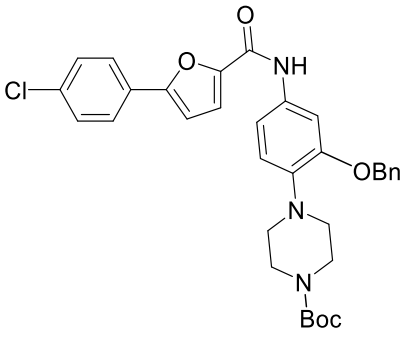

Chemical Formula: $C_{33}H_{34}ClN_3O_5$
Exact Mass: 587.21870
Molecular Weight: 588.10100

5-(4-Chlorophenyl)furan-2-carboxylic acid (**162**, 250 mg, 1.12 mmol, 1.00 eq.) and HATU (427 mg, 1.12 mmol, 1.00 eq.) were dissolved in DMF (15 mL). Subsequently, *tert*-butyl 4-(4-amino-2-(benzyloxy)phenyl)piperazine-1-carboxylate (**144**, 474 mg, 1.24 mmol, 1.10 eq.) and DIPEA (400 µL, 2.29 mmol, 2.04 eq.) were added and the reaction was stirred at rt for 18 h. Sat. NH_4Cl (25 mL) was added, and the aq. phase was extracted with EtOAc (3 x 25 mL). After drying over Na_2SO_4, the solvent was removed under reduced pressure and the residue was purified by flash column chromatography (silica gel, 0 – 50 % hexane/EtOAc) to yield the product **145** (551 mg, 0.937 mmol, 84 %) as a beige solid.

^{1}H-NMR (400 MHz, $CDCl_3$) δ 8.07 (s, 1H), 7.71 – 7.63 (m, 3H), 7.50 – 7.44 (m, 2H), 7.43 – 7.37 (m, 4H), 7.36 – 7.30 (m, 1H), 7.29 (d, J = 3.6 Hz, 1H), 7.05 (dd, J = 8.5, 2.3 Hz, 1H), 6.89 (d, J = 8.5 Hz, 1H), 6.77 (d, J = 3.6 Hz, 1H), 5.15 (s, 2H), 3.57 (t, J = 4.9 Hz, 4H), 3.03 (t, J = 5.0 Hz, 4H), 1.48 (s, 9H). ^{13}C-NMR (101 MHz, $CDCl_3$) δ 156.1, 155.0, 154.8, 151.9, 147.3, 138.7,

137.0, 134.9, 133.0, 129.3, 128.7, 128.1, 128.0, 127.3, 125.9, 118.7, 117.4, 112.9, 108.3, 106.5, 79.9, 70.5, 50.9, 43.6, 28.6. TLC-MS: ESI(+) calcd. for $[M+Na]^+$: *m/z* = 610.2; found: 610.1. HPLC: t_{ret} = 13.49 min (98.3 % at 254 nm, 97.5 % at 230 nm, method A).

tert-Butyl 4-(2-(benzyloxy)-4-(5-(4-chlorophenyl)-N-(pyridin-2-ylmethyl)furan-2-carboxamido)phenyl)piperazine-1-carboxylate (146)

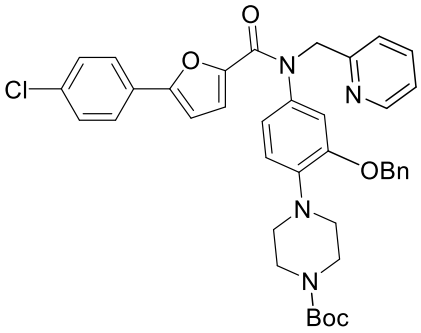

Chemical Formula: $C_{39}H_{39}ClN_4O_5$
Exact Mass: 678.26090
Molecular Weight: 679.21400

tert-Butyl 4-(2-(benzyloxy)-4-(5-(4-chlorophenyl)furan-2-carboxamido)phenyl)piperazine-1-carboxylate (**145**, 530 mg, 0.901 mmol, 1.00 eq.) was dissolved in DMF (12 mL). NaH (60 % dispersion in mineral oil, 80.0 mg, 1.98 mmol, 2.20 eq.) and 2-(bromomethyl)pyridine hydrobromide (274 mg, 1.08 mmol, 1.20 eq.) were added and the reaction was stirred at rt for 40 h. The solvent was then removed under reduced pressure and the residue was purified by flash column chromatography (silica gel, 0 – 80 % hexane/EtOAc) to yield the product **146** (349 mg, 0.514 mmol, 57 %) as a light yellow solid.

^{1}H-NMR (400 MHz, $CDCl_3$) δ 8.45 (ddd, J = 4.8, 1.8, 0.9 Hz, 1H), 7.59 (td, J = 7.6, 1.8 Hz, 1H), 7.42 (dt, J = 7.9, 1.1 Hz, 1H), 7.26 – 7.17 (m, 9H), 7.10 (ddd, J = 7.5, 4.9, 1.2 Hz, 1H), 6.82 – 6.72 (m, 3H), 6.41 (d, J = 3.6 Hz, 1H), 6.31 (d, J = 3.6 Hz, 1H), 5.09 (s, 2H), 4.89 (s, 2H), 3.50 (t, J = 5.0 Hz, 4H), 2.98 (t, J = 5.0 Hz, 4H), 1.42 (s, 9H). ^{13}C-NMR (101 MHz, $CDCl_3$) δ 159.2, 157.4, 155.0, 154.5, 151.9, 149.3, 146.6, 141.7, 138.0, 136.8, 136.6, 134.4, 129.0, 128.7, 128.3, 128.1, 127.1, 125.8, 123.0, 122.4, 121.1, 119.7, 118.7, 113.9, 106.9, 80.0, 70.7, 56.5, 50.7, 44.5, 28.6. TLC-MS: ESI(+) calcd. for $[M+Na]^+$: *m/z* = 701.3; found: 701.1. HPLC: t_{ret} = 13.49 min (91.2 % at 254 nm, 89.4 % at 230 nm, method A).

tert-Butyl 4-(4-(5-(4-chlorophenyl)-N-(pyridin-2-ylmethyl)furan-2-carboxamido)-2-hydroxyphenyl)piperazine-1-carboxylate

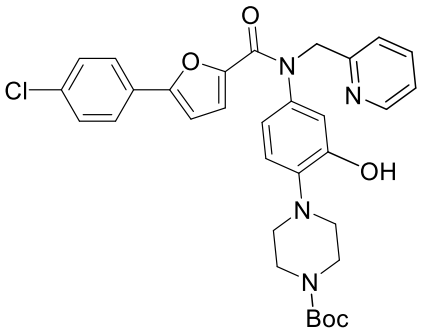

Chemical Formula: $C_{32}H_{33}ClN_4O_5$
Exact Mass: 588.21395
Molecular Weight: 589.08900

tert-Butyl 4-(2-(benzyloxy)-4-(5-(4-chlorophenyl)-*N*-(pyridin-2-ylmethyl)furan-2-carboxamido)phenyl)piperazine-1-carboxylate (**146**, 349 mg, 0.514 mmol, 1.00 eq.) was dissolved in MeOH (15 mL). Palladium on carbon (30 mg) was suspended in EtOAc (1.5 mL) and added to the first solution. H_2 was bubbled through the solution and the reaction was stirred under H_2 atmosphere for 2.5 h. The reaction mixture was filtered over celite, the solvent was then removed under reduced pressure and the residue was used in the next step without further purification.

TLC-MS: ESI(+) calcd. for $[M+Na]^+$: *m/z* = 611.2; found: 611.2.

tert-Butyl 4-(4-(5-(4-chlorophenyl)-N-(pyridin-2-ylmethyl)furan-2-carboxamido)-2-((fluorosulfonyl)oxy)phenyl)piperazine-1-carboxylate (147)

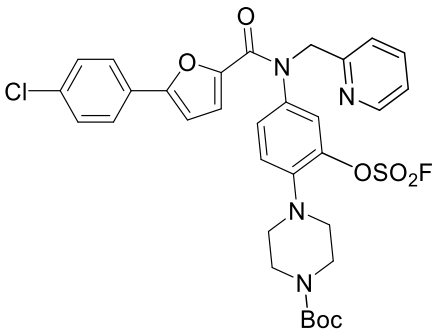

Chemical Formula: $C_{32}H_{32}ClFN_4O_7S$
Exact Mass: 670.16643
Molecular Weight: 671.13740

The residue from the previous step, *tert*-butyl 4-(4-(5-(4-chlorophenyl)-*N*-(pyridin-2-ylmethyl)furan-2-carboxamido)-2-hydroxyphenyl)piperazine-1-carboxylate (78.0 mg, 0.133 mmol, 1.00 eq.) and AISF (**64**, 51.3 mg, 0.163 mmol, 1.23 eq.) were dissolved in THF (7 mL). DBU (45.1 µL, 0.302 mmol, 2.28 eq.) was added and the reaction was stirred at rt for 5 h. Sat. NH_4Cl (15 mL) was added, and the aq. phase was extracted with EtOAc (3 x 25 mL). The organic phase was dried over Na_2SO_4, and the solvent was evaporated under reduced pressure. The residue was purified via flash column chromatography (silica gel, 0 – 100 % hexane/EtOAc) leading to the product **147** (53.5 mg, 79.7 µmol, 60 % over two steps) as a beige solid.

^{1}H-NMR (400 MHz, $CDCl_3$) δ 8.53 (ddd, J = 4.9, 1.8, 0.9 Hz, 1H), 7.71 (td, J = 7.7, 1.8 Hz, 1H), 7.50 (dt, J = 7.9, 1.2 Hz, 1H), 7.32 (d, J = 2.4 Hz, 1H), 7.27 (d, J = 2.5 Hz, 1H), 7.25 – 7.21 (m, 3H), 7.19 – 7.14 (m, 2H), 7.04 (d, J = 8.6 Hz, 1H), 6.78 (d, J = 3.7 Hz, 1H), 6.56 (d, J = 3.6 Hz, 1H), 5.17 (s, 2H), 3.63 – 3.55 (m, 4H), 2.97 (t, J = 4.9 Hz, 4H), 1.48 (s, 9H). ^{13}C-NMR (101 MHz, $CDCl_3$) δ 158.9, 156.5, 154.9 (d, J = 9.0 Hz), 149.2, 146.4, 144.5, 143.5, 138.7, 137.3, 134.6, 129.2, 129.0, 128.0, 125.7, 123.3, 122.9, 122.2, 121.3, 120.7, 107.0, 80.2, 56.1, 51.2,

43.9, 28.5. TLC-MS: ESI(+) [*m/z*]: calcd. mass $[M+Na]^+$ = 693.2; found = 693.0. HPLC: t_{ret} = 13.23 min (98.2 % at 254 nm, 98.8 % at 230 nm, method A).

5-(5-(4-Chlorophenyl)-N-(pyridin-2-ylmethyl)furan-2-carboxamido)-2-(piperazin-1-yl)phenyl sulfurofluoridate (121)

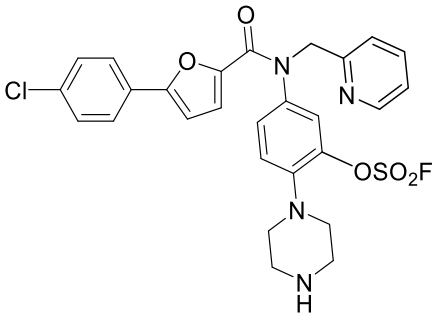

Chemical Formula: $C_{27}H_{24}ClFN_4O_5S$
Exact Mass: 570.11400
Molecular Weight: 571.02040

tert-Butyl 4-(4-(5-(4-chlorophenyl)-*N*-(pyridin-2-ylmethyl)furan-2-carboxamido)-2-((fluorosulfonyl)oxy)phenyl)piperazine-1-carboxylate (**147**, 53.5 mg, 79.7 µmol, 1.00 eq.), was dissolved in DCM (3 mL) and TFA (3 mL) and stirred at rt for 1 h. The solvent was evaporated and the residue was purified by reverse phase column chromatography (CHROMABOND® Flash RS 40 C18 ec, 10 – 55 % H_2O/MeCN, 0.2% TFA). The fractions containing product were lyophilized to afford the product **121** (TFA salt: 25.7 mg, 37.5 µmol, 47 %) as a beige solid.

^{1}H-NMR (400 MHz, DMSO) δ 8.86 (s, 2H), 8.52 (dt, J = 4.8, 1.5 Hz, 1H), 7.86 – 7.76 (m, 2H), 7.50 (dd, J = 8.6, 2.3 Hz, 2H), 7.43 – 7.37 (m, 2H), 7.36 – 7.30 (m, 2H), 7.29 – 7.23 (m, 2H), 7.05 (d, J = 3.7 Hz, 1H), 6.90 (d, J = 3.7 Hz, 1H), 5.14 (s, 2H), 3.27 – 3.15 (m, 8H).^{13}C-NMR (101 MHz, DMSO) δ 158.0, 156.0, 153.6, 148.6, 146.4, 142.6, 142.4, 138.8, 137.6, 133.2, 129.6, 128.9, 127.9, 125.6, 122.7, 122.5, 122.0, 121.7, 120.2, 108.1, 55.0, 47.7, 43.2. ^{19}F NMR (376 MHz, DMSO) δ 43.1, -74.4. HRMS: ESI(+) [*m/z*]: calcd. mass $[M+H]^+$ = 571.12127; found = 571.12147; rel. deviation 0.3 ppm. HPLC: t_{ret} = 11.27 min (98.2 % at 254 nm, 96.3 % at 230 nm, method A).

2-Fluoro-5-nitrobenzenesulfonyl fluoride (149)

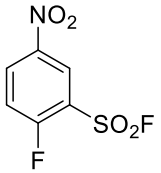

Chemical Formula: $C_6H_3F_2NO_4S$
Exact Mass: 222.97509
Molecular Weight: 223.14981

2-Fluoro-5-nitrobenzenesulfonyl chloride (**148**, 135 mg, 0.563 mmol, 1.00 eq.) was dissolved in MeCN (0.6 mL). KHF_2 (101 mg, 1.30 mmol, 2.30 eq.) was dissolved in H_2O (0.3 mL) and added to the first solution. The reaction mixture was stirred at rt for 18 h. Sat. NH_4Cl (10 mL) was added, and it was extracted with EtOAc (3 x 10 mL). After drying over Na_2SO_4, the solvent was removed under reduced pressure to afford the product **149** (125 mg, 0.560 mmol, quantitative) as a yellow oil.

^{1}H-NMR (400 MHz, $CDCl_3$) δ 8.88 (dd, J = 5.6, 2.8 Hz, 1H), 8.67 (ddd, J = 9.2, 4.1, 2.8 Hz, 1H), 7.57 (t, J = 8.7 Hz, 1H). ^{13}C-NMR (101 MHz, $CDCl_3$) δ 162.8 (d, J = 273.0 Hz), 133.1, 133.0, 127.3, 119.6, 119.4. ^{19}F NMR (376 MHz, $CDCl_3$) δ 64.9 (d, J = 12.3 Hz), -95.7 (d, J = 5.5 Hz). GC-MS: EI(+) calcd. for $[M]^+$: *m/z* = 223.0; found: 222.9. HPLC: t_{ret} = 9.50 min (95.9 % at 254 nm, 96.0 % at 230 nm, method A).

tert-Butyl 4-(2-(fluorosulfonyl)-4-nitrophenyl)piperazine-1-carboxylate (150)

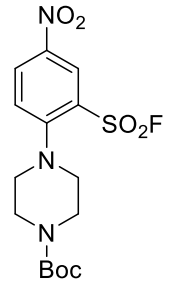

Chemical Formula: $C_{15}H_{20}FN_3O_6S$
Exact Mass: 389.10568
Molecular Weight: 389.39840

2-Fluoro-5-nitrobenzenesulfonyl fluoride (**149**, 118 mg, 0.529 mmol, 1.00 eq.) and 1-Boc-piperazine (149 mg, 0.798 mmol, 1.51 eq.) were dissolved in DMF (2.5 mL). DIPEA (220 µL, 1.26 mmol, 2.39 eq.) was added and the reaction was stirred at 80 °C for 3 h. After cooling to rt, H_2O (10 mL) was added and the aq. phase was extracted with EtOAc (4 x 10 mL). After drying over Na_2SO_4, the solvent was evaporated and the residue was purified by flash column chromatography (silica gel, 0 – 50 % hexane/EtOAc) to yield the product **150** (112 mg, 0.288 mmol, 54 %) as a yellow solid.

^{1}H-NMR (400 MHz, $CDCl_3$) δ 8.87 (d, J = 2.7 Hz, 1H), 8.48 (dd, J = 9.0, 2.7 Hz, 1H), 7.38 (d, J = 9.0 Hz, 1H), 3.68 – 3.61 (m, 4H), 3.23 – 3.16 (m, 4H), 1.48 (s, 9H). ^{13}C-NMR (101 MHz, $CDCl_3$) δ 157.6, 154.7, 142.5, 130.9, 128.5, 128.3, 123.8, 80.5, 53.1, 43.6, 28.5. TLC-MS: ESI(+) calcd. for $[M+Na]^+$: *m/z* = 412.1; found: 411.9. HPLC: t_{ret} = 12.06 min (97.6 % at 254 nm, 95.8 % at 230 nm, method A).

tert-Butyl 4-(4-amino-2-(fluorosulfonyl)phenyl)piperazine-1-carboxylate (151)

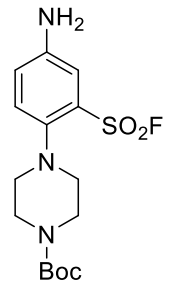

Chemical Formula: $C_{15}H_{22}FN_3O_4S$
Exact Mass: 359.13151
Molecular Weight: 359.41640

tert-Butyl 4-(2-(fluorosulfonyl)-4-nitrophenyl)piperazine-1-carboxylate (**150**, 112 mg, 0.288 mmol, 1.00 eq.) was dissolved in MeOH (10 mL). Palladium on carbon (15 mg) was suspended in EtOAc (2 mL) and added to the first solution. H_2 was bubbled through the solution and the reaction was stirred under H_2 atmosphere for 1 h. The reaction mixture was filtered over celite, and the solvent was removed to yield the product **151** (103 mg, 0.287 mmol, quantitative) as a yellow solid.

^{1}H-NMR (400 MHz, $CDCl_3$) δ 7.24 – 7.18 (m, 2H), 6.93 (dd, J = 8.5, 2.7 Hz, 1H), 3.95 (s, 2H), 3.55 (s, 4H), 2.88 – 2.79 (m, 4H), 1.47 (s, 9H). ^{13}C-NMR (101 MHz, $CDCl_3$) δ 154.9, 144.8, 143.0, 133.2 (d, J = 18.3 Hz), 126.3, 121.6, 115.0, 79.7, 53.2, 28.4. LC-MS: ESI(+) calcd. for $[M+Na]^+$: *m/z* = 360.1; found: 360.1. HPLC: t_{ret} = 11.25 min (97.5 % at 254 nm, 93.0 % at 230 nm, method A).

tert-Butyl 4-(4-(5-(4-chlorophenyl)furan-2-carboxamido)-2-(fluorosulfonyl)phenyl)piperazine-1-carboxylate (152)

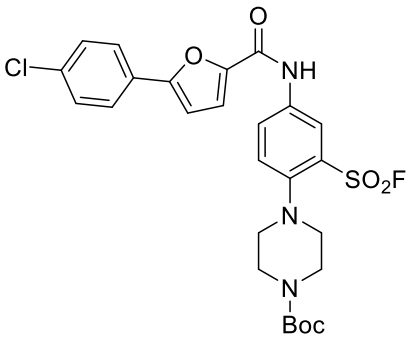

Chemical Formula: $C_{26}H_{27}ClFN_3O_6S$
Exact Mass: 563.12931
Molecular Weight: 564.02540

5-(4-Chlorophenyl)furan-2-carboxylic acid (**162**, 70.0 mg, 0.314 mmol, 1.00 eq.) and HATU (121 mg, 0.318 mmol, 1.01 eq.) were dissolved in DMF (2 mL). Subsequently, *tert*-butyl 4-(4-amino-2-(fluorosulfonyl)phenyl)piperazine-1-carboxylate (**151**, 113 mg, 0.314 mmol, 1.00 eq.) and DIPEA (110 µL, 0.632 mmol, 2.01 eq.) were added and the reaction was stirred at 80 °C for 17 h. After cooling to rt, sat. NH_4Cl (15 mL) was added, and the aq. phase was extracted with EtOAc (3 x 15 mL). After drying over Na_2SO_4, the solvent was removed under reduced pressure and the residue was purified by flash column chromatography (silica gel, 0 – 50 % hexane/EtOAc) to yield the product **152** (65.9 mg, 0.117 mmol, 37 %) as a white solid.

^{1}H-NMR (400 MHz, $CDCl_3$) δ 8.36 (s, 1H), 8.26 (dd, J = 8.7, 2.6 Hz, 1H), 8.11 (d, J = 2.6 Hz, 1H), 7.72 – 7.65 (m, 2H), 7.46 – 7.38 (m, 3H), 7.35 (d, J = 3.7 Hz, 1H), 6.79 (d, J = 3.6 Hz, 1H), 3.59 (t, J = 4.9 Hz, 4H), 2.92 (t, J = 4.8 Hz, 4H), 1.49 (s, 9H). ^{13}C-NMR (101 MHz, $CDCl_3$) δ 156.1, 155.4, 154.8, 148.8, 146.2, 135.3, 135.1, 132.3 (d, J = 19.8 Hz), 129.3, 127.7, 127.7, 126.0, 125.9, 121.6, 118.5, 108.3, 79.9, 53.2, 28.4. TLC-MS: ESI(+) calcd. for $[M+Na]^+$: *m/z* = 586.1; found: 585.9. HPLC: t_{ret} = 13.17 min (99.4 % at 254 nm, 97.5 % at 230 nm, method A).

tert-Butyl 4-(4-(5-(4-chlorophenyl)-N-(pyridin-2-ylmethyl)furan-2-carboxamido)-2-(fluorosulfonyl)phenyl)piperazine-1-carboxylate

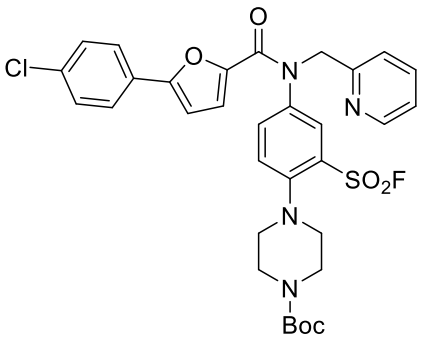

Chemical Formula: $C_{32}H_{32}ClFN_4O_6S$
Exact Mass: 654.17151
Molecular Weight: 655.13840

tert-Butyl 4-(4-(5-(4-chlorophenyl)furan-2-carboxamido)-2-(fluorosulfonyl)phenyl)piperazine-1-carboxylate (**152**, 57.0 mg, 0.101 mmol, 1.00 eq.) was dissolved in DMF (1.5 mL). NaH (60 % dispersion in mineral oil, 8.93 mg, 0.223 mmol, 2.21 eq.) and 2-(bromomethyl)pyridine hydrobromide (31.4 mg, 0.124 mmol, 1.23 eq.) were added and the reaction was stirred at rt for 20 h. The solvent was then removed under reduced pressure and the residue was used in the next step without further purification.

TLC-MS: ESI(+) calcd. for $[M+Na]^+$: *m/z* = 677.2; found: 677.1.

5-(5-(4-Chlorophenyl)-N-(pyridin-2-ylmethyl)furan-2-carboxamido)-2-(piperazin-1-yl)benzenesulfonyl fluoride (153)

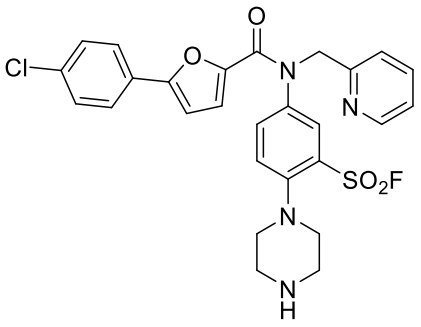

Chemical Formula: $C_{27}H_{24}ClFN_4O_4S$
Exact Mass: 554.11908
Molecular Weight: 555.02140

The residue from the previous step, *tert*-Butyl 4-(4-(5-(4-chlorophenyl)-*N*-(pyridin-2-ylmethyl)furan-2-carboxamido)-2-(fluorosulfonyl)phenyl)piperazine-1-carboxylate, was dissolved in DCM (3 mL) and TFA (3 mL) and stirred at rt for 2 h. The solvent was evaporated, and the residue was purified by reverse phase column chromatography (CHROMABOND® Flash RS 40 C18 ec, 10 – 60 % H_2O/MeCN, 0.2% TFA). The fractions containing product were lyophilized to afford the product **153** (TFA salt: 24.3 mg, 36.3 µmol, 42 % over two steps) as a light red solid.

^{1}H-NMR (400 MHz, DMSO) δ 8.76 (s, 2H), 8.52 (ddd, J = 4.9, 1.8, 0.9 Hz, 1H), 8.18 (d, J = 2.6 Hz, 1H), 7.93 (dd, J = 8.6, 2.6 Hz, 1H), 7.81 (td, J = 7.7, 1.8 Hz, 1H), 7.71 (d, J = 8.6 Hz, 1H), 7.50 (d, J = 7.9 Hz, 1H), 7.43 – 7.35 (m, 2H), 7.31 (ddd, J = 7.6, 4.9, 1.2 Hz, 1H), 7.25 – 7.17 (m, 2H), 7.13 – 7.04 (m, 2H), 5.18 (s, 2H), 3.24 – 3.20 (m, 4H), 3.11 – 3.04 (m, 4H). ^{13}C-NMR (101 MHz, DMSO) δ 157.9, 156.1, 153.6, 150.0, 148.8, 146.4, 141.1, 137.4, 136.8, 133.3, 130.4, 129.4, 129.0, 127.8, 126.4, 125.5, 122.8, 122.5, 120.6, 108.4, 55.0, 49.8, 43.4. ^{19}F NMR (376 MHz, DMSO) δ 58.8, -74.3. HRMS: ESI(+) [*m/z*]: calcd. mass $[M+H]^+$ = 555.12636; found = 555.12708; rel. deviation 1.3 ppm. HPLC: t_{ret} = 10.26 min (99.5 % at 254 nm, 96.4 % at 230 nm, method A).

tert-Butyl 4-(2-bromo-4-nitrophenyl)piperazine-1-carboxylate (155)

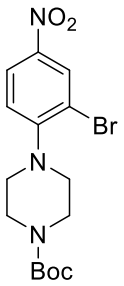

Chemical Formula: $C_{15}H_{20}BrN_3O_4$
Exact Mass: 385.06372
Molecular Weight: 386.24600

2-Bromo-1-fluoro-4-nitrobenzene (**154**, 500 mg, 2.27 mmol, 1.00 eq.) and 1-Boc-piperazine (466 mg, 2.50 mmol, 1.10 eq.) were dissolved in DMF (5 mL). K_2CO_3 (628 mg, 4.55 mmol, 2.00 eq.) was added and the reaction was stirred at 60 °C for 18 h. After cooling to rt, the solvent was evaporated and the residue was purified by flash column chromatography (silica gel, 0 – 20 % hexane/EtOAc) to yield the product **155** (803 mg, 2.08 mmol, 92 %) as an orange solid.

^{1}H-NMR (400 MHz, $CDCl_3$) δ 8.46 (d, J = 2.6 Hz, 1H), 8.16 (dd, J = 8.9, 2.7 Hz, 1H), 7.04 (d, J = 8.9 Hz, 1H), 3.67 – 3.60 (m, 4H), 3.13 (t, J = 5.0 Hz, 4H), 1.49 (s, 9H). ^{13}C-NMR (101 MHz, $CDCl_3$) δ 156.3, 154.9, 143.0, 130.0, 124.1, 120.1, 118.2, 80.3, 51.2, 44.3, 28.5. LC-MS: ESI(+) calcd. for $[M+Na]^+$: *m/z* = 408.1; found: 408.0. HPLC: t_{ret} = 12.74 min (99.7 % at 254 nm, 98.8 % at 230 nm, method A).

tert-Butyl 4-(4-amino-2-bromophenyl)piperazine-1-carboxylate (156)

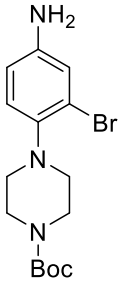

Chemical Formula: $C_{15}H_{22}BrN_3O_2$
Exact Mass: 355.08954
Molecular Weight: 356.26400

tert-Butyl 4-(2-bromo-4-nitrophenyl)piperazine-1-carboxylate (**155**, 780 mg, 2.02 mmol, 1.00 eq.) was dissolved in EtOH (7 mL) and H_2O (1.5 mL). Iron powder (343 mg, 6.14 mmol, 3.04 eq.) and NH_4Cl (650 mg, 12.2 mmol, 6.02 eq.) were added. The reaction mixture was then stirred at 70 °C for 22 h. After cooling to rt, all solids were filtered off. H_2O (25 mL) was added, and the aq. phase was extracted with EtOAc (3 x 25 mL). After drying over Na_2SO_4 and removing the solvent, the residue was purified by flash column chromatography (silica gel, 0 – 50 % hexane/EtOAc) to yield the product **156** (238 mg, 0.668 mmol, 33 %) as a yellow solid. 41 % of starting material were recovered which leads to an adjusted yield of the reaction of 56 %.

^{1}H-NMR (400 MHz, $CDCl_3$) δ 6.95 (d, J = 2.7 Hz, 1H), 6.85 (d, J = 8.5 Hz, 1H), 6.60 (dd, J = 8.5, 2.7 Hz, 1H), 3.60 – 3.55 (m, 6H), 2.86 (t, J = 4.9 Hz, 4H), 1.48 (s, 9H). ^{13}C-NMR (101 MHz, $CDCl_3$) δ 155.1, 143.7, 142.2, 121.9, 121.4, 120.2, 114.9, 79.8, 52.3, 28.6. TLC-MS: ESI(+) calcd. for $[M+Na]^+$: *m/z* = 378.1; found: 377.9. HPLC: t_{ret} = 11.12 min (99.1 % at 254 nm, 98.1 % at 230 nm, method A).

tert-Butyl 4-(2-bromo-4-(5-(4-chlorophenyl)furan-2-carboxamido)phenyl)piperazine-1-carboxylate (157)

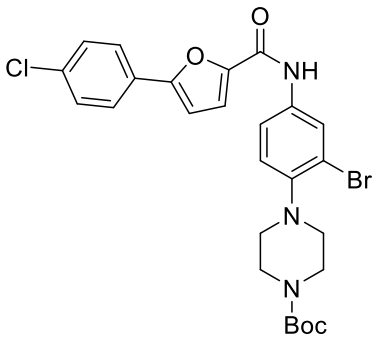

Chemical Formula: $C_{26}H_{27}BrClN_3O_4$
Exact Mass: 559.08735
Molecular Weight: 560.87300

5-(4-Chlorophenyl)furan-2-carboxylic acid (**162**, 130 mg, 0.519 mmol, 1.00 eq.) and HATU (201 mg, 0.529 mmol, 1.02 eq.) were dissolved in DMF (7 mL). Subsequently, *tert*-butyl 4-(4-amino-2-bromophenyl)piperazine-1-carboxylate (**156**, 231 mg, 0.648 mmol, 1.25 eq.) and DIPEA (190 µL, 1.09 mmol, 2.10 eq.) were added and the reaction was stirred at rt for 3.5 h. The solvent was removed under reduced pressure and the residue was purified by flash column chromatography (silica gel, 0 – 50 % hexane/EtOAc) to yield the product **157** (291 mg, 0.519 mmol, quantitative) as a beige solid.

^{1}H-NMR (400 MHz, $CDCl_3$) δ 8.01 (s, 1H), 7.90 (d, J = 2.5 Hz, 1H), 7.71 – 7.61 (m, 3H), 7.46 – 7.38 (m, 2H), 7.30 (d, J = 3.6 Hz, 1H), 7.02 (d, J = 8.7 Hz, 1H), 6.78 (d, J = 3.6 Hz, 1H), 3.61 (t, J = 4.9 Hz, 4H), 2.96 (t, J = 4.9 Hz, 4H), 1.49 (s, 9H). ^{13}C-NMR (101 MHz, $CDCl_3$) δ 155.8, 154.9, 147.2, 146.8, 134.9, 133.7, 129.3, 127.9, 125.8, 125.5, 121.1, 120.2, 120.2, 117.8, 108.2, 79.8, 51.8, 28.5. TLC-MS: ESI(+) calcd. for $[M+Na]^+$: *m/z* = 582.1; found: 582.2. HPLC: t_{ret} = 13.47 min (94.8 % at 254 nm, 97.5 % at 230 nm, method A).

tert-Butyl 4-(2-bromo-4-(5-(4-chlorophenyl)-N-(pyridin-2-ylmethyl)furan-2-carboxamido)phenyl)piperazine-1-carboxylate (158)

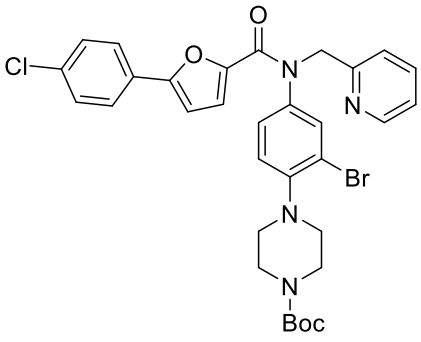

Chemical Formula: $C_{32}H_{32}BrClN_4O_4$
Exact Mass: 650.12955
Molecular Weight: 651.98600

tert-Butyl 4-(2-bromo-4-(5-(4-chlorophenyl)furan-2-carboxamido)phenyl)piperazine-1-carboxylate (**157**, 290 mg, 0.517 mmol, 1.00 eq.) was dissolved in DMF (7 mL). NaH (60 % dispersion in mineral oil, 45.0 mg, 1.14 mmol, 2.20 eq.) and 2-(bromomethyl)pyridine hydrobromide (157 mg, 0.620 mmol, 1.20 eq.) were added and the reaction was stirred at rt for 19 h. The solvent was then removed under reduced pressure and the residue was purified by flash column chromatography (silica gel, 0 – 100 % hexane/EtOAc) to yield the product **158** (244 mg, 0.374 mmol, 72 %) as a white solid.

^{1}H-NMR (400 MHz, $CDCl_3$) δ 8.53 (ddd, J = 4.9, 1.8, 0.9 Hz, 1H), 7.70 (td, J = 7.7, 1.8 Hz, 1H), 7.58 (d, J = 2.4 Hz, 1H), 7.51 (dt, J = 7.8, 1.0 Hz, 1H), 7.26 – 7.22 (m, 2H), 7.22 – 7.19 (m,

1H), 7.19 – 7.14 (m, 2H), 7.12 (dd, J = 8.5, 2.5 Hz, 1H), 6.92 (d, J = 8.4 Hz, 1H), 6.75 (d, J = 3.6 Hz, 1H), 6.54 (d, J = 3.7 Hz, 1H), 5.15 (s, 2H), 3.61 (t, J = 5.0 Hz, 4H), 2.94 (t, J = 4.9 Hz, 4H), 1.48 (s, 9H). ^{13}C-NMR (101 MHz, $CDCl_3$) δ 159.0, 156.8, 155.0, 154.7, 150.4, 149.0, 146.6, 139.2, 137.3, 134.5, 133.6, 129.0, 128.2, 128.1, 125.7, 123.1, 122.7, 121.2, 120.4, 120.0, 106.9, 80.1, 56.2, 51.8, 28.6. TLC-MS: ESI(+) calcd. for $[M+Na]^+$: *m/z* = 673.1; found: 673.2. HPLC: t_{ret} = 13.48 min (98.4 % at 254 nm, 98.6 % at 230 nm, method A).

Ethyl 5-(4-chlorophenyl)furan-2-carboxylate (161)

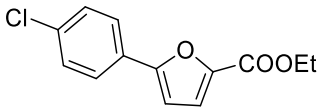

Chemical Formula: $C_{13}H_{11}ClO_3$
Exact Mass: 250.03967
Molecular Weight: 250.67800

Ethyl 5-bromofuran-2-carboxylate (**123**, 2.26 g, 10.3 mmol, 1.00 eq.) was dissolved in 1,4-dioxane (27 mL) and (4-chlorophenyl)boronic acid (1.86 g, 11.9 mmol, 1.15 eq.) was added. K_2CO_3 (2.85 g, 10.6 mmol, 2.00 eq.) was dissolved in H_2O (9 mL) and this solution was added to the first. $Pd(PPh_3)_4$ (358 mg, 0.310 mmol, 0.03 eq.) was added and the solution was stirred at 60 °C. After 20 h, the solution was cooled to rt and diluted with sat. NH_4Cl (25 mL). The aq. phase was extracted with EtOAc (3 x 30 mL). After drying over Na_2SO_4 and evaporating the solvent, the residue was purified by flash column chromatography (silica gel, 0 – 20 % hexane/EtOAc) to yield the product **161** (2.43 g, 9.69 mmol, 94 %) as a white solid.

^{1}H-NMR (400 MHz, $CDCl_3$) δ 7.75 – 7.67 (m, 2H), 7.43 – 7.35 (m, 2H), 7.23 (d, J = 3.6 Hz, 1H), 6.72 (d, J = 3.6 Hz, 1H), 4.38 (q, J = 7.1 Hz, 2H), 1.40 (t, J = 7.1 Hz, 3H). ^{13}C-NMR (101 MHz, $CDCl_3$) δ 158.9, 156.4, 144.3, 134.9, 128.2, 126.2, 119.9, 107.3, 61.1, 14.5. TLC-MS: ESI(+) calcd. for $[M+Na]^+$: *m/z* = 273.0; found: 272.8. HPLC: t_{ret} = 12.27 min (97.6 % at 254 nm, 97.3 % at 230 nm, method A).

5-(4-Chlorophenyl)furan-2-carboxylic acid (162)

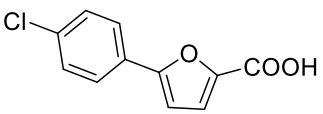

Chemical Formula: $C_{11}H_7ClO_3$
Exact Mass: 222.00837
Molecular Weight: 222.62400

Ethyl 5-(4-chlorophenyl)furan-2-carboxylate (**161**, 2.43 g, 9.69 mmol, 1.00 eq.) was dissolved in MeOH (30 mL) and H_2O (15 mL). NaOH (3.88 g, 96.9 mmol, 10.0 eq.) was dissolved in H_2O (10 mL) and added to the first solution. The reaction was stirred at rt for 3 h and then MeOH was removed. The solution was acidified with conc. HCl until the product precipitated. The precipitate was filtered off, washed with H_2O and dried to afford the product **162** (2.02 g, 9.07 mmol, 94 %) as a white solid.

^{1}H-NMR (400 MHz, DMSO) δ 13.18 (s, 1H), 7.87 – 7.77 (m, 2H), 7.60 – 7.50 (m, 2H), 7.36 – 7.28 (m, 1H), 7.24 – 7.15 (m, 1H). ^{13}C-NMR (101 MHz, DMSO) δ 159.2, 155.1, 144.5, 133.4, 129.2, 128.0, 126.1, 119.9, 108.6. LC-MS: ESI(-) calcd. for $[M-H]^+$: *m/z* = 221.0; found: 221.1. HPLC: t_{ret} = 10.75 min (98.5 % at 254 nm, 97.3 % at 230 nm, method A).

tert-Butyl 4-(4-(5-(4-chlorophenyl)furan-2-carboxamido)phenyl)piperazine-1-carboxylate (163)

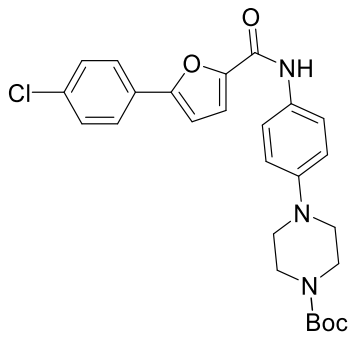

Chemical Formula: $C_{26}H_{28}ClN_3O_4$
Exact Mass: 481.17683
Molecular Weight: 481.97700

5-(4-Chlorophenyl)furan-2-carboxylic acid (**162**, 250 mg, 1.12 mmol, 1.00 eq.) and HATU (436 mg, 1.15 mmol, 1.02 eq.) were dissolved in DMF (10 mL). Subsequently, 1-Boc-4-(4′-aminophenyl)piperazine (467 mg, 1.68 mmol, 1.50 eq.) and DIPEA (400 µL, 2.29 mmol, 2.04 eq.) were added and the reaction was stirred at rt for 18 h. The solvent was removed under reduced pressure and the residue was purified by flash column chromatography (silica gel, 0 – 75 % hexane/EtOAc) to yield the product **163** (400 mg, 0.830 mmol, 74 %) as a beige solid.

^{1}H-NMR (400 MHz, $CDCl_3$) δ 8.04 (s, 1H), 7.68 – 7.64 (m, 2H), 7.60 – 7.55 (m, 2H), 7.42 – 7.37 (m, 2H), 7.27 (d, J = 3.6 Hz, 1H), 6.94 (d, J = 8.6 Hz, 2H), 6.76 (d, J = 3.6 Hz, 1H), 3.59 (t, J = 5.1 Hz, 4H), 3.11 (t, J = 5.1 Hz, 4H), 1.49 (s, 9H). ^{13}C-NMR (101 MHz, $CDCl_3$) δ 156.0, 154.8, 154.7, 148.4, 147.3, 134.7, 130.4, 128.2, 125.9, 121.7, 117.4, 117.3, 108.2, 80.1, 49.9, 28.4. TLC-MS: ESI(+) calcd. for $[M+Na]^+$: *m/z* = 504.2; found: 504.7. HPLC: t_{ret} = 12.77 min (99.0 % at 254 nm, 97.8 % at 230 nm, method A).

tert-Butyl 4-(4-(5-(4-chlorophenyl)-N-(pyridin-2-ylmethyl)furan-2-carboxamido)phenyl)piperazine-1-carboxylate

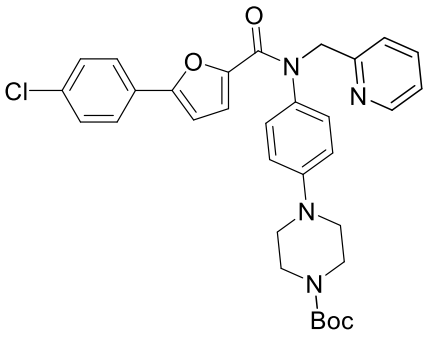

Chemical Formula: $C_{32}H_{33}ClN_4O_4$
Exact Mass: 572.21903
Molecular Weight: 573.09000

tert-Butyl 4-(4-(5-(4-chlorophenyl)furan-2-carboxamido)phenyl)piperazine-1-carboxylate (**163**, 300 mg, 0.622 mmol, 1.00 eq.) was dissolved in DMF (8.5 mL). NaH (60 % dispersion in mineral oil, 55.0 mg, 1.37 mmol, 2.20 eq.) and 2-(bromomethyl)pyridine hydrobromide (190 mg, 0.753 mmol, 1.21 eq.) were added and the reaction was stirred at rt for 18 h. The solvent was then removed under reduced pressure and the residue was used in the next step without further purification.

TLC-MS: ESI(+) calcd. for $[M+Na]^+$: *m/z* = 595.2; found: 595.8.

5-(4-Chlorophenyl)-N-(4-(piperazin-1-yl)phenyl)-N-(pyridin-2-ylmethyl)furan-2-carboxamide (119)

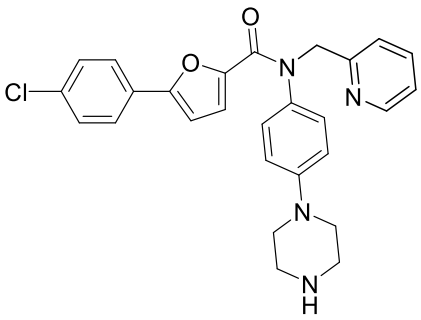

Chemical Formula: $C_{27}H_{25}ClN_4O_2$
Exact Mass: 472.16660
Molecular Weight: 472.97300

The residue from the previous reaction, *tert*-utyl 4-(4-(5-(4-chlorophenyl)-*N*-(pyridin-2-ylmethyl)furan-2-carboxamido)phenyl)piperazine-1-carboxylate, was dissolved in DCM (5 mL) and TFA (5 mL) and stirred at rt for 2 h. The solvent was evaporated, and the residue was purified by flash column chromatography (silica gel, 0 – 10 % DCM/MeOH, 1 % NH_3) to yield the product **119** (220 mg, 0.465 mmol, 89 % over two steps) as a yellow solid.

^{1}H-NMR (400 MHz, $CDCl_3$) δ 8.51 (ddd, J = 4.9, 1.9, 0.9 Hz, 1H), 7.66 (td, J = 7.7, 1.8 Hz, 1H), 7.51 (dt, J = 7.8, 1.1 Hz, 1H), 7.36 – 7.28 (m, 2H), 7.28 – 7.23 (m, 2H), 7.16 (ddd, J = 7.5, 4.9, 1.2 Hz, 1H), 7.12 – 7.08 (m, 2H), 6.92 – 6.82 (m, 2H), 6.49 (d, J = 3.6 Hz, 1H), 6.38 (d, J = 3.6 Hz, 1H), 5.16 (s, 2H), 3.24 – 3.13 (m, 4H), 3.08 – 3.01 (m, 4H).^{13}C-NMR (101 MHz, $CDCl_3$) δ 159.3, 157.5, 154.5, 151.4, 149.3, 146.8, 136.7, 134.7, 134.3, 128.9, 128.9, 125.9, 122.9, 122.4, 119.7, 116.4, 106.8, 56.6, 50.1, 46.2. HRMS: ESI(+) [*m/z*]: calcd. mass $[M+H]^+$ = 473.1739; found = 473.1742; rel. deviation 0.6 ppm. HPLC: t_{ret} = 10.02 min (96.0 % at 254 nm, 95.9 % at 230 nm, method A).

1-Fluoro-2-(methoxymethoxy)-4-nitrobenzene (164)

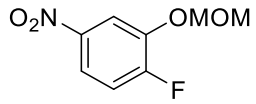

Chemical Formula: $C_8H_8FNO_4$
Exact Mass: 201.04374
Molecular Weight: 201.15340

2-Fluoro-5-nitrophenol (**141**, 500 mg, 3.18 mmol, 1.00 eq.) was dissolved in THF (20 mL) and cooled to 0 °C. NaH (60 % dispersion in mineral oil, 140 mg, 3.50 mmol, 1.10 eq.) was added and the reaction was warmed up to rt. MOMCl (270 µL, 3.56 mmol, 1.12 eq.) was added dropwise and the solution was stirred at rt for 2 h. Subsequently, the reaction was quenched with sat. NH_4Cl (40 mL), extracted with DCM (3 x 40 mL) and dried over Na_2SO_4. The solvent was removed under reduced pressure and the residue was purified by flash column chromatography (silica gel, 0 – 20 % hexane/EtOAc) to yield the product **164** (590 mg, 2.93 mmol, 92 %) as a light yellow oil.

^{1}H-NMR (400 MHz, $CDCl_3$) δ 8.11 (dd, J = 7.1, 2.7 Hz, 1H), 7.92 (ddd, J = 9.0, 4.0, 2.7 Hz, 1H), 7.22 (dd, J = 9.8, 9.0 Hz, 1H), 5.30 (s, 2H), 3.54 (s, 3H). ^{13}C-NMR (101 MHz, $CDCl_3$) δ 157.1 (d, J = 258.2 Hz), 145.5 (d, J = 11.8 Hz), 144.5, 118.4 (d, J = 8.4 Hz), 116.7 (d, J = 20.9 Hz), 113.4 (d, J = 3.1 Hz), 95.8, 56.9. LC-MS: ESI(+) calcd. for $[M+Na]^+$: *m/z* = 224.0; found: 224.0. HPLC: t_{ret} = 9.86 min (99.3 % at 254 nm, 97.5 % at 230 nm, method A).

tert-Butyl 4-(2-(methoxymethoxy)-4-nitrophenyl)piperazine-1-carboxylate (165)

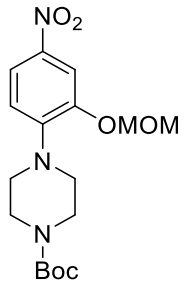

Chemical Formula: $C_{17}H_{25}N_3O_6$
Exact Mass: 367.17434
Molecular Weight: 367.40200

1-Fluoro-2-(methoxymethoxy)-4-nitrobenzene (**164**, 572 mg, 2.84 mmol, 1.00 eq.) was dissolved in MeCN (6 mL). 1-Boc-piperazine (794 mg, 4.27 mmol, 1.50 eq.) and DIPEA (750 µL, 4.29 mmol, 1.51 eq.) were added and the reaction was refluxed for 16 h. The solvent was evaporated, and the residue was purified by flash column chromatography (silica gel, 0 – 50 % hexane/EtOAc) to yield the product **165** (1.04 g, 2.83 mmol, quantitative) as an orange oil.

^{1}H-NMR (400 MHz, $CDCl_3$) δ 7.92 (d, J = 2.6 Hz, 1H), 7.86 (dd, J = 8.8, 2.6 Hz, 1H), 6.87 (d, J = 8.9 Hz, 1H), 5.26 (s, 2H), 3.58 (t, J = 4.0 Hz, 4H), 3.52 (s, 3H), 3.17 (t, J = 5.1 Hz, 4H), 1.46 (s, 9H). ^{13}C-NMR (101 MHz, $CDCl_3$) δ 154.8, 148.9, 148.1, 142.4, 119.0, 117.4, 111.5, 95.5, 80.2, 56.8, 50.1, 28.6. TLC-MS: ESI(+) calcd. for $[M+Na]^+$: *m/z* = 390.2; found: 390.2. HPLC: t_{ret} = 11.75 min (99.6 % at 254 nm, 99.3 % at 230 nm, method A).

tert-Butyl 4-(4-amino-2-(methoxymethoxy)phenyl)piperazine-1-carboxylate (166)

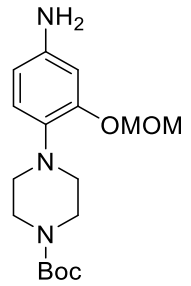

Chemical Formula: $C_{17}H_{27}N_3O_4$
Exact Mass: 337.20016
Molecular Weight: 337.42000

tert-Butyl 4-(2-(methoxymethoxy)-4-nitrophenyl)piperazine-1-carboxylate (**165**, 975 mg, 2.65 mmol, 1.00 eq.) was dissolved in MeOH (30 mL). Palladium on carbon (100 mg) was suspended in EtOAc (1.5 mL) and added to the first solution. H_2 was bubbled through the solution and the reaction was stirred under H_2 atmosphere for 1.5 h. The reaction mixture was filtered over celite and was purified by flash column chromatography (silica gel, 0 – 10 % DCM/MeOH) to yield the product **166** (814 mg, 2.41 mmol, 91 %) as a light pink solid.

^{1}H-NMR (400 MHz, $CDCl_3$) δ 6.77 (d, J = 8.4 Hz, 1H), 6.51 (d, J = 2.5 Hz, 1H), 6.31 (dd, J = 8.4, 2.6 Hz, 1H), 5.19 (s, 2H), 3.60 – 3.53 (m, 4H), 3.50 (s, 3H), 2.91 (t, J = 5.1 Hz, 4H), 1.47 (s, 9H). ^{13}C-NMR (101 MHz, $CDCl_3$) δ 155.0, 151.4, 143.1, 134.3, 120.2, 108.9, 104.6, 95.3, 79.8, 56.4, 51.5, 28.6. HPLC: t_{ret} = 8.11 min (98.8 % at 254 nm, 99.1 % at 230 nm, method A).

tert-Butyl 4-(4-(5-(4-chlorophenyl)furan-2-carboxamido)-2-(methoxymethoxy)phenyl)piperazine-1-carboxylate (167)

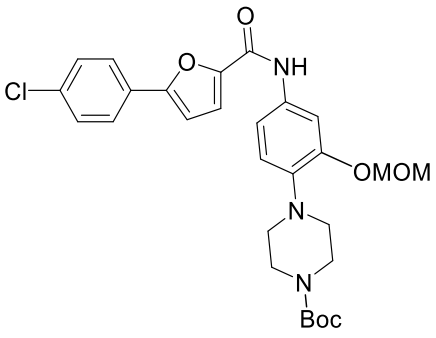

Chemical Formula: $C_{28}H_{32}ClN_3O_6$
Exact Mass: 541.19796
Molecular Weight: 542.02900

5-(4-Chlorophenyl)furan-2-carboxylic acid (**162**, 478 mg, 1.91 mmol, 1.00 eq.) and HATU (725 mg, 1.91 mmol, 1.00 eq.) were dissolved in DMF (25 mL). Subsequently, *tert*-Butyl 4-(4-amino-2-(methoxymethoxy)phenyl)piperazine-1-carboxylate (**166**, 804 mg, 2.38 mmol, 1.25 eq.) and DIPEA (678 µL, 3.89 mmol, 2.04 eq.) were added and the reaction was stirred at rt for 3.5 h. The solvent was removed under reduced pressure and the residue was purified by flash column chromatography (silica gel, 0 – 80 % hexane/EtOAc) to yield the product **167** (913 mg, 1.68 mmol, 88 %) as a light yellow solid.

^{1}H-NMR (400 MHz, $CDCl_3$) δ 7.97 (s, 1H), 7.73 – 7.65 (m, 2H), 7.49 – 7.39 (m, 3H), 7.36 – 7.31 (m, 1H), 7.29 (d, J = 3.6 Hz, 1H), 6.92 (d, J = 8.6 Hz, 1H), 6.77 (d, J = 3.6 Hz, 1H), 5.28 (s, 2H), 3.60 (s, 4H), 3.55 (s, 3H), 3.01 (s, 4H), 1.49 (s, 9H). ^{13}C-NMR (101 MHz, $CDCl_3$) δ 156.0, 155.0, 154.9, 150.4, 147.2, 139.1, 134.9, 133.0, 129.4, 128.1, 126.0, 119.2, 117.6, 114.5, 109.1, 108.3, 95.4, 79.9, 56.7, 51.0, 28.6. TLC-MS: ESI(+) calcd. for $[M+Na]^+$: *m/z* = 564.2; found: 564.0. HPLC: t_{ret} = 12.92 min (98.7 % at 254 nm, 98.2 % at 230 nm, method A).

tert-Butyl 4-(4-(5-(4-chlorophenyl)-N-(pyridin-2-ylmethyl)furan-2-carboxamido)-2-(methoxymethoxy)phenyl)piperazine-1-carboxylate

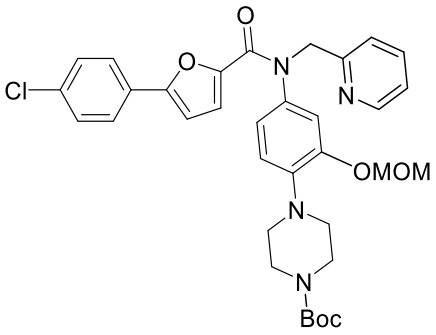

Chemical Formula: $C_{34}H_{37}ClN_4O_6$
Exact Mass: 632.24016
Molecular Weight: 633.14200

tert-Butyl 4-(4-(5-(4-chlorophenyl)furan-2-carboxamido)-2-(methoxymethoxy)phenyl)piperazine-1-carboxylate (**167**, 414 mg, 0.764 mmol, 1.00 eq.) was dissolved in DMF (10 mL). NaH (60 % dispersion in mineral oil, 67.0 mg, 1.68 mmol, 2.20 eq.) and 2-(bromomethyl)pyridine hydrobromide (232 mg, 0.917 mmol, 1.20 eq.) were added and the reaction was stirred at rt for 20 h. The solvent was then removed under reduced pressure and the residue was used in the next step without further purification.

TLC-MS: ESI(+) calcd. for $[M+Na]^+$: *m/z* = 655.2; found: 655.2.

5-(4-Chlorophenyl)-N-(3-hydroxy-4-(piperazin-1-yl)phenyl)-N-(pyridin-2-ylmethyl)furan-2-carboxamide (168)

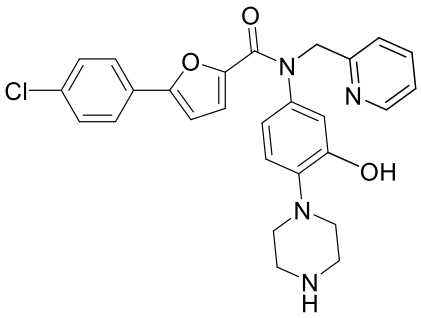

Chemical Formula: $C_{27}H_{25}ClN_4O_3$
Exact Mass: 488.16152
Molecular Weight: 488.97200

The residue from the previous reaction, *tert*-Butyl 4-(4-(5-(4-chlorophenyl)-*N*-(pyridin-2-ylmethyl)furan-2-carboxamido)-2-(methoxymethoxy)phenyl)piperazine-1-carboxylate, was dissolved in DCM (2 mL) and TFA (4 mL) and stirred at rt for 3 h. The solvent was evaporated and the residue was purified by flash column chromatography (silica gel, 0 – 10 % DCM/MeOH) to yield the product **168** (327 mg, 0.669 mmol, 88 % over two steps) as a beige solid.

^{1}H-NMR (400 MHz, DMSO) δ 9.55 (s, 1H), 8.73 (s, 2H), 8.50 (ddd, J = 4.9, 1.8, 0.9 Hz, 1H), 7.78 (td, J = 7.7, 1.8 Hz, 1H), 7.47 – 7.39 (m, 3H), 7.39 – 7.33 (m, 2H), 7.28 (ddd, J = 7.6, 4.9, 1.2 Hz, 1H), 7.01 (d, J = 3.6 Hz, 1H), 6.90 (d, J = 8.4 Hz, 1H), 6.81 (d, J = 2.4 Hz, 1H), 6.76 (dd, J = 8.3, 2.4 Hz, 1H), 6.63 (d, J = 3.7 Hz, 1H), 5.03 (s, 2H), 3.24 (t, J = 5.1 Hz, 4H), 3.19 – 3.06 (m, 4H). ^{13}C-NMR (101 MHz, DMSO) δ 158.0, 156.9, 153.2, 150.3, 149.0, 146.7, 138.3, 138.3, 136.8, 133.1, 128.9, 128.1, 125.7, 122.4, 121.9, 119.3, 118.8, 115.2, 108.0, 55.6, 46.9, 43.2. HRMS: ESI(+) [*m/z*]: calcd. mass $[M+H]^+$ = 489.1688; found = 489.1692; rel. deviation 0.9 ppm. HPLC: t_{ret} = 8.58 min (96.0 % at 254 nm, 97.7 % at 230 nm, method A).

Ethyl 5-(4-chloro-3-(methoxymethoxy)phenyl)furan-2-carboxylate (169)

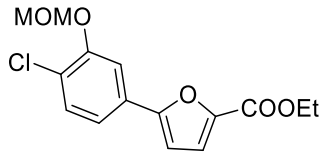

Chemical Formula: $C_{15}H_{15}ClO_5$
Exact Mass: 310.06080
Molecular Weight: 310.73000

Ethyl 5-(4-chloro-3-hydroxyphenyl)furan-2-carboxylate (**125**, 126 mg, 0.472 mmol, 1.00 eq.) was dissolved in THF (3.5 mL) and cooled to 0 °C. NaH (60 % dispersion in mineral oil, 20.0 mg, 0.520 mmol, 1.10 eq.) was added and the reaction mixture was warmed up to rt. MOMCl (39.8 µL, 0.524 mmol, 1.11 eq.) was added and the solution was stirred at rt for another 3 h. The reaction was quenched with sat. NH_4Cl (10 mL), extracted with DCM (3 x 15 mL) and dried over Na_2SO_4. After evaporating the solvent, the residue was purified by flash column chromatography (silica gel, 0 – 15 % hexane/EtOAc) to yield the product **169** (119 mg, 0.383 mmol, 81 %) as an off-white solid.

^{1}H-NMR (400 MHz, $CDCl_3$) δ 7.53 (d, J = 1.6 Hz, 1H), 7.45 – 7.35 (m, 2H), 7.22 (d, J = 3.7 Hz, 1H), 6.73 (d, J = 3.6 Hz, 1H), 5.32 (s, 2H), 4.38 (q, J = 7.1 Hz, 2H), 3.55 (s, 3H), 1.40 (t, J = 7.1 Hz, 3H). ^{13}C-NMR (101 MHz, $CDCl_3$) δ 158.9, 156.4, 153.3, 144.3, 130.8, 129.5, 124.5, 119.9, 119.3, 112.7, 107.7, 95.4, 61.1, 56.7, 14.5. TLC-MS: ESI(+) calcd. for $[M+Na]^+$: *m/z* = 333.1; found: 333.2. HPLC: t_{ret} = 12.18 min (98.3 % at 254 nm, 98.3 % at 230 nm, method A).

5-(4-Chloro-3-(methoxymethoxy)phenyl)furan-2-carboxylic acid (170)

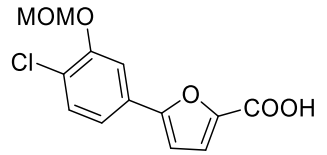

Chemical Formula: $C_{13}H_{11}ClO_5$
Exact Mass: 282.02950
Molecular Weight: 282.67600

Ethyl 5-(4-chloro-3-(methoxymethoxy)phenyl)furan-2-carboxylate (**169**, 168 mg, 0.329 mmol, 1.00 eq.) was dissolved in THF (2.5 mL) and H_2O (2.5 mL) and LiOH (68.3 mg, 1.63 mmol, 3.01 eq.) was added. The reaction mixture was stirred at rt for 4 h and then acidified with HCl (2 M) to achieve pH 4-5. The solution was extracted with DCM (4 x 20 mL), dried over Na_2SO_4 and the solvent was removed under reduced pressure. This residue was combined with the precipitate from the aq. phase that had formed overnight and triturated from water to afford the product **170** (69.7 mg, 0.257 mmol, 75 %) as a white solid.

^{1}H-NMR (400 MHz, $CDCl_3$) δ 7.56 (d, J = 1.7 Hz, 1H), 7.45 – 7.40 (m, 2H), 7.37 (d, J = 3.6 Hz, 1H), 6.78 (d, J = 3.6 Hz, 1H), 5.33 (s, 2H), 3.56 (s, 3H).^{13}C-NMR (101 MHz, $CDCl_3$) δ 167.0, 157.5, 153.4, 143.4, 130.9, 129.2, 124.9, 122.1, 119.5, 112.8, 108.0, 95.4, 56.7. LC-MS: ESI(-) calcd. for $[M-H]^+$: *m/z* = 281.0; found: 281.2. HPLC: t_{ret} = 10.70 min (98.3 % at 254 nm, 95.6 % at 230 nm, method A).

tert-Butyl 4-(4-(5-(4-chloro-3-(methoxymethoxy)phenyl)furan-2-carboxamido)phenyl)piperazine-1-carboxylate (171)

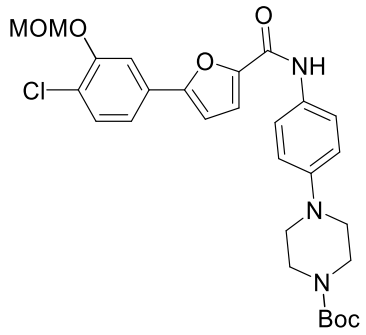

Chemical Formula: $C_{28}H_{32}ClN_3O_6$
Exact Mass: 541.19796
Molecular Weight: 542.02900

5-(4-Chloro-3-(methoxymethoxy)phenyl)furan-2-carboxylic acid (**170**, 64.0 mg, 0.226 mmol, 1.00 eq.) and HATU (87.0 mg, 0.229 mmol, 1.01 eq.) were dissolved in DMF (1 mL). Subsequently, 1-Boc-4-(4′-aminophenyl)piperazine (95.5 mg, 0.344 mmol, 1.52 eq.) and DIPEA (78.9 µL, 0.453 mmol, 2.00 eq.) were added and the reaction was stirred at rt for 6.5 h. The solvent was removed under reduced pressure and the residue was purified by flash column chromatography (silica gel, 0 – 80 % hexane/EtOAc) to yield the product **171** (120 mg, 0.221 mmol, 98 %) as a beige solid.

^{1}H-NMR (400 MHz, $CDCl_3$) δ 7.97 (s, 1H), 7.62 – 7.53 (m, 2H), 7.51 (d, J = 1.9 Hz, 1H), 7.43 (d, J = 8.3 Hz, 1H), 7.34 (dd, J = 8.3, 1.9 Hz, 1H), 7.28 (d, J = 3.6 Hz, 1H), 6.98 – 6.91 (m, 2H), 6.78 (d, J = 3.6 Hz, 1H), 5.33 (s, 2H), 3.62 – 3.57 (m, 4H), 3.57 (s, 3H), 3.12 (t, J = 5.1 Hz, 4H), 1.49 (s, 9H). ^{13}C-NMR (101 MHz, $CDCl_3$) δ 156.0, 154.9, 154.6, 153.5, 148.7, 147.4, 130.9, 130.2, 129.5, 124.4, 121.7, 119.0, 117.4, 117.3, 112.4, 108.6, 95.5, 80.1, 56.7, 49.9, 28.6. TLC-MS: ESI(+) calcd. for $[M+Na]^+$: *m/z* = 564.2; found: 564.3. HPLC: t_{ret} = 12.02 min (99.5 % at 254 nm, 97.6 % at 230 nm, method A).

tert-Butyl 4-(4-(5-(4-chloro-3-(methoxymethoxy)phenyl)-N-(pyridin-2-ylmethyl)furan-2-carboxamido)phenyl)piperazine-1-carboxylate

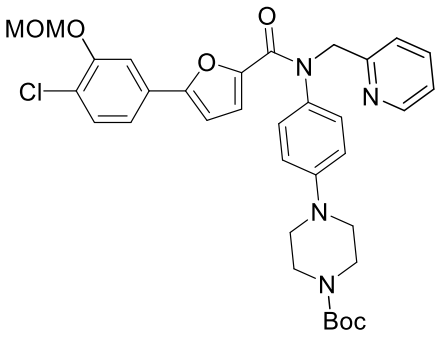

Chemical Formula: $C_{34}H_{37}ClN_4O_6$
Exact Mass: 632.24016
Molecular Weight: 633.14200

tert-Butyl 4-(4-(5-(4-chloro-3-(methoxymethoxy)phenyl)furan-2-carboxamido)phenyl)piperazine-1-carboxylate (**171**, 109 mg, 0.201 mmol, 1.00 eq.) was dissolved in DMF (3 mL). NaH (60 % dispersion in mineral oil, 18.0 mg, 0.442 mmol, 2.20 eq.) and 2-(bromomethyl)pyridine hydrobromide (62.1 mg, 0.245 mmol, 1.22 eq.) were added and the reaction was stirred at rt for 3 h. The solvent was then removed under reduced pressure and the residue was used in the next step without further purification.

TLC-MS: ESI(+) calcd. for $[M+Na]^+$: *m/z* = 655.2; found: 655.6.

5-(4-Chloro-3-hydroxyphenyl)-N-(4-(piperazin-1-yl)phenyl)-N-(pyridin-2-ylmethyl)furan-2-carboxamide (172)

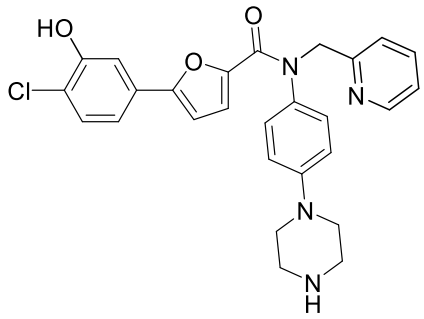

Chemical Formula: $C_{27}H_{25}ClN_4O_3$
Exact Mass: 488.16152
Molecular Weight: 488.97200

The residue from the previous reaction, *tert*-butyl 4-(4-(5-(4-chloro-3-(methoxymethoxy)phenyl)-*N*-(pyridin-2-ylmethyl)furan-2-carboxamido)phenyl)piperazine-1-carboxylate, was dissolved in DCM (1 mL) and TFA (2.5 mL) and stirred at rt for 1.5 h. The solvent was evaporated and the residue was purified by flash column chromatography (silica gel, 0 – 10 % DCM/MeOH) to yield the product **172** (TFA salt: 90.1 mg, 0.149 mmol, 66 % over two steps) as an off-white solid.

^{1}H-NMR (400 MHz, DMSO) δ 10.43 (s, 1H), 8.88 (s, 2H), 8.53 – 8.47 (m, 1H), 7.80 (td, J = 7.7, 1.8 Hz, 1H), 7.47 (d, J = 7.8 Hz, 1H), 7.35 – 7.27 (m, 2H), 7.25 – 7.20 (m, 2H), 7.16 (d, J = 2.0 Hz, 1H), 7.06 – 6.95 (m, 2H), 6.86 – 6.78 (m, 2H), 6.20 (s, 1H), 5.06 (s, 2H), 3.34 (dd, J = 6.7, 3.7 Hz, 4H), 3.26 – 3.19 (m, 4H). ^{13}C-NMR (101 MHz, DMSO) δ 158.3, 156.7, 153.5, 153.4, 149.4, 148.7, 146.3, 137.1, 134.6, 130.3, 129.0, 128.7, 122.5, 122.3, 120.1, 118.9, 116.3, 115.9, 111.9, 107.5, 55.3, 45.2, 42.7. HRMS: ESI(+) [*m/z*]: calcd. mass $[M+H]^+$ = 489.16873; found = 489.16879; rel. deviation 0.1 ppm. HPLC: t_{ret} = 7.91 min (95.6 % at 254 nm, 97.5 % at 230 nm, method A).

6.2.3. Synthesis of Covalent-First Library

3-(2-Aminopyridin-4-yl)phenol (174)

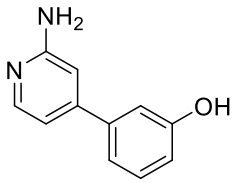

Chemical Formula: $C_{11}H_{10}N_2O$
Exact Mass: 186.07931
Molecular Weight: 186.21400

4-Bromopyridin-2-amine (**173**, 250 mg, 1.45 mmol, 1.00 eq.), (3-hydroxyphenyl)boronic acid (219 mg, 1.59 mmol, 1.10 eq.) and XPhos Pd G4 (37.3 mg, 43.4 µmol, 0.03 eq.) were dissolved in 1,4-dioxane (14.5 mL). K_2CO_3 (599 mg, 4.34 mmol, 3.00 eq.) was dissolved in H_2O (8.5 mL) and was added to the first solution. The mixture was heated to 80 °C and stirred at this temperature for 18 h. It was then cooled to rt and sat. NH_4Cl (20 mL) was added. The solution was extracted with EtOAc (3 x 20 mL). The combined org. phases were dried over Na_2SO_4, the solvent was evaporated, and the residue was purified by flash column chromatography (silica gel, 0 – 10 % DCM/MeOH) to yield the product **174** (228 mg, 1.22 mmol, 85 %) as a beige solid.

^{1}H-NMR (400 MHz, DMSO) δ 9.61 (s, 1H), 7.97 – 7.90 (m, 1H), 7.26 (t, J = 7.9 Hz, 1H), 7.07 – 7.01 (m, 1H), 6.99 (t, J = 2.0 Hz, 1H), 6.81 (ddd, J = 8.1, 2.4, 1.0 Hz, 1H), 6.70 (dd, J = 5.3, 1.7 Hz, 1H), 6.66 – 6.60 (m, 1H), 5.95 (s, 2H). ^{13}C-NMR (101 MHz, DMSO) δ 160.4, 157.8, 148.4, 148.3, 139.9, 130.1, 117.1, 115.7, 113.1, 110.0, 105.0. HRMS: ESI(+) [*m/z*]: calcd. mass $[M+H]^+$ = 187.08659; found = 187.08686; rel. deviation 1.4 ppm. HPLC: t_{ret} = 4.11 min (99.7 % at 254 nm, 99.6 % at 230 nm, method A).

3-(2-Aminopyridin-4-yl)phenyl sulfurofluoridate (176)

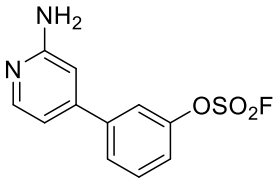

Chemical Formula: $C_{11}H_9FN_2O_3S$
Exact Mass: 268.03179
Molecular Weight: 268.26240

3-(2-Aminopyridin-4-yl)phenol (**174**, 100 mg, 0.537 mmol, 1.00 eq.) and AISF (**64**, 203 mg, 0.644 mmol, 1.20 eq.) were dissolved in THF (27 mL). DBU (176 µL, 1.18 mmol, 2.20 eq.) was added and the reaction was stirred at rt for 1.5 h. Sat. NH_4Cl (30 mL) was used to stop the reaction and it was extracted with EtOAc (3 x 30 mL). The org. phases were dried over Na_2SO_4, the solvent was evaporated, and the residue was purified by reverse phase column chromatography (CHROMABOND® Flash RS 40 C18 ec, 10 – 55 % H_2O/MeCN, 0.2% TFA). The fractions containing product were lyophilized to afford the product **176** (TFA salt: 46.2 mg, 0.121 mmol, 23 %) as a white solid.

^{1}H-NMR (400 MHz, DMSO) δ 8.18 – 7.98 (m, 3H), 7.97 – 7.88 (m, 1H), 7.85 – 7.75 (m, 2H), 7.25 – 7.18 (m, 2H). ^{13}C-NMR (101 MHz, DMSO) δ 155.0, 151.2, 150.2, 138.6, 138.1, 132.0, 128.0, 123.1, 120.1, 110.6, 110.0. ^{19}F NMR (376 MHz, DMSO) δ 39.2, -73.8. HRMS: ESI(+) [*m/z*]: calcd. mass $[M+H]^+$ = 269.03907; found = 269.03932; rel. deviation 0.9 ppm. HPLC: t_{ret} = 7.64 min (99.7 % at 254 nm, 99.1 % at 230 nm, method A).

4-(2-Aminopyridin-4-yl)phenol (175)

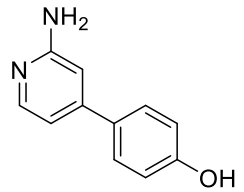

Chemical Formula: $C_{11}H_{10}N_2O$
Exact Mass: 186.07931
Molecular Weight: 186.21400

4-Bromopyridin-2-amine (**173**, 250 mg, 1.45 mmol, 1.00 eq.), (4-hydroxyphenyl)boronic acid (219 mg, 1.59 mmol, 1.10 eq.) and XPhos Pd G4 (37.3 mg, 43.4 µmol, 0.03 eq.) were dissolved in 1,4-dioxane (14.5 mL). K_2CO_3 (599 mg, 4.34 mmol, 3.00 eq.) was dissolved in H_2O (8.5 mL) and was added to the first solution. The mixture was heated to 80 °C and stirred at this temperature for 18 h. It was then cooled to rt and sat. NH_4Cl (20 mL) was added. The solution was extracted with EtOAc (3 x 20 mL). The combined org. phases were dried over Na_2SO_4, the solvent was evaporated, and the residue was purified by flash column chromatography (silica gel, 0 – 10 % DCM/MeOH) to yield the product **175** (234 mg, 1.26 mmol, 87 %) as a yellow solid.

^{1}H-NMR (400 MHz, DMSO) δ 9.72 (s, 1H), 7.92 – 7.86 (m, 1H), 7.52 – 7.43 (m, 2H), 6.89 – 6.82 (m, 2H), 6.71 (dd, J = 5.4, 1.7 Hz, 1H), 6.67 – 6.59 (m, 1H), 5.86 (s, 2H). ^{13}C-NMR (101 MHz, DMSO) δ 160.4, 158.2, 148.2, 148.0, 128.9, 127.6, 115.8, 109.6, 104.1. HRMS: ESI(+) [*m/z*]: calcd. mass $[M+H]^+$ = 187.08659; found = 187.08691; rel. deviation 1.7 ppm. HPLC: t_{ret} = 4.04 min (99.7 % at 254 nm, 99.5 % at 230 nm, method A).

4-(2-Aminopyridin-4-yl)phenyl sulfurofluoridate (177)

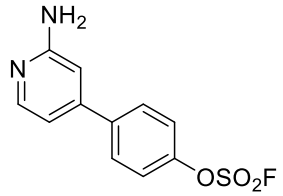

Chemical Formula: $C_{11}H_9FN_2O_3S$
Exact Mass: 268.03179
Molecular Weight: 268.26240

4-(2-Aminopyridin-4-yl)phenol (**175**, 70.1 mg, 0.376 mmol, 1.00 eq.) and AISF (**64**, 143 mg, 0.456 mmol, 1.21 eq.) were dissolved in THF (19 mL). DBU (124 µL, 0.828 mmol, 2.20 eq.) was added and the reaction was stirred at rt for 4.5 h. Sat. NH_4Cl (25 mL) was used to stop the reaction and it was extracted with EtOAc (3 x 25 mL). The org. phases were dried over Na_2SO_4, the solvent was evaporated, and the residue was purified by flash column chromatography (silica gel, 0 – 6.75 % DCM/MeOH) to yield the product **177** (61.9 mg, 0.231 mmol, 61 %) as a beige solid.

^{1}H-NMR (400 MHz, DMSO) δ 7.99 (dd, J = 5.4, 0.7 Hz, 1H), 7.87 – 7.78 (m, 2H), 7.74 – 7.66 (m, 2H), 6.80 (dd, J = 5.4, 1.7 Hz, 1H), 6.70 (dd, J = 1.8, 0.8 Hz, 1H), 6.04 (s, 2H). ^{13}C-NMR (101 MHz, DMSO) δ 160.5, 149.8, 148.7, 146.5, 139.5, 128.9, 121.8, 110.1, 105.3. ^{19}F NMR (376 MHz, DMSO) δ 38.8. HRMS: ESI(+) [*m/z*]: calcd. mass $[M+H]^+$ = 269.03907; found = 269.03942; rel. deviation 1.3 ppm. HPLC: t_{ret} = 7.45 min (98.0 % at 254 nm, 98.6 % at 230 nm, method A).

3-(2-Aminopyridin-4-yl)benzenesulfonyl fluoride (181)

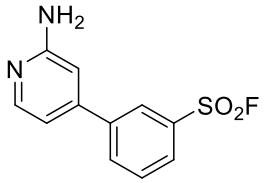

Chemical Formula: $C_{11}H_9FN_2O_2S$
Exact Mass: 252.03688
Molecular Weight: 252.26340

4-Bromopyridin-2-amine (**173**, 250 mg, 1.45 mmol, 1.00 eq.), (3-(fluorosulfonyl)phenyl)boronic acid (**69**, 448 mg, 2.20 mmol, 1.52 eq.), $Pd(OAc)_2$ (16.2 mg, 72.3 µmol, 0.05 eq.) and XPhos (69.0 mg, 0.145 mmol, 0.10 eq.) were suspended in 1,4-dioxane (5.8 mL). K_3PO_4 (613 mg, 2.89 mmol, 2.00 eq.) was dissolved in H_2O (2.9 mL) and this was added to the first solution. The solution was heated to 40 °C and stirred for 16 h. It was diluted with EtOAc (20 mL) and dried over Na_2SO_4. After evaporation of the solvent, the residue was purified by flash column chromatography (silica gel, 0 – 5 % DCM/MeOH) to yield the product **181** (118 mg, 0.468 mmol, 32 %) as an off-white solid.

^{1}H-NMR (400 MHz, DMSO) δ 8.27 – 8.16 (m, 3H), 8.04 (dd, J = 5.4, 0.8 Hz, 1H), 7.91 (t, J = 7.9 Hz, 1H), 6.89 (dd, J = 5.3, 1.7 Hz, 1H), 6.80 (dd, J = 1.8, 0.8 Hz, 1H), 6.11 (s, 2H). ^{13}C-NMR (101 MHz, DMSO) δ 160.6, 149.0, 145.5, 140.6, 134.5, 132.5 (d, J = 23.9 Hz), 131.4, 128.3, 125.7, 109.9, 105.4. ^{19}F NMR (376 MHz, DMSO) δ 66.3. HRMS: ESI(+) [m/z]: calcd. mass $[M+H]^+$ = 253.04415; found = 253.04442; rel. deviation 1.1 ppm. HPLC: t_{ret} = 6.34 min (99.2 % at 254 nm, 98.1 % at 230 nm, method A).

4-Bromobenzenesulfonyl fluoride (179)

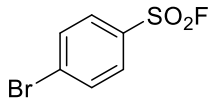

Chemical Formula: $C_6H_4BrFO_2S$
Exact Mass: 237.90994
Molecular Weight: 239.05840

4-Bromobenzenesulfonyl chloride (**178**, 2.00 g, 7.83 mmol, 1.00 eq.) was dissolved in MeCN (8 mL). KHF_2 (1.41 g, 18.0 mmol, 2.31 eq.) was dissolved in H_2O (4 mL) and added to the first solution. After stirring at rt for 18 h, the mixture was extracted with EtOAc (3 x 10 mL) and dried over Na_2SO_4. The solvent was evaporated under reduced pressure which afforded the product **179** (1.84 g, 7.70 mmol, 99 %) as a white solid.

^{1}H-NMR (400 MHz, $CDCl_3$) δ 7.92 – 7.83 (m, 2H), 7.83 – 7.74 (m, 2H). ^{13}C-NMR (101 MHz, $CDCl_3$) δ 133.27, 132.12 (d, J = 25.7 Hz), 131.46, 129.97. ^{19}F NMR (376 MHz, $CDCl_3$) δ 66.4. GC-MS: EI(+) calcd. for $[M]^+$: *m/z* = 237.9; found: 237.9. HPLC: t_{ret} = 10.80 min (96.9 % at 254 nm, 98.9 % at 230 nm, method A).

4-(4,4,5,5-Tetramethyl-1,3,2-dioxaborolan-2-yl)benzenesulfonyl fluoride (180)

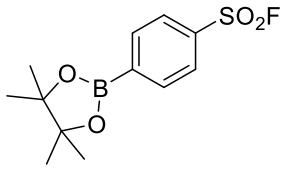

Chemical Formula: $C_{12}H_{16}BFO_4S$
Exact Mass: 286.08464
Molecular Weight: 286.12440

4-Bromobenzenesulfonyl fluoride (**179**, 1.83 g, 7.65 mmol, 1.00 eq.), bis(pinacolato)diboron (2.14 g, 8.42 mmol, 1.10 eq.), KOAc (2.25 g, 23.0 mmol, 3.00 eq.) and $Pd(dppf)Cl_2$ (168 mg, 0.230 mmol, 0.03 eq.) were suspended in 1,4-dioxane (24 mL) and heated to 80 °C. After 18 h, the solution was cooled to rt, and the solvent was evaporated. The residue was picked up in EtOAc (50 mL), washed with H_2O (50 mL) and brine (50 mL) and dried over Na_2SO_4. The solvent was removed under reduced pressure and the residue was purified by flash column chromatography (silica gel, 5 – 35 % hexane/EtOAc) to yield the product **180** (1.66 g, 5.80 mmol, 76 %) as a white solid.

^{1}H-NMR (400 MHz, $CDCl_3$) δ 8.06 – 8.01 (m, 2H), 8.01 – 7.96 (m, 2H), 1.36 (s, 12H). ^{13}C-NMR (101 MHz, $CDCl_3$) δ 135.9, 135.2 (d, J = 24.2 Hz), 127.4, 84.9, 83.7, 25.0. GC-MS: EI(+) calcd.

for $[M]^+$: *m/z* = 286.1; found: 286.1. HPLC: t_{ret} = 9.89 min (98.1 % at 254 nm, 99.8 % at 230 nm, method A).

4-(2-Aminopyridin-4-yl)benzenesulfonyl fluoride (182)

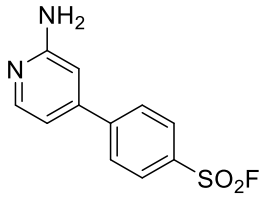

Chemical Formula: $C_{11}H_9FN_2O_2S$
Exact Mass: 252.03688
Molecular Weight: 252.26340

4-Bromopyridin-2-amine (**173**, 250 mg, 1.45 mmol, 1.00 eq.), 4-(4,4,5,5-tetramethyl-1,3,2-dioxaborolan-2-yl)benzenesulfonyl fluoride (**180**, 496 mg, 1.73 mmol, 1.20 eq.), $Pd(OAc)_2$ (16.2 mg, 72.3 µmol, 0.05 eq.) and XPhos (69.0 mg, 0.145 mmol, 0.10 eq.) were suspended in 1,4-dioxane (6 mL). K_3PO_4 (613 mg, 2.89 mmol, 2.00 eq.) was dissolved in H_2O (3 mL) and this was added to the first solution. The solution was heated to 40 °C and stirred for 19 h. Sat. NH_4Cl (20 mL) was added. The solution was extracted with EtOAc (3 x 20 mL) and dried over Na_2SO_4. After evaporation of the solvent, the residue was purified by flash column chromatography (silica gel, 20 – 100 % hexane/EtOAc) to yield the product **182** (21.3 mg, 84.4 µmol, 5.8 %) as an off-white solid.

^{1}H-NMR (400 MHz, DMSO) δ 8.27 – 8.19 (m, 2H), 8.05 (dd, J = 5.4, 0.8 Hz, 1H), 8.03 – 7.99 (m, 2H), 6.86 (dd, J = 5.4, 1.7 Hz, 1H), 6.77 (dd, J = 1.8, 0.8 Hz, 1H), 6.15 (s, 2H). ^{13}C-NMR (101 MHz, DMSO) δ 160.6, 149.0, 146.3, 145.8, 131.2 (d, J = 23.4 Hz), 129.2, 128.4, 110.0, 105.6. ^{19}F NMR (376 MHz, DMSO) δ 66.0. HRMS: ESI(+) [m/z]: calcd. mass $[M+H]^+$ = 253.04415; found = 253.04438; rel. deviation 0.9 ppm. HPLC: t_{ret} = 6.39 min (98.6 % at 254 nm, 98.7 % at 230 nm, method A).

4-(3-Methoxyphenoxy)pyridin-2-amine (184)

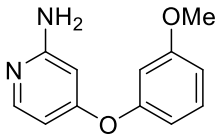

Chemical Formula: $C_{12}H_{12}N_2O_2$
Exact Mass: 216.08988
Molecular Weight: 216.24000

NaH (60 % dispersion in mineral oil, 46.7 mg, 1.17 mmol, 1.31 eq.) was suspended in NMP (4.5 mL). 3-Methoxyphenol (125 µL, 1.16 mmol, 1.30 eq.) was added and the solution was stirred at rt for 10 min. Subsequently, 4-fluoropyridin-2-amine (**183**, 100 mg, 0.892 mmol, 1.00 eq.) was added and the solution was stirred at 180 °C for 3 h. After cooling to rt, H_2O (20 mL) was added, and the solution was extracted with EtOAc (3 x 20 mL). The combined org. phases were washed with H_2O (3 x 50 mL) and dried over Na_2SO_4. The solvent was evaporated, and the residue was purified by flash column chromatography (silica gel, 0 – 10 % DCM/MeOH) to yield the product **184** (170 mg, 0.786 mmol, 88 %) as a beige solid.

^{1}H-NMR (400 MHz, $CDCl_3$) δ 7.93 (d, J = 5.9 Hz, 1H), 7.28 (t, J = 8.2 Hz, 1H), 6.77 (ddd, J = 8.4, 2.5, 0.9 Hz, 1H), 6.67 (ddd, J = 8.0, 2.2, 0.9 Hz, 1H), 6.63 (t, J = 2.3 Hz, 1H), 6.30 (dd, J = 5.8, 2.2 Hz, 1H), 5.97 (d, J = 2.1 Hz, 1H), 4.41 (s, 2H), 3.80 (s, 3H). ^{13}C-NMR (101 MHz, $CDCl_3$) δ 166.4, 161.2, 160.3, 155.6, 149.8, 130.5, 113.1, 111.0, 106.9, 104.6, 95.7, 55.6. LC-MS: ESI(+) [*m/z*]: calcd. mass $[M+H]^+$ = 217.1; found = 217.1. HPLC: t_{ret} = 6.35 min (98.0 % at 254 nm, 98.0 % at 230 nm, method A).

3-((2-Aminopyridin-4-yl)oxy)phenol (186)

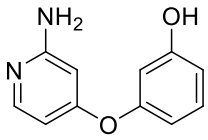

Chemical Formula: $C_{11}H_{10}N_2O_2$
Exact Mass: 202.07423
Molecular Weight: 202.21300

4-(3-Methoxyphenoxy)pyridin-2-amine (**184**, 138 mg, 0.638 mmol, 1.00 eq.) was dissolved in DCM (6.5 mL). The solution was cooled to 0 °C and BBr_3 (1 M in DCM, 1.61 mL, 1.61 mmol, 2.52 eq.) was added dropwise and the reaction was stirred at rt for 3 h. It was then quenched carefully with MeOH, and the solvent was evaporated. The residue was purified by flash column chromatography (silica gel, 5 – 10 % DCM/MeOH) leading to the product **186** (128 mg, 0.638 mmol, quant.) as a beige solid.

^{1}H-NMR (400 MHz, DMSO) δ 9.94 (s, 1H), 7.92 (d, J = 7.1 Hz, 1H), 7.52 (s, 2H), 7.32 (t, J = 8.1 Hz, 1H), 6.77 (ddd, J = 8.2, 2.3, 0.9 Hz, 1H), 6.64 (ddd, J = 8.0, 2.3, 0.9 Hz, 1H), 6.59 (t, J = 2.3 Hz, 1H), 6.57 (dd, J = 7.1, 2.5 Hz, 1H), 6.10 (d, J = 2.4 Hz, 1H). ^{13}C-NMR (101 MHz, DMSO) δ 168.5, 159.3, 156.6, 153.3, 139.9, 131.1, 113.7, 111.2, 108.0, 104.2, 94.7. LC-MS: ESI(+) [*m/z*]: calcd. mass $[M+H]^+$ = 203.1; found = 203.0. HPLC: t_{ret} = 4.42 min (95.7 % at 254 nm, 98.0 % at 230 nm, method A).

tert-Butyl (4-(3-hydroxyphenoxy)pyridin-2-yl)carbamate (190)

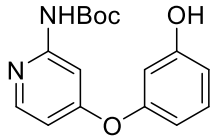

Chemical Formula: $C_{16}H_{18}N_2O_4$
Exact Mass: 302.12666
Molecular Weight: 302.33000

3-((2-Aminopyridin-4-yl)oxy)phenol (**186**, 129 mg, 0.638 mmol, 1.00 eq.) was dissolved in *t*BuOH (1 mL). Boc_2O (191 µL, 0.829 mmol, 1.30 eq.) was added and the reaction was stirred at 40 °C for 3 h. The solvent was evaporated, and the residue was purified by flash column chromatography (silica gel, 0 – 10 % DCM/MeOH) to yield the product **190** (122 mg, 0.404 mmol, 63 %) as a yellow oil.

^{1}H-NMR (400 MHz, $CDCl_3$) δ 7.94 (d, *J* = 5.9 Hz, 1H), 7.42 – 7.35 (m, 1H), 7.08 – 7.02 (m, 1H), 6.98 – 6.91 (m, 2H), 6.32 (dd, *J* = 5.9, 2.2 Hz, 1H), 5.99 (d, *J* = 2.2 Hz, 1H), 4.49 (s, 2H), 1.56 (s, 9H). ^{13}C-NMR (101 MHz, $CDCl_3$) δ 166.1, 160.3, 155.1, 152.2, 151.6, 149.7, 130.4,

118.1, 114.4, 104.6, 95.9, 84.1, 27.8. LC-MS: ESI(+) [*m/z*]: calcd. mass $[M+H]^+$ = 303.1; found = 303.2. HPLC: t_{ret} = 8.72 min (93.9 % at 254 nm, 87.6 % at 230 nm, method A).

4-(4-Methoxyphenoxy)pyridin-2-amine (185)

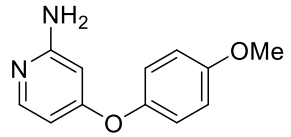

Chemical Formula: $C_{12}H_{12}N_2O_2$
Exact Mass: 216.08988
Molecular Weight: 216.24000

NaH (60 % dispersion in mineral oil, 46.7 mg, 1.17 mmol, 1.31 eq.) was suspended in NMP (4.5 mL). 4-Methoxyphenol (144 mL, 1.16 mmol, 1.30 eq.) was added and the solution was stirred at rt for 10 min. Subsequently, 4-fluoropyridin-2-amine (**183**, 100 mg, 0.892 mmol, 1.00 eq.) was added and the solution was stirred at 180 °C for 4 h. After cooling to rt, H_2O (20 mL) was added, and the solution was extracted with EtOAc (3 x 20 mL). The combined org. phases were washed with H_2O (3 x 50 mL) and dried over Na_2SO_4. The solvent was evaporated, and the residue was purified by flash column chromatography (silica gel, 0 – 10 % DCM/MeOH) to yield the product **185** (151 mg, 0.698 mmol, 78 %) as an off-white solid.

^{1}H-NMR (400 MHz, $CDCl_3$) δ 7.91 (d, J = 5.9 Hz, 1H), 7.05 – 6.97 (m, 2H), 6.95 – 6.87 (m, 2H), 6.25 (dd, J = 5.9, 2.2 Hz, 1H), 5.90 (d, J = 2.2 Hz, 1H), 4.37 (s, 2H), 3.82 (s, 3H). ^{13}C-NMR (101 MHz, $CDCl_3$) δ 167.3, 160.3, 157.1, 149.7, 147.6, 122.3, 115.1, 104.1, 95.0, 55.8. LC-MS: ESI(+) [*m/z*]: calcd. mass $[M+H]^+$ = 217.1; found = 217.1. HPLC: t_{ret} = 6.15 min (98.0 % at 254 nm, 99.1 % at 230 nm, method A).

4-((2-Aminopyridin-4-yl)oxy)phenol (187)

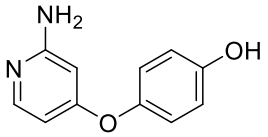

Chemical Formula: $C_{11}H_{10}N_2O_2$
Exact Mass: 202.07423
Molecular Weight: 202.21300

4-(4-Methoxyphenoxy)pyridin-2-amine (**185**, 153 mg, 0.708 mmol, 1.00 eq.) was dissolved in DCM (7 mL). The solution was cooled to 0 °C and BBr_3 (1 M in DCM, 1.77 mL, 1.77 mmol, 2.50 eq.) was added dropwise and the reaction was stirred at rt for 2 h. It was then quenched carefully with MeOH, and the solvent was evaporated. The residue was purified by flash column chromatography (silica gel, 5 – 10 % DCM/MeOH) leading to the product **187** (143 mg, 0.708 mmol, quant.) as a beige solid.

^{1}H-NMR (400 MHz, DMSO) δ 9.62 (s, 1H), 7.88 (d, *J* = 6.8 Hz, 1H), 7.20 (s, 2H), 7.06 – 6.97 (m, 2H), 6.91 – 6.82 (m, 2H), 6.46 (dd, *J* = 6.8, 2.4 Hz, 1H), 5.98 (d, *J* = 2.4 Hz, 1H). ^{13}C-NMR (101 MHz, DMSO) δ 168.8, 157.4, 155.5, 144.6, 141.4, 122.1, 116.6, 103.7, 94.1. LC-MS: ESI(+) [*m/z*]: calcd. mass $[M+H]^+$ = 203.1; found = 203.2. HPLC: t_{ret} = 3.96 min (99.5 % at 254 nm, 99.2 % at 230 nm, method A).

tert-Butyl (4-(4-hydroxyphenoxy)pyridin-2-yl)carbamate (191)

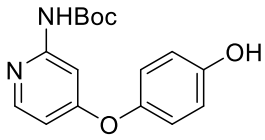

Chemical Formula: $C_{16}H_{18}N_2O_4$
Exact Mass: 302.12666
Molecular Weight: 302.33000

4-((2-Aminopyridin-4-yl)oxy)phenol (**187**, 143 mg, 0.708 mmol, 1.00 eq.) was dissolved in *t*BuOH (1.5 mL). Boc_2O (210 µL, 0.916 mmol, 1.30 eq.) was added and the reaction was stirred at 40 °C for 3.5 h. The solvent was evaporated, and the residue was purified by flash column chromatography (silica gel, 0 – 10 % DCM/MeOH) to yield the product **191** (93.0 mg, 0.308 mmol, 44 %) as a light yellow solid.

^{1}H-NMR (400 MHz, $CDCl_3$) δ 7.93 (d, J = 5.9 Hz, 1H), 7.24 – 7.15 (m, 2H), 7.12 – 7.03 (m, 2H), 6.29 (dd, J = 5.9, 2.2 Hz, 1H), 5.94 (d, J = 2.1 Hz, 1H), 4.43 (s, 2H), 1.57 (s, 9H). ^{13}C-NMR (101 MHz, $CDCl_3$) δ 166.5, 160.3, 152.1, 151.8, 149.9, 148.1, 122.9, 121.8, 104.4, 95.4, 84.0, 27.8. LC-MS: ESI(+) [*m/z*]: calcd. mass $[M+H]^+$ = 303.1; found = 303.1. HPLC: t_{ret} = 8.59 min (99.4 % at 254 nm, 97.6 % at 230 nm, method A).

4-(3-Bromophenoxy)pyridin-2-amine (194)

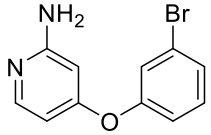

Chemical Formula: $C_{11}H_9BrN_2O$
Exact Mass: 263.98983
Molecular Weight: 265.11000

3-Bromophenol (1.00 g, 5.80 mmol, 1.30 eq.) was dissolved in NMP (15 mL). NaH (60 % dispersion in mineral oil, 232 mg, 5.80 mmol, 1.30 eq.) was added and the suspension was stirred at rt for 10 min. 4-Fluoropyridin-2-amine (**183**, 500 mg, 4.46 mmol, 1.00 eq.) was then added and the solution was stirred at 180 °C for 4 h. After cooling to rt, sat. NH_4Cl (30 mL) was added, and the solution was extracted with EtOAc (3 x 40 mL). The combined org. phases were washed with H_2O (3 x 75 mL) and dried over Na_2SO_4. The solvent was evaporated, and the residue was purified by flash column chromatography (silica gel, 0 – 10 % DCM/MeOH) leading to the product **194** (837 mg, 3.16 mmol, 71 %) as a beige solid.

^{1}H-NMR (400 MHz, $CDCl_3$) δ 7.96 (d, J = 5.9 Hz, 1H), 7.35 (d, J = 8.0 Hz, 1H), 7.30 – 7.22 (m, 2H), 7.02 (dd, J = 8.2, 2.3 Hz, 1H), 6.28 (dd, J = 6.0, 2.1 Hz, 1H), 5.97 (s, 1H), 4.46 (s, 2H). ^{13}C-NMR (101 MHz, $CDCl_3$) δ 165.7, 160.3, 155.2, 149.9, 131.1, 128.2, 124.1, 123.0, 119.4, 104.5, 95.8. TLC-MS: ESI(+) [*m/z*]: calcd. mass $[M+H]^+$ = 265.0; found = 265.1. HPLC: t_{ret} = 7.49 min (98.2 % at 254 nm, 98.1 % at 230 nm, method A).

tert-Butyl (4-(3-bromophenoxy)pyridin-2-yl)carbamate (196)

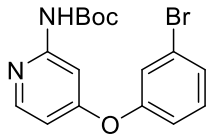

Chemical Formula: $C_{16}H_{17}BrN_2O_3$
Exact Mass: 364.04226
Molecular Weight: 365.22700

4-(3-Bromophenoxy)pyridin-2-amine (**194**, 837 mg, 3.16 mmol, 1.00 eq.) was dissolved in *t*BuOH (5 mL). Boc_2O (957 µL, 4.17 mmol, 1.32 eq.) was added and the reaction was stirred at 40 °C for 4 h. The solvent was evaporated, and the residue was purified by flash column chromatography (silica gel, 0 – 25 % hexane/EtOAc) to yield the product **196** (653 mg, 1.79 mmol, 57 %) as a white solid.

^{1}H-NMR (400 MHz, $CDCl_3$) δ 9.40 (s, 1H), 8.22 (d, J = 5.8 Hz, 1H), 7.65 (s, 1H), 7.39 – 7.32 (m, 1H), 7.31 – 7.23 (m, 2H), 7.04 (dd, J = 8.0, 2.4 Hz, 1H), 6.48 (dd, J = 5.8, 2.3 Hz, 1H), 1.51 (s, 9H). ^{13}C-NMR (101 MHz, $CDCl_3$) δ 165.9, 155.5, 154.8, 152.7, 149.4, 131.3, 128.3, 124.0, 123.2, 119.3, 107.5, 101.4, 81.2, 28.5. TLC-MS: ESI(+) [*m/z*]: calcd. mass $[M+Na]^+$ = 387.0; found = 387.4. HPLC: t_{ret} = 12.70 min (93.4 % at 254 nm, 94.0 % at 230 nm, method A).

tert-Butyl (4-(3-(benzylthio)phenoxy)pyridin-2-yl)carbamate (198)

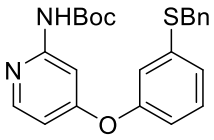

Chemical Formula: $C_{23}H_{24}N_2O_3S$
Exact Mass: 408.15076
Molecular Weight: 408.51600

tert-Butyl (4-(3-bromophenoxy)pyridin-2-yl)carbamate (**196**, 518 mg, 1.42 mmol, 1.00 eq.) was dissolved in 1,4-dioxane (7 mL). Benzyl mercaptane (166 µL, 1.42 mmol, 1.00 eq), DIPEA (485 µL, 2.85 mmol, 2.01 eq.), Pd_2dba_3 ($CHCl_3$ adduct, 73.4 mg, 709 µmol, 0.05 eq.) and Xantphos (82.1 mg, 0.142 mmol, 0.10 eq.) were added and the reaction was stirred at 90 °C for 18 h. After cooling to rt, H_2O (20 mL) was added, and the solution was extracted with EtOAc (3 x 25 mL). The combined org. phases were dried over Na_2SO_4, the solvent was evaporated, and the residue was purified by flash column chromatography (silica gel, 0 – 40 % hexane/EtOAc) leading to the product **198** (472 mg, 1.16 mmol, 81 %) as a yellow solid.

^{1}H-NMR (400 MHz, $CDCl_3$) δ 8.09 (d, J = 5.8 Hz, 1H), 7.95 (s, 1H), 7.60 – 7.55 (m, 1H), 7.32 – 7.27 (m, 5H), 7.25 – 7.21 (m, 1H), 7.13 (ddd, J = 7.8, 1.8, 1.0 Hz, 1H), 7.02 (t, J = 2.1 Hz, 1H), 6.89 (ddd, J = 8.1, 2.3, 1.0 Hz, 1H), 6.39 (dd, J = 5.8, 2.3 Hz, 1H), 4.12 (s, 2H), 1.50 (s, 9H). ^{13}C-NMR (101 MHz, $CDCl_3$) δ 166.1, 154.7, 153.9, 152.2, 149.2, 138.7, 137.0, 130.2, 128.8, 128.6, 127.3, 126.2, 121.3, 118.4, 107.5, 100.9, 81.1, 38.7, 28.3. TLC-MS: ESI(+) [*m/z*]: calcd. mass $[M+K]^+$ = 447.1; found = 447.4. HPLC: t_{ret} = 13.51 min (97.5 % at 254 nm, 93.8 % at 230 nm, method A).

tert-Butyl (4-(3-(chlorosulfonyl)phenoxy)pyridin-2-yl)carbamate (200)

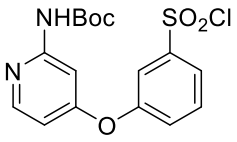

Chemical Formula: $C_{16}H_{17}ClN_2O_5S$
Exact Mass: 384.05467
Molecular Weight: 384.83100

tert-Butyl (4-(3-(benzylthio)phenoxy)pyridin-2-yl)carbamate (**198**, 100 mg, 0.245 mmol, 1.00 eq.) was dissolved in AcOH (1.8 mL) and H_2O (0.6 mL). NCS (98.4 mg, 0.737 mmol, 3.01 eq.) was added and the reaction was stirred at rt for 3.5 h. The solution was diluted with EtOAc (25 mL) and washed with brine (25 mL). The org. phase was dried over Na_2SO_4, the solvent was evaporated, and the residue was purified by flash column chromatography (silica gel, 0 – 50 % hexane/EtOAc) leading to the product **200** (64.7 mg, 0.168 mmol, 69 %) as a beige solid.

^{1}H-NMR (400 MHz, $CDCl_3$) δ 8.33 (s, 1H), 8.22 (d, J = 5.7 Hz, 1H), 7.88 (ddd, J = 8.0, 1.8, 1.0 Hz, 1H), 7.74 (t, J = 2.1 Hz, 1H), 7.72 – 7.63 (m, 2H), 7.46 (ddd, J = 8.3, 2.4, 1.0 Hz, 1H), 6.57 (dd, J = 5.7, 2.3 Hz, 1H), 1.50 (s, 9H). ^{13}C-NMR (101 MHz, $CDCl_3$) δ 164.9, 155.7, 154.6, 152.4, 149.8, 145.9, 131.6, 126.8, 123.1, 118.4, 108.3, 101.6, 81.6, 28.4. LC-MS: ESI(+) [*m/z*]: calcd. mass $[M+H]^+$ = 385.1; found = 385.1. HPLC: t_{ret} = 12.61 min (91.1 % at 254 nm, 93.1 % at 230 nm, method A).

tert-Butyl (4-(3-(fluorosulfonyl)phenoxy)pyridin-2-yl)carbamate

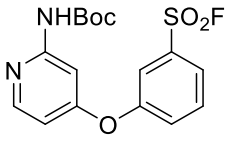

Chemical Formula: $C_{16}H_{17}FN_2O_5S$
Exact Mass: 368.08422
Molecular Weight: 368.37940

tert-Butyl (4-(3-(chlorosulfonyl)phenoxy)pyridin-2-yl)carbamate (**200**, 56.0 mg, 0.146 mmol, 1.00 eq.) was dissolved in THF (5 mL). KHF_2 (26.5 mg, 0.339 mmol, 2.33 eq.) was dissolved in H_2O (2.5 mL) and this was added to the first solution. After stirring at rt for 2 h, H_2O (10 mL) was added, and the solution was extracted with EtOAc (3 x 10 mL). The combined org. phases were dried over Na_2SO_4, and the solvent was evaporated. The crude product, a colorless oil, was used like this in the next step.

TLC-MS: ESI(+) calcd. for $[M+Na]^+$: *m/z* = 391.3; found: 391.3.

3-((2-Aminopyridin-4-yl)oxy)benzenesulfonyl fluoride (202)

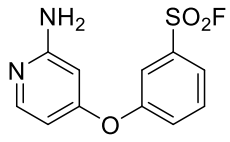

Chemical Formula: $C_{11}H_9FN_2O_3S$
Exact Mass: 268.03179
Molecular Weight: 268.26240

tert-Butyl (4-(3-(fluorosulfonyl)phenoxy)pyridin-2-yl)carbamate from the previous step was dissolved in HCl in dioxane (4 M, 5 mL). The reaction was stirred at 95 °C for 3.5 h and the solvent was evaporated. The residue was purified by flash column chromatography (silica gel, 0 – 50 % hexane/EtOAc) yielding the product **202** (HCl salt: 39.2 mg, 0.129 mmol, 88 % over two steps) as an off-white solid.

^{1}H-NMR (400 MHz, DMSO) δ 8.21 – 8.13 (m, 2H), 8.04 – 7.89 (m, 5H), 6.69 (dd, J = 7.2, 2.5 Hz, 1H), 6.21 (d, J = 2.5 Hz, 1H). ^{13}C-NMR (101 MHz, DMSO) δ 168.4, 156.7, 153.6, 139.2, 134.0 (d, J = 24.7 Hz), 133.6, 130.3, 127.1, 121.9, 104.9, 96.5. ^{19}F NMR (376 MHz, DMSO) δ 65.9. HRMS: ESI(+) [*m/z*]: calcd. mass $[M+H]^+$ = 309.03398; found = 309.03438; rel. deviation 1.3 ppm. HPLC: t_{ret} = 6.84 min (98.6 % at 254 nm, 98.4 % at 230 nm, method B).

4-(4-Bromophenoxy)pyridin-2-amine (195)

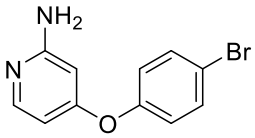

Chemical Formula: $C_{11}H_9BrN_2O$
Exact Mass: 263.98983
Molecular Weight: 265.11000

4-Bromophenol (1.00 g, 5.80 mmol, 1.30 eq.) was dissolved in NMP (15 mL). NaH (60 % dispersion in mineral oil, 232 mg, 5.80 mmol, 1.30 eq.) was added and the suspension was stirred at rt for 10 min. 4-Fluoropyridin-2-amine (**183**, 500 mg, 4.46 mmol, 1.00 eq.) was then added and the solution was stirred at 180 °C for 4 h. After cooling to rt, sat. NH_4Cl (30 mL) was added, and the solution was extracted with EtOAc (3 x 40 mL). The combined org. phases were washed with H_2O (3 x 75 mL) and dried over Na_2SO_4. The solvent was evaporated, and the residue was purified by flash column chromatography (silica gel, 0 – 10 % DCM/MeOH) and subsequently washed with hexane, leading to the product **195** (913 mg, 3.44 mmol, 77 %) as a beige solid.

^{1}H-NMR (400 MHz, $CDCl_3$) δ 7.94 (d, J = 5.9 Hz, 1H), 7.55 – 7.46 (m, 2H), 7.01 – 6.93 (m, 2H), 6.27 (dd, J = 5.9, 2.2 Hz, 1H), 5.95 (d, J = 2.2 Hz, 1H), 4.44 (s, 2H). ^{13}C-NMR (101 MHz, $CDCl_3$) δ 166.1, 160.3, 153.7, 149.9, 133.2, 122.7, 118.0, 104.4, 95.7. LC-MS: ESI(+) [*m/z*]: calcd. mass $[M+H]^+$ = 265.0; found = 265.1. HPLC: t_{ret} = 7.56 min (98.9 % at 254 nm, 97.5 % at 230 nm, method A).

tert-Butyl (4-(4-bromophenoxy)pyridin-2-yl)carbamate (197)

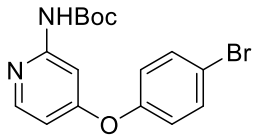

Chemical Formula: $C_{16}H_{17}BrN_2O_3$
Exact Mass: 364.04226
Molecular Weight: 365.22700

4-(4-Bromophenoxy)pyridin-2-amine (**195**, 913 mg, 3.44 mmol, 1.00 eq.) was dissolved in *t*BuOH (5 mL). Boc_2O (1.00 mL, 4.37 mmol, 1.27 eq.) was added and the reaction was stirred at 40 °C for 4 h. The solvent was evaporated, and the residue was purified by flash column chromatography (silica gel, 0 – 25 % hexane/EtOAc) to yield the product **197** (948 mg, 3.58 mmol, 76 %) as a white solid.

^{1}H-NMR (400 MHz, DMSO) δ 9.84 (s, 1H), 8.14 (d, J = 5.7 Hz, 1H), 7.70 – 7.61 (m, 2H), 7.34 (d, J = 2.3 Hz, 1H), 7.20 – 7.12 (m, 2H), 6.62 (dd, J = 5.7, 2.3 Hz, 1H), 1.41 (s, 9H). ^{13}C-NMR (101 MHz, DMSO) δ 165.1, 154.4, 153.3, 152.6, 149.7, 133.3, 122.9, 117.4, 107.6, 99.7, 79.9, 28.0. LC-MS: ESI(+) [*m/z*]: calcd. mass $[M+Na]^+$ = 387.0; found = 386.6. HPLC: t_{ret} = 12.49 min (95.1 % at 254 nm, 97.6 % at 230 nm, method A).

tert-Butyl (4-(4-(benzylthio)phenoxy)pyridin-2-yl)carbamate (199)

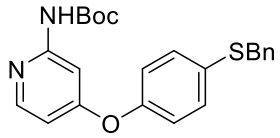

Chemical Formula: $C_{23}H_{24}N_2O_3S$
Exact Mass: 408.15076
Molecular Weight: 408.51600

tert-Butyl (4-(4-bromophenoxy)pyridin-2-yl)carbamate (**197**, 50.0 mg, 0.137 mmol, 1.00 eq.) was dissolved in 1,4-dioxane (1 mL). Benzyl mercaptane (16.0 µL, 0.137 mmol, 1.00 eq), DIPEA (47.0 µL, 0.277 mmol, 2.02 eq.), Pd_2dba_3 (6.27 mg, 6.85 µmol, 0.05 eq.) and Xantphos (7.92 mg, 13.7 µmol, 0.10 eq.) were added and the reaction was stirred at 90 °C for 18 h. After cooling to rt, H_2O (10 mL) was added and the solution was extracted with EtOAc (3 x 10 mL). The combined org. phases were dried over Na_2SO_4, the solvent was evaporated, and the residue was purified by flash column chromatography (silica gel, 0 – 30 % hexane/EtOAc) leading to the product **199** (45.0 mg, 0.110 mmol, 80 %) as a yellow solid.

^{1}H-NMR (400 MHz, $CDCl_3$) δ 9.21 (s, 1H), 8.01 (d, J = 6.4 Hz, 1H), 7.74 (d, J = 2.3 Hz, 1H), 7.44 – 7.33 (m, 2H), 7.33 – 7.20 (m, 5H), 7.03 – 6.95 (m, 2H), 6.61 (dd, J = 6.5, 2.3 Hz, 1H), 4.11 (s, 2H), 1.50 (s, 9H). ^{13}C-NMR (101 MHz, $CDCl_3$) δ 169.0, 152.6, 152.1, 151.3, 137.3, 134.2, 132.9, 129.0, 128.7, 127.5, 121.2, 107.8, 100.9, 83.0, 39.8, 28.2. LC-MS: ESI(+) [*m/z*]: calcd. mass $[M+Na]^+$ = 431.2; found = 430.8. HPLC: t_{ret} = 13.06 min (95.9 % at 254 nm, 96.3 % at 230 nm, method A).

tert-Butyl (4-(4-(chlorosulfonyl)phenoxy)pyridin-2-yl)carbamate (201)

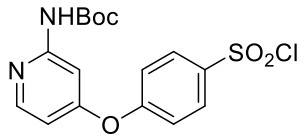

Chemical Formula: $C_{16}H_{17}ClN_2O_5S$
Exact Mass: 384.05467
Molecular Weight: 384.83100

tert-Butyl (4-(4-(benzylthio)phenoxy)pyridin-2-yl)carbamate (**199**, 130 mg, 0.318 mmol, 1.00 eq.) was dissolved in AcOH (2.4 mL) and H_2O (0.8 mL). NCS (127 mg, 0.955 mmol, 3.00 eq.) was added and the reaction was stirred at rt for 3.5 h. The solution was diluted with EtOAc (25 mL) and washed with brine (25 mL). The org. phase was dried over Na_2SO_4, the solvent was evaporated, and the residue was purified by flash column chromatography (silica gel, 0 – 50 % hexane/EtOAc) leading to the product **201** (72.2 mg, 0.188 mmol, 59 %) as a white solid.

^{1}H-NMR (400 MHz, $CDCl_3$) δ 8.28 – 8.22 (m, 1H), 8.14 – 8.01 (m, 2H), 7.99 (s, 1H), 7.73 (d, J = 2.2 Hz, 1H), 7.27 – 7.20 (m, 2H), 6.65 (dd, J = 5.7, 2.3 Hz, 1H), 1.51 (s, 9H). ^{13}C-NMR (101 MHz, $CDCl_3$) δ 163.8, 161.0, 154.6, 152.3, 150.0, 139.6, 129.9, 119.7, 109.5, 102.8, 81.7, 28.4. LC-MS: ESI(+) [*m/z*]: calcd. mass $[M+Na]^+$ = 407.1; found = 406.7. HPLC: t_{ret} = 18.65 min (95.5 % at 254 nm, 91.0 % at 230 nm, method B).

tert-Butyl (4-(4-(fluorosulfonyl)phenoxy)pyridin-2-yl)carbamate

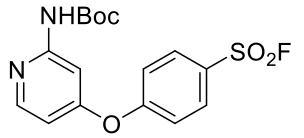

Chemical Formula: $C_{16}H_{17}FN_2O_5S$
Exact Mass: 368.08422
Molecular Weight: 368.37940

tert-Butyl (4-(4-(chlorosulfonyl)phenoxy)pyridin-2-yl)carbamate (**201**, 70.0 mg, 0.182 mmol, 1.00 eq.) was dissolved in THF (5 mL). KHF_2 (32.7 mg, 0.418 mmol, 2.30 eq.) was dissolved in H_2O (2.5 mL) and this was added to the first solution. After stirring at rt for 1 h, H_2O (10 mL) was added, and the solution was extracted with EtOAc (3 x 10 mL). The combined org. phases were dried over Na_2SO_4, and the solvent was evaporated. The crude product, a white solid, was used like this in the next step.

^{19}F NMR (376 MHz, $CDCl_3$) δ 66.9.

4-((2-Aminopyridin-4-yl)oxy)benzenesulfonyl fluoride (203)

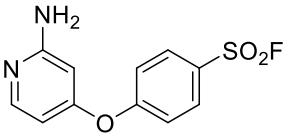

Chemical Formula: $C_{11}H_9FN_2O_3S$
Exact Mass: 268.03179
Molecular Weight: 268.26240

tert-Butyl (4-(4-(fluorosulfonyl)phenoxy)pyridin-2-yl)carbamate from the previous step was dissolved in HCl in dioxane (4 M, 5 mL). The reaction was stirred at 90 °C for 1 h and the solvent was evaporated. The residue was purified by flash column chromatography (silica gel, 0 – 10 %

DCM/MeOH) yielding the product **203** (HCl salt: 5.00 mg, 14.6 µmol, 4.6 % over two steps) as an off-white solid.

^{1}H-NMR (400 MHz, MeOD) δ 8.25 (d, J = 8.7 Hz, 2H), 7.90 (d, J = 7.2 Hz, 1H), 7.61 (d, J = 8.6 Hz, 2H), 6.71 (dd, J = 7.2, 2.4 Hz, 1H), 6.34 (d, J = 2.3 Hz, 1H). ^{13}C-NMR (101 MHz, MeOD) δ 169.8, 159.9, 157.8, 139.5, 132.8, 132.1, 131.8, 123.8, 106.3, 98.3. ^{19}F NMR (376 MHz, MeOD) δ 64.4. HRMS: ESI(+) [*m/z*]: calcd. mass $[M+H]^+$ = 269.03907; found = 269.03943; rel. deviation 1.4 ppm. HPLC: t_{ret} = 6.48 min (99.0 % at 254 nm, 99.5 % at 230 nm, method B).

3-(Pyridin-3-yl)phenol (205)

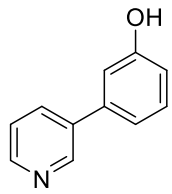

Chemical Formula: $C_{11}H_9NO$
Exact Mass: 171.06841
Molecular Weight: 171.19900

3-Bromopyridine (**204**, 250 mg, 1.58 mmol, 1.00 eq.), (3-hydroxyphenyl)boronic acid (240 mg, 1.74 mmol, 1.10 eq.) and XPhos Pd G4 (40.9 mg, 47.5 µmol, 0.03 eq.) were suspended in 1,4-dioxane (15 mL). K_2CO_3 (656 mg, 4.75 mmol, 3.00 eq.) was dissolved in H_2O (9 mL) and this was added to the first solution. The reaction was stirred at 80 °C for 18 h and then cooled to rt. Sat. NH_4Cl (20 mL) was added, and it was extracted with EtOAc (3 x 20 mL). The combined org. phases were dried over Na_2SO_4, the solvent was evaporated, and the residue was purified by flash column chromatography (silica gel, 0 – 10 % DCM/MeOH) leading to the product **205** (246 mg, 1.44 mmol, 91 %) as a light red solid.

^{1}H-NMR (400 MHz, DMSO) δ 9.63 (s, 1H), 8.82 (dd, J = 2.4, 0.9 Hz, 1H), 8.55 (dd, J = 4.8, 1.6 Hz, 1H), 7.99 (ddd, J = 7.9, 2.4, 1.6 Hz, 1H), 7.46 (ddd, J = 7.9, 4.8, 0.9 Hz, 1H), 7.30 (t, J = 7.9 Hz, 1H), 7.12 (ddd, J = 7.7, 1.8, 1.0 Hz, 1H), 7.06 (t, J = 2.1 Hz, 1H), 6.83 (ddd, J = 8.1, 2.4, 1.0 Hz, 1H). ^{13}C-NMR (101 MHz, DMSO) δ 158.0, 148.5, 147.5, 138.5, 135.7, 134.0, 130.2, 123.8, 117.6, 115.1, 113.6. TLC-MS: ESI(-) [*m/z*]: calcd. mass $[M-H]^-$ = 170.1; found = 169.9. HPLC: t_{ret} = 4.49 min (99.9 % at 254 nm, 99.7 % at 230 nm, method A).

3-(Pyridin-3-yl)phenyl sulfurofluoridate (207)

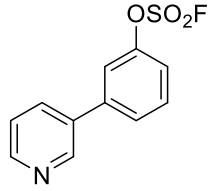

Chemical Formula: $C_{11}H_8FNO_3S$
Exact Mass: 253.02089
Molecular Weight: 253.24740

3-(Pyridin-3-yl)phenol (**205**, 75.0 mg, 0.438 mmol, 1.00 eq.) and AISF (**64**, 165 mg, 0.526 mmol, 1.20 eq.) were dissolved in THF (2.5 mL). DBU (145 µL, 0.968 mmol, 2.21 eq.) was added and the reaction was stirred at rt for 20 h. Sat. NH_4Cl (10 mL) was added and the solution was extracted with EtOAc (3 x 15 mL). After drying over Na_2SO_4 and evaporating the

solvent, the residue was purified by flash column chromatography (silica gel, 0 – 100 % hexane/EtOAc). The resulting oil was dissolved in HCl in dioxane (4 M, 5 mL) which was evaporated, leading to the product **207** (HCl salt: 111 mg, 0.383 mmol, 87 %) as a white solid.

^{1}H-NMR (400 MHz, DMSO) δ 9.27 (d, J = 2.2 Hz, 1H), 8.88 (dd, J = 5.5, 1.4 Hz, 1H), 8.78 (ddd, J = 8.2, 2.2, 1.4 Hz, 1H), 8.24 – 8.19 (m, 1H), 8.09 – 7.99 (m, 2H), 7.84 – 7.73 (m, 2H). ^{13}C-NMR (101 MHz, DMSO) δ 150.3, 143.2, 142.2, 141.5, 137.4, 135.9, 131.8, 128.2, 126.5, 121.9, 120.2. ^{19}F NMR (376 MHz, DMSO) δ 39.3. HRMS: ESI(+) [*m/z*]: calcd. mass $[M+H]^+$ = 254.02817; found = 254.02837; rel. deviation 0.8 ppm. HPLC: t_{ret} = 13.93 min (99.6 % at 254 nm, 98.6 % at 230 nm, method B).

4-(Pyridin-3-yl)phenol (206)

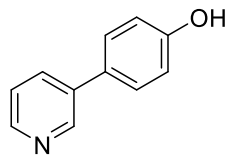

Chemical Formula: $C_{11}H_9NO$
Exact Mass: 171.06841
Molecular Weight: 171.19900

3-Bromopyridine (**204**, 250 mg, 1.58 mmol, 1.00 eq.), (4-hydroxyphenyl)boronic acid (240 mg, 1.74 mmol, 1.10 eq.) and XPhos Pd G4 (40.9 mg, 47.5 µmol, 0.03 eq.) were suspended in 1,4-dioxane (15 mL). K_2CO_3 (656 mg, 4.75 mmol, 3.00 eq.) was dissolved in H_2O (9 mL) and this was added to the first solution. The reaction was stirred at 80 °C for 18 h and then cooled to rt. Sat. NH_4Cl (20 mL) was added, and it was extracted with EtOAc (3 x 20 mL). The combined org. phases were dried over Na_2SO_4, the solvent was evaporated, and the residue was purified by flash column chromatography (silica gel, 0 – 10 % DCM/MeOH) leading to the product **206** (238 mg, 1.39 mmol, 88 %) as a light red solid.

^{1}H-NMR (400 MHz, DMSO) δ 9.67 (s, 1H), 8.81 (dd, J = 2.5, 0.9 Hz, 1H), 8.48 (dd, J = 4.8, 1.6 Hz, 1H), 7.97 (ddd, J = 7.9, 2.5, 1.6 Hz, 1H), 7.60 – 7.51 (m, 2H), 7.41 (ddd, J = 7.9, 4.8, 0.9 Hz, 1H), 6.92 – 6.84 (m, 2H). ^{13}C-NMR (101 MHz, DMSO) δ 157.7, 147.4, 147.1, 135.6, 133.2, 128.0, 127.7, 123.7, 116.0. TLC-MS: ESI(-) [*m/z*]: calcd. mass $[M-H]^-$ = 170.1; found = 169.9. HPLC: t_{ret} = 3.74 min (99.5 % at 254 nm, 99.1 % at 230 nm, method A).

4-(Pyridin-3-yl)phenyl sulfurofluoridate (208)

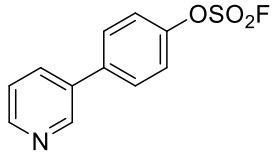

Chemical Formula: $C_{11}H_8FNO_3S$
Exact Mass: 253.02089
Molecular Weight: 253.24740

4-(Pyridin-3-yl)phenol (**206**, 75.0 mg, 0.438 mmol, 1.00 eq.) and AISF (**64**, 165 mg, 0.526 mmol, 1.20 eq.) were dissolved in THF (2.5 mL). DBU (145 µL, 0.968 mmol, 2.21 eq.) was added and the reaction was stirred at rt for 20 h. Sat. NH_4Cl (10 mL) was added, and the solution was extracted with EtOAc (3 x 15 mL). After drying over Na_2SO_4 and evaporating the

solvent, the residue was purified by flash column chromatography (silica gel, 0 – 100 % hexane/EtOAc) leading to the product **208** (110 mg, 0.438 mmol, quant.) as a white solid.

^{1}H-NMR (400 MHz, $CDCl_3$) δ 8.83 (dd, J = 2.4, 0.9 Hz, 1H), 8.65 (dd, J = 4.9, 1.6 Hz, 1H), 7.86 (ddd, J = 7.9, 2.4, 1.6 Hz, 1H), 7.73 – 7.63 (m, 2H), 7.51 – 7.44 (m, 2H), 7.41 (ddd, J = 7.9, 4.8, 0.9 Hz, 1H). ^{13}C-NMR (101 MHz, $CDCl_3$) δ 150.1, 149.5, 148.4, 138.8, 135.0, 134.6, 129.3, 123.9, 121.8. ^{19}F NMR (376 MHz, $CDCl_3$) δ 37.9. HRMS: ESI(+) [*m/z*]: calcd. mass $[M+H]^+$ = 254.02817; found = 254.02862; rel. deviation 1.8 ppm. HPLC: t_{ret} = 13.36 min (97.7 % at 254 nm, 95.3 % at 230 nm, method B).

4-(Pyridin-3-yl)phenyl trifluoromethanesulfonate (209)

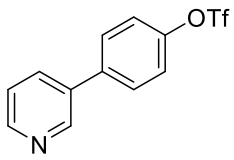

Chemical Formula: $C_{12}H_8F_3NO_3S$
Exact Mass: 303.01770
Molecular Weight: 303.25521

4-(Pyridin-3-yl)phenol (**206**, 75.0 mg, 0.438 mmol, 1.00 eq.) and pyridine (70.4 µL, 0.872 mmol, 1.99 eq.) were dissolved in DCM (1 mL). The solution was cooled to 0 °C. Tf_2O (89.2 µL, 0.530 mmol, 1.21 eq.) was dissolved in DCM (0.5 mL) and this solution was added dropwise to the cooled one. The reaction was stirred at rt for 1 h and was then quenched with HCl (1 M, 5 mL). The solution was extracted with EtOAc (3 x 10 mL), dried over Na_2SO_4 and the solvent was evaporated. The residue was purified by flash column chromatography (silica gel, 0 – 5 % DCM/MeOH) leading to the product **209** (107 mg, 0.353 mmol, 81 %) as a yellow oil.

^{1}H-NMR (400 MHz, $CDCl_3$) δ 8.84 (s, 1H), 8.68 – 8.62 (m, 1H), 7.86 (ddd, J = 7.9, 2.4, 1.6 Hz, 1H), 7.70 – 7.61 (m, 2H), 7.45 – 7.36 (m, 3H). ^{13}C-NMR (101 MHz, $CDCl_3$) δ 149.7, 149.4, 148.4, 138.5, 134.7, 129.2, 123.9, 122.2, 117.3 (q, J = 320.7 Hz). TLC-MS: ESI(+) [*m/z*]: calcd. mass $[M+H]^+$ = 304.0; found = 304.2. HPLC: t_{ret} = 11.56 min (99.1 % at 254 nm, 98.4 % at 230 nm, method A).

3-(4-(Benzylthio)phenyl)pyridine (210)

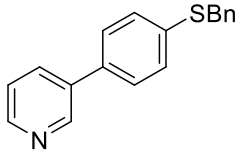

Chemical Formula: $C_{18}H_{15}NS$
Exact Mass: 277.09252
Molecular Weight: 277.38500

4-(Pyridin-3-yl)phenyl trifluoromethanesulfonate (**209**, 101 mg, 0.333 mmol, 1.00 eq.) was dissolved in 1,4-dioxane (2 mL). Benzyl mercaptane (39.0 µL, 0.333 mmol, 1.00 eq), DIPEA (113 µL, 0.666 mmol, 2.00 eq.), Pd_2dba_3 ($CHCl_3$ adduct, 17.2 mg, 16.7 µmol, 0.05 eq.) and Xantphos (19.3 mg, 33.3 µmol, 0.10 eq.) were added and the reaction was stirred at 90 °C for 19 h. After cooling to rt, H_2O (10 mL) was added, and the solution was extracted with EtOAc (3 x 10 mL). The combined org. phases were dried over Na_2SO_4, the solvent was evaporated, and the

residue was purified by flash column chromatography (silica gel, 0 – 55 % hexane/EtOAc) leading to the product **210** (76.3 mg, 0.275 mmol, 83 %) as a yellow solid.

^{1}H-NMR (400 MHz, $CDCl_3$) δ 8.83 (dd, J = 2.4, 0.9 Hz, 1H), 8.58 (dd, J = 4.9, 1.6 Hz, 1H), 7.86 (ddd, J = 7.9, 2.4, 1.7 Hz, 1H), 7.52 – 7.44 (m, 2H), 7.44 – 7.20 (m, 8H), 4.18 (s, 2H). ^{13}C-NMR (101 MHz, $CDCl_3$) δ 148.4, 148.0, 137.3, 137.2, 136.2, 135.6, 134.4, 130.0, 129.0, 128.7, 127.6, 127.5, 123.8, 38.8. TLC-MS: ESI(+) [*m/z*]: calcd. mass $[M+H]^+$ = 278.1; found = 278.1. HPLC: t_{ret} = 12.46 min (89.1 % at 254 nm, 92.4 % at 230 nm, method A).

Thieno[2,3-b]pyridine 7-oxide (212)

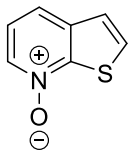

Chemical Formula: C_7H_5NOS
Exact Mass: 151.00918
Molecular Weight: 151.18300

Thieno[2,3-*b*]pyridine (**211**, 1.00 g, 7.40 mmol, 1.00 eq.) was dissolved in DCM (10 mL) and EtOAc (10 mL). The solution was cooled to 0 °C. *m*CPBA (1.79 g, 10.4 mmol, 1.40 eq.) was equally dissolved in DCM (10 mL) and EtOAc (10 mL) and this was slowly added to the first solution. After stirring at rt for 24 h, the solvent was evaporated. Aq. NaOH (2 M, 20 mL) was added, and it was extracted with DCM (2 x 25 mL). The org. phases were dried over Na_2SO_4, the solvent was evaporated, and the residue was purified by flash column chromatography (silica gel, 0 – 10 % DCM/MeOH) leading to the product **212** (963 mg, 6.37 mmol, 86 %) as an off-white solid.

^{1}H-NMR (400 MHz, $CDCl_3$) δ 8.32 (d, J = 6.2, 1H), 7.74 (dd, J = 8.1, 0.9 Hz, 1H), 7.59 – 7.56 (m, 1H), 7.39 – 7.29 (m, 2H). ^{13}C-NMR (101 MHz, $CDCl_3$) δ 137.0, 134.4, 128.6, 123.2, 122.1, 121.5. TLC-MS: ESI(+) [*m/z*]: calcd. mass $[M+Na]^+$ = 174.0; found = 174.0. HPLC: t_{ret} = 4.01 min (99.7 % at 254 nm, 99.3 % at 230 nm, method A).

4-Bromothieno[2,3-b]pyridine (213)

Chemical Formula: C_7H_4BrNS
Exact Mass: 212.92478
Molecular Weight: 214.08000

Thieno[2,3-*b*]pyridine 7-oxide (**212**, 821 mg, 5.43 mmol, 1.00 eq.) and TBAB (2.63 g, 8.15 mmol, 1.50 eq.) were dissolved in DCM (25 mL) and the solution was cooled to 0 °C. Tf_2O (1.83 mL, 10.9 mmol, 2.00 eq.) was added dropwise and the reaction was stirred at rt for 16 h. H_2O (10 mL) was added and the pH was adjusted to 7 using aq. NaOH (2 M). The solution was extracted with DCM (3 x 25 mL), dried over Na_2SO_4 and the solvent was evaporated. The residue was purified by flash column chromatography (silica gel, 0 – 30 % hexane/EtOAc) to yield the product **213** (989 mg, 4.62 mmol, 85 %) as a yellow solid.

^{1}H-NMR (400 MHz, $CDCl_3$) δ 8.36 (d, J = 5.0 Hz, 1H), 7.60 (d, J = 6.0 Hz, 1H), 7.50 (d, J = 5.0 Hz, 1H), 7.39 (d, J = 6.1 Hz, 1H). ^{13}C-NMR (101 MHz, $CDCl_3$) δ 161.9, 146.8, 133.6, 128.0, 123.1, 121.8. TLC-MS: ESI(+) [*m/z*]: calcd. mass $[M+H]^+$ = 213.9; found = 213.9. HPLC: t_{ret} = 11.04 min (99.5 % at 254 nm, 99.7 % at 230 nm, method A).

3-(Thieno[2,3-b]pyridin-4-yl)phenol (214)

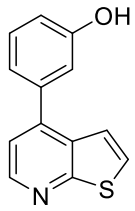

Chemical Formula: $C_{13}H_9NOS$
Exact Mass: 227.04049
Molecular Weight: 227.28100

4-Bromothieno[2,3-*b*]pyridine (**213**, 55.0 mg, 0.257 mmol, 1.00 eq.), (3-hydroxyphenyl)boronic acid (39.0 mg, 0.283 mmol, 1.10 eq.) and XPhos Pd G4 (6.63 mg, 7.71 µmol, 0.03 eq.) were suspended in 1,4-dioxane (3 mL). K_2CO_3 (107 mg, 0.771 mmol, 3.00 eq.) was dissolved in H_2O (1.5 mL) and this was added to the first solution. The reaction was stirred at 80 °C for 17 h and then cooled to rt. Sat. NH_4Cl (10 mL) was added, and it was extracted with EtOAc (3 x 15 mL). The combined org. phases were dried over Na_2SO_4, the solvent was evaporated, and the residue was purified by flash column chromatography (silica gel, 0 – 60 % hexane/EtOAc) leading to the product **214** (39.1 mg, 0.172 mmol, 67 %) as a white solid.

^{1}H-NMR (400 MHz, DMSO) δ 9.74 (s, 1H), 8.61 (d, J = 4.8 Hz, 1H), 7.93 (d, J = 6.1 Hz, 1H), 7.47 (d, J = 6.0 Hz, 1H), 7.42 (d, J = 4.8 Hz, 1H), 7.37 (t, J = 7.9 Hz, 1H), 7.07 (ddd, J = 7.6, 1.7, 1.0 Hz, 1H), 7.04 (t, J = 2.0 Hz, 1H), 6.96 – 6.88 (m, 1H). ^{13}C-NMR (101 MHz, DMSO) δ 161.9, 157.8, 146.8, 144.4, 138.9, 130.2, 129.9, 128.0, 120.8, 119.3, 119.0, 115.9, 115.4. TLC-MS: ESI(-) [*m/z*]: calcd. mass $[M-H]^-$ = 226.0; found = 226.0. HPLC: t_{ret} = 10.61 min (85.6 % at 254 nm, 95.2 % at 230 nm, method A).

3-(Thieno[2,3-b]pyridin-4-yl)phenyl sulfurofluoridate (216)

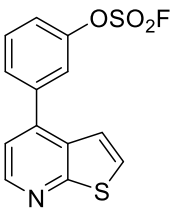

Chemical Formula: $C_{13}H_8FNO_3S_2$
Exact Mass: 308.99296
Molecular Weight: 309.32940

3-(Thieno[2,3-*b*]pyridin-4-yl)phenol (**214**, 34.2 mg, 0.150 mmol, 1.00 eq.) and AISF (**64**, 56.8 mg, 0.181 mmol, 1.20 eq.) were dissolved in THF (1.5 mL). DBU (49.9 µL, 0.334 mmol, 2.22 eq.) was added and the reaction was stirred at rt for 1 h. Sat. NH_4Cl (10 mL) was added, and the solution was extracted with EtOAc (3 x 10 mL). After drying over Na_2SO_4 and evaporating the solvent, the residue was purified by flash column chromatography (silica gel, 0 – 40 % hexane/EtOAc) to yield the product **216** (40.1 mg, 0.133 mmol, 86 %) as a white solid.

^{1}H-NMR (400 MHz, $CDCl_3$) δ 8.66 (d, J = 4.8 Hz, 1H), 7.71 – 7.58 (m, 4H), 7.47 (dtd, J = 6.2, 2.7, 1.0 Hz, 1H), 7.37 (d, J = 6.1 Hz, 1H), 7.31 (d, J = 4.8 Hz, 1H). ^{13}C-NMR (101 MHz, $CDCl_3$) δ 163.0, 150.4, 146.9, 142.6, 141.3, 131.2, 130.5, 129.1, 128.2, 121.5, 121.2, 120.2, 119.1. ^{19}F NMR (376 MHz, $CDCl_3$) δ 38.1. HRMS: ESI(+) [*m/z*]: calcd. mass $[M+H]^+$ = 310.00024; found = 310.00044; rel. deviation 0.7 ppm. HPLC: t_{ret} = 17.82 min (94.8 % at 254 nm, 95.9 % at 230 nm, method B).

4-(Thieno[2,3-b]pyridin-4-yl)phenol (215)

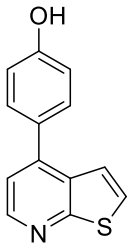

Chemical Formula: $C_{13}H_9NOS$
Exact Mass: 227.04049
Molecular Weight: 227.28100

4-Bromothieno[2,3-*b*]pyridine (**213**, 55.0 mg, 0.257 mmol, 1.00 eq.), (4-hydroxyphenyl)boronic acid (39.3 mg, 0.285 mmol, 1.11 eq.) and XPhos Pd G4 (6.63 mg, 7.71 µmol, 0.03 eq.) were suspended in 1,4-dioxane (3 mL). K_2CO_3 (107 mg, 0.771 mmol, 3.00 eq.) was dissolved in H_2O (1.5 mL) and this was added to the first solution. The reaction was stirred at 80 °C for 17 h and then cooled to rt. Sat. NH_4Cl (10 mL) was added, and it was extracted with EtOAc (3 x 15 mL). The combined org. phases were dried over Na_2SO_4, the solvent was evaporated, and the residue was purified by flash column chromatography (silica gel, 0 – 60 % hexane/EtOAc) leading to the product **215** (52.5 mg, 0.231 mmol, 90 %) as an off-white solid.

^{1}H-NMR (400 MHz, DMSO) δ 9.86 (s, 1H), 8.56 (d, J = 4.8 Hz, 1H), 7.89 (d, J = 6.1 Hz, 1H), 7.56 – 7.47 (m, 3H), 7.38 (d, J = 4.8 Hz, 1H), 7.00 – 6.91 (m, 2H). ^{13}C-NMR (101 MHz, DMSO) δ 162.0, 158.3, 146.7, 144.4, 130.1, 129.8, 128.2, 127.4, 121.0, 118.7, 115.9. TLC-MS: ESI(-) [*m/z*]: calcd. mass $[M-H]^-$ = 226.0; found = 226.0. HPLC: t_{ret} = 10.53 min (91.4 % at 254 nm, 92.0 % at 230 nm, method A).

4-(Thieno[2,3-b]pyridin-4-yl)phenyl sulfurofluoridate (217)

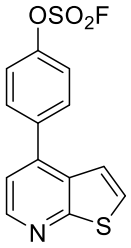

Chemical Formula: $C_{13}H_8FNO_3S_2$
Exact Mass: 308.99296
Molecular Weight: 309.32940

4-(Thieno[2,3-*b*]pyridin-4-yl)phenol (**215**, 45.5 mg, 0.200 mmol, 1.00 eq.) and AISF (**64**, 75.5 mg, 0.240 mmol, 1.20 eq.) were dissolved in THF (1.5 mL). DBU (65.7 µL, 0.440 mmol, 2.20 eq.) was added and the reaction was stirred at rt for 1 h. Sat. NH_4Cl (10 mL) was added, and the solution was extracted with EtOAc (3 x 10 mL). After drying over Na_2SO_4 and evaporating the solvent, the residue was purified by flash column chromatography (silica gel, 0 – 40 % hexane/EtOAc) leading to the product **217** (54.9 mg, 0.177 mmol, 89 %) as a white solid.

^{1}H-NMR (400 MHz, $CDCl_3$) δ 8.65 (d, J = 4.8 Hz, 1H), 7.76 – 7.68 (m, 2H), 7.60 (d, J = 6.1 Hz, 1H), 7.56 – 7.48 (m, 2H), 7.36 (d, J = 6.1 Hz, 1H), 7.29 (d, J = 4.8 Hz, 1H). ^{13}C-NMR (101 MHz, $CDCl_3$) δ 163.0, 150.3, 146.9, 143.0, 139.3, 130.9, 130.6, 127.9, 121.7, 120.3, 119.2. ^{19}F NMR (376 MHz, $CDCl_3$) δ 38.2. HRMS: ESI(+) [*m/z*]: calcd. mass $[M+H]^+$ = 310.00024; found = 310.00062; rel. deviation 1.2 ppm. HPLC: t_{ret} = 17.37 min (98.8 % at 254 nm, 99.3 % at 230 nm, method B).

tert-Butyl 6-bromo-1H-indazole-1-carboxylate (221)

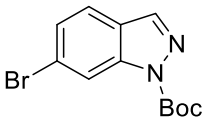

Chemical Formula: $C_{12}H_{13}BrN_2O_2$
Exact Mass: 296.01604
Molecular Weight: 297.15200

6-Bromo-1*H*-indazole (**220**, 2.00 g, 10.2 mmol, 1.00 eq.) and DMAP (248 mg, 2.03 mmol, 0.20 eq.) were dissolved in MeCN (25 mL). Boc_2O (2.40 mL, 11.3 mmol, 1.11 eq.) and TEA (2.80 mL, 20.2 mmol, 1.99 eq.) were added and the solution was stirred at rt for 2 h. The solvent was evaporated, and the crude was purified by flash column chromatography (silica gel, 0 – 50 % hexane/EtOAc) to yield the product **221** (2.89 g, 9.73 mmol, 95 %) as an off-white solid.

^{1}H-NMR (400 MHz, DMSO) δ 8.41 (d, J = 0.9 Hz, 1H), 8.22 (dt, J = 1.7, 0.7 Hz, 1H), 7.83 (dd, J = 8.4, 0.6 Hz, 1H), 7.52 (dd, J = 8.4, 1.7 Hz, 1H), 1.64 (s, 9H). ^{13}C-NMR (101 MHz, DMSO) δ 148.2, 139.8, 139.7, 126.9, 124.7, 123.4, 122.5, 116.6, 85.0, 27.6. LC-MS: ESI(+) [*m/z*]: calcd. mass $[M+Na]^+$ = 319.0; found = 319.0. HPLC: t_{ret} = 13.00 min (98.6 % at 254 nm, 98.0 % at 230 nm, method A).

tert-Butyl 6-((3-methoxybenzyl)thio)-1H-indazole-1-carboxylate (222)

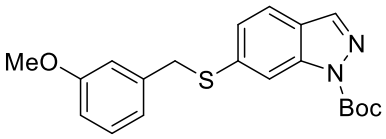

Chemical Formula: $C_{20}H_{22}N_2O_3S$
Exact Mass: 370.13511
Molecular Weight: 370.46700

tert-Butyl 6-bromo-1*H*-indazole-1-carboxylate (**221**, 150 mg, 0.505 mmol, 1.00 eq.) was dissolved in 1,4-dioxane (5 mL). (3-Methoxyphenyl)methanethiol (72.6 µL, 0.505 mmol, 1.00 eq), DIPEA (170 µL, 0.999 mmol, 1.98 eq.), Pd_2dba_3 (23.1 mg, 25.2 µmol, 0.05 eq.) and Xantphos (29.2 mg, 50.5 µmol, 0.10 eq.) were added and the reaction was stirred at 90 °C for 6 h. After cooling to rt, H_2O (15 mL) was added, and the solution was extracted with EtOAc (3 x 15 mL). The combined org. phases were dried over Na_2SO_4, the solvent was evaporated, and the residue was purified by flash column chromatography (silica gel, 0 – 25 % hexane/EtOAc) leading to the product **222** (124 mg, 0.335 mmol, 66 %) as a colorless oil.

^{1}H-NMR (400 MHz, $CDCl_3$) δ 8.17 (s, 1H), 8.08 (d, J = 0.9 Hz, 1H), 7.58 (dd, J = 8.3, 0.7 Hz, 1H), 7.26 – 7.17 (m, 2H), 6.99 – 6.89 (m, 2H), 6.79 (ddd, J = 8.3, 2.6, 0.9 Hz, 1H), 4.22 (s, 2H),

3.78 (s, 3H), 1.71 (s, 9H). ^{13}C-NMR (101 MHz, $CDCl_3$) δ 159.9, 149.3, 140.4, 139.4, 139.3, 138.3, 129.7, 124.8, 124.1, 121.4, 121.1, 114.5, 113.6, 113.3, 85.1, 55.3, 38.5, 28.3. LC-MS: ESI(+) [*m/z*]: calcd. mass $[M+Na]^+$ = 393.1; found = 393.1. HPLC: t_{ret} = 13.34 min (99.2 % at 254 nm, 100 % at 230 nm, method A).

3-(((1H-Indazol-6-yl)thio)methyl)phenol

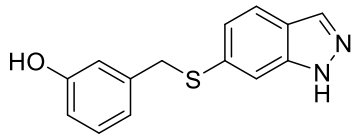

Chemical Formula: $C_{14}H_{12}N_2OS$
Exact Mass: 256.06703
Molecular Weight: 256.32300

tert-Butyl 6-((3-methoxybenzyl)thio)-1*H*-indazole-1-carboxylate (**222**, 97.0 mg, 0.262 mmol, 1.00 eq.) was dissolved in DCM (3 mL). BBr_3 (1 M in DCM, 790 µL, 0.785 mmol, 3.00 eq.) was added dropwise and the reaction was stirred at rt for 18 h. It was then quenched carefully with MeOH, and the solvent was evaporated. The crude was used in the next step without further purification.

LC-MS: ESI(+) [*m/z*]: calcd. mass $[M+H]^+$ = 257.1; found = 257.1.

3-(((1H-Indazol-6-yl)thio)methyl)phenyl sulfurofluoridate (223)

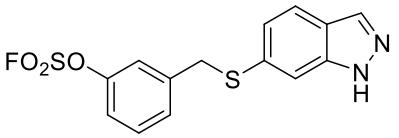

Chemical Formula: $C_{14}H_{11}FN_2O_3S_2$
Exact Mass: 338.01951
Molecular Weight: 338.37140

The crude from the previous step, 3-(((1*H*-indazol-6-yl)thio)methyl)phenol (29.0 mg, 0.113 mmol, 1.00 eq.) and AISF (**64**, 42.7 mg, 0.136 mmol, 1.20 eq.) were dissolved in DMF (1.5 mL). DBU (37.2 µL, 0.249 mmol, 2.20 eq.) was added and the reaction war stirred at rt for 18 h. Sat. NH_4Cl (10 mL) was added and the solution was extracted with DCM (3 x 10 mL). The combined org. phases were dried over Na_2SO_4, the solvent was evaporated, and the residue was purified by flash column chromatography (silica gel, 0 – 100 % hexane/EtOAc) to yield the product **223** (11.0 mg, 32.5 µmol, 29 %) as a beige solid.

^{1}H-NMR (400 MHz, MeOD) δ 7.54 – 7.41 (m, 4H), 7.35 – 7.26 (m, 1H), 7.22 (d, *J* = 8.3 Hz, 1H), 6.74 (d, *J* = 1.8 Hz, 1H), 6.60 (dd, *J* = 8.3, 1.7 Hz, 1H), 4.27 (s, 2H). ^{13}C-NMR (101 MHz, MeOD) δ 153.2, 152.4, 146.1, 143.1, 134.5, 132.6, 131.3, 123.2, 121.7, 119.6, 118.4, 115.5, 94.3, 37.6. ^{19}F NMR (376 MHz, MeOD) δ 35.8. HRMS: ESI(+) [*m/z*]: calcd. mass $[M+Na]^+$ = 361.00873; found = 361.00881; rel. deviation 0.2 ppm. HPLC: t_{ret} = 11.75 min (89.6 % at 254 nm, 90.5 % at 230 nm, method B).

3-(1H-Pyrrolo[2,3-b]pyridin-4-yl)phenol (225)

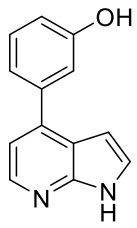

Chemical Formula: $C_{13}H_{10}N_2O$
Exact Mass: 210.07931
Molecular Weight: 210.23600

4-Chloro-1*H*-pyrrolo[2,3-*b*]pyridine (**224**, 250 mg, 1.64 mmol, 1.00 eq.), (3-hydroxyphenyl)boronic acid (249 mg, 1.80 mmol, 1.10 eq.) and XPhos Pd G4 (42.3 mg, 49.2 µmol, 0.03 eq.) were dissolved in 1,4-dioxane (16.5 mL). K_2CO_3 (679 mg, 4.92 mmol, 3.00 eq.) was dissolved in H_2O (9.8 mL) and was added to the first solution. The mixture was heated to 80 °C and stirred at this temperature for 18 h. It was then cooled to rt and sat. NH_4Cl (20 mL) was added. The solution was extracted with EtOAc (3 x 20 mL). The combined org. phases were dried over Na_2SO_4, the solvent was evaporated, and the residue was purified by flash column chromatography (silica gel, 0 – 100 % hexane/EtOAc) to yield the product **225** (94.0 mg, 0.447 mmol, 27 %) as a yellow solid.

^{1}H-NMR (400 MHz, DMSO) δ 11.77 (s, 1H), 9.64 (s, 1H), 8.26 (d, J = 4.9 Hz, 1H), 7.53 (dd, J = 3.5, 2.5 Hz, 1H), 7.34 (t, J = 8.1 Hz, 1H), 7.21 – 7.15 (m, 2H), 7.13 (d, J = 4.9 Hz, 1H), 6.86 (ddd, J = 8.1, 2.4, 1.1 Hz, 1H), 6.59 (dd, J = 3.5, 1.8 Hz, 1H). ^{13}C-NMR (101 MHz, DMSO) δ 157.8, 149.2, 142.9, 140.4, 139.8, 130.0, 126.5, 118.9, 117.2, 115.4, 115.0, 114.0, 99.1. HRMS: ESI(+) [*m/z*]: calcd. mass $[M+H]^+$ = 211.08659; found = 211.08686; rel. deviation 1.3 ppm. HPLC: t_{ret} = 7.87 min (98.0 % at 254 nm, 99.2 % at 230 nm, method A).

3-(1H-Pyrrolo[2,3-b]pyridin-4-yl)phenyl sulfurofluoridate (227)

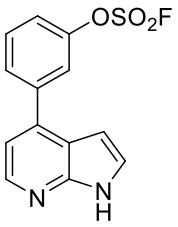

Chemical Formula: $C_{13}H_9FN_2O_3S$
Exact Mass: 292.03179
Molecular Weight: 292.28440

3-(1*H*-Pyrrolo[2,3-*b*]pyridin-4-yl)phenol (**225**, 71.0 mg, 0.338 mmol, 1.00 eq.) and AISF (**64**, 127 mg, 0.405 mmol, 1.20 eq.) were dissolved in THF (17 mL). DBU (111 µL, 0.743 mmol, 2.20 eq.) was added and the reaction was stirred at rt for 3.5 h. Sat. NH_4Cl (25 mL) was used to stop the reaction and it was extracted with EtOAc (3 x 25 mL). The org. phases were dried over Na_2SO_4, the solvent was evaporated, and the residue was purified by flash column chromatography (silica gel, 0 – 6.75 % DCM/MeOH) to yield the product **227** (67.8 mg, 0.232 mmol, 69 %) as a white solid.

^{1}H-NMR (400 MHz, DMSO) δ 11.91 (s, 1H), 8.33 (d, J = 4.9 Hz, 1H), 8.00 – 7.90 (m, 2H), 7.78 (t, J = 8.0 Hz, 1H), 7.70 (ddt, J = 8.3, 2.0, 0.9 Hz, 1H), 7.61 (dd, J = 3.5, 2.5 Hz, 1H), 7.26 (d, J = 4.9 Hz, 1H), 6.62 (dd, J = 3.5, 1.9 Hz, 1H). ^{13}C-NMR (101 MHz, DMSO) δ 150.1, 149.3, 143.1, 141.3, 137.9, 131.7, 129.1, 127.5, 120.9, 120.8, 117.1, 114.5, 98.6. ^{19}F NMR (376 MHz, DMSO) δ 38.8. HRMS: ESI(+) [*m/z*]: calcd. mass $[M+H]^+$ = 293.03907; found = 293.03942; rel. deviation 1.2 ppm. HPLC: t_{ret} = 11.67 min (96.0 % at 254 nm, 98.4 % at 230 nm, method A).

4-(1H-Pyrrolo[2,3-b]pyridin-4-yl)phenol (226)

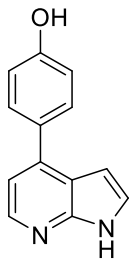

Chemical Formula: $C_{13}H_{10}N_2O$
Exact Mass: 210.07931
Molecular Weight: 210.23600

4-Chloro-1*H*-pyrrolo[2,3-*b*]pyridine (**224**, 250 mg, 1.64 mmol, 1.00 eq.), (4-hydroxyphenyl)boronic acid (249 mg, 1.80 mmol, 1.10 eq.) and XPhos Pd G4 (42.3 mg, 49.2 µmol, 0.03 eq.) were dissolved in 1,4-dioxane (16.5 mL). K_2CO_3 (679 mg, 4.92 mmol, 3.00 eq.) was dissolved in H_2O (9.8 mL) and was added to the first solution. The mixture was heated to 80 °C and stirred at this temperature for 18 h. It was then cooled to rt and sat. NH_4Cl (20 mL) was added. The solution was extracted with EtOAc (3 x 20 mL). The combined org. phases were dried over Na_2SO_4, the solvent was evaporated, and the residue was purified by flash column chromatography (silica gel, 0 – 10 % DCM/MeOH) to yield the product **226** (255 mg, 1.21 mmol, 74 %) as a white solid.

^{1}H-NMR (400 MHz, DMSO) δ 11.97 (s, 1H), 8.27 (d, J = 5.3 Hz, 1H), 7.70 – 7.62 (m, 2H), 7.59 – 7.53 (m, 1H), 7.22 (d, J = 5.3 Hz, 1H), 6.99 – 6.91 (m, 2H), 6.70 (d, J = 3.4 Hz, 1H). ^{13}C-NMR (101 MHz, DMSO) δ 158.5, 146.8, 142.6, 140.9, 129.9, 128.6, 127.0, 118.2, 116.1, 113.8, 100.1. HRMS: ESI(+) [m/z]: calcd. mass $[M+H]^+$ = 211.08659; found = 211.08692; rel. deviation 1.6 ppm. HPLC: t_{ret} = 6.87 min (97.7 % at 254 nm, 99.0 % at 230 nm, method A).

4-(1H-Pyrrolo[2,3-b]pyridin-4-yl)phenyl sulfurofluoridate (228)

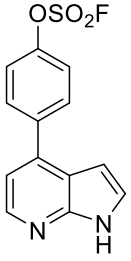

Chemical Formula: $C_{13}H_9FN_2O_3S$
Exact Mass: 292.03179
Molecular Weight: 292.28440

4-(1*H*-Pyrrolo[2,3-*b*]pyridin-4-yl)phenol (**226**, 100 mg, 0.476 mmol, 1.00 eq.) and AISF (**64**, 179 mg, 0.571 mmol, 1.20 eq.) were dissolved in THF (24 mL). DBU (156 µL, 1.05 mmol, 2.20 eq.) was added and the reaction was stirred at rt for 3 h. Sat. NH_4Cl (30 mL) was used to stop the reaction, and it was extracted with EtOAc (3 x 30 mL). The org. phases were dried over Na_2SO_4, the solvent was evaporated, and the residue was purified by flash column chromatography (silica gel, 0 – 6.75 % DCM/MeOH) to yield the product **228** (95.8 mg, 0.328 mmol, 69 %) as an off-white solid.

^{1}H-NMR (400 MHz, DMSO) δ 11.87 (s, 1H), 8.31 (d, J = 4.9 Hz, 1H), 8.02 – 7.94 (m, 2H), 7.83 – 7.73 (m, 2H), 7.59 (dd, J = 3.6, 2.5 Hz, 1H), 7.24 (d, J = 4.9 Hz, 1H), 6.62 (dd, J = 3.5, 1.9 Hz, 1H). ^{13}C-NMR (101 MHz, DMSO) δ 149.5, 149.2, 143.0, 139.4, 138.2, 130.6, 127.2, 121.8, 117.2, 114.5, 98.7. ^{19}F NMR (376 MHz, DMSO) δ 38.9. HRMS: ESI(+) [m/z]: calcd. mass $[M+H]^+$ = 293.03907; found = 293.03966; rel. deviation 2.0 ppm. HPLC: t_{ret} = 11.35 min (97.8 % at 254 nm, 98.2 % at 230 nm, method A).

3-(1H-Pyrrolo[2,3-b]pyridin-3-yl)phenol (230)

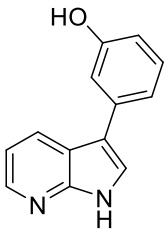

Chemical Formula: $C_{13}H_{10}N_2O$
Exact Mass: 210.07931
Molecular Weight: 210.23600

3-Bromo-1*H*-pyrrolo[2,3-*b*]pyridine (**229**, 250 mg, 1.27 mmol, 1.00 eq.), (3-hydroxyphenyl)boronic acid (193 mg, 1.40 mmol, 1.10 eq.) and XPhos Pd G4 (32.8 mg, 38.1 µmol, 0.03 eq.) were suspended in 1,4-dioxane (12.5 mL). K_2CO_3 (526 mg, 3.81 mmol, 3.00 eq.) was dissolved in H_2O (7 mL) and this was added to the first solution. The reaction was stirred at 80 °C for 2 d and then cooled to rt. Sat. NH_4Cl (20 mL) was added, and it was extracted with EtOAc (3 x 25 mL). The combined org. phases were dried over Na_2SO_4, the solvent was evaporated, and the residue was purified by flash column chromatography (silica gel, 0 – 8 % DCM/MeOH) leading to the product **230** (31.0 mg, 0.147 mmol, 12 %) as a beige solid.

^{1}H-NMR (400 MHz, DMSO) δ 11.85 (s, 1H), 9.37 (s, 1H), 8.26 (dd, J = 4.6, 1.6 Hz, 1H), 8.22 (dd, J = 7.9, 1.5 Hz, 1H), 7.78 (d, J = 2.6 Hz, 1H), 7.22 (t, J = 7.7 Hz, 1H), 7.18 – 7.09 (m, 3H), 6.66 (ddd, J = 8.1, 2.3, 1.1 Hz, 1H). ^{13}C-NMR (101 MHz, DMSO) δ 157.7, 149.0, 142.8, 136.2, 129.8, 127.3, 123.5, 117.3, 117.1, 115.9, 114.4, 113.1, 112.8. TLC-MS: ESI(-) [*m/z*]: calcd. mass $[M-H]^-$ = 209.1; found = 209.1. HPLC: t_{ret} = 9.41 min (99.4 % at 254 nm, 97.3 % at 230 nm, method A).

3-(1H-Pyrrolo[2,3-b]pyridin-3-yl)phenyl sulfurofluoridate (232)

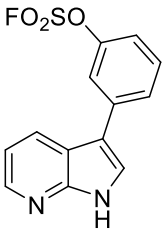

Chemical Formula: $C_{13}H_9FN_2O_3S$
Exact Mass: 292.03179
Molecular Weight: 292.28440

3-(1*H*-Pyrrolo[2,3-*b*]pyridin-3-yl)phenol (**230**, 36.0 mg, 0.171 mmol, 1.00 eq.) and AISF (**64**, 64.6 mg, 0.205 mmol, 1.20 eq.) were dissolved in THF (2 mL). DBU (56.2 µL, 0.377 mmol, 2.20 eq.) was added and the reaction was stirred at rt for 1 h. Sat. NH_4Cl (10 mL) was added, and the solution was extracted with EtOAc (3 x 10 mL). After drying over Na_2SO_4 and evaporating the solvent, the residue was purified by flash column chromatography (silica gel, 0 – 8 % DCM/MeOH) leading to the product **232** (5.67 mg, 19.4 µmol, 11 %) as a white solid.

^{1}H-NMR (400 MHz, MeOD) δ 8.32 (dd, J = 8.0, 1.5 Hz, 1H), 8.28 (dd, J = 4.8, 1.5 Hz, 1H), 7.85 – 7.77 (m, 2H), 7.73 (dt, J = 2.5, 1.2 Hz, 1H), 7.62 (t, J = 8.1 Hz, 1H), 7.33 (ddt, J = 8.3, 2.3, 1.1 Hz, 1H), 7.24 (dd, J = 8.0, 4.8 Hz, 1H), 4.59 (s, 1H). ^{13}C-NMR (101 MHz, MeOD) δ 152.2, 149.9, 144.1, 139.5, 132.1, 129.4, 128.1, 125.5, 119.8, 119.6, 119.0, 117.7, 115.1. ^{19}F NMR (376 MHz, MeOD) δ 35.6. HRMS: ESI(+) [*m/z*]: calcd. mass $[M+H]^+$ = 293.03907;

found = 293.03948; rel. deviation 1.4 ppm. HPLC: t_{ret} = 17.76 min (99.6 % at 254 nm, 99.5 % at 230 nm, method B).

4-(1H-Pyrrolo[2,3-b]pyridin-3-yl)phenol (231)

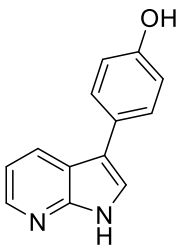

Chemical Formula: $C_{13}H_{10}N_2O$
Exact Mass: 210.07931
Molecular Weight: 210.23600

3-Bromo-1*H*-pyrrolo[2,3-*b*]pyridine (**229**, 250 mg, 1.27 mmol, 1.00 eq.), (4-hydroxyphenyl)boronic acid (193 mg, 1.40 mmol, 1.10 eq.) and XPhos Pd G4 (32.8 mg, 38.1 µmol, 0.03 eq.) were suspended in 1,4-dioxane (12.5 mL). K_2CO_3 (526 mg, 3.81 mmol, 3.00 eq.) was dissolved in H_2O (7 mL) and this was added to the first solution. The reaction was stirred at 80 °C for 2 d and then cooled to rt. Sat. NH_4Cl (20 mL) was added, and it was extracted with EtOAc (3 x 25 mL). The combined org. phases were dried over Na_2SO_4, the solvent was evaporated, and the residue was purified by flash column chromatography (silica gel, 0 – 100 % hexane/EtOAc) leading to the product **231** (40.0 mg, 0.190 mmol, 15 %) as a beige solid.

^{1}H-NMR (400 MHz, DMSO) δ 11.71 (s, 1H), 9.34 (s, 1H), 8.24 (dd, J = 4.7, 1.6 Hz, 1H), 8.19 (dd, J = 7.9, 1.6 Hz, 1H), 7.66 (d, J = 2.5 Hz, 1H), 7.55 – 7.46 (m, 2H), 7.11 (dd, J = 7.9, 4.6 Hz, 1H), 6.88 – 6.80 (m, 2H). ^{13}C-NMR (101 MHz, DMSO) δ 155.6, 148.9, 142.6, 127.5, 127.3, 125.9, 122.2, 117.4, 115.7, 114.5. TLC-MS: ESI(-) [*m/z*]: calcd. mass $[M-H]^-$ = 209.1; found = 209.1. HPLC: t_{ret} = 8.29 min (99.6 % at 254 nm, 97.9 % at 230 nm, method A).

4-(1H-Pyrrolo[2,3-b]pyridin-3-yl)phenyl sulfurofluoridate (233)

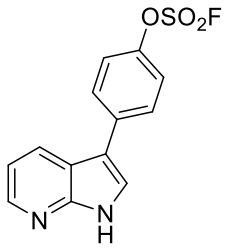

Chemical Formula: $C_{13}H_9FN_2O_3S$
Exact Mass: 292.03179
Molecular Weight: 292.28440

4-(1*H*-Pyrrolo[2,3-*b*]pyridin-3-yl)phenol (**231**, 28.0 mg, 0.133 mmol, 1.00 eq.) and AISF (**64**, 50.2 mg, 0.160 mmol, 1.20 eq.) were dissolved in THF (2 mL). DBU (43.7 µL, 0.293 mmol, 2.20 eq.) was added and the reaction was stirred at rt for 16 h. Sat. NH_4Cl (10 mL) was added, and the solution was extracted with EtOAc (3 x 10 mL). After drying over Na_2SO_4 and evaporating the solvent, the residue was purified by reverse phase column chromatography (CHROMABOND® Flash RS 40 C18 ec, 10 – 55 % H_2O/MeCN, 0.2% TFA). The fractions containing product were lyophilized to afford the product **233** (TFA salt: 5.70 mg, 15.5 µmol, 12 %) as a white solid.

^{1}H-NMR (400 MHz, $CDCl_3$) δ 8.61 (d, J = 8.1 Hz, 1H), 8.28 (d, J = 5.8 Hz, 1H), 7.74 – 7.66 (m, 3H), 7.53 – 7.44 (m, 3H). ^{13}C-NMR (101 MHz, $CDCl_3$) δ 149.2, 142.6, 134.9, 133.9, 133.4,

129.3, 126.4, 123.4, 121.9, 115.9. ^{19}F NMR (376 MHz, $CDCl_3$) δ 37.9, -76.2. HRMS: ESI(+) [*m/z*]: calcd. mass $[M+H]^+$ = 293.03907; found = 293.03958; rel. deviation 1.8 ppm. HPLC: t_{ret} = 17.38 min (95.2 % at 254 nm, 96.7 % at 230 nm, method B).

3-(1H-Pyrrolo[2,3-b]pyridin-5-yl)phenol (235)

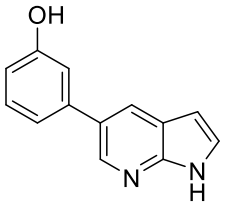

Chemical Formula: $C_{13}H_{10}N_2O$
Exact Mass: 210.07931
Molecular Weight: 210.23600

5-Bromo-1*H*-pyrrolo[2,3-*b*]pyridine (**234**, 250 mg, 1.27 mmol, 1.00 eq.), (3-hydroxyphenyl)boronic acid (193 mg, 1.40 mmol, 1.10 eq.) and XPhos Pd G4 (32.8 mg, 38.1 µmol, 0.03 eq.) were suspended in 1,4-dioxane (12.5 mL). K_2CO_3 (526 mg, 3.81 mmol, 3.00 eq.) was dissolved in H_2O (7 mL) and this was added to the first solution. The reaction was stirred at 80 °C for 3.5 h and then cooled to rt. Sat. NH_4Cl (20 mL) was added, and it was extracted with EtOAc (3 x 25 mL). The combined org. phases were dried over Na_2SO_4, the solvent was evaporated, and the residue was purified by flash column chromatography (silica gel, 0 – 8 % DCM/MeOH) leading to the product **235** (214 mg, 1.14 mmol, 80 %) as a yellow solid.

^{1}H-NMR (400 MHz, DMSO) δ 11.69 (s, 1H), 9.51 (s, 1H), 8.43 (d, J = 2.2 Hz, 1H), 8.12 (dd, J = 2.2, 0.7 Hz, 1H), 7.50 (dd, J = 3.5, 2.5 Hz, 1H), 7.26 (t, J = 7.8 Hz, 1H), 7.10 (ddd, J = 7.7, 1.8, 1.1 Hz, 1H), 7.05 (t, J = 2.1 Hz, 1H), 6.76 (ddd, J = 8.1, 2.5, 1.0 Hz, 1H), 6.49 (dd, J = 3.4, 1.8 Hz, 1H). ^{13}C-NMR (101 MHz, DMSO) δ 157.8, 148.1, 141.4, 140.5, 130.0, 128.3, 126.9, 126.0, 119.6, 117.7, 113.8, 113.7, 100.2. TLC-MS: ESI(-) [*m/z*]: calcd. mass $[M-H]^-$ = 209.1; found = 208.9. HPLC: t_{ret} = 9.55 min (96.7 % at 254 nm, 98.4 % at 230 nm, method A).

3-(1H-Pyrrolo[2,3-b]pyridin-5-yl)phenyl sulfurofluoridate (237)

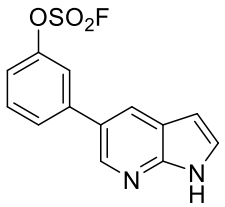

Chemical Formula: $C_{13}H_9FN_2O_3S$
Exact Mass: 292.03179
Molecular Weight: 292.28440

3-(1*H*-Pyrrolo[2,3-*b*]pyridin-5-yl)phenol (**235**, 100 mg, 0.476 mmol, 1.00 eq.) and AISF (**64**, 179 mg, 0.571 mmol, 1.20 eq.) were dissolved in THF (2.5 mL). DBU (156 µL, 1.05 mmol, 2.20 eq.) was added and the reaction was stirred at rt for 3 h. Sat. NH_4Cl (15 mL) was added, and the solution was extracted with EtOAc (3 x 15 mL). After drying over Na_2SO_4 and evaporating the solvent, the residue was purified by flash column chromatography (silica gel, 0 – 7.5 % DCM/MeOH) leading to the product **237** (105 mg, 0.359 mmol, 76 %) as an off-white solid.

^{1}H-NMR (400 MHz, DMSO) δ 11.81 (s, 1H), 8.59 (d, J = 2.3 Hz, 1H), 8.32 (dd, J = 2.3, 0.8 Hz, 1H), 7.99 (t, J = 2.1 Hz, 1H), 7.91 (ddd, J = 7.8, 1.8, 1.0 Hz, 1H), 7.69 (t, J = 8.0 Hz, 1H), 7.60 – 7.52 (m, 2H), 6.53 (dd, J = 3.4, 1.8 Hz, 1H). ^{13}C-NMR (101 MHz, DMSO) δ 150.9, 148.9, 142.5, 142.0, 131.8, 127.9, 127.9, 127.0, 126.4, 120.2, 119.7, 119.6, 100.9. ^{19}F NMR (376 MHz, DMSO) δ 38.9. HRMS: ESI(+) [*m/z*]: calcd. mass $[M+H]^+$ = 293.03907; found = 293.03946; rel. deviation 1.3 ppm. HPLC: t_{ret} = 17.18 min (99.1 % at 254 nm, 97.3 % at 230 nm, method B).

4-(1H-Pyrrolo[2,3-b]pyridin-5-yl)phenol (236)

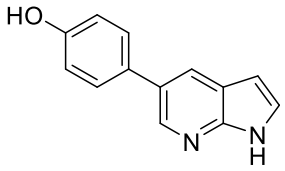

Chemical Formula: $C_{13}H_{10}N_2O$
Exact Mass: 210.07931
Molecular Weight: 210.23600

5-Bromo-1*H*-pyrrolo[2,3-*b*]pyridine (**234**, 250 mg, 1.27 mmol, 1.00 eq.), (4-hydroxyphenyl)boronic acid (193 mg, 1.40 mmol, 1.10 eq.) and XPhos Pd G4 (32.8 mg, 38.1 µmol, 0.03 eq.) were suspended in 1,4-dioxane (12.5 mL). K_2CO_3 (526 mg, 3.81 mmol, 3.00 eq.) was dissolved in H_2O (7 mL) and this was added to the first solution. The reaction was stirred at 80 °C for 3.5 h and then cooled to rt. Sat. NH_4Cl (20 mL) was added, and it was extracted with EtOAc (3 x 25 mL). The combined org. phases were dried over Na_2SO_4, the solvent was evaporated, and the residue was purified by flash column chromatography (silica gel, 0 – 100 % hexane/EtOAc) leading to the product **236** (240 mg, 1.14 mmol, 90 %) as a yellow solid.

^{1}H-NMR (400 MHz, DMSO) δ 11.62 (s, 1H), 9.48 (s, 1H), 8.42 (d, J = 2.2 Hz, 1H), 8.07 (d, J = 2.2 Hz, 1H), 7.54 – 7.43 (m, 3H), 6.91 – 6.82 (m, 2H), 6.46 (dd, J = 3.4, 1.8 Hz, 1H). ^{13}C-NMR (101 MHz, DMSO) δ 156.7, 147.6, 141.2, 129.9, 128.4, 127.9, 126.7, 125.3, 119.7, 115.8, 100.0. TLC-MS: ESI(+) [*m/z*]: calcd. mass $[M+H]^+$ = 211.1; found = 211.0. HPLC: t_{ret} = 9.01 min (96.5 % at 254 nm, 96.7 % at 230 nm, method A).

4-(1H-Pyrrolo[2,3-b]pyridin-5-yl)phenyl sulfurofluoridate (238)

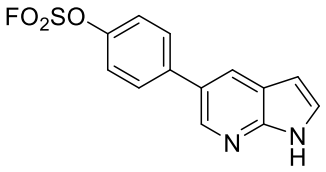

Chemical Formula: $C_{13}H_9FN_2O_3S$
Exact Mass: 292.03179
Molecular Weight: 292.28440

3-(1*H*-Pyrrolo[2,3-*b*]pyridin-5-yl)phenol (**236**, 100 mg, 0.476 mmol, 1.00 eq.) and AISF (**64**, 179 mg, 0.571 mmol, 1.20 eq.) were dissolved in THF (2.5 mL). DBU (156 µL, 1.05 mmol, 2.20 eq.) was added and the reaction was stirred at rt for 3 h. Sat. NH_4Cl (15 mL) was added, and the solution was extracted with EtOAc (3 x 15 mL). After drying over Na_2SO_4 and evaporating the solvent, the residue was purified by flash column chromatography (silica gel, 0 – 7.5 % DCM/MeOH) leading to the product **238** (99.1 mg, 0.339 mmol, 71 %) as an off-white solid.

^{1}H-NMR (400 MHz, DMSO) δ 11.79 (s, 1H), 8.55 (d, J = 2.3 Hz, 1H), 8.27 (dd, J = 2.3, 0.8 Hz, 1H), 7.96 – 7.87 (m, 2H), 7.73 – 7.64 (m, 2H), 7.54 (dd, J = 3.5, 2.5 Hz, 1H), 6.53 (dd, J = 3.4, 1.8 Hz, 1H). ^{13}C-NMR (101 MHz, DMSO) δ 148.8, 148.3, 141.6, 140.2, 129.1, 127.3, 126.5, 126.4, 121.6, 119.7, 100.3. ^{19}F NMR (376 MHz, DMSO) δ 38.5. HRMS: ESI(+) [*m/z*]: calcd. mass $[M+H]^+$ = 293.03907; found = 293.03959; rel. deviation 1.8 ppm. HPLC: t_{ret} = 17.55 min (98.1 % at 254 nm, 96.5 % at 230 nm, method B).

3-(1H-Pyrrolo[2,3-b]pyridin-4-yl)benzenesulfonyl fluoride (239)

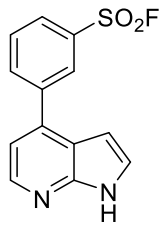

Chemical Formula: $C_{13}H_9FN_2O_2S$
Exact Mass: 276.03688
Molecular Weight: 276.28540

4-Chloro-1*H*-pyrrolo[2,3-*b*]pyridine (**224**, 95.0 mg, 0.623 mmol, 1.00 eq.), (3-(fluorosulfonyl)phenyl)boronic acid (**69**, 191 mg, 0.934 mmol, 1.50 eq.), $Pd(OAc)_2$ (7.00 mg, 31.1 µmol, 0.05 eq.) and XPhos (29.7 mg, 62.3 µmol, 0.10 eq.) were suspended in 1,4-dioxane (2.5 mL). K_3PO_4 (264 mg, 1.25 mmol, 2.00 eq.) was dissolved in H_2O (1.25 mL) and this was added to the first solution. The solution was heated to 40 °C and stirred for 18 h. It was diluted with EtOAc (15 mL) and sat. NH_4Cl (15 mL). The aq. phase was extracted with EtOAc (3 x 15 mL). The org. phases were dried over Na_2SO_4, the solvent was evaporated, and the residue was purified by flash column chromatography (silica gel, 0 – 100 % hexane/EtOAc) to yield the product **239** (34.2 mg, 0.124 mmol, 20 %) as an off-white solid.

^{1}H-NMR (400 MHz, DMSO) δ 11.96 (s, 1H), 8.39 – 8.31 (m, 3H), 8.28 – 8.21 (m, 1H), 7.98 (td, J = 8.1, 1.0 Hz, 1H), 7.64 (dd, J = 3.5, 2.6 Hz, 1H), 7.34 (d, J = 4.9 Hz, 1H), 6.61 (dd, J = 3.5, 1.9 Hz, 1H). ^{13}C-NMR (101 MHz, DMSO) δ 149.2, 143.1, 140.5, 137.2, 136.2, 132.5 (d, J = 23.5 Hz), 131.4, 128.0, 127.7, 127.4, 117.1, 114.6, 98.3. ^{19}F NMR (376 MHz, DMSO) δ 66.4. HRMS: ESI(+) [*m/z*]: calcd. mass $[M+H]^+$ = 277.04415; found = 277.04443; rel. deviation 1.0 ppm. HPLC: t_{ret} = 11.32 min (98.2 % at 254 nm, 98.6 % at 230 nm, method A).

4-(1H-Pyrrolo[2,3-b]pyridin-4-yl)benzenesulfonyl fluoride (240)

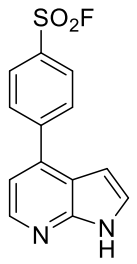

Chemical Formula: $C_{13}H_9FN_2O_2S$
Exact Mass: 276.03688
Molecular Weight: 276.28540

4-Chloro-1*H*-pyrrolo[2,3-*b*]pyridine (**224**, 100 mg, 0.655 mmol, 1.00 eq.), 4-(4,4,5,5-tetramethyl-1,3,2-dioxaborolan-2-yl)benzenesulfonyl fluoride (**180**, 225 mg, 0.786 mmol, 1.20 eq.), $Pd(OAc)_2$ (7.36 mg, 32.8 µmol, 0.05 eq.) and XPhos (31.2 mg, 65.5 µmol, 0.10 eq.) were suspended in 1,4-dioxane (2.6 mL). K_3PO_4 (278 mg, 2.89 mmol, 2.00 eq.) was dissolved in H_2O (1.3 mL) and this was added to the first solution. The solution was heated to 40 °C and stirred for 20 h. Sat. NH_4Cl (20 mL) was then added. The solution was extracted with EtOAc (3 x 20 mL) and dried over Na_2SO_4. After evaporation of the solvent, the residue was purified by flash column chromatography (silica gel, 0 – 5 % DCM/MeOH) to yield the product **240** (22.6 mg, 81.8 µmol, 12 %) as a beige solid.

^{1}H-NMR (400 MHz, DMSO) δ 11.99 (s, 1H), 8.37 (d, J = 4.9 Hz, 1H), 8.33 – 8.26 (m, 2H), 8.21 – 8.13 (m, 2H), 7.65 (dd, J = 3.5, 2.6 Hz, 1H), 7.33 (d, J = 5.0 Hz, 1H), 6.67 (dd, J = 3.5, 1.9 Hz, 1H). ^{13}C-NMR (101 MHz, DMSO) δ 149.2, 146.3, 143.0, 137.4, 130.8 (d, J = 23.9 Hz), 130.1, 129.2, 127.9, 117.1, 114.7, 98.6. ^{19}F NMR (376 MHz, DMSO) δ 66.7. HRMS: ESI(+) [*m/z*]: calcd. mass $[M+H]^+$ = 277.04415; found = 277.04465; rel. deviation 1.8 ppm. HPLC: t_{ret} = 11.17 min (97.7 % at 254 nm, 94.7 % at 230 nm, method A).

3-(1H-Pyrrolo[2,3-b]pyridin-5-yl)benzenesulfonyl fluoride (241)

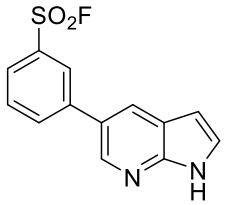

Chemical Formula: $C_{13}H_9FN_2O_2S$
Exact Mass: 276.03688
Molecular Weight: 276.28540

5-Bromo-1*H*-pyrrolo[2,3-*b*]pyridine (**234**, 100 mg, 0.508 mmol, 1.00 eq.), (3-(fluorosulfonyl)phenyl)boronic acid (**69**, 155 mg, 0.761 mmol, 1.50 eq.), $Pd(OAc)_2$ (5.70 mg, 25.4 µmol, 0.05 eq.) and XPhos (24.2 mg, 50.8 µmol, 0.10 eq.) were suspended in 1,4-dioxane (2 mL). K_3PO_4 (215 mg, 1.02 mmol, 2.00 eq.) was dissolved in H_2O (1 mL) and this was added to the first solution. The solution was heated to 40 °C and stirred for 36 h. Sat. NH_4Cl (20 mL) was then added. The solution was extracted with EtOAc (3 x 20 mL) and dried over Na_2SO_4. After evaporation of the solvent, the residue was purified by flash column chromatography (silica gel, 0 – 100 % hexane/EtOAc) to yield the product **241** (5.01 mg, 18.1 µmol, 3.6 %) as a white solid.

^{1}H-NMR (400 MHz, $CDCl_3$) δ 10.10 (s, 1H), 8.59 (d, *J* = 2.2 Hz, 1H), 8.27 (t, *J* = 1.9 Hz, 1H), 8.19 (d, *J* = 2.1 Hz, 1H), 8.08 – 7.97 (m, 2H), 7.74 (td, *J* = 7.9, 1.0 Hz, 1H), 7.46 (dd, *J* = 3.5, 2.3 Hz, 1H), 6.62 (dd, *J* = 3.5, 1.9 Hz, 1H). ^{13}C-NMR (101 MHz, $CDCl_3$) δ 148.8, 142.1, 141.9,

134.4, 134.0 (d, J = 24.3 Hz), 130.4, 127.8, 127.3, 127.1, 126.8, 126.6, 120.6, 101.7. ^{19}F NMR (376 MHz, $CDCl_3$) δ 66.0. HRMS: ESI(+) [*m/z*]: calcd. mass $[M+H]^+$ = 277.04415; found = 277.04361; rel. deviation 2.0 ppm. HPLC: t_{ret} = 16.61 min (99.5 % at 254 nm, 98.7 % at 230 nm, method B).

4-Bromo-1-(triisopropylsilyl)-1H-pyrrolo[2,3-b]pyridine (243)

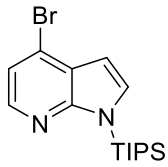

Chemical Formula: $C_{16}H_{25}BrN_2Si$
Exact Mass: 352.09704
Molecular Weight: 353.37900

4-Bromo-1*H*-pyrrolo[2,3-*b*]pyridine (**242**, 1.00 g, 5.03 mmol, 1.00 eq.) was suspended in THF (10 mL). NaH (60 % dispersion in mineral oil, 223 mg, 5.58 mmol, 1.10 eq.) was added portion wise and the suspension was stirred at rt for 10 min. TIPSCl (1.20 mL, 5.58 mmol, 1.10 eq.) was added and the reaction was stirred at 50 °C for 2.5 h. It was quenched with sat. NH_4Cl (15 mL) and extracted with DCM (3 x 20 mL). The org. phases were dried over Na_2SO_4, and the solvent was evaporated. The residue was purified by flash column chromatography (silica gel, hexane) to yield the product **243** (1.58 g, 4.47 mmol, 88 %) as a white solid.

^{1}H-NMR (400 MHz, $CDCl_3$) δ 8.05 (d, J = 5.1 Hz, 1H), 7.34 (d, J = 3.5 Hz, 1H), 7.22 (d, J = 5.1 Hz, 1H), 6.59 (d, J = 3.5 Hz, 1H), 1.84 (hept, J = 7.5 Hz, 3H), 1.11 (d, J = 7.6 Hz, 18H). ^{13}C-NMR (101 MHz, $CDCl_3$) δ 142.6, 131.8, 124.2, 124.0, 119.2, 103.1, 18.2, 12.4. TLC-MS: ESI(+) [*m/z*]: calcd. mass $[M+H]^+$ = 352.2; found = 352.8. HPLC: t_{ret} = 14.06 min (96.6 % at 254 nm, 97.2 % at 230 nm, method A).

4-Fluoro-1-(triisopropylsilyl)-1H-pyrrolo[2,3-b]pyridine (244)

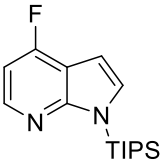

Chemical Formula: $C_{16}H_{25}FN_2Si$
Exact Mass: 292.17710
Molecular Weight: 292.47340

4-Bromo-1-(triisopropylsilyl)-1*H*-pyrrolo[2,3-*b*]pyridine (**243**, 750 mg, 1.84 mmol, 1.00 eq.) was dissolved in THF (9 mL) and the solution was cooled to -78 °C. *n*BuLi (2.5 M in hexane, 1.62 mL, 4.04 mmol, 2.20 eq.) was slowly added and the reaction was stirred for 30 min. NFSI (753 mg, 2.39 mmol, 1.30 eq.) was dissolved in Et_2O (9 mL) and this was added to the first solution. The reaction was stirred at -78 °C another 3 h and then warmed up to rt. It was quenched by the addition of sat. $NaHCO_3$ (20 mL) and extracted with EtOAc (3 x 25 mL). The org. phases were dried over Na_2SO_4, the solvent was evaporated, and the residue was purified by flash column chromatography (silica gel, hexane) to yield the product **244** (515 mg, 1.76 mmol, 96 %) as a colorless oil.

^{1}H-NMR (400 MHz, $CDCl_3$) δ 8.18 (dd, J = 8.3, 5.4 Hz, 1H), 7.25 – 7.25 (m, 1H), 6.75 (dd, J = 9.7, 5.4 Hz, 1H), 6.63 (d, J = 3.5 Hz, 1H), 1.85 (hept, J = 7.6 Hz, 3H), 1.12 (d, J = 7.6 Hz, 18H). ^{13}C-NMR (101 MHz, $CDCl_3$) δ 161.9 (d, J = 261.7 Hz), 157.3 (d, J = 10.2 Hz), 143.8 (d, J = 5.9 Hz), 130.7, 111.5, 102.4 (d, J = 14.9 Hz), 98.9, 18.1, 13.4. TLC-MS: ESI(+) [*m/z*]: calcd. mass $[M+H]^+$ = 293.2; found = 293.0.

4-Fluoro-1H-pyrrolo[2,3-b]pyridine (245)

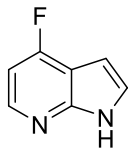

Chemical Formula: $C_7H_5FN_2$
Exact Mass: 136.04368
Molecular Weight: 136.12940

4-Fluoro-1-(triisopropylsilyl)-1*H*-pyrrolo[2,3-*b*]pyridine (**244**, 503 mg, 1.72 mmol, 1.00 eq.) was dissolved in THF (8.6 mL) and the solution was cooled to 0 °C. TBAF (1 M in THF, 1.89 mL, 1.89 mmol, 1.10 eq.) was added dropwise and the reaction was stirred for 16 h. It was quenched with sat. $NaHCO_3$ (15 mL), extracted with EtOAc (3 x 20 mL) and dried over Na_2SO_4. The solvent was evaporated, and the residue was purified by flash column chromatography (silica gel, 0 – 100 % hexane/EtOAc) to yield the product **245** (223 mg, 1.64 mmol, 95 %) as a white solid.

^{1}H-NMR (400 MHz, $CDCl_3$) δ 10.98 (s, 1H), 8.28 (dd, J = 7.7, 5.5 Hz, 1H), 7.35 (d, J = 3.6 Hz, 1H), 6.84 (dd, J = 9.7, 5.5 Hz, 1H), 6.61 (d, J = 3.5 Hz, 1H). ^{13}C-NMR (101 MHz, $CDCl_3$) δ 162.7 (d, J = 264.0 Hz), 152.4 (d, J = 12.4 Hz), 144.6 (d, J = 6.6 Hz), 124.9, 109.8 (d, J = 18.7 Hz), 102.7 (d, J = 16.1 Hz), 97.3. ^{19}F NMR (376 MHz, $CDCl_3$) δ -110.2. LC-MS: ESI(+) [*m/z*]: calcd. mass $[M+H]^+$ = 137.1; found = 137.1. HPLC: t_{ret} = 8.58 min (97.4 % at 254 nm, 74.3 % at 230 nm, method A).

4-(3-Methoxyphenoxy)-1H-pyrrolo[2,3-b]pyridine (246)

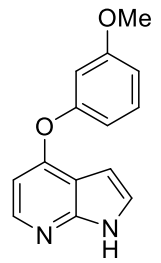

Chemical Formula: $C_{14}H_{12}N_2O_2$
Exact Mass: 240.08988
Molecular Weight: 240.26200

3-Methoxyphenol (94.8 mg, 0.764 mmol, 1.30 eq.) was dissolved in NMP (3 mL) and NaH (60 % dispersion in mineral oil, 30.5 mg, 0.764 mmol, 1.30 eq.) was added. The suspension was stirred at rt for 10 min. Subsequently, 4-fluoro-1H-pyrrolo[2,3-*b*]pyridine (**245**, 80.0 mg, 0.588 mmol, 1.0 eq.) was added and the reaction was stirred at 180 °C for 3.5 h. After cooling to rt, H_2O (10 mL) was added, and it was extracted with EtOAc (3 x 15 mL). The combined org. phases were washed with H_2O (3 x 30 mL), dried over Na_2SO_4 and the solvent was evaporated. The residue was purified by flash column chromatography (silica gel, 0 – 100 % hexane/EtOAc) to yield the product **246** (30.1 mg, 0.125 mmol, 21 %) as a yellow solid.

^{1}H-NMR (400 MHz, $CDCl_3$) δ 11.18 (s, 1H), 8.20 (d, J = 5.5 Hz, 1H), 7.31 (t, J = 8.1 Hz, 1H), 7.28 – 7.26 (m, 1H), 6.83 – 6.72 (m, 3H), 6.55 (d, J = 5.5 Hz, 1H), 6.41 (d, J = 3.5 Hz, 1H), 3.80 (s, 3H). ^{13}C-NMR (101 MHz, $CDCl_3$) δ 161.2, 158.3, 156.4, 151.6, 144.3, 130.4, 123.8, 112.8, 111.5, 110.8, 106.5, 103.2, 98.5, 55.6. TLC-MS: ESI(+) [*m/z*]: calcd. mass $[M+H]^+$ = 241.1; found = 241.1. HPLC: t_{ret} = 10.37 min (96.6 % at 254 nm, 95.4 % at 230 nm, method A).

3-((1H-Pyrrolo[2,3-b]pyridin-4-yl)oxy)phenol (248)

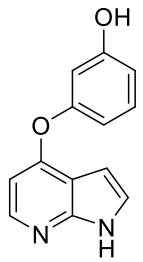

Chemical Formula: $C_{13}H_{10}N_2O_2$
Exact Mass: 226.07423
Molecular Weight: 226.23500

4-(3-Methoxyphenoxy)-1*H*-pyrrolo[2,3-*b*]pyridine (**246**, 30.0 mg, 0.125 mmol, 1.00 eq.) was dissolved in DCM (1.5 mL) and cooled to 0 °C. BBr_3 (1 M in DCM, 310 µL, 0.312 mmol, 2.50 eq.) was added dropwise and the reaction was stirred at rt for 3 h. It was then quenched carefully with MeOH, and the solvent was evaporated. The residue was purified by flash column chromatography (silica gel, 0 – 10 % DCM/MeOH) to yield the product **248** (24.2 mg, 0.107 mmol, 86 %) as a yellow solid.

^{1}H-NMR (400 MHz, DMSO) δ 11.71 (s, 1H), 9.77 (s, 1H), 8.08 (d, J = 5.4 Hz, 1H), 7.34 (t, J = 3.0 Hz, 1H), 7.23 (t, J = 8.1 Hz, 1H), 6.65 (dd, J = 8.1, 2.3 Hz, 1H), 6.58 (dd, J = 8.1, 2.3 Hz, 1H), 6.51 (t, J = 2.4 Hz, 1H), 6.47 (d, J = 5.4 Hz, 1H), 6.19 (dd, J = 3.7, 1.9 Hz, 1H). ^{13}C-NMR (101 MHz, DMSO) δ 158.9, 156.9, 156.0, 151.2, 144.3, 130.7, 124.9, 112.1, 110.7, 110.5, 107.2, 102.8, 97.3. TLC-MS: ESI(+) [*m/z*]: calcd. mass $[M+H]^+$ = 227.1; found = 227.0. HPLC: t_{ret} = 7.72 min (97.4 % at 254 nm, 97.6 % at 230 nm, method A).

3-((1H-Pyrrolo[2,3-b]pyridin-4-yl)oxy)phenyl sulfurofluoridate (250)

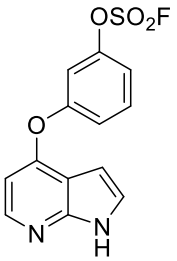

Chemical Formula: $C_{13}H_9FN_2O_4S$
Exact Mass: 308.02671
Molecular Weight: 308.28340

3-((1*H*-Pyrrolo[2,3-*b*]pyridin-4-yl)oxy)phenol (**248**, 20.0 mg, 88.4 µmol, 1.00 eq.) and AISF (**64**, 33.3 mg, 0.106 mmol, 1.20 eq.) were dissolved in THF (0.5 mL). DBU (29.0 µL, 0.194 mmol, 2.20 eq.) was added and the reaction was stirred at rt for 1 h. Sat. NH_4Cl (10 mL) was added, and the solution was extracted with EtOAc (3 x 10 mL). After drying over Na_2SO_4 and evaporating the solvent, the residue was purified by flash column chromatography (silica gel, 0 – 100 % hexane/EtOAc) leading to the product **250** (18.3 mg, 59.4 µmol, 67 %) as a white solid.

^{1}H-NMR (400 MHz, $CDCl_3$) δ 10.39 (s, 1H), 8.26 (d, J = 5.5 Hz, 1H), 7.50 (t, J = 8.3 Hz, 1H), 7.29 (d, J = 3.6 Hz, 1H), 7.21 (dtd, J = 8.2, 2.3, 1.0 Hz, 2H), 7.16 (td, J = 2.3, 0.8 Hz, 1H), 6.63 (d, J = 5.5 Hz, 1H), 6.34 (d, J = 3.5 Hz, 1H). ^{13}C-NMR (101 MHz, $CDCl_3$) δ 157.0, 156.7, 151.6, 150.6, 144.7, 131.4, 124.4, 120.1, 116.8, 113.1, 111.7, 104.3, 98.5. ^{19}F NMR (376 MHz, $CDCl_3$) δ 38.2. HRMS: ESI(+) [*m/z*]: calcd. mass $[M+H]^+$ = 309.03398; found = 309.03420; rel. deviation 0.7 ppm. HPLC: t_{ret} = 16.54 min (96.7 % at 254 nm, 97.2 % at 230 nm, method B).

4-(4-Methoxyphenoxy)-1H-pyrrolo[2,3-b]pyridine (247)

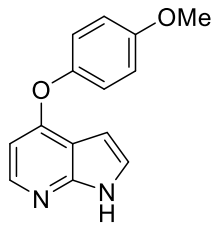

Chemical Formula: $C_{14}H_{12}N_2O_2$
Exact Mass: 240.08988
Molecular Weight: 240.26200

4-Methoxyphenol (94.8 mg, 0.764 mmol, 1.30 eq.) was dissolved in NMP (3 mL) and NaH (60 % dispersion in mineral oil, 30.5 mg, 0.764 mmol, 1.30 eq.) was added. The suspension was stirred at rt for 10 min. Subsequently, 4-fluoro-1H-pyrrolo[2,3-*b*]pyridine (**245**, 80.0 mg, 0.588 mmol, 1.0 eq.) was added and the reaction was stirred at 180 °C for 3.5 h. After cooling to rt, H_2O (10 mL) was added, and it was extracted with EtOAc (3 x 15 mL). The combined org. phases were washed with H_2O (3 x 30 mL), dried over Na_2SO_4 and the solvent was evaporated. The residue was purified by flash column chromatography (silica gel, 0 – 7.5 % DCM/MeOH) to yield the product **247** (58.3 mg, 0.243 mmol, 41 %) as a yellow solid.

^{1}H-NMR (400 MHz, $CDCl_3$) δ 10.61 (s, 1H), 8.14 (d, J = 5.6 Hz, 1H), 7.23 (d, J = 3.5 Hz, 1H), 7.17 – 7.08 (m, 2H), 7.01 – 6.91 (m, 2H), 6.42 (d, J = 5.6 Hz, 1H), 6.40 (d, J = 3.5 Hz, 1H), 3.85 (s, 3H). ^{13}C-NMR (101 MHz, $CDCl_3$) δ 159.4, 157.0, 151.4, 148.5, 144.5, 123.4, 122.1, 115.1, 110.9, 102.3, 98.6, 55.8. LC-MS: ESI(+) [*m/z*]: calcd. mass $[M+H]^+$ = 241.1; found = 240.8. HPLC: t_{ret} = 9.16 min (92.7 % at 254 nm, 94.7 % at 230 nm, method A).

4-((1H-Pyrrolo[2,3-b]pyridin-4-yl)oxy)phenol (249)

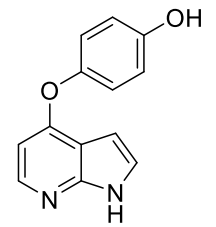

Chemical Formula: $C_{13}H_{10}N_2O_2$
Exact Mass: 226.07423
Molecular Weight: 226.23500

4-(4-Methoxyphenoxy)-1*H*-pyrrolo[2,3-*b*]pyridine (**247**, 58.3 mg, 0.243 mmol, 1.00 eq.) was dissolved in DCM (2.5 mL) and cooled to 0 °C. BBr_3 (1 M in DCM, 610 µL, 0.607 mmol, 2.50 eq.) was added dropwise and the reaction was stirred at rt for 1.5 h. It was then quenched carefully with MeOH, and the solvent was evaporated. The residue was purified by flash column chromatography (silica gel, 0 – 10 % DCM/MeOH) to yield the product **249** (46.9 mg, 0.207 mmol, 85 %) as a yellow solid.

^{1}H-NMR (400 MHz, DMSO) δ 11.65 (s, 1H), 9.52 (s, 1H), 8.02 (d, J = 5.4 Hz, 1H), 7.31 (dd, J = 3.5, 2.4 Hz, 1H), 7.06 – 6.97 (m, 2H), 6.87 – 6.78 (m, 2H), 6.29 (d, J = 5.4 Hz, 1H), 6.19 (dd, J = 3.4, 1.8 Hz, 1H). ^{13}C-NMR (101 MHz, DMSO) δ 158.4, 154.7, 151.1, 146.5, 144.2, 124.3, 122.0, 116.3, 109.8, 101.2, 97.2. LC-MS: ESI(+) [*m/z*]: calcd. mass $[M+H]^+$ = 227.1; found = 226.8. HPLC: t_{ret} = 6.59 min (93.5 % at 254 nm, 95.5 % at 230 nm, method A).

4-((1H-Pyrrolo[2,3-b]pyridin-4-yl)oxy)phenyl sulfurofluoridate (251)

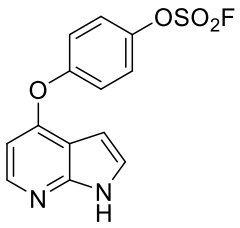

Chemical Formula: $C_{13}H_9FN_2O_4S$
Exact Mass: 308.02671
Molecular Weight: 308.28340

4-((1*H*-Pyrrolo[2,3-*b*]pyridin-4-yl)oxy)phenol (**249**, 38.0 mg, 0.168 mmol, 1.00 eq.) and AISF (**64**, 63.3 mg, 0.202 mmol, 1.20 eq.) were dissolved in THF (1 mL). DBU (55.2 µL, 0.370 mmol, 2.20 eq.) was added and the reaction was stirred at rt for 1 h. Sat. NH_4Cl (10 mL) was added, and the solution was extracted with EtOAc (3 x 10 mL). After drying over Na_2SO_4 and evaporating the solvent, the residue was purified by flash column chromatography (silica gel, 0 – 100 % hexane/EtOAc) leading to the product **251** (29.8 mg, 96.7 µmol, 58 %) as a white solid.

^{1}H-NMR (400 MHz, $CDCl_3$) δ 10.52 (s, 1H), 8.24 (d, J = 5.5 Hz, 1H), 7.43 – 7.34 (m, 2H), 7.29 (d, J = 3.6 Hz, 1H), 7.26 – 7.21 (m, 2H), 6.59 (d, J = 5.4 Hz, 1H), 6.36 (d, J = 3.5 Hz, 1H). ^{13}C-NMR (101 MHz, $CDCl_3$) δ 157.2, 155.5, 151.6, 146.2, 144.6, 124.3, 122.7, 121.6, 111.6, 104.1, 98.5. ^{19}F NMR (376 MHz, $CDCl_3$) δ 37.3. HRMS: ESI(+) [*m/z*]: calcd. mass $[M+H]^+$ = 309.03398; found = 309.03438; rel. deviation 1.3 ppm. HPLC: t_{ret} = 15.73 min (95.9 % at 254 nm, 97.8 % at 230 nm, method B).

tert-Butyl 4-bromo-1H-pyrrolo[2,3-b]pyridine-1-carboxylate (252)

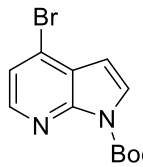

Chemical Formula: $C_{12}H_{13}BrN_2O_2$
Exact Mass: 296.01604
Molecular Weight: 297.15200

4-Bromo-1*H*-pyrrolo[2,3-*b*]pyridine (**242**, 250 mg, 1.27 mmol, 1.00 eq.) and DMAP (7.75 mg, 63.4 µmol, 0.05 eq.) were dissolved in DCM (15 mL). Boc_2O (301 µL, 1.41 mmol, 1.11 eq.) and TEA (176 µL, 1.27 mmol, 1.00 eq.) were added and the solution was stirred at rt for 2 h. The solvent was evaporated, and the crude was purified by flash column chromatography (silica gel, 0 – 30 % hexane/EtOAc) to yield the product **252** (348 g, 1.17 mmol, 92 %) as a colorless oil.

^{1}H-NMR (400 MHz, $CDCl_3$) δ 8.31 (d, J = 5.2 Hz, 1H), 7.69 (d, J = 4.1 Hz, 1H), 7.38 (d, J = 5.2 Hz, 1H), 6.57 (d, J = 4.1 Hz, 1H), 1.67 (s, 9H). ^{13}C-NMR (101 MHz, $CDCl_3$) δ 148.2,

147.8, 145.4, 127.3, 125.6, 124.7, 121.9, 104.3, 84.8, 28.2. TLC-MS: ESI(+) [*m/z*]: calcd. mass $[M+Na]^+$ = 319.0; found = 319.0. HPLC: t_{ret} = 12.62 min (98.0 % at 254 nm, 97.1 % at 230 nm, method A).

tert-Butyl 4-((3-methoxyphenyl)amino)-1H-pyrrolo[2,3-b]pyridine-1-carboxylate (253)

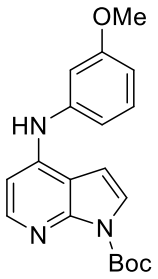

Chemical Formula: $C_{19}H_{21}N_3O_3$
Exact Mass: 339.15829
Molecular Weight: 339.39500

tert-Butyl 4-bromo-1*H*-pyrrolo[2,3-*b*]pyridine-1-carboxylate (**252**, 100 mg, 0.337 mmol, 1.00 eq.) was dissolved in toluene (3.5 mL). 3-Methoxyaniline (62.1 mg, 0.505 mmol, 1.50 eq.), Xantphos Pd G4 (16.2 mg, 16.8 µmol, 0.05 eq.) and Cs_2CO_3 (439 mg, 1.35 mmol, 4.00 eq.) were added and the reaction was stirred at 55 °C for 2 d. Sat. $NaHCO_3$ (10 mL) was added and the reaction was extracted with DCM (3 x 15 mL). The org. phases were dried over Na_2SO_4, the solvent was evaporated, and the residue was purified by flash column chromatography (silica gel, 0 – 65 % hexane/EtOAc) to yield the product **253** (11.5 mg, 33.9 µmol, 10 %) as a beige solid. 75 % of starting material were recovered which leads to an adjusted yield of the reaction of 41 %.

^{1}H-NMR (400 MHz, $CDCl_3$) δ 8.25 (d, J = 5.6 Hz, 1H), 7.49 (d, J = 4.1 Hz, 1H), 7.31 – 7.22 (m, 1H), 6.90 (d, J = 5.6 Hz, 1H), 6.83 (dd, J = 8.0, 2.1 Hz, 1H), 6.79 (t, J = 2.3 Hz, 1H), 6.68 (dd, J = 8.3, 2.4 Hz, 1H), 6.41 (d, J = 4.1 Hz, 1H), 6.23 (s, 1H), 3.80 (s, 3H), 1.66 (s, 9H). ^{13}C-NMR (101 MHz, $CDCl_3$) δ 160.8, 149.9, 148.1, 146.7, 144.1, 141.4, 130.4, 124.0, 113.9, 111.6, 109.4, 107.4, 103.2, 101.1, 84.0, 55.5, 28.2. TLC-MS: ESI(+) [*m/z*]: calcd. mass $[M+Na]^+$ = 362.2; found = 362.3. HPLC: t_{ret} = 9.28 min (95.9 % at 254 nm, 96.4 % at 230 nm, method A).

3-((1H-Pyrrolo[2,3-b]pyridin-4-yl)amino)phenol (259)

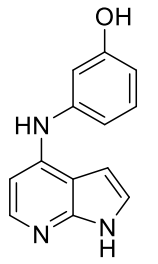

Chemical Formula: $C_{13}H_{11}N_3O$
Exact Mass: 225.09021
Molecular Weight: 225.25100

tert-Butyl 4-((3-methoxyphenyl)amino)-1*H*-pyrrolo[2,3-*b*]pyridine-1-carboxylate (**253**, 11.5 mg, 33.9 µmol, 1.00 eq.) was dissolved in DCM (1 mL) and cooled to 0 °C. BBr_3 (1 M in DCM, 10.2 µL, 84.7 µmol, 2.50 eq.) was added and the reaction was stirred at rt for 2 h. It was then quenched carefully with MeOH, and the solvent was evaporated. The crude product, a beige solid, was used as is in the next step.

TLC-MS: ESI(+) [*m/z*]: calcd. mass $[M+H]^+$ = 226.1; found = 226.1.

tert-Butyl 4-((4-methoxyphenyl)amino)-1H-pyrrolo[2,3-b]pyridine-1-carboxylate (254)

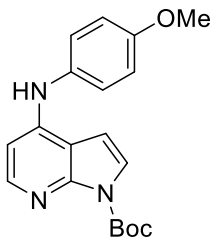

Chemical Formula: $C_{19}H_{21}N_3O_3$
Exact Mass: 339.15829
Molecular Weight: 339.39500

tert-Butyl 4-bromo-1*H*-pyrrolo[2,3-*b*]pyridine-1-carboxylate (**252**, 100 mg, 0.337 mmol, 1.00 eq.) was dissolved in toluene (3.5 mL). 4-Methoxyaniline (62.1 mg, 0.505 mmol, 1.50 eq.), Xantphos Pd G4 (16.2 mg, 16.8 µmol, 0.05 eq.) and Cs_2CO_3 (439 mg, 1.35 mmol, 4.00 eq.) were added and the reaction was stirred at 55 °C for 2 d. Sat. $NaHCO_3$ (10 mL) was added and the reaction was extracted with DCM (3 x 15 mL). The org. phases were dried over Na_2SO_4, the solvent was evaporated, and the residue was purified by flash column chromatography (silica gel, 0 – 65 % hexane/EtOAc) to yield the product **254** (16.1 mg, 47.4 µmol, 14 %) as a beige solid. 71 % of starting material were recovered which leads to an adjusted yield of the reaction of 48 %.

^{1}H-NMR (400 MHz, $CDCl_3$) δ 8.17 (d, J = 5.6 Hz, 1H), 7.45 (d, J = 4.2 Hz, 1H), 7.23 – 7.15 (m, 2H), 6.96 – 6.88 (m, 2H), 6.60 (d, J = 5.6 Hz, 1H), 6.34 (d, J = 4.1 Hz, 1H), 6.08 (s, 1H), 3.83 (s, 3H), 1.65 (s, 9H). ^{13}C-NMR (101 MHz, $CDCl_3$) δ 157.3, 149.8, 148.2, 146.7, 145.9, 132.6, 125.4, 123.5, 114.9, 110.5, 101.9, 101.0, 83.9, 55.7, 28.2. TLC-MS: ESI(+) [*m/z*]: calcd. mass $[M+Na]^+$ = 362.2; found = 362.3. HPLC: t_{ret} = 9.20 min (97.4 % at 254 nm, 98.0 % at 230 nm, method A).

4-((1H-Pyrrolo[2,3-b]pyridin-4-yl)amino)phenol (260)

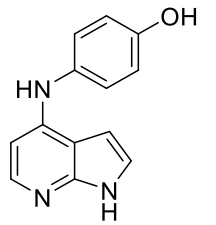

Chemical Formula: $C_{13}H_{11}N_3O$
Exact Mass: 225.09021
Molecular Weight: 225.25100

tert-Butyl 4-((4-methoxyphenyl)amino)-1*H*-pyrrolo[2,3-*b*]pyridine-1-carboxylate (**254**, 16.1 mg, 47.4 µmol, 1.00 eq.) was dissolved in DCM (1 mL) and cooled to 0 °C. BBr_3 (1 M in DCM, 14.3 µL, 0.119 mmol, 2.50 eq.) was added and the reaction was stirred at rt for 2 h. It was then quenched carefully with MeOH, and the solvent was evaporated. The crude product, a beige solid, was used as is in the next step.

TLC-MS: ESI(+) [*m/z*]: calcd. mass $[M+H]^+$ = 226.1; found = 226.1.

***tert*-Butyl 4-hydroxy-1H-pyrrolo[2,3-b]pyridine-1-carboxylate (256)**

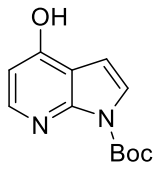

Chemical Formula: $C_{12}H_{14}N_2O_3$
Exact Mass: 234.10044
Molecular Weight: 234.25500

1*H*-Pyrrolo[2,3-*b*]pyridin-4-ol (**255**, 200 mg, 1.49 mmol, 1.00 eq.) and DMAP (9.11 mg, 74.5 µmol, 0.05 eq.) were dissolved in DMF (6 mL) and DCM (7.5 mL) and cooled to 0 °C. Boc_2O (351 µL, 1.64 mmol, 1.10 eq.) was added and the reaction was stirred at rt for 2.5 h. The solvent was evaporated, and the residue was purified by flash column chromatography (silica gel, 0 – 8 % DCM/MeOH) to yield the product **256** (202 mg, 0.862 mmol, 58 %) as a white solid.

^{1}H-NMR (400 MHz, $CDCl_3$) δ 10.13 (s, 1H), 7.84 (d, J = 8.3 Hz, 1H), 6.81 (dd, J = 3.4, 2.2 Hz, 1H), 6.73 (dd, J = 3.4, 2.7 Hz, 1H), 6.18 (d, J = 8.2 Hz, 1H), 1.66 (s, 9H). ^{13}C-NMR (101 MHz, $CDCl_3$) δ 176.8, 149.5, 135.0, 130.5, 117.1, 115.1, 114.7, 103.3, 87.5, 28.1. TLC-MS: ESI(-) [*m/z*]: calcd. mass $[M\text{-}H\text{-}Boc]^-$ = 133.1; found = 133.0. HPLC: t_{ret} = 8.73 min (93.0 % at 254 nm, 98.8 % at 230 nm, method A).

***N*-(3-Methoxyphenyl)-1H-pyrrolo[2,3-b]pyridin-4-amine (257)**

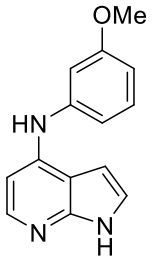

Chemical Formula: $C_{14}H_{13}N_3O$
Exact Mass: 239.10586
Molecular Weight: 239.27800

3-Methoxyaniline (**264**, 61.5 mg, 0.499 mmol, 1.30 eq.), K_3PO_4 (408 mg, 1.92 mmol, 5.00 eq.) and 5,6-dichloropyrazine-2,3-dicarbonitrile (**263**, 91.7 mg, 0.461 mmol, 1.20 eq.) were suspended in 1,4-dioxane (1.5 mL) and stirred at 50 °C for 2 h. Subsequently, *tert*-butyl 4-hydroxy-1*H*-pyrrolo[2,3-*b*]pyridine-1-carboxylate (**255**, 90.0 mg, 0.384 mmol, 1.00 eq.) and DMSO (2.2 mL) were added, and the reaction was heated at 100 °C for 1 h. At rt, zinc powder (251 mg, 3.84 mmol, 10.0 eq.) and AcOH (4.3 mL) were added, and the solution was stirred at 80 °C for another 30 min. The reaction was then diluted with EtOAc (50 mL), filtered over celite and washed with H_2O (3 x 25 mL). The org. phase was dried over Na_2SO_4, the solvent was evaporated, and the residue was purified by flash column chromatography (silica gel, 0 – 10 % DCM/MeOH) leading to the product **257** (45.0 mg, 0.188 mmol, 49 %) as a beige solid.

^{1}H-NMR (400 MHz, DMSO) δ 12.40 (s, 1H), 10.19 (s, 1H), 8.03 (d, J = 7.0 Hz, 1H), 7.46 – 7.36 (m, 2H), 7.02 – 6.89 (m, 3H), 6.84 (s, 1H), 6.75 (d, J = 7.0 Hz, 1H). ^{13}C-NMR (101 MHz, DMSO) δ 160.7, 150.8, 139.5, 138.7, 135.6, 131.0, 124.4, 116.8, 112.5, 110.5, 109.7, 101.2, 98.9, 55.8. TLC-MS: ESI(+) [*m/z*]: calcd. mass $[M+H]^+$ = 240.1; found = 240.2. HPLC: t_{ret} = 7.15 min (97.6 % at 254 nm, 97.8 % at 230 nm, method A).

N-(4-Methoxyphenyl)-1H-pyrrolo[2,3-b]pyridin-4-amine (258)

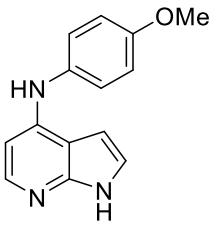

Chemical Formula: $C_{14}H_{13}N_3O$
Exact Mass: 239.10586
Molecular Weight: 239.27800

4-Methoxyaniline (68.3 mg, 0.555 mmol, 1.30 eq.), K_3PO_4 (453 mg, 2.13 mmol, 5.00 eq.) and 5,6-dichloropyrazine-2,3-dicarbonitrile (**263**, 102 mg, 0.512 mmol, 1.20 eq.) were suspended in 1,4-dioxane (1.8 mL) and stirred at 50 °C for 2 h. Subsequently, *tert*-butyl 4-hydroxy-1*H*-pyrrolo[2,3-*b*]pyridine-1-carboxylate (**255**, 100 mg, 0.427 mmol, 1.00 eq.) and DMSO (2.2 mL) were added, and the reaction was heated at 100 °C for 1 h. At rt, zinc powder (279 mg, 4.27 mmol, 10.0 eq.) and AcOH (4.8 mL) were added, and the solution was stirred at 80 °C for another 30 min. The reaction was then diluted with EtOAc (50 mL), filtered over celite and washed with H_2O (3 x 25 mL). The org. phase was dried over Na_2SO_4, the solvent was evaporated, and the residue was purified by flash column chromatography (silica gel, 0 – 10 % DCM/MeOH) leading to the product **258** (96.6 mg, 0.404 mmol, 95 %) as a brown solid.

^{1}H-NMR (400 MHz, $CDCl_3$) δ 7.95 (d, *J* = 5.9 Hz, 1H), 7.27 – 7.20 (m, 3H), 7.16 (d, *J* = 3.6 Hz, 1H), 6.99 – 6.91 (m, 2H), 6.50 (d, *J* = 5.9 Hz, 1H), 6.41 (s, 1H), 6.36 (d, *J* = 3.6 Hz, 1H), 3.85 (s, 3H). ^{13}C-NMR (101 MHz, $CDCl_3$) δ 157.6, 147.5, 141.8, 132.1, 126.0, 122.5, 114.9, 108.6, 98.8, 97.9, 55.7. TLC-MS: ESI(+) [*m/z*]: calcd. mass $[M+H]^+$ = 240.1; found = 240.1. HPLC: t_{ret} = 6.99 min (85.6 % at 254 nm, 97.4 % at 230 nm, method A).

tert-Butyl 4-((3-methoxybenzyl)thio)-1H-pyrrolo[2,3-b]pyridine-1-carboxylate (269)

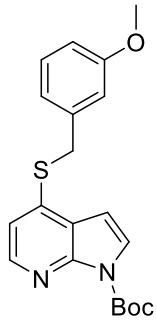

Chemical Formula: $C_{20}H_{22}N_2O_3S$
Exact Mass: 370.13511
Molecular Weight: 370.46700

tert-Butyl 4-bromo-1*H*-pyrrolo[2,3-*b*]pyridine-1-carboxylate (**252**, 150 mg, 0.505 mmol, 1.00 eq.) was dissolved in 1,4-dioxane (5 mL). (3-Methoxyphenyl)methanethiol (72.6 µL, 0.505 mmol, 1.00 eq), DIPEA (170 µL, 0.999 mmol, 1.98 eq.), Pd_2dba_3 (23.1 mg, 25.2 µmol, 0.05 eq.) and Xantphos (29.2 mg, 50.5 µmol, 0.10 eq.) were added and the reaction was stirred at 90 °C for 6 h. After cooling to rt, H_2O (15 mL) was added, and the solution was extracted with EtOAc (3 x 15 mL). The combined org. phases were dried over Na_2SO_4, the solvent was evaporated, and the residue was purified by flash column chromatography (silica gel, 0 – 60 % hexane/EtOAc) leading to the product **269** (107 mg, 0.289 mmol, 57 %) as a colorless oil.

^{1}H-NMR (400 MHz, $CDCl_3$) δ 8.34 (d, J = 5.2 Hz, 1H), 7.59 (d, J = 4.1 Hz, 1H), 7.26 – 7.20 (m, 1H), 7.03 (d, J = 5.2 Hz, 1H), 7.00 – 6.93 (m, 2H), 6.82 (ddd, J = 8.3, 2.6, 0.9 Hz, 1H), 6.54 (d,

J = 4.1 Hz, 1H), 4.28 (s, 2H), 3.79 (s, 3H), 1.66 (s, 9H). ^{13}C-NMR (101 MHz, $CDCl_3$) δ 160.0, 147.9, 147.5, 145.1, 141.4, 137.5, 129.9, 125.9, 121.3, 121.2, 115.0, 114.5, 113.4, 103.0, 84.4, 55.4, 36.2, 28.2. LC-MS: ESI(+) [*m/z*]: calcd. mass $[M+H]^+$ = 371.1; found = 371.1. HPLC: t_{ret} = 13.23 min (96.4 % at 254 nm, 92.0 % at 230 nm, method A).

3-(((1H-Pyrrolo[2,3-b]pyridin-4-yl)thio)methyl)phenol (271)

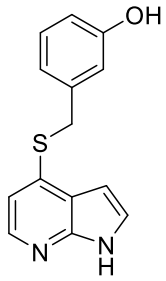

Chemical Formula: $C_{14}H_{12}N_2OS$
Exact Mass: 256.06703
Molecular Weight: 256.32300

tert-Butyl 4-((3-methoxybenzyl)thio)-1*H*-pyrrolo[2,3-*b*]pyridine-1-carboxylate (**269**, 97.0 mg, 0.262 mmol, 1.00 eq.) was dissolved in DCM (3 mL) and cooled to 0 °C. BBr_3 (1 M in DCM, 0.80 mL, 0.799 mmol, 3.05 eq.) was added dropwise and the reaction was stirred at rt for 18 h. It was then quenched carefully with MeOH, and the solvent was evaporated. The crude was purified by flash column chromatography (silica gel, 0 – 10 % DCM/MeOH) leading to the product **271** (49.2 mg, 0.192 mmol, 73 %) as an off-white solid.

^{1}H-NMR (400 MHz, DMSO) δ 11.71 (s, 1H), 9.41 (s, 1H), 8.07 (d, J = 5.1 Hz, 1H), 7.41 (dd, J = 3.5, 2.5 Hz, 1H), 7.11 (t, J = 7.8 Hz, 1H), 7.02 (d, J = 5.1 Hz, 1H), 6.91 – 6.83 (m, 2H), 6.65 (ddd, J = 8.2, 2.3, 1.1 Hz, 1H), 6.39 (dd, J = 3.5, 1.8 Hz, 1H), 4.34 (s, 2H). ^{13}C-NMR (101 MHz, DMSO) δ 157.4, 147.0, 142.5, 139.3, 138.1, 129.4, 125.3, 119.5, 117.3, 115.6, 114.3, 111.3, 98.1, 34.1. LC-MS: ESI(+) [*m/z*]: calcd. mass $[M+H]^+$ = 257.1; found = 257.0. HPLC: t_{ret} = 10.17 min (91.1 % at 254 nm, 94.6 % at 230 nm, method A).

3-(((1H-Pyrrolo[2,3-b]pyridin-4-yl)thio)methyl)phenyl sulfurofluoridate (273)

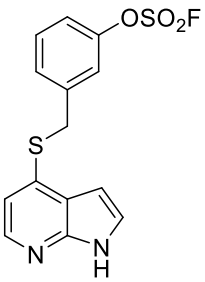

Chemical Formula: $C_{14}H_{11}FN_2O_3S_2$
Exact Mass: 338.01951
Molecular Weight: 338.37140

3-(((1*H*-Pyrrolo[2,3-*b*]pyridin-4-yl)thio)methyl)phenol (**271**, 43.0 mg, 0.168 mmol, 1.00 eq.) and AISF (**64**, 63.3 mg, 0.201 mmol, 1.20 eq.) were dissolved in DMF (1.5 mL). DBU (55.1 µL, 0.369 mmol, 2.20 eq.) was added and the reaction was stirred at rt for 16 h. Sat. NH_4Cl (10 mL) was added, and the solution was extracted with EtOAc (3 x 10 mL). After drying over Na_2SO_4 and evaporating the solvent, the residue was purified by flash column chromatography (silica gel, 0 – 100 % hexane/EtOAc) leading to the product **273** (10.8 mg, 31.9 µmol, 19 %) as a white solid.

^{1}H-NMR (400 MHz, MeOD) δ 8.02 (d, J = 5.3 Hz, 1H), 7.59 – 7.42 (m, 3H), 7.35 (d, J = 3.6 Hz, 1H), 7.31 (ddt, J = 8.2, 2.4, 1.1 Hz, 1H), 7.02 (d, J = 5.3 Hz, 1H), 6.51 (d, J = 3.5 Hz, 1H), 4.45 (s, 2H). ^{13}C-NMR (101 MHz, MeOD) δ 151.6, 147.8, 142.9, 142.1, 141.4, 131.7, 130.4, 126.5, 122.4, 120.8, 120.7, 113.9, 100.0, 35.6. ^{19}F NMR (376 MHz, MeOD) δ 35.6. HRMS: ESI(+) [*m/z*]: calcd. mass $[M+H]^+$ = 339.02679; found = 339.02688; rel. deviation 0.3 ppm. HPLC: t_{ret} = 17.54 min (89.0 % at 254 nm, 95.7 % at 230 nm, method B).

tert-Butyl 4-((4-methoxybenzyl)thio)-1H-pyrrolo[2,3-b]pyridine-1-carboxylate (270)

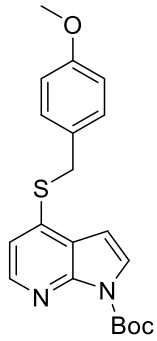

Chemical Formula: $C_{20}H_{22}N_2O_3S$
Exact Mass: 370.13511
Molecular Weight: 370.46700

tert-Butyl 4-bromo-1*H*-pyrrolo[2,3-*b*]pyridine-1-carboxylate (**252**, 250 mg, 0.841 mmol, 1.00 eq.) was dissolved in 1,4-dioxane (9 mL). (4-Methoxyphenyl)methanethiol (121 µL, 0.841 mmol, 1.00 eq), DIPEA (286 µL, 1.68 mmol, 2.00 eq.), Pd_2dba_3 (38.5 mg, 42.1 µmol, 0.05 eq.) and Xantphos (48.7 mg, 84.1 µmol, 0.10 eq.) were added and the reaction was stirred at 90 °C for 5 h. After cooling to rt, H_2O (20 mL) was added, and the solution was extracted with EtOAc (3 x 20 mL). The combined org. phases were dried over Na_2SO_4, the solvent was evaporated, and the residue was purified by flash column chromatography (silica gel, 0 – 60 % hexane/EtOAc) leading to the product **270** (300 mg, 0.810 mmol, 96 %) as an off-white solid.

^{1}H-NMR (400 MHz, $CDCl_3$) δ 8.34 (d, J = 5.2 Hz, 1H), 7.58 (d, J = 4.1 Hz, 1H), 7.35 – 7.26 (m, 2H), 7.03 (d, J = 5.3 Hz, 1H), 6.89 – 6.81 (m, 2H), 6.53 (d, J = 4.1 Hz, 1H), 4.26 (s, 2H), 3.79 (s, 3H), 1.66 (s, 9H). ^{13}C-NMR (101 MHz, $CDCl_3$) δ 159.3, 148.0, 147.5, 145.2, 141.6, 130.1, 127.8, 125.9, 121.3, 115.0, 114.3, 103.0, 84.3, 55.4, 35.7, 28.2. LC-MS: ESI(+) [*m/z*]: calcd. mass $[M+H]^+$ = 371.1; found = 371.2. HPLC: t_{ret} = 13.22 min (99.0 % at 254 nm, 97.1 % at 230 nm, method A).

4-(((1H-Pyrrolo[2,3-b]pyridin-4-yl)thio)methyl)phenol (272)

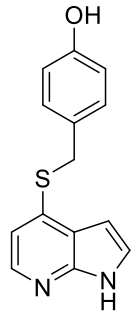

Chemical Formula: $C_{14}H_{12}N_2OS$
Exact Mass: 256.06703
Molecular Weight: 256.32300

tert-Butyl 4-((4-methoxybenzyl)thio)-1*H*-pyrrolo[2,3-*b*]pyridine-1-carboxylate (**270**, 300 mg, 0.810 mmol, 1.00 eq.) was dissolved in DCM (8 mL) and cooled to 0 °C. BBr_3 (1 M in DCM, 2.00 mL, 2.00 mmol, 2.47 eq.) was added dropwise and the reaction was stirred at rt for 2 h. It was then quenched carefully with MeOH, and the solvent was evaporated. The crude was purified by flash column chromatography (silica gel, 0 – 10 % DCM/MeOH) leading to the product **272** (133 mg, 0.519 mmol, 64 %) as a yellow solid.

^{1}H-NMR (400 MHz, DMSO) δ 11.67 (s, 1H), 9.38 (s, 1H), 8.07 (d, J = 5.1 Hz, 1H), 7.40 (dd, J = 3.5, 2.5 Hz, 1H), 7.29 – 7.21 (m, 2H), 7.03 (d, J = 5.1 Hz, 1H), 6.75 – 6.67 (m, 2H), 6.37 (dd, J = 3.5, 1.9 Hz, 1H), 4.31 (s, 2H). ^{13}C-NMR (101 MHz, DMSO) δ 156.6, 147.1, 142.5, 139.4, 130.0, 126.4, 125.2, 117.2, 115.2, 111.3, 98.1, 33.9. LC-MS: ESI(+) [*m/z*]: calcd. mass $[M+H]^+$ = 257.1; found = 257.1. HPLC: t_{ret} = 9.41 min (99.3 % at 254 nm, 96.9 % at 230 nm, method A).

4-(((1H-Pyrrolo[2,3-b]pyridin-4-yl)thio)methyl)phenyl sulfurofluoridate (274)

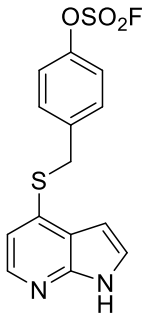

Chemical Formula: $C_{14}H_{11}FN_2O_3S_2$
Exact Mass: 338.01951
Molecular Weight: 338.37140

4-(((1*H*-Pyrrolo[2,3-*b*]pyridin-4-yl)thio)methyl)phenol (**272**, 61.0 mg, 0.238 mmol, 1.00 eq.) and AISF (**64**, 112 mg, 0.357 mmol, 1.50 eq.) were dissolved in DMF (2.5 mL). DBU (78.1 µL, 0.524 mmol, 2.20 eq.) was added and the reaction was stirred at rt for 16 h. Sat. NH_4Cl (10 mL) was added, and the solution was extracted with EtOAc (3 x 10 mL). After drying over Na_2SO_4 and evaporating the solvent, the residue was purified by reverse phase column chromatography (CHROMABOND® Flash RS 40 C18 ec, 10 – 55 % H_2O/MeCN, 0.2% TFA). The fractions containing product were lyophilised to afford the product **274** (TFA salt: 5.71 mg, 13.8 µmol, 3.9 %) as an off-white solid.

^{1}H-NMR (400 MHz, $CDCl_3$) δ 13.81 (s, 1H), 7.98 (d, J = 6.3 Hz, 1H), 7.62 – 7.54 (m, 2H), 7.46 (dd, J = 3.6, 1.7 Hz, 1H), 7.42 – 7.33 (m, 2H), 7.06 (d, J = 6.3 Hz, 1H), 6.69 (s, 1H), 4.48 (s, 2H). ^{13}C-NMR (101 MHz, $CDCl_3$) δ 151.4, 149.8, 139.1, 135.2, 132.0, 130.9, 128.2, 121.9, 109.9, 101.0, 35.0. ^{19}F NMR (376 MHz, $CDCl_3$) δ 38.0, -76.1. HRMS: ESI(+) [*m/z*]: calcd. mass $[M+H]^+$ = 339.02679; found = 339.02712; rel. deviation 1.0 ppm. HPLC: t_{ret} = 17.46 min (97.5 % at 254 nm, 97.0 % at 230 nm, method B).

3-Methoxy-N-(1H-pyrrolo[2,3-b]pyridin-4-yl)benzamide (276)

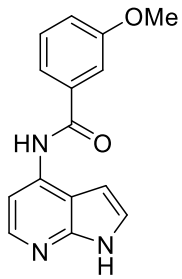

Chemical Formula: $C_{15}H_{13}N_3O_2$
Exact Mass: 267.10078
Molecular Weight: 267.28800

3-Methoxybenzoic acid (100 mg, 0.617 mmol, 1.00 eq.), 1*H*-pyrrolo[2,3-*b*]pyridin-4-amine (**275**, 131 mg, 0.986 mmol, 1.50 eq.) and HATU (500 mg, 1.31 mmol, 2.00 eq.) were dissolved in DMF (3.5 mL). DIPEA (335 µL, 1.97 mmol, 3.00 eq.) was added and the reaction was stirred at rt for 18 h. H_2O (15 mL) was added, and the solution was extracted with DCM (3 x 20 mL). The combined org. phases were dried over Na_2SO_4, the solvent was evaporated, and the residue was purified by flash column chromatography (silica gel, 20 – 100 % hexane/EtOAc) to yield the product **276** (102 mg, 0.381 mmol, 58 %) as an off-white solid.

^{1}H-NMR (400 MHz, DMSO) δ 11.91 (s, 1H), 10.38 (s, 1H), 8.37 (d, *J* = 4.9 Hz, 1H), 7.65 – 7.59 (m, 1H), 7.53 – 7.46 (m, 2H), 7.44 – 7.36 (m, 1H), 7.27 (t, *J* = 8.1 Hz, 1H), 6.76 (dd, *J* = 3.4, 1.9 Hz, 1H), 6.71 (ddd, *J* = 8.2, 2.6, 0.9 Hz, 1H), 3.77 (s, 3H). ^{13}C-NMR (101 MHz, DMSO) δ 165.4, 159.5, 149.6, 142.2, 140.2, 133.9, 129.4, 127.8, 117.3, 113.4, 112.5, 109.3, 106.0, 100.1, 55.0. LC-MS: ESI(+) [*m/z*]: calcd. mass $[M+H]^+$ = 268.3; found = 268.1. HPLC: t_{ret} = 9.33 min (98.7 % at 254 nm, 98.5 % at 230 nm, method A).

3-Hydroxy-N-(1H-pyrrolo[2,3-b]pyridin-4-yl)benzamide

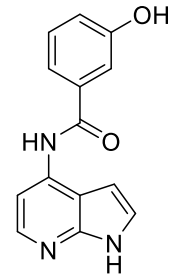

Chemical Formula: $C_{14}H_{11}N_3O_2$
Exact Mass: 253.08513
Molecular Weight: 253.26100

3-Methoxy-*N*-(1*H*-pyrrolo[2,3-*b*]pyridin-4-yl)benzamide (**276**, 90.0 mg, 0.337 mmol, 1.00 eq.) was dissolved in DCM (5 mL) and cooled to 0 °C. BBr_3 (1 M in DCM, 1.00 mL, 1.00 mmol, 2.98 eq.) was added dropwise and the reaction was stirred at rt for 18 h. It was then quenched carefully with MeOH, and the solvent was evaporated. The crude product, a beige solid, was used as is in the next step.

TLC-MS: ESI(-) [*m/z*]: calcd. mass $[M-H]^-$ = 252.1; found = 251.9.

3-((1H-Pyrrolo[2,3-b]pyridin-4-yl)carbamoyl)phenyl sulfurofluoridate (278)

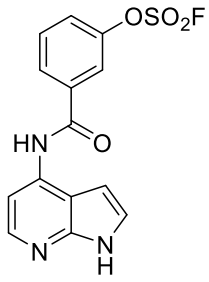

Chemical Formula: $C_{14}H_{10}FN_3O_4S$
Exact Mass: 335.03761
Molecular Weight: 335.30940

The crude from the previous step, 3-hydroxy-*N*-(1*H*-pyrrolo[2,3-*b*]pyridin-4-yl)benzamide, and AISF (**64**, 127 mg, 0.403 mmol, 1.20 eq.) were dissolved in DMF (3.5 mL). DBU (110 µL, 0.738 mmol, 2.20 eq.) was added and the reaction was stirred at rt for 7 h. Sat. $NaHCO_3$ (10 mL) was added, and the solution was extracted with DCM (3 x 10 mL). After drying over Na_2SO_4 and evaporating the solvent, the residue was purified by flash column chromatography (silica gel, 0 – 7 % DCM/MeOH) to yield the product **278** (36.0 mg, 0.107 mmol, 32 % over two steps) as a white solid.

^{1}H-NMR (400 MHz, MeOD) δ 8.20 – 8.15 (m, 1H), 8.13 (dt, J = 7.0, 1.7 Hz, 1H), 8.09 – 8.06 (m, 1H), 7.80 – 7.68 (m, 3H), 7.36 (d, J = 3.6 Hz, 1H), 6.74 (d, J = 3.6 Hz, 1H), 4.59 (s, 2H). ^{13}C-NMR (101 MHz, MeOD) δ 166.9, 151.5, 150.7, 143.9, 139.8, 138.7, 132.1, 129.4, 125.8, 125.6, 121.9, 114.3, 109.0, 100.0. ^{19}F NMR (376 MHz, MeOD) δ 36.3. HRMS: ESI(+) [*m/z*]: calcd. mass $[M+H]^+$ = 336.04488; found = 336.04526; rel. deviation 1.1 ppm. HPLC: t_{ret} = 13.40 min (97.8 % at 254 nm, 99.4 % at 230 nm, method B).

4-Methoxy-N-(1H-pyrrolo[2,3-b]pyridin-4-yl)benzamide (277)

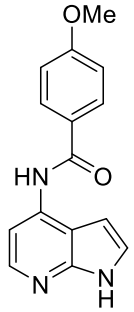

Chemical Formula: $C_{15}H_{13}N_3O_2$
Exact Mass: 267.10078
Molecular Weight: 267.28800

4-Methoxybenzoic acid (100 mg, 0.617 mmol, 1.00 eq.), 1*H*-pyrrolo[2,3-*b*]pyridin-4-amine (**275**, 131 mg, 0.986 mmol, 1.50 eq.) and HATU (500 mg, 1.31 mmol, 2.00 eq.) were dissolved in DMF (3.5 mL). DIPEA (335 µL, 1.97 mmol, 3.00 eq.) was added and the reaction was stirred at rt for 18 h. H_2O (15 mL) was added, and the solution was extracted with DCM (3 x 20 mL). The combined org. phases were dried over Na_2SO_4, the solvent was evaporated, and the residue was purified by flash column chromatography (silica gel, 0 – 6 % DCM/MeOH) to yield the product **277** (20.0 mg, 74.8 µmol, 11 %) as a white solid.

^{1}H-NMR (400 MHz, MeOD) δ 8.18 (d, J = 5.8 Hz, 1H), 8.04 – 7.93 (m, 2H), 7.84 (d, J = 5.8 Hz, 1H), 7.39 (d, J = 3.6 Hz, 1H), 7.12 – 7.04 (m, 2H), 6.84 (d, J = 3.6 Hz, 1H), 3.90 (s, 3H). ^{13}C-NMR (101 MHz, MeOD) δ 168.8, 164.8, 142.9, 141.2, 132.8, 131.3, 127.5, 126.2, 115.0, 114.7, 108.2, 100.8, 56.1. TLC-MS: ESI(+) [*m/z*]: calcd. mass $[M+Na]^+$ = 290.1; found = 290.0. HPLC: t_{ret} = 8.22 min (95.0 % at 254 nm, 97.1 % at 230 nm, method A).

4-Hydroxy-N-(1H-pyrrolo[2,3-b]pyridin-4-yl)benzamide

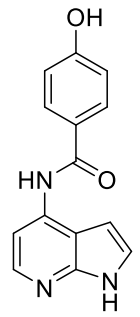

Chemical Formula: $C_{14}H_{11}N_3O_2$
Exact Mass: 253.08513
Molecular Weight: 253.26100

4-Methoxy-*N*-(1*H*-pyrrolo[2,3-*b*]pyridin-4-yl)benzamide (**277**, 20.0 mg, 74.8 µmol, 1.00 eq.) was dissolved in DCM (1 mL) and cooled to 0 °C. BBr_3 (1 M in DCM, 0.20 mL, 0.202 mmol, 2.70 eq.) was added dropwise and the reaction was stirred at rt for 18 h. It was then quenched carefully with MeOH, and the solvent was evaporated. The crude product, a beige solid, was used as is in the next step.

TLC-MS: ESI(-) [*m/z*]: calcd. mass $[M-H]^-$ = 252.1; found = 252.0.

4-((1H-Pyrrolo[2,3-b]pyridin-4-yl)carbamoyl)phenyl sulfurofluoridate (279)

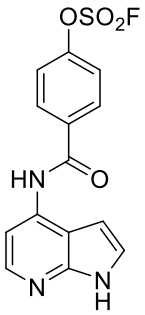

Chemical Formula: $C_{14}H_{10}FN_3O_4S$
Exact Mass: 335.03761
Molecular Weight: 335.30940

The crude from the previous step, 4-hydroxy-*N*-(1*H*-pyrrolo[2,3-*b*]pyridin-4-yl)benzamide, and AISF (**64**, 28.3 mg, 90.0 µmol, 1.20 eq.) were dissolved in DMF (1 mL). DBU (24.6 µL, 0.165 mmol, 2.20 eq.) was added and the reaction was stirred at rt for 5 h. H_2O (10 mL) was added, and the solution was extracted with EtOAc (3 x 10 mL). After drying over Na_2SO_4 and evaporating the solvent, the residue was purified by flash column chromatography (silica gel, 0 – 10 % DCM/MeOH) to yield the product **279** (7.30 mg, 21.8 µmol, 29 % over two steps) as a white solid.

^{1}H-NMR (400 MHz, MeOD) δ 8.21 – 8.13 (m, 3H), 7.74 (d, *J* = 5.5 Hz, 1H), 7.69 – 7.60 (m, 2H), 7.35 (d, *J* = 3.6 Hz, 1H), 6.75 (d, *J* = 3.6 Hz, 1H), 4.59 (s, 2H). ^{13}C-NMR (101 MHz, MeOD) δ 167.6, 153.6, 150.7, 143.9, 139.9, 136.8, 131.7, 125.7, 122.4, 114.9, 108.7, 99.9. ^{19}F NMR (376 MHz, MeOD) δ 36.5. HRMS: ESI(+) [*m/z*]: calcd. mass $[M+H]^+$ = 336.04488; found = 336.04545; rel. deviation 1.7 ppm. HPLC: t_{ret} = 16.16 min (93.2 % at 254 nm, 93.6 % at 230 nm, method B).

4-Iodo-N-(1H-pyrrolo[2,3-b]pyridin-4-yl)benzamide (280)

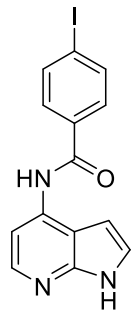

Chemical Formula: $C_{14}H_{10}IN_3O$
Exact Mass: 362.98686
Molecular Weight: 363.15847

4-Iodobenzoic acid (250 mg, 1.01 mmol, 1.00 eq.), 1*H*-pyrrolo[2,3-*b*]pyridin-4-amine (**275**, 201 mg, 1.51 mmol, 1.50 eq.) and HATU (767 mg, 2.02 mmol, 2.00 eq.) were dissolved in DMF (5 mL). DIPEA (519 µL, 3.05 mmol, 3.03 eq.) was added and the reaction was stirred at rt for 2 d. Sat. $NaHCO_3$ (20 mL) was added, and the solution was extracted with DCM (3 x 25 mL). The combined org. phases were dried over Na_2SO_4, the solvent was evaporated, and the residue was purified by flash column chromatography (silica gel, 0 – 10 % DCM/MeOH) to yield the product **280** (117 mg, 0.322 mmol, 32 %) as a light pink solid.

^{1}H-NMR (400 MHz, DMSO) δ 11.61 (s, 1H), 10.41 (s, 1H), 8.15 (d, J = 5.4 Hz, 1H), 7.99 – 7.91 (m, 2H), 7.81 – 7.72 (m, 2H), 7.66 (d, J = 5.4 Hz, 1H), 7.37 (dd, J = 3.5, 2.4 Hz, 1H), 6.77 (dd, J = 3.5, 1.9 Hz, 1H). ^{13}C-NMR (101 MHz, DMSO) δ 165.8, 149.9, 143.1, 137.9, 137.2, 134.1, 130.0, 124.2, 111.6, 107.0, 99.5, 99.0. TLC-MS: ESI(+) [*m/z*]: calcd. mass $[M+H]^+$ = 364.0; found = 363.8. HPLC: t_{ret} = 10.45 min (98.7 % at 254 nm, 99.4 % at 230 nm, method A).

tert-Butyl 4-(4-iodobenzamido)-1H-pyrrolo[2,3-b]pyridine-1-carboxylate (281)

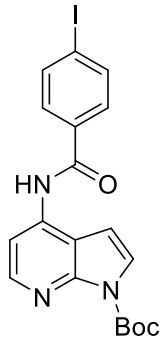

Chemical Formula: $C_{19}H_{18}IN_3O_3$
Exact Mass: 463.03929
Molecular Weight: 463.27547

4-Iodo-*N*-(1*H*-pyrrolo[2,3-*b*]pyridin-4-yl)benzamide (**280**, 111 mg, 0.306 mmol, 1.00 eq.) and DMAP (7.47 mg, 61.1 µmol, 0.20 eq.) were dissolved in DMF (1.5 mL). Boc_2O (77.2 µL, 0.336 mmol, 1.10 eq.) and TEA (84.7 µL, 0.611 mmol, 2.00 eq.) were added and the reaction was stirred at rt for 1 h. The solvent was then evaporated, and the residue was purified by flash column chromatography (silica gel, 0 – 50 % hexane/EtOAc) to yield the product **281** (52.0 mg, 0.122 mmol, 37 %) as a white solid.

^{1}H-NMR (400 MHz, $CDCl_3$) δ 8.49 (d, J = 5.5 Hz, 1H), 8.08 (s, 1H), 8.04 (d, J = 5.5 Hz, 1H), 7.93 – 7.85 (m, 2H), 7.68 – 7.60 (m, 3H), 6.53 (d, J = 4.2 Hz, 1H), 1.68 (s, 9H). ^{13}C-NMR (101 MHz, $CDCl_3$) δ 165.2, 149.5, 147.9, 146.8, 138.4, 137.8, 133.8, 128.8, 125.9, 113.4, 109.2, 100.3, 99.9, 84.6, 28.2. ASAP: APCI(+) [*m/z*]: calcd. mass $[M+H]^+$ = 464.0; found = 463.9. HPLC: t_{ret} = 12.42 min (98.9 % at 254 nm, 97.4 % at 230 nm, method A).

tert-Butyl 4-(4-(fluorosulfonyl)benzamido)-1H-pyrrolo[2,3-b]pyridine-1-carboxylate (282)

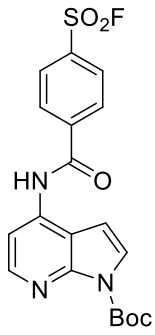

Chemical Formula: $C_{19}H_{18}FN_3O_5S$
Exact Mass: 419.09512
Molecular Weight: 419.42740

tert-Butyl 4-(4-iodobenzamido)-1*H*-pyrrolo[2,3-*b*]pyridine-1-carboxylate (**281**, 50.0 mg, 0.106 mmol, 1.00 eq.), DABSO (15.6 mg, 64.6 µmol, 0.60 eq.), $Pd(OAc)_2$ (1.21 mg, 5.40 µmol, 0.05 eq.) and cataCXium A (3.87 mg, 10.8 µmol, 0.10 eq.) were suspended in *i*PrOH (0.5 mL). TEA (45.0 µL, 0.325 mmol, 3.01 eq.) was added and the reaction was stirred at 75 °C for 6 h. After cooling to rt, Selectfluor (76.5 mg, 0.216 mmol, 2.00 eq.) and MeCN (0.5 mL) were added, and the reaction was stirred a further 1.5 h at rt. The solvent was evaporated, and the residue was purified by flash column chromatography (silica gel, 0 – 60 % hexane/EtOAc) to yield the product **282** (14.8 mg, 35.3 µmol, 33 %) as a beige solid.

^{1}H-NMR (400 MHz, $CDCl_3$) δ 8.50 (d, J = 5.5 Hz, 1H), 8.30 (s, 1H), 8.15 (s, 4H), 8.02 (d, J = 5.5 Hz, 1H), 7.66 (d, J = 4.2 Hz, 1H), 6.58 (d, J = 4.2 Hz, 1H), 1.67 (s, 9H). ^{13}C-NMR (101 MHz, $CDCl_3$) δ 163.9, 149.5, 147.8, 146.7, 141.0, 137.4, 136.2, 129.2, 128.7, 126.2, 113.7, 109.5, 100.5, 84.8, 28.2. ^{19}F NMR (376 MHz, $CDCl_3$) δ 66.0. LC-MS: ESI(+) [*m/z*]: calcd. mass $[M+H]^+$ = 420.1; found = 420.1. HPLC: t_{ret} = 11.92 min (96.1 % at 254 nm, 98.3 % at 230 nm, method A).

4-((1H-Pyrrolo[2,3-b]pyridin-4-yl)carbamoyl)benzenesulfonyl fluoride (283)

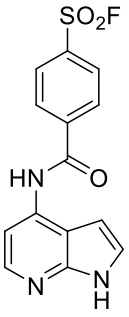

Chemical Formula: $C_{14}H_{10}FN_3O_3S$
Exact Mass: 319.04269
Molecular Weight: 319.31040

tert-Butyl 4-(4-(fluorosulfonyl)benzamido)-1*H*-pyrrolo[2,3-*b*]pyridine-1-carboxylate (**282**, 14.0 mg, 34.4 µmol, 1.00 eq.) was dissolved in DCM (5 mL) and TFA (5 mL). It was stirred at rt for 18 h and the solvent was evaporated. The resulting solid was washed with hexane to yield the product **283** (TFA salt: 9.00 mg, 20.8 µmol, 60 %) as a beige solid.

^{1}H-NMR (400 MHz, MeOD) δ 8.34 – 8.23 (m, 6H), 7.56 (d, J = 3.6 Hz, 1H), 7.13 (d, J = 3.7 Hz, 1H). ^{13}C-NMR (101 MHz, MeOD) δ 167.6, 145.3, 143.9, 142.3, 137.9, 130.9, 129.8, 127.5, 115.8, 107.8, 101.8, 68.1. ^{19}F NMR (376 MHz, MeOD) δ 63.7, -76.8. HRMS: ESI(+) [*m/z*]: calcd. mass $[M+H]^+$ = 320.04997; found = 320.05021; rel. deviation 0.8 ppm. HPLC: t_{ret} = 12.12 min (96.6 % at 254 nm, 97.2 % at 230 nm, method B).

2-Methoxy-N-(1H-pyrrolo[2,3-b]pyridin-5-yl)benzamide (285)

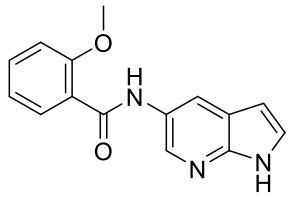

Chemical Formula: $C_{15}H_{13}N_3O_2$
Exact Mass: 267.10078
Molecular Weight: 267.28800

2-Methoxybenzoic acid (200 mg, 1.31 mmol, 1.00 eq.), 1*H*-pyrrolo[2,3-*b*]pyridin-5-amine (**284**, 263 mg, 1.97 mmol, 1.50 eq.) and HATU (1.00 g, 2.63 mmol, 2.00 eq.) were dissolved in DMF (6.5 mL). DIPEA (671 µL, 3.94 mmol, 3.00 eq.) was added and the reaction was stirred at rt for 18 h. Sat. $NaHCO_3$ (10 mL) was added, and the solution was extracted with DCM (3 x 15 mL). The combined org. phases were dried over Na_2SO_4, the solvent was evaporated, and the residue was purified by flash column chromatography (silica gel, 35 – 100 % hexane/EtOAc) to yield the product **285** (295 mg, 1.10 mmol, 84 %) as a white solid.

^{1}H-NMR (400 MHz, $CDCl_3$) δ 9.91 – 9.85 (m, 2H), 8.52 (d, J = 2.2 Hz, 1H), 8.42 (d, J = 2.3 Hz, 1H), 8.34 (dt, J = 7.9, 1.3 Hz, 1H), 7.52 (dddd, J = 8.2, 7.2, 1.9, 0.9 Hz, 1H), 7.36 (t, J = 2.7 Hz, 1H), 7.20 – 7.11 (m, 1H), 7.07 (d, J = 8.3 Hz, 1H), 6.51 (dd, J = 3.4, 1.7 Hz, 1H), 4.10 (s, 3H). ^{13}C-NMR (101 MHz, $CDCl_3$) δ 163.8, 157.4, 146.0, 137.2, 133.4, 132.7, 128.7, 126.1, 122.0, 121.9, 121.7, 120.3, 111.7, 101.4, 56.4. TLC-MS: ESI(+) [*m/z*]: calcd. mass $[M+H]^+$ = 268.1; found = 268.0. HPLC: t_{ret} = 9.80 min (99.8 % at 254 nm, 99.1 % at 230 nm, method A).

2-Hydroxy-N-(1H-pyrrolo[2,3-b]pyridin-5-yl)benzamide

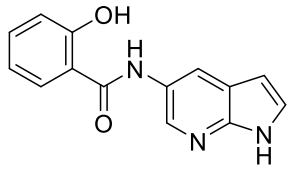

Chemical Formula: $C_{14}H_{11}N_3O_2$
Exact Mass: 253.08513
Molecular Weight: 253.26100

2-Methoxy-*N*-(1*H*-pyrrolo[2,3-*b*]pyridin-5-yl)benzamide (**285**, 283 mg, 1.06 mmol, 1.00 eq.) was dissolved in DCM (10 mL). BBr_3 (1 M in DCM, 3.20 mL, 3.20 mmol, 3.02 eq.) was added dropwise and the reaction was stirred at rt for 18 h. It was then quenched carefully with MeOH, and the solvent was evaporated. The crude product, a beige solid, was used like this in the next step.

LC-MS: ESI(+) calcd. for $[M+H]^+$: *m/z* = 254.1; found: 254.1.

2-((1H-Pyrrolo[2,3-b]pyridin-5-yl)carbamoyl)phenyl sulfurofluoridate (286)

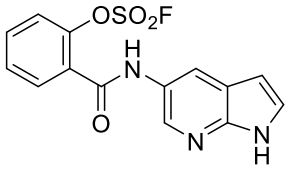

Chemical Formula: $C_{14}H_{10}FN_3O_4S$
Exact Mass: 335.03761
Molecular Weight: 335.30940

The crude product from the previous step, 2-Hydroxy-*N*-(1*H*-pyrrolo[2,3-*b*]pyridin-5-yl)benzamide, and AISF (**64**, 495 mg, 1.57 mmol, 1.20 eq.) were dissolved in DMF (6.5 mL). DBU (432 µL, 2.90 mmol, 2.21 eq.) was added and the reaction war stirred at rt for 18 h. Sat. NH_4Cl (15 mL) was added, and the solution was extracted with DCM (3 x 15 mL). The combined org. phases were dried over Na_2SO_4, the solvent was evaporated, and the residue was purified by flash column chromatography (silica gel, 0 – 50 % hexane/EtOAc) to yield the product **286** (112 mg, 0.334 mmol, 25 % over two steps) as a white solid.

^{1}H-NMR (400 MHz, $CDCl_3$) δ 8.60 (d, J = 2.3 Hz, 1H), 8.23 (dd, J = 7.8, 1.7 Hz, 1H), 8.12 (d, J = 2.3 Hz, 1H), 7.82 (ddd, J = 8.3, 7.5, 1.8 Hz, 1H), 7.68 (d, J = 4.1 Hz, 1H), 7.55 (td, J = 7.6, 1.1 Hz, 1H), 7.43 (dd, J = 8.3, 1.0 Hz, 1H), 6.83 (d, J = 4.1 Hz, 1H). ^{13}C-NMR (101 MHz, $CDCl_3$) δ 160.8, 150.5, 147.6, 146.7, 137.2, 131.8, 131.1, 128.7, 127.7, 125.7, 123.5, 118.8, 116.9, 107.7. ^{19}F NMR (376 MHz, $CDCl_3$) δ 56.6. HRMS: ESI(+) [*m/z*]: calcd. mass $[M+MeCN+Na]^+$ = 399.05338; found = 397.99146. HPLC: t_{ret} = 16.67 min (94.9 % at 254 nm, 89.4 % at 230 nm, method B).

3-Aminophenyl sulfurofluoridate (289)

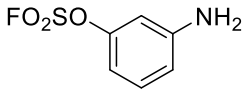

Chemical Formula: $C_6H_6FNO_3S$
Exact Mass: 191.00524
Molecular Weight: 191.17640

3-Aminophenol (**287**, 250 mg, 0.229 mmol, 1.00 eq.) and AISF (**64**, 864 mg, 0.275 mmol, 1.20 eq.) were dissolved in DMF (12 mL). DBU (752 µL, 0.504 mmol, 2.20 eq.) was added and the reaction was stirred at rt for 2 h. H_2O (15 mL) was added, and the solution was extracted with EtOAc (3 x 20 mL). After drying over Na_2SO_4 and evaporating the solvent, the residue was purified by flash column chromatography (silica gel, 0 – 50 % hexane/EtOAc) leading to the product **289** (313 mg, 1.64 mmol, 72 %) as a yellow oil.

^{1}H-NMR (400 MHz, $CDCl_3$) δ 7.20 (t, J = 8.2 Hz, 1H), 6.73 – 6.63 (m, 2H), 6.63 – 6.57 (m, 1H), 3.81 (s, 2H). ^{13}C-NMR (101 MHz, $CDCl_3$) δ 151.3, 148.6, 131.0, 115.0, 110.1, 107.0. LC-MS: ESI(+) [*m/z*]: calcd. mass $[M+H]^+$ = 192.0; found = 192.0. HPLC: t_{ret} = 9.73 min (99.6 % at 254 nm, 95.3 % at 230 nm, method A).

4-Aminophenyl sulfurofluoridate (290)

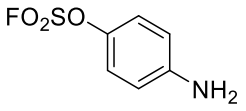

Chemical Formula: $C_6H_6FNO_3S$
Exact Mass: 191.00524
Molecular Weight: 191.17640

4-Aminophenol (**288**, 250 mg, 2.29 mmol, 1.00 eq.) and AISF (**64**, 864 mg, 2.75 mmol, 1.20 eq.) were dissolved in DMF (12 mL). DBU (752 µL, 5.04 mmol, 2.20 eq.) was added and the reaction was stirred at rt for 2 h. H_2O (15 mL) was added, and the solution was extracted with EtOAc (3 x 20 mL). After drying over Na_2SO_4 and evaporating the solvent, the residue was purified by flash column chromatography (silica gel, 0 – 50 % hexane/EtOAc) leading to the product **290** (287 mg, 1.50 mmol, 65 %) as a yellow oil.

^{1}H-NMR (400 MHz, $CDCl_3$) δ 7.15 – 7.06 (m, 2H), 6.72 – 6.63 (m, 2H), 3.82 (s, 2H). ^{13}C-NMR (101 MHz, $CDCl_3$) δ 146.8, 142.3, 121.9, 115.7. LC-MS: ESI(+) [*m/z*]: calcd. mass $[M+H]^+$ = 192.0; found = 192.0. HPLC: t_{ret} = 9.39 min (97.9 % at 254 nm, 95.5 % at 230 nm, method A).

N-(3-Methoxybenzyl)-1H-pyrrolo[2,3-b]pyridine-4-carboxamide (293)

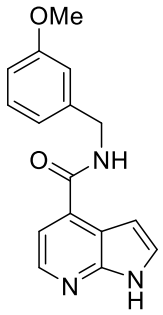

Chemical Formula: $C_{16}H_{15}N_3O_2$
Exact Mass: 281.11643
Molecular Weight: 281.31500

1*H*-Pyrrolo[2,3-*b*]pyridine-4-carboxylic acid (**291**, 250 mg, 1.54 mmol, 1.00 eq.) and HATU (1.17 g, 3.08 mmol, 2.00 eq.) were dissolved in DMF (8 mL). (3-Methoxyphenyl)methanamine (411 µL, 3.08 mmol, 2.00 eq.) and TEA (641 µL, 4.63 mmol, 3.00 eq.) were added and the reaction was stirred at rt for 17 h. Sat. $NaHCO_3$ (15 mL) was added, and the solution was extracted with DCM (3 x 20 mL). The combined org. phases were dried over Na_2SO_4, the solvent was evaporated, and the residue was purified by flash column chromatography (silica gel, 50 – 100 % hexane/EtOAc) to yield the product **293** (216 mg, 0.768 mmol, 50 %) as an off-white solid.

^{1}H-NMR (400 MHz, DMSO) δ 11.85 (s, 1H), 9.06 (t, J = 6.0 Hz, 1H), 8.31 (d, J = 4.9 Hz, 1H), 7.59 (dd, J = 3.4, 2.5 Hz, 1H), 7.41 (d, J = 5.0 Hz, 1H), 7.30 – 7.22 (m, 1H), 6.99 – 6.91 (m, 2H), 6.86 – 6.76 (m, 2H), 4.50 (d, J = 6.0 Hz, 2H), 3.74 (s, 3H). ^{13}C-NMR (101 MHz, DMSO) δ 166.3, 159.3, 149.6, 142.2, 141.2, 133.4, 129.4, 127.5, 119.4, 117.2, 113.1, 112.9, 112.1, 100.3, 54.9, 42.5. TLC-MS: ESI(+) [*m/z*]: calcd. mass $[M+Na]^+$ = 304.1; found = 304.0. HPLC: t_{ret} = 8.92 min (90.4 % at 254 nm, 95.1 % at 230 nm, method A).

N-(3-Hydroxybenzyl)-1H-pyrrolo[2,3-b]pyridine-4-carboxamide

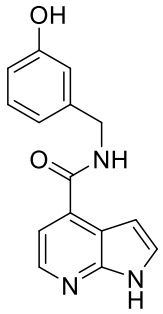

Chemical Formula: $C_{15}H_{13}N_3O_2$
Exact Mass: 267.10078
Molecular Weight: 267.28800

N-(3-Methoxybenzyl)-1*H*-pyrrolo[2,3-*b*]pyridine-4-carboxamide (**293**, 205 mg, 0.729 mmol, 1.00 eq.) was dissolved in DCM (7.5 mL) and cooled to 0 °C. BBr_3 (1 M in DCM, 2.20 mL, 2.20 mmol, 3.02 eq.) was added dropwise and the reaction was stirred at rt for 16 h. It was then quenched carefully with MeOH, and the solvent was evaporated. The crude product was used as is in the next step.

TLC-MS: ESI(+) [*m/z*]: calcd. mass $[M+Na]^+$ = 290.1; found = 289.9.

3-((1H-Pyrrolo[2,3-b]pyridine-4-carboxamido)methyl)phenyl sulfurofluoridate (295)

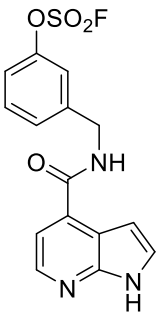

Chemical Formula: $C_{15}H_{12}FN_3O_4S$
Exact Mass: 349.05326
Molecular Weight: 349.33640

The crude from the previous step, *N*-(3-hydroxybenzyl)-1*H*-pyrrolo[2,3-*b*]pyridine-4-carboxamide (100 mg, 0.374 mmol, 1.00 eq.), and AISF (**64**, 141 mg, 0.449 mmol, 1.20 eq.) were dissolved in DMF (3.8 mL). DBU (123 µL, 0.823 mmol, 2.20 eq.) was added and the reaction was stirred at rt for 16 h. Sat. $NaHCO_3$ (15 mL) was added, and the solution was extracted with DCM (3 x 20 mL). After drying over Na_2SO_4 and evaporating the solvent, the residue was purified by flash column chromatography (silica gel, 0 – 10 % DCM/MeOH) to yield the product **295** (70.4 mg, 0.202 mmol, 54 %) as an off-white solid.

^{1}H-NMR (400 MHz, DMSO) δ 11.88 (s, 1H), 9.20 (t, *J* = 6.1 Hz, 1H), 8.35 – 8.30 (m, 1H), 7.62 – 7.59 (m, 1H), 7.59 – 7.55 (m, 2H), 7.52 (dt, *J* = 7.6, 1.2 Hz, 1H), 7.49 (dd, *J* = 8.1, 2.5 Hz, 1H), 7.43 (dd, *J* = 5.0, 1.2 Hz, 1H), 6.78 (dt, *J* = 3.4, 1.6 Hz, 1H), 4.60 (d, *J* = 5.9 Hz, 2H). ^{13}C-NMR (101 MHz, DMSO) δ 166.5, 149.8, 149.7, 143.2, 142.3, 133.1, 130.8, 127.9, 127.7, 119.5, 119.4, 117.2, 113.2, 100.3, 42.0. ^{19}F NMR (376 MHz, DMSO) δ 38.6. HRMS: ESI(+) [*m/z*]: calcd. mass $[M+H]^+$ = 350.06053; found = 350.06103; rel. deviation 1.4 ppm. HPLC: t_{ret} = 13.49 min (98.6 % at 254 nm, 97.9 % at 230 nm, method B).

N-(4-Methoxybenzyl)-1H-pyrrolo[2,3-b]pyridine-4-carboxamide (294)

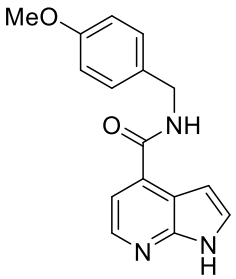

Chemical Formula: $C_{16}H_{15}N_3O_2$
Exact Mass: 281.11643
Molecular Weight: 281.31500

1*H*-Pyrrolo[2,3-*b*]pyridine-4-carboxylic acid (**291**, 100 mg, 0.617 mmol, 1.00 eq.) and HATU (469 mg, 1.23 mmol, 2.00 eq.) were dissolved in DMF (3 mL). (4-Methoxyphenyl)methanamine (160 µL, 1.23 mmol, 2.00 eq.) and TEA (257 µL, 1.85 mmol, 3.00 eq.) were added and the reaction was stirred at rt for 3 h. Sat. $NaHCO_3$ (15 mL) was added, and the solution was extracted with DCM (3 x 15 mL). The combined org. phases were dried over Na_2SO_4, the solvent was evaporated, and the residue was purified by flash column chromatography (silica gel, EtOAc) to yield the product **294** (56.0 mg, 0.199 mmol, 32 %) as an off-white solid.

^{1}H-NMR (400 MHz, DMSO) δ 11.88 (s, 1H), 9.04 (t, J = 6.0 Hz, 1H), 8.32 (s, 1H), 7.58 (dd, J = 3.4, 2.4 Hz, 1H), 7.40 (d, J = 4.9 Hz, 1H), 7.33 – 7.25 (m, 2H), 6.94 – 6.86 (m, 2H), 6.78 (dd, J = 3.5, 1.8 Hz, 1H), 4.45 (d, J = 6.0 Hz, 2H), 3.73 (s, 3H). ^{13}C-NMR (101 MHz, DMSO) δ 166.1, 158.2, 149.5, 142.1, 133.7, 131.5, 128.6, 127.6, 117.4, 113.7, 113.2, 100.4, 55.1, 42.0. TLC-MS: ESI(+) [*m/z*]: calcd. mass $[M+Na]^+$ = 304.1; found = 304.4. HPLC: t_{ret} = 8.87 min (98.3 % at 254 nm, 98.8 % at 230 nm, method A).

N-(4-Hydroxybenzyl)-1H-pyrrolo[2,3-b]pyridine-4-carboxamide

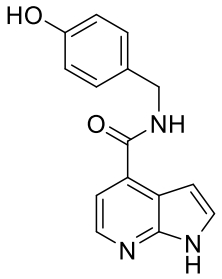

Chemical Formula: $C_{15}H_{13}N_3O_2$
Exact Mass: 267.10078
Molecular Weight: 267.28800

N-(4-Methoxybenzyl)-1*H*-pyrrolo[2,3-*b*]pyridine-4-carboxamide (**294**, 56.0 mg, 0.199 mmol, 1.00 eq.) was dissolved in DCM (2 mL) and cooled to 0 °C. BBr_3 (1 M in DCM, 0.50 mL, 0.498 mmol, 2.50 eq.) was added dropwise and the reaction was stirred at rt for 3 h. It was then quenched carefully with MeOH, and the solvent was evaporated. The crude product was used as is in the next step.

Conversion was ensured via HPLC. HPLC: t_{ret} = 6.35 min (method A).

4-((1H-Pyrrolo[2,3-b]pyridine-4-carboxamido)methyl)phenyl sulfurofluoridate (296)

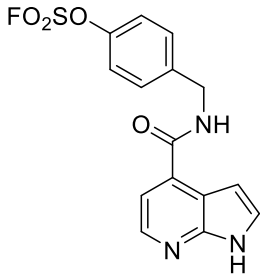

Chemical Formula: $C_{15}H_{12}FN_3O_4S$
Exact Mass: 349.05326
Molecular Weight: 349.33640

The crude from the previous step, *N*-(4-hydroxybenzyl)-1*H*-pyrrolo[2,3-*b*]pyridine-4-carboxamide, and AISF (**64**, 74.8 mg, 0.238 mmol, 1.20 eq.) were dissolved in DMF (2 mL). DBU (65.1 µL, 0.436 mmol, 2.20 eq.) was added and the reaction was stirred at rt for 16 h. Sat. NH_4Cl (10 mL) was added, and the solution was extracted with EtOAc (3 x 15 mL). After drying over Na_2SO_4 and evaporating the solvent, the residue was purified by flash column chromatography (silica gel, 0 – 10 % DCM/MeOH) to yield the product **296** (12.0 mg, 34.4 µmol, 17 % over two steps) as an off-white solid.

^{1}H-NMR (400 MHz, MeOD) δ 8.30 (d, J = 5.0 Hz, 1H), 7.65 – 7.56 (m, 2H), 7.53 (d, J = 3.5 Hz, 1H), 7.47 – 7.42 (m, 2H), 7.40 (d, J = 5.1 Hz, 1H), 6.83 (d, J = 3.5 Hz, 1H), 4.69 (s, 2H), 4.57 (s, 2H). ^{13}C-NMR (101 MHz, MeOD) δ 169.8, 150.7, 143.1, 141.4, 135.4, 130.8, 128.8, 122.2, 119.5, 114.5, 101.5, 43.7. ^{19}F NMR (376 MHz, MeOD) δ 35.4. HRMS: ESI(+) [*m/z*]: calcd. mass $[M+H]^+$ = 350.06053; found = 350.06076; rel. deviation 0.7 ppm. HPLC: t_{ret} = 13.58 min (94.9 % at 254 nm, 98.0 % at 230 nm, method B).

N-(4-Iodobenzyl)-1H-pyrrolo[2,3-b]pyridine-4-carboxamide (297)

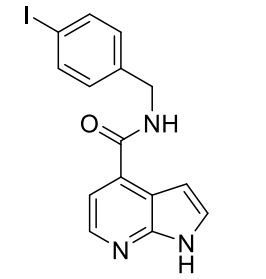

Chemical Formula: $C_{15}H_{12}IN_3O$
Exact Mass: 377.00251
Molecular Weight: 377.18547

1*H*-Pyrrolo[2,3-*b*]pyridine-4-carboxylic acid (**291**, 400 mg, 2.47 mmol, 1.00 eq.), (4-iodophenyl)methanamine (690 mg, 2.96 mmol, 1.20 eq.) and HATU (1.41 g, 3.70 mmol, 1.50 eq.) were dissolved in DMF (12 mL). DIPEA (839 µL, 4.93 mmol, 2.00 eq.) was added and the reaction was stirred at rt for 6 h. The solvent was evaporated, and the residue was purified by flash column chromatography (silica gel, 0 – 100 % hexane/EtOAc) to yield the product **297** (750 mg, 1.99 mmol, 81 %) as an off-white solid.

^{1}H-NMR (400 MHz, DMSO) δ 11.87 (s, 1H), 9.12 (t, J = 6.0 Hz, 1H), 8.34 – 8.29 (m, 1H), 7.74 – 7.63 (m, 2H), 7.58 (dd, J = 3.4, 2.4 Hz, 1H), 7.42 (d, J = 4.8 Hz, 1H), 7.22 – 7.14 (m, 2H), 6.78 (dd, J = 3.5, 1.7 Hz, 1H), 4.47 (d, J = 6.0 Hz, 2H). ^{13}C-NMR (101 MHz, DMSO) δ 166.3, 149.7, 142.2, 139.5, 137.1, 133.2, 129.7, 127.7, 117.3, 113.2, 100.3, 92.5, 42.1. ASAP: APCI(+) [*m/z*]: calcd. mass $[M+H]^+$ = 378.0; found = 377.9. HPLC: t_{ret} = 10.79 min (95.5 % at 254 nm, 93.9 % at 230 nm, method A).

tert-Butyl 4-((4-iodobenzyl)carbamoyl)-1H-pyrrolo[2,3-b]pyridine-1-carboxylate (298)

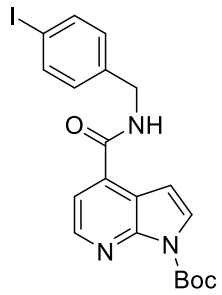

Chemical Formula: $C_{20}H_{20}IN_3O_3$
Exact Mass: 477.05494
Molecular Weight: 477.30247

N-(4-Iodobenzyl)-1*H*-pyrrolo[2,3-*b*]pyridine-4-carboxamide (**297**, 750 mg, 1.99 mmol, 1.00 eq.) and DMAP (48.6 mg, 0.398 mmol, 0.20 eq.) were dissolved in DMF (10 mL). Boc_2O (503 µL, 2.19 mmol, 1.10 eq.) and TEA (551 µL, 3.98 mmol, 2.00 eq.) were added and the reaction was stirred at rt for 2 h. H_2O (20 mL) was added, and the solution was extracted with DCM (3 x 25 mL). The org. phases were dried over Na_2SO_4, the solvent was evaporated, and the residue was purified by flash column chromatography (silica gel, 0 – 60 % hexane/EtOAc) to yield the product **298** (281 mg, 0.589 mmol, 30 %) as a white solid.

^{1}H-NMR (400 MHz, DMSO) δ 9.31 (t, *J* = 6.0 Hz, 1H), 8.51 (d, *J* = 5.0 Hz, 1H), 7.89 (d, *J* = 4.0 Hz, 1H), 7.75 – 7.67 (m, 2H), 7.62 (d, *J* = 5.0 Hz, 1H), 7.22 – 7.14 (m, 2H), 7.01 (d, *J* = 4.1 Hz, 1H), 4.47 (d, *J* = 5.9 Hz, 2H), 1.62 (s, 9H). ^{13}C-NMR (101 MHz, DMSO) δ 165.3, 148.4, 147.4, 144.5, 139.1, 137.1, 134.2, 129.7, 128.4, 120.5, 116.1, 104.8, 92.6, 83.8, 42.2, 27.6. LC-MS: ESI(+) [*m/z*]: calcd. mass $[M+H]^+$ = 478.1; found = 478.0. HPLC: t_{ret} = 12.59 min (95.9 % at 254 nm, 94.2 % at 230 nm, method A).

tert-Butyl 4-((4-(fluorosulfonyl)benzyl)carbamoyl)-1H-pyrrolo[2,3-b]pyridine-1-carboxylate

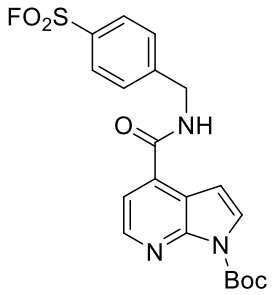

Chemical Formula: $C_{20}H_{20}FN_3O_5S$
Exact Mass: 433.11077
Molecular Weight: 433.45440

tert-Butyl 4-((4-iodobenzyl)carbamoyl)-1*H*-pyrrolo[2,3-*b*]pyridine-1-carboxylate (**298**, 262 mg, 0.549 mmol, 1.00 eq.), DABSO (79.1 mg, 0.329 mmol, 0.60 eq.), $Pd(OAc)_2$ (6.16 mg, 27.4 µmol, 0.05 eq.) and cataCXium A (19.7 mg, 54.9 µmol, 0.10 eq.) were suspended in *i*PrOH (2 mL). TEA (228 µL, 1.65 mmol, 3.00 eq.) was added and the reaction was stirred at 90 °C for 16 h. After cooling to rt, Selectfluor (389 mg, 1.10 mmol, 2.00 eq.) and MeCN (2 mL) were added, and the reaction was stirred a further 2 h at rt. The solution was filtered over celite, the solvent was evaporated, and the crude was used like this in the next step.

Conversion was ensured via HPLC. HPLC: t_{ret} = 11.76 min (method A).

4-((1H-Pyrrolo[2,3-b]pyridine-4-carboxamido)methyl)benzenesulfonyl fluoride (299)

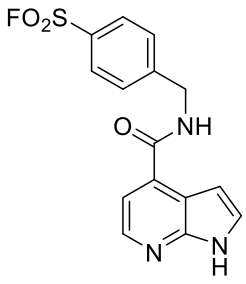

Chemical Formula: $C_{15}H_{12}FN_3O_3S$
Exact Mass: 333.05834
Molecular Weight: 333.33740

The crude from the previous step, *tert*-butyl 4-((4-(fluorosulfonyl)benzyl)carbamoyl)-1*H*-pyrrolo[2,3-*b*]pyridine-1-carboxylate was dissolved in DCM (10 mL) and TFA (10 mL). It was stirred at rt for 18 h and the solvent was evaporated. The residue was purified by flash column chromatography (silica gel, 0 – 7.5 % DCM/MeOH) to yield the product **299** (22.6 mg, 67.8 µmol, 12 % over two steps) as a white solid.

^{1}H-NMR (400 MHz, MeOD) δ 9.27 (s, 1H), 8.33 (d, J = 5.1 Hz, 1H), 8.11 – 8.02 (m, 2H), 7.85 – 7.73 (m, 2H), 7.55 (d, J = 3.5 Hz, 1H), 7.46 (d, J = 5.1 Hz, 1H), 6.86 (d, J = 3.5 Hz, 1H), 4.79 (d, J = 5.3 Hz, 2H). ^{13}C-NMR (101 MHz, MeOD) δ 169.7, 150.3, 149.4, 142.8, 135.5, 132.9 (d, J = 24.9 Hz), 129.9, 129.8, 129.0, 119.8, 114.5, 101.6, 44.1. ^{19}F NMR (376 MHz, MeOD) δ 64.2. HRMS: ESI(+) [*m/z*]: calcd. mass $[M+H]^+$ = 334.06562; found = 334.06585; rel. deviation 0.7 ppm. HPLC: t_{ret} = 12.31 min (89.8 % at 254 nm, 95.7 % at 230 nm, method B).

N-(4-Nitrophenyl)-1H-pyrrolo[2,3-b]pyridin-4-amine (300)

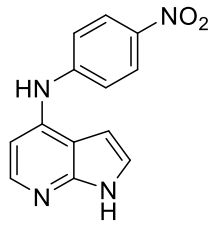

Chemical Formula: $C_{13}H_{10}N_4O_2$
Exact Mass: 254.08038
Molecular Weight: 254.24900

4-Bromo-1*H*-pyrrolo[2,3-*b*]pyridine (**242**, 1.00 g, 5.08 mmol, 1.00 eq.), 4-nitroaniline (1.05 g, 7.61 mmol, 1.50 eq.), Pd_2dba_3 (232 mg, 0.254 mmol, 0.05 eq.), XPhos (242 mg, 0.508 mmol, 0.10 eq.) and K_2CO_3 (2.10 g, 15.2 mmol, 3.00 eq.) were suspended in *t*BuOH (30 mL). The reaction was stirred at 80 °C for 16 h, after which the solvent was evaporated and the residue was purified by flash column chromatography (silica gel, 0 – 10 % DCM/MeOH) to yield the product **300** (815 mg, 3.21 mmol, 63 %) as an orange solid.

^{1}H-NMR (400 MHz, DMSO) δ 11.61 (s, 1H), 9.52 (s, 1H), 8.22 – 8.12 (m, 2H), 8.09 (d, J = 5.3 Hz, 1H), 7.38 – 7.30 (m, 3H), 6.97 (d, J = 5.3 Hz, 1H), 6.53 (dd, J = 3.5, 1.7 Hz, 1H). ^{13}C-NMR (101 MHz, DMSO) δ 150.1, 149.0, 143.6, 140.1, 139.5, 125.7, 123.9, 116.4, 111.0, 103.3, 98.3. LC-MS: ESI(+) [*m/z*]: calcd. mass $[M+H]^+$ = 255.1; found = 255.1. HPLC: t_{ret} = 6.38 min (95.6 % at 254 nm, 97.1 % at 230 nm, method A).

N^1-(1H-Pyrrolo[2,3-b]pyridin-4-yl)benzene-1,4-diamine (301)

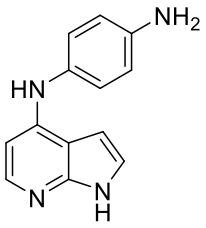

Chemical Formula: $C_{13}H_{12}N_4$
Exact Mass: 224.10620
Molecular Weight: 224.26700

N-(4-Nitrophenyl)-1*H*-pyrrolo[2,3-*b*]pyridin-4-amine (**300**, 815 mg, 3.21 mmol, 1.00 eq.) was dissolved in MeOH (45 mL). Palladium on carbon (100 mg) was suspended in EtOAc (2 mL) and added to the first solution. H_2 was bubbled through the solution and the reaction was stirred under H_2 atmosphere for 18 h. The reaction mixture was filtered over celite, and the solvent was evaporated to afford the product **301** (717 mg, 3.18 mmol, 99 %) as a brown solid.

^{1}H-NMR (400 MHz, DMSO) δ 11.13 (s, 1H), 8.09 (s, 1H), 7.75 (d, J = 5.5 Hz, 1H), 7.10 – 7.03 (m, 1H), 6.99 – 6.91 (m, 2H), 6.64 – 6.56 (m, 2H), 6.51 (dd, J = 3.4, 1.3 Hz, 1H), 6.24 (d, J = 5.5 Hz, 1H), 4.95 (s, 2H). ^{13}C-NMR (101 MHz, DMSO) δ 149.5, 146.1, 145.5, 143.9, 129.1, 125.1, 121.0, 114.4, 107.6, 98.1, 96.9. LC-MS: ESI(+) [*m/z*]: calcd. mass $[M+H]^+$ = 225.1; found = 225.1. HPLC: t_{ret} = 2.96 min (95.5 % at 254 nm, 95.0 % at 230 nm, method A).

Ethyl 3-((fluorosulfonyl)oxy)benzoate (304)

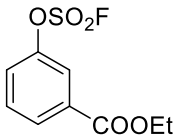

Chemical Formula: $C_9H_9FO_5S$
Exact Mass: 248.01547
Molecular Weight: 248.22440

Ethyl 3-hydroxybenzoate (**302**, 750 mg, 4.51 mmol, 1.00 eq.) and AISF (**64**, 1.70 g, 5.42 mmol, 1.20 eq.) were dissolved in THF (23 mL). DBU (1.50 mL, 10.1 mmol, 2.23 eq.) was added and the reaction was stirred at rt for 5 h. Sat. NH_4Cl (35 mL) was added, and the solution was extracted with EtOAc (3 x 40 mL). After drying over Na_2SO_4 and evaporating the solvent, the residue was purified by flash column chromatography (silica gel, 0 – 30 % hexane/EtOAc) to afford the product **304** (985 mg, 3.97 mmol, 88 %) as a colorless oil.

^{1}H-NMR (400 MHz, $CDCl_3$) δ 8.11 (dt, J = 7.4, 1.5 Hz, 1H), 8.04 – 7.98 (m, 1H), 7.62 – 7.50 (m, 2H), 4.42 (q, J = 7.2 Hz, 2H), 1.42 (t, J = 7.2 Hz, 3H). ^{13}C-NMR (101 MHz, $CDCl_3$) δ 164.7, 150.1, 133.5, 130.6, 129.9, 125.3, 122.2, 61.9, 14.4. LC-MS: ESI(+) [*m/z*]: calcd. mass $[M+Na]^+$ = 271.0; found = 271.0. HPLC: t_{ret} = 12.03 min (92.8 % at 254 nm, 98.9 % at 230 nm, method A).

3-((Fluorosulfonyl)oxy)benzoic acid (306)

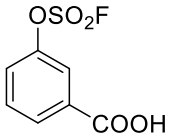

Chemical Formula: $C_7H_5FO_5S$
Exact Mass: 219.98417
Molecular Weight: 220.17040

Ethyl 3-((fluorosulfonyl)oxy)benzoate (**304**, 985 mg, 3.97 mmol, 1.00 eq.) was dissolved in aq. HCl (1 M, 50 mL) and HCl in dioxane (4 M, 5 mL). The reaction was refluxed for 16 h and subsequently the solvent was evaporated to afford the product **306** (658 mg, 2.99 mmol, 75 %) as a white solid.

^{1}H-NMR (400 MHz, DMSO) δ 13.55 (s, 1H), 8.11 – 8.01 (m, 2H), 7.89 (ddt, J = 8.3, 2.2, 1.0 Hz, 1H), 7.75 (t, J = 8.0 Hz, 1H). ^{13}C-NMR (101 MHz, DMSO) δ 165.5, 149.5, 133.6, 131.4, 129.9, 125.5, 121.5. LC-MS: ESI(-) [*m/z*]: calcd. mass $[M-H]^-$ = 219.0; found = 219.0. HPLC: t_{ret} = 10.33 min (89.8 % at 254 nm, 91.2 % at 230 nm, method A).

3-((4-((1H-Pyrrolo[2,3-b]pyridin-4-yl)amino)phenyl)carbamoyl)phenyl sulfurofluoridate (308)

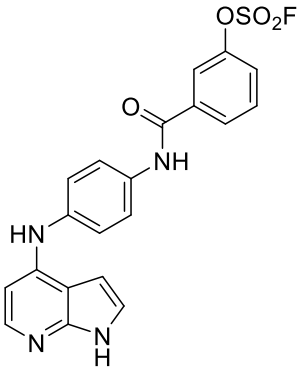

Chemical Formula: $C_{20}H_{15}FN_4O_4S$
Exact Mass: 426.07980
Molecular Weight: 426.42240

3-((Fluorosulfonyl)oxy)benzoic acid (**306**, 34.0 mg, 0.154 mmol, 1.00 eq.), *N*^{1}-(1*H*-pyrrolo[2,3-*b*]pyridin-4-yl)benzene-1,4-diamine (**301**, 38.1 mg, 0.170 mmol, 1.10 eq.) and HATU (117 mg, 0.309 mmol, 2.00 eq.) were dissolved in DMF (1 mL). DIPEA (78.8 µL, 0.463 mmol, 3.00 eq.) was added and the reaction was stirred at rt for 6 h. H_2O (10 mL) was added, and the aq. phase was extracted with DCM (3 x 15 mL). The combined org. phases were dried over Na_2SO_4, the solvent was evaporated, and the residue was purified by flash column chromatography (silica gel, 50 – 100 % hexane/EtOAc) to afford the product **308** (21.7 mg, 50.9 µmol, 33 %) as a yellow solid.

^{1}H-NMR (400 MHz, MeOD) δ 8.10 (dt, J = 7.4, 1.5 Hz, 1H), 8.06 – 8.02 (m, 1H), 7.87 (d, J = 5.8 Hz, 1H), 7.77 – 7.65 (m, 4H), 7.39 – 7.31 (m, 2H), 7.16 (d, J = 3.6 Hz, 1H), 6.72 (d, J = 5.8 Hz, 1H), 6.61 (d, J = 3.6 Hz, 1H). ^{13}C-NMR (101 MHz, MeOD) δ 166.1, 151.6, 149.1, 147.5, 143.5, 139.1, 138.9, 135.3, 132.1, 129.0, 125.2, 123.6, 123.4, 123.2, 121.5, 110.6, 99.7, 99.6. ^{19}F NMR (376 MHz, MeOD) δ 36.2. HRMS: ESI(+) [*m/z*]: calcd. mass $[M+H]^+$ = 427.08708; found = 427.08735; rel. deviation 0.6 ppm. HPLC: t_{ret} = 9.30 min (96.5 % at 254 nm, 96.9 % at 230 nm, method A).

Ethyl 4-((fluorosulfonyl)oxy)benzoate (305)

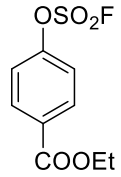

Chemical Formula: $C_9H_9FO_5S$
Exact Mass: 248.01547
Molecular Weight: 248.22440

Ethyl 4-hydroxybenzoate (**303**, 150 mg, 0.903 mmol, 1.00 eq.) and AISF (**64**, 341 mg, 1.08 mmol, 1.20 eq.) were dissolved in DMF (5 mL). DBU (296 µL, 1.99 mmol, 2.20 eq.) was added and the reaction was stirred at rt for 5 h. Sat. NH_4Cl (15 mL) was added, and the solution was extracted with EtOAc (3 x 20 mL). After drying over Na_2SO_4 and evaporating the solvent, the residue was purified by flash column chromatography (silica gel, 0 – 30 % hexane/EtOAc) to afford the product **305** (179 mg, 0.721 mmol, 80 %) as a colorless oil.

^{1}H-NMR (400 MHz, $CDCl_3$) δ 8.22 – 8.13 (m, 2H), 7.46 – 7.37 (m, 2H), 4.41 (q, J = 7.1 Hz, 2H), 1.41 (t, J = 7.1 Hz, 3H). ^{13}C-NMR (101 MHz, $CDCl_3$) δ 165.0, 153.0, 132.2, 131.2, 121.0, 61.8, 14.4. LC-MS: ESI(+) [*m/z*]: calcd. mass $[M+Na]^+$ = 271.0; found = 271.0. HPLC: t_{ret} = 11.90 min (97.8 % at 254 nm, 98.9 % at 230 nm, method A).

4-((Fluorosulfonyl)oxy)benzoic acid (307)

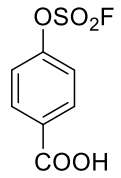

Chemical Formula: $C_7H_5FO_5S$
Exact Mass: 219.98417
Molecular Weight: 220.17040

Ethyl 4-((fluorosulfonyl)oxy)benzoate (**305**, 179 mg, 0.721 mmol, 1.00 eq.) was dissolved in aq. HCl (1 M, 10 mL) and HCl in dioxane (4 M, 1 mL). The reaction was refluxed for 16 h and subsequently the solvent was evaporated to afford the product **307** (133 mg, 0.604 mmol, 84 %) as a white solid.

^{1}H-NMR (400 MHz, DMSO) δ 13.35 (s, 1H), 8.17 – 8.09 (m, 2H), 7.73 (d, J = 8.4 Hz, 2H). ^{13}C-NMR (101 MHz, DMSO) δ 165.8, 152.2, 132.0, 131.6, 121.4. LC-MS: ESI(-) [*m/z*]: calcd. mass $[M-H]^-$ = 219.0; found = 219.0. HPLC: t_{ret} = 10.21 min (78.5 % at 254 nm, 97.8 % at 230 nm, method A).

4-((4-((1H-Pyrrolo[2,3-b]pyridin-4-yl)amino)phenyl)carbamoyl)phenyl sulfurofluoridate (309)

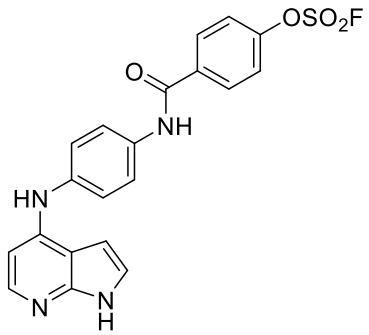

Chemical Formula: $C_{20}H_{15}FN_4O_4S$
Exact Mass: 426.07980
Molecular Weight: 426.42240

4-((Fluorosulfonyl)oxy)benzoic acid (**307**, 35.0 mg, 0.159 mmol, 1.00 eq.), *N*[1]-(1*H*-pyrrolo[2,3-*b*]pyridin-4-yl)benzene-1,4-diamine (**301**, 39.2 mg, 0.175 mmol, 1.10 eq.) and HATU (121 mg, 0.318 mmol, 2.00 eq.) were dissolved in DMF (1 mL). DIPEA (81.1 µL, 0.477 mmol, 3.00 eq.) was added and the reaction was stirred at rt for 18 h. H_2O (10 mL) was added, and the aq. phase was extracted with DCM (3 x 15 mL). The combined org. phases were dried over Na_2SO_4, the solvent was evaporated, and the residue was purified by flash column chromatography (silica gel, 25 – 100 % hexane/EtOAc) to afford the product **309** (7.20 mg, 16.9 µmol, 11 %) as a yellow solid.

^{1}H-NMR (400 MHz, acetone) δ 8.26 – 8.17 (m, 2H), 7.99 – 7.92 (m, 1H), 7.89 – 7.81 (m, 2H), 7.74 – 7.68 (m, 2H), 7.39 – 7.31 (m, 2H), 7.23 (d, J = 3.6 Hz, 1H), 6.74 (dd, J = 5.5, 2.9 Hz, 1H), 6.59 (d, J = 3.5 Hz, 1H). ^{13}C-NMR (101 MHz, DMSO) δ 177.1, 163.8, 151.2, 149.7, 143.9, 139.7, 137.2, 136.0, 131.9, 130.4, 127.4, 121.9, 121.3, 121.2, 112.4, 108.6, 98.2. ^{19}F NMR (376 MHz, acetone) δ 37.2. HRMS: ESI(+) [*m/z*]: calcd. mass $[M+H]^+$ = 427.08708; found = 427.08772; rel. deviation 1.5 ppm. HPLC: t_{ret} = 12.01 min (98.8 % at 254 nm, 99.6 % at 230 nm, method B).

6.2.4. Synthesis of Putative ACVR1 Inhibitors

tert-Butyl (4-((4-nitrophenyl)amino)pyridin-2-yl)carbamate (311)

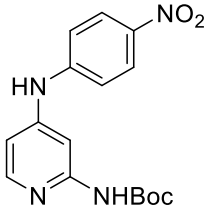

Chemical Formula: $C_{16}H_{18}N_4O_4$
Exact Mass: 330.13281
Molecular Weight: 330.34400

tert-Butyl (4-bromopyridin-2-yl)carbamate (**310**, 500 mg, 1.83 mmol, 1.00 eq.), 4-nitroaniline (379 mg, 2.75 mmol, 1.50 eq.), Pd_2dba_3 (83.8 mg, 91.5 µmol, 0.05 eq.), XantPhos (106 mg, 0.183 mmol, 0.10 eq.) and Cs_2CO_3 (1.79 g, 5.49 mmol, 3.00 eq.) were suspended in 1,4-dioxane (9 mL). The reaction was stirred at 95 °C for 18 h. After cooling to rt, H_2O (15 mL) was added, and the reaction was extracted with DCM (3 x 15 mL). The org. phase was dried over Na_2SO_4, the solvent was evaporated, and the residue was purified by flash column chromatography (silica gel, 0 – 7 % DCM/MeOH) to yield the product **311** (525 mg, 1.59 mmol, 87 %) as a yellow solid.

^{1}H-NMR (400 MHz, DMSO) δ 9.68 (d, J = 10.2 Hz, 2H), 8.22 – 8.14 (m, 2H), 8.07 (d, J = 5.7 Hz, 1H), 7.68 (d, J = 2.2 Hz, 1H), 7.35 – 7.26 (m, 2H), 6.86 (dd, J = 5.7, 2.1 Hz, 1H), 1.47 (s, 9H). ^{13}C-NMR (101 MHz, DMSO) δ 153.6, 152.7, 149.1, 148.8, 148.1, 140.0, 125.7, 116.6, 107.0, 99.9, 79.5, 28.0. TLC-MS: ESI(+) [*m/z*]: calcd. mass $[M+Na]^+$ = 353.1; found = 353.1. HPLC: t_{ret} = 8.79 min (99.5 % at 254 nm, 99.4 % at 230 nm, method A).

tert-Butyl (4-((4-aminophenyl)amino)pyridin-2-yl)carbamate (312)

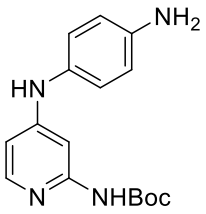

Chemical Formula: $C_{16}H_{20}N_4O_2$
Exact Mass: 300.15863
Molecular Weight: 300.36200

tert-Butyl (4-((4-nitrophenyl)amino)pyridin-2-yl)carbamate (**311**, 510 mg, 1.54 mmol, 1.00 eq.) was dissolved in MeOH (20 mL). Palladium on carbon (100 mg) was suspended in EtOAc (2 mL) and added to the first solution. H_2 was bubbled through the solution and the reaction was stirred under H_2 atmosphere for 16 h. The reaction mixture was filtered over celite, the solvent was evaporated to afford the product **312** (330 mg, 1.10 mmol, 71 %) as a brown solid.

^{1}H-NMR (400 MHz, DMSO) δ 9.63 (s, 1H), 8.23 (s, 1H), 7.77 (d, J = 5.8 Hz, 1H), 7.25 – 7.20 (m, 1H), 6.85 (d, J = 8.1 Hz, 2H), 6.57 (d, J = 8.2 Hz, 2H), 6.33 – 6.27 (m, 1H), 4.95 (s, 2H), 1.44 (s, 9H). ^{13}C-NMR (101 MHz, DMSO) δ 154.0, 153.1, 152.6, 147.6, 145.5, 128.6, 124.4, 114.5, 103.7, 95.1, 79.1, 28.1. TLC-MS: ESI(+) [*m/z*]: calcd. mass $[M+H]^+$ = 301.2; found = 301.0. HPLC: t_{ret} = 5.27 min (90.5 % at 254 nm, 91.6 % at 230 nm, method A).

3-((4-((2-((tert-Butoxycarbonyl)amino)pyridin-4-yl)amino)phenyl)carbamoyl)phenyl sulfurofluoridate (313)

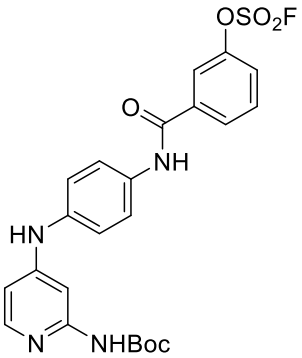

Chemical Formula: $C_{23}H_{23}FN_4O_6S$
Exact Mass: 502.13223
Molecular Weight: 502.51740

3-((Fluorosulfonyl)oxy)benzoic acid (**306**, 120 mg, 0.545 mmol, 1.00 eq.), *tert*-butyl (4-((4-aminophenyl)amino)pyridin-2-yl)carbamate (**312**, 180 mg, 0.600 mmol, 1.10 eq.) and HATU (311 mg, 0.818 mmol, 2.00 eq.) were dissolved in DMF (3 mL). DIPEA (278 µL, 1.64 mmol, 3.00 eq.) was added and the reaction was stirred at rt for 24 h. Sat. NH_4Cl (10 mL) was added, and the aq. phase was extracted with DCM (3 x 15 mL). The combined org. phases were dried over Na_2SO_4, the solvent was evaporated, and the residue was purified by flash column chromatography (silica gel, 0 – 100 % hexane/EtOAc) to afford the product **313** (251 mg, 0.499 mmol, 92 %) as an off-white solid.

^{1}H-NMR (400 MHz, DMSO) δ 10.41 (s, 1H), 9.46 (s, 1H), 8.81 (s, 1H), 8.13 (td, J = 3.5, 1.6 Hz, 2H), 7.90 – 7.82 (m, 2H), 7.79 (d, J = 8.1 Hz, 1H), 7.77 – 7.69 (m, 2H), 7.43 (d, J = 2.1 Hz, 1H), 7.24 – 7.16 (m, 2H), 6.57 (dd, J = 5.8, 2.2 Hz, 1H), 1.45 (s, 9H). ^{13}C-NMR (101 MHz, DMSO) δ 163.1, 153.0, 152.6, 152.1, 149.5, 147.8, 137.6, 136.7, 133.6, 131.1, 128.3, 124.0, 121.6, 120.9, 120.2, 104.7, 96.3, 79.3, 28.0. TLC-MS: ESI(+) [*m/z*]: calcd. mass $[M+H]^+$ = 503.1; found = 503.0. HPLC: t_{ret} = 10.42 min (98.3 % at 254 nm, 99.2 % at 230 nm, method A).

3-((4-((2-Aminopyridin-4-yl)amino)phenyl)carbamoyl)phenyl sulfurofluoridate (314)

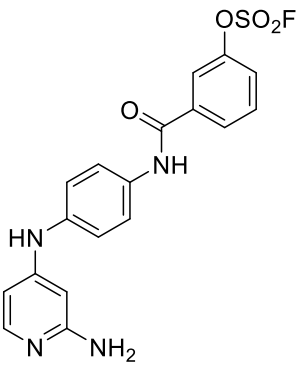

Chemical Formula: $C_{18}H_{15}FN_4O_4S$
Exact Mass: 402.07980
Molecular Weight: 402.40040

3-((4-((2-((*tert*-Butoxycarbonyl)amino)pyridin-4-yl)amino)phenyl)carbamoyl)phenyl sulfurofluoridate (**313**, 193 mg, 0.384 mmol, 1.00 eq.) was dissolved in DCM (10 mL) and TFA (2 mL). The reaction was stirred at 4 h. The solvent was evaporated, and the residue was purified by flash column chromatography (silica gel, 0 – 10 % DCM/MeOH) to afford the product **314** (TFA salt: 130 mg, 0.252 mmol, 66 %) as a white solid.

^{1}H-NMR (400 MHz, DMSO) δ 10.57 (s, 1H), 9.64 (s, 1H), 8.17 – 8.10 (m, 2H), 7.90 – 7.82 (m, 3H), 7.79 (t, J = 8.2 Hz, 1H), 7.62 (d, J = 7.2 Hz, 1H), 7.32 – 7.23 (m, 4H), 6.35 (dd, J = 7.3, 2.3 Hz, 1H), 6.11 (d, J = 2.3 Hz, 1H). ^{13}C-NMR (101 MHz, DMSO) δ 163.4, 155.4, 154.3, 149.5, 137.4, 136.1, 136.1, 131.2, 128.4, 124.3, 123.8, 121.6, 120.3, 102.6, 87.5. ^{19}F NMR (376 MHz, DMSO) δ 39.3, -73.6. HRMS: ESI(+) [*m/z*]: calcd. mass $[M+H]^+$ = 403.08700; found = 403.0880; rel. deviation 2.5 ppm. HPLC: t_{ret} = 10.94 min (95.6 % at 254 nm, 96.4 % at 230 nm, method B).

Methyl 4-((1H-pyrrolo[2,3-b]pyridin-4-yl)amino)benzoate (315)

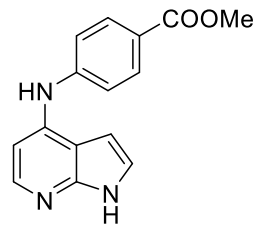

Chemical Formula: $C_{15}H_{13}N_3O_2$
Exact Mass: 267.10078
Molecular Weight: 267.28800

4-Bromo-1*H*-pyrrolo[2,3-*b*]pyridine (**242**, 500 mg, 2.54 mmol, 1.00 eq.), methyl 4-aminobenzoate (575 mg, 3.81 mmol, 1.50 eq.), Pd_2dba_3 (116 mg, 0.127 mmol, 0.05 eq.), XPhos (121 mg, 0.254 mmol, 0.10 eq.) and K_2CO_3 (1.16 g, 7.61 mmol, 3.00 eq.) were suspended in *t*BuOH (17 mL). The reaction was stirred at 80 °C for 16 h, after which the solvent was evaporated and the residue was purified by flash column chromatography (silica gel, 0 – 10 % DCM/MeOH) to yield the product **315** (546 mg, 2.04 mmol, 80 %) as a yellow solid.

^{1}H-NMR (400 MHz, DMSO) δ 11.49 (s, 1H), 9.09 (s, 1H), 8.02 (d, J = 5.4 Hz, 1H), 7.95 – 7.86 (m, 2H), 7.37 – 7.31 (m, 2H), 7.29 (dd, J = 3.5, 1.9 Hz, 1H), 6.90 (d, J = 5.5 Hz, 1H), 6.57 (dd, J = 3.6, 1.4 Hz, 1H), 3.82 (s, 3H). ^{13}C-NMR (101 MHz, DMSO) δ 165.9, 150.0, 146.6, 143.7, 141.3, 130.7, 123.1, 121.3, 117.4, 110.2, 101.4, 98.3, 51.7. TLC-MS: ESI(+) [*m/z*]: calcd. mass $[M+H]^+$ = 268.1; found = 268.0. HPLC: t_{ret} = 7.21 min (99.8 % at 254 nm, 99.8 % at 230 nm, method A).

4-((1H-Pyrrolo[2,3-b]pyridin-4-yl)amino)benzoic acid (316)

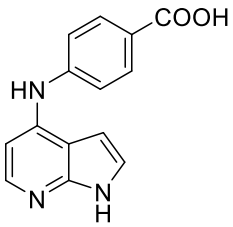

Chemical Formula: $C_{14}H_{11}N_3O_2$
Exact Mass: 253.08513
Molecular Weight: 253.26100

Methyl 4-((1*H*-pyrrolo[2,3-*b*]pyridin-4-yl)amino)benzoate (**315**, 529 mg, 1.98 mmol, 1.00 eq.) and LiOH (142 mg, 5.94 mmol, 3.00 eq.) were dissolved in H_2O (10 mL) and THF (10 mL). The reaction was stirred at rt for 16 h. The org. solvent was then removed, and the aq. solution was acidified with aq. HCl (1 M). The resulting precipitate was filtered off and washed with H_2O to afford the product **316** (498 mg, 1.97 mmol, quant.) as an off-white solid.

^{1}H-NMR (400 MHz, DMSO) δ 12.94 (s, 1H), 12.60 (s, 1H), 10.66 (s, 1H), 8.12 – 7.99 (m, 3H), 7.58 – 7.50 (m, 2H), 7.48 – 7.38 (m, 1H), 7.04 (dd, J = 3.6, 1.4 Hz, 1H), 6.94 (d, J = 6.9 Hz, 1H). ^{13}C-NMR (101 MHz, DMSO) δ 166.7, 149.0, 142.5, 138.5, 135.2, 130.8, 127.2, 124.4, 122.6, 110.2, 101.1, 98.9. ASAP: APCI(+) [*m/z*]: calcd. mass $[M+H]^+$ = 254.1; found = 253.9. HPLC: t_{ret} = 4.95 min (97.8 % at 254 nm, 99.1 % at 230 nm, method A).

3-(4-((1H-Pyrrolo[2,3-b]pyridin-4-yl)amino)benzamido)phenyl sulfurofluoridate (317)

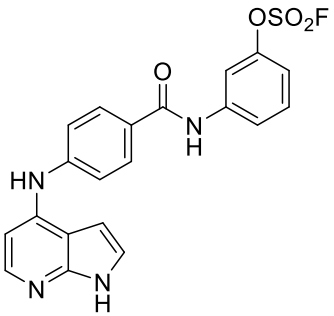

Chemical Formula: $C_{20}H_{15}FN_4O_4S$
Exact Mass: 426.07980
Molecular Weight: 426.42240

4-((1*H*-Pyrrolo[2,3-*b*]pyridin-4-yl)amino)benzoic acid (**316**, 100 mg, 0.395 mmol, 1.00 eq.), 3-aminophenyl sulfurofluoridate (**289**, 98.1 mg, 0.513 mmol, 1.30 eq.) and HATU (225 mg, 0.592 mmol, 2.00 eq.) were dissolved in DMF (2 mL). DIPEA (202 µL, 1.18 mmol, 3.00 eq.) was added and the reaction was stirred at rt for 18 h. H_2O (10 mL) was added, and the aq. phase was extracted with DCM (3 x 15 mL). The combined org. phases were dried over Na_2SO_4, the solvent was evaporated, and the residue was purified by preparative HPLC (10 – 60 % H_2O/MeCN, 0.1 % TFA) to afford the product **317** (TFA salt: 13.8 mg, 25.5 µmol, 6.5 %) as a white solid.

^{1}H-NMR (400 MHz, DMSO) δ 12.46 (s, 1H), 10.67 (s, 1H), 10.35 (s, 1H), 8.18 – 8.07 (m, 4H), 7.88 (ddd, J = 8.3, 2.0, 0.9 Hz, 1H), 7.64 – 7.53 (m, 3H), 7.46 (dd, J = 3.5, 2.2 Hz, 1H), 7.34 (dd, J = 8.3, 2.6 Hz, 1H), 6.94 – 6.87 (m, 2H). ^{13}C-NMR (101 MHz, DMSO) δ 165.1, 149.6, 149.1, 141.7, 141.2, 139.0, 135.7, 130.9, 130.8, 129.4, 124.5, 122.7, 120.4, 115.7, 112.1, 110.0, 100.7, 98.9. ^{19}F NMR (376 MHz, DMSO) δ 38.7, -73.9. HRMS: ESI(+) [*m/z*]: calcd. mass $[M+H]^+$ = 427.08700; found = 427.0867; rel. deviation 0.7 ppm. HPLC: t_{ret} = 12.71 min (98.7 % at 254 nm, 98.4 % at 230 nm, method B).

N-(3-Fluoro-4-nitrophenyl)-1H-pyrrolo[2,3-b]pyridin-4-amine (318)

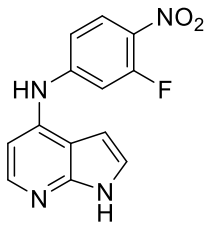

Chemical Formula: $C_{13}H_9FN_4O_2$
Exact Mass: 272.07095
Molecular Weight: 272.23940

4-Bromo-1*H*-pyrrolo[2,3-*b*]pyridine (**242**, 400 mg, 2.03 mmol, 1.00 eq.), 3-fluoro-4-nitroaniline (475 mg, 3.05 mmol, 1.50 eq.), Pd_2dba_3 (93.0 mg, 0.102 mmol, 0.05 eq.), XPhos (96.8 mg, 0.203 mmol, 0.10 eq.) and K_2CO_3 (842 mg, 6.09 mmol, 3.00 eq.) were suspended in *t*BuOH (14 mL). The reaction was stirred at 80 °C for 18 h, after which the solvent was evaporated and the residue was purified by flash column chromatography (silica gel, 0 – 10 % DCM/MeOH) to yield the product **318** (466 mg, 1.71 mmol, 84 %) as a yellow solid.

^{1}H-NMR (400 MHz, DMSO) δ 11.63 (s, 1H), 9.31 (d, J = 1.4 Hz, 1H), 8.17 (dd, J = 11.4, 2.6 Hz, 1H), 8.09 (d, J = 5.3 Hz, 1H), 8.03 (ddd, J = 9.0, 2.6, 0.9 Hz, 1H), 7.38 – 7.28 (m, 2H), 6.80 (dd, J = 5.3, 1.0 Hz, 1H), 6.38 (dd, J = 3.5, 1.6 Hz, 1H). ^{13}C-NMR (101 MHz, DMSO) δ 151.8 (d, J = 246.5 Hz), 150.6, 144.0, 140.5, 140.2 (d, J = 8.1 Hz), 138.1 (d, J = 11.4 Hz), 124.6, 121.7 (d, J = 2.6 Hz), 118.8 (d, J = 3.4 Hz), 112.4 (d, J = 23.9 Hz), 111.7, 105.5, 99.2. TLC-MS: ESI(+) [*m/z*]: calcd. mass $[M+H]^+$ = 273.1; found = 272.9. HPLC: t_{ret} = 6.51 min (99.9 % at 254 nm, 99.7 % at 230 nm, method A).

3-Fluoro-N^1-(1H-pyrrolo[2,3-b]pyridin-4-yl)benzene-1,4-diamine (320)

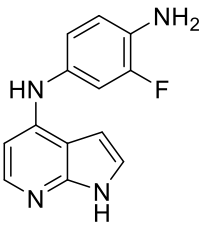

Chemical Formula: $C_{13}H_{11}FN_4$
Exact Mass: 242.09677
Molecular Weight: 242.25740

N-(3-Fluoro-4-nitrophenyl)-1*H*-pyrrolo[2,3-*b*]pyridin-4-amine (**318**, 445 mg, 1.63 mmol, 1.00 eq.) was dissolved in MeOH (15 mL). Palladium on carbon (100 mg) was suspended in EtOAc (2 mL) and added to the first solution. H_2 was bubbled through the solution and the reaction was stirred under H_2 atmosphere for 18 h. The reaction mixture was filtered over celite, the solvent was evaporated, and the residue was purified by flash column

chromatography (silica gel, 0 – 10 % DCM/MeOH) to afford the product **320** (349 mg, 1.44 mmol, 88 %) as a beige solid.

^{1}H-NMR (400 MHz, DMSO) δ 11.18 (s, 1H), 7.96 (s, 1H), 7.75 (d, J = 5.5 Hz, 1H), 7.09 (d, J = 3.5 Hz, 1H), 7.00 (t, J = 8.8 Hz, 1H), 6.50 – 6.39 (m, 3H), 5.94 (dd, J = 5.5, 1.5 Hz, 1H), 5.38 (s, 2H). ^{13}C-NMR (101 MHz, DMSO) δ 148.5 (d, *J* = 242.8 Hz), 139.5, 138.6 (d, J = 10.9 Hz), 136.9, 133.8, 119.6 (d, J = 3.4 Hz), 111.3, 105.2 (d, J = 13.3 Hz), 100.0 (d, J = 2.5 Hz), 97.4, 90.9 (d, J = 23.1 Hz), 88.1, 87.3. TLC-MS: ESI(+) [*m/z*]: calcd. mass $[M+H]^+$ = 243.1; found = 242.9. HPLC: t_{ret} = 3.57 min (99.3 % at 254 nm, 99.6 % at 230 nm, method A).

3-((4-((1H-Pyrrolo[2,3-b]pyridin-4-yl)amino)-2-fluorophenyl)carbamoyl)phenyl sulfurofluoridate (322)

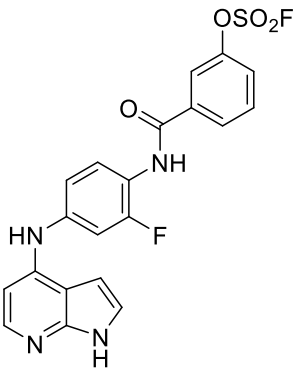

Chemical Formula: $C_{20}H_{14}F_2N_4O_4S$
Exact Mass: 444.07038
Molecular Weight: 444.41281

3-((Fluorosulfonyl)oxy)benzoic acid (**306**, 80.0 mg, 0.363 mmol, 1.00 eq.), 3-Fluoro-*N*^{1}-(1*H*-pyrrolo[2,3-*b*]pyridin-4-yl)benzene-1,4-diamine (**320**, 96.8 mg, 0.400 mmol, 1.10 eq.) and HATU (276 mg, 0.727 mmol, 2.00 eq.) were dissolved in DMF (2 mL). DIPEA (185 µL, 1.09 mmol, 3.00 eq.) was added and the reaction was stirred at rt for 18 h. H_2O (10 mL) was added, and the aq. phase was extracted with DCM (3 x 15 mL). The combined org. phases were dried over Na_2SO_4, the solvent was evaporated, and the residue was purified by preparative HPLC (10 – 70 % H_2O/MeCN, 0.1 % TFA) to afford the product **322** (TFA salt: 15.4 mg, 31.9 µmol, 8.8 %) as an off-white solid.

^{1}H-NMR (400 MHz, DMSO) δ 11.54 (s, 1H), 10.66 (s, 1H), 8.81 (s, 1H), 8.17 – 8.10 (m, 2H), 7.96 – 7.84 (m, 3H), 7.81 (t, J = 8.2 Hz, 1H), 7.60 (dd, J = 8.7, 2.3 Hz, 1H), 7.44 (t, J = 8.9 Hz, 1H), 7.23 (d, J = 3.5 Hz, 1H), 6.58 (d, J = 3.5 Hz, 1H), 6.25 (dd, J = 5.8, 1.9 Hz, 1H). ^{13}C-NMR (101 MHz, DMSO) δ 163.6, 157.2, 154.8, 149.5, 146.3, 141.7, 137.3, 137.1 (d, J = 9.7 Hz), 131.2, 128.4, 127.2, 124.4, 123.2 (d, J = 12.9 Hz), 122.5, 120.4, 116.6, 108.4 (d, J = 17.9 Hz), 98.7, 98.4. ^{19}F NMR (376 MHz, DMSO) δ 39.3, -69.2, -71.1. HRMS: ESI(+) [*m/z*]: calcd. mass $[M+H]^+$ = 445.07758; found = 445.0773; rel. deviation 0.6 ppm. HPLC: t_{ret} = 12.54 min (96.9 % at 254 nm, 97.0 % at 230 nm, method B).

N-(2-Fluoro-4-nitrophenyl)-1H-pyrrolo[2,3-b]pyridin-4-amine (319)

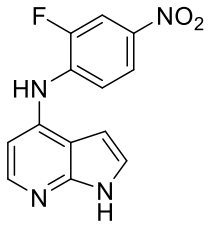

Chemical Formula: $C_{13}H_9FN_4O_2$
Exact Mass: 272.07095
Molecular Weight: 272.23940

4-Bromo-1*H*-pyrrolo[2,3-*b*]pyridine (**242**, 400 mg, 2.03 mmol, 1.00 eq.), 2-fluoro-4-nitroaniline (475 mg, 3.05 mmol, 1.50 eq.), Pd_2dba_3 (93.0 mg, 0.102 mmol, 0.05 eq.), XPhos (96.8 mg, 0.203 mmol, 0.10 eq.) and K_2CO_3 (842 mg, 6.09 mmol, 3.00 eq.) were suspended in *t*BuOH (14 mL). The reaction was stirred at 80 °C for 18 h, after which the solvent was evaporated and the residue was purified by flash column chromatography (silica gel, 0 – 10 % DCM/MeOH) to yield the product **319** (395 mg, 1.45 mmol, 72 %) as a yellow solid.

^{1}H-NMR (400 MHz, DMSO) δ 11.69 (s, 1H), 9.73 (s, 1H), 8.17 – 8.06 (m, 2H), 7.39 (dd, J = 3.5, 2.3 Hz, 1H), 7.16 – 7.06 (m, 2H), 7.01 (d, J = 5.4 Hz, 1H), 6.50 (dd, J = 3.5, 1.7 Hz, 1H). ^{13}C-NMR (101 MHz, DMSO) δ 156.9 (d, *J* = 260.1 Hz), 150.4 (d, *J* = 11.8 Hz), 150.1, 143.6, 139.3, 128.2, 128.1 (d, *J* = 6.5 Hz), 124.4, 112.2 (d, *J* = 2.2 Hz), 111.4, 104.3, 103.6 (d, *J* = 24.9 Hz), 98.2. TLC-MS: ESI(+) [*m/z*]: calcd. mass $[M+H]^+$ = 273.1; found = 272.9. HPLC: t_{ret} = 6.72 min (98.7 % at 254 nm, 97.5 % at 230 nm, method A).

2-Fluoro-N^1-(1H-pyrrolo[2,3-b]pyridin-4-yl)benzene-1,4-diamine (321)

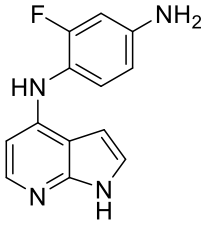

Chemical Formula: $C_{13}H_{11}FN_4$
Exact Mass: 242.09677
Molecular Weight: 242.25740

N-(2-Fluoro-4-nitrophenyl)-1*H*-pyrrolo[2,3-*b*]pyridin-4-amine (**319**, 375 mg, 1.38 mmol, 1.00 eq.) was dissolved in MeOH (15 mL). Palladium on carbon (100 mg) was suspended in EtOAc (2 mL) and added to the first solution. H_2 was bubbled through the solution and the reaction was stirred under H_2 atmosphere for 18 h. The reaction mixture was filtered over celite, the solvent was evaporated, and the residue was purified by flash column chromatography (silica gel, 0 – 10 % DCM/MeOH) to afford the product **321** (273 mg, 1.13 mmol, 82 %) as a violet solid.

^{1}H-NMR (400 MHz, DMSO) δ 11.24 (s, 1H), 8.27 (s, 1H), 7.81 (d, J = 5.5 Hz, 1H), 7.13 (d, J = 3.5 Hz, 1H), 6.93 (dd, J = 12.8, 2.3 Hz, 1H), 6.86 (dd, J = 8.5, 2.3 Hz, 1H), 6.83 – 6.74 (m, 1H), 6.53 (d, J = 3.4 Hz, 1H), 6.37 (d, J = 5.5 Hz, 1H), 4.98 (s, 2H). ^{13}C-NMR (101 MHz, DMSO) δ 150.5 (d, J = 238.0 Hz), 149.6, 145.3, 143.9, 132.6 (d, J = 13.1 Hz), 129.8 (d, J = 8.6 Hz), 121.5, 119.7 (d, J = 2.9 Hz), 116.4 (d, J = 5.7 Hz), 110.6 (d, J = 19.9 Hz), 107.9, 98.1, 97.2. TLC-MS: ESI(+) [*m/z*]: calcd. mass $[M+H]^+$ = 243.1; found = 243.0. HPLC: t_{ret} = 3.93 min (94.5 % at 254 nm, 93.7 % at 230 nm, method A).

3-((4-((1H-Pyrrolo[2,3-b]pyridin-4-yl)amino)-3-fluorophenyl)carbamoyl)phenyl sulfurofluoridate (323)

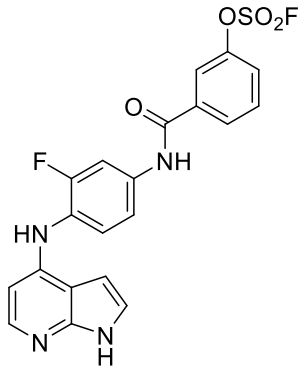

Chemical Formula: $C_{20}H_{14}F_2N_4O_4S$
Exact Mass: 444.07038
Molecular Weight: 444.41281

3-((Fluorosulfonyl)oxy)benzoic acid (**306**, 80.0 mg, 0.363 mmol, 1.00 eq.), 2-Fluoro-*N*[1]-(1*H*-pyrrolo[2,3-*b*]pyridin-4-yl)benzene-1,4-diamine (**321**, 96.8 mg, 0.400 mmol, 1.10 eq.) and HATU (276 mg, 0.727 mmol, 2.00 eq.) were dissolved in DMF (2 mL). DIPEA (185 µL, 1.09 mmol, 3.00 eq.) was added and the reaction was stirred at rt for 18 h. H_2O (10 mL) was added, and the aq. phase was extracted with DCM (3 x 15 mL). The combined org. phases were dried over Na_2SO_4, the solvent was evaporated, and the residue was purified by flash column chromatography (silica gel, 0 – 100 % hexane/EtOAc) to afford the product **323** (15.1 mg, 34.0 µmol, 9.4 %) as a white solid.

^{1}H-NMR (400 MHz, DMSO) δ 12.41 (s, 1H), 10.47 (s, 1H), 10.24 (s, 1H), 8.19 – 8.12 (m, 2H), 8.08 (d, J = 6.9 Hz, 1H), 7.94 – 7.86 (m, 1H), 7.86 – 7.77 (m, 1H), 7.73 (t, J = 8.6 Hz, 1H), 7.47 – 7.39 (m, 2H), 7.34 – 7.26 (m, 1H), 6.88 – 6.79 (m, 2H). ^{13}C-NMR (101 MHz, DMSO) δ 163.6, 157.0, 154.6, 149.6 (d, J = 5.6 Hz), 138.8, 136.8 (d, J = 9.7 Hz), 136.4, 135.7, 131.3, 128.6, 127.8, 124.6, 124.2, 122.8 (d, J = 12.5 Hz), 120.5, 119.9, 111.7 (d, J = 22.6 Hz), 109.5, 100.6, 98.5. ^{19}F NMR (376 MHz, DMSO) δ 39.3, -73.7. HRMS: ESI(+) [*m/z*]: calcd. mass $[M+H]^+$ = 445.07758; found = 445.0785; rel. deviation 2.1 ppm. HPLC: t_{ret} = 11.69 min (95.3 % at 254 nm, 95.8 % at 230 nm, method B).

Methyl 3-hydroxy-5-methylbenzoate (326)

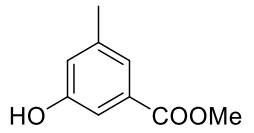

Chemical Formula: $C_9H_{10}O_3$
Exact Mass: 166.06299
Molecular Weight: 166.17600

3-Hydroxy-5-methylbenzoic acid (**324**, 500 mg, 3.29 mmol, 1.00 eq.) was dissolved in MeOH (6.5 mL) and conc. H_2SO_4 (16.0 µL, 0.164 mmol, 0.05 eq.) was added. The reaction was refluxed for 20 h and then neutralized with aq. NaOH (2 M). The solvent was evaporated leading to the product **326** (532 mg, 3.20 mmol, 97 %) as an off-white solid.

^{1}H-NMR (400 MHz, DMSO) δ 9.69 (s, 1H), 7.24 – 7.19 (m, 1H), 7.15 (ddd, J = 2.2, 1.5, 0.6 Hz, 1H), 6.84 (ddd, J = 2.3, 1.5, 0.8 Hz, 1H), 3.80 (s, 3H), 2.27 (s, 3H). ^{13}C-NMR (101 MHz, DMSO) δ 166.3, 157.4, 139.4, 130.6, 120.8, 120.5, 112.9, 52.0, 20.8. LC-MS: ESI(+) [*m/z*]: calcd. mass $[M+H]^+$ = 167.1; found = 167.1. HPLC: t_{ret} = 9.57 min (97.2 % at 254 nm, 95.7 % at 230 nm, method A).

Methyl 3-((fluorosulfonyl)oxy)-5-methylbenzoate (333)

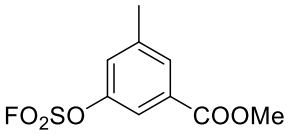

Chemical Formula: $C_9H_9FO_5S$
Exact Mass: 248.01547
Molecular Weight: 248.22440

Methyl 3-hydroxy-5-methylbenzoate (**326**, 525 mg, 3.16 mmol, 1.00 eq.) and AISF (**64**, 1.19 g, 3.79 mmol, 1.20 eq.) were dissolved in THF (15 mL). DBU (1.00 mL, 6.73 mmol, 2.13 eq.) was added and the reaction was stirred at rt for 16 h. Sat. NH_4Cl (25 mL) was added, and the solution was extracted with DCM (3 x 30 mL). After drying over Na_2SO_4 and evaporating the solvent, the residue was purified by flash column chromatography (silica gel, 0 – 30 % hexane/EtOAc) to afford the product **333** (269 mg, 1.08 mmol, 34 %) as a colorless oil.

^{1}H-NMR (400 MHz, $CDCl_3$) δ 7.95 – 7.89 (m, 1H), 7.83 – 7.77 (m, 1H), 7.37 – 7.31 (m, 1H), 3.94 (s, 3H), 2.47 (s, 3H). ^{13}C-NMR (101 MHz, $CDCl_3$) δ 165.4, 150.0, 141.6, 132.6, 130.6, 125.8, 119.2, 52.8, 21.4. ASAP: APCI(+) [*m/z*]: calcd. mass $[M+H]^+$ = 249.0; found = 248.7. HPLC: t_{ret} = 12.08 min (94.3 % at 254 nm, 95.2 % at 230 nm, method A).

3-((Fluorosulfonyl)oxy)-5-methylbenzoic acid (340)

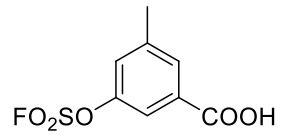

Chemical Formula: $C_8H_7FO_5S$
Exact Mass: 233.99982
Molecular Weight: 234.19740

Methyl 3-((fluorosulfonyl)oxy)-5-methylbenzoate (**333**, 269 mg, 1.08 mmol, 1.00 eq.) was dissolved in aq. HCl (1 M, 10 mL) and HCl in dioxane (4 M, 2 mL) and was refluxed for 18 h. The solvent was evaporated and the crude product, an off-white solid, was used in the next step without further purification.

LC-MS: ESI(-) [*m/z*]: calcd. mass $[M-H]^-$ = 233.0; found = 233.1.

3-((4-((1H-Pyrrolo[2,3-b]pyridin-4-yl)amino)phenyl)carbamoyl)-5-methylphenyl sulfurofluoridate (349)

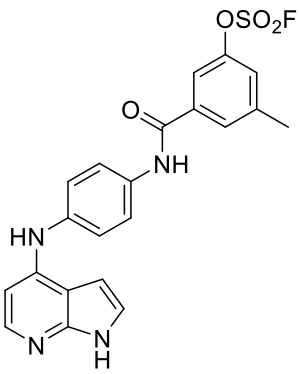

Chemical Formula: $C_{21}H_{17}FN_4O_4S$
Exact Mass: 440.09545
Molecular Weight: 440.44940

3-((Fluorosulfonyl)oxy)-5-methylbenzoic acid (**340**, 120 mg, 0.512 mmol, 1.00 eq.), *N*^{1}-(1*H*-pyrrolo[2,3-*b*]pyridin-4-yl)benzene-1,4-diamine (**301**, 126 mg, 0.564 mmol, 1.10 eq.) and HATU (292 mg, 0.769 mmol, 1.50 eq.) were dissolved in DMF (2.5 mL). DIPEA (174 µL, 1.02 mmol, 2.00 eq.) was added and the reaction was stirred at rt for 18 h. H_2O (10 mL) was added, and the aq. phase was extracted with DCM (3 x 15 mL). The combined org. phases were dried over Na_2SO_4, the solvent was evaporated, and the residue was

purified by preparative HPLC (10 – 60 % H_2O/MeCN, 0.1 % TFA) to afford the product **349** (TFA salt: 101 mg, 0.195 mmol, 38 %) as a white solid.

^{1}H-NMR (400 MHz, DMSO) δ 12.39 (s, 1H), 10.57 (s, 1H), 10.19 (s, 1H), 8.02 (d, *J* = 6.9 Hz, 1H), 7.99 – 7.96 (m, 1H), 7.96 – 7.87 (m, 3H), 7.71 (t, *J* = 1.8 Hz, 1H), 7.46 – 7.36 (m, 3H), 6.81 (s, 1H), 6.66 (d, *J* = 7.0 Hz, 1H), 2.50 (s, 3H). ^{13}C-NMR (101 MHz, DMSO) δ 163.6, 158.0, 150.5, 149.5, 141.6, 138.3, 137.1, 135.2, 133.5, 129.0, 125.1, 124.4, 123.8, 121.5, 117.4, 108.9, 100.7, 98.1, 20.8. ^{19}F NMR (376 MHz, DMSO) δ 39.3, -73.7. HRMS: ESI(+) [*m/z*]: calcd. mass $[M+H]^+$ = 441.10265; found = 441.1021; rel. deviation 1.2 ppm. HPLC: t_{ret} = 13.12 min (99.1 % at 254 nm, 98.2 % at 230 nm, method B).

Methyl 3-hydroxy-5-(trifluoromethyl)benzoate (327)

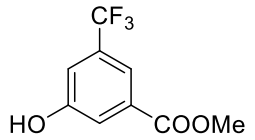

Chemical Formula: $C_9H_7F_3O_3$
Exact Mass: 220.03473
Molecular Weight: 220.14721

3-Hydroxy-5-(trifluoromethyl)benzoic acid (**325**, 500 mg, 2.43 mmol, 1.00 eq.) was dissolved in MeOH (5 mL) and conc. H_2SO_4 (11.8 µL, 0.121 mmol, 0.05 eq.) was added. The reaction was refluxed for 20 h and then neutralized with aq. NaOH (2 M). The solvent was evaporated leading to the product **327** (531 mg, 2.41 mmol, 99 %) as a white solid.

^{1}H-NMR (400 MHz, DMSO) δ 10.61 (s, 1H), 7.63 – 7.54 (m, 2H), 7.31 (ddd, J = 2.3, 1.6, 0.6 Hz, 1H), 3.87 (s, 3H). ^{13}C-NMR (101 MHz, DMSO) δ 164.9, 158.4, 132.1, 130.7 (q, J = 32.1 Hz), 123.5 (q, J = 272.5 Hz), 119.6, 116.2 (q, J = 3.7 Hz), 115.7 (q, J = 4.1 Hz), 52.6. LC-MS: ESI(-) [*m/z*]: calcd. mass $[M-H]^-$ = 219.0; found = 219.1. HPLC: t_{ret} = 11.39 min (92.8 % at 254 nm, 93.4 % at 230 nm, method A).

Methyl 3-((fluorosulfonyl)oxy)-5-(trifluoromethyl)benzoate (334)

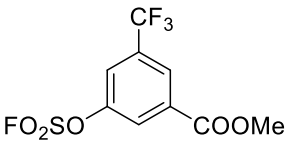

Chemical Formula: $C_9H_6F_4O_5S$
Exact Mass: 301.98721
Molecular Weight: 302.19561

Methyl 3-hydroxy-5-(trifluoromethyl)benzoate (**327**, 530 mg, 2.41 mmol, 1.00 eq.) and AISF (**64**, 908 mg, 2.89 mmol, 1.20 eq.) were dissolved in THF (12 mL). DBU (819 µL, 5.30 mmol, 2.20 eq.) was added and the reaction was stirred at rt for 16 h. Sat. NH_4Cl (25 mL) was added, and the solution was extracted with DCM (3 x 30 mL). After drying over Na_2SO_4 and evaporating the solvent, the residue was purified by flash column chromatography (silica gel, 0 – 30 % hexane/EtOAc) to afford the product **334** (218 mg, 0.721 mmol, 30 %) as a colorless oil.

^{1}H-NMR (400 MHz, $CDCl_3$) δ 8.45 – 8.35 (m, 1H), 8.24 – 8.18 (m, 1H), 7.83 – 7.77 (m, 1H), 4.01 (s, 3H). ^{13}C-NMR (101 MHz, DMSO) δ 164.9, 158.4, 132.1, 130.7 (q, J = 32.1 Hz), 123.5 (q, J = 272.5 Hz), 119.6, 116.2 (q, J = 3.7 Hz), 115.7 (q, J = 4.1 Hz), 52.6. ASAP: APCI(+) [*m/z*]: calcd. mass $[M+H]^+$ = 303.0; found = 302.7. HPLC: t_{ret} = 12.48 min (92.1 % at 254 nm, 98.7 % at 230 nm, method A).

3-((Fluorosulfonyl)oxy)-5-(trifluoromethyl)benzoic acid (341)

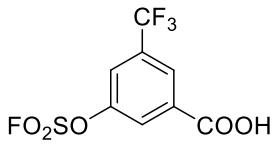

Chemical Formula: $C_8H_4F_4O_5S$
Exact Mass: 287.97156
Molecular Weight: 288.16861

Methyl 3-((fluorosulfonyl)oxy)-5-(trifluoromethyl)benzoate (**334**, 218 mg, 0.721 mmol, 1.00 eq.) was dissolved in aq. HCl (1 M, 10 mL) and HCl in dioxane (4 M, 2 mL) and was refluxed for 18 h. The solvent was evaporated and the crude product, a white solid, was used in the next step without further purification.

LC-MS: ESI(-) [*m/z*]: calcd. mass $[M-H]^-$ = 287.0; found = 287.0.

3-((4-((1H-Pyrrolo[2,3-b]pyridin-4-yl)amino)phenyl)carbamoyl)-5-(trifluoromethyl)phenyl sulfurofluoridate (350)

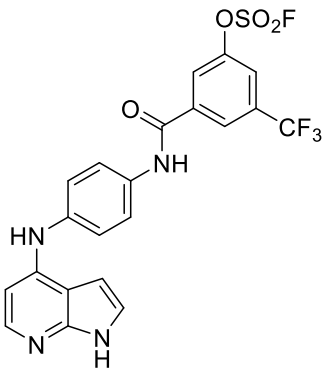

Chemical Formula: $C_{21}H_{14}F_4N_4O_4S$
Exact Mass: 494.06719
Molecular Weight: 494.42061

3-((Fluorosulfonyl)oxy)-5-(trifluoromethyl)benzoic acid (**341**, 100 mg, 0.347 mmol, 1.00 eq.), *N*^{1}-(1*H*-pyrrolo[2,3-*b*]pyridin-4-yl)benzene-1,4-diamine (**301**, 85.6 mg, 0.382 mmol, 1.10 eq.) and HATU (198 mg, 0.521 mmol, 1.50 eq.) were dissolved in DMF (1.8 mL). DIPEA (118 µL, 0.694 mmol, 2.00 eq.) was added and the reaction was stirred at rt for 18 h. H_2O (10 mL) was added, and the aq. phase was extracted with DCM (3 x 15 mL). The combined org. phases were dried over Na_2SO_4, the solvent was evaporated, and the residue was purified by preparative HPLC (10 – 60 % H_2O/MeCN, 0.1 % TFA) to afford the product **350** (TFA salt: 26.6 mg, 46.6 µmol, 13 %) as a white solid.

^{1}H-NMR (400 MHz, DMSO) δ 12.38 (s, 1H), 10.80 (s, 1H), 10.22 (s, 1H), 8.54 – 8.43 (m, 3H), 8.03 (d, J = 7.0 Hz, 1H), 7.95 – 7.87 (m, 2H), 7.49 – 7.34 (m, 3H), 6.82 (s, 1H), 6.68 (d, J = 7.0 Hz, 1H). ^{13}C-NMR (151 MHz, DMSO) δ 162.2, 158.5 (q, J = 31.7 Hz), 150.5, 149.5, 138.7, 136.0 (q, J = 200.0 Hz), 131.5 (q, J = 33.7 Hz), 125.2, 125.1, 125.0, 123.9, 122.8 (q, J = 273.1 Hz), 122.1, 121.7, 109.0, 100.7, 98.1, 66.4. ^{19}F NMR (376 MHz, DMSO) δ 40.3, -

61.1, -73.7. HRMS: ESI(+) [*m/z*]: calcd. mass $[M+H]^+$ = 495.07439; found = 495.0755; rel. deviation 2.2 ppm. HPLC: t_{ret} = 14.68 min (95.4 % at 254 nm, 95.4 % at 230 nm, method B).

Methyl 3-((fluorosulfonyl)oxy)-5-methoxybenzoate (335)

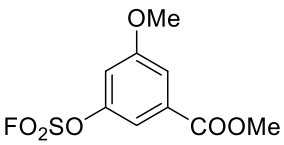

Chemical Formula: $C_9H_9FO_6S$
Exact Mass: 264.01039
Molecular Weight: 264.22340

Methyl 3-hydroxy-5-methoxybenzoate (**328**, 200 mg, 1.10 mmol, 1.00 eq.) and AISF (**64**, 414 mg, 1.32 mmol, 1.20 eq.) were dissolved in THF (5.5 mL). DBU (361 µL, 2.42 mmol, 2.20 eq.) was added and the reaction was stirred at rt for 2 h. Sat. NH_4Cl (15 mL) was added, and the solution was extracted with DCM (3 x 20 mL). After drying over Na_2SO_4 and evaporating the solvent, the residue was purified by flash column chromatography (silica gel, 0 – 30 % hexane/EtOAc) to afford the product **335** (247 mg, 0.935 mmol, 85 %) as a colorless oil.

^{1}H-NMR (400 MHz, $CDCl_3$) δ 7.62 (dd, J = 2.4, 1.3 Hz, 1H), 7.59 (dt, J = 2.3, 1.2 Hz, 1H), 7.06 (td, J = 2.4, 0.8 Hz, 1H), 3.95 (s, 3H), 3.89 (s, 3H). ^{13}C-NMR (101 MHz, $CDCl_3$) δ 165.2, 161.0, 150.5, 133.4, 115.0, 114.1, 112.0, 56.3, 52.9. LC-MS: ESI(+) [*m/z*]: calcd. mass $[M+H]^+$ = 265.0; found = 265.0. HPLC: t_{ret} = 11.98 min (90.2 % at 254 nm, 98.7 % at 230 nm, method A).

3-((Fluorosulfonyl)oxy)-5-methoxybenzoic acid (342)

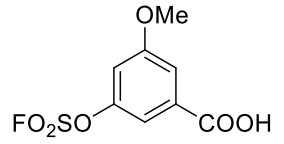

Chemical Formula: $C_8H_7FO_6S$
Exact Mass: 249.99474
Molecular Weight: 250.19640

Methyl 3-((fluorosulfonyl)oxy)-5-methoxybenzoate (**335**, 247 mg, 0.935 mmol, 1.00 eq.) was dissolved in aq. HCl (1 M, 10 mL) and HCl in dioxane (4 M, 2 mL) and was refluxed for 24 h. The solvent was evaporated and the crude product, a white solid, was used in the next step without further purification.

LC-MS: ESI(-) [*m/z*]: calcd. mass $[M-H]^-$ = 249.0; found = 249.1.

3-((4-((1H-Pyrrolo[2,3-b]pyridin-4-yl)amino)phenyl)carbamoyl)-5-methoxyphenyl sulfurofluoridate (351)

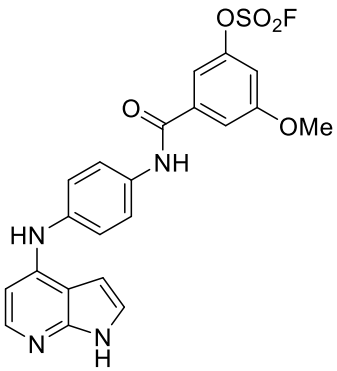

Chemical Formula: $C_{21}H_{17}FN_4O_5S$
Exact Mass: 456.09037
Molecular Weight: 456.44840

3-((Fluorosulfonyl)oxy)-5-methoxybenzoic acid (**342**, 80.0 mg, 0.320 mmol, 1.00 eq.), *N*[1]-(1*H*-pyrrolo[2,3-*b*]pyridin-4-yl)benzene-1,4-diamine (**301**, 78.9 mg, 0.352 mmol, 1.10 eq.) and HATU (182 mg, 0.480 mmol, 1.50 eq.) were dissolved in DMF (1.5 mL). DIPEA (163 µL, 0.959 mmol, 3.00 eq.) was added and the reaction was stirred at rt for 18 h. H_2O (10 mL) was added, and the aq. phase was extracted with DCM (3 x 15 mL). The combined org. phases were dried over Na_2SO_4, the solvent was evaporated, and the residue was purified by preparative HPLC (10 – 55 % H_2O/MeCN, 0.1 % TFA) to afford the product **351** (TFA salt: 35.8 mg, 67.2 µmol, 21 %) as a white solid.

^{1}H-NMR (400 MHz, DMSO) δ 12.40 (s, 1H), 10.57 (s, 1H), 10.18 (s, 1H), 8.03 (d, J = 7.0 Hz, 1H), 7.95 – 7.87 (m, 2H), 7.74 – 7.68 (m, 2H), 7.52 (t, J = 2.3 Hz, 1H), 7.47 – 7.36 (m, 3H), 6.81 (s, 1H), 6.67 (d, J = 7.0 Hz, 1H), 3.93 (s, 3H). ^{13}C-NMR (101 MHz, DMSO) δ 163.3, 160.6, 150.4, 150.2, 138.5, 137.9, 136.9, 135.3, 133.6, 125.0, 123.8, 121.6, 114.4, 112.1, 110.3, 108.9, 100.7, 98.1, 56.4. ^{19}F NMR (376 MHz, DMSO) δ 39.5, -73.6. HRMS: ESI(+) [*m/z*]: calcd. mass $[M+H]^+$ = 457.09757; found = 457.0979; rel. deviation 0.7 ppm. HPLC: t_{ret} = 13.16 min (96.0 % at 254 nm, 96.0 % at 230 nm, method B).

Methyl 3-fluoro-5-((fluorosulfonyl)oxy)benzoate (336)

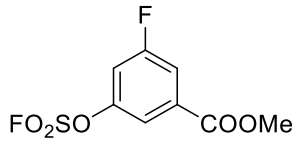

Chemical Formula: $C_8H_6F_2O_5S$
Exact Mass: 251.99040
Molecular Weight: 252.18781

Methyl 3-fluoro-5-hydroxybenzoate (**329**, 200 mg, 1.18 mmol, 1.00 eq.) and AISF (**64**, 443 mg, 1.41 mmol, 1.20 eq.) were dissolved in THF (6 mL). DBU (386 µL, 2.59 mmol, 2.20 eq.) was added and the reaction was stirred at rt for 2 h. Sat. NH_4Cl (15 mL) was added, and the solution was extracted with DCM (3 x 20 mL). After drying over Na_2SO_4 and evaporating the solvent, the residue was purified by flash column chromatography (silica gel, 0 – 30 % hexane/EtOAc) to afford the product **336** (259 mg, 1.03 mmol, 87 %) as a colorless oil.

^{1}H-NMR (400 MHz, $CDCl_3$) δ 7.87 – 7.78 (m, 2H), 7.31 (dtd, J = 7.9, 2.4, 0.8 Hz, 1H), 3.97 (s, 3H). ^{13}C-NMR (101 MHz, $CDCl_3$) δ 164.2 (d, J = 3.3 Hz), 162.7 (d, J = 253.3 Hz), 150.0 (d, J = 10.6 Hz), 134.3 (d, J = 8.4 Hz), 118.2 (d, J = 3.9 Hz), 117.4 (d, J = 22.9 Hz), 113.8 (d,

J = 25.8 Hz). LC-MS: ESI(+) [*m/z*]: calcd. mass $[M+Na]^+$ = 275.0; found = 275.0. HPLC: t_{ret} = 11.74 min (99.2 % at 254 nm, 99.3 % at 230 nm, method A).

3-Fluoro-5-((fluorosulfonyl)oxy)benzoic acid (343)

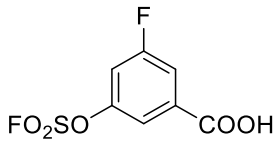

Chemical Formula: $C_7H_4F_2O_5S$
Exact Mass: 237.97475
Molecular Weight: 238.16081

Methyl 3-fluoro-5-((fluorosulfonyl)oxy)benzoate (**336**, 259 mg, 1.03 mmol, 1.00 eq.) was dissolved in aq. HCl (1 M, 10 mL) and HCl in dioxane (4 M, 2 mL) and was refluxed for 16 h. The solvent was evaporated and the crude product, a white solid, was used in the next step without further purification.

LC-MS: ESI(-) [*m/z*]: calcd. mass $[M-H]^-$ = 237.0; found = 237.0.

3-((4-((1H-Pyrrolo[2,3-b]pyridin-4-yl)amino)phenyl)carbamoyl)-5-fluorophenyl sulfurofluoridate (352)

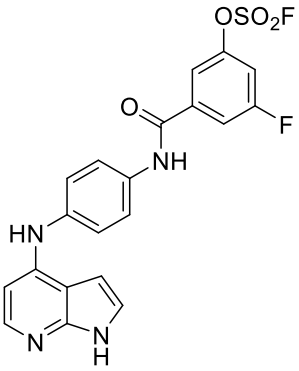

Chemical Formula: $C_{20}H_{14}F_2N_4O_4S$
Exact Mass: 444.07038
Molecular Weight: 444.41281

3-Fluoro-5-((fluorosulfonyl)oxy)benzoic acid (**343**, 55.8 mg, 0.234 mmol, 1.00 eq.), N^1-(1*H*-pyrrolo[2,3-*b*]pyridin-4-yl)benzene-1,4-diamine (**301**, 57.8 mg, 0.258 mmol, 1.10 eq.) and HATU (134 mg, 0.351 mmol, 1.50 eq.) were dissolved in DMF (1.5 mL). DIPEA (120 µL, 0.703 mmol, 3.00 eq.) was added and the reaction was stirred at rt for 18 h. H_2O (10 mL) was added, and the aq. phase was extracted with DCM (3 x 15 mL). The combined org. phases were dried over Na_2SO_4, the solvent was evaporated, and the residue was purified by preparative HPLC (10 – 75 % H_2O/MeCN, 0.1 % TFA) to afford the product **352** (TFA salt: 25.0 mg, 51.8 µmol, 22 %) as a white solid.

^{1}H-NMR (400 MHz, DMSO) δ 12.39 (s, 1H), 10.65 (s, 1H), 10.20 (s, 1H), 8.09 – 8.00 (m, 4H), 7.94 – 7.86 (m, 2H), 7.46 – 7.40 (m, 2H), 7.39 (dd, J = 3.5, 2.1 Hz, 1H), 6.81 (s, 1H), 6.67 (d, J = 7.0 Hz, 1H). ^{13}C-NMR (101 MHz, DMSO) δ 162.7 (d, J = 83.0 Hz), 160.7, 150.5, 149.5 (d, J = 11.4 Hz), 138.8, 138.3, 136.7, 135.2, 133.7, 125.1, 123.8, 121.6, 117.0, 115.9 (d, J = 23.1 Hz), 113.0 (d, J = 27.2 Hz), 108.9, 100.7, 98.1. ^{19}F NMR (376 MHz, DMSO) δ 40.0, -73.4. HRMS: ESI(+) [*m/z*]: calcd. mass $[M+H]^+$ = 445.07758; found = 445.0773; rel. deviation 0.6 ppm. HPLC: t_{ret} = 12.76 min (98.5 % at 254 nm, 97.9 % at 230 nm, method B).

Methyl 3-bromo-5-((fluorosulfonyl)oxy)benzoate (337)

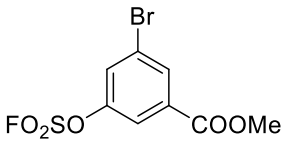

Chemical Formula: $C_8H_6BrFO_5S$
Exact Mass: 311.91034
Molecular Weight: 313.09340

Methyl 3-bromo-5-hydroxybenzoate (**330**, 200 mg, 0.866 mmol, 1.00 eq.) and AISF (**64**, 327 mg, 1.04 mmol, 1.20 eq.) were dissolved in THF (4.5 mL). DBU (284 µL, 1.90 mmol, 2.20 eq.) was added and the reaction was stirred at rt for 2 h. Sat. NH_4Cl (15 mL) was added, and the solution was extracted with DCM (3 x 20 mL). After drying over Na_2SO_4 and evaporating the solvent, the residue was purified by flash column chromatography (silica gel, 0 – 30 % hexane/EtOAc) to afford the product **337** (223 mg, 0.712 mmol, 82 %) as a white solid.

^{1}H-NMR (400 MHz, $CDCl_3$) δ 8.24 (t, J = 1.6 Hz, 1H), 7.95 (dt, J = 2.2, 1.1 Hz, 1H), 7.71 (ddd, J = 2.5, 1.8, 0.8 Hz, 1H), 3.97 (s, 3H). ^{13}C-NMR (101 MHz, $CDCl_3$) δ 164.0, 149.9, 134.1, 133.2, 128.7, 123.5, 121.1, 53.2. LC-MS: ESI(+) [*m/z*]: calcd. mass $[M+H]^+$ = 313.0; found = 312.9. HPLC: t_{ret} = 12.47 min (96.2 % at 254 nm, 98.7 % at 230 nm, method A).

3-Bromo-5-((fluorosulfonyl)oxy)benzoic acid (344)

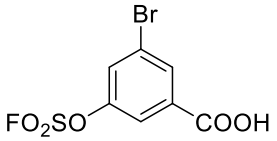

Chemical Formula: $C_7H_4BrFO_5S$
Exact Mass: 297.89469
Molecular Weight: 299.06640

Methyl 3-bromo-5-((fluorosulfonyl)oxy)benzoate (**337**, 223 mg, 0.712 mmol, 1.00 eq.) was dissolved in aq. HCl (1 M, 10 mL) and HCl in dioxane (4 M, 2 mL) and was refluxed for 16 h. The solvent was evaporated and the crude product, a white solid, was used in the next step without further purification.

LC-MS: ESI(-) [*m/z*]: calcd. mass $[M-H]^-$ = 296.9; found = 297.0.

3-((4-((1H-Pyrrolo[2,3-b]pyridin-4-yl)amino)phenyl)carbamoyl)-5-bromophenyl sulfurofluoridate (353)

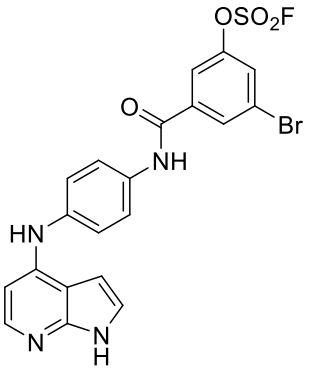

Chemical Formula: $C_{20}H_{14}BrFN_4O_4S$
Exact Mass: 503.99032
Molecular Weight: 505.31840

3-Bromo-5-((fluorosulfonyl)oxy)benzoic acid (**344**, 36.5 mg, 0.122 mmol, 1.00 eq.), *N*^{1}-(1*H*-pyrrolo[2,3-*b*]pyridin-4-yl)benzene-1,4-diamine (**301**, 30.1 mg, 0.134 mmol, 1.10 eq.) and HATU (69.6 mg, 0.183 mmol, 1.50 eq.) were dissolved in DMF (0.6 mL). DIPEA (41.5 µL, 0.244 mmol, 2.00 eq.) was added and the reaction was stirred at rt for 18 h. H_2O (10 mL) was added, and the aq. phase was extracted with DCM (3 x 15 mL). The combined org. phases were dried over Na_2SO_4, the solvent was evaporated, and the residue was purified by preparative HPLC (10 – 60 %

H_2O/MeCN, 0.1 % TFA) to afford the product **353** (TFA salt: 35.8 mg, 20.8 µmol, 17 %) as an off-white solid.

^{1}H-NMR (400 MHz, DMSO) δ 12.35 (s, 1H), 10.67 (s, 1H), 10.19 (s, 1H), 8.36 (t, J = 1.6 Hz, 1H), 8.29 (t, J = 2.0 Hz, 1H), 8.17 (t, J = 1.9 Hz, 1H), 8.02 (d, J = 7.0 Hz, 1H), 7.94 – 7.78 (m, 2H), 7.47 – 7.34 (m, 3H), 6.81 (s, 1H), 6.67 (d, J = 7.0 Hz, 1H). ^{13}C-NMR (101 MHz, DMSO) δ 162.1, 150.4, 149.5, 138.7, 138.3, 136.7, 135.2, 133.7, 131.3, 127.5, 125.0, 123.8, 122.6, 121.5, 120.0, 108.9, 100.7, 98.1. ^{19}F NMR (376 MHz, DMSO) δ 40.1, -73.6. HRMS: ESI(+) [*m/z*]: calcd. mass $[M+H]^+$ = 504.99752; found = 504.9979; rel. deviation 0.8 ppm. HPLC: t_{ret} = 14.30 min (95.1 % at 254 nm, 96.1 % at 230 nm, method B).

Methyl 3-cyano-5-hydroxybenzoate (331)

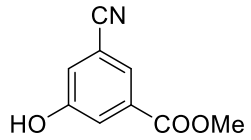

Chemical Formula: $C_9H_7NO_3$
Exact Mass: 177.04259
Molecular Weight: 177.15900

Methyl 3-bromo-5-hydroxybenzoate (**330**, 250 mg, 1.08 mmol, 1.00 eq.) and CuCN (116 mg, 1.30 mmol, 1.20 eq.) were dissolved in NMP (2 mL). The reaction was stirred at 180 °C for 6 h and then cooled to rt. The solution was poured onto sat. $NaHCO_3$ (10 mL) and extracted with EtOAc (3 x 15 mL). The combined org. phases were washed with H_2O (3 x 30 mL), brine (30 mL) and dried over Na_2SO_4. The solvent was evaporated, and the residue was purified by flash column chromatography (silica gel, 0 – 50 % hexane/EtOAc) to yield the product **331** (149 mg, 0.841 mmol, 78 %) as a white solid.

^{1}H-NMR (400 MHz, DMSO) δ 10.68 (s, 1H), 7.72 (t, J = 1.5 Hz, 1H), 7.61 (dd, J = 2.5, 1.5 Hz, 1H), 7.41 (dd, J = 2.5, 1.4 Hz, 1H), 3.86 (s, 3H). ^{13}C-NMR (101 MHz, DMSO) δ 164.6, 158.2, 132.3, 123.1, 122.8, 120.6, 117.9, 112.8, 52.6. LC-MS: ESI(-) [*m/z*]: calcd. mass $[M-H]^-$ = 176.0; found = 176.1. HPLC: t_{ret} = 9.25 min (98.6 % at 254 nm, 99.6 % at 230 nm, method A).

Methyl 3-cyano-5-((fluorosulfonyl)oxy)benzoate (338)

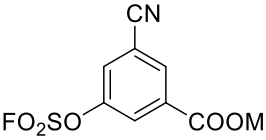

Chemical Formula: $C_9H_6FNO_5S$
Exact Mass: 258.99507
Molecular Weight: 259.20740

Methyl 3-cyano-5-hydroxybenzoate (**331**, 139 mg, 0.785 mmol, 1.00 eq.) and AISF (**64**, 296 mg, 0.942 mmol, 1.20 eq.) were dissolved in THF (3 mL). DBU (258 µL, 1.73 mmol, 2.20 eq.) was added and the reaction was stirred at rt for 1.5 h. Sat. NH_4Cl (15 mL) was added, and the solution was extracted with DCM (3 x 20 mL). After drying over Na_2SO_4 and evaporating the solvent, the residue was purified by flash column chromatography (silica gel, 0 – 30 % hexane/EtOAc) to afford the product **338** (138 mg, 0.532 mmol, 88 %) as a white solid.

^{1}H-NMR (400 MHz, $CDCl_3$) δ 8.39 (t, J = 1.4 Hz, 1H), 8.24 (ddd, J = 2.4, 1.4, 0.8 Hz, 1H), 7.83 (ddd, J = 2.3, 1.4, 0.7 Hz, 1H), 4.01 (s, 3H). ^{13}C-NMR (101 MHz, $CDCl_3$) δ 163.3, 149.8, 134.5, 133.4, 128.6, 126.7, 116.0, 115.4, 53.5. LC-MS: ESI(+) [*m/z*]: calcd. mass $[M+H]^+$ = 260.0; found = 260.0. HPLC: t_{ret} = 10.59 min (98.9 % at 254 nm, 95.3 % at 230 nm, method A).

3-Cyano-5-((fluorosulfonyl)oxy)benzoic acid (345)

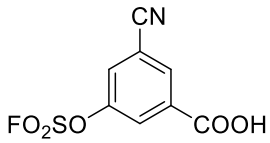

Chemical Formula: $C_8H_4FNO_5S$
Exact Mass: 244.97942
Molecular Weight: 245.18040

Methyl 3-cyano-5-((fluorosulfonyl)oxy)benzoate (**338**, 138 mg, 0.532 mmol, 1.00 eq.) was dissolved in aq. HCl (1 M, 10 mL) and HCl in dioxane (4 M, 2 mL) and was refluxed for 18 h. The solvent was evaporated and the crude product, a white solid, was used in the next step without further purification.

LC-MS: ESI(-) [*m/z*]: calcd. mass $[M-H]^-$ = 244.0; found = 244.0.

3-((4-((1H-Pyrrolo[2,3-b]pyridin-4-yl)amino)phenyl)carbamoyl)-5-cyanophenyl sulfurofluoridate (354)

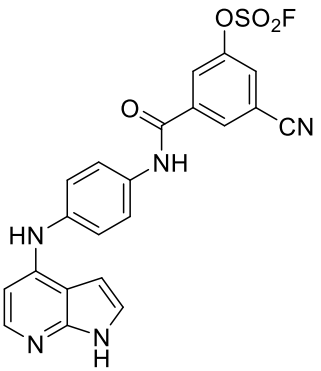

Chemical Formula: $C_{21}H_{14}FN_5O_4S$
Exact Mass: 451.07505
Molecular Weight: 451.43240

3-Cyano-5-((fluorosulfonyl)oxy)benzoic acid (**345**, 80.0 mg, 0.326 mmol, 1.00 eq.), *N*^{1}-(1*H*-pyrrolo[2,3-*b*]pyridin-4-yl)benzene-1,4-diamine (**301**, 80.5 mg, 0.359 mmol, 1.10 eq.) and HATU (186 mg, 0.489 mmol, 1.50 eq.) were dissolved in DMF (1.6 mL). DIPEA (111 µL, 0.653 mmol, 2.00 eq.) was added and the reaction was stirred at rt for 18 h. H_2O (10 mL) was added, and the aq. phase was extracted with DCM (3 x 15 mL). The combined org. phases were dried over Na_2SO_4, the solvent was evaporated, and the residue was purified by preparative HPLC (10 – 60 % H_2O/MeCN, 0.1 % TFA) to afford the product **354** (TFA salt: 29.1 mg, 53.3 µmol, 16 %) as a yellow solid.

^{1}H-NMR (400 MHz, DMSO) δ 12.40 (s, 1H), 10.75 (s, 1H), 10.22 (s, 1H), 8.62 (t, J = 1.4 Hz, 1H), 8.59 (dd, J = 2.5, 1.3 Hz, 1H), 8.49 (dd, J = 2.5, 1.5 Hz, 1H), 8.03 (d, J = 7.0 Hz, 1H), 7.95 – 7.86 (m, 2H), 7.48 – 7.36 (m, 3H), 6.82 (s, 1H), 6.68 (d, J = 7.0 Hz, 1H). ^{13}C-NMR (101 MHz, DMSO) δ 161.9, 150.5, 149.1, 138.5, 138.1, 136.7, 135.1, 133.8, 132.3, 128.2, 125.8, 125.1, 123.9, 121.5, 116.6, 113.8, 109.0, 100.7, 98.1. ^{19}F NMR (376 MHz, DMSO) δ 40.6, -73.8. HRMS: ESI(+) [*m/z*]: calcd. mass $[M+H]^+$ = 452.08225; found = 452.0823; rel. deviation 0.1 ppm. HPLC: t_{ret} = 11.52 min (95.4 % at 254 nm, 95.7 % at 230 nm, method B).

Methyl 5-((fluorosulfonyl)oxy)nicotinate (339)

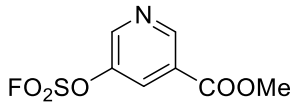

Chemical Formula: $C_7H_6FNO_5S$
Exact Mass: 234.99507
Molecular Weight: 235.18540

Methyl 5-hydroxynicotinate (**332**, 200 mg, 1.31 mmol, 1.00 eq.) and AISF (**64**, 493 mg, 1.57 mmol, 1.20 eq.) were dissolved in THF (6.5 mL). DBU (429 µL, 2.87 mmol, 2.20 eq.) was added and the reaction was stirred at rt for 2 h. Sat. NH_4Cl (15 mL) was added, and the solution was extracted with DCM (3 x 20 mL). After drying over Na_2SO_4 and evaporating the solvent, the residue was purified by flash column chromatography (silica gel, 0 – 30 % hexane/EtOAc) to afford the product **339** (197 mg, 0.838 mmol, 64 %) as a colorless oil.

^{1}H-NMR (400 MHz, $CDCl_3$) δ 9.28 (d, J = 1.7 Hz, 1H), 8.84 (d, J = 2.7 Hz, 1H), 8.30 (ddd, J = 2.7, 1.7, 0.9 Hz, 1H), 4.01 (s, 3H). ^{13}C-NMR (101 MHz, $CDCl_3$) δ 163.9, 150.8, 146.8, 146.4, 129.7, 127.9, 53.2. LC-MS: ESI(+) [*m/z*]: calcd. mass $[M+H]^+$ = 236.0; found = 236.0. HPLC: t_{ret} = 9.77 min (99.7 % at 254 nm, 96.7 % at 230 nm, method A).

5-((Fluorosulfonyl)oxy)nicotinic acid (346)

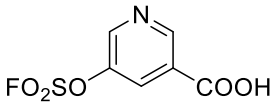

Chemical Formula: $C_6H_4FNO_5S$
Exact Mass: 220.97942
Molecular Weight: 221.15840

Methyl 5-((fluorosulfonyl)oxy)nicotinate (**339**, 197 mg, 0.838 mmol, 1.00 eq.) was dissolved in aq. HCl (1 M, 10 mL) and HCl in dioxane (4 M, 2 mL) and was refluxed for 7 h. The solvent was evaporated and the crude product, an off-white solid, was used in the next step without further purification.

LC-MS: ESI(-) [*m/z*]: calcd. mass $[M-H]^-$ = 220.0; found = 220.0.

5-((4-((1H-Pyrrolo[2,3-b]pyridin-4-yl)amino)phenyl)carbamoyl)pyridin-3-yl sulfurofluoridate (355)

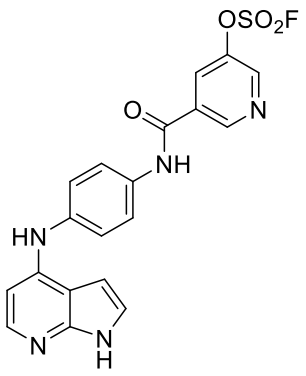

Chemical Formula: $C_{19}H_{14}FN_5O_4S$
Exact Mass: 427.07505
Molecular Weight: 427.41040

5-((Fluorosulfonyl)oxy)nicotinic acid (**346**, 80.0 mg, 0.362 mmol, 1.00 eq.), *N*^{1}-(1*H*-pyrrolo[2,3-*b*]pyridin-4-yl)benzene-1,4-diamine (**301**, 89.2 mg, 0.398 mmol, 1.10 eq.) and HATU (206 mg, 0.543 mmol, 1.50 eq.) were dissolved in DMF (2 mL). DIPEA (185 µL, 1.09 mmol, 3.00 eq.) was added and the reaction was stirred at rt for 18 h. H_2O (10 mL) was added, and the aq. phase was extracted with DCM (3 x 15 mL). The combined org. phases were dried over Na_2SO_4, the solvent was evaporated, and the residue was

purified by preparative HPLC (10 – 50 % H_2O/MeCN, 0.1 % TFA) to afford the product **355** (TFA salt: 13.3 mg, 24.6 µmol, 6.8 %) as a yellow solid.

^{1}H-NMR (400 MHz, DMSO) δ 12.38 (s, 1H), 10.80 (s, 1H), 10.23 (s, 1H), 9.28 (d, J = 1.7 Hz, 1H), 9.14 (d, J = 2.7 Hz, 1H), 8.62 (t, J = 2.3 Hz, 1H), 8.03 (d, J = 7.0 Hz, 1H), 7.95 – 7.87 (m, 2H), 7.48 – 7.37 (m, 3H), 6.82 (s, 1H), 6.67 (d, J = 7.0 Hz, 1H). ^{13}C-NMR (101 MHz, DMSO) δ 162.1, 157.9, 150.6, 149.1, 146.6, 145.2, 138.0, 136.8, 135.1, 133.7, 132.4, 128.7, 125.2, 123.9, 121.5, 112.5, 108.9, 100.7. ^{19}F NMR (376 MHz, DMSO) δ 40.4, -73.9. HRMS: ESI(+) [*m/z*]: calcd. mass $[M+H]^+$ = 428.08225; found = 428.0824; rel. deviation 0.4 ppm. HPLC: t_{ret} = 10.30 min (98.5 % at 254 nm, 98.7 % at 230 nm, method B).

3-(Fluorosulfonyl)benzoic acid (348)

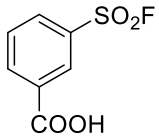

Chemical Formula: $C_7H_5FO_4S$
Exact Mass: 203.98926
Molecular Weight: 204.17140

3-(Chlorosulfonyl)benzoic acid (**347**, 500 mg, 2.27 mmol, 1.00 eq.) was dissolved in MeCN (11 mL). KHF_2 (1.95 g, 24.9 mmol, 11.0 eq.) was dissolved in H_2O (11 mL) and was added to the first solution. The reaction was stirred at rt for 20 h, after which sat. $NaHCO_3$ (15 mL) was added. The aq. phase was extracted with EtOAc (3 x 25 mL). The combined org. phases were dried over Na_2SO_4 and the solvent was evaporated to yield the product **348** (439 mg, 2.15 mmol, 95 %) as a white solid.

^{1}H-NMR (400 MHz, $CDCl_3$) δ 8.76 (t, J = 1.8 Hz, 1H), 8.52 (dt, J = 7.9, 1.4 Hz, 1H), 8.31 – 8.24 (m, 1H), 7.81 (t, J = 7.9 Hz, 1H). ^{13}C-NMR (101 MHz, $CDCl_3$) δ 169.3, 136.9, 134.3 (d, J = 25.9 Hz), 133.3, 131.2, 130.4, 130.4. LC-MS: ESI(-) [*m/z*]: calcd. mass $[M-H]^-$ = 203.0; found = 203.0. HPLC: t_{ret} = 9.47 min (100 % at 254 nm, 99.3 % at 230 nm, method A).

3-((4-((1H-Pyrrolo[2,3-b]pyridin-4-yl)amino)phenyl)carbamoyl)benzenesulfonyl fluoride (356)

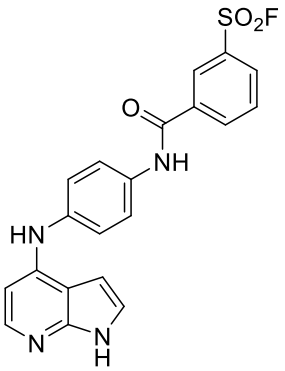

Chemical Formula: $C_{20}H_{15}FN_4O_3S$
Exact Mass: 410.08489
Molecular Weight: 410.42340

3-(Fluorosulfonyl)benzoic acid (**348**, 80.0 mg, 0.392 mmol, 1.00 eq.), *N*[1]-(1*H*-pyrrolo[2,3-*b*]pyridin-4-yl)benzene-1,4-diamine (**301**, 96.7 mg, 0.431 mmol, 1.10 eq.) and HATU (223 mg, 0.588 mmol, 1.50 eq.) were dissolved in DMF (2 mL). DIPEA (200 µL, 1.18 mmol, 3.00 eq.) was added and the reaction was stirred at rt for 16 h. H_2O (10 mL) was added, and the aq. phase was extracted with DCM (3 x 15 mL). The combined org. phases were dried over Na_2SO_4, the solvent was evaporated, and the residue was purified by preparative HPLC (10 – 55 % H_2O/MeCN, 0.1 % TFA) to afford the product **356** (TFA salt: 18.6 mg, 38.2 µmol, 9.8 %) as a white solid.

^{1}H-NMR (400 MHz, DMSO) δ 12.36 (s, 1H), 10.80 (s, 1H), 10.21 (s, 1H), 8.67 (t, J = 1.8 Hz, 1H), 8.52 (dt, J = 7.9, 1.4 Hz, 1H), 8.39 (ddd, J = 8.0, 2.0, 1.0 Hz, 1H), 8.06 – 7.96 (m, 2H), 7.96 – 7.88 (m, 2H), 7.47 – 7.36 (m, 3H), 6.82 (s, 1H), 6.67 (d, J = 7.0 Hz, 1H). ^{13}C-NMR (101 MHz, DMSO) δ 163.1, 150.6, 138.1, 136.9, 136.5, 135.7, 135.1, 133.6, 131.8, 131.2, 131.0, 127.3, 125.1, 123.8, 121.6, 108.9, 100.7, 98.1. ^{19}F NMR (376 MHz, DMSO) δ 66.4, -73.7. HRMS: ESI(+) [*m/z*]: calcd. mass $[M+H]^+$ = 411.09209; found = 411.0922; rel. deviation 0.3 ppm. HPLC: t_{ret} = 11.27 min (93.6 % at 254 nm, 93.4 % at 230 nm, method B).

N-(4-((1H-Pyrrolo[2,3-b]pyridin-4-yl)amino)phenyl)-3-hydroxybenzamide (357)

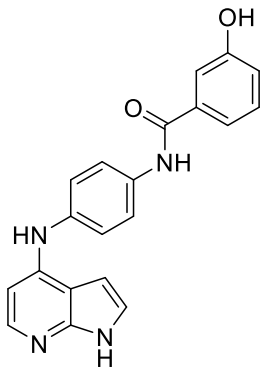

Chemical Formula: $C_{20}H_{16}N_4O_2$
Exact Mass: 344.12733
Molecular Weight: 344.37400

3-Hydroxybenzoic acid (80.0 mg, 0.579 mmol, 1.00 eq.), *N*[1]-(1*H*-pyrrolo[2,3-*b*]pyridin-4-yl)benzene-1,4-diamine (**301**, 143 mg, 0.637 mmol, 1.10 eq.) and HATU (330 mg, 0.869 mmol, 1.50 eq.) were dissolved in DMF (3 mL). DIPEA (197 µL, 1.16 mmol, 2.00 eq.) was added and the reaction was stirred at rt for 18 h. H_2O (10 mL) was added, and the aq. phase was extracted with DCM (3 x 15 mL). The combined org. phases were dried over Na_2SO_4, the solvent was evaporated, and the residue was purified by preparative HPLC (10 – 50 % H_2O/MeCN, 0.1 % TFA) to afford the product **357** (TFA salt: 30.8 mg, 59.6 µmol, 10 %) as a white solid.

^{1}H-NMR (400 MHz, DMSO) δ 12.33 (s, 1H), 10.33 (s, 1H), 10.14 (s, 1H), 9.79 (s, 1H), 8.01 (d, J = 7.0 Hz, 1H), 7.96 – 7.88 (m, 2H), 7.40 – 7.29 (m, 6H), 6.99 (ddd, J = 8.0, 2.5, 1.2 Hz, 1H),

6.80 (s, 1H), 6.64 (d, J = 7.0 Hz, 1H). ^{13}C-NMR (101 MHz, DMSO) δ 166.2, 157.9, 151.0, 138.9, 138.0, 136.8, 135.8, 133.5, 130.0, 125.5, 124.2, 121.7, 119.1, 118.7, 115.0, 109.3, 101.1, 98.5. ^{19}F NMR (376 MHz, DMSO) δ -73.6. HRMS: ESI(+) [*m/z*]: calcd. mass $[M+H]^+$ = 345.13453; found = 345.1352; rel. deviation 1.9 ppm. HPLC: t_{ret} = 7.28 min (98.3 % at 254 nm, 96.5 % at 230 nm, method B).

N-(4-((1H-Pyrrolo[2,3-b]pyridin-4-yl)amino)phenyl)benzamide (358)

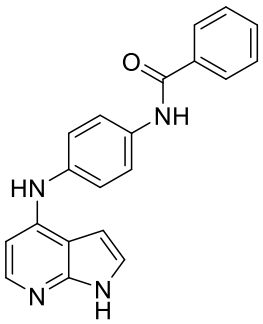

Chemical Formula: $C_{20}H_{16}N_4O$
Exact Mass: 328.13241
Molecular Weight: 328.37500

Benzoic acid (75.0 mg, 0.614 mmol, 1.00 eq.), *N*^{1}-(1*H*-pyrrolo[2,3-*b*]pyridin-4-yl)benzene-1,4-diamine (**301**, 152 mg, 0.676 mmol, 1.10 eq.) and HATU (350 mg, 0.921 mmol, 1.50 eq.) were dissolved in DMF (3 mL). DIPEA (209 µL, 1.23 mmol, 2.00 eq.) was added and the reaction was stirred at rt for 18 h. H_2O (10 mL) was added, and the aq. phase was extracted with DCM (3 x 15 mL). The combined org. phases were dried over Na_2SO_4, the solvent was evaporated, and the residue was purified by preparative HPLC (10 – 50 % H_2O/MeCN, 0.1 % TFA) to afford the product **358** (TFA salt: 91.8 mg, 0.208 mmol, 34 %) as an off-white solid.

^{1}H-NMR (400 MHz, DMSO) δ 12.38 (s, 1H), 10.43 (s, 1H), 10.08 (s, 1H), 8.06 – 7.95 (m, 3H), 7.95 – 7.89 (m, 2H), 7.66 – 7.50 (m, 3H), 7.43 – 7.33 (m, 3H), 6.81 (s, 1H), 6.65 (d, J = 6.6 Hz, 1H). ^{13}C-NMR (101 MHz, DMSO) δ 165.6, 158.1, 150.0, 139.2, 137.3, 135.8, 134.9, 133.4, 131.7, 128.4, 127.7, 124.8, 123.6, 121.3, 100.5, 98.0. ^{19}F NMR (376 MHz, DMSO) δ -73.6. HRMS: ESI(+) [*m/z*]: calcd. mass $[M+H]^+$ = 329.13961; found = 329.1380; rel. deviation 4.9 ppm. HPLC: t_{ret} = 9.08 min (95.8 % at 254 nm, 97.0 % at 230 nm, method B).

6.3. Overview of Test Compounds

Table 7: Overview of all test compounds.

#	Structure	#	Structure
JAK3			
61	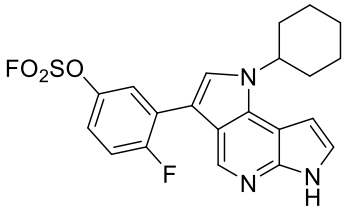	**81**	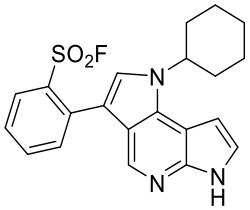
62	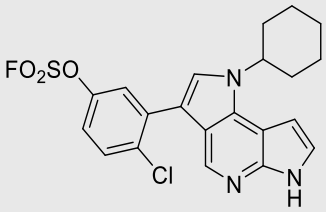	**100**	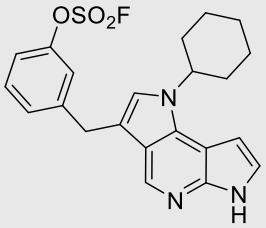
63	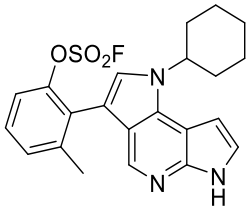	**112**	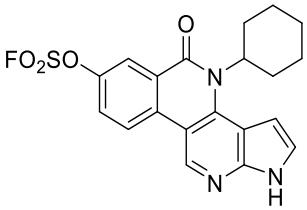
80	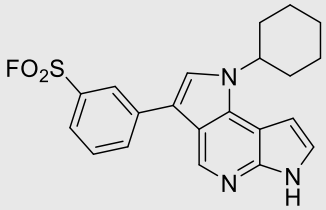		
MK2			
120	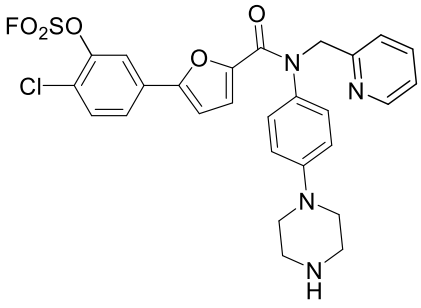	**119**	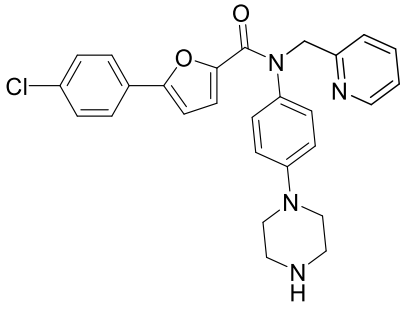

121	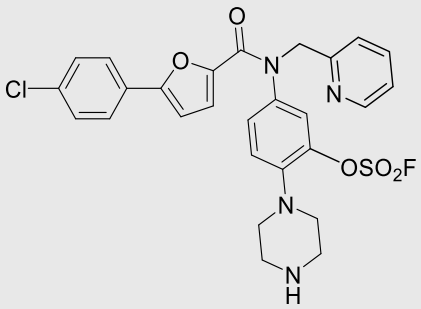	**168**	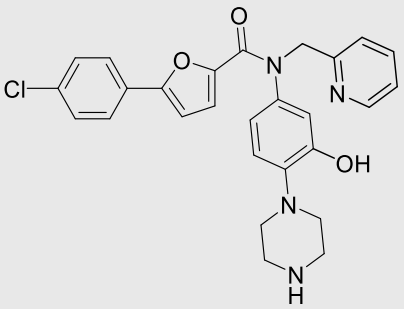
153	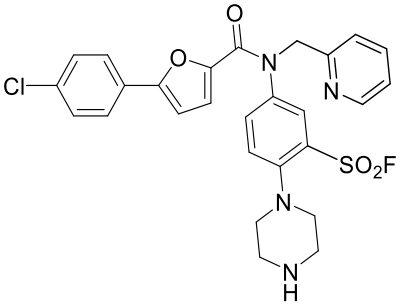	**172**	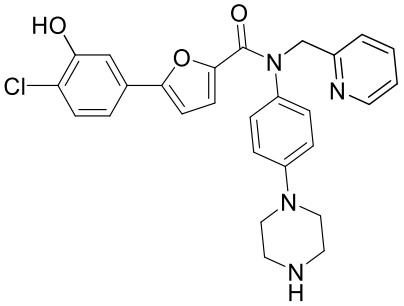

Covalent-First Library

176	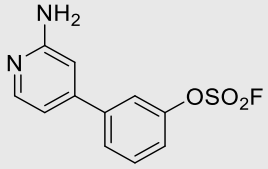	**181**	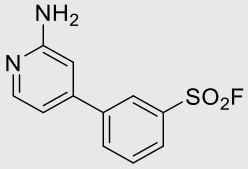
177	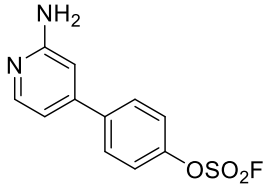	**182**	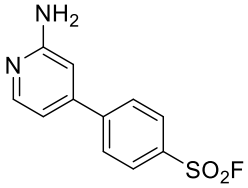
202	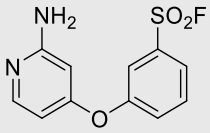	**228**	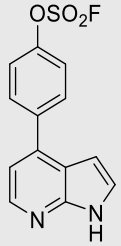
203	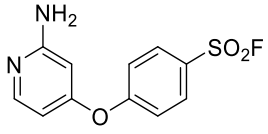	**232**	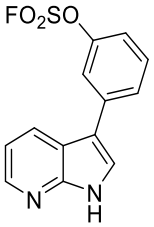
207	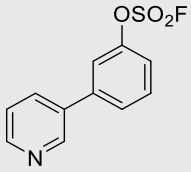	**233**	

208	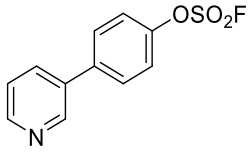	**237**	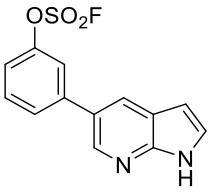
216	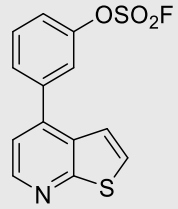	**238**	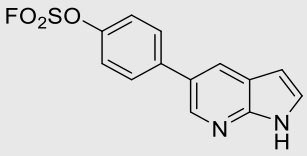
217	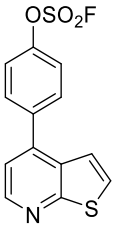	**239**	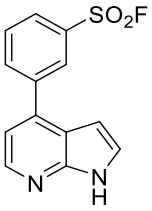
223	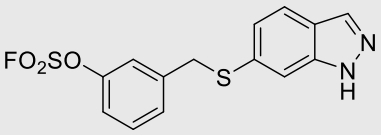	**240**	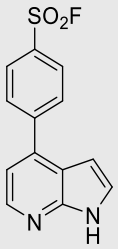
227	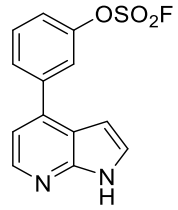	**241**	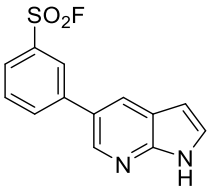
250	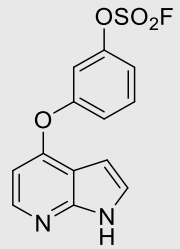	**279**	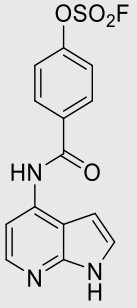
251	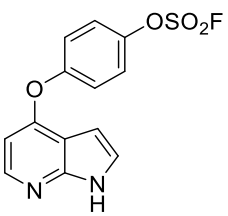	**283**	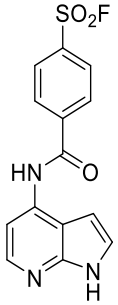

273	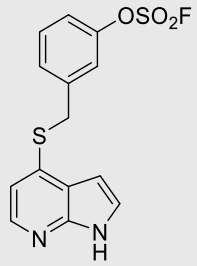	**286**	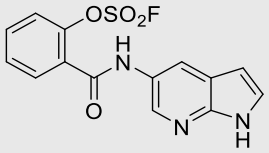
274	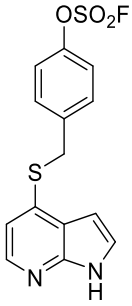	**295**	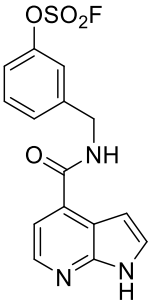
278	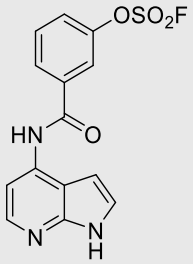	**296**	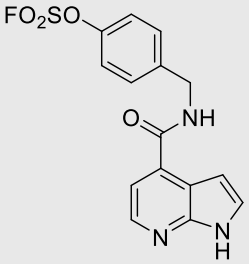
299	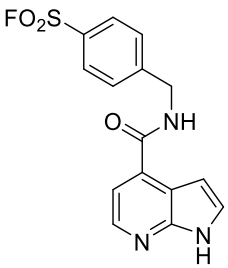	**309**	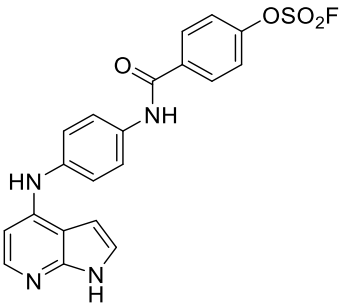
308	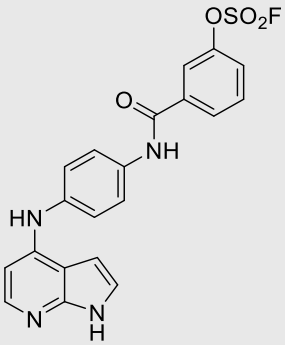		

ALK2			
314	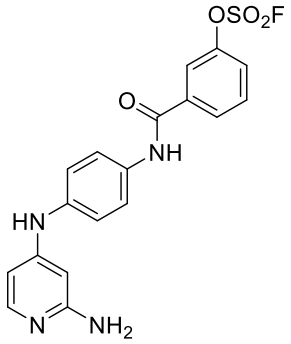	**322**	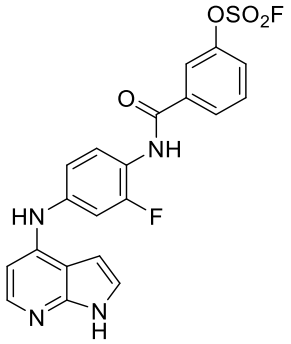
317	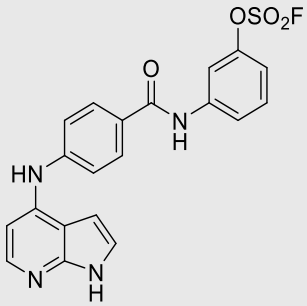	**323**	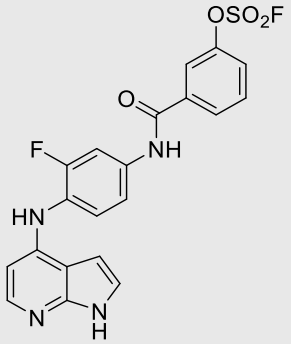
351	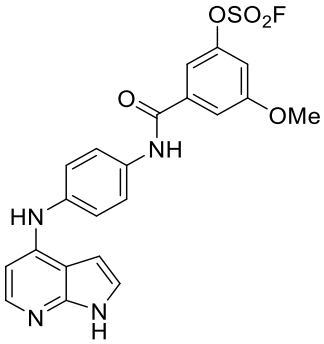	**352**	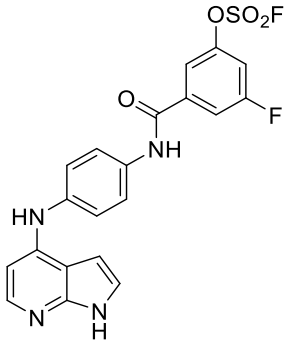
349	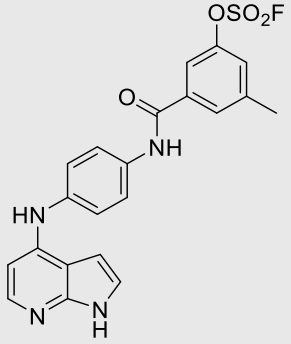	**355**	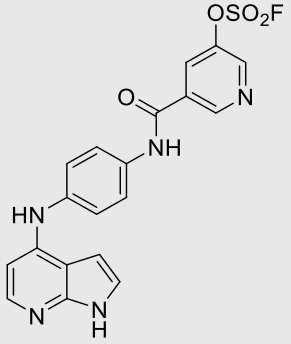

350	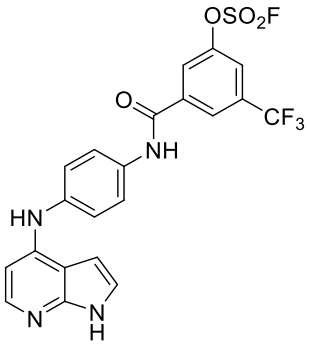	**353**	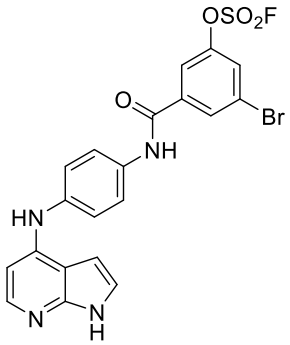
354	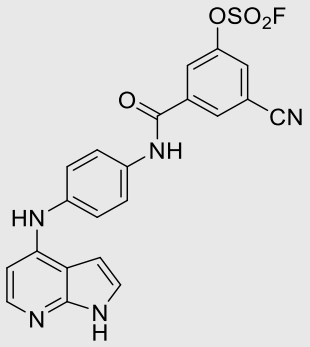	**357**	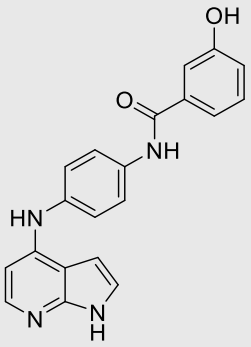
356	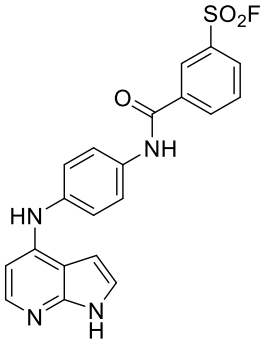	**358**	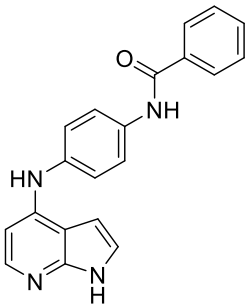

7. Literature

[1] L. N. Johnson, R. J. Lewis, *Chem Rev* **2001**, *101*, 2209–2242.

[2] K.-K. Han, A. Martinage, *Int. J. Biochem.* **1992**, *24*, 19–28.

[3] G. Manning, D. B. Whyte, R. Martinez, T. Hunter, S. Sudarsanam, *Science (1979)* **2002**, *298*, 1912–1934.

[4] D. Fabbro, S. W. Cowan-Jacob, H. Moebitz, *Br J Pharmacol* **2015**, *172*, 2675–2700.

[5] P. Cohen, *Eur J Biochem* **2001**, *268*, 5001–5010.

[6] P. Blume-Jensen, T. Hunter, *Nature* **2001**, *411*, 355–365.

[7] N. Dhanasekaran, E. Premkumar Reddy, *Oncogene* **1998**, *17*, 1447–1455.

[8] P. M. Wolanin, P. A. Thomason, J. B. Stock, *Genome Biol* **2002**, *3*, 1–8.

[9] L. J. Wilson, A. Linley, D. E. Hammond, F. E. Hood, J. M. Coulson, D. J. MacEwan, S. J. Ross, J. R. Slupsky, P. D. Smith, P. A. Eyers, I. A. Prior, *Cancer Res* **2018**, *78*, 15–29.

[10] S. S. Taylor, A. P. Kornev, *Trends Biochem Sci* **2011**, *36*, 65–77.

[11] E. D. Scheeff, P. E. Bourne, *PLoS Comput Biol* **2005**, *1*, e49.

[12] S. K. Hanks, T. Hunter, *The FASEB Journal* **1995**, *9*, 576–596.

[13] S. K. Hanks, A. Marie Quinn, T. Hunter, *Science (1979)* **1988**, *241*, 42–52.

[14] L. N. Johnson, M. E. M. Noble, *Cell* **1996**, *85*, 149–158.

[15] L. N. Johnson, E. D. Lowe, M. E. M. Noble, D. J. Owen, *FEBS Lett* **1998**, *430*, 1–11.

[16] P. Traxler, P. Furet, *Pharmacol. Ther.* **1999**, *82*, 195–206.

[17] Y. Zhou, S. Xiang, F. Yang, X. Lu, *J Med Chem* **2022**, *65*, 15540–15558.

[18] L. Hillebrand, M. Gehringer, *Chimia (Aarau)* **2022**, *76*, 435–447.

[19] Z. Zhao, P. E. Bourne, *Med Res Rev* **2024**, *45*, 629–653.

[20] J. Singh, R. C. Petter, T. A. Baillie, A. Whitty, *Nat Rev Drug Discov* **2011**, *10*, 307–317.

[21] J. Singh, *J Med Chem* **2022**, *65*, 5886–5901.

[22] L. Hillebrand, X. J. Liang, R. A. M. Serafim, M. Gehringer, *J Med Chem* **2024**, *67*, 7668–7758.

[23] K. B. Patel, D. E. Heppner, *RSC Med Chem* **2025**, *16*, 1049–1066.

[24] M. Gehringer, in *Proteinkinase Inhibitors*, Springer, Cham, Switzerland, **2020**, pp. 43–94.

[25] D. E. Heppner, B. C. Ogboo, D. A. Urul, E. W. May, E. M. Schaefer, A. S. Murkin, M. Gehringer, *J Med Chem* **2024**, *67*, 14693–14696.

[26] M. Gehringer, S. A. Laufer, *J Med Chem* **2019**, *62*, 5673–5724.

[27] N. Shindo, A. Ojida, K. Tokunaga, M. Sato, K. Kuwata, C. Miura, H. Fuchida, N. Matsunaga, S. Koyanagi, S. Ohdo, *J Am Chem Soc* **2020**, *142*, 18522–18531.

[28] A. Chaikuad, P. Koch, S. A. Laufer, S. Knapp, *Angewandte Chemie - International Edition* **2018**, *57*, 4372–4385.

[29] Z. Zhang, K. Z. Guiley, K. M. Shokat, *Nat Chem Biol* **2022**, *18*, 1177–1183.

[30] Z. Zhang, J. Morstein, A. K. Ecker, K. Z. Guiley, K. M. Shokat, *J Am Chem Soc* **2022**, *144*, 15916–15921.

[31] Q. Zheng, Z. Zhang, K. Z. Guiley, K. M. Shokat, *Nat Chem Biol* **2024**, *20*, 1114–1122.

[32] Z. Yu, X. He, R. Wang, X. Xu, Z. Zhang, K. Ding, Z. M. Zhang, Y. Tan, Z. Li, *J Am Chem Soc* **2023**, DOI 10.1021/jacs.3c05899.

[33] L. S. Sirocchi, M. Scharnweber, S. Oberndorfer, G. Siszler, K. M. Zak, K. Rumpel, R. A. Neumüller, B. Wilding, *J Am Chem Soc* **2025**, DOI 10.1021/jacs.5c03562.

[34] J. E. Knox, G. L. Burnett, C. Weller, L. Jiang, D. Zhang, N. Vita, A. Marquez, K. J. Seamon, A. Gould, M. Menard, E. Quintana, Z. Chen, Z. Wang, Z. Wang, E. S. Koltun, M. Singh, J. Jiang, D. Wildes, J. A. M. Smith, A. L. Gill, *Cancer Res* **2024**, *84*, ND03–ND03.

[35] G. Platzer, M. Okon, L. P. McIntosh, *J Biomol NMR* **2014**, *60*, 109–129.

[36] D. G. Isom, C. A. Castañed, B. R. Cannon, B. E. García-Moreno, *Proc Natl Acad Sci U S A* **2011**, *108*, 5260–5265.

[37] A. Jones, X. Zhang, X. Lei, *Cell Chem Biol* **2017**, *24*, 537–539.

[38] R. Liu, Z. Yue, C. C. Tsai, J. Shen, *J Am Chem Soc* **2019**, *141*, 6553–6560.

[39] G. H. Iyer, S. Garrod, V. L. Woods, S. S. Taylor, *J Mol Biol* **2005**, *351*, 1110–1122.

[40] H. Mukherjee, J. Debreczeni, J. Breed, S. Tentarelli, B. Aquila, J. E. Dowling, A. Whitty, N. P. Grimster, *Org Biomol Chem* **2017**, *15*, 9685–9695.

[41] K. E. Gilbert, A. Vuorinen, A. Aatkar, P. Pogány, J. Pettinger, E. K. Grant, J. M. Kirkpatrick, K. Rittinger, D. House, G. A. Burley, J. T. Bush, *ACS Chem Biol* **2023**, DOI 10.1021/acschembio.2c00633.

[42] J. Dong, L. Krasnova, M. G. Finn, K. Barry Sharpless, *Angewandte Chemie - International Edition* **2014**, *53*, 9430–9448.

[43] D. E. Moss, P. Berlanga, M. M. Hagan, H. Sandoval, C. Ishida, *Alzheimer Dis Assoc Disord* **1999**, *13*.

[44] B. R. Baker, *Acc Chem Res* **1969**, *2*, 129–136.

[45] A. A. Kumar, J. H. Mangum, D. T. Blankenship, J. H. Freisheim, *Journal of Biological Chemistry* **1981**, *256*, 8970–8976.

[46] S. Ohnuma, E. Chufan, K. Nandigama, L. M. M. Jenkins, S. R. Durell, E. Appella, Z. E. Sauna, S. V Ambudkar, *Biochemistry* **2011**, *50*, 3724–3735.

[47] A. E. Annamalai, J. M. Tomich, M. T. Mas, R. F. Colman, *Arch Biochem Biophys* **1982**, *219*, 47–57.

[48] J. Y. C. Lim, P. D. Beer, *Chem* **2018**, *4*, 731–783.

[49] A. L. Borne, J. W. Brulet, K. Yuan, K. L. Hsu, *RSC Chem Biol* **2021**, *2*, 322–337.

[50] J. W. Brulet, A. L. Borne, K. Yuan, A. H. Libby, K. L. Hsu, *J Am Chem Soc* **2020**, *142*, 8270–8280.

[51] R. L. McCloud, K. Yuan, K. E. Mahoney, D. L. Bai, J. Shabanowitz, M. M. Ross, D. F. Hunt, K. L. Hsu, *Anal Chem* **2021**, *93*, 11946–11955.

[52] T. Huang, S. Hosseinibarkooie, A. L. Borne, M. E. Granade, J. W. Brulet, T. E. Harris, H. A. Ferris, K. L. Hsu, *Chem Sci* **2021**, *12*, 3295–3307.

[53] H. S. Hahm, E. K. Toroitich, A. L. Borne, J. W. Brulet, A. H. Libby, K. Yuan, T. B. Ware, R. L. McCloud, A. M. Ciancone, K. L. Hsu, *Nat Chem Biol* **2020**, *16*, 150–159.

[54] I. S. Moreira, P. A. Fernandes, M. J. Ramos, **2007**, 803–812.

[55] C. Baggio, L. Gambini, P. Udompholkul, A. F. Salem, A. Aronson, A. Dona, E. Troadec, F. Pichiorri, M. Pellecchia, *J Med Chem* **2018**, *61*, 6350–6363.

[56] L. Gambini, C. Baggio, P. Udompholkul, J. Jossart, A. F. Salem, J. J. P. Perry, M. Pellecchia, *J Med Chem* **2019**, *62*, 5616–5627.

[57] C. Baggio, P. Udompholkul, L. Gambini, A. F. Salem, J. Jossart, J. J. P. Perry, M. Pellecchia, *J Med Chem* **2019**, *3*, 9188–9200.

[58] P. Udompholkul, A. Garza-Granados, G. Alboreggia, C. Baggio, J. McGuire, S. D. Pegan, M. Pellecchia, *J Med Chem* **2023**, *66*, 8159–8169.

[59] P. Udompholkul, C. Baggio, L. Gambini, G. Alboreggia, M. Pellecchia, *J Med Chem* **2021**, *64*, 16147–16158.

[60] L. Gambini, P. Udompholkul, A. F. Salem, C. Baggio, M. Pellecchia, *ChemMedChem* **2020**, *15*, 2176–2184.

[61] H. Mukherjee, N. Su, M. A. Belmonte, D. Hargreaves, J. Patel, S. Tentarelli, B. Aquila, N. P. Grimster, *Bioorg Med Chem Lett* **2019**, *29*, 126682.

[62] X. Wan, T. Yang, A. Cuesta, X. Pang, T. E. Balius, J. J. Irwin, B. K. Shoichet, J. Taunton, *J Am Chem Soc* **2020**, *142*, 4960–4964.

[63] A. Cuesta, X. Wan, A. L. Burlingame, J. Taunton, *J Am Chem Soc* **2020**, *142*, 3392–3400.

[64] X. Yang, M. A. Dilweg, D. Osemwengie, L. Burggraaff, D. van der Es, L. H. Heitman, A. P. IJzerman, *Biochem Pharmacol* **2020**, *180*, DOI 10.1016/j.bcp.2020.114144.

[65] X. Yang, J. P. D. Van Veldhoven, J. Offringa, B. J. Kuiper, E. B. Lenselink, L. H. Heitman, D. Van Der Es, A. P. Ijzerman, *J Med Chem* **2019**, *62*, 3539–3552.

[66] B. L. H. Beerkens, Ç. Koç, R. Liu, B. I. Florea, S. E. Le Dévédec, L. H. Heitman, A. P. Ijzerman, D. Van Der Es, *ACS Chem Biol* **2022**, *17*, 3131–3139.

[67] B. L. H. Beerkens, X. Wang, M. Avgeropoulou, L. N. Adistia, J. P. D. van Veldhoven, W. Jespers, R. Liu, L. H. Heitman, A. P. IJzerman, D. van der Es, *RSC Med Chem* **2022**, *13*, 850–856.

[68] M. L. J. Doornbos, X. Wang, S. C. Vermond, L. Peeters, L. Pérez-Benito, A. A. Trabanco, H. Lavreysen, J. M. Cid, L. H. Heitman, G. Tresadern, A. P. Ijzerman, *J Med Chem* **2019**, *62*, 223–233.

[69] K. Bum-Erdene, D. Liu, G. Gonzalez-Gutierrez, M. K. Ghozayel, D. Xu, S. O. Meroueh, *Proc Natl Acad Sci U S A* **2020**, *117*, 7131–7139.

[70] J. A. Ippolito, H. Niu, N. Bertoletti, Z. J. Carter, S. Jin, K. A. Spasov, J. A. Cisneros, M. Valhondo, K. J. Cutrona, K. S. Anderson, W. L. Jorgensen, *ACS Med Chem Lett* **2021**, *12*, 249–255.

[71] J. E. Bolding, P. Martín-Gago, N. Rajabi, L. F. Gamon, T. N. Hansen, C. R. O. Bartling, K. Strømgaard, M. J. Davies, C. A. Olsen, *Angewandte Chemie - International Edition* **2022**, *61*, e202204565.

[72] J. T. Cruite, R. P. Nowak, K. A. Donovan, S. B. Ficarro, H. Huang, H. Liu, Y. Liu, J. A. Marto, R. J. Metivier, E. S. Fischer, L. H. Jones, *ACS Med Chem Lett* **2023**, *14*, 1576–1581.

[73] R. P. Nowak, L. Ragosta, F. Huerta, H. Liu, S. B. Ficarro, J. T. Cruite, R. J. Metivier, K. A. Donovan, J. A. Marto, E. S. Fischer, B. L. Zerfas, L. H. Jones, *RSC Chem Biol* **2023**, *4*, 906–912.

[74] Q. Zhao, X. Ouyang, X. Wan, K. S. Gajiwala, J. C. Kath, L. H. Jones, A. L. Burlingame, J. Taunton, *J Am Chem Soc* **2017**, *139*, 680–685.

[75] J. M. Hatcher, G. Wu, C. Zeng, J. Zhu, F. Meng, S. Patel, W. Wang, S. B. Ficarro, A. L. Leggett, C. E. Powell, J. A. Marto, K. Zhang, J. C. Ki Ngo, X. D. Fu, T. Zhang, N. S. Gray, *Cell Chem Biol* **2018**, *25*, 460-470.e6.

[76] F. Ferlenghi, L. Scalvini, F. Vacondio, R. Castelli, N. Bozza, G. Marseglia, S. Rivara, A. Lodola, S. La Monica, R. Minari, P. G. Petronini, R. Alfieri, M. Tiseo, M. Mor, *Eur J Med Chem* **2021**, *225*, DOI 10.1016/j.ejmech.2021.113786.

[77] B. Cosgrove, E. K. Grant, S. Bertrand, K. D. Down, D. O. Somers, J. P. Evans, N. C. O. Tomkinson, M. D. Barker, *RSC Chem Biol* **2023**, *4*, 1111–1122.

[78] H. Mukherjee, N. P. Grimster, *Curr Opin Chem Biol* **2018**, *44*, 30–38.

[79] J. Engel, J. Lategahn, D. Rauh, *ACS Med Chem Lett* **2016**, *7*, 2–5.

[80] T. Barf, A. Kaptein, *J Med Chem* **2012**, *55*, 6243–6262.

[81] R. Bischoff, H. Schlüter, *J Proteomics* **2012**, *75*, 2275–2296.

[82] L. H. Jones, *Angewandte Chemie - International Edition* **2018**, *57*, 9220–9223.

[83] J. Che, L. H. Jones, *RSC Med Chem* **2022**, *13*, 1121–1126.

[84] S. Guth, S. Hüser, A. Roth, G. Degen, P. Diel, K. Edlund, G. Eisenbrand, K. H. Engel, B. Epe, T. Grune, V. Heinz, T. Henle, H. U. Humpf, H. Jäger, H. G. Joost, S. E. Kulling, A. Lampen, A. Mally, R. Marchan, D. Marko, E. Mühle, M. A. Nitsche, E. Röhrdanz, R. Stadler, C. van Thriel, S. Vieths, R. F. Vogel, E. Wascher, C. Watzl, U. Nöthlings, J. G. Hengstler, *Toxicity of Fluoride: Critical Evaluation of Evidence for Human Developmental Neurotoxicity in Epidemiological Studies, Animal Experiments and in Vitro Analyses*, Springer Berlin Heidelberg, **2020**.

[85] W. Xu, C. Kang, *J Med Chem* **2025**, DOI 10.1021/acs.jmedchem.5c00424.

[86] K. McAulay, A. Bilsland, M. Bon, *Pharmaceuticals* **2022**, *15*, DOI 10.3390/ph15111366.

[87] N. S. Troelsen, M. H. Clausen, *Chemistry - A European Journal* **2020**, *26*, 11391–11403.

[88] W. Lu, M. Kostic, T. Zhang, J. Che, M. P. Patricelli, L. H. Jones, E. T. Chouchani, N. S. Gray, *RSC Chem Biol* **2021**, *2*, 354–367.

[89] R. Lonsdale, R. A. Ward, *Chem Soc Rev* **2018**, *47*, 3816–3830.

[90] D. E. Mortenson, G. J. Brighty, L. Plate, G. Bare, W. Chen, S. Li, H. Wang, B. F. Cravatt, S. Forli, E. T. Powers, K. B. Sharpless, I. A. Wilson, J. W. Kelly, *J Am Chem Soc* **2018**, *140*, 200–210.

[91] G. J. Brighty, R. C. Botham, S. Li, L. Nelson, D. E. Mortenson, G. Li, C. Morisseau, H. Wang, B. D. Hammock, K. B. Sharpless, J. W. Kelly, *Nat Chem* **2020**, *12*, 906–913.

[92] C. Liongue, T. Ratnayake, F. Basheer, A. C. Ward, *Int J Mol Sci* **2024**, *25*, 2977.

[93] M. Forster, M. Gehringer, S. A. Laufer, *Bioorg Med Chem Lett* **2017**, *27*, 4229–4237.

[94] M. Forster, A. Chaikuad, T. Dimitrov, E. Döring, J. Holstein, B. T. Berger, M. Gehringer, K. Ghoreschi, S. Müller, S. Knapp, S. A. Laufer, *J Med Chem* **2018**, *61*, 5350–5366.

[95] H. A. Blair, *Drugs* **2023**, *83*, 1315–1321.

[96] M. Gehringer, M. Forster, E. Pfaffenrot, S. M. Bauer, S. A. Laufer, *ChemMedChem* **2014**, *9*, 2516–2527.

[97] M. Forster, A. Chaikuad, S. M. Bauer, J. Holstein, M. B. Robers, C. R. Corona, M. Gehringer, E. Pfaffenrot, K. Ghoreschi, S. Knapp, S. A. Laufer, *Cell Chem Biol* **2016**, *23*, 1335–1340.

[98] R. Gaur, K. A. Mensah, J. Stricker, M. Adams, A. Parton, D. Cedzik, J. Connarn, M. Thomas, G. Horan, P. Schafer, S. Mair, M. Palmisano, F. Ramírez-Valle, *Arthritis Res Ther* **2022**, *24*, DOI 10.1186/s13075-022-02850-6.

[99] P. Ganguly, T. Macleod, C. Wong, M. Harland, D. McGonagle, *Pharmaceuticals* **2023**, *16*, 1286.

[100] J. Malona, C. Chuaqui, B. M. Seletsky, L. Beebe, S. Cantin, D. Van Kalken, K. Fahnoe, Z. Wang, B. Browning, H. Szabo, L. A. Koopman, T. Oravecz, J. J. McDonald, F. Ramirez-Valle, R. Gaur, K. A. Mensah, M. Thomas, J. N. Connarn, H. Hu, M. D. Alexander, A. F. Corin, *Translational Research* **2022**, *249*, 49–73.

[101] L. Rooney, C. Jones, *ACS Omega* **2021**, *6*, 20729–20734.

[102] H. González-Álvarez, D. Ensan, T. Xin, J. F. Wong, C. A. Zepeda-Velázquez, J. Cros, M. N. Sweeney, L. Hoffer, T. Kiyota, B. J. Wilson, A. Aman, O. Roberts, M. B. Isaac, A. N. Bullock, D. Smil, R. Al-Awar, *J Med Chem* **2024**, *67*, 4707–4725.

[103] T. Katagiri, S. Tsukamoto, M. Kuratani, *Biomedicines* **2021**, *9*, 736.

[104] K. Sekimata, T. Sato, N. Sakai, *Chem. Pharm. Bull* **2020**, *68*, 194–200.

[105] A. J. Davis, N. Brooijmans, J. D. Brubaker, F. Stevison, T. P. LaBranche, F. Albayya, P. Fleming, B. L. Hodous, J. L. Kim, S. Kim, R. Lobbardi, M. Palmer, M. P. Sheets, J. Vassiliadis, R. Wang, B. D. Williams, D. Wilson, L. Xu, X. Julia Zhu, K. Bouchard, J. W. Hunter, C. Graul, E. Greenblatt, A. Hussein, M. Lyon, J. Russo, R. Stewart, M. Dorsch, T. J. Guzi, V. Kadambi, C. Lengauer, A. P. Garner, *Sci. Transl. Med* **2024**, *16*, eabp8334.

[106] S. Ito, S. Otsuki, H. Ohsawa, A. Hirano, H. Kazuno, S. Yamashita, K. Egami, Y. Shibata, I. Yamamiya, F. Yamashita, Y. Kodama, K. Funabashi, H. Kazuno, T. Komori, S. Suzuki, H. Sootome, H. Hirai, T. Sagara, *ACS Med Chem Lett* **2023**, *14*, 396–404.

[107] M. Gehringer, E. Pfaffenrot, S. Bauer, S. A. Laufer, *ChemMedChem* **2014**, *9*, 277–281.

[108] E. Pfaffenrot, Design, Synthese Und Optimierung Neuer Trizyklischer Januskinase 3 Inhibitoren, Eberhard Karls Universität Tübingen, **2016**.

[109] L. Hillebrand, G. Wang, A. Rasch, B. Masberg, A. Chaikuad, T. Kronenberger, E. Günther, M. Forster, A. Poso, M. Lämmerhofer, S. A. Laufer, S. Knapp, M. Gehringer, *RSC Med Chem* **2025**, *accepted*.

[110] A. Rasch, Synthese Trizyklischer JAK3-Inhibitoren Zur Kovalenten Adressierung von Tyrosinen in Der Hinge-Region Mit Fluorosulfat-Warheads, Masterarbeit, Eberhard Karls Universität Tübingen, **2021**.

[111] H. Zhou, P. Mukherjee, R. Liu, E. Evrard, D. Wang, J. M. Humphrey, T. W. Butler, L. R. Hoth, J. B. Sperry, S. K. Sakata, C. J. Helal, C. W. Am Ende, *Org Lett* **2018**, *20*, 812–815.

[112] T. S. B. Lou, M. C. Willis, *Tetrahedron* **2020**, *76*, 130782.

[113] J. M. Murphy, C. C. Tzschucke, J. F. Hartwig, *Org Lett* **2007**, *9*, 757–760.

[114] A. Talko, D. Antoniak, M. Barbasiewicz, *Synthesis (Stuttg)* **2019**, *51*, 2278–2286.

[115] X. Wang, X. Li, J. Xue, Y. Zhao, Y. Zhang, *Tetrahedron Lett* **2009**, *50*, 413–415.

[116] D. C. Batesky, M. J. Goldfogel, D. J. Weix, *Journal of Organic Chemistry* **2017**, *82*, 9931–9936.

[117] B. Xu, L. Troian-gautier, R. Dykstra, R. T. Martin, O. Gutierrez, U. K. Tambar, *J Am Chem Soc* **2020**, *142*, 6206–6215.

[118] T. Konno, T. Takehana, M. Mishima, T. Ishihara, *Journal of Organic Chemistry* **2006**, *71*, 3545–3550.

[119] D. Guérin, A. C. Gaumont, I. Dez, M. Mauduit, S. Couve-Bonnaire, X. Pannecoucke, *ACS Catal* **2014**, *4*, 2374–2378.

[120] I. R. Nascimento, L. M. X. Lopes, L. B. Davin, N. G. Lewis, *Tetrahedron* **2000**, *56*, 9181–9193.

[121] F. Krätzschmar, M. Kaßel, D. Delony, A. Breder, *Chemistry - A European Journal* **2015**, *21*, 7030–7034.

[122] L. Adak, K. Chattopadhyay, B. C. Ranu, *Journal of Organic Chemistry* **2009**, *74*, 3982–3985.

[123] M. S. A. Elsayed, J. J. Nielsen, S. Park, J. Park, Q. Liu, C. H. Kim, Y. Pommier, K. Agama, P. S. Low, M. Cushman, *J Med Chem* **2018**, *61*, 10440–10462.

[124] X. Huang, G. W. Shipps, C. C. Cheng, P. Spacciapoli, X. Zhang, M. A. McCoy, D. F. Wyss, X. Yang, A. Achab, K. Soucy, D. K. Montavon, D. M. Murphy, C. E. Whitehurst, *ACS Med Chem Lett* **2011**, *2*, 632–637.

[125] M. Mori, G. Stelitano, A. Gelain, E. Pini, L. R. Chiarelli, J. C. Sammartino, G. Poli, T. Tuccinardi, G. Beretta, A. Porta, M. Bellinzoni, S. Villa, F. Meneghetti, *J Med Chem* **2020**, *63*, 7066–7080.

[126] A. L. Tribby, I. Rodríguez, S. Shariffudin, N. D. Ball, *Journal of Organic Chemistry* **2017**, *82*, 2294–2299.

[127] A. T. Davies, J. M. Curto, S. W. Bagley, M. C. Willis, *Chem Sci* **2017**, *8*, 1233–1237.

[128] Y. Liu, T. Okazoe, T. Gatzenmeier, K. Nozaki, *ChemistryEurope* **2024**, *2*, DOI 10.1002/ceur.202400053.

[129] G. Wang, N. J. Seidler, S. Röhm, Y. Pan, X. J. Liang, L. Haarer, B. T. Berger, S. A. Sivashanmugam, V. R. Wydra, M. Forster, S. A. Laufer, A. Chaikuad, M. Gehringer, S. Knapp, *Angewandte Chemie - International Edition* **2025**, DOI 10.1002/anie.202419736.

[130] J. T. Cruite, G. P. Dann, J. Che, K. A. Donovan, S. Ferrao, S. B. Ficarro, E. S. Fischer, N. S. Gray, F. Huerta, N. R. Kong, H. Liu, J. A. Marto, R. J. Metivier, R. P. Nowak, B. L. Zerfas, L. H. Jones, *RSC Chem Biol* **2022**, *3*, 1105–1110.

[131] K. L. Wilson, J. Murray, C. Jamieson, A. J. B. Watson, *Synlett* **2018**, *29*, 650–654.

[132] N. Marion, O. Navarro, J. Mei, E. D. Stevens, N. M. Scott, S. P. Nolan, *J Am Chem Soc* **2006**, *128*, 4101–4111.

[133] A. L. S. Thompson, G. W. Kabalka, M. R. Akula, J. W. Huffman, *Synthesis (Stuttg)* **2005**, 547–550.

[134] I. Pevet, C. Brulé, A. Tizot, A. Gohier, F. Cruzalegui, J. A. Boutin, S. Goldstein, *Bioorg Med Chem* **2011**, *19*, 2517–2528.

[135] B. J. Eduful, S. N. O'Byrne, L. Temme, C. R. M. Asquith, Y. Liang, A. Picado, J. R. Pilotte, M. A. Hossain, C. I. Wells, W. J. Zuercher, C. M. C. Catta-Preta, P. Zonzini Ramos, A. D. S. Santiago, R. M. Couñago, C. G. Langendorf, K. Nay, J. S. Oakhill, T. L. Pulliam, C. Lin, D. Awad, T. M. Willson, D. E. Frigo, J. W. Scott, D. H. Drewry, *J Med Chem* **2021**, *64*, 10849–10877.

[136] L. J. Gao, S. Kovackova, M. Šála, A. T. Ramadori, S. De Jonghe, P. Herdewijn, *J Med Chem* **2014**, *57*, 7624–7643.

[137] K. Kristian, J. Fanfrlík, M. Lepšík, *ChemPhysChem* **2018**, *19*, 2540–2548.

[138] S. C. C. Lucas, J. E. Moore, C. S. Donald, J. L. Hawkins, *Journal of Organic Chemistry* **2015**, *80*, 12594–12598.

[139] S. Gerstenecker, Design and Synthesis of Covalent Inhibitors Targeting Cysteines in the Hinge Region of S6K2 and MPS1, Eberhard Karls Universität Tübingen, **2023**.

[140] P. S. Fier, S. Kim, *J Am Chem Soc* **2024**, *146*, 6476–6480.

[141] S. M. Bauer, M. Gehringer, S. A. Laufer, *Analytical Methods* **2014**, *6*, 8817–8822.

[142] L. H. Jones, *Chem Sci* **2025**, DOI 10.1039/D5SC02647D.

[143] T. Anastassiadis, S. W. Deacon, K. Devarajan, H. Ma, J. R. Peterson, *Nat Biotechnol* **2011**, *29*, 1039–1045.

[144] Y. Wang, H. Ma, *Drug Discov Today Technol* **2015**, *18*, 1–8.

[145] M. D. Shults, K. A. Janes, D. A. Lauffenburger, B. Imperiali, *Nat Methods* **2005**, *2*, 277–283.

[146] M. D. Shults, D. Carrico-Moniz, B. Imperiali, *Anal Biochem* **2006**, *352*, 198–207.

[147] E. Luković, J. A. González-Vera, B. Imperiali, *J Am Chem Soc* **2008**, *130*, 12821–12827.

[148] A. Aatkar, A. Vuorinen, O. E. Longfield, K. Gilbert, R. Peltier-Heap, C. D. Wagner, F. Zappacosta, K. Rittinger, C. W. Chung, D. House, N. C. O. Tomkinson, J. T. Bush, *ACS Chem Biol* **2023**, *18*, 1926–1937.

[149] S. C. Koeberle, J. Romir, S. Fischer, A. Koeberle, V. Schattel, W. Albrecht, C. Grütter, O. Werz, D. Rauh, T. Stehle, S. A. Laufer, *Nat Chem Biol* **2012**, *8*, 141–143.

[150] H. Mukherjee, J. Debreczeni, J. Breed, S. Tentarelli, B. Aquila, J. E. Dowling, A. Whitty, N. P. Grimster, *Org Biomol Chem* **2017**, *15*, 9685–9695.

[151] G. R. Grimsley, J. M. Scholtz, C. N. Pace, *Protein Science* **2009**, *18*, 247–251.

[152] S. Pahari, L. Sun, E. Alexov, *Database* **2019**, *2019*, 1–7.

[153] G. K. Kanev, C. de Graaf, B. A. Westerman, I. J. P. de Esch, A. J. Kooistra, *Nucleic Acids Res* **2021**, *49*, D562–D569.

[154] M. E. Berginski, N. Moret, C. Liu, D. Goldfarb, P. K. Sorger, S. M. Gomez, *Nucleic Acids Res* **2021**, *49*, D529–D535.

[155] H. Huang, L. H. Jones, *Expert Opin Drug Discov* **2023**, *18*, 725–735.

[156] E. Vandermarliere, M. Mueller, L. Martens, *Mass Spectrom Rev* **2013**, *32*, 453–465.

[157] M. Teng, M. Teng, S. B. Ficarro, S. B. Ficarro, S. B. Ficarro, H. Yoon, H. Yoon, J. Che, J. Che, J. Zhou, E. S. Fischer, E. S. Fischer, J. A. Marto, J. A. Marto, J. A. Marto, T. Zhang, T. Zhang, N. S. Gray, N. S. Gray, *ACS Med Chem Lett* **2020**, *11*, 1269–1273.

[158] P. Giansanti, L. Tsiatsiani, T. Y. Low, A. J. R. Heck, *Nat Protoc* **2016**, *11*, 993–1006.

[159] T. Dau, G. Bartolomucci, J. Rappsilber, *Anal Chem* **2020**, *92*, 9523–9527.

[160] M. Holderfield, T. E. Nagel, D. D. Stuart, *Br J Cancer* **2014**, *111*, 640–645.

[161] U. M. Battisti, C. Gao, O. Nilsson, F. Akladios, A. Lulla, A. Bogucka, A. Nain-Perez, L. Håversen, W. Kim, J. Boren, M. Hyvönen, M. Uhlen, A. Mardinoglu, M. Grøtli, *ChemBioChem* **2023**, *24*, DOI 10.1002/cbic.202200339.

[162] F. H. Niesen, H. Berglund, M. Vedadi, *Nat Protoc* **2007**, *2*, 2212–2221.

[163] K. Gao, R. Oerlemans, M. R. Groves, *Biophys Rev* **2020**, *12*, 85–104.

[164] B. L. Roman, A. P. Hinck, *Cellular and Molecular Life Sciences* **2017**, *74*, 4539–4560.

[165] L. Rooney, C. Jones, *ACS Omega* **2021**, *6*, 20729–20734.

[166] G. R. Fulmer, A. J. M. Miller, N. H. Sherden, H. E. Gottlieb, A. Nudelman, B. M. Stoltz, J. E. Bercaw, K. I. Goldberg, *Organometallics* **2010**, *29*, 2176–2179.

[167] J. Rappsilber, Y. Ishihama, M. Mann, *Anal Chem* **2003**, *75*, 663–670.

[168] K. S. Li, J. G. Quinn, M. J. Saabye, J. F. S. Guerrero, J. Nonomiya, Q. Lian, W. Phung, Y. Izrayelit, B. T. Walters, A. Gustafson, N. F. Endres, M. H. Beresini, M. M. Mulvihill, *Anal Chem* **2022**, *94*, 1230–1239.

[169] A. Keeley, P. Ábrányi-Balogh, G. M. Keseru, *Medchemcomm* **2019**, *10*, 263–267.

[170] O. Fedorov, F. H. Niesen, S. Knapp, in *Kinase Inhibitors: Methods and Protocols* (Ed.: B. Kuster), Humana Press, Totowa, NJ, **2012**, pp. 109–118.

[171] C. H. Heldin, A. Moustakas, *Cold Spring Harb Perspect Biol* **2016**, *8*, DOI 10.1101/cshperspect.a022053.